Published in final edited form as:
Clin Trials. 2011 October ; 8(5): 591–600. doi:10.1177/1740774511419683.

Challenges to accrual predictions to phase III cancer clinical trials: a survey of study chairs and lead statisticians of 248 NCI sponsored trials

Anneke T. Schroen, MD, MPH[1,2], **Gina R. Petroni**[2], **Hongkun Wang**[2], **Monika J. Thielen**[1], **Daniel J. Sargent**[3], **Jacqueline Benedetti**[4], **Walter M. Cronin**[5], **Donald L. Wickerham**[6], **Xiaofei F. Wang**[7], **Robert Gray**[8], **Wendy F Cohn**[2], **Craig L. Slingluff Jr.**[1], and **Benjamin Djulbegovic**[9]

[1]Department of Surgery, University of Virginia, Charlottesville, Virginia, USA

[2]Department of Public Health Sciences, University of Virginia, Charlottesville, Virginia, USA

[3]Department of Health Sciences Research, Mayo Clinic, Rochester, Minnesota, USA

[4]Southwest Oncology Group Statistical Center, Seattle, Washington, USA

[5]Department of Biostatistics, University of Pittsburgh, Pittsburgh, PA

[6]National Surgical Adjuvant Breast and Bowel Project Operating Center, Pittsburgh, Pennsylvania, USA

[7]Department of Biostatistics & Bioinformatics, Duke University, Durham, North Carolina, USA

[8]Department of Biostatistics, Dana Farber Cancer Institute, Boston, MA USA

[9]Department of Medicine, University of South Florida, Tampa, Florida, USA

Introduction

Low accrual to adult oncology clinical trials is a major obstacle to progress in cancer therapy. Research in barriers to trial accrual has focused primarily on physician and patient deterrents to trial participation - deterrents that affect accrual after a trial has opened.[1-7] Research in processes prior to trial activation that may impact accrual has been far less common. Operational studies of trial development processes have illustrated the lengthy sequence of steps involved in the progression from concept submission to trial activation.[8] Factors related to trial design may also impact accrual.[9] This has not been well studied but we believe identifying factors related to accrual that are present prior to trial opening has relevant and immediate ramifications for clinical trial conduct.

We conducted a survey of study chairs and lead statisticians involved in phase III cancer trials, in order to define issues that may affect clinical trial accrual but are recognizable during protocol development. This survey complements data collected as part of a larger study, entitled the Oncology Clinical Trial Accrual Study (OCTAS), which entails a systematic evaluation of combined phase III trial experiences from five National Cancer Institute (NCI) - sponsored Clinical Trials Cooperative Groups (CTCG) performed over a ten-year time period. The perceptions of national clinical trial leaders on trial design processes and accrual influences have not been previously studied. Survey questions

Corresponding Author Anneke T Schroen, MD, MPH Department of Surgery University of Virginia P.O. Box 800709 Charlottesville, VA USA 22908-0709 ats2x@virginia.edu.

concentrated on investigator experience, trial design elements, accrual prediction practices, and perceived accrual influences. These responses were then evaluated in light of each trial's actual accrual experience.

Methods

The study population was created by identifying the study chair and lead statistician for each phase III trial open between January 1, 1993 and December 31, 2002, by one of five participating CTCGs. A total of 248 phase III trials were included, sponsored by the Cancer and Leukemia Group B (CALGB), Eastern Cooperative Oncology Group (ECOG), North Central Cancer Treatment Group (NCCTG), National Surgical Adjuvant Breast and Bowel Project (NSABP), or Southwest Oncology Group (SWOG). Participation was limited to U.S. CTCGs offering therapeutic trials for adult cancer patients to reduce variability in accrual experiences. Of the 8 applicable CTCGs, one (American College of Surgeons Oncology Group) was not open for the entire study period and two (Gynecology Oncology Group and Radiation Therapy Oncology Group) were not strongly pursued since less specialized groups were ideally sought. The remaining five CTCGs agreed to participate and offered a heterogeneous mix in disease sites and treatment modalities to meet the goals of this study. Protocols were reviewed to identify the study chair and lead statistician for each trial. For intergroup trials, the study chair and lead statistician were derived from the originating CTCG. Cooperative group input was sought to determine the most appropriate persons as study chair and lead statistician for trials where the person filling this role was unclear. NSABP substituted the protocol officer for the study chair in their trials; within the organizational structure of NSABP, the protocol officer assumes responsibilities commonly performed by the study chair. Since this substitution only pertains to a small number of trials (n=18), the responses from protocol officers and study chairs are reported together. Updated contact information and email addresses were confirmed for each survey recipient prior to this study. An introductory email notifying recipients of the upcoming survey was also used to help verify active email addresses. The final survey recipient population consisted of 179 unique study chairs and 49 unique statisticians since an individual could be associated with more than one trial.

A self-administered, web-based survey consisting of 28 questions for lead statisticians and 29 questions for study chairs was developed using published guidelines for question writing and survey construction.[10] The survey questions were evaluated by oncologists, statisticians, and a survey methodologist from the University of Virginia (WFC) affiliated with this project. The survey instrument then underwent a pilot test among a convenience sample of five medical, surgical, and radiation oncologists with experience as clinical trial principal investigators as well as a biostatistician with cooperative group experience. Revisions were made based on comments received from expert review and the pilot test.

Each survey was unique to a specific trial with questions adapted to the study chair or lead statistician role. Questions focused on perceptions about the following: accrual prediction influences, feasibility of predicted accrual, presence of clinical equipoise, and factors contributing to accrual success for an individual trial. Additional questions queried perceptions about control arm selection and appropriateness of eligibility criteria. General questions examined prior clinical trial experience, academic rank, medical specialty, and gender. A 5-point Likert scale quantified respondents' perceptions of influences on accrual predictions and accrual success. The scale used 1 to indicate a factor had strong influence, 3 to indicate some influence, and 5 to indicate no influence. An option to indicate that a factor was not applicable or its influence was unknown was provided.

After the introductory email, each recipient received a separate invitation to participate in the survey. The survey included a sequential roll-out among the five CTCGs between April 8 and May 5, 2008. The survey was closed on June 25, 2008. Each recipient received three reminder emails spaced two weeks apart. The email provided a link to a web-based survey for each trial assigned to a recipient. The study included a novel deferral process, allowing a recipient to defer a survey for any assigned trial and recommend another individual who could better represent the trial. This process was instituted to ensure that each survey was sent to the most appropriate person and to maximize response rates. The survey website also featured endorsement letters from the five CTCG chairmen as well as assurance regarding confidentiality of responses.

Accrual sufficiency categorization was based on the reason for trial termination documented by the CTCG, not survey responses. Target and actual accrual data were available for each trial. Sufficient accrual was defined as any of the following: (1) meeting target accrual, (2) CTCG documentation stating the trial had closed with complete or adequate accrual, (3) closure at interim analysis with conclusive results, or (4) closure due to toxicity. Target accrual comprised either the original sample size as documented in the initial protocol or a revised sample size if the trial underwent a major revision during its course which affected the statistical considerations. Insufficient accrual was defined as any of the following: (1) CTCG documentation indicating closure due to poor accrual, or (2) closure due to factors external to the trial rendering it likely unable to address the primary endpoint, such as discontinuation of a test agent or loss of equipoise resulting from new data. Five trials remained open to accrual at the time of the survey. At analysis, two more had closed with sufficient accrual and the other three remained open with 71%, 76%, and 90% of the target accrual met. Given these good accrual rates, these five trials were included in the analysis as trials with sufficient accrual. Eligible survey responses required 10 or more answered questions, excluding questions about respondent gender or medical specialty. This cutoff for eligibility was determined by distinct patterns in number of questions answered among the respondents.

Prior clinical trial experience of the study chair or lead statistician was categorized as 0, 1, 2-10, 11-20, or greater than 21 trials in which the respondent had had a leading role. This allowed consistent trial experience categorization to be used for the study chairs and lead statisticiansLS, while distinguishing limited trial experience from moderate or high levels of prior trial experience. Responses for therapeutic versus non-therapeutic trials were compared due to inherent differences between these trial types and due to a propensity for unique respondents representing the greatest number of trials to be involved with non-therapeutic trials. Therapeutic trials were defined as testing treatments specifically for cancer. Non-therapeutic trials included cancer prevention trials, behavior modification trials, quality of life trials, and trials testing treatments for cancer-related symptoms or cancer treatment-related symptoms. A measure of recalled equipoise was obtained by asking about the perceived value of experimental treatment(s) versus control treatment(s) when the trial opened and closed to accrual. This perceived value was reported in six categories: (1) control treatment highly preferred to experimental treatment, (2) control treatment preferred to experimental treatment, (3) about equal with experimental treatment expected to be disappointing, (4) about equal with experimental treatment expected to be successful, (5) experimental treatment preferred to control treatment, and (6) experimental treatment highly preferred to control treatment. Analysis of these responses was conducted both for all six categories and by reduction to three categories in which responses 1 and 2 showed lack of equipoise favoring the control arm, 3 and 4 showed equipoise, 5 and 6 showed lack of equipoise favoring the experimental arm.

Analysis of each questionnaire item was performed by respondent role (lead statistician vs. study chair), trial type (therapeutic vs. non-therapeutic), and accrual sufficiency status (sufficient vs. insufficient). The Pearson's chi-square test was used for categorical data and the Student t-test or one-way analysis of variance for continuous data. Likert scale data were viewed as ordinal with median values reported. Since respondents could indicate that a factor was not used or applicable, the proportion of respondents actually citing a factor on the Likert scale is reported with each response category. A test for paired binomials was used to evaluate perceptions of equipoise at trial opening and closing for the same respondents. Results are reported only in aggregate form. Analytic tests were performed with SAS 9.0 (SAS, Cary, NC). Although this survey was conducted with CTCG cooperation, the survey design and conduct, data analysis, and results interpretation were performed independently of the CTCGs by study personnel at the University of Virginia. This study was approved by the University of Virginia Institutional Review Board (IRB-HSR # 12582) and granted waiver of consent.

Results

Response Rate

Of 496 total surveys sent out, responses were received for 335 (68%). Twenty-six responses (8%) were ineligible due to fewer than 10 questions being answered. Of the remaining 309 responses (63% overall eligible response rate), 199 came from lead statisticians (81% eligible response rate) and 110 from study chairs (45% eligible response rate). 223 (90%) of 248 trials were represented by at least one response with matched pair responses received from both the study chair and lead statistician for 86 trials (35%). Of the 25 trials for which no survey response was received, sixteen (64%) were classified as having sufficient accrual, which is similar to the rate of accrual sufficiency seen overall in this trial cohort.

Respondent and Trial Characteristics

Respondent gender and medical specialty are reported by unique respondent rather than by response. Study chairs most commonly were medical oncologists (75%) with the remaining study chairs representing surgical oncology (5%), radiation oncology (4%), or other (16%). Study chairs were less often female (19%) than were lead statisticians (56%). Eligible responses were received from 77 unique study chairs, representing a median of 1 trial per respondent (range 1-12), and from 34 unique lead statisticians, representing a median of 4 trials per respondent (range 1-44). Of note, only 4 lead statistician respondents represented nine or more trials. Considerable variability in responses for trial-specific questions was noted in respondents representing high numbers of trials.

Among the 223 trials for which survey responses were received, 140 (63%) were classified as sufficient accrual and 83 (37%) as insufficient accrual. Only three trials categorized as insufficient accrual were closed due to external factors. Among these 223 trials, 163 (73%) were classified as therapeutic. These classifications of accrual sufficiency and trial type were obtained from CTCG documentation and were not dependent on survey responses. There was no significant difference between therapeutic and non-therapeutic trials in proportions categorized as having sufficient accrual.

Investigator Experience

The remaining results are presented by response because these characteristics may have changed for an individual respondent representing multiple trials. Academic rank, prior trial leadership experience, and continuity of involvement in a trial's course from design to closure for study chairs and lead statisticians are depicted in Table 1. Clear and expected differences exist between study chairs and lead statisticians overall. However, no association

between these respondent characteristics and trial accrual sufficiency status was identified within these two respondent groups. Specifically, seniority was not associated with greater likelihood of attaining sufficient accrual. Among study chairs who were assistant professors at the start of their trial, 74% led trials with sufficient accrual. For study chairs who were associate professors or professors, 69% and 63% respectively completed their trials with sufficient accrual. Similarly, prior trial leadership experience was not associated with greater likelihood of accrual success.

Trial Design Elements

Trial design factors as reported by the study chairs are listed in Table 2, including use of a placebo or observation arm, time elapsed from trial concept to activation, and appropriateness of eligibility criteria. No significant associations were found between these reported trial design factors and accrual sufficiency. In particular, study chairs were no more likely to recall overly restrictive eligibility criteria with trials having insufficient as compared to sufficient accrual.

When given the option of marking all choices that apply, study chairs indicated that the following factors most commonly influenced selection of the control intervention:(1) systematic literature review (57%), (2) expert opinion within the CTCG (57%), and (3) standard of care within one's community based on personal experience (45%). Clinician surveys regarding the standard of care (22%), best judgment of the study chair (19%), meta-analysis of relevant trials (8%), and other (7%) were selected much less often. The reported influences in control arm selection were nearly identical between study chairs of trials with sufficient and insufficient accrual. Control arm selection in therapeutic trials was more commonly influenced by expert opinion within the CTCG than in non-therapeutic trials (65% vs. 29% respectively, $p=0.002$). Non-therapeutic trials were more often influenced by study chair experiences than therapeutic trials. The standard of care within one's community based on personal experience of the study chair was reported as influential in 63% of non-therapeutic compared to 41% of therapeutic trials ($p=0.06$). The best judgment of the study chair was cited as influential in 50% of non-therapeutic compared to 11% of therapeutic trials ($p=<0.001$). Lastly, only 9% of respondents thought that a redesign or contingency plan had been prepared during the initial trial design for use in the event of poor accrual. Disparity in this response was noted with 15 of 67 matched pairs disagreeing on the presence of a contingency plan. Study chairs were more likely to think a plan existed than were lead statisticians.

Accrual Prediction Practices

Both study chairs and lead statisticians were queried about perceived influences on accrual predictions during a trial's design. A CTCG's accrual experience in a particular disease, disease stage, or intervention was viewed as the strongest influence on accrual predictions by both study chairs and lead statisticians (Table 3). CTCG experience was reported equally as the top influence on patient accrual predictions for trials with sufficient and insufficient accrual. Direct input from prospective participating clinicians or patients was reported as not having a role in informing accrual predictions (Table 3).

Perceived Equipoise

Both study chairs and lead statisticians were asked to select one of six statements describing their recalled, perceived relative value of the experimental treatment(s) versus the control treatment(s) at opening and closing of their trial. These responses, shown in Table 4, reflect that study chairs were more prone to optimism about the experimental treatments than were lead statisticians. This relative optimism of the study chairs persisted when comparing study chair and lead statistician responses for the 75 matched pairs (data not shown). Furthermore,

over 40% of study chairs report having preferred one arm over another before trial opening. Perceived equipoise was largely maintained from opening to closing with no major shifts in preference recalled for one treatment arm over another during the course of a trial. There appeared to be a greater shift in perceptions among the lead statisticians when evaluating perceptions at trial opening and closing for the same respondent, although still only in the minority of respondents. Among lead statisticians, 16% more respondents had reported about equal relative value at trial closing ($p<.001$). Among study chairs, 7.5% more respondents had reported the relative value of the experimental and control arms as about equal at trial closing than at opening ($p=.19$). The change was more often noted in respondents becoming less enthusiastic about the experimental arm over the trial course. No statistically significant difference was identified in perceptions of equipoise between trials with sufficient or insufficient accrual for both lead statisticians and study chairs (data not shown). This was noted when responses were evaluated both in the original six and reduced three categories. Similarly no significant differences were found in perceptions of equipoise between therapeutic and non-therapeutic trials (data not shown).

Perceived Accrual Influences

Overall, 41% of respondents indicated that their trial experienced significant accrual difficulties. No significant differences were seen between therapeutic (44%) and non-therapeutic trials (35%) in reporting accrual difficulties. Positive accrual experience was credited to three factors: perceived clinical relevance of the study question, lack of competing trials, and protocol designed to parallel normal practice (Table 5). In contrast, a negative accrual experience was not strongly attributed to any of sixteen specific factors offered as choices (Table 5). Although respondents were offered the opportunity to record other reasons to explain poor accrual, no persistent themes emerged in these responses.

Discussion

Phase III trial experiences from the vantage point of study chairs and lead statisticians offer unusual insight into accrual prediction practices and perceived accrual influences. Our study showed considerable unanimity, particularly among study chairs, in attributing accrual success to (1) perceived clinical relevance of the study question, (2) lack of competing trials, and (3) a protocol designed to parallel normal practice. However, the trial leaders did not identify consistent factors to explain accrual difficulties. This suggests that reasons for poor accrual are not well understood, are variable and complex, or are not necessarily consistent with commonly accepted accrual barriers. Commonly described barriers such as inadequate recruitment resources, excessive expense to patients or institutions, inadequate clinician incentives, significant deviation of the protocol from usual practice, restrictive entry criteria, and an uninteresting research question, were offered as survey response options but were not viewed by trial leaders to have contributed significantly to accrual difficulties. Interestingly, the barriers noted above are typically described in studies of recruiting clinicians active in clinical trial research.[3-5] In our study of senior trial leadership, the perceived reasons for low patient participation may not be reflective of factors affecting accrual on a local level. Alternately, reasons for low accrual may be multifactorial or may be actually different when viewed from the global perspective of trial leadership. These survey results will lead to additional study of this group of trials to establish trial-level factors associated with accrual success that are identifiable prior to trial activation.

Trial-level factors linked to accrual success are reflective of effective trial design, prioritization, and accrual prediction practices. Gauging clinical trial interest among physicians and patients in a relevant timeframe may be particularly challenging. Our findings on equipoise, although limited in that these represented recalled perceptions, suggested that perceptions of equipoise by trial leadership were not necessarily good

indicators of accrual success. However, perceived equipoise did appear to be largely maintained over the course of the trials, which is important to ethical trial conduct.[11] Influences in selecting the control intervention were no different between trials with sufficient and insufficient accrual. The importance credited to the protocol mirroring normal practice and the clinical relevance of the study question, however, support the importance of appropriate control arm selection in framing a question of clinically relevant uncertainty.[12] Ability to appreciate clinical relevance of a study question or appeal of a study design may hypothetically increase with seniority or experience. However, our study showed no association of quantity of trial leadership experience or academic seniority with accrual success. Prior studies have shown that physicians overestimate their ability to accrue patients by a factor of six.[13] This again speaks to the challenges of measuring the clinical relevance and acceptability of a trial among its target patients and enrolling physicians. Time elapsed from development of a trial concept to trial activation may serve as one proxy measure for clinical relevance.[14] However, measuring clinical relevance is likely more complex. Studying means to reliably measure interest in a trial concept during its planning phases would prove highly valuable both in trial prioritization and in accrual predictions. Development of such methodologies could find applications among numerous stakeholders in the trial design and prioritization processes.

In our study, trials with sufficient as well as insufficient accrual were reported as having relied primarily on cooperative group experience to inform accrual predictions. Alternate strategies for accrual prediction could prove useful and should be explored. Our results further demonstrate that the perceived role of prospective clinicians and patients in the accrual prediction process appears very limited. This may offer an important opportunity for process improvement. Issued in 2005, the Report of the Clinical Trials Working Group (CTWG) of the National Cancer Advisory Board entitled "Restructuring the National Cancer Clinical Trials Enterprise," outlines recommendations and implementation strategies to take effect over the subsequent five years in restructuring the national oncology clinical trials effort.[15] Among these recommendations, the CTWG introduced an initiative to increase community physician and patient advocate representation on Scientific Steering Committees tasked with promoting development of clinical trials that address relevant and feasible study questions in the community setting.[15] The three factors to which accrual success was most strongly attributed in this survey are surely considered by the Scientific Steering Committees. However, the subjectivity of clinical relevance and similarities to normal practice limits formal incorporation of these three criteria into the trial prioritization process. The actual impact of these Scientific Steering Committees in effective trial concept prioritization will need to be assessed in more current trials. As another potential opportunity for process improvement, a contingency plan in the event of poor accrual could be determined prior to trial opening. A greater emphasis on accrual strategy as part of the trial design process would allow better allocation of resources in prioritizing trials and quicker reallocation of resources if accrual still proves insufficient.[16]

Our study has several limitations. Most notably, perceptions of study chairs and lead statisticians may not accurately reflect accrual barriers encountered by enrolling physicians or patients. However, these clinical trial leaders were the most appropriate people to report influences on accrual predictions and trial design, a primary focus of this work. A second limitation relates to possible recall bias particularly among older trials. The study chairs and lead statisticians work so intently with a trial over its entire course that it seems that many aspects of the trial would be well-remembered. Nonetheless, questions reflecting recalled perceptions, such as those related to perceived equipoise, may be particularly sensitive to alterations over time. This survey is part of a larger study systematically examining the accrual experience of these 248 trials. To help address the degree of discordance between perception and "actuality," a comparison of these select survey results with data abstracted

about each trial from CTCG documentation may be useful. Third, the OCTAS definition of accrual sufficiency based on ability to address the primary endpoint grouped trials closed due to external factors with trials closed due to inadequate accrual. These external factors, such as discontinuation of a study agent or new data from another study, may be entirely separate from accrual. However, since closure due to external factors only related to three survey responses, these results were not reported separately. Fourth, this study's response rate for study chairs was lower than that for lead statisticians. The overall response rate was consistent with that reported for this survey genre but the study chairs' eligible response rate fell slightly below that of the mean reported for physician surveys of 54%.[17]

This limited the ability to perform matched pair analyses. Importantly, the response rate did not appear biased by the trial's accrual sufficiency. Study chair and lead statistician responses also varied in some important ways and therefore were not reported in aggregate. For instance, in questions using a Likert scale, lead statisticians were more likely to cluster responses in the middle of the scale, whereas study chairs were more likely to utilize the scale's extremes. Lastly, wording of survey questions can profoundly affect the results. In our study, it is plausible that consistent factors associated with accrual difficulties may have been found if respondents had been asked to rank the provided factors in order of perceived influence rather than rate the factors' strength of influence. However, we maintain that our study provides a more telling result by not masking whether respondents consider the factor's influence unimportant overall.

The low rate of patient participation in cancer clinical trials and the common problem of trial closure due to inadequate accrual underscore the need for critical appraisal of accrual prediction practices, trial design choices, and trial prioritization. Alternate strategies for accrual prediction that augment cooperative group experience and improved measures of clinical relevance that accurately reflect the interests of participating physicians and potential patients will be instrumental in effectively testing new advances in cancer care.

Acknowledgments

This work was supported by a grant from the National Institutes of Health [R01 CA118232] to Dr. Schroen.

This work was supported in part by: Public Health Service Grants U10CA-12027, U10CA-69974, U10CA-37377, U10CA-69651, and U24-CA-114732 from the National Cancer Institute, Department of Health and Human Services

Glossary of Abbreviations

OCTAS	Oncology Clinical Trial Accrual Study
NCI	National Cancer Institute
CTCG	Clinical Trials Cooperative Group
CALGB	Cancer and Leukemia Group B
ECOG	Eastern Cooperative Oncology Group
NCCTG	North Central Cancer Treatment Group
NSABP	National Surgical Adjuvant Breast and Bowel Project
SWOG	Southwest Oncology Group
CTWG	Clinical Trials Working Group of the National Cancer Advisory Board

References

1. Lara PN Jr, Higdon R, Lim N, Kwan K, Tanaka M, Lau DHM, et al. Prospective evaluation of cancer clinical trial accrual patterns: identifying potential barriers to enrollment. J Clin Oncol. 2001; 19:1728–33. [PubMed: 11251003]
2. Prescott RJ, Counsell CE, Gillespie WJ, Grant AM, Russell IT, Kiauka S, et al. Factors that limit the quality, number and progress of randomized controlled trials. Health Technol Assess. 1999; 3(20)
3. Grunfeld E, Zitzelsberger L, Coristine M, Aspelund F. Barriers and facilitators to enrollment in cancer clinical trials: qualitative study of the perspectives of clinical research associates. Cancer. 2002; 95:1577–83. [PubMed: 12237928]
4. Ross S, Grant A, Counsell C, Gillespie W, Russell I, Prescott R. Barriers to participation in randomized controlled trials: a systematic review. J Clin Epidemiol. 1999; 52:1143–56. [PubMed: 10580777]
5. Ellis PM. Attitudes towards and participation in randomized clinical trials in oncology: a review of the literature. Ann Oncol. 2000; 11:939–45. [PubMed: 11038029]
6. Mapstone J, Elbourne D, Roberts IG. Strategies to improve recruitment to research studies. Cochrane Database of Systematic Reviews. 2007; (Issue 2) Art. No.:MR000013. [DOI: 10.1002/14651858.MR000013.pub3.].
7. Mills EJ, Seely D, Rachlis B, Griffith L, et al. Barriers to participation in clinical trials of cancer: a meta-analysis and systematic review of patient-reported factors. Lancet Oncol. 2006; 7:141–8. [PubMed: 16455478]
8. Dilts DM, Sandler AB, Baker M, Cheng SK, et al. Processes to activate phase III clinical trials in a cooperative oncology group: the case of Cancer and Leukemia Group B. J Clin Oncol. 2006; 24:4553–7. [PubMed: 17008694]
9. Schroen AT, Petroni GR, Wang H, Grey R, et al. Preliminary evaluation of factors associated with premature trial closure and feasibility of accrual benchmarks in phase III oncology trials. Clin Trials. 2010; 7:312–21. [PubMed: 20595245]
10. Dillman, DA. Mail and internet surveys: the tailored design method. 2nd edition. Wiley & Sons; New York: 2000.
11. Freedman B. Equipoise and the ethics of clinical research. NEJM. 1987; 317:141–5. [PubMed: 3600702]
12. Matn H, Djulbegovic B. Choosing a control intervention for a randomized clinical trial. BMC Medical Research Methodology. 2003; 3:7–12. [PubMed: 12709266]
13. Taylor KM, Feldstein ML, Skeel RT, Pandya KJ, NG P, Carbone PP. Fundamental dilemmas of the randomized clinical trial process: results of a survey of the 1,737 Eastern Cooperative Oncology Group investigators. J Clin Oncol. 1994; 12:1796–1805. [PubMed: 8083703]
14. Cheng SK, Dietrich MS, Dilts DM. A sense of urgency: evaluating the link between clinical trial development time and the accrual performance of Cancer Therapy Evaluation Program (NCI-CTEP) sponsored studies. Clin Cancer Res. 2010; 16:5557–63. [PubMed: 21062929]
15. Clinical Trials Working Group of the National Cancer Advisory Board. Restructuring the National Cancer Clinical Trials Enterprise. Jun. 2005 Accessed at http://integratedtrials.nci.nih.gov/ict/CTWG_report_June2005.pdf
16. Demmy TL, Yasko JM, Collyar DE, Katz ML, et al. Managing accrual in cooperative group trials. J Clin Oncol. 2005; 22:2997–3002. [PubMed: 15284251]
17. Asch DA, Jedrziewski MK, Christakis NA. Response rates to mail surveys published in medical journals. J Clin Epidemiol. 1997; 50:1129–36. [PubMed: 9368521]

Clin Trials. Author manuscript; available in PMC 2012 October 17.

Table 1

Association of trial accrual sufficiency status with respondent academic rank, prior clinical trial experience, and continuity of trial involvement for study chairs and lead statisticians

Respondent characteristic at trial opening	Overall, %		By trial accrual sufficiency status, %			
			Study Chair		Lead Statistician	
	Study Chair (n=110)	Lead Statistician (n=199)	Sufficient(n=75)	Insufficient (n=35)	Sufficient (n=126)	Insufficient (n=73)
Academic Rank						
Asst. Prof.	31	23	33	26	24	21
Assoc Prof.	35	16	36	34	18	14
Prof.	27	20	25	31	19	20
Other	7	33	6	9	33	33
Missing	-	8			6	12
No. of prior trials served as study chair / lead statistician in cooperative group setting						
0	34	11	39	26	14	7
1	21	1	19	26	0	3
2-10	29	26	28	31	27	23
11-20	4	17	4	3	18	17
≥ 21	9	34	9	8	33	34
Missing	3	11	1	6	8	16
Involved with trial from design to closure						
Yes	80[a]	55	76	89	55	55

[a] NSABP substituted protocol officers for study chair respondents. Protocol officers frequently answered this question as "No" since they technically were not the study chair but they were involved throughout the course of the trial.

Table 2

The association of study chair responses on trial design factors and accrual sufficiency status

	Overall, % (n=110)	By trial accrual status, %		
		Sufficient (n=75)	Insufficient (n=35)	p-value
Time elapsed from trial concept introduction to trial activation				
≤12 mos	43	45	37	
>12 - ≤ 24 mos	40	41	37	
>24 - ≤ 36 mos	11	7	20	
> 36 mos	6	7	6	0.11
Perception of eligibility criteria				
Appropriate	86	88	83	
Overly restrictive	13	11	17	
Overly permissive	1	1	0	0.54
	Therapeutic trials only, % (n= 86)	By trial accrual status, %		
		Sufficient (n= 60)	Insufficient (n= 26)	p-value
Use of placebo, observation, or non-treatment control arm reported				
Yes	31	27	42	
No	69	73	58	0.15
Best descriptor of treatments compared in trial				
Novel therapy vs established therapy	65	70	54	
Two or more novel therapies	8	7	11	
Head-to-head comparison of well-established therapies	27	23	35	0.36

Table 3

Reported influences on accrual predictions during trial design stratified by final accrual sufficiency status

Potential factor influencing patient accrual predictions	Median score and percent citing factor					
	Study Chairs			Lead Statisticians		
	Percent citing factor	Accrual status		Percent citing factor	Accrual status	
		Sufficient	Insufficient		Sufficient	Insufficient
SCs experience in disease, disease stage, or intervention	95%	2	3	94%	3	3
Cooperative group's experience in disease, disease stage, or intervention	99%	1	1	97%	2	2
Accrual estimates by experts on disease sub-committee	94%	3	3	87%	3	3
Accrual estimates by local investigators at participating institutions	93%	3	3	81%	3	3
Survey or focus group of prospective participating *clinicians*	58%	4	4	65%	4	4
Survey or focus group of prospective participating *patients*	41%	5	5	58%	5	5
Published accounts of accrual experience in *similar* trials	70%	3	3	76%	3	3

Results presented by median score on five-point Likert score for respondents considering factor relevant to trial and by percent factor not used for respondents considering factor not relevant to trial.

Likert scale from 1-5 used to rate strength of influence

1=Strong influence; 3=Some influence; 5=No influence

Table 4

Perceptions of the relative value of experimental versus control treatments at opening and closing of trial

	Study Chairs, %		Lead Statisticians, %	
	Opening	Closing	Opening	Closing
Control arm highly preferred	3	7	0	3
Control arm preferred	5	10	1	10
About equal, experimental arm expected to be disappointing	7	12	5	28
About equal, experimental arm expected to be successful	47	34	65	31
Experimental arm preferred	31	22	17	16
Experimental arm highly preferred	4	11	2	5

Column percents do not equal 100% because a small number of respondents failed to answer the question. This may be more common with lead statisticians since change in statisticians over trial duration was more common.

Table 5

Strength of factors' perceived influence on positive and negative patient accrual experiences

	Median score and percent citing factor			
	Study Chairs		Lead Statisticians	
	Percent citing factor	Median score	Percent citing factor	Median score
Potential Factors with Positive Accrual Influence				
Recruitment resources devoted to this trial	90%	4	88%	3
Clinical relevance of study question	100%	1	100%	2
Control arm selection	100%	3	99%	3
No other trials competing for similar patient population	98%	2	95%	3
Participation of other cooperative groups	61%	3	46%	2
Study protocol designed to parallel normal practice	98%	2	96%	4
Supplemental funding from a non-federal source	56%	4	32%	5
New data emerged enhancing the value of this trial's research question	71%	4	73%	5
Potential Factors with Negative Accrual Influence				
Restrictive entry criteria	91%	4	92%	4
Inadequate formal planning of patient recruitment	94%	5	87%	4
Inadequate patient recruitment resources, incl. personnel	96%	4	89%	4
Diminished clinical relevance of study question by time of trial opening	96%	4	90%	5
Control arm selection	96%	5	92%	5
Unrealistic patient accrual estimates	96%	4	97%	3
Competition from another trial entering similar patient population	94%	4	90%	5
Participation of other cooperative groups	81%	3	77%	4
Study protocol deviated too much from normal practice	96%	5	93%	4
Lack of supplemental funding	85%	5	77%	5
New data emerged diminishing the value of this trial's research question	87%	5	87%	5
Financial costs of participation too high for patients	94%	5	81%	5
Financial costs of participation too high for institutions/ clinicians	96%	5	83%	5
Inadequate incentive for institutions/clinicians to enroll patients	98%	4	83%	4

Likert scale from 1-5 used to rate strength of influence

1=Strong influence; 3=Some influence; 5=No influence

Neuro-Oncology 13(12):1288–1295, 2011.
doi:10.1093/neuonc/nor139
Advance Access publication September 27, 2011

Investigation of intravenous delivery of nanoliposomal topotecan for activity against orthotopic glioblastoma xenografts

Laura P. Serwer, Charles O. Noble, Karine Michaud, Daryl C. Drummond, Dmitri B. Kirpotin, Tomoko Ozawa, Michael D. Prados, John W. Park, and C. David James

Department of Neurological Surgery, University of California–San Francisco (L.P.S., K.M., T.O., M.D.P., C.D.J.); Pharmaceutical Sciences and Pharmacogenomics Graduate Program, University of California–San Francisco (L.P.S.); Merrimack Pharmaceuticals, Cambridge, Massachusetts (C.O.N., D.C.D., D.B.K.); Division of Hematology-Oncology, University of California–San Francisco (J.W.P.)

Achieving effective treatment outcomes for patients with glioblastoma (GBM) has been impeded by many obstacles, including the pharmacokinetic limitations of antitumor agents, such as topotecan (TPT). Here, we demonstrate that intravenous administration of a novel nanoliposomal formulation of TPT (nLS-TPT) extends the survival of mice with intracranial GBM xenografts, relative to administration of free TPT, because of improved biodistribution and pharmacokinetics of the liposome-formulated drug. In 3 distinct orthotopic GBM models, 3 weeks of biweekly intravenous therapy with nLS-TPT was sufficient to delay tumor growth and significantly extend animal survival, compared with treatment with free TPT ($P \leq .03$ for each tumor tested). Analysis of intracranial tumors showed increased activation of cleaved caspase-3 and increased DNA fragmentation, both indicators of apoptotic response to treatment with nLS-TPT. These results demonstrate that intravenous delivery of nLS-TPT is a promising strategy in the treatment of GBM and support clinical investigation of this therapeutic approach.

Keywords: bioluminescence imaging, glioma, liposome, topotecan, xenograft.

Topotecan (TPT), an analogue of the chemotherapeutic camptothecin, is an approved treatment for many types of cancer, including recurrent small cell lung and ovarian tumors.[1–4] With respect to brain tumors, TPT has shown significant activity against the most common and malignant type of primary brain tumor, glioblastoma (GBM), both in vitro and in subcutaneous xenograft models of GBM.[5,6] Results from preclinical studies, in combination with encouraging results regarding the distribution of TPT in cerebrospinal fluid (CSF) after systemic TPT administration, prompted clinical investigations of TPT monotherapy efficacy in treating patients with GBM.[5–7] Unfortunately, results from phase II clinical trials involving TPT treatment of both newly diagnosed and recurrent GBM revealed only modest patient responses.[8–10] Although no longer being investigated as a monotherapy for treating GBM, TPT continues to be used in GBM clinical trials as a part of combination therapy approaches.

The minor efficacy of TPT as a monotherapy for GBM has been attributed to a rapid rate of TPT clearance from the CSF ($t_{1/2CSF} = 4.8$ h) and rapid TPT inactivation in plasma (active form $t_{1/2} = 23$ min).[11] Liposomal encapsulation is a strategy being explored for improving the antitumor efficacy of camptothecin derivatives,[12,13] including TPT,[14] and has been shown to increase drug circulatory half-life while helping maintain drug activity by providing an appropriate pH.[12,15]

In fact, systemic injection of nanoliposomal TPT has shown enhanced activity, relative to free TPT, against subcutaneous xenografts for several types of human cancer.[13,16] Moreover, nanoliposomal TPT has demonstrated superior efficacy in treating orthotopic (intracranial) xenograft models of GBM when administered directly into the tumor by convection-enhanced delivery (CED).[12,14] Specifically, in a rat orthotopic GBM xenograft model, CED of nanoliposomal TPT increased TPT half-life in the brain, relative to free TPT, and conferred a highly significant survival advantage. In spite of such demonstrations, the invasive nature of CED, combined

Received February 2, 2011; accepted June 23, 2011.

Corresponding Author: C. David James, PhD, Department of Neurological Surgery, University of California–San Francisco, 1450 Third St, Rm 283, San Francisco, CA 94158 (david.james@ucsf.edu).

with the limited success of CED-associated clinical trials to date, has restrained enthusiasm for more widespread use of this route of therapeutic administration in treating patients with brain tumor.

Here, we show for the first time, to our knowledge, the enhanced efficacy of systemically administered nanoliposomal TPT in 3 orthotopic xenograft models of GBM. The interpretation of enhanced efficacy is based on bioluminescence monitoring of tumor growth and therapeutic response, survival benefit to animal subjects, and immunohistochemical analysis of tumor apoptotic response to therapy, with the results from each consistent in their support for clinical investigation of this approach for treating GBM.

Materials and Methods

Cell Cultures

U87-MG cells were maintained as monolayers in high-glucose Dulbecco's minimal essential medium (DMEM) supplemented with 10% fetal calf serum, 1% nonessential amino acids, penicillin, and streptomycin. Cells were cultured at 37°C with 5% carbon dioxide. GBM43 and GBM6 cells were maintained as serially passaged subcutaneous xenografts in athymic mice. U87-MG, GBM43, and GBM6 were each modified by lentiviral infection for stable expression of firefly luciferase.[17] For intracranial injection of GBM43 and GBM6, a subcutaneous tumor was removed, minced with a scalpel, and subjected to 3 rounds of passage through a 40- μm pore filter with centrifugation after each round of filtering (increasing speed: 158 g, 355 g, 631 g for 10 min each). After the final round of centrifugation, the cells were resuspended in 1 mL of sterile DMEM media (without antibiotics), counted, and diluted to 1×10^8 cells/mL for intracranial injection. U87-MG cells were harvested for intracranial injection by monolayer trypsinization and resuspended in DMEM at 1×10^8 cells/mL.

Tumor Implantation

All animal experiments were conducted using protocols approved by the University of California, San Francisco, Institutional Animal Care and Use Committee. Four to six-week-old female athymic nu/nu mice (Simonsen Labs) were anesthetized by intraperitoneal injection of ketamine (100 mg/kg) and xylazine (10 mg/kg). A 1-cm sagittal incision was made along the scalp, and the skull suture lines were exposed. A small hole was created by puncture with a 25-g needle at 2 mm to the right of the bregma and 0.5 mm anterior of the coronal suture. With use of a sterile Hamilton syringe (Stoelting), 3×10^5 cells in 3 μL were injected at a depth of 3 mm over a 60-s period. After injection, the syringe was held in place for 1 min and then slowly removed. The skull was cleaned with 3% hydrogen peroxide and then sealed with bone wax. The scalp was closed using 7-mm surgical staples (Stoelting). Mice were monitored daily and euthanized when exhibiting significant neurological deficit or >15% reduction from their initial body weight.

Preparation of Nanoliposomal TPT

A detailed description of nanoliposomal TPT preparation is given elsewhere.[13] In brief, liposomes for packaging TPT consisted of hydrogenated soy phosphocholine and 1,2-distearoyl-*sn*-glycero-3-phosphoethanolamine-N-[methoxy(polyethylene glycol)-2000] at a molar ratio of 3:2:0.015. A sucrose octasulfate gradient was used for loading TPT into the liposomes. Unencapsulated TPT was removed by Sephadex G-25 gel filtration chromatography, eluting with HEPES buffered saline (pH, 6.5). The phospholipid concentration of the purified solution was measured spectrophotometrically using a standard phosphate assay.[18] Before HPLC column injection for TPT quantitation, liposome samples were solubilized in a solution containing 1% trifluoroacetic acid in methanol. TPT was detected by fluorescence (excitation, 370 nm; emission, 535 nm) with a retention time of 11.5 min. The nanoliposomal TPT (nLS-TPT) had a final drug to phospholipid ratio of 327.7 ± 5.31 g TPT HCl per mol phospholipid. Liposome size was determined by photon correlation spectroscopy using a Coulter N4 Plus particle size analyzer (Beckman Coulter) and was reported as the volume-weighted mean diameter ± standard deviation of the liposome size distribution (100.1 ± 8.4 nm).

Biodistribution Studies

Mice with intracranial U87-MG tumors were injected with 5 mg/kg of either free TPT or nLS-TPT via tail vein, then euthanized at 1, 8, 24, or 48 h after injection by trans-cardiac perfusion with phosphate-buffered saline (PBS). Blood samples were obtained immediately before perfusion via cardiac puncture and were centrifuged for 10 min at 8154 *g*. The plasma was then removed and frozen at −80°C. After perfusion with PBS, the tumor-bearing brain hemispheres were resected and frozen at −80°C. TPT was extracted from 10–20 μL of plasma with 980–990 μL of 1% trifluoroacetic acid in methanol. The mixture was vortexed for 5 s and stored at −80°C for 2 h, followed by centrifugation at 13 400 *g* for 10 min. The supernatant was transferred to an HPLC autosampler vial and stored at 4°C until analyzed for TPT content. HPLC analysis was performed as described in "Preparation of Nanoliposomal TPT." Brain tissues were processed with a mechanical homogenizer in water at 20% wt/wt ratio; 100 μL of the tissue homogenate was added to 400 μL of 1% trifluoroacetic acid in methanol and subjected to the same extraction and analysis procedure that was used for plasma. The spiked extraction recovery from tumor-containing brain tissue was 97.8%. The standard curve linearity was a mean of >0.998 with a detection limit of 0.1 ng/mL. TPT

concentrations shown include both free and encapsulated TPT. Area under curve (AUC) calculations used the trapezoidal rule.[19]

Blood Cell Analysis

Athymic mice were treated with 1 mg/kg doses of either free TPT or nLS-TPT as described in "TPT Treatment." Blood samples were collected weekly from the submandibular vein into EDTA-coated tubes, according to the University of California, San Francisco Institutional Animal Care and Use Committee/Laboratory Animal Resource Center (UCSF IACUC/LARC) standard procedure,[20] and were analyzed using a Hemavet 850 (Drew Scientific) within 2 h after collection.

In Vitro Luciferase Assay

Luciferase-modified U87-MG cells were plated in a 96-well plate at a concentration of 5000 cells/well. Twenty-four hour later, cells were treated for either 24 h or 48 h with 2.67×10^{-3} mg/mL free TPT or nLS-TPT. After incubation, the cells were washed in prewarmed PBS, and fresh media without phenol red was added to the cells. D-luciferin was added to each well at a final concentration of 0.6 mg/mL. After a 10-min incubation, cells were examined for luminescence on the IVIS Lumina System (Caliper Life Sciences), as described in the next section.

Bioluminescence Imaging

Mice were anesthetized by intraperitoneal injection of ketamine (100 mg/kg) and xylazine (10 mg/kg) and then were injected intraperitoneally with 33.3 mg of D-luciferin (potassium salt; Gold Biotechnology) dissolved in sterile saline. Tumor bioluminescence was determined 10 min after luciferin injection using the IVIS Lumina System (Caliper Life Sciences) and Livingimage software, as the sum of photon counts per second in regions of interest defined by a lower threshold value of 25% of peak pixel intensity. Imaging was performed biweekly from 3 days after tumor implantation to completion of study.

TPT Treatment

TPT (Fisher) was dissolved in pyrogen-free sterile water and stored at −20°C. Before treatment, mice were randomized according to bioluminescence imaging score at most recent imaging. Both nLS-TPT and free TPT were administered to mice via tail vein injection.[21] Immediately before injection, nLS-TPT and free TPT were diluted to a concentration of 0.2 mg/mL in either 5 mM HEPES (nLS-TPT) or sterile water (free TPT). Mice received TPT administrations twice weekly (Tuesday and Friday), for a maximum of 6 administrations.

Immunohistochemistry

After resection, mouse brains were fixed for 48 h in 10% buffered formalin. Brains were then paraffin-embedded and sectioned (10 μm) for hematoxylin and eosin staining and immunohistochemical analysis. To assay DNA fragmentation, TUNEL staining was performed using the DeadEnd Colorimetric TUNEL system (Promega) according to the manufacturer's protocol for paraffin-embedded tissues. For the determination of cleaved caspase-3 reactivity, unstained sections were processed using a Ventana BenchMark XT automated system and a protocol consisting of pretreatment with 3% ethanolic hydrogen peroxide for 16 min at room temperature, epitope retrieval in Tris buffer (pH, 8) for 8 min at 90°C, and incubation with primary antibody to cleaved caspase-3 (Cell Signaling Tech) at 0.2 μg/mL for 32 min at 37°C.

Statistical Analysis

PRISM 5, Version 5.03 (GraphPad Software) was used to conduct all statistical analyses. For survival analysis, significance was determined by the log-rank (Mantel-Cox) test. For all other analyses, a 2-tailed unpaired *t* test was applied.

Results

Biodistribution of nLS-TPT and Free TPT

Athymic mice with intracranial U87-MG tumors were injected with a single dose of nLS-TPT or free TPT and sacrificed at 1, 8, 24, and 48 h after injection, with tissue samples removed for HPLC analysis of TPT content. At all times after injection, there was significantly more TPT in tumor-bearing brain from mice treated with nLS-TPT than in brain from mice treated with free TPT ($P < .05$, all time points) (Fig. 1A). In fact, after 24 h, mice treated with free TPT had no detectable TPT in tumor-bearing brain samples (limit of detection = 1.67 ng TPT/g tissue), whereas mice treated with nLS-TPT continued to show detectable TPT in brain samples at 48 h after administration of nLS-TPT, the last time point assayed. Furthermore, AUC calculations, indicating total drug exposure, revealed that brain tissue from mice receiving nLS-TPT was 5-fold greater than for mice receiving free TPT (Table 1).

Corresponding results for the analysis of plasma TPT showed that nLS-TPT treatment significantly increased the duration of and total exposure to TPT in circulation (Fig. 1B, Table 1). The plasma AUC∞ for mice treated with nLS-TPT was 197 μg*h/mL, over 200-fold higher than the AUC∞ in mice treated with free TPT (0.655 μg*h/mL). With respect to duration, TPT was not detectable in plasma samples from mice 48 h after administration of free TPT, whereas the 48-h concentration of TPT in mice receiving nLS-TPT was readily

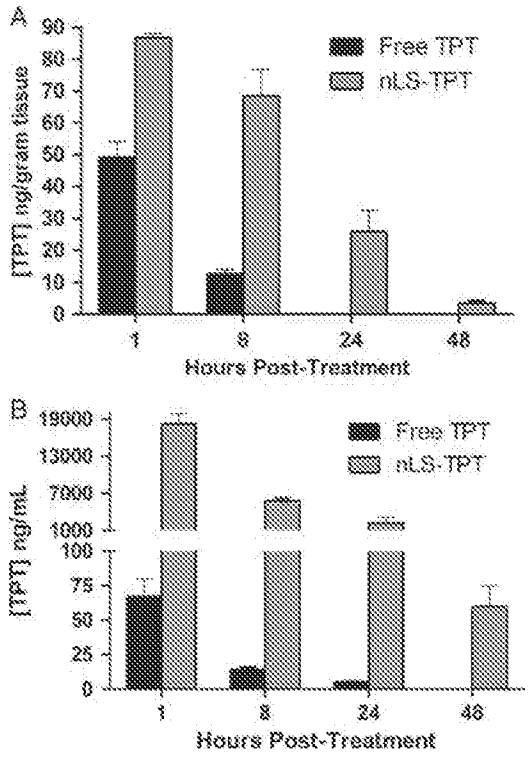

Fig. 1. Pharmacokinetic analysis of nLS-TPT retention in tumor-bearing brain and plasma. A single dose of 5 mg/kg of free TPT or nLS-TPT was administered intravenously, with mice euthanized at the indicated time points subsequent to TPT administration. (A) Brains were resected, and the hemisphere containing the tumor was dissected for isolation of TPT. (B) Blood samples were obtained from mice immediately before sacrifice, with plasma separated and analyzed for TPT content as described in the Materials and Methods. Group means with SEM are indicated. Free TPT versus nanoliposomal TPT concentration comparisons are significantly different for each time point and for each type of tissue ($P < .05$ for all comparisons).

Table 1. AUC_{∞} of TPT in tumor-bearing mice

	Brain w/Tumor (ng*h/g)	Plasma (ug*h/mL)
Free TPT	342	0.655
nLS-TPT	1745.7	197

detectable and significantly greater than the 8- and 24-h plasma concentrations for mice receiving free TPT.

Effect of nLS-TPT on Tumor Growth

Mice receiving treatment with free TPT or nLS-TPT and bearing intracranial U87-MG xenografts experienced a reduced tumor growth rate relative to untreated controls (Fig. 2A), with nLS-TPT significantly outperforming free TPT. To address the consistency of nLS-TPT efficacy in vivo, we applied the same experimental design as used with the U87-MG experiment to orthotopic GBM models in which the tumor cell sources were obtained from serially propagated

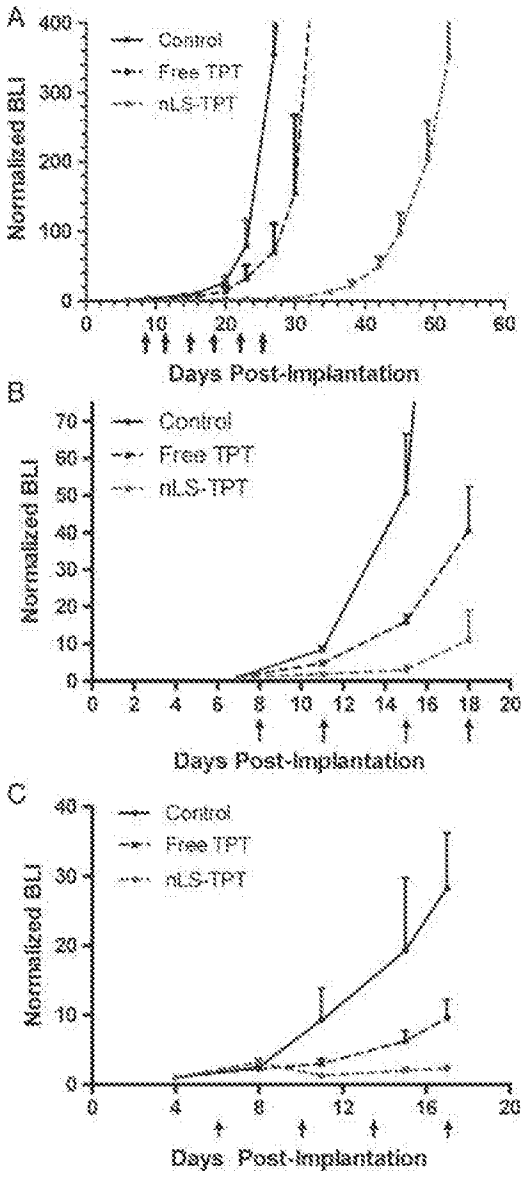

Fig. 2. Effects of nLS-TPT treatment on tumor growth in vivo. Results from bioluminescence monitoring of intracranial tumor growth and response to intravenous TPT, either free or nanoliposomal; 1 mg/kg administrations are indicated by arrows (maximum of 6 administrations). Group means are plotted, with SEM indicated for each. (A) U87-MG xenograft model of GBM. (B) and (C) Results for subcutaneously propagated GBM43 and GBM6, classified as proneural and classical subtypes of GBM, respectively.[24]

subcutaneous xenografts (Fig. 2B and C). This approach for tumor maintenance has been previously shown to promote retention of patient GBM molecular and biologic characteristics.[22,23] Bioluminescence monitoring of response to treatment for xenografts GBM43 (proneural subtype) and GBM6 (classical subtype)[24] (Fig. 2B and C) revealed antitumor activity of nLS-TPT consistent with that indicated for the U87-MG model, supporting the finding that nLS-TPT is more effective in suppressing tumor growth.

Effect of nLS-TPT on Animal Survival

Consistent with our prior experience in using bioluminescence imaging for monitoring intracranial tumor response to therapy,[17,25] corresponding survival analysis for all 3 GBM models tested (U87-MG, GBM43, GBM6) showed that suppression of tumor growth is predictive of survival benefit. Mice treated with free TPT experienced increased median and mean survival, relative to control group mice, but of lesser extent than mice treated with nLS-TPT (Fig. 3). Of importance, in all 3 xenograft models, there was a statistically significant survival benefit from nLS-TPT treatment, compared with free TPT treatment ($P \leq .03$ for all models).

Effect of Liposomal Packaging on Drug Efficacy In Vitro

To rule out any intrinsic differences in TPT efficacy related to liposomal packaging, we compared free TPT and nLS-TPT antitumor effects in vitro employing the same luciferase-modified U87-MG cells as used in vivo (Figs 2A and 3A). Results for 24- and 48-h incubations indicated similar activities for free TPT and nLS-TPT (Supplemental Figure 2), supporting the differential efficacy observed in vivo as being attributable to improved drug distribution and stability from nanoliposomal formulation.

Analysis of Biologic Effect from TPT Treatment In Vivo

To assess mode of action and biologic consequences of nLS-TPT treatment in vivo, athymic mice bearing GBM43 tumors were injected with a single dose of either free TPT or nLS-TPT and were sacrificed 24 h after treatment. Brains were removed, fixed, embedded, and then sectioned for molecular analysis of intracranial xenograft response to therapy. In contrast to tumors from untreated mice, tumors from mice treated with free TPT or nLS-TPT showed significantly higher levels of TUNEL staining (Fig. 4A–C), indicative of more extensive DNA fragmentation, with cellular positivity in tumors exposed to nLS-TPT significantly higher than in tumors exposed to free TPT ($P < .01$ for all 2-way comparisons). Cleaved caspase-3 staining showed a similar pattern of results, confirming the highest tumor apoptotic response from nLS-TPT (Supplemental Figure 1). Staining for Ki67, to address the effects of therapy on tumor cell proliferation, showed no significant difference in cellular positivity between treatment groups (data not shown).

Toxicity

For each in vivo experiment, the body weight of all animal subjects was monitored. There was no significant difference in mean body weights between free TPT– and nLS-TPT–treated mice during the period in which mice remained asymptomatic of tumor burden, irrespective of tumor model being tested (Supplemental Figure 3).

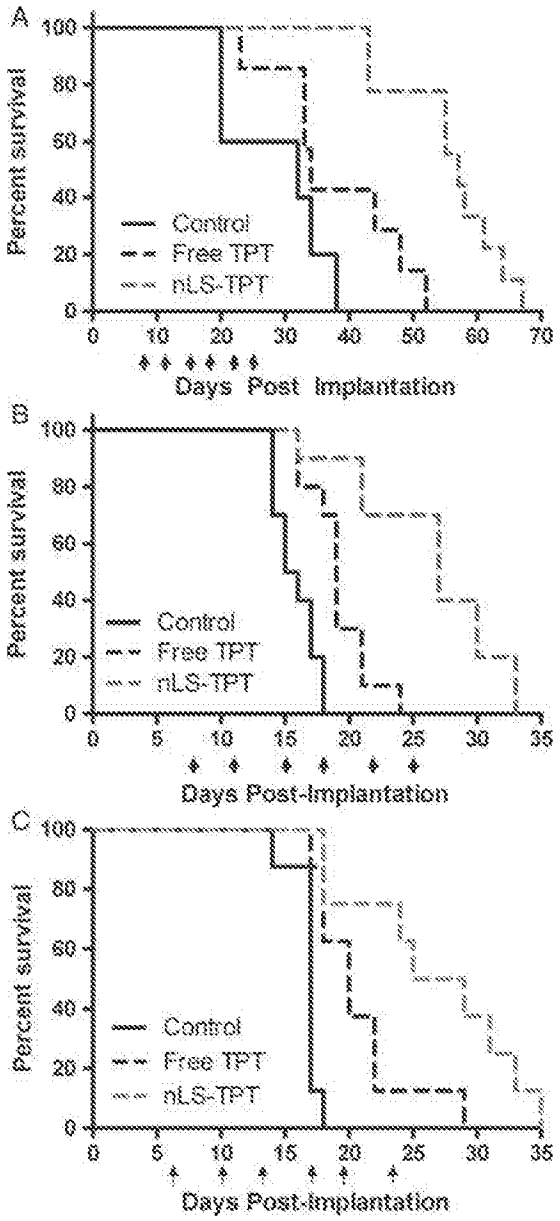

Fig. 3. Effect of nLS-TPT treatment on survival in mice bearing intracranial tumors. Kaplan-Meier survival curves for mice bearing tumors described in Fig. 2; 1 mg/kg doses are indicated by arrows (maximum of 6 administrations). (A) U87-MG model ($N_{control} = 5$, $N_{freeTPT} = 7$, $N_{nLS-TPT} = 9$). (B) GBM43 model ($n = 10$, all groups). (C) GBM6 model ($n = 8$, all groups). In each set of survival plots, survival comparisons for free TPT– versus nLS-TPT–treated mice indicate a statistically significant difference: $P = .001$ for A (U87-MG) and B (GBM43); $P = .03$ for C (GBM6).

To compare the myelosuppressive effects of free TPT and liposomal TPT and to contrast TPT myelosuppressive effects against the most frequently used cytotoxic chemotherapeutic for treating GBM, athymic mice were either given 10 mg/kg of temozolomide (TMZ) for 5 consecutive days or TPT using the same free TPT and nLS-TPT regimens as in the efficacy experiments (Figs 2 and 3). Peripheral blood samples were collected weekly, and blood cell counts were determined. For all

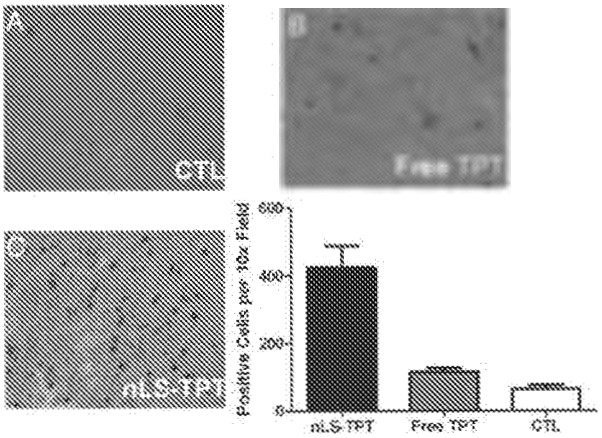

Fig. 4. Comparison of free TPT versus nLS-TPT pro-apoptotic activity as indicated by DNA fragmentation analysis. Mice bearing GBM43 tumors were treated with a single dose of free TPT or nLS-TPT and euthanized 24 h following treatment. Brains were immediately resected following euthanasia, fixed in formalin, and then embedded in paraffin and sectioned for immunohistochemical analysis of TUNEL positivity. Counting of positive cells in four 10× fields per tumor indicated a significant difference of effect of treatment on tumor apoptosis for all 2-way comparisons ($P < .01$).

time points tested, neither free TPT nor nLS-TPT treatment had a significant effect on hematocrit or hemoglobin levels (Supplemental Figure 4), suggesting that nLS-TPT treatment is unlikely to cause anemia. In contrast, mice receiving TMZ experienced a near-significant decrease in hemoglobin levels (control vs TMZ: $P = .08$). Platelet levels were unaffected by TPT or TMZ treatments (Supplemental Figure 5). There was a significant decrease in neutrophil levels at the first time point after initiation of TMZ or TPT therapy (day 4: control vs free TPT, $P = .01$; control vs nLS-TPT, $P = .05$; control vs TMZ, $P = .01$) (Fig. 5). Of importance, neutrophil levels recovered rapidly after completion of the treatment cycle, with baseline levels achieved within 7 days after the last administration of TPT. In addition, there was no significant difference in neutrophil levels between nLS-TPT and free TPT–treated mice at any time point.

After recovery of blood cell counts to pretreatment levels for mice receiving TMZ, the same mice were administered nLS-TPT to investigate myelosuppressive effects of nLS-TPT when used as a salvage therapy for recurrent GBM. Results show that administration of nLS-TPT after blood cell recovery from TMZ monotherapy has a lesser myelosuppressive effect than does the initial TMZ treatment (Fig. 6).

Discussion

Although the use of camptothecins in treating primary brain tumors has been widely researched, these compounds have yet to be used routinely in clinical practice, in large part because of their toxicity and related pharmacokinetic

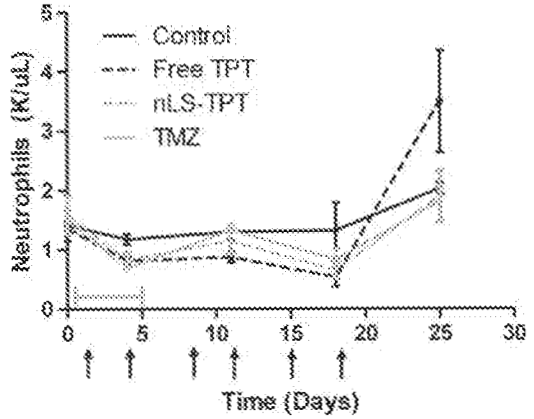

Fig. 5 Neutrophil levels in mice treated with nLS-TPT. Athymic mice were treated with 1-mg/kg doses of either free TPT or nLS-TPT (arrows), according to the same schedule used in the efficacy experiments (biweekly administration for 3 consecutive weeks). Mice in the TMZ group were administered 10 mg/kg of TMZ daily for 5 consecutive days (days 1–5 *[grey bracket]*), a regimen previously determined to be well-tolerated and demonstrating antitumor activity against most GBM intracranial xenografts. Blood samples were collected weekly, with complete blood cell counts obtained for each sample. Group means are plotted ($n = 5$, all groups), with SEMs indicated.

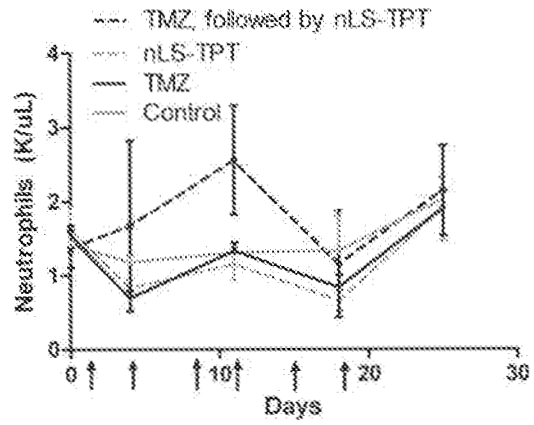

Fig. 6. Neutrophil levels in mice treated with nLS-TPT with or without prior TMZ treatment. Athymic mice were treated with 1-mg/kg doses of free TPT or nLS-TPT (arrows) following no treatment or treatment and recovery from 10 mg/kg TMZ for 5 days. Blood samples were collected weekly and complete blood cell counts obtained. Group means are plotted ($n = 5$, all groups), with SEMs indicated.

shortcomings.[8,26] Liposomal encapsulation of chemotherapeutics has been shown to increase tumor drug exposure and to reduce systemic toxicity.[27–30] Because of the size of therapeutic liposomes, previous brain tumor studies have often focused on their direct, local delivery to tumors by CED.[31–34] Although nLS-TPT CED has shown efficacy in preclinical investigations using rodent models of GBM,[14] enthusiasm for use of this route of administration has been restrained because of the invasive nature of CED and the limited success of CED-associated clinical trials conducted to date.[35]

In contrast to CED, intravenous delivery is less invasive and promotes a more uniform drug distribution throughout the brain, which is an important consideration because of the invasive nature of GBM. In our study, we investigated intravenous administration of nanoliposomal TPT for efficacy against 3 types of GBM xenografts and report for the first time, to our knowledge, that liposomal encapsulation enhanced TPT concentration in the brain, resulting in increased antitumor activity. We have previously shown that empty liposomes do not have antitumor activity,[36] indicating that it is the liposomal packaging of TPT, and not the liposomes, that is responsible for improved antitumor activity in relation to free TPT.

By intercalating into DNA, TPT inhibits an essential process in proliferating cells, namely the role of topoisomerase I (TOPI) in DNA replication, ultimately resulting in DNA strand breaks that initiate programmed cell death. Indeed, the results of our TUNEL analysis show increased DNA strand breaks in TPT-treated tumors (Fig. 4) and a corresponding increase in activated caspase-3 (Supplemental Figure 1), a marker of programmed cell death. Of importance, DNA strand breaks and activated caspase-3 were significantly elevated by liposomal packaging of TPT. These results complement our previously published data indicating that TPT treatment depletes topoisomerase I in tumor cells[36] and, in combination, address the mode of action and biologic consequence of TPT activity.

In contrast to targeted therapeutics, such as Tarceva, for which an antitumor effect has been shown to be specific to a subclass of GBM,[37] TPT is expected to have a more generalized effect against GBM because of the essential nature of topoisomerase I in tumor growth. In fact, an analysis of The Cancer Genome Atlas (TCGA) data for DNA TOPI expression shows significantly elevated TOPI mRNA levels irrespective of GBM subclassification (Supplemental Figure 6). Results from our analysis of 3 distinct GBM cell sources (U87-MG and serially propagated subcutaneous xenografts GBM6 and GBM43) for TPT treatment response (Figs 2 and 3) support the antitumor effect of this cytotoxic chemotherapeutic as being generalizable to most if not all subtypes of GBM.

The increased efficacy of nLS-TPT did not come at the expense of increased toxicity; there was not a significant difference in either mouse body weights or in neutrophil counts in mice treated with nLS-TPT, compared with mice treated with free TPT (Supplemental Figure 3, Fig. 5). Moreover, our analysis of blood cell counts in mice treated with TMZ followed by treatment with nLS-TPT indicate that nLS-TPT has a favorable safety profile for use in treating recurrent GBM.

Previous studies have not shown a significant advantage to adding TPT to radiation therapy.[38,39] However, because of the dramatic improvements in distribution and efficacy seen with nLS-TPT, further study into nLS-TPT combined with radiation seems warranted. In addition, it would be of interest to examine the efficacy of TPT when used in combination with inhibitors of proteins that prevent apoptosis, such as obatoclax mesylate (GX15-070MS), a small-molecule pan-Bcl-2 family inhibitor recently shown to be well-tolerated when administered with TPT to patients with cancer.[40]

In total, our study results and previous results from others indicate several promising possibilities for maximizing benefit from intravenous administration of nLS-TPT and support additional investigation of this therapeutic agent and approach.

Supplementary Material

Supplementary material is available online at *Neuro-Oncology* (http://neuro-oncology.oxfordjournals.org/).

Acknowledgments

We thank Raquel Santos, the UCSF Brain Tumor Tissue Core, and the UCSF Mouse Pathology Core for technical assistance.

Conflict of interest statement. D.C.D. and D.B.K. are employees of Merrimack Pharmaceuticals. C.O.N. is a former employee of Merrimack Pharmaceuticals.

Funding

This work was supported by NS065819-02 (to C.D.J.) and CA097257 (to M.D.P., J.W.P., C.D.J.).

References

1. Bookman MA, Malmstrom H, Bolis G, et al. Topotecan for the treatment of advanced epithelial ovarian cancer: an open-label phase II study in patients treated after prior chemotherapy that contained cisplatin or carboplatin and paclitaxel. *J Clin Oncol*. 1998;16:3345–3352.
2. Depierre A, von Pawel J, Hans K, et al. Evaluation of topotecan (Hycamtin) in relapsed small cell lung cancer (SCLC). A multicentre phase II study. *Lung Cancer*. 1997;18(suppl 1):35.
3. ten Bokkel Huinink W, Gore M, Carmichael J, et al. Topotecan vs paclitaxel for the treatment of recurrent epithelial ovarian cancer. *J Clin Oncol*. 1997;15:2183–2193.
4. ten Bokkel Huinink W, Lane SR, Ross GA, the International Topotecan Study Group. Long-term survival in a phase III, randomised study of topotecan vs paclitaxel in advanced epithelial ovarian carcinoma. *Ann Oncol*. 2004;15:100–103.
5. Ciusani E, Croci D, Gelati M, et al. In vitro effects of topotecan and ionizing radiation on TRAIL/Apo2L-mediated apoptosis in malignant glioma. *J Neuro-Oncol*. 2005;71:19–25.
6. Rapisarda A, Zalek J, Hollingshead M, et al. Schedule-dependent inhibition of hypoxia-inducible factor-1alpha protein accumulation, angiogenesis, and tumor growth by topotecan in U251-HRE glioblastoma xenografts. *Cancer Res*. 2004;64:6845–6848.

7. Baker SD, Heideman RL, Crom WR, et al. Cerebrospinal fluid pharmacokinetics and penetration of continuous infusion topotecan in children with central nervous system tumors. *Cancer Chemother Pharmacol*. 1996;37:195–202.
8. Macdonald D, Cairncross G, Stewart D, et al. Phase II study of topotecan in patients with recurrent malignant glioma. National Clinical Institute of Canada Clinical Trials Group. *Ann Oncol*. 1996;7(2):205–207.
9. Friedman HS, Kerby T, Fields S, et al. Topotecan treatment of adults with primary malignant glioma. The Brain Tumor Center at Duke. *Cancer*. 1999;85(5):1160–1165.
10. Blaney SM, Phillips PC, Packer RJ, et al. Phase II evaluation of topotecan for pediatric central nervous system tumors. *Cancer*. 1996;78(3):527–531.
11. Mi Z, Malak H, Burke TG. Reduced albumin binding promotes the stability and activity of topotecan in human blood. *Biochemistry*. 1995;34(42):13722–13728.
12. Tardi P, Choice E, Masin D, Redelmeier T, Bally M, Madden TD. Liposomal encapsulation of topotecan enhances anticancer efficacy in murine and human xenograft models. *Clin Cancer Res*. 2001;60:3389–3393.
13. Drummond DC, Noble CO, Guo Z, et al. Development of a highly stable and targetable nanoliposomal formulation of topotecan. *J Control Release*. 2010;141(1):13–21.
14. Saito R, Krauze MT, Noble CO, et al. Convection-enhanced delivery of Ls-TPT enables an effective continuous, low dose chemotherapy against malignant glioma xenograft model. *Neuro Oncol*. 2006;8(3):205–214.
15. Burke TG, Gao X. Stabilization of topotecan in low pH liposomes composed of distearoylphosphatidylcholine. *J Pharm Sci*. 1994;83:967–969.
16. Tardi P, Choice E, Masin D, Redelmeier T, Bally M, Madden TD. Liposomal encapsulation of topotecan enhances anticancer efficacy in murine and human xenograft models. *Clin Cancer Res*. 2000;60:3389–3393.
17. Dinca EB, Sarkaria JN, Schroeder MA, et al. Bioluminescence monitoring of intracranial glioblastoma xenograft: response to primary and salvage temozolomide therapy. *J Neurosurg*. 2007;108(3):610–616.
18. Bartlett GR. Phosphorus assay in column chromatography. *J Biol Chem*. 1959;234(3):466–468.
19. Roland M, Tozer T. Clinical Pharmacokinetics: Concepts and Applications. 3rd ed. Philadelphia, PA: Lippincott Williams & Wilkins; 1995.
20. UCSF Animal Care and Use Program. Standard Procedures and Guidelines. http://www.iacuc.ucsf.edu/Policies/awStandardProcedures.asp. Accessed June 9, 2011.
21. Serwer L, Hashizume R, Ozawa T, James CD. Systemic and local drug delivery for treating diseases of the central nervous system in rodent models. *J Vis Exp*. 2010;42. http://www.jove.com/Details.php?ID=1992.
22. Sarkaria JN, Yang L, Grogan PT, et al. Identification of molecular characteristics correlated with glioblastoma sensitivity to EGFR kinase inhibition through use of an intracranial xenograft test panel. *Mol Cancer Ther*. 2007;6:1167–1174.
23. Giannini C, Sarkaria JN, Saito A, et al. Patient tumor EGFR and PDGFRA gene amplifications retained in an invasive intracranial xenograft model of glioblastoma multiforme. *Neuro Oncol*. 2005;7(2):164–176.
24. Verhaak RG, Hoadley KA, Purdom E, et al. Cancer Genome Atlas Research Network. Integrated genomic analysis identifies clinically relevant subtypes of glioblastoma characterized by abnormalities in PDGFRA, IDH1, EGFR, and NF1. *Cancer Cell*. 2010;17(1):98–110.
25. Michaud K, Solomon DA, Oermann E, et al. Pharmacologic inhibition of cyclin-dependent kinases 4 and 6 arrests the growth of glioblastoma multiforme intracranial xenografts. *Cancer Res*. 2010;70(8):3228–3238.
26. Quinn JA, Jiang SX, Reardon DA, et al. Phase II trial of temozolomide (TMZ) plus irinotecan (CPT-11) in adults with newly diagnosed glioblastoma multiforme before radiotherapy. *J Neuro-Oncol*. 2009;95(3):393–400.
27. Drummond DC, Noble CO, Guo Z, Hong K, Park JW, Kirpotin DB. Development of a Highly Active Nanoliposomal Irinotecan Using a Novel Intraliposomal Stabilization Strategy. *Cancer Res*. 2006;66:3271–3277.
28. Allen TM, Cullis PR. Drug delivery systems: Entering the mainstream. *Science*. 2004;303:1818–1822.
29. Drummond DC, Meyer O, Hong KL, Kirpotin DB, Papahadjopoulos D. Optimizing liposomes for delivery of chemotherapeutic agents to solid tumors. *Pharmacol Rev*. 1999;51:691–743.
30. Drummond DC, Noble CO, Hayes ME, Park JW, Kirpotin DB. Pharmacokinetics and in vivo drug release rates in liposomal nanocarrier development. *J Pharm Sci*. 2008;97(11):4696–4740.
31. Dickinson PJ, LeCouteur RA, Higgins RJ, et al. Canine model of convection-enhanced delivery of liposomes containing CPT-11 monitored with real-time magnetic resonance imaging: laboratory investigation. *J Neurosurg*. 2008;108(5):989–998.
32. Noble CO, Krauze MT, Drummond DC, et al. Novel nanoliposomal CPT-11 infused by convection-enhanced delivery in intracranial tumors: pharmacology and efficacy. *Cancer Res*. 2006;66(5):2801–2806.
33. Saito R, Bringas JR, McKnight TR, et al. Distribution of liposomes into brain and rat brain tumor models by convection-enhanced delivery monitored with magnetic resonance imaging. *Cancer Res*. 2004;64:2572–2579.
34. Mamot C, Nguyen JB, Pourdehnad M, et al. Extensive distribution of liposomes in rodent brains and brain tumors following convection-enhanced delivery. *J Neuro-Oncol*. 2004;68:1–9.
35. Sampson JH, Akabani G, Archer GE, et al. Intracerebral infusion of an EGFR-targeted toxin in recurrent malignant brain tumors. *Neuro Oncol*. 2008;10(3):320–329.
36. Yamashita Y, Krauze MT, Kawaguchi T, et al. Convection-enhanced delivery of a topoisomerase I inhibitor (nanoliposomal topotecan) and a topoisomerase II inhibitor (pegylated liposomal doxorubicin) in intracranial brain tumor xenografts. *Neuro Oncol*. 2007;9(1):20–28.
37. Mellinghoff IK, Wang MY, Vivanco I, et al. Molecular determinants of the response of glioblastomas to EGFR kinase inhibitors. *N Engl J Med*. 2005;353:2012–2024.
38. Neuhaus T, Ko Y, Muller RP, et al. A phase III trial of topotecan and whole brain radiation therapy for patients with CNS-metastases due to lung cancer. *Br J Cancer*. 2009;100(2):291–297.
39. Fisher B, Won M, Macdonald D, Johnson DW, Roa W. Phase II study of topotecan plus cranial radiation for glioblastoma multiforme: results of Radiation Therapy Oncology Group 9513. *Int J Radiat Oncol Biol Phys*. 2002;53(4):980–986.
40. Paik PK, Rudin CM, Brown A, et al. A phase I study of obatoclax mesylate, a Bcl-2 antagonist, plus topotecan in solid tumor malignancies. *Cancer Chemother Pharmacol*. 2010;66:1079–1085.

BMC Cancer

BioMed Central

Research article

Open Access

Capecitabine plus Irinotecan (XELIRI regimen) compared to 5-FU/LV plus Irinotecan (FOLFIRI regimen) as neoadjuvant treatment for patients with unresectable liver-only metastases of metastatic colorectal cancer: a randomised prospective phase II trial

Erik Skof†, Martina Rebersek†, Zvezdana Hlebanja† and Janja Ocvirk*†

Address: Institute of Oncology, Division of Medical Oncology, Zaloska 2, 1000 Ljubljana, Slovenia

Email: Erik Skof - eskof@onko-i.si; Martina Rebersek - mrebersek@onko-i.si; Zvezdana Hlebanja - zhlebanja@onko-i.si; Janja Ocvirk* - jocvirk@onko-i.si

* Corresponding author †Equal contributors

Published: 22 April 2009

BMC Cancer 2009, 9:120 doi:10.1186/1471-2407-9-120

Received: 6 August 2008
Accepted: 22 April 2009

This article is available from: http://www.biomedcentral.com/1471-2407/9/120

Abstract

Background: Phase II studies have shown that the combination of capecitabine and irinotecan (the XELIRI regimen) is active in metastatic colorectal cancer (MCRC). There are, however, no data about the use of the XELIRI regimen in the neoadjuvant treatment.

Methods: Patients with unresectable liver-only metastases of MCRC with ≤ 75 years of age were randomised to either the XELIRI (irinotecan 250 mg/m^2 given on day one and capecitabine 1000 mg/m^2 twice daily from day 2--15, every 21 days) or the FOLFIRI arm (irinotecan 180 mg/m^2, 5-FU 400 mg/m^2, LV 200 mg/m^2, 5-FU 2400 mg/m^2 (46-h infusion) -- all given on day one, every 14 days). Primary end points were objective response rate (ORR) and rate of radical (R0) surgical resection. Secondary end points were progression-free survival (PFS), overall survival (OS) and safety.

Results: Altogether 87 patients were enrolled (41 pts in the XELIRI and 46 pts in the FOLFIRI arm). The median age was 63 years (63 years in the XELIRI and 62 years in the FOLFIRI arm) (p = 0.33). ORR was 49% in the XELIRI and 48% in the FOLFIRI arm (p = 0.76). The rate of radical R0 resection was 24% in both arms of patients. At the end of treatment, 37% of patients in the XELIRI and 26% of patients in the FOLFIRI arm were without evidence of the disease (CR+R0 resection) (p = 0.56). There were no statistical differences in grade 3 or 4 adverse events between both arms: diarrhoea 7% vs. 6%, neutropenia 5% vs. 13%, ischemic stroke 0 vs. 2%, acute coronary syndrome 2% vs. 4%, respectively. At the median follow up of 17 (range 1--39) months, the median PFS was 10.3 months in the XELIRI and 9.3 months in the FOLFIRI arm (p = 0.78), the median OS was 30.7 months in the XELIRI arm and 16.6 months in the FOLFIRI arm (p = 0.16).

Conclusion: The XELIRI regimen showed similar ORR as the FOLFIRI regimen in the neoadjuvant treatment of patients with MCRC. In addition, the XELIRI regimen showed similar PFS and OS with acceptable toxicity compared to the FOLFIRI regimen.

Trial Registration: Current Controlled Trials ISRCTN19912492

Background

The majority of patients with metastatic colorectal cancer (MCRC) have liver metastases. Radical (R0) resection of liver metastases offers the greatest likelihood of cure in the patients with liver-only metastases of MCRC. The five-year survival rates after radical resection are 24–58% [1-4], whereas the five-year survival rates for unresectable disease with most active systemic chemotherapy regimens are <5% [5]. Since the majority of patients with MCRC have unresectable liver metastases, neoadjuvant (or preoperative) chemotherapy is an appropriate treatment choice with intent to reduce the number and/or size of the liver metastases to make the radical (R0) resection of liver metastases possible. This can be achieved in 12–33% of patients [6-8]. In the neoadjuvant chemotherapy, combinations of fluoropyrimidines (5-FU/leucovorin (LV)) with irinotecan and/or oxaliplatin are usually used. Among the combinations of fluoropyrimidines with irinotecan, the FOLFIRI regimen is preferred, whereas the FOLFOX regimen is preferred among the combinations of fluoropyrimidines with oxaliplatin. Randomised studies have shown that the combination of capecitabine with oxaliplatin (XELOX regimen) in the first-line treatment of patients with MCRC shows similar efficacy and tolerability compared to the combinations of 5-FU/LV with oxaliplatin [9,10]. There are, however, only few published data about the combination of capecitabine with irinotecan in the treatment of patients with MCRC. Phase I/II studies have demonstrated that the combination of capecitabine (1000 mg/m2 twice daily for 14 days) with irinotecan (250 mg/m2 i.v. on day one, every 21 days) (the XELIRI regimen) is active [11-14]. The XELIRI regimen showed response rates of 35–54% and time to progression 8–9 months. Most common treatment-related grade 3 or grade 4 adverse events reported from a phase II study were neutropenia (25%), diarrhoea (20%), vomiting (16%), dehydration (10%), nausea (6%), abdominal pain (6%), and hand-foot syndrome (6%) [11].

To our knowledge, there has been no study published with the XELIRI regimen in the neoadjuvant setting of patients with unresectable liver-only metastases of MCRC. The aim of our study was to compare the efficacy, safety and survival of the XELIRI regimen to the standard FOLFIRI regimen in the neoadjuvant setting of patients with unresectable liver-only metastases of MCRC.

Our hypothesis was that there are no statistically significant differences in efficacy, survival and safety of the XELIRI regimen compared to the standard FOLFIRI regimen. However, the XELIRI regimen seems to be more convenient when compared to the FOLFIRI regimen since capecitabine is an oral drug; therefore, there is no need for central venous catheters implantation (risk for bleeding, infection, thrombosis) and no need for hospitalisation. The treatment is performed in out-patient clinic. The cycles are applied every 21 days compared to every 14 days in the FOLFIRI regimen.

In the year 2004, at the time when our study was initiated, bevacizumab was not yet registered for the treatment of patients with MCRC in Slovenia. However, in 2006, while our study was ongoing, bevacizumab became a standard in the first-line treatment of patients with MCRC. This was the main reason why the study was prematurely closed for the accrual at the end of the year 2006 with only 43% of initially planned accrual.

Methods

The study was performed at the Institute of Oncology Ljubljana, Slovenia, after it had been approved by National Medical Ethics Committee. This was a prospective randomised phase II study.

Eligibility criteria were: age 18–75 years, performance status of 0–1 according to WHO, unresectable liver metastases of colorectal adenocarcinoma – determined by liver surgeon either because of the size, number, or unfavourable location of metastases that did not allow a complete resection of disease leaving at least 25% of normal liver parenchyma, no prior chemotherapy for metastatic disease, >6 months since adjuvant treatment, at least one measurable lesion of ≥ 1 cm visible on spiral computed tomography (CT), bilirubin < 2× times the upper limit of normal (ULN), aspartate aminotransferase (AST) < 5× ULN, alanine aminotransferase (ALT) < 5× ULN, adequate haematological and renal function, and signed informed consent.

Exclusion criteria were: extra-hepatic disease (either metastases outside liver or loco-regional recurrence), other malignancy within the past 5 years (except limited basal cell or squamous cell carcinoma of the skin or in situ cervical carcinoma), inadequately controlled hypertension (blood pressure >150/100 mmHg on antihypertensive medications), unstable angina pectoris, history of myocardial infarction or stroke within 6 months, clinically significant peripheral vascular disease, inflammatory bowel disease. Patients that fulfilled eligibility criteria were randomly assigned to either the XELIRI or FOLFIRI arm with no prior stratification.

Patient evaluation

Pre-treatment evaluation included a detailed medical history, physical examination, a complete blood count with differential and platelet count, blood chemistry, serum levels of carcinoembryonic antigen (CEA) and baseline tumour measurements by CT. The pre-treatment evaluation had to be performed within 14 days before the treatment was initiated. The patients were assessed for toxicity

before each application of cytotoxic drugs. Repeat imaging was required every three months during treatment. Chemotherapy was discontinued prior to the expiry of six months if liver metastases became resectable (patients were referred to liver surgeon) or if there was either progression of the disease or serious adverse event occurred during chemotherapy. After the discontinuation of study treatment, a follow-up examination, including clinical examination, blood samples (liver enzymes, CEA), CT or ultrasound of the abdomen, was performed every 3 months, until the progression of the disease or death.

Chemotherapy

The XELIRI regimen consisted of irinotecan 250 mg/m^2 given on day one and capecitabine 1000 mg/m^2 twice daily from day 2–15, every 21 days. The FOLFIRI regimen consisted of irinotecan 180 mg/m^2, 5-FU 400 mg/m^2, LV 200 mg/m^2, 5-FU 2400 mg/m^2 (46-h infusion) – all given on day one, every 14 days. The patients in both arms received premedication with dexamethason 20 mg i.v., granisetron 1 mg i.v. and diazepam 10 mg i.v. on day 1 of each chemotherapy cycle. To initiate a cycle of cytotoxic chemotherapy, an absolute neutrophil count of at least 1500/μl, platelets at least 100000/μl and resolution of other toxic effects to at least CTC grade 1 were required. A resolution of toxicity to at least CTC grade 1 was required within 3 weeks of the intended start of a cycle or patients were withdrawn from the study. All patients were advised to use emollients with urea to manage hand-foot syndrome of grade I and II. The maximum planned duration of the treatment was six months in both arms. Postoperative chemotherapy was not planned.

Surgery

At evaluation, surgical resection of metastases was reconsidered by a team of experts, consisting of a liver surgeon, radiologist and medical oncologist. Liver surgery was attempted when technically feasible and potentially curative in the patients fit for operative procedure. During surgery, a complete exploration of the abdomen, including intraoperative ultrasound, was performed. Different surgical techniques were used for the resection of metastases.

The primary end points were: overall objective response (ORR) and rate of radical surgical resection (R0 resection). The evaluation of response was based on RECIST [15]. The radical surgical resection (R0 resection) of liver metastases was defined as tumour-free margin of >10 mm at histology specimen and no signs of residual metastases during exploration of the abdomen. In case of complete response (CR), liver surgery was not performed; regular follow-up was performed in these patients.

Secondary end points were: progression-free survival (PFS), overall survival (OS) and safety. PFS was defined as the time between the randomisation and the progression of the disease or death of any cause; the patients who were withdrawn from the study treatment for other reasons were censored at the discontinuation of study therapy. OS was defined as the time between the randomisation and death. Treatment-related death was defined as the death within 30 days after the last cycle of chemotherapy or liver surgery. All toxic effects were graded according to the National Cancer Institute (NCI) – Common Toxicity Criteria (CTC), version 3.0. The histology reports documented any signs of steatohepatitis.

Statistical considerations

For the statistical power calculation, online DSS Research toolkit was used. For the FOLFIRI arm, a response rate of 40% and a R0 resection rate of 15% was expected. The statistical power for initially planned 200 patients, with Alpha Error level of 5% (a 95% Confidence Interval) to show 10% difference between arms, was calculated to be 41% for the objective response rate, and 55% for the R0 resection rate. With 87 patients enrolled, the statistical power for the objective response rate was 24%, and for the R0 resection rate 32%.

Statistical analysis was performed with the program SPSS – Version 1.3. For the comparison of the two arms, two-sided Pearson chi-square test and Student's t-test were used. Objective response rate was assessed on intention to treat (ITT) population. Safety analysis was performed on the group of patients who received at least one dose of protocol medication. Overall survival and progression-free survival were estimated according to Kaplan-Meier method [16]. Survival curves were compared with the log-rank test. Statistical difference between the arms was determined as $p < 0.05$.

Results

In the period of 1 January 2004 – 31 December 2006, altogether eighty-seven patients were enrolled. Forty-one patients were randomly assigned to the XELIRI and forty-six patients to the FOLFIRI arm. There were no statistically significant differences in baseline characteristics between the two arms (Table 1). Median duration of neoadjuvant treatment was 5.0 (range 1.1 – 9.6) months in the XELIRI arm and 5.1 (range 0.1 – 9.7) in the FOLFIRI arm ($p = 0.45$). The median follow up was 17 months (range 1–39). The efficacy of both treatment arms (ORR, R0 resection rate) is shown in Table 2. At the time of evaluation by CT scans after the conclusion of neoadjuvant chemotherapy, the disease was expected to be resectable in 29% of patients in the XELIRI arm and in 44% of patients in the FOLFIRI arm ($p = 0.16$). All of these patients underwent surgery. The R0 resection has been performed in 10 (24%) of all patients in the XELIRI arm and in 11 (24%) of all patients in the FOLFIRI arm ($p = 0.83$).

Table 1: Baseline clinical characteristics of patients in the XELIRI and FOLFIRI arms, data are shown as n (%) or as n (range)

	XELIRI n = 41	FOLFIRI n = 46	p
Median age-years	63 (47--75)	62 (34--75)	0.33
Gender			
Male	26 (63%)	27 (59%)	0.38
Female	15 (37%)	19 (41%)	0.40
WHO performance status			
Performance status 0	31 (75%)	36 (78%)	0.82
Performance status 1	10 (25%)	10 (22%)	0.85
Primary tumour			
Colon	30 (73%)	40 (87%)	0.23
Rectum	11 (27%)	6 (13%)	0.22
Initial stage of disease at diagnosis			
Stage 1	0	1 (2%)	-
Stage 2	7 (17%)	3 (7%)	0.21
Stage 3	6 (15%)	14 (30%)	0,07
Stage 4	28 (68%)	28 (61%)	1.0
Previous adjuvant treatment*			
Yes	6 (15%)	10 (22%)	0.32
No	35 (85%)	36 (78%)	0.91
Median time from diagnosis to randomisation (months)	1.87 (0.7--65.5)	2.1 (0.26--55.7)	0.77
Number of liver metastases			
1 -- 4	15 (37%)	11 (24%)	0.43
5 -- 10	8 (19%)	10 (22%)	0.81
> 10	18 (44%)	25 (54%)	0.28
Liver involvement (%)			
< 25	14 (34%)	10 (22%)	0.41
25 -- 50	13 (32%)	14 (30%)	0.85
> 50	14 (34%)	21 (45%)	0.24
Median size of liver metastases (cm)	4.0 (1.5 -- 12.4)	5.0 (0.5--15.0)	0.10
Bilateral liver metastases, n (%)	35 (85%)	37 (80%)	0.81
Baseline CEA			
Normal	8 (19%)	10 (22%)	0.64
> 3.5 μg/l	33 (81%)	36 (78%)	0.72
Baseline LDH			
Normal	25 (61%)	18 (39%)	0.28
> 4.12 μkat/l	15 (37%)	26 (56%)	0.09
Reasons for initial unresectability			
Location of metastases	10 (24%)	8 (17%)	0.52
Number of metastases	25 (61%)	30 (65%)	0.71
Size of metastases	6 (15%)	8 (17%)	0.84

* Adjuvant treatment with chemotherapy ± radiotherapy

Table 2: Efficacy of treatment in the XELIRI and FOLFIRI arms (response rate, R0 resection* rate), data are shown as n (%)

	XELIRI n = 41	FOLFIRI n = 46	p
Complete response	5 (12%)	1 (2%)	0.10
Partial response	15 (37%)	21 (46%)	0.32
Objective response	20 (49%)	22 (48%)	0.76
Stagnation	12 (29%)	10 (22%)	0.67
Progressive disease	7 (17%)	11 (24%)	0.35
R0 resection*	10 (24%)	11 (24%)	0.83
Complete response + R0 resection	15 (37%)	12 (26%)	0.56

R0 resection* -- > 10 mm tumour-free resection margin on histology

The PFS of patients in the XELIRI and FOLFIRI arms is shown in Figure 1. The median PFS for the patients in the XELIRI arm was 10.3 months (95% CI: 9.1–11.5) and 9.3 months (95% CI: 6.7–12.0) in the FOLFIRI arm (p = 0.78). The OS of patients in the XELIRI and FOLFIRI arms is shown in Figure 2. The median OS for the XELIRI arm was 30.7 months (95% CI: 19.5–41.9) and for the FOLFIRI arm 16.6 months (95% CI: 7.9–25.3) (p = 0.16).

At the time of the analysis, of 21 patients who underwent R0 resection of liver metastases, 19 (90%) were alive: in the XELIRI arm, 9 out of 10 (90%) patients, and in the FOLFIRI arm, 10 out of 11 (91%) (p = 0.82). At the time of the analysis, CR after chemotherapy was evident in 4 out of 6 (67%) patients: in the XELIRI arm, 3 out of 5 (60%) patients, and in the FOLFIRI arm, 1/1 patient (p = 0.32).

Adverse events of any grade in the treatment the XELIRI and FOLFIRI arms are shown in Table 3. The majority of adverse events were of grade I or II. The adverse events of grade 3 or 4 in the XELIRI arm were diarrhoea (7%), neutropenia (5%), and acute coronary syndrome (2%). In the FOLFIRI arm, the adverse events of grade 3 or 4 were neutropenia (13%), diarrhoea (6%), acute coronary syndrome (4%), and ischemic stroke (2%). No hand-foot syndrome of grade 3 occurred in any of the two arms. Dose reduction due to adverse events was required in 12% of patients in the XELIRI arm and in 22% of patients in the FOLFIRI arm (p = 0.20). The therapy was completed as planned in 90% of patients in the XELIRI arm and in 87% of patients in the FOLFIRI arm (p = 0.85). The diagnosis of steatohepatitis from histology reports at liver surgery was present in 6/12 (50%) of patients in the XELIRI arm and in 8/20 (40%) of patients in the FOLFIRI arm (p =

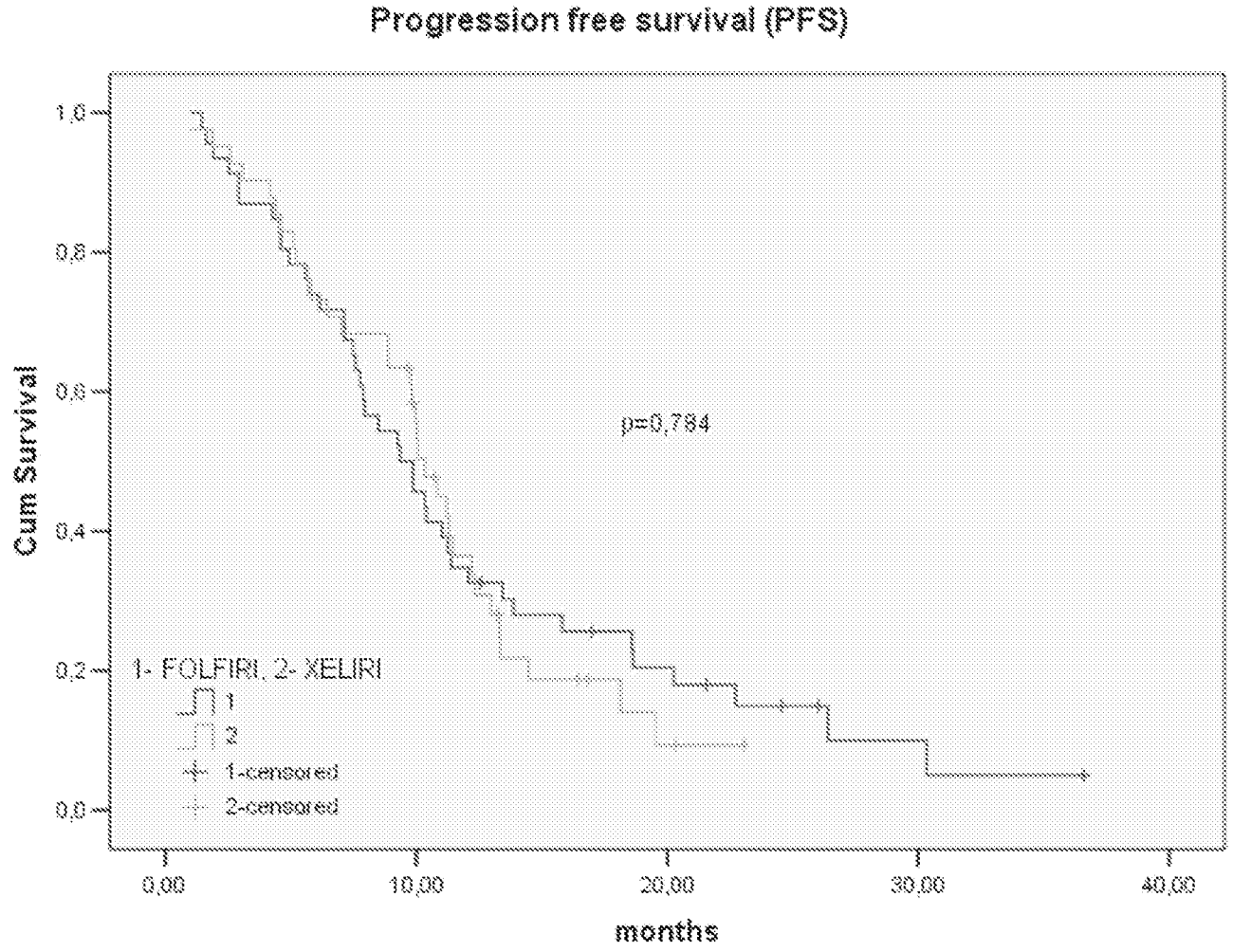

Figure 1
The PFS of patients in the XELIRI and FOLFIRI arms (months).

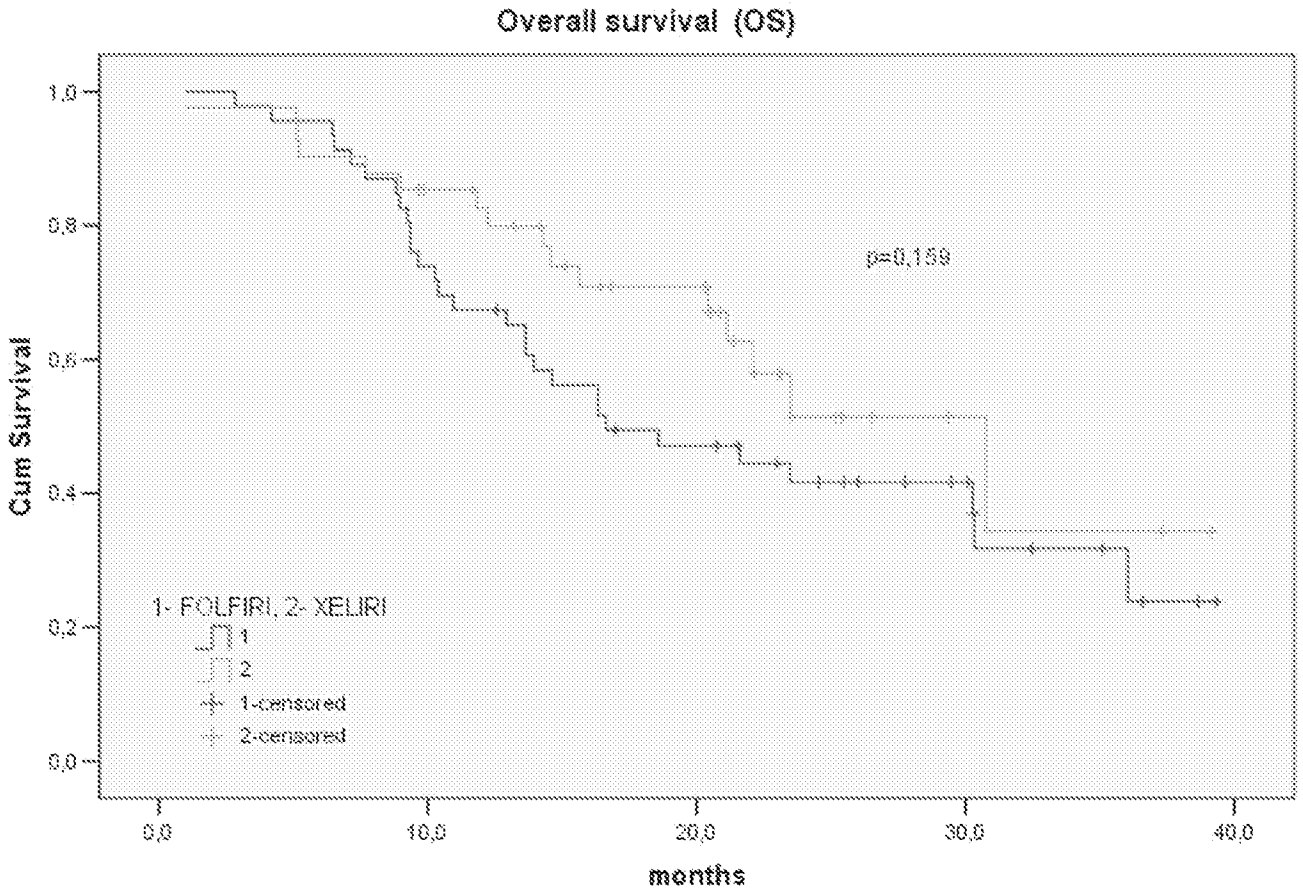

Figure 2
The OS of patients in the XELIRI and FOLFIRI arms (months).

0.59). Steatohepatitis was present in median of 65% (range 20% – 90%) of liver tissue in the XELIRI arm and in median of 55% (range 10% – 70%) in the FOLFIRI arm (p = 0.59). The intensity of steatohepatitis was either mild (3 patients) or modest (3 patients) in the XELIRI arm, and mild (5 patients), modest (1 patient) and severe (2 patients) in the FOLFIRI arm (p = 0.30). None of patients with steatohepatitis had any additional perioperative co-morbidity after liver surgery. There were no treatment-related deaths in any of the two arms of patients.

At relapse, all patients received at least one line of chemotherapy: oxaliplatin-based second-line therapy received 85% of patients in the XELIRI arm and 62% of patients in the FOLFIRI arm (p = 0.59), cetuximab-based second-line therapy received 5% of patients in the XELIRI arm and 12% of patients in the FOLFIRI arm (p = 0.32).

Discussion

The present study reports the comparison of efficacy, safety and survival between the XELIRI and FOLFIRI regimen in the neoadjuvant treatment of patients with MCRC.

The current single-institution randomised phase II trial demonstrated that the XELIRI regimen is effective in the neoadjuvant treatment of patients with MCRC and that it has acceptable toxicity, when compared to the FOLFIRI regimen. Both primary end-points were practically identical between the two arms. The relatively high rate of objective response (49% and 48%) in both arms is in the range of expected, since all patients had liver-only metastases. The rate of R0 resection (24%) of liver metastases in our study is one of the highest reported. We believe that both chemotherapy regimens are effective since, at the end of treatment, 37% of patients were without any evidence of the disease (either complete remission achieved with chemotherapy or R0 resection of liver metastases) in the XELIRI regimen and 26% of patients in the FOLFIRI regimen.

Table 3: Adverse events regarding CTCAE-3 in the XELIRI and FOLFIRI arms, data are shown as n (%)

	XELIRI N = 41	FOLFIRI n = 46	p
Hand-foot syndrome			
Grade 1	4 (10%)	0	0.18
Grade 2	2 (5%)	0	0.10
Grade 3	0	0	-
Diarrhoea			
Grade 1	1 (2%)	4 (8%)	0.18
Grade 2	4 (10%)	7 (15%)	0.37
Grade 3	1 (2%)	2 (4%)	0.56
Grade 4	2 (5%)	1 (2%)	0.56
Nausea			
Grade 1	3 (7%)	8 (17%)	0.13
Grade 2	6 (15%)	1 (2%)	0.06
Grade 3	0	0	-
Grade 4	0	0	-
Fatigue			
Grade 1	3 (7%)	4 (9%)	0.70
Grade 2	1 (2%)	2 (4%)	0.56
Grade 3	0	0	-
Grade 4	0	0	-
Neutropenia			
Grade 1	3 (7%)	2 (4%)	0.65
Grade 2	2 (5%)	12 (26%)	0.008
Grade 3	1 (2%)	5 (11%)	0.10
Grade 4	1 (2%)	1 (2%)	1.0
Thrombopenia of any grade	0	0	-
Ischemic stroke	0	1 (2%)	-
Acute coronary syndrome	1 (2%)	2 (4%)	0.56
Death*	0	0	-

* Patients who died within 30 days after the last cycle of chemotherapy or liver surgery

The PFS of 9–10 months in the patients in our study was similar to the PFS of patients with liver only metastases treated with the FOLFIRI regimen in a recently reported large randomised the CRYSTAL trial [17]. In the CRYSTAL trial, however, the secondary resection rate of liver metastases in 134 patients with liver-only metastases was only 4.5%. Since the majority of patients in the CRYSTAL trial had extra-hepatic disease, it is possible that the low rate of secondary resection of liver-only metastases was due to the lack of active searching for resectable liver metastases after neoadjuvant chemotherapy by the multidisciplinary team consisting of a liver surgeon, radiologist and medical oncologist. We believe that this multidisciplinary approach is essential for an optimal treatment outcome of patients with liver-only metastases of MCRC.

Despite the high R0 resection rate in both our study arms and high survival of patients following R0 resection in our study, the median OS of all patients in the FOLFIRI arm is one of the lowest ever reported for this regimen (16.6 months). It is possible that poor median OS in our FOLFIRI arm is due to the fact that only 62% of patients in this arm received an oxaliplatin-based second line regimen at progression of the disease. For the patients with MCRC who receive all three chemotherapeutic drugs (irinotecan, oxaliplatin, and fluoropyrimidine), the expected median OS is 20–22 months [18,19].

It is noteworthy that the XELIRI regimen showed acceptable toxicity. To our surprise, no grade 3 hand-foot syndrome, a well-known adverse event of capecitabine, occurred in the XELIRI arm. This is possibly due to the lower daily dose of capecitabine in the XELIRI regimen than in the capecitabine monotherapy. During the treatment with irinotecan and capecitabine, diarrhoea is a frequent adverse event when these drugs are used as single agents. In our study, the rate of grade 3 or 4 diarrhoea in the XELIRI arm was also low. This is in concordance with the European CAIRO trial [20], which showed no additional grade 3 or 4 diarrhoea in the patients in the XELIRI arm as compared to the sequential therapy with capecitabine and irinotecan monotherapy. In contrast, in the recently published American trial BICC-C [21], the incidence of grade 3 or 4 diarrhoea was present in 48% of patients in the XELIRI arm. The reason for these differences in diarrhoea incidences among these trials is not known.

The neoadjuvant chemotherapy is known to cause liver toxicity. For the irinotecan-based regimens, the usual pathological abnormality of liver cells is steatohepatitis. Because of liver toxicity, the resection of liver metastases should be performed as soon as the metastases become resectable with neoadjuvant chemotherapy. There were signs of steatohepatitis in both arms of patients, but no additional co-morbidities were observed after liver resections in the patients of either arm.

In the recent years, three targeted drugs became available for the treatment of patients with MCRC (bevacizumab, cetuximab, panitumumab). Since best clinical benefit of these drugs is achieved in combination with chemotherapy, they are usually used with different chemotherapy regimens. The combination of targeted therapy with different chemotherapy regimens showed favourable objective response rates when compared to chemotherapy alone in phase II/III studies [17,22]. In the neoadjuvant setting, the regimens with higher objective response rates are preferred as it is believed that higher objective response rates lead to higher R0 resection rates of liver metastases. Therefore, the combination of targeted agents with chemotherapy is generally applied in the neoadjuvant setting. Because of this, our study was prematurely closed soon after bevacizumab had become available in our country. We believe that the XELIRI regimen should be considered to be part of phase II trials where the targeted drugs, like cetuximab or bevacizumab, are used in

combination with chemotherapy. Outside clinical trials, in small subset of patients, where the targeted agents are contraindicated or not available to the patients, the XELIRI regimen could be used as an alternative to the FOLFIRI regimen in the neoadjuvant setting of patients with liver-only metastases of MCRC.

Conclusion

Our study showed that the XELIRI regimen is effective with acceptable toxicity when compared to the FOLFIRI regimen in neoadjuvant treatment of patients with unresectable liver-only metastases of MCRC. XELIRI regimen merits further evaluation in phase II trials in combination with targeted drugs in patients with MCRC.

Competing interests

The authors declare that they have no competing interests.

Authors' contributions

ES made a substantial contribution to the conception, design, and coordination of the study, to the treatment of patients, interpretation of data; he performed statistical analysis, and was involved in drafting the manuscript. MR made a substantial contribution to the treatment of patients and helped to draft the manuscript. ZH made a substantial contribution to the treatment of patients and helped to draft the manuscript. JO made a substantial contribution to the conception, design and coordination of the study and to the treatment of patients, and helped to draft the manuscript. All authors read and approved the final manuscript.

References

1. Abdalla EK, Vauthey JN, Ellis LM, Ellis V, Pollock R, Broglio KR, Hess K, Curley SA: **Recurrence and outcomes following hepatic resection, radiofrequency ablation, and combined resection/ablation for colorectal liver metastases.** *Ann Surg* 2004, **239**:818-825.
2. Wei AC, Greig PD, Grant D, Taylor B, Langer B, Gallinger S: **Survival after hepatic resection for colorectal metastases: a 10-year experience.** *Ann Surg Oncol* 2006, **13**:668-676.
3. Simmonds PC, Primrose JN, Colquitt JL, Garden OJ, Poston GJ, Rees M: **Surgical resection of hepatic metastases from colorectal cancer: a systematic review of published studies.** *Br J Cancer* 2006, **94**:982-999.
4. Cummings LC, Payes JD, Cooper GS: **Survival after hepatic resection in metastatic colorectal cancer: a population-based study.** *Cancer* 2007, **109**:718-726.
5. Van Cutsem E, Nordlinger B, Adam R, Köhne CH, Pozzo C, Poston G, Ychou M, Rougier P: **European Colorectal Metastases Treatment. Towards a pan-European consensus on the treatment of patients with colorectal liver metastases.** *Eur J Cancer* 2006, **42**:2212-2221.
6. Masi G, Cupini S, Marcucci L, Cerri E, Loupakis F, Allegrini G, Brunetti IM, Pfanner E, Viti M, Goletti O, Filipponi F, Falcone : **Treatment with 5-fluorouracil/folinic acid, oxaliplatin, and irinotecan enables surgical resection of metastases in patients with initially unresectable metastatic colorectal cancer.** *Ann Surg Oncol* 2006, **13**:58-56.
7. Alberts SR, Horvath WL, Sternfeld WC, Goldberg RM, Mahoney MR, Dakhil SR, Levitt R, Rowland K, Nair S, Sargent DJ, Donohue : **Oxaliplatin, Fluorouracil, and Leucovorin for Patients With Unresectable Liver-Only Metastases From Colorectal Cancer: A North Central Cancer Treatment Arm Phase II Study.** *J Clin Oncol* 2005, **23**:9243-9249.
8. Barone C, Nuzzo G, Cassano A, Basso M, Schinzari G, Giuliante F, D'Argento E, Trigila N, Astone A, Pozzo : **Final analysis of colorectal cancer patients treated with irinotecan and 5-fluorouracil plus folinic acid neoadjuvant chemotherapy for unresectable liver metastases.** *Br J Cancer* 2007, **97**:1035-1039.
9. Porschen R, Arkenau HT, Kubicka S, Greil R, Seufferlein T, Freier W, Kretzschmar A, Graeven U, Grothey A, Hinke A, Schmiegel W, Schmoll HJ, AIO Colorectal Study Arm: **Capecitabine Plus Oxaliplatin Compared With Fluorouracil and Leucovorin Plus Oxaliplatin: A Randomized Comparison in Metastatic Colorectal Cancer – A Final Report of the AIO Colorectal Study Arm.** *J Clin Oncol* 2007, **25**:4217-4223.
10. Diaz-Rubio E, Tabernero J, Gomez-Espana A, Massuti B, Sastre J, Chaves M, Abad A, Carrato A, Queralt B, Reina JJ, Maurel J, González-Flores E, Aparicio J, Rivera F, Losa F, Aranda E, Spanish Cooperative Arm for the Treatment of Digestive Tumors Trial: **Phase III Study of Capecitabine Plus Oxaliplatin Versus Continuous-Infusion Fluorouracil Plus Oxaliplatin As First-Line Therapy in Metastatic Colorectal Cancer: Final Report of the Spanish Cooperative Arm for the Treatment of Digestive Tumors Trial.** *J Clin Oncol* 2007, **25**:4224-4230.
11. Patt YZ, Lee FC, Leibmann JE, Diamandidis D, Eckhardt SG, Javle M, Justice GR, Keiser W, Salvatore JR, Bexon A, Lin E: **Capecitabine plus 3-weekly irinotecan (XELIRI regimen) as first-line chemotherapy for metastatic colorectal cancer.** *Am J Clin Oncol* 2007, **30**:350-357.
12. Bajetta E, Di Bartolomeo M, Mariani L, Cassata A, Artale S, Frustaci S, Pinotti G, Bonetti A, Carreca I, Biasco G, Bonaglia L, Marini G, Iannelli A, Cortinovis D, Ferrario E, Beretta E, Lambiase A, Buzzoni R, Italian Trials in Medical Oncology (I.T.M.O.) Arm: **Randomized multicenter Phase II trial of two different schedules of irinotecan combined with capecitabine as first-line treatment in metastatic colorectal carcinoma.** *Cancer* 2004, **100**:279-287.
13. Borner MM, Bernhard J, Dietrich D, Popescu R, Wernli M, Saletti P, Rauch D, Herrmann R, Koeberle D, Honegger H, Brauchli P, Lanz D, Roth AD, Swiss Arm for Clinical Cancer Research (SAKK), Berne, Switzerland: **A randomized phase II trial of capecitabine and two different schedules of irinotecan in first-line treatment of metastatic colorectal cancer: efficacy, quality-of-life and toxicity.** *Ann Oncol* 2005, **16**:282-288.
14. Rea DW, Nortier JW, Ten Bokkel Huinink WW, Falk S, Richel DJ, Maughan T, Groenewegen G, Smit JM, Steven N, Bakker JM, Semiond D, Kerr DJ, Punt CJ: **A phase I/II and pharmacokinetic study of irinotecan in combination with capecitabine as first-line therapy for advanced colorectal cancer.** *Ann Oncol* 2005, **16**:1123-1132.
15. Therasse P, Arbuck SG, Eisenhauer EA, Wanders J, Kaplan RS, Rubinstein L, Verweij J, Van Glabbeke M, van Oosterom AT, Christian MC, Gwyther SG: **New guidelines to evaluate the response to treatment in solid tumors. European Organization for Research and Treatment of Cancer, National Cancer Institute of the United States, National Cancer Institute of Canada.** *J Natl Cancer Inst* 2000, **92**:205-216.
16. Kaplan E, Meier P: **Nonparametric estimation from incomplete observations.** *J Am Stat Assoc* 1958, **53**:457-481.
17. Van Cutsem E, Bodoky G, Roh JK, Folprecht G, Park YS, Van Laethem JL, Raoul JL, Ciardiello F, Lebrun P, Rougier P: **CRYSTAL, a randomized phase III trial of cetuximab plus FOLFIRI vs. FOLFIRI in first-line metastatic colorectal cancer (mCRC) [abstract].** *Eur J Cancer* 2007, **5(Suppl 4)**:235.
18. Tournigand C, Andre T, Achille E, Lledo G, Flesh M, Mery-Mignard D, Quinaux E, Couteau C, Buyse M, Ganem G, Landi B, Colin P, Louvet C, de Gramont A: **FOLFIRI followed by FOLFOX6 or the reverse sequence in advanced colorectal cancer: a randomized GERCOR study.** *J Clin Oncol* 2004, **22**:229-237.
19. Colucci G, Gebbia V, Paoletti G, Giuliani F, Caruso M, Gebbia N, Cartenì G, Agostara B, Pezzella G, Manzione L, Borsellino N, Misino A, Romito S, Durini E, Cordio S, Di Seri M, Lopez M, Maiello E, Montemurro S, Cramarossa A, Lorusso V, Di Bisceglie M, Chiarenza M, Valerio MR, Guida T, Leonardi V, Pisconti S, Rosati G, Carrozza F, Nettis G, Valdesi M, Filippelli G, Fortunato S, Mancarella S, Brunetti C: **Phase III randomized trial of FOLFIRI versus FOLFOX4 in the treatment of advanced colorectal cancer: a multicenter**

study of the Gruppo Oncologico Dell'Italia Meridionale. *J Clin Oncol* 2005, **23**:4866-75.
20. Koopman M, Antonini NF, Douma J, Wals J, Honkoop AH, Erdkamp FL, de Jong RS, Rodenburg CJ, Vreugdenhil G, Loosveld OJ, van Bochove A, Sinnige HA, Creemers GJ, Tesselaar ME, Slee PH, Werter MJ, Mol L, Dalesio O, Punt CJ: **Sequential versus combination chemotherapy with capecitabine, irinotecan, and oxaliplatin in advanced colorectal cancer (CAIRO): a phase III randomised controlled trial.** *Lancet* 2007, **370**:135-142.
21. Fuchs CS, Marshall J, Mitchell E, Wierzbicki R, Ganju V, Jeffery M, Schulz J, Richards D, Soufi-Mahjoubi R, Wang B, Barrueco J: **Randomized, controlled trial of irinotecan plus infusional, bolus, or oral fluoropyrimidines in first-line treatment of metastatic colorectal cancer: results from the BICC-C Study.** *J Clin Oncol* 2007, **25**:4779-4786.
22. Folprecht G, Gruenberger T, Hartmann JT, Lordick F, Stoehlmacher J, Bechstein W, Ockert D, Hermann T, Liersch T, Koehne C: **Randomized multicenter study of cetuximab plus FOLFOX of plus FOLFIRI in neoadjuvant treatment of non-resectable colorectal liver metastases (CELIM-study).** *Ann Oncol* 2007, **19(Suppl 8)**:viii168.

Pre-publication history

The pre-publication history for this paper can be accessed here:

http://www.biomedcentral.com/1471-2407/9/120/prepub

Liposomal irinotecan in adults with small cell lung cancer who progressed on platinum-based therapy: subgroup analyses by platinum sensitivity

David R Spigel MD,[1] Luis G Paz-Ares MD,[2] Yuanbin Chen MD,[3] Maria Jove MD,[4] Oscar Juan-Vidal MD,[5] Patricia Rich MD,[6] Theresa Hayes MD,[7] Vanesa Gutiérrez-Calderón MD,[8] Reyes Bernabe Caro MD,[9] Alejandro Navarro MD,[10] Afshin Dowlati MD,[11] Bin Zhang MD,[12] Yan Moore MD,[12] Tiffany Wang MSc,[12] Natalya Nazarenko MD,[12] Jaba Kokhreidze MD,[12] Santiago Ponce MD,[2] Paul Bunn MD[13]

[1]Sarah Cannon Research Institute, Tennessee Oncology, Nashville, TN, USA; [2]Hospital Universitario 12 de Octubre, Madrid, Spain; [3]Cancer & Hematology Centers of Western Michigan, Grand Rapids, MI, USA; [4]Institut Català d'Oncologia, Hospital Duran i Reinals, Barcelona, Spain; [5]Hospital Universitari i Politècnic La Fe, Valencia, Spain; [6]Cancer Treatment Centers of America, Atlanta, GA, USA; [7]South West Healthcare, Warrnambool, VIC, Australia; [8]Hospital Regional Universitario de Malaga, Malaga, Spain; [9]Hospital Universitario Virgen del Rocio, Sevilla, Spain; [10]Hospital Universitari Vall d'Hebron, Barcelona, Spain; [11]Case Western Reserve University, Cleveland, OH, USA; [12]Ipsen Bioscience, Boston, MA, USA; [13]University of Colorado, Cancer Center and Department of Medicine, Denver, CO, USA

BACKGROUND

- The mainstay of first-line (1L) treatment for patients with small-cell lung cancer (SCLC) is platinum-based combination therapy – carboplatin or cisplatin, typically administered with the topoisomerase 2 inhibitor etoposide.[1,2]
  - However, many patients who are receiving platinum-based therapy develop drug resistance to it or discontinue it for other reasons.[2]
- Topoisomerase 1 is an alternative therapeutic target in SCLC, with proven mechanistic rationale.[3]
- Liposomal irinotecan (ONIVYDE, ONIVYDE pegylated liposomal) encapsulates the topoisomerase 1 inhibitor irinotecan in a lipid-bilayer vesicle, leading to prolonged circulation compared with the non-liposomal form.[4]
  - Liposomal irinotecan is approved in the USA in combination with 5-fluorouracil/leucovorin for use in patients with metastatic pancreatic adenocarcinoma following progression with gemcitabine-based therapy.[5]
- RESILIENT (NCT03088813) is a two-part phase 2/3 study assessing the safety, tolerability and efficacy of second-line (2L) liposomal irinotecan monotherapy in adults with SCLC who progressed while or after receiving 1L platinum-based therapy.
- Preliminary data from the phase 2 RESILIENT part 1 study (data cut off May 8, 2019) showed that intravenous liposomal irinotecan 70 mg/m^2 free base, given every 2 weeks:
  - was generally well tolerated (primary endpoint)
  - achieved an objective response rate (ORR) of 44.0% (11/25) (secondary endpoint).[6]

OBJECTIVE

- To report preliminary efficacy analyses from RESILIENT part 1 in *post hoc* subgroups categorized by sensitivity to platinum-based therapy.

METHODS

Study design

- RESILIENT part 1 was an open-label, single-arm, phase 2 study comprising dose-finding and dose-expansion phases.[6,7]

Study population

- Patients were adults (aged ≥ 18 years) with:[6,7]
  - progression while or after receiving 1L treatment for limited- or extensive-stage SCLC with platinum-based chemotherapy (carboplatin or cisplatin) or chemoradiation including platinum-based chemotherapy
  - disease evaluable by Response Evaluation Criteria in Solid Tumors version 1.1 (RECIST v1.1)
  - Eastern Cooperative Oncology Group Performance Status of 0 or 1
  - adequate organ function
  - life expectancy of more than 12 weeks.
- Additional permitted criteria were:[7]
  - a single line of prior immunotherapy
  - asymptomatic central nervous system metastases.

Treatment regimen

- **Administration:** intravenous liposomal irinotecan over 90 minutes every 2 weeks.[7]
- **Dose-finding phase.**
  - Cohort 1: liposomal irinotecan 85 mg/m^2 free base (n = 5); deemed not tolerable owing to dose-limiting toxicity[6] (diarrhea in three patients, abnormal liver function test in one patient).
  - Cohort 2: liposomal irinotecan 70 mg/m^2 free base (deemed tolerable and recommended for dose expansion; n = 12).[6]
- **Dose-expansion phase:** liposomal irinotecan 70 mg/m^2 free base (n = 13).[6]

Post hoc subgroup analyses by platinum sensitivity

- Analyses were conducted in a pooled population of patients who received liposomal irinotecan 70 mg/m^2 during either study phase (dose-finding cohort 2 or dose expansion; n = 25).

- Date of data cut off was May 8, 2019, to ensure at least 12 weeks of follow-up.
- Subgroups were defined by patients' platinum sensitivity.
  - Platinum sensitive: patients without progression while receiving, or in the 90 days after completion of, 1L platinum-based therapy.
  - Platinum resistant: patients with progression while receiving, or in the 90 days after completion of, 1L platinum-based therapy.

Table 1. Baseline and treatment characteristics by platinum-sensitivity subgroup

Baseline characteristics	Liposomal irinotecan 70 mg/m²		
	Pooled population (n = 25)	Platinum-sensitive subgroup (n = 15)	Platinum-resistant subgroup (n = 10)
Age, years			
Median (range)	59.8 (48–73)	62.0 (49–70)	58.0 (48–73)
Gender, n (%)			
Male	10 (40)	5 (33)	5 (50)
Race, n (%)			
White	25 (100)	15 (100)	10 (100)
Disease status, n (%)			
Locally advanced	2 (8)	2 (13)	0
Metastatic	23 (92)	13 (87)	10 (100)
ECOG Performance Status, n (%)			
Fully active (ECOG 0)	3 (12)	2 (13)	1 (10)
Restricted activity (ECOG 1)	22 (88)	13 (87)	9 (90)
Treatment characteristics			
Duration of exposure, weeks			
Mean (SD)	14 (7.2)	12 (7.9)	12 (6.5)
Median	15	17	11
Disposition at data cut-off, n (%)			
Receiving treatment	7 (28)	6 (40)	1 (10)
Discontinued	18 (72)	9 (60)	9 (90)

ECOG, Eastern Cooperative Oncology Group; SD, standard deviation.

- Tumor assessments were conducted every 6 weeks, using RECIST v1.1 to evaluate:
  - ORR, based on the proportion of patients with a best overall response of complete response (CR) or partial response (PR)
  - disease control rate at 12 weeks (DCR_{12wks}), based on the proportion of patients with CR, PR or stable disease at 12 weeks.
- Overall and progression-free survival were not mature at the time of data cut-off.[6]

Safety

- Adverse events were coded using Medical Dictionary for Regulatory Activities version 22.0.

RESULTS

Patient characteristics and drug exposure

- Baseline characteristics were balanced between the platinum-sensitivity subgroups (**Table 1**).
- Median duration of exposure was numerically higher in the platinum-sensitive subgroup than in the platinum-resistant subgroup, and a higher proportion of patients in the platinum-sensitive subgroup remained on treatment at the data cut-off (**Table 1**).

Post hoc subgroup analyses by platinum sensitivity

- ORR and DCR_{12wks} were 53.3% and 60.0%, respectively, in the platinum-sensitive subgroup compared with 30% for both measures in the platinum-resistant subgroup (**Table 2**); tumor response over time is shown in **Figure 1**.

Table 2. Clinical response by platinum-sensitivity subgroup

	Liposomal irinotecan 70 mg/m²		
	Pooled population (n = 25)[a]	Platinum-sensitive subgroup (n = 15)	Platinum-resistant subgroup (n = 10)
Best overall response, n (%)			
CR	0	0	0
PR	11 (44.0)	8 (53.3)	3 (30.0)
SD	7 (28.0)	3 (20.0)	4 (40.0)
PD	5 (20.0)	2 (13.3)	3 (30.0)
Not evaluable	2 (8.0)	2 (13.3)	0
Objective response,[a] n (rate, %)	11 (44.0)	8 (53.3)	3 (30.0)
Disease control at 12 weeks,[b] n (rate, %)	12 (48.0)	9 (60.0)	3 (30.0)

Percentages are subject to rounding.
[a]Defined as CR + PR. [b]Defined as CR + PR + SD at 12 weeks.
CR, complete response; PD, progressive disease; PR, partial response; SD, stable disease.

Figure 1. Duration of response by platinum-sensitivity subgroup

Small numbers indicate the dose of liposomal irinotecan (mg/m² free base) received at each time point.
FU, follow-up; NonCR, non-complete response; NonPR, non-partial response; PD, progressive disease; OS, overall survival; PR, partial response; SD, stable disease.

Safety

- The proportion of patients with treatment-emergent adverse events (TEAEs) of grade 3 or higher that were considered to be related to study drug was numerically higher in the platinum-sensitive subgroup than in the platinum-resistant subgroup (**Table 3**).

Table 3. Treatment-related TEAEs of grade 3 or higher by platinum-sensitivity subgroup

	Liposomal irinotecan 70 mg/m²		
	Pooled population (n = 25)	Platinum-sensitive subgroup (n = 15)	Platinum-resistant subgroup (n = 10)
Any TEAE, n (%)	25 (100)	15 (100)	10 (100)
Grade ≥ 3 treatment-related TEAEs, n (%)	10 (40)	8 (53)	2 (20)
Diarrhea	5 (20)	5 (33)	0
Neutropenia	4 (16)	4 (27)	0
Abdominal sepsis	2 (8)	2 (13)	0
Anemia	2 (8)	2 (13)	0
Asthenia	2 (8)	1 (7)	1 (10)
Thrombocytopenia	2 (8)	2 (13)	0
Fatigue	1 (4)	1 (7)	0
Hypokalemia	1 (4)	0	1 (10)
Alanine aminotransferase increased	1 (4)	1 (7)	0
Dysphagia	1 (4)	0	1 (10)
Gamma-glutamyltransferase increased	1 (4)	1 (7)	0
Death from AE related to study drug, n (%)	2[a] (8)	2 (13)	0

Coded using Medical Dictionary for Regulatory Activities version 22.0.
[a]Abdominal sepsis, n = 2.
AE, adverse event; TEAE, treatment-related adverse event.

CONCLUSIONS

- In this *post hoc* subgroup analysis of RESILIENT part 1, ORR and DCR_{12wks} were numerically higher in platinum-sensitive (than in platinum-resistant) patients with SCLC who received 2L liposomal irinotecan 70 mg/m^2 after progression while or after receiving 1L platinum-based therapy.
  - Nevertheless, partial response was observed in 3 out of 10 patients with resistance to 1L platinum-based therapy.
- RESILIENT part 2, an ongoing, randomized, controlled, phase 3 study of liposomal irinotecan versus topotecan, will provide further efficacy and safety data for the use of liposomal irinotecan in patients with SCLC.

References

1. National Comprehensive Cancer Network. Guidelines: small cell lung cancer v3.2020. Feb 5, 2020. Available from: https://www.nccn.org/professionals/physician_gls/pdf/sclc.pdf (Accessed September 2020).
2. Jett JR *et al. Chest* 2013;143(5 Suppl):e400S–19S.
3. Horita N *et al. Sci Rep* 2015;5:15437.
4. Drummond DC *et al. Cancer Res* 2006;66:3271–7.
5. Ipsen Biopharmaceuticals, Inc. Prescribing information. ONIVYDE (irinotecan liposome injection). US Food and Drug Administration. July 2017. Available from: https://www.ipsen.com/websites/Ipsen_Online/wp-content/uploads/sites/9/2020/04/10140532/ONV-US-000771-Onivyde-Promotional-PI-8.5-x-11.pdf (Accessed September 2020).
6. Paz-Ares LG *et al.* Efficacy and safety of irinotecan liposome injection (nal-IRI) in patients with small cell lung cancer (SCLC). Presented at WCLC 2019, Oct 12, 2019, Barcelona, Spain. Oral presentation.
7. Paz-Ares LG *et al.* RESILIENT: study of irinotecan liposome injection (nal-IRI) in patients with small cell lung cancer: preliminary findings from part 1 dose-defining phase. Presented at ASCO 2019, May 31–June 4, 2019, Chicago, IL, USA. Poster 318.

Acknowledgments

The authors thank all patients involved in the study, as well as their caregivers and care teams, and the investigators and research staff in participating institutions.

The authors thank Dr Heather Lang of Oxford PharmaGenesis, Oxford, UK, for providing medical writing support, which was sponsored by Ipsen in accordance with Good Publication Practice (GPP3) guidelines.

Author contributions

All authors have contributed to study conception/design, drafting the publication or revising it critically for scientific accuracy and important intellectual content, and final approval of the publication.

Disclosures

DRS – consultant/advisor (all to institution): Aptitude Health, AstraZeneca, Bayer, Bristol-Myers Squibb, Celgene, Dracen Pharmaceuticals, EMD Serono, Evelo Biosciences, Genentech, GlaxoSmithKline, Iksuda Therapeutics, Illumina, Merck, Molecular Templates, Nektar Therapeutics, Novartis, Pfizer, PharmaMar, Roche, Seattle Genetics, Takeda, Triptych Health Partners, TRM Oncology, Williams & Connolly; travel/accommodation/expenses: Amgen, AstraZeneca, Celgene, Daiichi Sankyo, Bristol-Myers Squibb, Genentech/Roche, GlaxoSmithKline, Janssen, Merck, Novartis, Seattle Genetics, Spectrum Pharmaceuticals, Takeda; research funding (all to institution): Aegiea BioTherapeutics, Astellas, AstraZeneca, Bind Therapeutics, Bristol-Myers Squibb, Celgene, Celldex Therapeutics, Clovis Oncology, Daiichi Sankyo, Eisai, Eli Lilly, EMD Serono, G1 Therapeutics, Genentech, GRAIL, ImClone Systems, ImmunoGen, Ipsen, Janssen, MedImmune, Merck, Molecular Partners, Nektar Therapeutics, Neon Therapeutics, Novartis, Takeda, Transgene, UT Southwestern, LGP-A – leadership: Altum Sequencing, European Medicines Agency Scientific Advisory Groups, Genomica S.A.U.; honoraria: Advanced Accelerator Applications, Amgen, AstraZeneca, Bayer, Blueprint Medicines, Bristol-Myers Squibb, Boehringer Ingelheim, Celgene, Incyte, Ipsen, Lilly, Merck Serono, Merck Sharp & Dohme, Novartis, Pfizer, PharmaMar, Roche/Genentech, Sanofi, Servier, Sysmex; research funding: AstraZeneca, Bristol-Myers Squibb; travel/accommodation/expenses: AstraZeneca, Bristol-Myers Squibb, Merck Sharp & Dohme, Pfizer, Roche, Takeda; other relationships: Amgen, Ipsen, Merck, Novartis, Pfizer, Roche, Sanofi, Servier. YC – honoraria: AstraZeneca, Bristol-Myers Squibb, Genentech, Guardant Health, Lilly, Merck, Novartis, Takeda; consultant/advisor: Array BioPharma, AstraZeneca, Bristol-Myers Squibb, Genentech, Heron Therapeutics, Lilly, Novartis, Pfizer, Takeda; speakers' bureau: AstraZeneca, Bristol-Myers Squibb, Genentech, Guardant Health, Lilly, Merck, Novartis, Takeda; research funding: AstraZeneca, Bristol-Myers Squibb, Guardant Health, Helsinn, Ipsen, Roche; expert testimony: AstraZeneca, Takeda. MJ – honoraria: Boehringer Ingelheim; travel/accommodation/expenses: Merck Sharp & Dohme, Roche, Takeda. QJ-V – consultant/advisor: Abbvie, AstraZeneca, Boehringer Ingelheim, Bristol-Myers Squibb, Eli Lilly, Merck Sharp & Dohme, Pfizer, Roche/Genentech, Takeda. RBC – consultant/advisor: AstraZeneca, Bristol-Myers Squibb, Merck Sharp & Dohme, Roche, Takeda. AN – consultant/advisor: Boehringer Ingelheim, Pfizer; speaker's bureau: Roche; expert testimony: Oryzon Genomics; travel/accommodation/expenses: Boehringer Ingelheim, Pfizer, Roche. AD – consultant/advisor: Abbvie, AstraZeneca, Bristol-Myers Squibb, Seattle Genetics, Takeda; research funding: Abbvie, Amgen, Bayer, Incuron, Ipsen, Loxo, Regeneron, Seattle Genetics, Symphogen, Takeda, Tesaro. BZ – employment, stock/other ownership and patents/royalties/other intellectual property: Ipsen. YM – employment, leadership, stock/other ownership and travel/accommodation/expenses: Ipsen. TW – employment and stock/other ownership: Ipsen Bioscience. NN – employment and stock/other ownership: Ipsen. JK – employment: Ipsen; consultant/advisor: Bristol-Myers Squibb, Constellation Pharmaceuticals, JKMD Global Medical Solutions, Tocagen. SP – consultant/advisor: Bristol-Myers Squibb, Merck, Roche; speakers' bureau: Bristol-Myers Squibb, Merck, Roche; travel/accommodation/expenses: AstraZeneca, Merck, Roche. PR, TH, VGC and PB – nothing to disclose.

Corresponding author: dspigel@tnonc.com

Presented at the International Association for the Study of Lung Cancer (IASLC) 2020 North America Conference on Lung Cancer (NACLC 2020), virtual format, October 16–17, 2020 (#NACLC2020)

Originally presented at the Annual Meeting of the American Society of Clinical Oncology (ASCO), virtual format, May 29–June 2, 2020 (#ASCO20)

This study was sponsored by Ipsen

Liposomal irinotecan in adults with small cell lung cancer who progressed on platinum-based therapy: subgroup analyses by platinum sensitivity

[redacted]

BACKGROUND

[redacted]

OBJECTIVE

[redacted]

METHODS

[redacted]

RESULTS

[redacted]

CONCLUSIONS

[redacted]

RESILIENT part 1, an open-label, safety run-in of liposomal irinotecan in adults with small-cell lung cancer who have progressed with platinum-based first-line therapy: subgroup analyses by platinum sensitivity

David R Spigel MD,[1] Luis G Paz-Ares MD,[2] Yuanbin Chen MD,[3] Maria Jove MD,[4] Oscar Juan-Vidal MD,[5] Patricia Rich MD,[6] Theresa Hayes MD,[7] Vanesa Gutiérrez-Calderón MD,[8] Reyes Bernabe Caro MD,[9] Alejandro Navarro MD,[10] Afshin Dowlati MD,[11] Bin Zhang MD,[12] Yan Moore MD,[12] Tiffany Wang MSc,[12] Natalya Nazarenko MD,[12] Jaba Kokhreidze MD,[12] Santiago Ponce MD,[7] Paul Bunn MD[13]

[1]Sarah Cannon Research Institute, Tennessee Oncology, Nashville, TN, USA; [2]Hospital Universitario 12 de Octubre, Madrid, Spain; [3]Cancer & Hematology Centers of Western Michigan, Grand Rapids, MI, USA; [4]Institut Català d' Oncologia, Hospital Duran i Reinals, Barcelona, Spain; [5]Hospital Universitari i Politècnic La Fe, Valencia, Spain; [6]Cancer Treatment Centers of America, Atlanta, GA, USA; [7]South West Healthcare, Warrnambool, VIC, Australia; [8]Hospital Regional Universitario de Malaga, Malaga, Spain; [9]Hospital Universitario Virgen del Rocío, Sevilla, Spain; [10]Hospital Universitari Vall d'Hebron, Barcelona, Spain; [11]Case Western Reserve University, Cleveland, OH, USA; [12]Ipsen Bioscience, Boston, MA, USA; [13]University of Colorado, Cancer Center and Department of Medicine, Denver, CO, USA

BACKGROUND

- The mainstay of first-line (1L) treatment for patients with small-cell lung cancer (SCLC) is platinum-based combination therapy – carboplatin or cisplatin, typically administered with the topoisomerase 2 inhibitor etoposide.[1,2]
  - However, many patients who are receiving platinum-based therapy develop drug resistance to it or discontinue it for other reasons.[2]
- Topoisomerase 1 is an alternative therapeutic target in SCLC, with proven mechanistic rationale.[3]
- Liposomal irinotecan (ONIVYDE, ONIVYDE pegylated liposomal) encapsulates the topoisomerase 1 inhibitor irinotecan in a lipid-bilayer vesicle, leading to prolonged circulation compared with the non-liposomal form.[4]
  - Liposomal irinotecan is approved in the USA in combination with 5-fluorouracil/leucovorin for use in patients with metastatic pancreatic adenocarcinoma following progression with gemcitabine-based therapy.[5]
- RESILIENT (NCT03088813) is a two-part phase 2/3 study assessing the safety, tolerability and efficacy of second-line (2L) liposomal irinotecan monotherapy in adults with SCLC who progressed while or after receiving 1L platinum-based therapy.
- Preliminary data from the phase 2 RESILIENT part 1 study (data cut off May 8, 2019) showed that intravenous liposomal irinotecan 70 mg/m^2 free base, given every 2 weeks:
  - was generally well tolerated (primary endpoint)
  - achieved an objective response rate (ORR) of 44.0% (11/25) (secondary endpoint).[6]

OBJECTIVE

- To report preliminary efficacy analyses from RESILIENT part 1 in *post hoc* subgroups categorized by sensitivity to platinum-based therapy.

METHODS

Study design

- RESILIENT part 1 was an open-label, single-arm, phase 2 study comprising dose-finding and dose-expansion phases.[6,7]

Study population

- Patients were adults (aged ≥ 18 years) with:[6,7]
  - progression while or after receiving 1L treatment for limited- or extensive-stage SCLC with platinum-based chemotherapy (carboplatin or cisplatin) or chemoradiation including platinum-based chemotherapy
  - disease evaluable by Response Evaluation Criteria in Solid Tumors version 1.1 (RECIST v1.1)
  - Eastern Cooperative Oncology Group Performance Status of 0 or 1
  - adequate organ function
  - life expectancy of more than 12 weeks.
- Additional permitted criteria were:[7]
  - a single line of prior immunotherapy
  - asymptomatic central nervous system metastases.

Treatment regimen

- **Administration:** intravenous liposomal irinotecan over 90 minutes every 2 weeks.[7]
- **Dose-finding phase.**
  - Cohort 1: liposomal irinotecan 85 mg/m^2 free base (n = 5); deemed not tolerable owing to dose-limiting toxicity[6] (diarrhea in three patients, abnormal liver function test in one patient).
  - Cohort 2: liposomal irinotecan 70 mg/m^2 free base (deemed tolerable and recommended for dose expansion; n = 12).[6]
- **Dose-expansion phase:** liposomal irinotecan 70 mg/m^2 free base (n = 13).[6]

Post hoc subgroup analyses by platinum sensitivity

- Analyses were conducted in a pooled population of patients who received liposomal irinotecan 70 mg/m^2 during either study phase (dose-finding cohort 2 or dose expansion; n = 25).
- Date of data cut off was May 8, 2019, to ensure at least 12 weeks of follow-up.
- Subgroups were defined by patients' platinum sensitivity.
  - Platinum sensitive: patients without progression while receiving, or in the 90 days after completion of, 1L platinum-based therapy.
  - Platinum resistant: patients with progression while receiving, or in the 90 days after completion of, 1L platinum-based therapy.
- Tumor assessments were conducted every 6 weeks, using RECIST v1.1 to evaluate:
  - ORR, based on the proportion of patients with a best overall response of complete response (CR) or partial response (PR)
  - disease control rate at 12 weeks (DCR_{12wks}), based on the proportion of patients with CR, PR or stable disease at 12 weeks.
- Overall and progression-free survival were not mature at the time of data cut-off.[6]

Safety

- Adverse events were coded using Medical Dictionary for Regulatory Activities version 22.0.

RESULTS

Patient characteristics and drug exposure

- Baseline characteristics were balanced between the platinum-sensitivity subgroups (**Table 1**).
- Median duration of exposure was numerically higher in the platinum-sensitive subgroup than in the platinum-resistant subgroup, and a higher proportion of patients in the platinum-sensitive subgroup remained on treatment at the data cut-off (**Table 1**).

Post hoc subgroup analyses by platinum sensitivity

- ORR and DCR_{12wks} were 53.3% and 60.0%, respectively, in the platinum-sensitive subgroup compared with 30% for both measures in the platinum-resistant subgroup (**Table 2**); tumor response over time is shown in **Figure 1**.

Safety

- The proportion of patients with treatment-emergent adverse events (TEAEs) of grade 3 or higher that were considered to be related to study drug was numerically higher in the platinum-sensitive subgroup than in the platinum-resistant subgroup (**Table 3**).

Table 1. Baseline and treatment characteristics by platinum-sensitivity subgroup

Baseline characteristics	Liposomal irinotecan 70 mg/m²		
	Pooled population (n = 25)	Platinum-sensitive subgroup (n = 15)	Platinum-resistant subgroup (n = 10)
Age, years			
Median (range)	59.6 (48–73)	62.0 (49–70)	58.0 (48–73)
Gender, n (%)			
Male	10 (40)	5 (33)	5 (50)
Race, n (%)			
White	25 (100)	15 (100)	10 (100)
Disease status, n (%)			
Locally advanced	2 (8)	2 (13)	0
Metastatic	23 (92)	13 (87)	10 (100)
ECOG Performance Status, n (%)			
Fully active (ECOG 0)	3 (12)	2 (13)	1 (10)
Restricted activity (ECOG 1)	22 (88)	13 (87)	9 (90)
Treatment characteristics			
Duration of exposure, weeks			
Mean (SD)	14 (7.2)	12 (7.9)	12 (6.5)
Median	15	17	11
Disposition at data cut-off, n (%)			
Receiving treatment	7 (28)	6 (40)	1 (10)
Discontinued	18 (72)	9 (60)	9 (90)

ECOG, Eastern Cooperative Oncology Group; SD, standard deviation.

Table 2. Clinical response by platinum-sensitivity subgroup

	Liposomal irinotecan 70 mg/m²		
	Pooled population (n = 25)[a]	Platinum-sensitive subgroup (n = 15)	Platinum-resistant subgroup (n = 10)
Best overall response, n (%)			
CR	0	0	0
PR	11 (44.0)	8 (53.3)	3 (30.0)
SD	7 (28.0)	3 (20.0)	4 (40.0)
PD	5 (20.0)	2 (13.3)	3 (30.0)
Not evaluable	2 (8.0)	2 (13.3)	0
Objective response,[b] n (rate, %)	11 (44.0)	8 (53.3)	3 (30.0)
Disease control at 12 weeks,[c] n (rate, %)	12 (48.0)	9 (60.0)	3 (30.0)

Percentages are subject to rounding.
[a]Defined as CR + PR. [b]Defined as CR + PR + SD at 12 weeks.
CR, complete response; PD, progressive disease; PR, partial response; SD, stable disease.

Figure 1. Duration of response by platinum-sensitivity subgroup

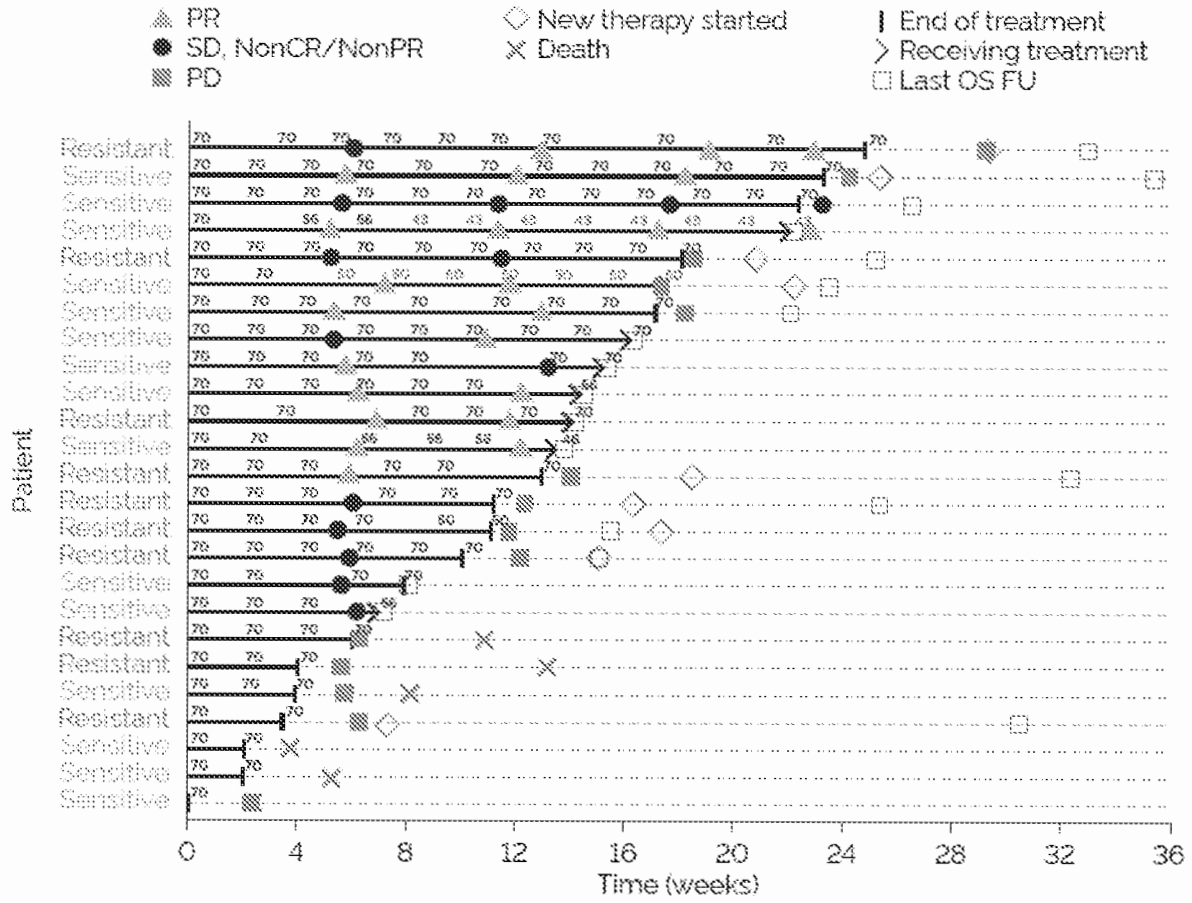

Small numbers indicate the dose of liposomal irinotecan (mg/m² free base) received at each time point.
FU, follow-up; NonCR, non-complete response; NonPR, non-partial response; PD, progressive disease; OS, overall survival; PR, partial response; SD, stable disease.

Table 3. Treatment-related TEAEs of grade 3 or higher by platinum-sensitivity subgroup

	Liposomal irinotecan 70 mg/m²		
	Pooled (n = 25)	Platinum-sensitive subgroup (n = 15)	Platinum-resistant subgroup (n = 10)
Any TEAE, n (%)	25 (100)	15 (100)	10 (100)
Grade ≥ 3 treatment-related TEAEs, n (%)	10 (40)	8 (53)	2 (20)
Diarrhea	5 (20)	5 (33)	0
Neutropenia	4 (16)	4 (27)	0
Abdominal sepsis	2 (8)	2 (13)	0
Anemia	2 (8)	2 (13)	0
Asthenia	2 (8)	1 (7)	1 (10)
Thrombocytopenia	2 (8)	2 (13)	0
Fatigue	1 (4)	1 (7)	0
Hypokalemia	1 (4)	0	1 (10)
Alanine aminotransferase increased	1 (4)	1 (7)	0
Dysphagia	1 (4)	0	1 (10)
Gamma-glutamyltransferase increased	1 (4)	1 (7)	0
Death from AE related to study drug, n (%)	2[a] (8)	2 (13)	0

Coded using Medical Dictionary for Regulatory Activities version 22.0.
[a]Abdominal sepsis, n = 2.
AE, adverse event; TEAE, treatment-related adverse event.

CONCLUSIONS

- In this *post hoc* subgroup analysis of RESILIENT part 1, ORR and DCR_{12wks} were numerically higher in platinum-sensitive (than in platinum-resistant) patients with SCLC who received 2L liposomal irinotecan 70 mg/m^2 after progression while or after receiving 1L platinum-based therapy.
  - Nevertheless, a partial response was observed in 3/10 patients with resistance to 1L platinum-based therapy.
- RESILIENT part 2, an ongoing, randomized, controlled, phase 3 study of liposomal irinotecan versus topotecan, will provide further efficacy and safety data for the use of liposomal irinotecan in patients with SCLC (further details can be found in poster 274).

References

1. National Comprehensive Cancer Network. Guidelines: small cell lung cancer v3.2020. Feb 5, 2020. Available from: https://www.nccn.org/professionals/physician_gls/pdf/sclc.pdf (Accessed April 2020).
2. Jett JR *et al. Chest* 2013;143(5 Suppl):e400S–19S.
3. Horita N *et al. Sci Rep* 2015;5:15437.
4. Drummond DC *et al. Cancer Res* 2006;66:3271–7.
5. Ipsen Biopharmaceuticals, Inc. Prescribing information, ONIVYDE (irinotecan liposome injection). US Food and Drug Administration, July 2017. Available from: https://www.ipsen.com/websites/Ipsen_Online/wp-content/uploads/sites/9/2020/04/10140532/ONV-US-000771-Onivyde-Promotional-PI-8.5-x-11.pdf (Accessed April 2020).
6. Paz-Ares LG *et al.* Efficacy and safety of irinotecan liposome injection (nal-IRI) in patients with small cell lung cancer (SCLC). Presented at WCLC 2019, Oct 12, 2019, Barcelona, Spain. Oral presentation.
7. Paz-Ares LG *et al.* RESILIENT, study of irinotecan liposome injection (nal-IRI) in patients with small cell lung cancer: preliminary findings from part 1 dose-defining phase. Presented at ASCO 2019, May 31–June 4, 2019, Chicago, IL, USA. Poster 318.

Acknowledgments

The authors thank all patients involved in the study, as well as their caregivers and care teams, and the investigators and research staff in participating institutions.

The authors thank Dr Heather Lang of Oxford PharmaGenesis, Oxford, UK, for providing medical writing support, which was sponsored by Ipsen in accordance with Good Publication Practice (GPP3) guidelines.

Author contributions

All authors have contributed to study conception/design, drafting the publication or revising it critically for scientific accuracy and important intellectual content, and final approval of the publication.

Disclosures

DRS – consultant/advisor (all to institution): Aptitude Health, AstraZeneca, Bayer, Bristol-Myers Squibb, Celgene, Dracen Pharmaceuticals, EMD Serono, Evelo Biosciences, Genentech, GlaxoSmithKline, Ikuuda Therapeutics, Illumina, Merck, Molecular Templates, Nektar Therapeutics, Novartis, Pfizer, PharmaMar, Roche, Seattle Genetics, Takeda, Triptych Health Partners, TRM Oncology, Williams & Connolly; travel/accommodation/expenses: Amgen, AstraZeneca, Celgene, Daiichi Sankyo, Bristol-Myers Squibb, Genentech/Roche, GlaxoSmithKline, Janssen, Merck, Novartis, Seattle Genetics, Spectrum Pharmaceuticals, Takeda; research funding (all to institution): Aeglea BioTherapeutics, Astellas, AstraZeneca, Bind Therapeutics, Bristol-Myers Squibb, Celgene, Celldex Therapeutics, Clovis Oncology, Daiichi Sankyo, Eisai, Eli Lilly, EMD Serono, G1 Therapeutics, Genentech, GRAIL, ImClone Systems, ImmunoGen, Ipsen, Janssen, Medimmune, Merck, Molecular Partners, Nektar Therapeutics, Neon Therapeutics, Novartis, Takeda, Transgene, UT Southwestern; LGP-A – leadership: Altum Sequencing; European Medicines Agency Scientific Advisory Groups; Genomica S.A.U.; honoraria: Advanced Accelerator Applications, Amgen, AstraZeneca, Bayer, Blueprint Medicines, Bristol-Myers Squibb, Boehringer Ingelheim, Celgene, Incyte, Ipsen, Lilly, Merck Serono, Merck Sharp & Dohme, Novartis, Pfizer, PharmaMar, Roche/Genentech, Sanofi, Servier, Sysmex; research funding: AstraZeneca, Bristol-Myers Squibb; travel/accommodation/expenses: AstraZeneca, Bristol-Myers Squibb, Merck Sharp & Dohme, Pfizer, Roche, Takeda; other relationships: Amgen, Ipsen, Merck, Novartis, Pfizer, Roche, Sanofi Servier; YC – honoraria: AstraZeneca, Bristol-Myers Squibb, Genentech, Guardant Health, Lilly, Merck, Novartis, Takeda; consultant/advisor: Array BioPharma, AstraZeneca, Bristol-Myers Squibb, Genentech, Heron Therapeutics, Lilly, Novartis, Pfizer, Takeda; speakers' bureau: AstraZeneca, Bristol-Myers Squibb, Genentech, Guardant Health, Lilly, Merck, Novartis, Takeda; research funding: AstraZeneca, Bristol-Myers Squibb, Guardant Health, Helsinn, Ipsen, Roche; expert testimony: AstraZeneca, Takeda; MJ – honoraria: Boehringer Ingelheim; travel/accommodation/expenses: Merck Sharp & Dohme, Roche, Takeda; OJ-V – consultant/advisor: Abbvie, AstraZeneca, Boehringer Ingelheim, Bristol-Myers Squibb, Eli Lilly, Merck Sharp & Dohme, Pfizer, Roche/Genentech, Takeda; RBC – consultant/advisor: AstraZeneca, Bristol-Myers Squibb, Merck Sharp & Dohme, Roche, Takeda; AN – consultant/advisor: Boehringer Ingelheim, Pfizer; speaker's bureau: Roche; expert testimony: Oryzon Genomics; travel/accommodation/expenses: Boehringer Ingelheim, Pfizer, Roche; AD – consultant/advisor: Abbvie, AstraZeneca, Bristol-Myers Squibb, Seattle Genetics, Takeda; research funding: Abbvie, Amgen, Bayer, Incyron, Ipsen, Loxo, Regeneron, Seattle Genetics, Symphogen, Takeda, Tesaro; EZ – employment, stock/other ownership and patents/royalties/other intellectual property: Ipsen; YM – employment, leadership, stock/other ownership and travel/accommodation/expenses: Ipsen; TW – employment and stock/other ownership: Ipsen Bioscience; NN – employment and stock/other ownership: Ipsen; JK – employment: Ipsen; consultant/advisor: Bristol-Myers Squibb, Constellation Pharmaceuticals; JKMD Global Medical Solutions, Tocagen; SP – consultant/advisor: Bristol-Myers Squibb, Merck, Roche; speakers' bureau: Bristol-Myers Squibb, Merck, Roche; travel/accommodation/expenses: AstraZeneca, Merck, Roche; PR, TH, VGC and PB – nothing to disclose

Corresponding author: dspigel@tnonc.com

Presented at the Annual Meeting of the American Society of Clinical Oncology (ASCO), virtual format, May 29–June 2, 2020 (#ASCO20)

This study was sponsored by Ipsen

RESILIENT part 1, an open-label, safety run-in of liposomal irinotecan in adults with small-cell lung cancer who have progressed with platinum-based first-line therapy: subgroup analyses by platinum sensitivity

262

BACKGROUND

OBJECTIVE

METHODS

RESULTS

CONCLUSIONS

LUNG CANCER—NON-SMALL CELL LOCAL-REGIONAL/SMALL CELL/OTHER THORACIC CANCERS

RESILIENT part I, an open-label, safety run-in of liposomal irinotecan in adults with small cell lung cancer (SCLC) who have progressed with platinum-based first-line (1L) therapy: Subgroup analyses by platinum sensitivity.

David R. Spigel, Luis G. Paz-Ares, Yuanbin Chen, Maria Jove, Oscar Juan-Vidal, Patricia Rich, Theresa M. Hayes, M Vanessa Gutierrez Calderon, Reyes Bernabe Caro, Alejandro Navarro, Afshin Dowlati, Bin Zhang, Yan Moore, Haofei Tiffany Wang, Jaba Kokhreidze, Natalya Nazarenko, Santiago Ponce Aix, Paul Sunn

Sarah Cannon Research Institute, Nashville, TN; Hospital Universitario 12 de Octubre, Madrid, Spain; Cancer and Hematology Centers of Western Michigan, Grand Rapids, MI; Institut Català d'Oncologia, Barcelona, Spain; Hospital Universitario y Politécnico La Fe, Valencia, Spain; Cancer Treatment Centers of America, Atalanta, GA; South West Healthcare, Warrnambool, VIC, Australia; Hospital Regional Universitario de Málaga, Málaga, Spain; Hospital Universitario Virgen Del Rocio, Seville, Spain; Hospital Universitari Vall d'Hebron, Barcelona, Spain; Case Western Reserve University, Cleveland, OH; Ipsen Bioscience, Boston, MA; Hospital Universitario 12 De Octubre, Madrid, Spain; University of Colorado, Denver, CO

Show Less

Abstract Disclosures

Abstract

9069

Background: Most patients with extensive SCLC develop drug resistance to platinum-based 1L therapy or discontinue for other reasons, and second-line (2L) therapies are limited. RESILIENT (NCT03088813) is a two-part phase 2/3 study assessing the safety, tolerability and efficacy of 2L liposomal irinotecan monotherapy in adults with SCLC who progressed with platinum-based 1L therapy. Preliminary data from RESILIENT part 1 (cut-off May 8 2019; ≥ 12 weeks follow-up) showed that liposomal irinotecan 70 mg/m^2 free base every 2 weeks was generally well tolerated and had encouraging antitumor activity (Paz-Ares *et al.* WCLC 2019 OA03.03). Objective response rate (ORR; secondary endpoint) was 44% (11/25). Here we report efficacy analyses in *post hoc* subgroups by platinum sensitivity. **Methods:** RESILIENT part 1 was an open-label, single-arm study comprising dose-finding and dose-expansion phases. Eligible patients were aged ≥ 18 y, with an ECOG performance status score of 0/1 and adequate organ function; a single line of prior immunotherapy was allowed. Participants received liposomal irinotecan 70

mg/m^2 or 85 mg/m^2 free base every 2 weeks, with tumor assessments every 6 weeks (RECIST v1.1). Analyses were undertaken for the dose-finding phase recommended dose (RD) in subgroups of platinum-resistant/sensitive patients (with/without progression within 90 days from completion of 1L therapy). **Results:** During dose finding, 5 patients received liposomal irinotecan 85 mg/m^2 (deemed not tolerable; dose-limiting toxicity) and 12 received 70 mg/m^2 (deemed tolerable; RD for dose-expansion phase in which 13 more patients were included). Analyses included all 25 patients receiving the RD (mean exposure, 13.95 weeks [median 14.86; SD 7.222]). In the platinum-sensitive subgroup (33.3% men; median age 62.0 y) ORR was 53.3% (8/15) and 12-week disease control rate (DCR12wks) was 60% (9/15); in the platinum-resistant subgroup (50% men, median age 58.0 y) both ORR and DCR12wks were 30% (3/10). Overall and progression-free survival (secondary endpoints) are not yet mature. **Conclusions:** ORR and DCR12wks were numerically higher in platinum-sensitive than in platinum-resistant patients with SCLC who had progressed with platinum-based 1L therapy before receiving 2L liposomal irinotecan 70 mg/m^2 in this phase 2 study. RESILIENT part 2, an ongoing, phase 3, randomized controlled trial vs topotecan, will provide further data. Clinical trial information: NCT03088813.

Research Sponsor:

Ipsen

MO01.39

Liposomal Irinotecan in Adults with Small Cell Lung Cancer who Progressed on Platinum-Based Therapy: Subgroup Analyses by Platinum Sensitivity

David R. Spigel[1], Luis G. Paz-Ares[2], Yuanbin Chen[3], Maria Jove[4], Oscar Juan-Vidal[5], Patricia Rich[6], Theresa Hayes[7], Vanesa Gutiérrez Calderón[8], Reyes Bernabe Caro[9], Alejandro Navarro[10], Afshin Dowlati[11], Bin Zhang[12], Yan Moore[12], Tiffany Wang[12], Natalya Nazarenko[12], Jaba Kokhreidze[12], Santiago Ponce[2], Paul Bunn[13]
[1]Sarah Cannon Research Institute, Nashville, USA, [2]Hospital Universitario 12 de Octubre, Madrid, Spain, [3]Cancer & Hematology Centers of Western Michigan, Grand Rapids, USA, [4]Institut Català d'Oncologia, Hospital Duran i Reinals, Barcelona, Spain, [5]Hospital Universitari i Politècnic La Fe, Valencia, Spain, [6]Cancer Treatment Centers of America, Atlanta, USA, [7]South West Healthcare, Warrnambool, Australia, [8]Hospital Regional Universitario de Malaga, Malaga, Spain, [9]Hospital Universitario Virgen del Rocio, Seville, Spain, [10]Hospital Universitari Vall d'Hebron, Barcelona, Spain, [11]Case Western Reserve University, Cleveland, USA, [12]Ipsen, Boston, USA, [13]University of Colorado, Cancer Center and Department of Medicine, Denver, USA

Background: Most patients with extensive small cell lung cancer (SCLC) develop drug resistance to platinum-based first-line therapy or discontinue for other reasons, and second-line therapies are limited. RESILIENT (ClinicalTrials.gov identifier NCT03088813) is a two-part phase 2/3 study assessing the safety, tolerability and efficacy of second-line liposomal irinotecan monotherapy in adults with SCLC who progressed with platinum-based first-line therapy. Preliminary data from RESILIENT part 1 (cut off May 8 2019; ≥ 12 weeks follow-up) showed that liposomal irinotecan 70 mg/m2 free base every 2 weeks was generally well tolerated and had encouraging antitumor activity (Paz-Ares et al. WCLC 2019; OA03.03). Objective response rate (ORR; secondary endpoint) was 44% (11/25 patients). Here we report efficacy analyses in post hoc subgroups by platinum sensitivity. **Methods:** RESILIENT part 1 was an open-label, single-arm study comprising dose-finding and dose-expansion phases. Eligible patients were aged ≥ 18 years, with an Eastern Cooperative Oncology Group performance status score of 0/1 and adequate organ function; a single line of prior immunotherapy was permitted. Participants received liposomal irinotecan 70 mg/m2 or 85 mg/m2 free base every 2 weeks, with disease assessments every 6 weeks (Response Evaluation Criteria in Solid Tumors v1.1). Analyses were undertaken for the dose-finding phase recommended dose in subgroups of platinum-resistant/platinum-sensitive patients (with/without disease progression within 90 days from completion of first-line therapy). **Results:** During dose finding, 5 patients received liposomal irinotecan 85 mg/m2 (deemed not tolerable owing to dose-limiting toxicity) and 12 received 70 mg/m2 (deemed tolerable; recommended dose for dose-expansion phase in which 13 additional patients were included). Analyses included all 25 patients receiving the recommended dose (mean exposure, 13.95 weeks [median 14.86; standard deviation 7.222]). In the platinum-sensitive subgroup (33.3% men; median age 62.0 years), ORR was 53.3% (8/15 patients) and 12-week disease control rate (DCR12wks) was 60% (9/15 patients); in the platinum-resistant subgroup (50.0% men, median age 58.0 years) both ORR and DCR12wks were 30% (3/10 patients). Overall survival and progression-free survival (secondary endpoints) are not yet mature. **Conclusions:** ORR and DCR12wks were numerically higher in platinum-sensitive than in platinum-resistant patients with SCLC who had progressed with platinum-based first-line therapy before receiving second-line liposomal irinotecan 70 mg/m2 in this phase 2 study. RESILIENT part 2, an ongoing, phase 3, randomized controlled trial versus topotecan, will provide further data.

IASLC

2020 North America Conference on Lung Cancer

OCTOBER 16-17, 2020 | WORLDWIDE VIRTUAL EVENT

ABSTRACTS

Electronic Acknowledgement Receipt

EFS ID:	42154199
Application Number:	15809815
International Application Number:	
Confirmation Number:	5137
Title of Invention:	Methods for Treating Metastatic Pancreatic Cancer Using Combination Therapies Comprising Liposomal Irinotecan and Oxaliplatin
First Named Inventor/Applicant Name:	Eliel Bayever
Customer Number:	153749
Filer:	Mary Rucker Henninger/Richard King
Filer Authorized By:	Mary Rucker Henninger
Attorney Docket Number:	263266-421428
Receipt Date:	12-MAR-2021
Filing Date:	10-NOV-2017
Time Stamp:	16:25:35
Application Type:	Utility under 35 USC 111(a)

Payment information:

Submitted with Payment	no

File Listing:

Document Number	Document Description	File Name	File Size(Bytes)/ Message Digest	Multi Part /.zip	Pages (if appl.)
1	Information Disclosure Statement (IDS) Form (SB08)	2021-03-12_01208-0007-01US_SB08_5_OF_6_as_filed.pdf	1057991 a34c327304156e76d0e433619c11b00c22eb22bc	no	8

Warnings:

Information:					
A U.S. Patent Number Citation or a U.S. Publication Number Citation is required in the Information Disclosure Statement (IDS) form for autoloading of data into USPTO systems. You may remove the form to add the required data in order to correct the Informational Message if you are citing U.S. References. If you chose not to include U.S. References, the image of the form will be processed and be made available within the Image File Wrapper (IFW) system. However, no data will be extracted from this form. Any additional data such as Foreign Patent Documents or Non Patent Literature will be manually reviewed and keyed into USPTO systems.					
2	Non Patent Literature	Park_1998a.pdf	400422 5d340dcaefadef884c89ec70c935ae9468e881f6	no	9
Warnings:					
Information:					
3	Non Patent Literature	Patankar_2013.pdf	238760 185bf8fff32943ea4ffe5e76ae6ab2fcaf8572cd	no	13
Warnings:					
Information:					
4	Non Patent Literature	Patel_2004.pdf	93851 00829eff10c16b0fdc1ae3ec0265a19222fc9136	no	7
Warnings:					
Information:					
5	Non Patent Literature	Pavai_2003.pdf	706500 544ffcd2813a1c1286659db93b896ff100050a3a	no	6
Warnings:					
Information:					
6	Non Patent Literature	Pavillard_2002.pdf	114841 fa134f1ee862d226558ab08889a6f72f0b0b6608	no	7
Warnings:					
Information:					
7	Non Patent Literature	Paz_2012_poster.pdf	1516765 b4d93f66fd4eff891aa209e5f588ac6cf43036b5	no	9
Warnings:					
Information:					

8	Non Patent Literature	Paz_2012_abstract.pdf	158461 c9175f4b2bc59b8a60975d23197bfda7e06563ee	no	3
Warnings:					
Information:					
9	Non Patent Literature	Paz-Ares_2019_presentation.pdf	395653 5cdf6d956f84544c09e9304fd99c5dbc72cfa427	no	9
Warnings:					
Information:					
10	Non Patent Literature	Paz-Ares_ASCO_2020_poster.pdf	4281771 17b4416131e3e573b2666c7400d459fc086ffb4f	no	7
Warnings:					
Information:					
11	Non Patent Literature	Paz-Ares_ASCO_2020_abstract.pdf	75823 76fd4b88334e5a01fb9ef8e54a9e7ed3765e6ba8	no	2
Warnings:					
Information:					
12	Non Patent Literature	Paz-Ares_Rodriguez_2019_abstract.pdf	225334 84a5b334b601f4237cec145aa7c4fd5912c82d29	no	3
Warnings:					
Information:					
13	Foreign Reference	PCTGB2017053293_IPRP.pdf	82264 a37badb2abbdce637359f4a3181b61aee3455155	no	7
Warnings:					
Information:					
14	Foreign Reference	PCTGB2017053293_ISR_WO.pdf	449996 71c054290cd1f9cf786aed6e9309bf649b8a24e7	no	12
Warnings:					
Information:					

15	Foreign Reference	PCTUS200515349_ISR_WO.pdf	617149 0c3cd672c9c4434c191cc3d2ab29740cc5d71084	no	14
Warnings:					
Information:					
16	Foreign Reference	PCTUS2016027515_IPRP.pdf	311526 c2e3334fd8540637b8398cdf98102854c2d68473	no	8
Warnings:					
Information:					
17	Foreign Reference	PCTUS2016027515_ISR.pdf	148631 909303e54475d672c0fd10fb7ac894c7bdd d37d1	no	4
Warnings:					
Information:					
18	Foreign Reference	PCTUS2016057247_IPRP.pdf	288742 7c5a043110cf98a6695b6ceeea18db06502 e0c40	no	8
Warnings:					
Information:					
19	Foreign Reference	PCTUS2016057247_ISR.pdf	111546 0b2c3d4a5bccb4b4a2400ce11ce3048ba57 73e1b	no	4
Warnings:					
Information:					
20	Non Patent Literature	Peikov_2005.pdf	615576 7cbb0e76e12519e4eedb54b7bb9a6c05f3a a877f	no	8
Warnings:					
Information:					
21	Non Patent Literature	Peinert_2010.pdf	151202 ebe816142a48423a28c1f0f84415be82ae41 c58d	no	14
Warnings:					
Information:					

22	Non Patent Literature	Pharmaengine_PEP02_2011.pdf	184543 b7612c6e98ff11b80ae4fe6786aa907647f55da9	no	4
Warnings:					
Information:					
23	Non Patent Literature	Pillai_2014.pdf	1606759 3ae39a72db9423d38f69d8a60b56715827b0593d	no	13
Warnings:					
Information:					
24	Non Patent Literature	Ponce_ESMO_2020_poster.pdf	6094939 64313e5e526d93d2de3d00e6780cceb58dec5352	no	8
Warnings:					
Information:					
25	Non Patent Literature	Ponce_ESMO_2020_abstract.pdf	60833 36fa638a8d3bb84144bd81145f7549950ef86498	no	2
Warnings:					
Information:					
26	Non Patent Literature	Poplin_2005.pdf	158916 72b7148a6ecd84d5d84031f90d07b789d6b40213	no	7
Warnings:					
Information:					
27	Non Patent Literature	Ramsay_2008b.pdf	306922 a2981aa188528e0e1271a2f7b2d4a5a3a5e115d4	no	11
Warnings:					
Information:					
28	Non Patent Literature	Raymond_2003.pdf	834270 1bafdec97e16942f4e5cbdc1a5da90b821615256	no	12
Warnings:					
Information:					

29	Non Patent Literature	Rea_2005.pdf	107181 5d817c0a86ed8feddaa5c2f438cc00a85016bfe2	no	10
Warnings:					
Information:					
30	Non Patent Literature	Reynolds_2012.pdf	747645 f2e54d72e555005e97cf3e9a7369388cd8d64a90	no	10
Warnings:					
Information:					
31	Non Patent Literature	Riviere_2011_V2pdf.pdf	446094 29d4afa366bd8ce54ba6ae161398b223d7b506df	no	19
Warnings:					
Information:					
32	Non Patent Literature	Rosenecker_1996.pdf	1357471 5b1a665f7cd59108f8da73ee0f2cdbe2e2b0b1ab	no	6
Warnings:					
Information:					
33	Non Patent Literature	Roth_2007.pdf	553618 ccbfd690e0d400d0fb5a686ecb2e95a12b84f72a	no	11
Warnings:					
Information:					
34	Non Patent Literature	Rothenberg_1998.pdf	807952 5cf87ef43bf36b87cd685865c411c1c395369d66	no	16
Warnings:					
Information:					
35	Non Patent Literature	Roy_2013.pdf	139855 d20c83f60d35130630b8f3eedd15cfe6441ad190	no	7
Warnings:					
Information:					

36	Non Patent Literature	Rubesova_2002.pdf	108355 ec144405900ecc65963ece46cd4daa072c3912f7	no	3
Warnings:					
Information:					
37	Non Patent Literature	Sachdev_2019_poster.pdf	1738258 9b381828e2adddcdb8671a891ca9f2adf4e6853d	no	9
Warnings:					
Information:					
38	Non Patent Literature	Sachdev_2019_abstract.pdf	227792 fe641792883688c1ea8ea26cd14735492cd83b4c	no	4
Warnings:					
Information:					
39	Non Patent Literature	Sadzuka_1999.pdf	421150 11bffce2c3b0d13936f3e5ab2a08f0e36c607785	no	7
Warnings:					
Information:					
40	Non Patent Literature	Saif_2009.pdf	192138 e364909a9c70163dd1a6219d8c6ccda1d45569b7	no	10
Warnings:					
Information:					
41	Non Patent Literature	Saltz_1997.pdf	170344 9386964326901caddb0c966b2d0854bb4341e3e9	no	8
Warnings:					
Information:					
42	Non Patent Literature	Saltz_1996.pdf	796856 941d31672149482b347eea6f3e888e69401ca51f	no	9
Warnings:					
Information:					

43	Non Patent Literature	Satoh_2013.pdf	235650 04a9d1652a2bf8da933ecb9056ef20c4aaa2d2d7	no	9
Warnings:					
Information:					
44	Non Patent Literature	Scheithauer_1997.pdf	539526 fc58f6c9943116f258cc937e29498231a1f201a5	no	7
Warnings:					
Information:					
45	Non Patent Literature	Schroen_2011.pdf	221564 9dc3bc76be6affab7b7c2c8f17e59dfc71d1ea1f	no	14
Warnings:					
Information:					
46	Non Patent Literature	Serwer_2011.pdf	262648 b3aa5cda6c9ccec5bdd8365103f1bdef2a282497	no	8
Warnings:					
Information:					
47	Non Patent Literature	Skof_2009.pdf	229402 595df104b351cf193bdf1656d6865c5801824a27	no	9
Warnings:					
Information:					
48	Non Patent Literature	Spigel_NACLC_2020_poster.pdf	6528911 4858761dc68429bbc1c87b3aea8463173672cab8	no	9
Warnings:					
Information:					
49	Non Patent Literature	Spigel_ASCO_2020_poster.pdf	3671753 13a1e427da8b61c61b5d7c3e9f0ae726990322bb	no	6
Warnings:					
Information:					

50	Non Patent Literature	Spigel_ASCO_2020_abstract.pdf	84901 ad2f305cf8f9db1744dccd14c525252af1d34340	no	2
Warnings:					
Information:					
51	Non Patent Literature	Spigel_NACLC_2020_abstract.pdf	1425707 e76daf3a8aaf5bb59c9fbddc42a9f2d611dd103c	no	2
Warnings:					
Information:					
			Total Files Size (in bytes):	42304757	

This Acknowledgement Receipt evidences receipt on the noted date by the USPTO of the indicated documents, characterized by the applicant, and including page counts, where applicable. It serves as evidence of receipt similar to a Post Card, as described in MPEP 503.

New Applications Under 35 U.S.C. 111

If a new application is being filed and the application includes the necessary components for a filing date (see 37 CFR 1.53(b)-(d) and MPEP 506), a Filing Receipt (37 CFR 1.54) will be issued in due course and the date shown on this Acknowledgement Receipt will establish the filing date of the application.

National Stage of an International Application under 35 U.S.C. 371

If a timely submission to enter the national stage of an international application is compliant with the conditions of 35 U.S.C. 371 and other applicable requirements a Form PCT/DO/EO/903 indicating acceptance of the application as a national stage submission under 35 U.S.C. 371 will be issued in addition to the Filing Receipt, in due course.

New International Application Filed with the USPTO as a Receiving Office

If a new international application is being filed and the international application includes the necessary components for an international filing date (see PCT Article 11 and MPEP 1810), a Notification of the International Application Number and of the International Filing Date (Form PCT/RO/105) will be issued in due course, subject to prescriptions concerning national security, and the date shown on this Acknowledgement Receipt will establish the international filing date of the application.

PTO/SB/08a (02-18)
Approved for use through 11/30/2020. OMB 0651-0031
U.S. Patent and Trademark Office; U.S. DEPARTMENT OF COMMERCE

INFORMATION DISCLOSURE STATEMENT BY APPLICANT

(Not for submission under 37 CFR 1.99)

Application Number	15809815
Filing Date	2017-11-10
First Named Inventor	Eliel Bayever
Art Unit	1612
Examiner Name	Celeste A. RONEY
Attorney Docket Number	01208-0007-01US

U.S.PATENTS Remove

Examiner Initial*	Cite No	Patent Number	Kind Code[1]	Issue Date	Name of Patentee or Applicant of cited Document	Pages,Columns,Lines where Relevant Passages or Relevant Figures Appear
	1					

If you wish to add additional U.S. Patent citation information please click the Add button. Add

U.S.PATENT APPLICATION PUBLICATIONS Remove

Examiner Initial*	Cite No	Publication Number	Kind Code[1]	Publication Date	Name of Patentee or Applicant of cited Document	Pages,Columns,Lines where Relevant Passages or Relevant Figures Appear
	1					

If you wish to add additional U.S. Published Application citation information please click the Add button. Add

FOREIGN PATENT DOCUMENTS Remove

Examiner Initial*	Cite No	Foreign Document Number[3]	Country Code[2] i	Kind Code[4]	Publication Date	Name of Patentee or Applicant of cited Document	Pages,Columns,Lines where Relevant Passages or Relevant Figures Appear	T[5]
	1							

If you wish to add additional Foreign Patent Document citation information please click the Add button Add

NON-PATENT LITERATURE DOCUMENTS Remove

Examiner Initials*	Cite No	Include name of the author (in CAPITAL LETTERS), title of the article (when appropriate), title of the item (book, magazine, journal, serial, symposium, catalog, etc), date, pages(s), volume-issue number(s), publisher, city and/or country where published.	T[5]

INFORMATION DISCLOSURE STATEMENT BY APPLICANT (Not for submission under 37 CFR 1.99)		
	Application Number	15809815
	Filing Date	2017-11-10
	First Named Inventor	Eliel Bayever
	Art Unit	1612
	Examiner Name	Celeste A. RONEY
	Attorney Docket Number	01208-0007-01US

	1	STATHOPOULOS G and BOULIKAS T, "Lipoplatin Formulation Review Article," J Drug Deliv. 2012:581363, Article ID 581363, doi:10.1155/2012/581363, Epub 2011, 10 pages.
	2	STATHOPOULOS G, et. al., "Liposomal Oxaliplatin in the Treatment of Advanced Cancer: A Phase I Study," Anticancer Res. 26(2B):1489-93 (2006).
	3	STYLIANOPOULOS T and JAIN R, "Combining Two Strategies to Improve Perfusion and Drug Delivery in Solid Tumors," Proc Natl Acad Sci USA. 110(46):18632-7 (2013).
	4	TAKANO S, et. al., "Metronomic Treatment of Malignant Glioma Xenografts with Irinotecan (CPT-11) Inhibits Angiogenesis and Tumor Growth," J Neurooncol. 99(2):177-85 (2010).
	5	TARDI P, et al., "Liposomal Encapsulation of Topotecan Enhances Anticancer Efficacy in Murine and Human Xenograft Models," Cancer Res. 60(13):3389-93 (2000).
	6	TARDI P, et. al., "Coencapsulation of Irinotecan and Floxuridine Into Low Cholesterol-Containing Liposomes That Coordinate Drug Release In Vivo," Biochim Biophys Acta. 1768(3):678–87 (2007). Epub 2006.
	7	TOUTAIN P and BOUSQUET-MELOU A, "Plasma terminal half-life," J Vet Pharmacol Ther. 27(6):427-39 (2004).
	8	U.S. Patent Application No. 15/664,976: 2019-11-04 Nonfinal Office Action, 9 pages.
	9	U.S. Patent Application No. 15/664,976: 2020-05-18 Final Office Action, 11 pages.
	10	U.S. Patent Application No. 15/664,976: 2020-10-13 Notice of Allowance including Examiner's Reasons for Allowance, 13 pages.
	11	U.S. Patent Application No. 15/809,815: 2020-02-27 Final Office Action, 16 pages.

INFORMATION DISCLOSURE STATEMENT BY APPLICANT (Not for submission under 37 CFR 1.99)		
	Application Number	15809815
	Filing Date	2017-11-10
	First Named Inventor	Eliel Bayever
	Art Unit	1612
	Examiner Name	Celeste A. RONEY
	Attorney Docket Number	01208-0007-01US

	12	U.S. Patent Application No. 15/896,389: 2020-01-31 Final Office Action, 28 pages.
	13	U.S. Patent Application No. 15/896,389: 2020-03-26 Examiner Interview Summary and Applicant slides, 22 pages.
	14	U.S. Patent Application No. 15/896,389: 2020-04-09 Advisory Action, 3 pages.
	15	U.S. Patent Application No. 15/896,389: 2020-06-05 Notice of Allowance including Examiner's Reasons for Allowance and Examiner Interview Summary, 13 pages.
	16	U.S. Patent Application No. 16/012,351: 2020-01-07 Final Office Action, 9 pages.
	17	U.S. Patent Application No. 16/012,372: 2020-01-07 Final Office Action, 9 pages.
	18	U.S. Patent Application No. 16/012,372: 2020-07-27 Non-Final Office Action, 8 pages.
	19	U.S. Patent Application No. 16/302,050: 2020-01-17 Non-Final Office Action, 17 pages.
	20	U.S. Patent Application No. 16/510,394: 2020-03-06 Non-Final Office Action, 15 pages.
	21	U.S. Patent Application No. 16/567,902: 2020-04-27 Non-Final Office Action, 20 pages.
	22	U.S. Patent Application No. 16/567,902: 2020-08-10 Final Office Action, 21 pages.

INFORMATION DISCLOSURE STATEMENT BY APPLICANT (Not for submission under 37 CFR 1.99)		
	Application Number	15809815
	Filing Date	2017-11-10
	First Named Inventor	Eliel Bayever
	Art Unit	1612
	Examiner Name	Celeste A. RONEY
	Attorney Docket Number	01208-0007-01US

	23	U.S. Patent Application No. 16/586,609: 2020-10-05 Non-Final Office Action, 5 pages.
	24	VAAGE J, et. al., "Therapy of a Xenografted Human Colonic Carcinoma Using Cisplatin or Doxorubicin Encapsulated in Long-Circulating Pegylated Stealth Liposomes," Int J Cancer. 80(1):134–7 (1999).
	25	VEAL G, et. al., "A Phase I Study in Paediatric Patients to Evaluate the Safety and Pharmacokinetics of SPI-77, A Liposome Encapsulated Formulation of Cisplatin," Br J Cancer. 84(8):1029-35 (2001).
	26	VENOOK A, "Critical Evaluation of Current Treatments in Metastatic Colorectal Cancer," Oncologist. 10(4):250-61 (2005).
	27	VENTURA M, et al., "Ferumoxytol as an MR Imaging Surrogate Marker of Liposomal Drug Deposition and Longitudinal Efficacy in a Preclinical Model of Breast Cancer." Poster presented at World Molecular Imaging Congress, September 13-16, 2017, Philadelphia, Pennsylvania, 6 pages.
	28	VILLALONA-CALERO M, et. al., "Phase I Study of Low-Dose Suramin as a Chemosensitizer in Patients With Advanced Non-Small Cell Lung Cancer," Clin Cancer Res. 9(9):3303-11 (2003).
	29	WALKER S, et. al., "Simulation of Y-Site Compatibility of Irinotecan and Leucovorin at Room Temperature in 5% Dextrose in Water in 3 Different Containers," Can J Hosp Pharm. 58(4):212-22 (2005).
	30	WANG W, et. al., "Weekly 24-Hour Infusion of High-dose 5-Fluorouracil and Leucovorin in Patients with Advanced Colorectal Cancer: Taiwan Experience," Jpn J Clin Oncol. 28(1):16-19 (1998).
	31	WEI H, et al, "Active Loading Liposomal Irinotecan Hydrochloride: Preparation, In Vitro and In Vivo Evaluation," Asian J Pharm Sci. 8(5):303-11 (2013).
	32	WENG K, et al., "Convection-Enhanced Delivery of Targeted Quantum Dot-Immunoliposome Hybrid Nanoparticles to Intracranial Brain Tumor Models," Nanomedicine (Lond). 8(12):1913-25. 2013.
	33	WENG K, et al., "Targeted Tumor Cell Internalization and Imaging of Multifunctional Quantum Dot-Conjugated Immunoliposomes in Vitro and in Vivo," Nano Lett. 8(9):2851-7 (2008).

INFORMATION DISCLOSURE STATEMENT BY APPLICANT (Not for submission under 37 CFR 1.99)		
	Application Number	15809815
	Filing Date	2017-11-10
	First Named Inventor	Eliel Bayever
	Art Unit	1612
	Examiner Name	Celeste A. RONEY
	Attorney Docket Number	01208-0007-01US

	34	WILLETT C, et. al., "Direct Evidence That the VEGF-Specific Antibody Bevacizumab Has Antivascular Effects in Human Rectal Cancer," Nat Med. 10(2):145-7 (2004), author manuscript version, 7 pages.
	35	WULANINGSIH W, et. al., "Irinotecan Chemotherapy Combined With Fluoropyrimidines Versus Irinotecan Alone for Overall Survival and Progression-Free Survival in Patients With Advanced and/or Metastatic Colorectal Cancer," Cochrane Database Syst Rev. 2:CD008593 doi: 10.1002/14651858.CD008593.pub3. (2016), 36 pages.
	36	Xeloda (capecitabine) package insert, Roche, revised November 2000, 19 pages.
	37	YAMASHITA Y, et al., "Convection-Enhanced Delivery of a Topoisomerase I Inhibitor (Nanoliposomal Topotecan) and a Topoisomerase II Inhibitor (Pegylated Liposomal Doxorubicin) in Intracranial Brain Tumor Xenografts," Neuro Oncol. 9(1):20-8 (2007). Epub 2006.
	38	YAMASHITA Y, et. al., "Convection-Enhanced Delivery of Liposomal Doxorubicin in Intracranial Brain Tumor Xenografts," Targ Oncol. 1:79-85 (2006).
	39	YANG W, et. al. "Development of a Method to Quantify Total and Free Irinotecan and 7-ethyl-10-hydroxycamptothecin (SN-38) for Pharmacokinetic and Bio-Distribution Studies After Administration of Irinotecan Liposomal Formulation," Asian J Pharm Sci. 14(6):687-97 (2019). Epub 2018.
	40	YANG W, et. al., "The Influence of Trapping Agents on the Antitumor Efficacy of Irinotecan Liposomes: Head-to-Head Comparison of Ammonium Sulfate, Sulfobutylether-β-Cyclodextrin and Sucrose Octasulfate," Biomater Sci., 7 (1):419-28 (2019).
	41	YANG, et. al., "Oxaliplatin Long-Circulating Liposomes Improved Therapeutic Index of Colorectal Carcinoma," BMC Biotechnology. 11:21 doi: 10.1186/1472-6750-11-21 (2011), 8 pages.
	42	YOO C, et al., "Multicenter Randomized Phase II Trial of 5-Fluorouracil/Leucovorin (5-FU/LV) With or Without Liposomal Irinotecan (nal-IRI) in Metastatic Biliary Tract Cancer (BTC) as Second-Line Therapy After Progression on Gemcitabine Plus Cisplatin (GemCis): NIFTY Trial." Poster presented at the European Society for Medical Oncology (ESMO) 2019 Congress, Barcelona, Spain, September 27-October 1, 2019, 6 pages.
	43	YOO C, et al., Abstract 829TiP. "Multicenter Randomized Phase II Trial of 5-Fluorouracil/Leucovorin (5-FU/LV) With or Without Liposomal Irinotecan (nal-IRI) in Metastatic Biliary Tract Cancer (BTC) as Second-Line Therapy After Progression on Gemcitabine Plus Cisplatin (GemCis): NIFTY Trial," Ann Oncol. 30(Supp_5):v318 /doi.org/10.1093/annonc/mdz247.155 (2019).
	44	YOUNIS I, et. al., "Enterohepatic Recirculation Model of Irinotecan (CPT-11) and Metabolite Pharmacokinetics in Patients With Glioma," Cancer Chemother Pharmacol. 63(3):517-24 (2009), author manuscript version, 16 pages.

INFORMATION DISCLOSURE STATEMENT BY APPLICANT (Not for submission under 37 CFR 1.99)		
	Application Number	15809815
	Filing Date	2017-11-10
	First Named Inventor	Eliel Bayever
	Art Unit	1612
	Examiner Name	Celeste A. RONEY
	Attorney Docket Number	01208-0007-01US

	45	ZAMBONI W, et. al., "Phase I and Pharmacokinetic Study of Pegylated Liposomal CKD-602 in Patients with Advanced Malignancies," Clin Cancer Res. 15(4):1466-72 (2009) and correction found at Clin Cancer Res. 15(8):2949-50 (2009).
	46	ZHANG K, et al., "Comprehensive Optimization of a Single-Chain Variable Domain Antibody Fragment as a Targeting Ligand for a Cytotoxic Nanoparticle," MAbs. 7(1):42-52 (2015).
	47	ZHANG L, et al., PEG-Coated Irinitecan Cationic Liposomes Improve the Therapeutic Efficacy of Breast Cancer in Animals," Eur Rev Med Pharmacol Sci. 17(24):3347-61 (2013).
	48	ZHOU X, et al., "Clinical Analysis of Bevacizumab Plus FOLFIRI Regimen as Front-Line Therapy for Chinese Patients with Advanced Colorectal Cancer," J Cancer Ther. 2(4):470-4 (2011).

If you wish to add additional non-patent literature document citation information please click the Add button Add

EXAMINER SIGNATURE

Examiner Signature		Date Considered	

*EXAMINER: Initial if reference considered, whether or not citation is in conformance with MPEP 609. Draw line through a citation if not in conformance and not considered. Include copy of this form with next communication to applicant.

[1] See Kind Codes of USPTO Patent Documents at www.USPTO.GOV or MPEP 901.04. [2] Enter office that issued the document, by the two-letter code (WIPO Standard ST.3). [3] For Japanese patent documents, the indication of the year of the reign of the Emperor must precede the serial number of the patent document. [4] Kind of document by the appropriate symbols as indicated on the document under WIPO Standard ST.16 if possible. [5] Applicant is to place a check mark here if English language translation is attached.

INFORMATION DISCLOSURE STATEMENT BY APPLICANT (Not for submission under 37 CFR 1.99)		
	Application Number	15809815
	Filing Date	2017-11-10
	First Named Inventor	Eliel Bayever
	Art Unit	1612
	Examiner Name	Celeste A. RONEY
	Attorney Docket Number	01208-0007-01US

CERTIFICATION STATEMENT

Please see 37 CFR 1.97 and 1.98 to make the appropriate selection(s):

That each item of information contained in the information disclosure statement was first cited in any communication from a foreign patent office in a counterpart foreign application not more than three months prior to the filing of the information disclosure statement. See 37 CFR 1.97(e)(1).

OR

☐ That no item of information contained in the information disclosure statement was cited in a communication from a foreign patent office in a counterpart foreign application, and, to the knowledge of the person signing the certification after making reasonable inquiry, no item of information contained in the information disclosure statement was known to any individual designated in 37 CFR 1.56(c) more than three months prior to the filing of the information disclosure statement. See 37 CFR 1.97(e)(2).

See attached certification statement.

The fee set forth in 37 CFR 1.17 (p) has been submitted herewith.

☒ A certification statement is not submitted herewith.

SIGNATURE

A signature of the applicant or representative is required in accordance with CFR 1.33, 10.18. Please see CFR 1.4(d) for the form of the signature.

Signature	/Mary R. Henninger/	Date (YYYY-MM-DD)	2021-03-12
Name/Print	Mary R. Henninger	Registration Number	56992

This collection of information is required by 37 CFR 1.97 and 1.98. The information is required to obtain or retain a benefit by the public which is to file (and by the USPTO to process) an application. Confidentiality is governed by 35 U.S.C. 122 and 37 CFR 1.14. This collection is estimated to take 1 hour to complete, including gathering, preparing and submitting the completed application form to the USPTO. Time will vary depending upon the individual case. Any comments on the amount of time you require to complete this form and/or suggestions for reducing this burden, should be sent to the Chief Information Officer, U.S. Patent and Trademark Office, U.S. Department of Commerce, P.O. Box 1450, Alexandria, VA 22313-1450. DO NOT SEND FEES OR COMPLETED FORMS TO THIS ADDRESS. **SEND TO: Commissioner for Patents, P.O. Box 1450, Alexandria, VA 22313-1450.**

Privacy Act Statement

The Privacy Act of 1974 (P.L. 93-579) requires that you be given certain information in connection with your submission of the attached form related to a patent application or patent. Accordingly, pursuant to the requirements of the Act, please be advised that: (1) the general authority for the collection of this information is 35 U.S.C. 2(b)(2); (2) furnishing of the information solicited is voluntary; and (3) the principal purpose for which the information is used by the U.S. Patent and Trademark Office is to process and/or examine your submission related to a patent application or patent. If you do not furnish the requested information, the U.S. Patent and Trademark Office may not be able to process and/or examine your submission, which may result in termination of proceedings or abandonment of the application or expiration of the patent.

The information provided by you in this form will be subject to the following routine uses:

1. The information on this form will be treated confidentially to the extent allowed under the Freedom of Information Act (5 U.S.C. 552) and the Privacy Act (5 U.S.C. 552a). Records from this system of records may be disclosed to the Department of Justice to determine whether the Freedom of Information Act requires disclosure of these record s.

2. A record from this system of records may be disclosed, as a routine use, in the course of presenting evidence to a court, magistrate, or administrative tribunal, including disclosures to opposing counsel in the course of settlement negotiations.

3. A record in this system of records may be disclosed, as a routine use, to a Member of Congress submitting a request involving an individual, to whom the record pertains, when the individual has requested assistance from the Member with respect to the subject matter of the record.

4. A record in this system of records may be disclosed, as a routine use, to a contractor of the Agency having need for the information in order to perform a contract. Recipients of information shall be required to comply with the requirements of the Privacy Act of 1974, as amended, pursuant to 5 U.S.C. 552a(m).

5. A record related to an International Application filed under the Patent Cooperation Treaty in this system of records may be disclosed, as a routine use, to the International Bureau of the World Intellectual Property Organization, pursuant to the Patent Cooperation Treaty.

6. A record in this system of records may be disclosed, as a routine use, to another federal agency for purposes of National Security review (35 U.S.C. 181) and for review pursuant to the Atomic Energy Act (42 U.S.C. 218(c)).

7. A record from this system of records may be disclosed, as a routine use, to the Administrator, General Services, or his/her designee, during an inspection of records conducted by GSA as part of that agency's responsibility to recommend improvements in records management practices and programs, under authority of 44 U.S.C. 2904 and 2906. Such disclosure shall be made in accordance with the GSA regulations governing inspection of records for this purpose, and any other relevant (i.e., GSA or Commerce) directive. Such disclosure shall not be used to make determinations about individuals.

8. A record from this system of records may be disclosed, as a routine use, to the public after either publication of the application pursuant to 35 U.S.C. 122(b) or issuance of a patent pursuant to 35 U.S.C. 151. Further, a record may be disclosed, subject to the limitations of 37 CFR 1.14, as a routine use, to the public if the record was filed in an application which became abandoned or in which the proceedings were terminated and which application is referenced by either a published application, an application open to public inspections or an issued patent.

9. A record from this system of records may be disclosed, as a routine use, to a Federal, State, or local law enforcement agency, if the USPTO becomes aware of a violation or potential violation of law or regulation.

Hindawi Publishing Corporation
Journal of Drug Delivery
Volume 2012, Article ID 581363, 10 pages
doi:10.1155/2012/581363

Review Article

Lipoplatin Formulation Review Article

G. P. Stathopoulos[1] and T. Boulikas[2]

[1] *First Oncology Clinic, Errikos Dunant Hospital, Athens, Greece*
[2] *Regulon Inc. and Regulon A.E, Afxentiou 7, Alimos, 17455 Athens, Greece*

Correspondence should be addressed to G. P. Stathopoulos, dr-gps@ath.forthnet.gr

Received 29 May 2011; Accepted 24 June 2011

Academic Editor: Rassoul Dinarvand

Patented platform technologies have been used for the liposomal encapsulation of cisplatin (Lipoplatin) into tumor-targeted 110 nm (in diameter) nanoparticles. The molecular mechanisms, preclinical and clinical data concerning lipoplatin, are reviewed here. Lipoplatin has been successfully administered in three randomized Phase II and III clinical trials. The clinical data mainly include non-small-cell lung cancer but also pancreatic, breast, and head and neck cancers. It is anticipated that lipoplatin will replace cisplatin as well as increase its potential applications. For the first time, a platinum drug has shown superiority to cisplatin, at least in non-squamous non-small-cell lung cancer as reported in a Phase III study which documented a simultaneous lowering of all of the side effects of cisplatin.

1. Introduction

Over the last twenty years, the effort to produce new, more effective, and less toxic cytotoxic agents has been intensive, in order to ameliorate the treatment of cancer patients. One of the most effective agents since the late 1970s has been cisplatin (CDDP) in patients with testicular cancer [1], ovarian cancer [2], head and neck [3], and lung cancer [4] as well as bladder cancer [5] and in other malignancies [6, 7]. Cisplatin was established as being quite effective and as one of the most important cytotoxic agents. It has mainly been administered in combination with other agents. The toxicity rendered by cisplatin has been its main drawback, particularly nephrotoxicity [8–10]. After 1990, new agents that did not cause nephrotoxicity were produced as a substitute for cisplatin. Agents such as carboplatin [11] paclitaxel, docetaxel, gemcitabine, vinorelbine, and irinotecan [12–15] were used either in combination or as substitutes for cisplatin [16, 17]. These agents succeeded in producing no nephrotoxicity but did produce other toxicities such as myelotoxicity, in comparison to cisplatin. The main example was carboplatin, an analogue of cisplatin, which showed no renal toxicity but produced higher myelotoxicity than cisplatin. Carboplatin has often been used as a substitute for CDDP [11, 12] in lung [15], head and neck, and ovarian cancers [11]. The effectiveness of carboplatin was more or less equal to that of CDDP but not better. For instance, CDDP was shown to be more effective than carboplatin in the most common lung cancer, adenocarcinoma [18]. The other agents, previously mentioned, are mainly administered in combination with CDDP than as a substitute for it. Over all of the last twenty years, cisplatin has been in regular usage since most oncologists still believe it has priority with regard to effectiveness. Liposomal agents comprise another direction which research is taking and several of these have become part of clinical practice as is the case of liposomal anthracycline. None of these agents has managed to become a substitute for cisplatin, and they are used as second-line treatment.

Our review article is related to a new formulation of cisplatin, that is, liposomal cisplatin (lipoplatin). The purpose of this agent is to become a substitute for the original cisplatin, and, thus, the two drugs must be compared with regard to toxicity and effectiveness.

There are preclinical data in cancer cell cultures and in animals as well as clinical data which involve Phase I studies, pharmacokinetics and Phase II and Phase III studies. The data in 16 published studies are related to patients with pancreatic cancer, non-small-cell lung cancer (NSCLC), head and neck, and breast cancers.

2. Lipoplatin: Formulation, Mechanisms, and Technology

Cisplatin was formulated into liposomes as depicted in Figure 1. The lipids of lipoplatin are composed of soy phosphatidyl choline (SPC-3), cholesterol, dipalmitoyl phosphatidyl glycerol (DPPG), and methoxy-polyethylene glycol-distearoyl phosphatidylethanolamine (mPEG 2000-DSPE). The formulation was achieved by the formation of reverse micelles between cisplatin and DPPG under special conditions of pH, ethanol, ionic strength, and other parameters, and the cisplatin-DPPG reverse micelles were subsequently converted into liposomes by interaction with neutral lipids. About 15 extrusions are performed to give to the nanoparticles their final size of 110 nm, using a thermobarrel, extruder and membranes of 0.2, 0.1, 0.08 and 0.05 μm pore sizes under ultra pure nitrogen pressure.

The nanoparticles, 110 nm in diameter, have the ability to target tumors and metastasis following intravenous administration using the compromised endothelium of the tumor vasculature sprouted during neoangiogenesis; this process, known as extravasation, takes advantage of the compromised endothelium of the vasculature of the tumors generated during neoangiogenesis. Lipoplatin has shown an amazing concentration in tumors and metastases at levels up to 200-fold higher compared to the adjacent normal tissue in surgical specimens from patients [19].

3. Molecular Mechanisms of Cisplatin and Lipoplatin

After infusion, cisplatin is rapidly excreted in the urine causing renal tubular damage. When it reaches normal and malignant cells, it uses the major copper influx transporter Ctr1 for entry inside the cytoplasm (Figure 2). Ctr1 has been convincingly demonstrated to transport cisplatin and its analogues, carboplatin, and oxaliplatin. Two copper efflux transporters, ATP7A and ATP7B, regulate the efflux of cisplatin [21].

The S-containing tripeptide glutathione is present in cells at mM concentrations, and the formation of complexes with cisplatin plays an important role in its detoxification and biological activities. The depletion of glutathione levels has been shown to increase the toxicity of cisplatin to kidney cells. Cancer cells that are resistant to cisplatin often have elevated glutathione levels. Glutathione could quench DNA-Pt monofunctional adducts before they can rearrange toxic bifunctional adducts on DNA. Human glutathione S-transferase P1 (GSTP1) contributes to chemoresistance and its suppression, decreasing the cisplatin-induced activation of ERK1/2 and might have synergistic therapeutic effects [22].

Cisplatin and other apoptotic stimuli trigger the release of cytochrome c from the mitochondrial intermembrane space to the cytosol, which induces the formation of the apoptosome and the activation of procaspase-9, leading to apoptosis. The apoptosome is an Apaf-1 cytochrome c complex that activates procaspase-9. Cisplatin can also activate the proapoptotic protein Bax, resulting in cytochrome c release, caspase activation, and apoptosis; Bax activation is implicated in the nephrotoxicity of cisplatin [23]. Bcl-2 plays an important role in the mitochondrial apoptotic pathway. Although the general role of Bcl-2 is antiapoptotic, Bcl-2 fragments resulting by caspase cleavage after cisplatin treatment of cells in culture could promote the apoptotic process [24]. Lipoplatin, releasing cisplatin molecules in the cytoplasm of the tumor cell, is also proposed to activate the mitochondrial apoptotic cascade.

During signal transduction, a cell senses both the external and internal environment and converts a stimulus into an ordered sequence of phosphorylation-dephosphoryiation, protease degradation, gene regulation, or ion flux events, across the cell membrane. Receptor tyrosine kinases contribute to chemoresistance in tumors. A number of additional properties of cisplatin are now emerging including the activation of signal transduction pathways leading to apoptosis. The firing of such pathways may originate at the level of the cell membrane after damage of the receptor or lipid molecules by cisplatin, in the cytoplasm by modulation of proteins via the interaction of their thiol groups with cisplatin, (kinases, and other regulatory proteins and enzymes), or finally from DNA damage via the activation of the DNA repair pathways [25, 26].

Cisplatin induction of signaling is cell type, time and dose dependent. It induces oxidative stress and is an activator of stress-signaling pathways especially of the mitogen-activated protein (MAP) kinase cascades. The extracellular signal-regulated kinase (ERK) pathway is indeed activated by cisplatin. The acquisition of cisplatin resistance by ovarian carcinoma cells was associated with the loss of ERK activation in response to cisplatin [27]. ERK activation and DNA-damage induced apoptosis are tightly linked; p53 may act as one of the upstream regulators of ERK activation for the induction of apoptosis in carboplatin-treated cervical cancer cells [28]. The treatment of cells with high cisplatin concentrations (one order of magnitude higher than the IC_{50}) induces cellular superoxide formation and caspase activation independently of nuclear DNA damage. In contrast, cisplatin concentrations at IC_{50} doses, which do not induce acute apoptosis, are sufficient for the induction of DNA damage signaling [29].

The PI3K/Akt cascade has an important role in the resistance of ovarian cancer cells to cisplatin, and the inhibition of PI3K/Akt increases the efficacy of cisplatin [30]. The Akt-specific inhibitor LY294005 increased the efficacy of docetaxel, did not affect the efficacy of 6-thioguanine, and decreased the efficacy of cisplatin, lipoplatin, oxaliplatin, and lipoxal in human colorectal adenocarcinoma sublines, suggesting a novel property of Akt in aggravating drug sensitivity [31].

Cisplatin appears to exhibit synergistic effects with other potent inducers of apoptosis such as a synthetic isothiocyanate; the sequential administration of both agents led to increased intracellular platinum accumulation, glutathione depletion, poly (ADP-ribosyl) polymerase cleavage, stimulation of caspase-3 activity, upregulation of p53, FasL and Gadd45alpha, cyclin B1 downregulation, and an increase

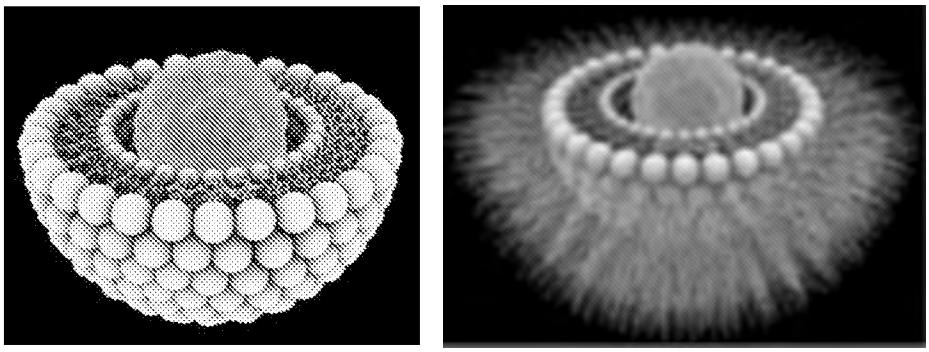

(a) (b)

Figure 1: Depiction of a lipoplatin nanoparticle (b). Cisplatin molecules are depicted as blue spheres surrounded by the lipid bilayer with the PEGylated lipid sticking out like hair from the outer surface. Thus, this toxic substance, cisplatin, is camouflaged by its lipid shell as a nutrient. This nanoparticle can pass undetected by macrophages after intravenous injection to human cancer patients because of its PEG coating thus escaping immune surveillance [20]. © CNRS Photothèque/SAGASCIENCE/CAILLAUD François.

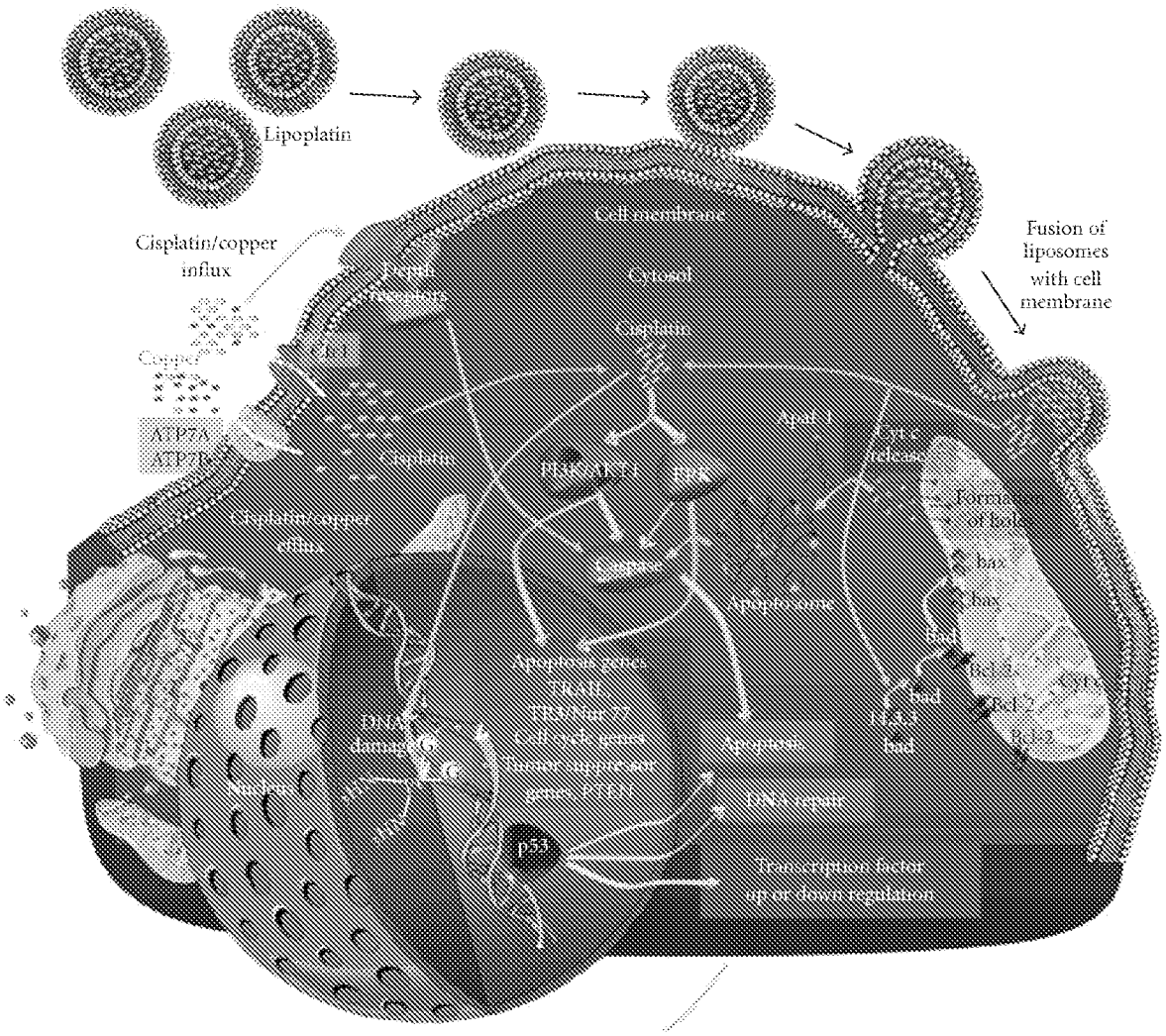

Figure 2: Penetration of lipoplatin nanoparticles through the cell membrane of tumor cells. lipoplatin nanoparticles once inside the tumor cell mass can fuse with the cell membrane because of the presence of the fusogenic lipid DPPG in their lipid bilayer; an alternative mechanism proposed is that lipoplatin is taken by *endocytosis* by tumor cells as shown from lipoplatin containing fluorescent lipids and imaging of the tumor cells in culture thus treated with fluorescent microscopy (see Figure 3). These processes occurring at the cell membrane level are promoted by the lipid shell of the nanoparticles (disguised as nutrients) [20].

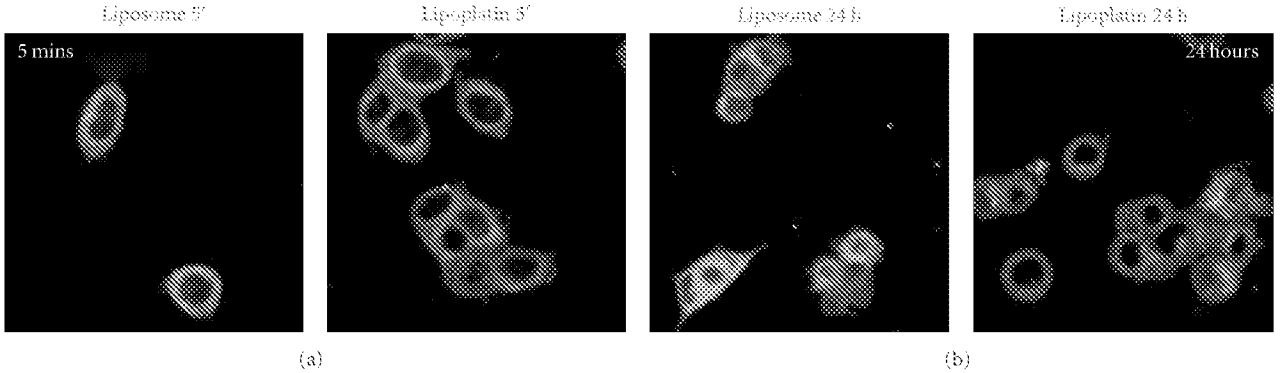

Figure 3: Lipoplatin or DPPG-liposomes with fluorescent lipids enter rapidly MCF-7 breast cancer cells in culture. Time-course processing of FITC-labeled DPPG-containing liposomes (a) and Lipoplatin (b) using confocal microscopy. At 5 min, the majority of the signal is localized in the membrane. Lipids are rapidly internalized and at 4–24 hours, a strong signal is observed in the cytoplasm and at the perinuclear area. These results demonstrate that *lipoplatin or DPPG-liposomes* nanoparticles are able to cross the cell membrane barrier [20].

in mitogen-activated protein kinases JNK, ERK, and p38 phosphorylation as well as PI3K level alterations [32].

4. Resistance of Tumor Cells to Cisplatin and a Role for Lipoplatin

The resistance of tumor cells to cisplatin is attributed to at least four different mechanisms: (i) decreased levels of cisplatin entrance to the cytoplasm or increased efflux through the cell membrane, (ii) increased levels of glutathione, (iii) modulation of signaling pathways, and (iv) enhanced levels of DNA repair.

However, additional pathways have been found for establishing the cisplatin resistant phenotype. For example, the selection of ovarian carcinoma cells in culture in the presence of cisplatin led to upregulated expression of the L1 adhesion molecule; this could constitute a mechanism for the establishment of chemoresistance and of a more malignant tumor phenotype [33].

The direct fusion of lipoplatin nanoparticles with the membrane of the tumor cell (Figure 2) suggests that lipoplatin can have applications after the failure of cisplatin front-line chemotherapy and the development of cisplatin resistance at the cell membrane level.

5. Preclinical Studies

A comparison of the cytotoxicity of lipoplatin and cisplatin in vitro in established cell lines (derived from NSCLC, renal cell carcinoma, and in normal hematopoietic cell precursors), as well as the identification of biological markers associated with sensitivity and resistance has rendered some interesting data. ERCC1 and LRP expression levels appeared to be valid predictors of sensitivity or resistance to both drugs. A superior cytotoxicity in all tumor cell models and a much lower toxicity in normal cells for lipoplatin compared with cisplatin were found, suggesting a higher therapeutic index for the liposomal compound [34].

Fedier et al. [35] investigated whether the cytotoxic effect of lipoplatin is dependent on the functional integrity of DNA mismatch repair (MMR). MMR is a postreplicative DNA repair mechanism implicated in cell cycle control and apoptosis. MMR function was found to be a relevant determinant accounting for the cytotoxicity of lipoplatin [35]. A possible relationship between MMR-mediated cisplatin DNA damage signaling, and the Akt signaling pathway was also found [31].

The fusion between liposomes and the cell membrane was suggested based on the fusogenic properties of DPPG and lipids integrated into the shell of lipoplatin (Figure 2). Subsequent cell culture studies where the lipids of the lipoplatin nanoparticle were labelled with fluorescein isothiocyanate (FITC) established the rapid uptake and internalization of the nanoparticles (Figure 3). In these studies the fluorescent nanoparticles were incubated with MCF-7 breast cancer cells in culture for various times ranging from 5 min to 24 h, and the cells were fixed and visualized by confocal microscopy (Figure 3). Liposomes containing DPPG without cisplatin were also used as a control. The study has provided proof that the lipids of lipoplatin labelled with FITC are transferred initially (in less than 5 min) to the cell membrane of MCF-7 cells in culture and are then (from 5 min to 24 h) docked to the interior of the cell. The membrane fusion is proposed to modulate signalling, an important process for cancer cell proliferation.

The lower nephrotoxicity of lipoplatin, compared to cisplatin, was shown in mice, rats, and SCID mice [36], whereas animals injected with cisplatin developed renal insufficiency with clear evidence of tubular damage, but those injected with the same dose of lipoplatin were almost completely free of kidney injury [36].

In order to explain the lower toxicity of lipoplatin compared to cisplatin, the levels of total platinum in rat tissue after cisplatin or lipoplatin injections were determined at different time intervals. The maximum levels of total platinum after cisplatin were found in the kidney followed by

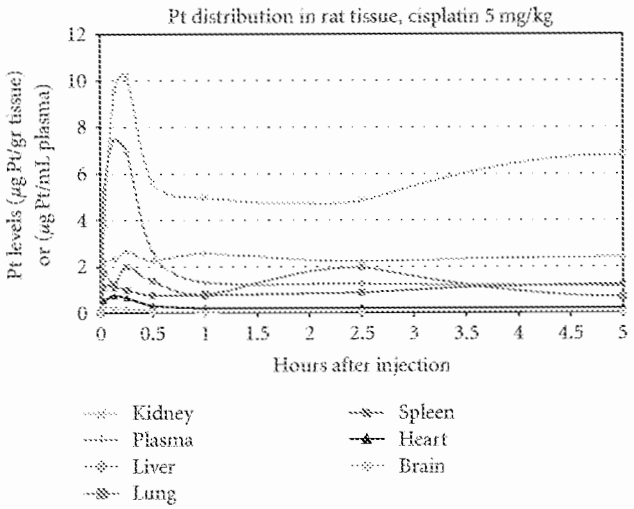

Figure 4: Kidney and other tissue accumulation of total platinum after *cisplatin* injection of rats (0–5h) [20].

the plasma, liver, lung, spleen, heart, and brain, in those tissues examined from 5 min to 5 h. At later times (up to 50 h), the order of the tissues with the highest levels of platinum was the kidney, liver spleen, plasma, lung, heart, and brain. A single treatment with 30 mg/kg lipoplatin in rats resulted in no toxicity, whereas 2 or 3 weekly administrations at 30 mg/kg in rats produced neutropenia but no nephrotoxicity. However, a single injection of 5 mg/kg cisplatin in rats resulted in severe nephrotoxicity. The levels of total platinum attained in animal kidneys after cisplatin administration are about the same as those after lipoplatin (Figure 4); however, at about 1 h and up to 5 days, the levels of total platinum are about 1 microgram after lipoplatin compared to 5 micrograms after cisplatin administration (Figure 4).

After cisplatin injection, the kidneys accumulate the highest levels of platinum among all of the animal tissues, followed by the liver and the lung. One hour after lipoplatin administration i.p., the kidney Pt levels drop from 13 to 3 μg/g tissue. The highest Pt levels among all of the animal tissues are in the liver and spleen after 4 h i.p. administration maintained for over 100 h.

The treatment of dogs with lipoplatin led to the conclusion that the drug can be safely administered to clinically normal dogs at dosages of up to 150 mg/m^2 without the need for concurrent hydration protocols. The maximum tolerated dose (MTD) of unencapsulated cisplatin in dogs has been established as 70 mg/m^2. Therefore, lipoplatin would allow the safe and repeated administration of doses higher than the MTD of unencapsulated cisplatin [37].

The intrapleural administration of lipoplatin in an animal model seems to offer a more effective therapeutic index while improving tolerability. Wistar rats were treated with doses of 10 mg/kg lipoplatin (intravenously) versus 10 or 20 mg/kg lipoplatin (intrapleurally) corresponding to 60 and 120 mg/m^2, respectively, in humans. The authors noted minor fibrotic changes in the pleura of rats injected intrapleurally, and mild kidney changes in rats injected intravenously, as expected [38].

6. Cellular Uptake and Cytoplasm/DNA Distribution of Cisplatin versus Lipoplatin

The antineoplastic or radio-sensitizing activity of platinum drugs is attributed to their binding to DNA. The time course of accumulation of cisplatin, lipoplatin, oxaliplatin, and lipoxal (liposomal oxaliplatin) in the human colorectal cancer HCT116 cell line and their distribution between the cytoplasm and DNA were measured by inductively coupled plasma mass spectrometry. The distribution of cytoplasm/DNA of free cisplatin and lipoplatin were similar. However, lipoxal displayed a higher accumulation in the cytoplasm compared to free oxaliplatin, consistent with its proposed mechanism of fusion with the cell membrane [39].

The cytotoxicity and synergic effect of platinum compounds with radiation were examined in F98 glioma cells. Lipoplatin improved the cell uptake of cisplatin by 3-fold, and its radiosensitizing potential was enhanced by 14-fold. Among the five platinum compounds tested, carboplatin and lipoplatin showed the best radiosensitizing effect. Lipoplatin seemed the most promising since it led to the best cellular incorporation and reduced all the toxicities of cisplatin [40].

7. Clinical Studies

7.1. Pharmacokinetics. In the administration of liposomal cisplatin to humans, the target was to determine the pharmacokinetics and adverse reactions. A Phase I study of 27 patients with different malignancies was performed. The drug was infused for 8 hrs every fourteen days at escalating doses. The drug levels started at 25 mg/m^2 and were increased by 25 mg/m^2 up to 125 mg/m^2. Three–5 patients were selected for each dosage. Blood was taken at certain time intervals in order to estimate the total platinum plasma levels. For pharmacokinetics, blood was drawn at 0, 3, 6, 8, 12, 24 hrs and 3, 5, 7 days, into tubes containing EDTA, and total platinum levels (i.e., free plus proteins bound plus liposomal) were analyzed by atomic absorption. Total platinum was also determined in the ultrafiltrate of less plasma. The maximum level attained in the plasma was 5.7 μg/mL at 8 hrs. The levels of platinum in the blood after lipoplatin infusion drop to normal on the fourth day at a dose of 100 mg/m^2, but at a dose of 125 mg/m^2 platinum can be detected in the blood for 7 days (Table 1) [41]. Renal function tests (blood urea, serum creatinine, and creatinine clearance) showed no change before and after treatment. The excretion of platinum in the urine in lipoplatin-treated patients attains a maximum within 8 hrs (infusion period) and declines thereafter. During the 3 following days (after infusion) 40.7% of the total platinum was excreted in the urine. Toxicity was very mild (grade 1 or 2 neutropenia and nausea/vomiting) at the 125 mg/m^2 dosage level. In another trial, the tumor uptake of lipoplatin was examined in comparison to normal tissue, in 4 patients with hepatocellular adenocarcinoma, gastric cancer, and colon cancer. Lipoplatin was administered to the patients 24 hours before the surgery [19]. This study showed liposomal cisplatin accumulation in tumors as compared to normal tissue after the intravenous infusion of lipoplatin.

Table 1: Pharmacokinetic parameters of total platinum in patients' sera at the different dose levels.

Dose mg/m^2	Pts (n)	$AUC_{0\text{-}\infty A}$ (h μg/mL)	C_{max} (μg/mL)	Cl (L/m^2 h)	K_{el} (L/h)	$t_{1/2}$ (h)	V_{ss} (L/m^2)
25	5	139.63	2.48 ± 1.18	0.18	0.0114	60.79	15.71
50	3	119.19	2.87 ± 0.59	0.42	0.0001	N/A	N/A
100	5	172.89	3.74 ± 1.18	0.58	0.0059	117.46	98.03
125	4	256.09	5.65 ± 2.67	0.49	0.0085	81.53	57.42

N/A, not applicable.

Among the various surgical specimens examined, gastric tumors revealed the highest levels of total platinum (up to 262 μg cisplatin/gr tissue). The liver metastatic specimen displayed a total amount of 131.15 μg platinum/gr of tissue compared to 20.94 μg platinum/gr of normal liver tissue. Both specimens of gastric tumors appeared to accumulate the highest amounts of platinum among all specimens analyzed in this study: 262.62 and 66.38 μg/gr of tissue. The total platinum levels in the colon tumor specimens were 11.26 and 7.69 μg platinum/gr of tissue compared to 0.06 μg/gr normal colon tissue [19].

7.2. Dose-Limited Toxicity and Maximum Tolerated Doses. The human testing of this new agent primarily required the definition of toxicity by investigating the MTD as well as the dose-limited toxicity (DLT). Two Phase I and I-II studies examined these objectives. The first trial was in patients with advanced pancreatic cancer. The results showed that the dosages which began to produce side effects were 100 mg/m^2 and 125 mg/m^2. But these dosages did not later prove that this was the DLT since lipoplatin was combined with gemcitabine, the latter which may have been responsible for the toxicity [42]. The second study defined similar doses as the DLT and MTD. This trial also used two agents, lipoplatin and gemcitabine in pretreated patients with NSCLC. The two drugs were repeated on day 8. The small number of 13 patients was not efficacious enough to determine ample data concerning toxicity [43]. In both these aforementioned studies, there was also a defect in that all of the patients had undergone chemotherapy pretreatment when they were recruited and the efficacy of lipoplatin was tested. A proper third Phase I trial was eventually performed. The main objective of this study was to determine the DLT and MTD of lipoplatin tested as a single agent and in combination with a second cytotoxic agent. The selected second agent was paclitaxel. All of the patients had NSCLC. Adverse reactions, mainly myelotoxicity, renal toxicity and gastrointestinal toxicity (nausea, vomiting, diarrhea) were determined. Sixty-six patients were recruited and evaluated. Thirty-nine patients comprised the group that received lipoplatin monotherapy, and 27 patients were given lipoplatin in combination with paclitaxel. In the first group, the dosage of lipoplatin started at the level of 125 mg/m^2 and the drug-dose escalation increased to 350 mg/m^2. It was determined that 350 mg/m^2 was the DLT and 300 mg/m^2 the MDT. In the group that received combination therapy, the escalation of paclitaxel started at 100 mg/m^2 and went up to 175 mg/m^2 and of lipoplatin from 100 mg/m^2 to 250 mg/m^2. The results of the combined treatment evaluation determined the DLT as 250 mg/m^2 and the MTD, 200 mg/m^2. Nausea, vomiting, fatigue, and neutropenia were not higher than grade 1-2, and other adverse reactions in a small percentage of patients reached grade 3. In the combined modality, other side effects, such as neurotoxicity, were observed, and this was attributed to paclitaxel. Grade 1 nephrotoxicity was observed in a small percentage of patients, but this was only temporary (Table 2) [44].

Over the last five years, several Phase II and III trials have been performed in different institutions and countries. Lipoplatin has been tested in the following malignancies: pancreatic cancer, head and neck cancer, mesothelioma, breast and gastric cancer, and NSCLC. In pancreatic cancer, lipoplatin was administered as second-line treatment in combination with gemcitabine. The patients had initially undergone gemcitabine monotherapy as first-line treatment and were experiencing disease progression. The combination of lipoplatin with gemcitabine rendered a response rate of 8% [42].

A trial was done concerning a combination of lipoplatin 120 mg/m^2 plus 5-fluorouracil 400 mg/m^2 and leucovorin, both cytotoxic drugs administered weekly along with radiotherapy. The cytotoxic agents were given on day 1 and radiotherapy (dosage 3.5 Gy / 3, days 2, 3, 4) for four or five weeks. This treatment was given to patients with advanced gastric cancer. No serious toxicity was observed, and the therapy was well tolerated; 18.2% patients developed grade 1 renal toxicity and nausea and 25% showed fatigue. A good response to the combined treatment was observed [45].

It is too early to confirm that lipoplatin is effective in mesothelioma. There is a case report indicating the responsiveness of mesothelioma to lipoplatin given in combination with gemcitabine as second-line treatment on disease recurrence [46].

The testing of the toxicity and effectiveness of liposomal cisplatin was done in patients with squamous cell carcinoma of the head and neck. This was a randomized study comparing lipoplatin combined with 5-fluorouracil versus cisplatin combined with 5-fluorouracil. The toxicity was well tolerated. Grade 3 renal toxicity was much lower after lipoplatin administration than after cisplatin. Higher myelotoxicity was observed in the cisplatin arm (31.7% versus 12% in the lipoplatin arm). Mucositis and peripheral neuropathy were also much higher in the cisplatin group. The response rate was higher in the cisplatin arm, but

Table 2: Toxicity: lipoplatin monotherapy.

Dosage lipoplatin mg/m^2	Toxicity	Grade 1	2	3	4
		n	n	n	n
150–250	Nausea-vomiting	----	----	----	----
	Fatigue	----	----	----	----
	Diarrhea	----	----	----	----
	Nephrotoxicity	----	----	----	----
	Neutropenia	----	----	----	----
	Neurotoxicity	----	----	----	----
300	Nausea-vomiting	2/4	1/4	----	----
	Fatigue	2/4	1/4	----	----
	Neutropenia	1/4	----	----	----
	Nephrotoxicity	1/4	----	----	----
350	Nausea-vomiting	1/4	3/4	----	----
	Fatigue	1/4	3/4	----	----
	Neutropenia	2/4	1/4	1/4	----
	Nephrotoxicity	2/4	1/4	1/4	----

stable disease was higher in the lipoplatin arm. This low responsiveness of the lipoplatin arm may be due to the quite low dosage administered and its short duration. One should take into account that the MTD is 200 mg/m^2 and not 100 mg/m^2 [47].

A Phase II trial combining lipoplatin with vinorelbine in first-line treatment of HER2/neu-negative metastatic breast cancer was done. The investigators administered the above agents on the basis of the rationale that the frequent use of anthracyclines and taxanes in the adjuvant setting of breast cancer has led to drug resistance and cardiac toxicity. This raised the need for new agents in the metastatic setting. Another reason for testing the aforementioned combination was that the use of cisplatin-vinorelbine showed interesting results with an overall response rate of 64%. The administered dose of lipoplatin was 120 mg/m^2 and of vinorelbine 30 mg/m^2. The objective response rate of the latter combination was 50% (one complete response). Stable disease was 45.5%. Toxicity was well tolerated [48].

One Phase II and two Phase III trials have been recently integrated and published. In these studies, lipoplatin was combined with a second agent in comparison with cisplatin also combined with the same second agent, and the objectives were to determine the side effects and efficacy. In the Phase II randomized study, lipoplatin (dosage 120 mg/m^2 given on days 1, 8, 15) combined with gemcitabine (1000 mg/m^2 given on days 1, 8) was compared with cisplatin (100 mg/m^2 day 1) combined with gemcitabine (1000 mg/m^2 given on days 1, 8). With respect to efficacy, the overall response rate of the lipoplatin arm was 31.7%, and the cisplatin arm 25.6%. Although the efficacy of lipoplatin was not statistically higher than that of cisplatin, a better response rate was achieved with lipoplatin, particularly in cases of adenocarcinoma. The more important finding was the toxicity outcome which was shown to be much lower in patients treated with lipoplatin versus in patients treated with cisplatin. Very low nephrotoxicity was observed in the patients who received lipoplatin. Although the aforementioned study [49] included a rather limited number of patients (88 in total), the results were confirmed by another study which was done in parallel to the above trial.

These results with respect to the study done in parallel, mentioned above, are as follows: this Phase III trial included 229 evaluable patients. The differences between this study and the previous one were, the number of patients, the dosage of the drugs, the repetition of the courses, and the second agent which was combined with lipoplatin and cisplatin. The dose of lipoplatin was 200 mg/m^2, which is the proper MTD combined with paclitaxel 135 mg/m^2 repeated every 2 weeks for a planned 9 courses. The control arm received cisplatin 75 mg/m^2 also combined with paclitaxel 135 mg/m^2, repeated every 2 weeks. The planned number of courses was 9. The treatment of both agents and arms was on day 1. The main objectives of this trial were to determine the toxicity and median survival. The results were quite impressive; nephrotoxicity, in particular, leukopenia, nausea/vomiting, and asthenia were statistically significantly lower after lipoplatin treatment ($P \leq 0.001$, 0.017, 0.042, 0.019, resp.) (Table 3). The comparison of efficacy was also important; the response rate was 59.7% for the lipoplatin arm, and 47% for the cisplatin arm (no statistically significant difference, $P = 0.073$) (Table 4). The median and overall survival for both arms was the same [50].

The data documented in the last two trials indicate that the cisplatin formulation (lipoplatin) could be considered as the best substitute for cisplatin, at least in NSCLC, with regard to efficacy and toxicity.

The next Phase III trial was based on certain indications from the previous trials, and this was the possibility that NSCLC subtypes may have a different response rate with the

Table 3: Toxicity/statistical differences.

Toxicity grade 1–4	Arm A *n* (%)	Arm B *n* (%)	*P* value*
Anemia	50 (43.9)	62 (54.9)	0.112
Leucopenia (neutropenia)	38 (33.3)	52 (45.2)	0.017
Thrombocytopenia	2 (1.8)	3 (2.6)	1.000†
Nephrotoxicity (renal)	7 (6.1)	46 (40.0)	<0.001
Neurotoxicity	52 (45.6)	63 (54.8)	0.145
GI toxic nausea/vomiting	37 (32.5)	52 (45.2)	0.042
GI diarrhea	2 (1.8)	3 (2.6)	1.000†
Asthenia	65 (57.0)	82 (71.3)	0.019
Alopecia	96 (84.2)	87 (75.7)	0.134

GI, gastrointestinal.
*Pearson's chi-square test.
†Fisher's exact test.

Table 4: Response rate/survival time (months), Log-rank test *P* value: 0.577.

		ARM			
Response rate		A	B	Total	*P* value*
CR					
n		1	0	1	----
% within ARM		0.9	0.0	0.4	----
PR					
n		67	54	121	
% within ARM		58.8	47.0	52.8	0.073
SD					
n		42	50	92	
% within ARM		36.8	43.5	40.2	0.306
PD					
n		4	11	15	
% within ARM		3.5	9.6	6.6	0.064
Total	*n*	114	115	229	
Survival time	*n*	Median		95% CI	
Arm A	114	9.0		6.2–11.8	
Arm B	115	10.0		6.8–13.2	
Total sample	229	10.0		8.3–11.7	

CR: complete response; PR: partial response; SD: stable disease; PD: progressive disease.
*Pearson's chi-square test.

Table 5: Response rate.

	Arm A ($n = 103$)	Arm B ($n = 99$)	*P* value
Partial response	61 (59.22%)	42 (42.42%)	0.036
Stable disease	35 (33.98%)	43 (43.43%)	0.220
Progressive disease	7 (6.80%)	14 (14.14%)	0.110

administration of lipoplatin or cisplatin. This study recruited patients with nonsquamous cell lung cancer, mainly adenocarcinomas, and they were treated with lipoplatin combined with paclitaxel versus cisplatin combined with paclitaxel. The dosage and administration of these two combined treatments was the same as in the previous study. It was found in 202 patients randomized into two groups, that the response rate was superior in the lipoplatin group. The difference was statistically significant ($P = 0.036$) (Table 5). The median survival for the lipoplatin group was 10 months and for

cisplatin group 8 months, approaching statistical significance ($P = 0.1551$) [51].

There are data examining the possibility of using lipoplatin in cancer patients with renal failure. The preliminary data show that patients with serum creatinine ranging from 1.6–3.5 mg/dL tolerate lipoplatin without increasing renal failure and without side effects such as neutropenia, nausea/vomiting, and fatigue.

8. Conclusion

The efforts over the last 20 years to produce a substitute for cisplatin, a very important and effective anticancer agent, with a similarly effective and less toxic agent, have not properly succeeded. The current data in a number of preclinical and clinical trials shed new light on the previous efforts to produce a substitute for cisplatin. Liposomal cisplatin (lipoplatin), is a new formulation of cisplatin and one would expect at least to achieve equal effectiveness. Phase I, II, and III trials have shown lipoplatin to produce similar efficacy to that of cisplatin in pancreatic, head and neck, breast cancers, and NSCLC (the latter has been more broadly tested). In a new substitute for cisplatin, what is more important, apart from effectiveness, is significant toxicity reduction. The reduction of toxicity, mainly nephrotoxicity, has been shown and confirmed in published trials. It will be important to use this new cisplatin formulation in future trials and to test it in malignancies such as ovarian and bladder cancers.

References

[1] L. H. Einhorn, S. D. Williams, P. J. Loehrer et al., "Evaluation of optimal duration of chemotherapy in favorable-prognosis disseminated germ cell tumors: a Southeastern Cancer Study Group protocol," *Journal of Clinical Oncology*, vol. 7, no. 3, pp. 387–391, 1989.

[2] K. Aabo, M. Adams, P. Adnitt et al., "Chemotherapy in advanced ovarian cancer: four systematic meta-analyses of individual patient data from 37 randomized trials," *British Journal of Cancer*, vol. 78, no. 11, pp. 1479–1487, 1998.

[3] J. P. Pignon, J. Bourhis, C. Domenge, and L. Designe, "Chemotherapy added to locoregional treatment for head and neck squamous-cell carcinoma: three meta-analyses of updated individual data," *The Lancet*, vol. 355, no. 9208, pp. 949–955, 2000.

[4] Non-small Cell Lung Cancer Collaborative Group, "Chemotherapy in non-small cell lung cancer, a meta-analysis using updated data on individual patients from 52 randomized clinical trials," *British Medical Journal*, vol. 311, no. 7010, pp. 899–909, 1995.

[5] D. Kaufman, D. Raghavan, M. Carducci et al., "Phase II trial of gemcitabine plus cisplatin in patients with metastatic urothelial cancer," *Journal of Clinical Oncology*, vol. 18, no. 9, pp. 1921–1927, 2000.

[6] B. Rosenberg, "Platinum complexes for the treatment of cancer: why the research goes on," in *Cisplatin: Chemistry of a Leading Anticancer Drug*, B. Lippert, Ed., pp. 3–12, Verlag Helvetica Chemica Acta, Zurich, Switzerland, 1999.

[7] D. M. Hayes, E. Cvitkovic, R. B. Golbey, E. Scheiner, L. Helson, and I. H. Krakoff, "High dose cis-platinum diamminedichloride: amelioration of renal toxicity by mannitol diuresis," *Cancer*, vol. 39, pp. 1372–1378, 1977.

[8] C. M. Sorenson and A. Eastman, "Mechanism of cis-diamminedichloroplatinum(II)-induced cytotoxicity: role of G2 arrest and DNA double-strand breaks," *Cancer Research*, vol. 48, no. 16, pp. 4484–4488, 1988.

[9] D. R. Gandara, N. A. Nahhas, M. D. Adelson et al., "Randomized placebo-controlled multicenter evaluation of diethyldithiocarbamate for chemoprotection against cisplatinum-induced toxicities," *Journal of Clinical Oncology*, vol. 13, no. 3, pp. 490–496, 1995.

[10] I. Arany and R. L. Safirstein, "Cisplatin nephrotoxicity," *Seminars in Nephrology*, vol. 23, no. 5, pp. 460–464, 2003.

[11] A. E. Taylor, E. Wiltshaw, M. E. Gore, I. Fryatt, and C. Fisher, "Long-term follow-up of the first randomized study of cisplatin versus carboplatin for advanced epithelial ovarian cancer," *Journal of Clinical Oncology*, vol. 12, no. 10, pp. 2066–2070, 1994.

[12] A. Tognoni, F. Pensa, E. Vaira et al., "A dose finding study of carboplatin and gemcitabine in advanced non-small cell lung cancer," *Journal of Chemotherapy*, vol. 14, no. 3, pp. 296–300, 2002.

[13] B. E. Johnson, "Integration of new agents into the treatment of advanced non-small cell lung cancer," in *American Society of Clinical Oncology Educational Book*, pp. 345–356, Lipincott Williams and Wilkins, Baltimore, Md, USA, 2000.

[14] F. A. Shepherd, J. Dancey, A. Arnold et al., "Phase II study of pemetrexed disodium, a multitargeted antifolate and cisplatin as first-line therapy in patients with advanced non-small cell lung cancer," *Cancer*, vol. 92, no. 3, pp. 595–600, 2001.

[15] F. Barlesi and J. L. Pujal, "Combination of chemotherapy without platinum compounds in the treatment of advanced non-small cell lung cancer: a systemic review of phase III trials," *Lung Cancer*, vol. 49, no. 3, pp. 289–298, 2005.

[16] G. P. Stathopoulos, M. Veslemes, N. Georgatou et al., "Paclitaxel and vinorelbine combination in advanced inoperable adenocarcinoma of the lung: a phase II study," *Anticancer Research*, vol. 23, no. 4, pp. 3479–3484, 2003.

[17] G. P. Stathopoulos, J. Dimitroulis, D. Antoniou et al., "Front-line paclitaxel and irinotecan combination chemotherapy in advanced non-small-cell lung cancer: a phase I-II trial," *British Journal of Cancer*, vol. 93, no. 10, pp. 1106–1111, 2005.

[18] A. Ardizzoni, L. Boni, M. Tiseo et al., "Cisplatin- versus carboplatin-based chemotherapy in first-line treatment of advanced non-small-cell lung cancer: an individual patient data meta-analysis," *Journal of the National Cancer Institute*, vol. 99, no. 11, pp. 847–857, 2007.

[19] T. Boulikas, G. P. Stathopoulos, N. Volakakis, and M. Vougiouka, "Systemic lipoplatin infusion results in preferential tumor uptake in human studies," *Anticancer Research*, vol. 25, no. 4, pp. 3031–3040, 2005.

[20] Boulikas Teni, "Lipoplatin: a successful cisplatin formulation," *Cancer Therapy*. In press.

[21] M. T. Kuo, H. H. W. Chen, I. S. Song, N. Savaraj, and T. Ishikawa, "The roles of copper transporters in cisplatin resistance," *Cancer and Metastasis Reviews*, vol. 26, no. 1, pp. 71–83, 2007.

[22] G. Huang, L. Mills, and L. L. Worth, "Expression of human glutathione S-transferase P1 mediates the chemosensitivity of osteosarcoma cells," *Molecular Cancer Therapeutics*, vol. 6, no. 5, pp. 1610–1619, 2007.

[23] Q. Wei, G. Dong, J. Franklin, and Z. Dong, "The pathological role of Bax in cisplatin nephrotoxicity," *Kidney International*, vol. 72, no. 1, pp. 53–62, 2007.

[24] J. Zhu, Y. Yang, and J. Wu, "Bcl-2 cleavages at two adjacent sites by different caspases promote cisplatin-induced apoptosis," *Cell Research*, vol. 17, no. 5, pp. 441–448, 2007.

[25] T. Boulikas and M. Vougiouka, "Cisplatin and platinum drugs at the molecular level. (Review)," *Oncology Reports*, vol. 10, no. 6, pp. 1663–1682, 2003.

[26] D. Wang and S. J. Lippard, "Cellular processing of platinum anticancer drugs," *Nature Reviews Drug Discovery*, vol. 4, no. 4, pp. 307–320, 2005.

[27] M. Villedieu, M. Briand, M. Duval, J. F. Heron, P. Gauduchon, and L. Poulain, "Anticancer and chemosensitizing effects of 2,3-DCPE in ovarian carcinoma cell lines: link with ERK activation and modulation of p21(WAF1/CIP1), Bcl-2 and Bcl-x(L) expression," *Gynecologic Oncology*, vol. 105, no. 2, pp. 373–384, 2007.

[28] M. Singh, H. Sharma, and N. Singh, "Hydrogen peroxide induces apoptosis in HeLa cells through mitochondrial pathway," *Mitochondrion*, vol. 7, no. 6, pp. 367–373, 2007.

[29] M. Berndtsson, M. Hägg, T. Panaretakis, A. M. Havelka, M. C. Shoshan, and S. Linder, "Acute apoptosis by cisplatin requires induction of reactive oxygen species but is not associated with damage to nuclear DNA," *International Journal of Cancer*, vol. 120, no. 1, pp. 175–180, 2007.

[30] T. Ohta, M. Ohmichi, T. Hayasaka et al., "Inhibition of phosphatidylinositol 3-kinase increases efficacy of cisplatin in in vivo ovarian cancer models," *Endocrinology*, vol. 147, no. 4, pp. 1761–1769, 2006.

[31] A. Fedier, R. Erdmann, T. Boulikas, and D. Fink, "Potential of the Akt inhibitor LY294005 to antagonize the efficacy of cisplatin against HCT116 tumor cells in a DNA mismatch repair-dependent manner," *International Journal of Oncology*, vol. 29, no. 5, pp. 1303–1310, 2006.

[32] J. Bodo, L. Hunakova, P. Kvasnicka et al., "Sensitisation for cisplatin-induced apoptosis by isothiocyanate E-41B leads to signalling pathways alterations," *British Journal of Cancer*, vol. 95, no. 10, pp. 1348–1353, 2006.

[33] A. Stoeck, D. Gast, M. P. Sanderson, Y. Issa, P. Gutwein, and P. Altevogt, "L1-CAM in a membrane-bound or soluble form augments protection from apoptosis in ovarian carcinoma cells," *Gynecologic Oncology*, vol. 104, no. 2, pp. 461–469, 2007.

[34] C. Arienti, A. Tesei, A. Ravaioli et al., "Activity of lipoplatin in tumor and in normal cells in vitro," *Anticancer Drugs*, vol. 19, no. 10, pp. 983–990, 2008.

[35] A. Fedier, C. Poyet, D. Perucchini, T. Boulikas, and D. Fink, "MLH1-deficient tumor cells are resistant to lipoplatin, but retain sensitivity to lipoxal," *Anticancer Drugs*, vol. 17, no. 3, pp. 315–323, 2006.

[36] P. Devarajan, R. Tarabishi, J. Mishra et al., "Low renal toxicity of lipoplatin compared to cisplatin in animals," *Anticancer Research*, vol. 24, no. 4, pp. 2193–2200, 2004.

[37] A. K. Marr, I. D. Kurzman, and D. M. Vail, "Preclinical evaluation of a liposome-encapsulated formulation of cisplatin in clinically normal dogs," *American Journal of Veterinary Research*, vol. 65, no. 11, pp. 1474–1478, 2004.

[38] M. E. Froudarakis, L. Greillier, S. Monjanel-Mouterde et al., "Intrapleural administration of lipoplatin in an animal model," *Lung Cancer*, vol. 72, no. 1, pp. 78–83, 2010.

[39] T. Tippayamontri, R. Kotb, B. Paquette, and L. Sanche, "Cellular uptake and cytoplasm/DNA distribution of cisplatin and oxaliplatin and their liposomal formulation in human colorectal cancer cell HCT116," *Investigational New Drugs*. In press.

[40] G. Charest, B. Paquette, D. Fortin, D. Mathieu, and L. Sanche, "Concomitant treatment of F98 glioma cells with new liposomal platinum compounds and ionizing radiation," *Journal of Neuro-Oncology*, vol. 97, no. 2, pp. 187–193, 2010.

[41] G. P. Stathopoulos, T. Boulikas, M. Vougiouka et al., "Pharmacokinetics and adverse reactions of a new liposomal cisplatin (lipoplatin): phase I study," *Oncology Reports*, vol. 13, no. 4, pp. 589–595, 2005.

[42] G. P. Stathopoulos, T. Boulikas, M. Vougiouka, S. K. Rigatos, and J. G. Stathopoulos, "Liposomal cisplatin combined with gemcitabine in pretreated advanced pancreatic cancer patients: a phase I-II study," *Oncology Reports*, vol. 15, no. 5, pp. 1201–1204, 2006.

[43] M. E. Froudarakis, A. Pataka, P. Pappas et al., "Phase I trial of lipoplatin and gemcitabine as a second-line chemotherapy in patients with nonsmall cell lung carcinoma," *Cancer*, vol. 113, no. 10, pp. 2752–2760, 2008.

[44] G. P. Stathopoulos, S. K. Rigatos, and J. Stathopoulos, "Liposomal cisplatin dose escalation for determining the maximum tolerated dose and dose-limiting toxicity: a phase I study," *Anticancer Research*, vol. 30, no. 4, pp. 1317–1321, 2010.

[45] M. I. Koukourakis, A. Giatromanolaki, M. Pitakoudis et al., "Concurrent liposomal cisplatin (lipoplatin), 5-fluorouracil and radiotherapy for the treatment of locally advanced gastric cancer: a phase I-II study," *International Journal of Radiation Oncology Biology Physics*, vol. 78, no. 1, pp. 150–155, 2009.

[46] G. Karpathiou, E. Argiana, A. Kontsopoulos, and M. E. Froudarakis, "Response of a patient with pleural and peritoneal mesothelioma after second-line chemotherapy with lipoplatin and gemcitabine," *Oncology*, vol. 73, no. 5-6, pp. 426–429, 2008.

[47] C. E. Jehn, T. Boulikas, A. Kourvetaris, K. Possinger, and D. Luftner, "Pharmacokinetics of liposomal cisplatin (lipoplatin) in combination with 5-FU in patients with advanced head and neck cancer: first results of a phase III study," *Anticancer Research*, vol. 27, no. 1, pp. 471–476, 2007.

[48] F. S. Farhat, K. Ibrahim, J. Kattan et al., "Preliminary results of phase II study of liposomal cisplatin—vinorelbine combination as first-line treatment in HER2/neu negative metastatic breast cancer (MBC)," in *Proceedings of the ASCO Annual Meeting*, 2009.

[49] N. Mylonakis, A. Athanasiou, N. Ziras et al., "Phase II study of liposomal cisplatin (lipoplatin) plus gemcitabine versus cisplatin plus gemcitabine as first line treatment in inoperable (stage IIIB/IV) non-small cell lung cancer," *Lung Cancer*, vol. 68, no. 2, pp. 240–247, 2010.

[50] G. P. Stathopoulos, D. Antoniou, J. Dimitroulis et al., "Liposomal cisplatin combined with paclitaxel versus cisplatin and paclitaxel in non-small-cell lung cancer: a randomized phase III multicenter trial," *Annals of Oncology*, vol. 21, no. 11, pp. 2227–2232, 2010.

[51] G. P. Stathopoulos, D. Antoniou, J. Dimitroulis, J. Stathopoulos, K. Marosis, and P. Michalopoulou, "Comparison of lipo-somal cisplatin versus cisplatin in non-squamous cell non-small cell lung cancer," *Cancer Chemotherapy and Pharmacology*. In press.

Liposomal Oxaliplatin in the Treatment of Advanced Cancer: A Phase I Study

GEORGE P. STATHOPOULOS[1], TENI BOULIKAS[2], ANDREAS KOURVETARIS[2] and JOHN STATHOPOULOS[1]

[1]*First Oncology Department Errikos Dunant Hospital, Athens, Greece;*
[2]*Regulon, Inc., 715 North Shoreline Blvd, Mountain View CA 94043, U.S.A. and Regulon A.E., 7 Grigoriou Afxentiou, 17455 Alimos, Greece*

Abstract. *Background: Lipoxal is a liposomal oxaliplatin, which reduces the cytotoxic agent's adverse reactions without reducing effectiveness. Our objectives were to determine the adverse reactions, dose-limiting toxicity (DLT) and the maximum tolerated dose (MTD) of lipoxal. Patients and Methods: Twenty-seven patients with advanced disease of the gastrointestinal system were included in the study. All patients had been pretreated with standard chemotherapy according to established guidelines. At entry, all patients had recurrent or progressive disease (stage IV gastrointestinal cancers: colorectal, gastric and pancreatic). Six lipoxal dose levels (100 mg/m^2, 150 mg/m^2, 200 mg/m^2, 250 mg/m^2, 300 mg/m^2 and 350 mg/m^2) were set and at least 3 patients were included at each level. Eight patients were treated at 300 mg/m^2 (MTD). The treatment was given once weekly for 8 weeks. Results: No serious side-effects were observed at the first 4 dose levels (100-250 mg/m^2). At levels 5 and 6, mild myelotoxicity and nausea were observed. The most common adverse reaction was grade 2-3 peripheral neuropathy, observed in all 4 patients treated at 350 mg/m^2. The 350 mg/m^2 dose level was therefore considered as DLT and the 300 mg/m^2 level as the MTD. Of the 27 patients, 3 achieved partial response and 18 had stable disease for 4 months, (range 2-9 months). Conclusion: The most common toxicity was peripheral neuropathy at the 300 and 350 mg/m^2 dose levels. Lipoxal was well-tolerated and greatly reduced all the other side-effects of oxaliplatin, especially myelotoxicity and gastrointestinal tract toxicities. These preliminary results showed adequate effectiveness in pretreated patients.*

Correspondence to: G.P. Stathopoulos, MD, Semitelou 2A, 115 28 Athens, Greece. Tel: + 30-210-7752600, Fax: + 30-210-7251736, e-mail: dr-gps@ath.forthnet.gr

Key Words: Liposomal oxaliplatin (lipoxal), gastrointestinal cancer.

Oxaliplatin, an analog of cisplatin, has shown a wide antitumor effect *in vitro* and *in vivo* and a better safety profile than cisplatin (1-7). The main adverse reactions are neurotoxicity and hematological and gastrointestinal (GI) toxicity (8). No nephrotoxicity has been observed, in contrast to cisplatin, and no hydration is needed during its administration. Kidney tubular necrosis has been rarely observed (8). The alkaline hydrolysis of oxaliplatin produces the oxalato monodentate intermediate complex (pKa 7.23) and the dihydrated oxaliplatin complex in 2 consecutive steps. The monodentate intermediate is assumed to rapidly react with endogenous compounds (9). The crystal structures of oxaliplatin bound to a DNA dodecamer duplex with the sequence 5'-d (CCTCTGGTCTCC) has been reported (10). The platinum atom forms a 1,2-intrastrand cross-link between 2 adjacent guanosine residues, bending the double helix by approximately 30 degrees toward the major groove. Crystallography has provided structural evidence for the importance of chirality in mediating the interaction between oxaliplatin and duplex DNA (10). With oxaliplatin, like cisplatin, adduct lesions are repaired by the nucleotide excision repair system. Oxaliplatin, like cisplatin, is detoxified by glutathione (GSH)-related enzymes. ERCC1 and XPA expressions were predictive of oxaliplatin sensitivity in 6 colon cell lines *in vitro* (11). Oxaliplatin combined with 5-Fluorouracil and folinic acid improved the response rate and progression-free and overall survival of patients with advanced colorectal cancer (12). The dose-limiting adverse reaction of oxaliplatin is neurotoxicity (sodium channel inactivation) and the kinetics are altered after exposure of animals to oxaliplatin. The results from preliminary clinical studies indicate that the sodium channel blockers carbamazepine and gabapentin may be effective in preventing neurotoxicity (13).

Liposomal encapsulation of oxaliplatin was achieved using Regulon's platform technology (data not shown). The new drug (lipoxal) has completed stability and chemical testing and one formulation was chosen for preclinical studies in January 2003.

Table I. *Liposal dose escalation.*

Dose level	No. of patients	Lipoxal (mg/m^2 per week)
First	3	100
Second	3	150
Third	5	200
Fourth	4	250
Fifth	4+4	300
Sixth	4	350

Animal Data

Animal studies of a liposomal oxaliplatin (lipoxal) have shown the following. Intraperitoneal (*i.p.*) injection of lipoxal, or oxaliplatin as a control, in rats was used to study tissue biodistribution from 10 min to 7 days post-injection. The maxima levels of total platinum (Pt) in the plasma at a dose of 15 mg/kg were 14.0 μg/ml after lipoxal injection compared to 7.5 μg/ml after oxaliplatin treatment; these levels were attained at 7-20 min after injection. Similar plasma pharmacokinetic behavior was observed for kidney tissue; the plasma and kidney had the highest levels of platinum during the first 20 min after injection. Spleen tissue exhibited over 2 times higher levels of platinum after oxaliplatin treatment, compared to lipoxal at the same dose level during an extended period of 40-190 h post-injection. Following 11 repetitive administrations of lipoxal in rats, the spleen attained astonishingly high levels of total Pt in all tissues examined (100 μg/g tissue). The liver exhibited similar pharmacokinetics of Pt accumulation as a function of time after oxaliplatin *versus* lipoxal treatment (data not shown). The liposomal form of oxaliplatin (lipoxal) reduces the adverse reactions of the encapsulated cytotoxic agent without reducing effectiveness.

The present study was a clinical trial with liposomal oxaliplatin (lipoxal) with the following primary objectives: a) to define the dose-limiting toxicity (DLT) and maximum tolerated dose (MTD) of escalating doses of weekly lipoxal administration and, b) to detect the toxicity profile and pharmacokinetics of lipoxal monotherapy in pretreated advanced GI tract cancer patients. The secondary objectives were to determine efficacy and survival.

Patients and Methods

The study was a phase I cohort, dose-escalation trial of lipoxal. The study protocol was reviewed and approved by our Institutional Review Board. An informed consent document satisfying all institutional requirements was read by the patients and signed as a condition of their registration.

Table II. *Patients' characteristics at baseline.*

		No.	%
Total No. of patients		27	100
Age (yr)			
Median	62		
Range	32-78		
Gender			
Male		18	66.7
Female		9	33.3
Performance status			
0		2	7.4
1		14	51.9
2		11	40.7
Stage IV		27	100
Primary tumor			
Colorectal		12	44.4
Pancreas		8	29.6
Stomach		4	14.8
Biliary		2	7.4
Liver		1	3.7
Histology			
Adenocarcinoma		27	100

Eligibility criteria. All patients were required to meet the following criteria: confirmed histological or cytological diagnosis of cancer, at least 1 bidimensionally measurable or evaluable disease, WHO performance status 0-2, a life expectancy greater than 3 months, previous treatment by standard chemotherapy at the time of entry and refractory to any prior cytotoxic treatment. Patients were eligible if they had had 2 or 3 previous courses, provided that they had been off treatment for at least 3 weeks.

Assessment. The eligible patients over 18 years of age were required to have adequate hematological, renal and hepatic functions as defined by WBC count $3.5x10^9/l$, absolute neutrophil count $1.5x10^9/l$, platelet count $100x10^9/l$, hemoglobin level 9 g/dl, total bilirubin level 1.5 mg/dl, ALT and AST twice the upper normal limit in the absence of liver metastases or 5 times the upper normal limit in the case of documented liver metastasis, and creatinine level 1.5 mg/dl. A medical history, physical examination, assessment of vital signs, electrocardiogram, chest and abdominal computed tomography (CT) or ultrasound were performed before treatment. During treatment (1 day before each course) blood count, blood urea and sugar, serum creatinine and uric acid tests, and ECG were done. CT scan assessments were done after at least 8 weekly drug infusions, or earlier in the case of disease progression.

Treatment plan. Lipoxal was supplied by Regulon Inc. Biotechnology Company, Mountain View, CA 94043, USA. Drug characteristics: provided in 3 mg/ml, 50 ml per glass vial, 150 mg of oxaliplatin per glass vial; stored at 4˚C, opaque appearance, characteristic of a liposomal drug. Lipoxal is diluted in 1 L 5% dextrose and given in a 3-hour intravenous (*i.v.*) infusion once weekly for 8 consecutive weeks. In case of side-effects and, in particular, myelotoxicity or neurotoxicity, a delay of treatment by

Table III. *Plasma pharmacokinetic parameter estimates for lipoxal in patients.*

Dose (mg/m^2)	C_{max} (μg Pt/ml)	AUC (μg Pt*h/ml)	Cl ($L/h*m^2$)	K_{el} (l/h)	$t_{1/2}$ (h)	V_{ss} (L/m^2)
250	9.175	424.4	0.289	0.028	24.3	9.7
350	12.087	782.3	0.219	0.020	35.5	10.9

Abbreviations and parameters as in the text.

1 week would take place. No pre- or post hydration was needed. No other drugs, such as antiemetic or anti-allergic, were planned to be given prophylactically. In case of nausea or vomiting, antiemetics (ondansetron) or antiallergic (dexamethasone) were used.

In preceding animal studies, approximately 400 mg/m^2 to 600 mg/m^2 were defined as the MTD. In humans, a dose of 100 mg/m^2 was introduced for level one and the dosage increase was decided at 50 mg/m^2 per level. The dose escalation of lipoxal per group is shown in Table I.

Drug-related toxicities were evaluated during each cycle of therapy and graded according to WHO criteria. The DLT was defined as any grade 3 or 4 toxicity, with a neutrophil count <500 ml associated with fever persisting longer than 72 h, in 50% of the patients. Other grade 2-3 toxicities, in particular neurotoxicity, were also considered as DLT if observed in at least 50% of the patients. One dose level lower than that of DLT was defined as the MTD. Cohorts of a minimum of 3 patients were scheduled for entry at each dose level. The dose was escalated to the next higher level after all 3 patients had received at least 1 cycle. The treatment was discontinued with the occurrence of a DLT and the patient continued at 1 dose level below.

Pharmacokinetics. For the pharmacokinetic study, blood samples were taken at the following hours: 0 (before drug infusion) and after the start of the infusion at 1, 3, 6, 24, 98, 120 (5 days) and 168 (7 days) h. Three ml of blood were drawn into EDTA or heparin-containing tubes and were then centrifuged and refrigerated at 2˚C before being sent for laboratory analysis for total Pt levels. Blood samples from 5 patients at 350 mg/m^2 dose levels were used for the pharmacokinetic studies. The Pt levels (total and serum ultrafiltrates) were measured by atomic absorption (Perkin Elmer AA 700 Graphite Furnace Atomic Absorption Spectrometer at Regulon A.E.); the area under the plasma concentration-time curve (AUC) and the C_{max} (maximum concentration of total Pt in serum) were calculated. The total body clearance (Cl) was calculated by $CL=D_{iv}/AUC$, where D_{iv} is the *i.v.* dose of lipoxal and AUC the relative Area Under the Curve for a specific dose. The K_{el} (elimination rate constant) was calculated by linear regression analysis of the logarithmic plasma concentration-time curve by the formula $K_{el}=[Ln(C_{p1})-Ln(C_{p2})]/(t_2-t_1)$, where t_1 and t_2 are the starting and ending time-points of measurements and C_{p1} and C_{p2} the starting and ending concentrations of total Pt in serum for t_1 and t_2, respectively.

The $t_{1/2}$ (elimination half-time) was calculated by the formula $t_{1/2}=0.693$ $(1/K_{el})$; $1/K_{el}$ is the MRT (mean residence time), the statistical moment analogy to half-life $t_{1/2}$ (14). In effect, the MRT represents the time for 63.2% of the administered dose to be eliminated.

Results

Patients. The patients' characteristics are shown in Table II. In total, 27 patients were enrolled (age range 32-78 years, median 62 years, males 18, females 9, performance status (PS) 0-2). All patients had undergone previous chemotherapy treatment.

Toxicity. Lipoxal GI tract toxicity was negligible. Without antiemetics (ondansetron), nausea or mild vomiting was observed, but with ondansetron administration, no nausea/vomiting was observed nor was diarrhea. Mild, grade 1 myelotoxicity (neutropenia) was only seen in 2 patients (7.4%) at the highest dose level (350 mg/m^2). There was no hepatotoxicity, renal toxicity or cardiotoxicity, nor was alopecia seen. Mild asthenia was observed in 3 patients.

The main side-effect was neurotoxicity, which was observed after at least 3 infusions of the agents; grade 1 neurotoxicity was seen at the 3rd and 4th dosage levels, grade 2 at the 5th level and grades 2-3 in 100% of the patients at the 6th level.

On the basis of these results, grade 2-3 neurotoxicity was considered as the DLT, which was observed in 100% of patients treated with 350 mg/m^2 of lipoxal; therefore, 300 mg/m^2 was defined as the MTD. The lipoxal dose escalation and the number of patients treated at each of the 6 levels are presented in Table I.

Pharmacokinetics. The results regarding the pharmacokinetics are presented in Table III and in Figures 1 and 2. The half-life of oxaliplatin in the plasma concentration was found to be 24.3 h at 250 mg/m^2 and 35.5 h at 350 mg/m^2 (Table III).

Compliance with treatment. A total number of 104 infusions (cycles) were administered, with a median of 4 cycles per patient (range 2-15). The median interval between cycles was 7 days. The dose intensity was 100% of that planned. No patient had a delay in treatment due to grade 3 or 4 hematological toxicity; however, patients at a dosage of 350 mg/m^2 after a maximum of 4 or 5 infusions (cycles) were given 2-week interval before the lower dose of 300 mg/m^2 was administered. Seventeen (63%) patients stopped

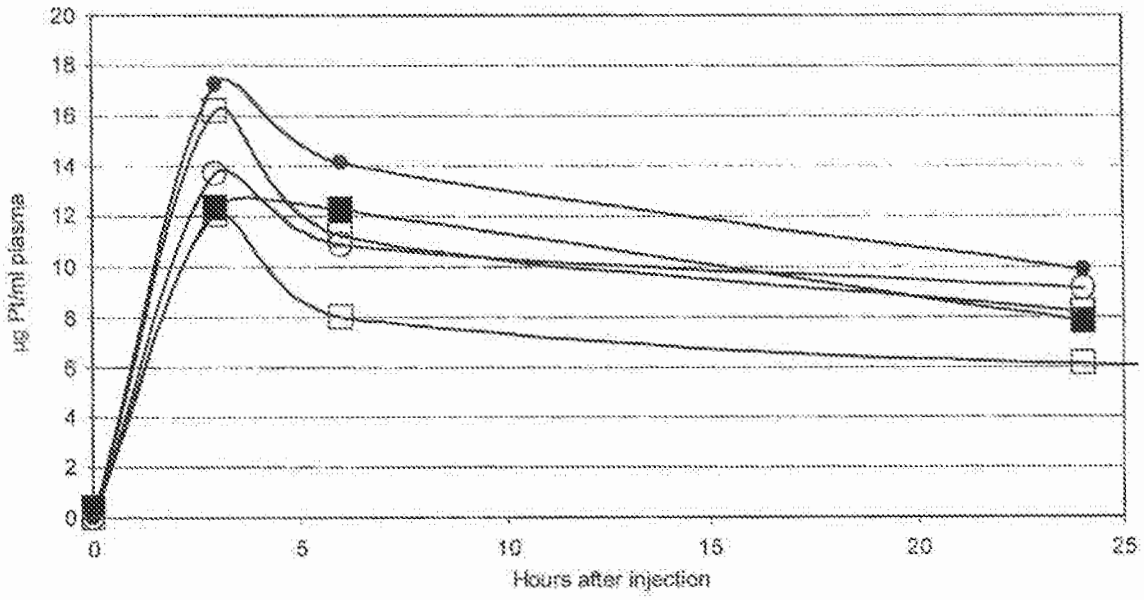

Figure 1. *Pt levels of 5 patients during lipoxal chemotherapy (0-25 hours). Lipoxal dose: 350 mg/m².*

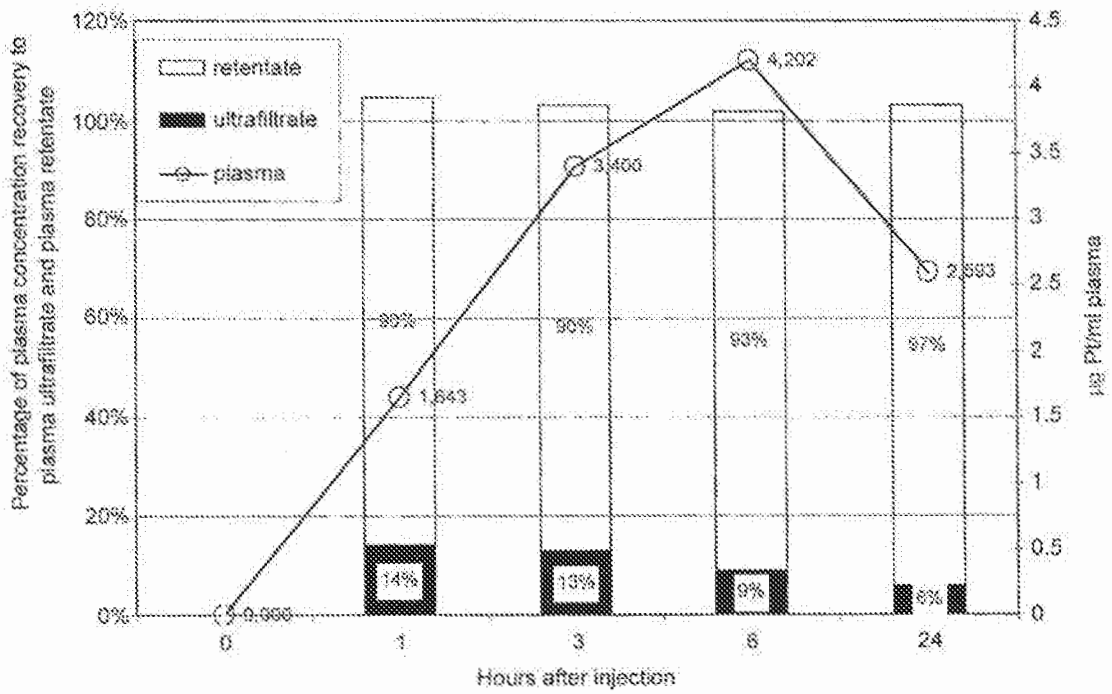

Figure 2. *Distribution of Pt levels in plasma during lipoxal chemotherapy treatment. Lipoxal dose: 420 mg (250 mg/m²).*

treatment due to disease progression after 4-6 cycles. Twelve patients (44.4%) were still alive at the end of the study.

Response to treatment. Responses were analyzed on an intention-to-treat basis. There were no complete responses. Three out of 27 patients (11.1%) achieved a partial response; 2 of these patients had gastric cancer, 1 of whom had pleural effusion and the other had bone metastases; the third was a patient with liver metastases from colon carcinoma. The determination of a partial response was

based on a CT-scan for the first patient, a bone scan for the second patient and a CT-scan and a bilirubin serum level value for the third patient. The third patient was treated while the serum bilirubin level was 51 mg/dl and, after 2 courses of treatment, the level dropped to 8 mg/dl and lasted for 5 weeks.

The duration of response was 4, 7 and 2 months for each of the above patients, respectively. Eighteen (66.7%) patients achieved stable disease with a median duration of 4 months (range 2-9 months). Six patients showed disease progression. In all 3 responders there was also a reduction of 50% or more of the marker CA-19-9 and performance status improved from 2 to 1.

Discussion

Liposomal oxaliplatin (lipoxal) was tested in the present trial as monotherapy in patients with advanced cancer of the gastrointestinal system. All patients had undergone standard pretreatment and all the included colorectal cancer patients had also been treated with oxaliplatin. The treatment with lipoxal has only had prior testing in preclinical studies and no other clinical trial has been previously performed. The present trial was based on preclinical study data and data on non-liposomal oxaliplatin. The latter mainly helped in focusing our present trial on estimating the similarities or differences of liposomal oxaliplatin *versus* standard oxaliplatin; GI tract and hematological side-effects were not observed with the former. The only side-effect that remained without any difference, *i.e.*, any reduction, was neurotoxicity. Neurotoxicity was often seen analogously with the increase in dosage of the agent; this became the only or main criterion for defining DLT. The MTD defined dose was 300 mg/m^2 administered weekly. There was also cumulative neurotoxicity, as is also the case with non-liposomal oxaliplatin. With respect to effectiveness, the 11% response rate observed in pretreated patients refractory to previously established tumors could be meaningful in future trials in a combined chemotherapy modality. It is also important to point out that the cancer types selected for this trial were not those which are the most sensitive to chemotherapy.

Liposomal oxaliplatin (lipoxal) is a well-tolerated agent. Although the MTD was established, further investigation is needed, particularly with other agents in combination.

References

1 De Gramont A, Vignond J, Tournigand C *et al*: Oxaliplatin with high-dose leucovorin and 5-fluorouracil 48-h continuous infusion in pretreated metastatic colorectal cancer. Eur J Cancer *33*: 214-219, 1997.

2 Giacchetti S, Perpoint B, Zidani R *et al*: Phase III multicentre randomized trial of oxaliplatin added to chronomodulated fluorouracil-leucovorin as first line treatment of metastatic colorectal cancer. J Clin Oncol *18*: 136-147, 2000.

3 De Gramont A, Figer A, Seymour M *et al*: Leucovorin and fluorouracil with or without oxaliplatin as first-line treatment in advanced colorectal cancer. J Clin Oncol *18*: 2938-2947, 2000.

4 Sougiakos J, Mavroudis D, Kakolyris S *et al*: Triplet combination with irinotecan plus oxaliplatin plus continuous-infusion fluorouracil and leucovorin as first-line treatment in metastatic colorectal cancer: a multicenter phase II trial. J Clin Oncol *20*: 2651-2657, 2002.

5 Scheithauer W, Kornek GV, Raderer M *et al*: Randomized multicenter phase II trial of two different schedules of capecitabine plus oxaliplatin as first-line treatment in advanced colorectal cancer. J Clin Oncol *21*: 1307-1312, 2003.

6 Goldberg RM, Sargent DJ, Morton RF *et al*: A randomized controlled trial of fluorouracil plus leucovorin, irinotecan, and oxaliplatin combinations in patients with previously untreated metastatic colorectal cancer. J Clin Oncol *22*: 23-30, 2004.

7 Sorbye H, Glimelius B, Berglund A *et al*: Multicenter phase II study of Nordic fluorouracil and folinic acid bolus schedule combined with oxaliplatin as first-line treatment of metastatic colorectal cancer. J Clin Oncol *22*: 31-38, 2004.

8 Cassidy J and Misset JL: Oxaliplatin-related side effects: characteristics and management. Semin Oncol *29(Suppl 15)*: 11-20, 2002.

9 Jerremalm E, Eksborg S and Ehrsson H: Hydrolysis of oxaliplatin-evaluation of the acid dissociation constant for the oxalato monodentate complex. J Pharm Sci *92*: 436-438, 2003.

10 Spingler B, Whittington DA and Lippard SJ: 2.4 crystal structure of an oxaliplatin 1,2-d (GpG) intrastrand cross-link in a DNA dodecamer duplex. Inorg Chem *40*: 5596-5602, 2001.

11 Arnould S, Hennebelle I, Canal P, Bugat R and Guichard S: Cellular determinants of oxaliplatin sensitivity in colon cancer cell lines. Eur J Cancer *39*: 112-119, 2003.

12 De Vita F, Orditura M, Matano E *et al*: A phase II study of biweekly oxaliplatin plus infusional 5-fluorouracil and folinic acid (FOLFOX-4) as first-line treatment of advanced gastric cancer patients. Br J Cancer *92(9)*: 1644-1649, 2005.

13 Lersch C, Schmelz R, Eckel F *et al*: Prevention of oxaliplatin-induced peripheral sensory neuropathy by carbamazepine in patients with advanced colorectal cancer. Clin Colorectal Cancer *2*: 54-58, 2002.

14 Gibaldi M and Perrier D: Non-compartmental analysis based on the statistical moment theory. *In*: Pharmacokinetics. 2nd edition. New York: Marcel Dekker, pp. 409-417, 1982.

Received October 12, 2005
Accepted December 6, 2005

Combining two strategies to improve perfusion and drug delivery in solid tumors

Triantafyllos Stylianopoulos[a] and Rakesh K. Jain[b,1]

[a]Department of Mechanical and Manufacturing Engineering, University of Cyprus, 1678 Nicosia, Cyprus; and [b]Edwin L. Steele Laboratory, Department of Radiation Oncology, Massachusetts General Hospital, Harvard Medical School, Boston, MA 02114

Contributed by Rakesh K. Jain, October 2, 2013 (sent for review June 7, 2013)

Blood perfusion in tumors can be significantly lower than that in the surrounding normal tissue owing to the leakiness and/or compression of tumor blood vessels. Impaired perfusion reduces oxygen supply and results in a hypoxic microenvironment. Hypoxia promotes tumor progression and immunosuppression, and enhances the invasive and metastatic potential of cancer cells. Furthermore, poor perfusion lowers the delivery of systemically administered drugs. Therapeutic strategies to improve perfusion include reduction in vascular permeability by vascular normalization and vascular decompression by alleviating physical forces (solid stress) inside tumors. Both strategies have shown promise, but guidelines on how to use these strategies optimally are lacking. To this end, we developed a mathematical model to guide the optimal use of these strategies. The model accounts for vascular, transvascular, and interstitial fluid and drug transport as well as the diameter and permeability of tumor vessels. Model simulations reveal an optimal perfusion region when vessels are uncompressed, but not very leaky. Within this region, intratumoral distribution of drugs is optimized, particularly for drugs 10 nm in diameter or smaller and of low binding affinity. Therefore, treatments should modify vessel diameter and/or permeability such that perfusion is optimal. Vascular normalization is more effective for hyperpermeable but largely uncompressed vessels (e.g., glioblastomas), whereas solid stress alleviation is more beneficial for compressed but less-permeable vessels (e.g., pancreatic ductal adenocarcinomas). In the case of tumors with hyperpermeable and compressed vessels (e.g., subset of mammary carcinomas), the two strategies need to be combined for improved treatment outcomes.

tumor microenvironment | vessel decompression | vessel permeability | mechanical forces | mathematical modeling

Perfused vessels are necessary for enabling adequate oxygenation and distribution of systemically administered drugs in solid tumors. However, perfusion rates in some regions of a tumor can be significantly lower than that in the peritumor normal tissue, leading to hypoxia, low pH, and inadequate drug delivery. Impaired blood perfusion in tumors could result from (*i*) excessive fluid loss from the vasculature to the interstitial space owing to vessel hyperpermeability (Fig. 1*A*), (*ii*) increased resistance to fluid flow caused by vessel tortuosity, and (*iii*) reduced effective cross-sectional area for blood flow due to vessel compression (Fig. 1*C*) (1, 2). Vessel hyperpermeability and tortuosity can be lowered using judicious doses of antiangiogenic agents (Table 1), which increases pericyte coverage and fortifies the leaky vessels without excessive pruning of vessels. This strategy—referred to as "vascular normalization"—can improve tumor perfusion and thereby increase oxygen and drug delivery as well as treatment efficacy (1, 3–6). Fig. 1 *A* and *B* shows a schematic of how vascular normalization can improve perfusion by improving the structure and composition of the vessel wall, and Table 1 summarizes evidence in various preclinical tumor models and in cancer patients.

Vessel compression is a result of physical forces—referred to as solid stress—accumulated within solid components of tumors (cancer and stromal cells, collagen, and hyaluronan) (23–25). Stress alleviation can be achieved by depletion of any or all of these components, which can reopen compressed vessels and improve perfusion and delivery of drugs (25, 26). The schematic in Fig. 1 *C* and *D* shows how depletion of cancer or stromal cells can decompress blood vessels, and Table 2 presents therapeutic agents that have been used to deplete components of tumors and decompress tumor vessels.

One challenge now is to better understand under what conditions vascular normalization and vessel decompression improve perfusion in solid tumors and to develop guidelines for optimal use alone and in combination. To this end, we use a mathematical model for fluid flow and drug transport in tumors that accounts explicitly for the geometry and leakiness of the blood vessels. Our model accounts for preclinical and clinical data and suggests guidelines for effective use of these two therapeutic strategies. The tumor vasculature is represented as a percolation network with one inlet and one outlet (31, 32) (Fig. S1). The baseline value for the diameter of the vessels is set at 15 μm (1), whereas the leakiness is defined by the size (i.e., diameter) of the pores of the vessel wall. The pore size in our analysis varies from 50 nm (poorly permeable tumor vessels) to 400 nm (hyperpermeable vessels) (33). To quantify vascular efficiency we calculate the fraction of perfused vessels and the effective vascular density. Perfused vessels are considered to be those with velocities greater than 0.1 mm/s (34), whereas the effective vascular density is the density of the perfused vessels. Perfusion is considered optimal when these two parameters are maximal.

Results

Vessel Decompression Improves Perfusion in Tumors with Abundant Compressed but Poorly or Moderately Permeable Vessels. We first investigated under what conditions decompression of blood vessels with stress-alleviation treatment can improve tumor perfusion. We modeled vessel decompression by increasing the diameter of the vessels to the baseline value. The effects for different vessel wall pore sizes are shown in Fig. 2, and in Figs. S2

Significance

Vascular normalization and stress-alleviation treatments are promising strategies to improve tumor perfusion and delivery of drugs. Vascular normalization is more effective for tumors with hyperpermeable but uncompressed vessels, whereas stress alleviation is more beneficial for compressed but low-permeable vessels. In the case of tumors with hyperpermeable and compressed vessels, the two strategies need to be combined for improved treatment.

Author contributions: T.S. and R.K.J. designed research; T.S. performed research; T.S. and R.K.J. analyzed data; and T.S. and R.K.J. wrote the paper.

Conflict of interest statement: R.K.J. received research grants from MedImmune and Roche; received consultant fees from Enlight, Noxxon, and Zyngenia; owns equity in Enlight, SynDevRx, and XTuit; and serves on the Board of Directors of XTuit and Boards of Trustees of H&Q Healthcare Investors and H&Q Life Sciences Investors. No reagents or funds from these organizations were used in this study.

Freely available online through the PNAS open access option.

[1]To whom correspondence should be addressed. E-mail: jain@steele.mgh.harvard.edu.

This article contains supporting information online at www.pnas.org/lookup/suppl/doi:10.1073/pnas.1318415110/-/DCSupplemental.

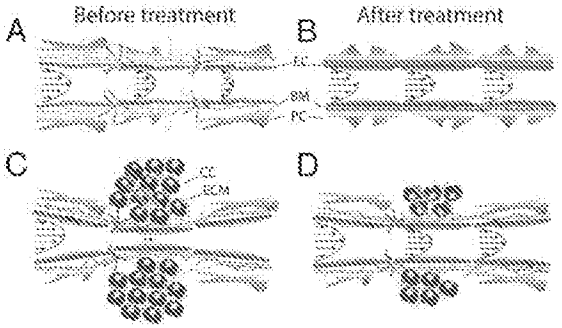

Fig. 1. Schematic of therapeutic strategies to improve tumor perfusion. (*A*) Abnormalities in interendothelial junctions, pericyte coverage, and/or basement membrane lead to hyperpermeability of tumor blood vessels and excessive fluid leakage that slows down blood flow. (*B*) Vascular normalization fortifies the vessel wall, resulting in smaller interendothelial gaps ("pores") and improved perfusion. (*C*) Structural components of the tumor microenvironment exert forces on blood vessels, resulting in vessel compression and reduced blood flow. (*D*) Alleviation of these forces by selective depletion of tumor constituents (e.g., cells or extracellular matrix) can decompress the vessels and improve vessel perfusion. BM, basement membrane; CC, cancer and/or stromal cell; EC, endothelial cell; ECM, extracellular matrix; PC, pericyte.

and S3 for compressed central regions occupying 80% and 30% of the tumor, respectively. The figures show that our results are qualitatively independent from the region of vessel compression. For pore sizes less than 200 nm (low or moderately permeable tumors), there is a strong dependence of the fraction of perfused vessels and the effective vascular density on increases in vessel diameter. Recently, we found that stress-alleviation therapy in murine pancreatic ductal adenocarcinomas increased vessel diameter by 20% (from 10 to 12 μm) and the perfused vessel fraction by 47% (from 0.32 to 0.47) (25). Our model predictions are within this range and, moreover, they show that perfusion is optimal for uncompressed vessels with low permeability. Therefore, vessel decompression would be most beneficial for tumors with abundant compressed but poorly or moderately permeable vessels (Fig. 2, dashed line), such as pancreatic ductal adenocarcinomas. However, decompression of tumor vessels is reversible and vessels can revert to their compressed state unless stress-alleviation treatment is continued.

The ease with which the interstitial fluid percolates through the extravascular space of a tissue is referred to as its hydraulic conductivity. Hydraulic conductivity affects blood velocity because of the communication between vascular and interstitial fluid (35). High hydraulic conductivity allows fluid to rapidly flow in the interstitial space and be drained by peripheral lymphatic vessels. This prevents accumulation of interstitial fluid and thus more fluid can leak from the vessel wall, which in turn decreases perfusion. Results shown in Fig. 2 and Fig. S2 suggest that tumors with a relatively high hydraulic conductivity, usually tumors with low collagen and hyaluronan levels such as some melanomas, would be less responsive to stress-alleviation treatment.

Vascular Normalization Improves Perfusion of Tumors with Hyperpermeable and Uncompressed Vessels. In parallel, we tested under what conditions vascular normalization can improve perfusion (Fig. 3). The tumor vessel was assigned an initial diameter of 15 μm and a vascular pore size of 400 nm (circle in the top right corner of Fig. 3). An ideal treatment to optimize perfusion in such a vessel would aim at decreasing its permeability while keeping the vessel open. In our previous animal study (36), the vessel diameter changed from 14.5 μm to 7.3, 9.5, and 9.5 μm at days 1, 3, and 5 after anti-VEGF treatment, a predominant angiogenic growth factor in many tumors. The solid lines in the figure show the potential paths of the treatment as the diameter decreased from 14.5 μm to 7.3 μm (day 1) or 9.5 μm (days 3 and 5). Even though the decrease in pore size was not measured, there is a large range of pore sizes for which treatment falls into the optimal perfusion region. One should note that vascular normalization is reversible and if anti-VEGF treatment is stopped the vascular structure will return to an abnormal, less-functional state (37). Indeed, in our clinical trial in recurrent glioblastoma patients we saw a similar reversal in tumor vessel structure and function (38).

In another study (10), we found that the increase in tumor perfusion was dependent on the dose of anti-VEGF receptor 2 (VEGFR2) antibody used. The lowest dose of anti-VEGFR2 antibody caused an increase in the perfused vessel fraction from 0.2 to 0.45, whereas the highest dose did not increase perfusion. These values of perfused vessel fraction are within the range of our study—the highest dose of the antibody led to a significant decrease in vessel diameter and/or pruning of tumor vessels, yielding

Table 1. Studies showing vascular normalization improves perfusion measured as improved oxygenation

Therapeutic agent	Tumor model	Effect on oxygenation (refs.)
Antibody		
Bevacizumab	Melanoma, breast and ovarian carcinomas, GBM	↑ (7, 8)
DC101	GBM, mammary carcinoma	↑ (9, 10)
TKI		
Cediranib	GBM	↕ (11–13)*
Sunitinib	Squamous carcinoma	↕ (14)
Semaxanib	Melanoma	↑ (15)
Other therapies		
PI-103 (PI3K inhibitor)	Fibrosarcoma, squamous carcinoma	↑ (16)
FTIs (Ras inhibitors)	Prostate carcinoma, bladder carcinoma, glioma, fibrosarcoma, squamous carcinoma	↕ (16–18)
Nelfinavir (AKT inhibitor)	Fibrosarcoma, squamous carcinoma	↑ (16)
PHD2 down-regulation	Lung carcinomas	↑ (19)
R-Ras up-regulation	Melanomas and lung carcinomas	↑ (20)
Cancer cells nitric oxide synthesis inhibition	Glioblastomas	↕ (21)
VE-PTP inhibition	Breast carcinomas	↕ (22)

Information given in the table is updated from ref. 5. FTI, farnesyltransferase inhibitors; GBM, glioblastoma multiforme; PHD2, prolyl hydroxylase domain protein 2; TKI, tyrosine kinase inhibitor; VE-PTP, vascular endothelial protein tyrosine phosphatase.
*Clinical evidence.

Table 2. Studies showing stress alleviation decompresses vessels and improves perfusion

Therapeutic agent	Target	Tumor model	Effect on vessel diameter/density (refs.)	Effect on perfusion (refs.)
Diptheria toxin	Cancer cells	Soft tissue sarcoma	↑ (24)	Not reported
Taxane	Cancer cells	Soft tissue sarcoma	↑ (23)	Not reported
Saridegib	Stromal cells	Pancreatic ductal carcinoma	↑ (25, 27)	↑ (25, 27)
PEGPH20	Hyaluronan	Pancreatic ductal carcinoma	↑ (28, 29)	↑ (28, 29)
1D11	Collagen	Mammary carcinoma	↑ (30)	↑ (30)
Losartan	Stromal cells, hyaluronan, collagen	Pancreatic ductal carcinoma	↑ (26)	↑ (26)

Diphtheria toxin is preferentially toxic to human cancer cells and thus preferentially kills cancer cells in a human tumor xenograft model. Taxane is a chemotherapeutic agent. Saridegib is an inhibitor of the Hedgehog cellular signaling pathway. PEGPH20 is a PEGylated human recombinant hyaluronidase. 1D11 is a TGF-β neutralizing antibody. Losartan is an angiotensin receptor blocker.

compromised perfusion (Figs. 3 and 4). Fig. 4 shows changes in perfusion as a function of time and dose. The region of improved perfusion is related to the window of normalization, and thus the higher the dose of treatment, the shorter the window of normalization, and excessive pruning would lead to hypoxia.

Other parameters that affect vascular normalization are the degree of vessel compression and the hydraulic conductivity. Our results suggest that effective anti-VEGF treatment requires tumor vessels to be open (Fig. 3). In cases where tumor vessels are compressed normalization of abnormal vessels and the resulting decrease in vascular permeability will not be sufficient to improve perfusion. Fig. S4 depicts the fraction of perfused vessels for three different values of the hydraulic conductivity. As for vessel decompression, a high conductivity compromises the therapeutic outcome. Taken all together, vascular normalization is expected to be more effective for tumors with hyperpermeable and uncompressed vessels with low or moderate values of hydraulic conductivity, such as a subset of glioblastomas, melanomas, and ovarian carcinomas.

Combined Treatment Improves Perfusion in Tumors with Compressed Yet Hyperpermeable Vessels. Our analysis thus far suggests that neither vessel decompression nor vascular normalization would be effective in treating tumors with compressed and hyperpermeable vessels, such as those seen in a subset of mammary carcinomas. In such a case, a combined treatment might be beneficial. A treatment to alleviate solid stress (depletion of cells or extracellular matrix) to decompress blood vessels would increase the effective vascular density without affecting significantly the fraction of perfused vessels (Fig. 2 and Fig. S2). Then, a subsequent or concurrent vascular normalization treatment would have the potential to improve perfusion (Fig. 3). Attention should be given, however, to the fact that stress-alleviation therapies, which aim to selectively deplete structural components of tumors, might increase the hydraulic conductivity of the interstitial space and thus reduce the therapeutic potential of vascular normalization. Indeed, the hydraulic conductivity depends on the concentration of collagen and hyaluronan, and empirical correlations to describe this relationship exist (39–41). In Fig. S5, we used these methodologies to calculate the hydraulic conductivity of tumors. Assuming that the optimal perfusion region is severely affected by conductivity values higher than 5×10^{-7} cm^2/mmHg-s (Fig. S4), data in Fig. S5 suggest that collagen or hyaluronan can be significantly decreased and still the tumors be responsive to anti-VEGF treatment. The schematic in Fig. 5 summarizes the guidelines for improving perfusion with these two strategies based on our baseline values. Fig. S6 provides examples from preclinical studies.

Improved Perfusion Enhances Delivery of Drugs. To elucidate the relationship between perfusion and drug delivery, we calculated the transport of drugs with sizes ranging from 1 nm (e.g., chemotherapeutic agents) to 10 nm (e.g., antibodies, nab-paclitaxel following disintegration in plasma) to 60 nm (e.g., liposomes and micelles). The model accounts for the transport of the drug from the vessels to the tumor interstitial space and for drug binding to and internalized by cancer cells (details are given in *Supporting Information*) (42–44). Fig. 6 shows the intratumoral distribution of the drug with low or high binding affinity as a function of the perfused vessel fraction. Intratumoral distribution is defined as the fraction of the tumor in which the drug is bound to cancer cells in amounts higher than 1% of the concentration at the inlet of the vascular network. Delivery is improved with improved perfusion for drugs of all sizes, and the effect is more prominent for small drugs with low binding affinity. Small drugs diffuse quickly in the tumor extracellular matrix and thus their transport is perfusion-limited. By contrast, large-size particles cannot effectively penetrate into the tumor tissue and a rate-limiting step is the interstitial transport. Binding to cells or matrix is an additional barrier to interstitial transport. The higher the binding affinity, the more difficult it is for the drug to spread into the tumor. Interestingly, for drugs binding with a high affinity, the distribution of the 10-nm and 60-nm drugs is the same. This suggests that drug binding to cells dominates interstitial diffusion, whereas for low binding affinity interstitial diffusion is important and for that reason 10-nm particles distribute better than 60-nm particles. Our results are in agreement with previous studies showing that delivery of 10-nm particles is superior compared with that of 60-nm and 120-nm particles in tumors following vascular normalization (32). In general, the smaller the drug, the better it will distribute into the tumor, unless binding dominates. This may explain why nab-paclitaxel (10 nm in size)

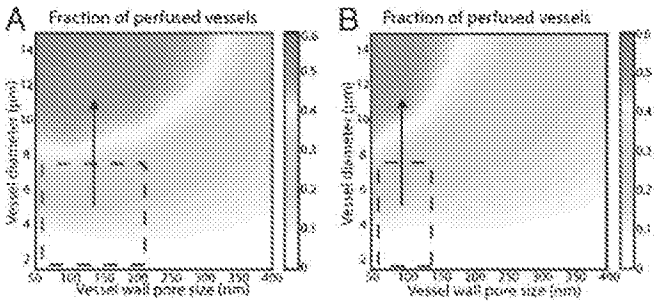

Fig. 2. Results for the fraction of perfused vessels as a function of the vessel diameter and the vessel wall pore size, a determinant of vascular permeability. Two values of the hydraulic conductivity of the interstitial space were used. (*A*) 1×10^{-7} cm^2/mmHg-s and (*B*) 1×10^{-6} cm^2/mmHg-s. The compressed central region occupies 80% of the tumor. The colors represent the values of the fraction of perfused vessels and the dashed line depicts the region within which vessel decompression is beneficial. The fraction of the well-perfused vessels becomes optimal for uncompressed (larger diameter) and low-permeable (smaller vessel wall pore size) vessels. The fraction of perfused vessels decreases if the tumor vessels are compressed or hyperpermeable. Vessel decompression is beneficial for compressed and low-permeable vessels.

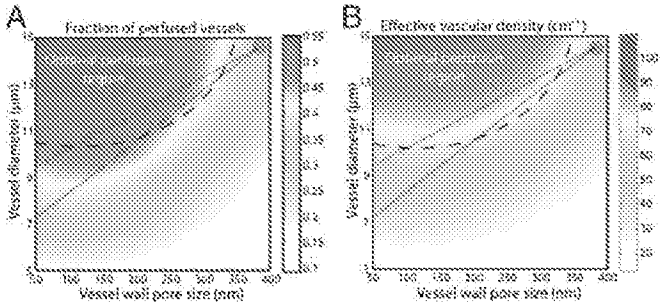

Fig. 3. Results for (*A*) fraction of perfused vessels and (*B*) effective vascular density as a function of vessel diameter and vessel wall pore size. The dashed line depicts the region within which vascular normalization is beneficial (referred to as optimal perfusion region), the circle shows the initial values, and the solid lines show potential paths of the treatment. The fraction of the well-perfused vessels and the effective vascular density become optimal for uncompressed (larger diameter) and low-permeable (smaller vessel wall pore size) vessels. The fraction of perfused vessels decreases if the tumor vessels are compressed or hyperpermeable. Vascular normalization is beneficial for compressed and hyperpermeable vessels.

improves overall survival of metastatic breast and pancreatic adenocarcinoma patients, whereas pegylated liposomal doxorubicin (100 nm in size) does not robustly improve survival over conventional chemotherapy (45–47).

Discussion

In this article, we used a mathematical framework for blood perfusion in solid tumors focusing on the effects of vessel leakiness and compression. In agreement with our model predictions,

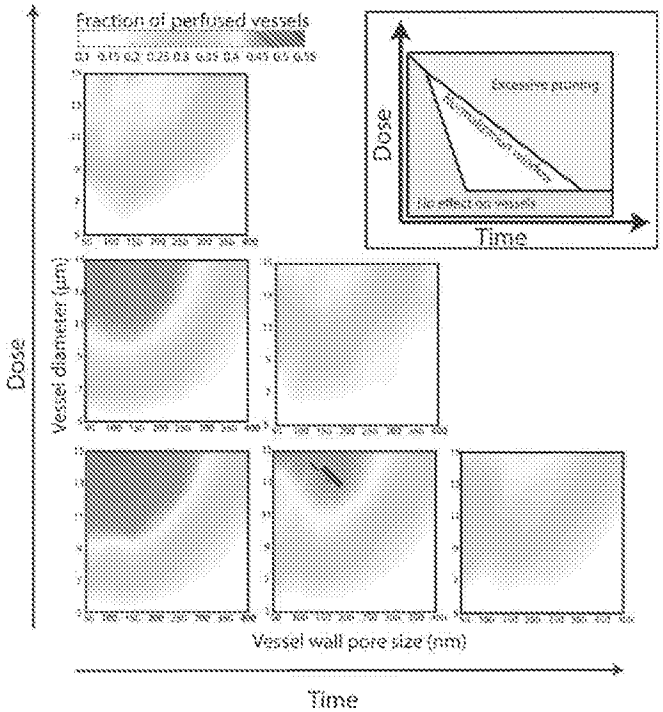

Fig. 4. Normalization window as a function of dose and time. Higher doses of antiangiogenic treatment over time increase vessel pruning, which in turn decreases the effective vascular density and impairs vascular efficiency. As a result the fraction of perfused vessels and the region of optimal perfusion decrease. These dose- and time-dependent effects create a normalization window within which drug delivery is optimized. (*Inset*) Schematic presents the effects of dose and time on the normalization window (adapted from ref. 2).

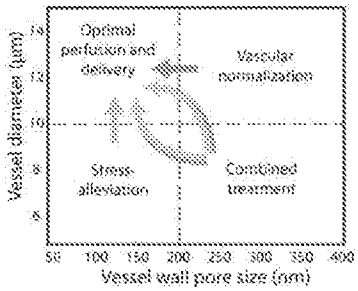

Fig. 5. Schematic of the proposed therapeutic strategies to improve perfusion and drug delivery. Tumors with hyperpermeable and uncompressed vessels benefit from vascular normalization strategy (red arrow). Tumors with compressed and low or moderately permeable vessels benefit from vessel decompression/stress-alleviation strategy (green arrow). Tumors with compressed and hyperpermeable vessels benefit from the application of stress-alleviation treatment to decompress vessels along with vascular normalization treatment to decrease permeability (two-color arrows).

vascular normalization has been shown to improve perfusion and therapeutic outcomes in both animal and human studies (9–13, 22, 32, 48) (Table 1). It is, however, effective mainly in the setting of leaky tumor vessels with open lumen (e.g., glioblastomas) and might not benefit compressed vessels. This would explain why antiangiogenic agents have failed thus far in desmoplastic tumors such as pancreatic ductal adenocarcinomas, with abundant compressed vessels (49, 50). Furthermore, anti-VEGF treatment has a dose-dependent effect, and a high dose or long-term treatment with anti-VEGF agents can cause excessive pruning of vessels and impairment of vascular efficiency (Fig. 4 and refs. 2 and 10). This could explain why in many studies antiangiogenic strategies reduce drug delivery (51–55). Monitoring of blood perfusion or oxygenation in tumors during treatment could be used to identify the right dose. This could be done, for instance, with a novel functional MRI approach termed "vessel architecture imaging" (13). Additionally, anti-VEGF treatment has a size-dependent effect because the decrease in vessel wall pore size might exclude the delivery of nanoscale drugs larger than the pore size. Indeed, we have recently shown that normalization treatment improved the delivery of small particles with a size of 10 nm but not the delivery of 60-nm and 120-nm particles (32). In our analysis anti-VEGF agents were considered to cause a decrease in vessel diameter and vascular density, which compromises the benefit of reducing vessel leakiness on perfusion. One notable exception is when vessels are normalized with restoring nitric oxide gradients, which increases both vessel density and diameter (21, 22, 56). Finally, vessel leakiness is a hallmark of inflammation as well. In inflammation, however, plasma extravasation and leukocyte adhesion occur in a coordinated manner to enable the immune response and to maintain tissue perfusion.

Our model suggests that treatment to alleviate solid stress in tumors has the potential to enhance blood flow. Many studies, indeed, support the idea that decompression of blood vessels by alleviating solid stress improves perfusion and treatment efficacy (Table 2). We have recently shown that depletion of hyaluronan or collagen can lower solid stress levels in a variety of tumors, including pancreatic cancers (25, 26). This reduction in solid stress may explain how enzymatic degradation of hyaluronan combined with cytotoxic agents can improve perfusion and the overall survival of mice bearing pancreatic ductal adenocarcinomas (28, 29). Furthermore, depletion of collagen using losartan, an angiotensin receptor blocker, or an anti–TGF-β antibody improved the in vivo delivery of therapeutics in a variety of tumors in mice (26, 30, 57). In addition, pharmacological depletion of stromal cells with saridegib, an inhibitor of the Sonic Hedgehog pathway, has been shown to decrease solid stress (25) and improve drug delivery and overall survival of mice bearing pancreatic tumors (27). This drug, however, recently failed in a phase-II

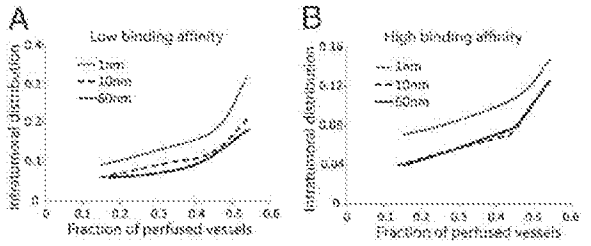

Fig. 6. Intratumoral distribution of therapeutic agents as a function of perfused vessel fraction for drugs with (*A*) low binding affinity and (*B*) high binding affinity (details in *Supporting Information*). Three curves in each panel show the intratumoral distribution of drugs of three sizes (1, 10, and 60 nm) versus the fraction of perfused vessels. The curves demonstrate that the intratumoral distribution of drugs of all three sizes increases with the fraction of perfused vessels, but in a nonlinear manner. The increase is more substantial for smaller drugs than for larger drugs. Intratumoral distribution is defined as the fraction of the tumor extravascular space that the drug is bound to cancer cells in amounts higher than 1% of the concentration at the inlet of the vascular network.

clinical trial for pancreatic cancer patients when combined with gemcitabine (58), presumably owing to intrinsic resistance to gemcitabine by these tumors. Increased delivery of a drug might not benefit patients if cancer cells are resistant to that drug.

Retrospective analysis of clinical data has shown that patients with pancreatic ductal adenocarcinomas receiving angiotensin receptor blockers survive approximately 6 mo longer than those who do not (59). Similar retrospective analyses have shown increased survival in patients with lung or renal cancers treated with such drugs (60, 61). Indeed, based on our preclinical findings (26), our Massachusetts General Hospital colleagues have initiated a phase-II trial with losartan and FOLFIRINOX in pancreatic ductal adenocarcinoma patients (clinicaltrials.gov identifier NCT01821729). Finally, depletion of cells with chemotherapeutics (or fractionated radiation) is another way to alleviate stresses and decompress vessels, which might explain the greater tumor response to chemotherapy in a subset of pancreatic cancer patients who are able to tolerate a combination of highly toxic drugs (62).

Our current study is of particular importance because it proposes new considerations for the use of treatments that modify the tumor microenvironment. Vessel compression is caused by physical forces exerted by the cells and extracellular matrix (25). Therefore, desmoplastic tumors should have a large amount of compressed vessels and thus anti-VEGF drugs (Table 1) most likely would not work, unless these drugs also alleviate solid stress by depleting stromal elements. If not, stress-alleviation drugs (Table 2) to decompress vessels should be considered either alone or in combination with anti-VEGF agents (Table 1). Less-desmoplastic tumors are expected to have a low fraction of compressed vessels, and thus stress-alleviation treatment would not be required. In this case, the use of anti-VEGF treatment with agents that target cancer cells should be considered (Table 3). To turn our theoretical predictions into practice, one needs to identify which tumors are leaky, compressed, both, or neither. This is a challenging task. Although we can make some broad statements (e.g., pancreatic ductal adenocarcinomas are desmoplastic), there are many tumors such as breast cancers in which the degree of desmoplasia is highly variable from one tumor to the next and potentially from the primary site to the metastatic site, and thus it could be hard to choose an appropriate strategy until the state of that individual tumor is known. Emerging imaging approaches have the potential to help in this selection (13).

It is conceivable that opening blood vessels could bring more nutrients to the tumor and increase its growth rate. Also, the opened vessels could allow more metastatic cells to leave the primary tumor and increase metastases. Indeed, this has been shown in a number of preclinical studies (63, 64). Therefore, drugs that open vessels should be given only with concurrent cytotoxic treatments, such as chemotherapy, radiation therapy, immune therapy, or another cancer-cell–targeted treatment. Finally, apart from vessel compression and hyperpermeability, other causes of decreased blood flow in tumors include heterogeneous distribution of blood vessels, intravascular coagulation/thrombosis, and formation of vascular shunts (65, 66). Our model accounts for vascular heterogeneity with the use of an irregular network structure and by permitting vessel pruning. Mathematically, thrombosis is similar to vascular compression because both phenomena reduce the effective cross-sectional area of tumor blood vessels. Vascular shunts are short, high-flow vascular pathways that bypass long downstream pathways and thus exclude downstream regions from blood supply (66). Our model does not recapitulate the high heterogeneity of path lengths of the vessels as well as the enlargement of short flow pathways.

Table 3. Summary of barriers to and strategies for improved drug delivery

Tumor microenvironment	Strategy
Desmoplastic, moderately permeable tumors (e.g., pancreatic ductal adenocarcinomas)	Stress alleviation
Hyperpermeable, nondesmoplastic tumors (e.g., subset of glioblastomas and ovarian carcinomas)	Vascular normalization
Hyperpermeable, desmoplastic tumors (e.g., a subset of mammary carcinomas)	Combined treatment
Drug	**Delivery barrier**
Small size (≤ 10 nm), low binding affinity	Perfusion-limited transport. Improved perfusion increases delivery.
Large size (> 10 nm), low binding affinity	Perfusion, transvascular, and interstitial limited transport. Improved perfusion increases delivery.
Any size, high binding affinity	Additional barrier to interstitial transport. Improved perfusion increases delivery but benefit may be compromised.

Methods

The current model builds on our recently published framework (32, 67). The baseline parameters of the model are summarized in Table S1. Description of model equations, methodology, and limitations (Figs. S7 and S8) can be found in *Supporting Information*.

ACKNOWLEDGMENTS. We thank J. Baish, V. Chauhan, D. Duda, K. Emblem, D. Fukumura, E. Gerstner, S. Goel, L. Munn, T. Padera, and M. Datta. This work was supported by National Cancer Institute Grants P01-CA080124, R01-CA126642, R01-CA115767, R01-CA096915, R01-CA085140, and R01-CA098706; Federal Share Income Grant T32-CA073479; Department of Defense Breast Cancer Research Innovator Award W81XWH-10-1-0016 (to R.K.J.); and European Commission Grants FP7-PIRG08-GA-2010-276894 and ERC-2013-StG-336839 (to T.S.).

1. Jain RK (1988) Determinants of tumor blood flow: A review. *Cancer Res* 48(10): 2641–2658.

2. Jain RK (2013) Normalizing tumor microenvironment to treat cancer: Bench to bedside to biomarkers. *J Clin Oncol* 31(17):2205–2218.

3. Jain RK (2001) Normalizing tumor vasculature with anti-angiogenic therapy: A new paradigm for combination therapy. *Nat Med* 7(9):987–989.
4. Jain RK (2005) Normalization of tumor vasculature: An emerging concept in anti-angiogenic therapy. *Science* 307(5706):58–62.
5. Goel S, et al. (2011) Normalization of the vasculature for treatment of cancer and other diseases. *Physiol Rev* 91(3):1071–1121.
6. Goel S, Fukumura D, Jain RK (2012) Normalization of the tumor vasculature through oncogenic inhibition: An emerging paradigm in tumor biology. *Proc Natl Acad Sci USA* 109(20):E1214.
7. Dings RP, et al. (2007) Scheduling of radiation with angiogenesis inhibitors anginex and Avastin improves therapeutic outcome via vessel normalization. *Clin Cancer Res* 13(11):3395–3402.
8. McGee MC, et al. (2010) Improved intratumoral oxygenation through vascular normalization increases glioma sensitivity to ionizing radiation. *Int J Radiat Oncol Biol Phys* 76(5):1537–1545.
9. Winkler F, et al. (2004) Kinetics of vascular normalization by VEGFR2 blockade governs brain tumor response to radiation: Role of oxygenation, angiopoietin-1, and matrix metalloproteinases. *Cancer Cell* 6(6):553–563.
10. Huang Y, et al. (2012) Vascular normalizing doses of antiangiogenic treatment reprogram the immunosuppressive tumor microenvironment and enhance immunotherapy. *Proc Natl Acad Sci USA* 109(43):17561–17566.
11. Batchelor TT, et al. (2013) Improved tumor oxygenation and survival in glioblastoma patients who show increased blood perfusion after cediranib and chemoradiation. *Proc Natl Acad Sci USA*, 10.1073/pnas.1318022110.
12. Sorensen AG, et al. (2012) Increased survival of glioblastoma patients who respond to antiangiogenic therapy with elevated blood perfusion. *Cancer Res* 72(2):402–407.
13. Emblem KE, et al. (2013) Vascular architecture imaging identifies patient responders to anti-angiogenic therapy. *Nat Med* 19(9):1178–1183.
14. Matsumoto S, et al. (2011) Antiangiogenic agent sunitinib transiently increases tumor oxygenation and suppresses cycling hypoxia. *Cancer Res* 71(20):6350–6359.
15. Eichhorn ME, et al. (2008) Contrast enhanced MRI and intravital fluorescence microscopy indicate improved tumor microcirculation in highly vascularized melanomas upon short-term anti-VEGFR treatment. *Cancer Biol Ther* 7(7):1006–1013.
16. Qayum N, et al. (2009) Tumor vascular changes mediated by inhibition of oncogenic signaling. *Cancer Res* 69(15):6347–6354.
17. Cohen-Jonathan E, et al (2001) The farnesyltransferase inhibitor L744,832 reduces hypoxia in tumors expressing activated H-ras. *Cancer Res* 61(5):2289–2293.
18. Delmas C, et al. (2003) The farnesyltransferase inhibitor R115777 reduces hypoxia and matrix metalloproteinase 2 expression in human glioma xenograft. *Clin Cancer Res* 9(16 Pt 1):6062–6068.
19. Leite de Oliveira R, et al. (2012) Gene-targeting of Phd2 improves tumor response to chemotherapy and prevents side-toxicity. *Cancer Cell* 22(2):263–277.
20. Sawada J, et al. (2012) Small GTPase R-Ras regulates integrity and functionality of tumor blood vessels. *Cancer Cell* 22(2):235–249.
21. Kashiwagi S, et al. (2008) Perivascular nitric oxide gradients normalize tumor vasculature. *Nat Med* 14(3):255–257.
22. Goel S, et al. (2013) Effects of vascular-endothelial protein tyrosine phosphatase inhibition on breast cancer vasculature and metastatic progression. *J Natl Cancer Inst* 105(16):1188–1201.
23. Griffon-Etienne G, Boucher Y, Brekken C, Suit HD, Jain RK (1999) Taxane-induced apoptosis decompresses blood vessels and lowers interstitial fluid pressure in solid tumors: clinical implications. *Cancer Res* 59(15):3776–3782.
24. Padera TP, et al. (2004) Pathology: Cancer cells compress intratumour vessels. *Nature* 427(6976):695.
25. Stylianopoulos T, et al. (2012) Causes, consequences, and remedies for growth-induced solid stress in murine and human tumors. *Proc Natl Acad Sci USA* 109(38):15101–15108.
26. Chauhan VP, et al. (2013) Angiotensin inhibition enhances drug delivery and potentiates chemotherapy by decompressing tumour blood vessels. *Nat Commun* 4:2516, 10.1038/ncomms3516.
27. Olive KP, et al. (2009) Inhibition of Hedgehog signaling enhances delivery of chemotherapy in a mouse model of pancreatic cancer. *Science* 324(5933):1457–1461.
28. Jacobetz MA, et al. (2013) Hyaluronan impairs vascular function and drug delivery in a mouse model of pancreatic cancer. *Gut* 62(1):112–120.
29. Provenzano PP, et al. (2012) Enzymatic targeting of the stroma ablates physical barriers to treatment of pancreatic ductal adenocarcinoma. *Cancer Cell* 21(3):418–429.
30. Liu J, et al. (2012) TGF-β blockade improves the distribution and efficacy of therapeutics in breast carcinoma by normalizing the tumor stroma. *Proc Natl Acad Sci USA* 109(41):16618–16623.
31. Baish JW, et al. (1996) Role of tumor vascular architecture in nutrient and drug delivery: An invasion percolation-based network model. *Microvasc Res* 51(3):327–346.
32. Chauhan VP, et al. (2012) Normalization of tumour blood vessels improves the delivery of nanomedicines in a size-dependent manner. *Nat Nanotechnol* 7(6):383–388.
33. Hobbs SK, et al. (1998) Regulation of transport pathways in tumor vessels: Role of tumor type and microenvironment. *Proc Natl Acad Sci USA* 95(8):4607–4612.
34. Kamoun WS, et al. (2010) Simultaneous measurement of RBC velocity, flux, hematocrit and shear rate in vascular networks. *Nat Methods* 7(8):655–660.
35. Netti PA, Roberge S, Boucher Y, Baxter LT, Jain RK (1996) Effect of transvascular fluid exchange on pressure-flow relationship in tumors: A proposed mechanism for tumor blood flow heterogeneity. *Microvasc Res* 52(1):27–46.
36. Yuan F, et al. (1996) Time-dependent vascular regression and permeability changes in established human tumor xenografts induced by an anti-vascular endothelial growth factor/vascular permeability factor antibody. *Proc Natl Acad Sci USA* 93(25):14765–14770.
37. Mancuso MR, et al. (2006) Rapid vascular regrowth in tumors after reversal of VEGF inhibition. *J Clin Invest* 116(10):2610–2621.
38. Batchelor TT, et al. (2007) AZD2171, a pan-VEGF receptor tyrosine kinase inhibitor, normalizes tumor vasculature and alleviates edema in glioblastoma patients. *Cancer Cell* 11(1):83–95.
39. Swabb EA, Wei J, Gullino PM (1974) Diffusion and convection in normal and neoplastic tissues. *Cancer Res* 34(10):2814–2822.
40. Jain RK (1987) Transport of molecules in the tumor interstitium: A review. *Cancer Res* 47(12):3039–3051.
41. Levick JR (1987) Flow through interstitium and other fibrous matrices. *Q J Exp Physiol* 72(4):409–437.
42. Baxter LT, Jain RK (1991) Transport of fluid and macromolecules in tumors. III. Role of binding and metabolism. *Microvasc Res* 41(1):5–23.
43. Thurber GM, Schmidt MM, Wittrup KD (2008) Antibody tumor penetration: transport opposed by systemic and antigen-mediated clearance. *Adv Drug Deliv Rev* 60(12):1421–1434.
44. Mok W, Stylianopoulos T, Boucher Y, Jain RK (2009) Mathematical modeling of herpes simplex virus distribution in solid tumors: implications for cancer gene therapy. *Clin Cancer Res* 15(7):2352–2360.
45. O'Brien ME, et al., CAELYX Breast Cancer Study Group (2004) Reduced cardiotoxicity and comparable efficacy in a phase III trial of pegylated liposomal doxorubicin HCl (CAELYX/Doxil) versus conventional doxorubicin for first-line treatment of metastatic breast cancer. *Ann Oncol* 15(3):440–449.
46. Gradishar WJ, et al. (2005) Phase III trial of nanoparticle albumin-bound paclitaxel compared with polyethylated castor oil-based paclitaxel in women with breast cancer. *J Clin Oncol* 23(31):7794–7803.
47. Von Hoff DD, et al. (2013) Results of a randomized phase III trial (MPACT) of weekly nab-paclitaxel plus gemcitabine versus gemcitabine alone for patients with metastatic adenocarcinoma of the pancreas with PET and CA19-9 correlates. *J Clin Oncol Suppl* 31(abstr 4005).
48. Tong RT, et al. (2004) Vascular normalization by vascular endothelial growth factor receptor 2 blockade induces a pressure gradient across the vasculature and improves drug penetration in tumors. *Cancer Res* 64(11):3731–3736.
49. Kindler H, et al. (2007) A double-blind, placebocontrolled, randomized phase III trial of gemcitabine (G) plus bevacizumab (B) versus gemcitabine plus placebo (P) in patients (pts) with advanced pancreatic cancer (PC). A preliminary analysis of cancer and leukemia group B (CALGB). *J Clin Oncol* 25(18, Suppl):4508.
50. Philip PA (2008) Targeting angiogenesis in pancreatic cancer. *Lancet* 371(9630):2062–2064.
51. Daldrup-Link HE, et al. (2004) Decrease in tumor apparent permeability-surface area product to a MRI macromolecular contrast medium following angiogenesis inhibition with correlations to cytotoxic drug accumulation. *Microcirculation* 11(5):387–396.
52. Pastuskovas CV, et al. (2012) Effects of anti-VEGF on pharmacokinetics, biodistribution, and tumor penetration of trastuzumab in a preclinical breast cancer model. *Mol Cancer Ther* 11(3):752–762.
53. Chen Y, Balthasar JP (2012) Evaluation of a catenary PBPK model for predicting the in vivo disposition of mAbs engineered for high-affinity binding to FcRn. *AAPS J* 14(4):850–859.
54. Van der Veldt AA, et al. (2012) Rapid decrease in delivery of chemotherapy to tumors after anti-VEGF therapy: Implications for scheduling of anti-angiogenic drugs. *Cancer Cell* 21(1):82–91.
55. Arjaans M, et al. (2013) Bevacizumab-induced normalization of blood vessels in tumors hampers antibody uptake. *Cancer Res* 73(11):3347–3355.
56. Fukumura D, Yuan F, Endo M, Jain RK (1997) Role of nitric oxide in tumor microcirculation. Blood flow, vascular permeability, and leukocyte-endothelial interactions. *Am J Pathol* 150(2):713–725.
57. Diop-Frimpong B, Chauhan VP, Krane S, Boucher Y, Jain RK (2011) Losartan inhibits collagen I synthesis and improves the distribution and efficacy of nanotherapeutics in tumors. *Proc Natl Acad Sci USA* 108(7):2909–2914.
58. Hidalgo M, Von Hoff DD (2012) Translational therapeutic opportunities in ductal adenocarcinoma of the pancreas. *Clin Cancer Res* 18(16):4249–4256.
59. Nakai Y, et al. (2010) Inhibition of renin-angiotensin system affects prognosis of advanced pancreatic cancer receiving gemcitabine. *Br J Cancer* 103(11):1644–1648.
60. Wilop S, et al. (2009) Impact of angiotensin I converting enzyme inhibitors and angiotensin II type 1 receptor blockers on survival in patients with advanced non-small-cell lung cancer undergoing first-line platinum-based chemotherapy. *J Cancer Res Clin Oncol* 135(10):1429–1435.
61. Keizman D, et al. (2011) Angiotensin system inhibitors and outcome of sunitinib treatment in patients with metastatic renal cell carcinoma: A retrospective examination. *Eur J Cancer* 47(13):1955–1961.
62. Conroy T, et al.; Groupe Tumeurs Digestives of Unicancer; PRODIGE Intergroup (2011) FOLFIRINOX versus gemcitabine for metastatic pancreatic cancer. *N Engl J Med* 364(19):1817–1825.
63. Stockmann C, et al. (2008) Deletion of vascular endothelial growth factor in myeloid cells accelerates tumorigenesis. *Nature* 456(7223):814–818.
64. Rhim AD, et al. (2012) EMT and dissemination precede pancreatic tumor formation. *Cell* 148(1–2):349–361.
65. Folanga A, Marchetti M, Vignoli A (2013) Coagulation and cancer: Biological and clinical aspects. *J Thromb Haemost* 11(2):223–233.
66. Pries AR, Höpfner M, le Noble F, Dewhirst MW, Secomb TW (2010) The shunt problem: Control of functional shunting in normal and tumour vasculature. *Nat Rev Cancer* 10(8):587–593.
67. Stylianopoulos T, Soteriou K, Fukumura D, Jain RK (2013) Cationic nanoparticles have superior transvascular flux into solid tumors: Insights from a mathematical model. *Ann Biomed Eng* 41(1):68–77.

J Neurooncol (2010) 99:177–185
DOI 10.1007/s11060-010-0118-8

LABORATORY INVESTIGATION - HUMAN/ANIMAL TISSUE

Metronomic treatment of malignant glioma xenografts with irinotecan (CPT-11) inhibits angiogenesis and tumor growth

Shingo Takano · Hiroshi Kamiyama · Ryota Mashiko · Satoru Osuka · Eiichi Ishikawa · Akira Matsumura

Received: 3 November 2009 / Accepted: 4 January 2010 / Published online: 12 January 2010

Abstract Irinotecan (CPT-11) has shown emerging promise in the treatment of malignant gliomas. It is believed the mechanism of action of irinotecan is to sensitize glioma cells to the cytotoxic action of radiation therapy and alkylating agents. However, clinical trials using weekly or three-weekly doses of CPT-11 have demonstrated imaging responses in only 10–15% of patients. In this study, we evaluated another mechanism of action, angiosuppression by CPT-11 of ACNU-resistant gliomas, using a metronomic administration schedule. Two different types of treatment, (1) conventional and (2) metronomic, were applied to the subcutaneous U87 model. We found that metronomic administration of CPT-11 significantly inhibited malignant glioma growth by inhibiting angiogenesis; this treatment procedure reduced the number of tumor vessels and the area of hypoxic lesions and reduced expression of VEGF and HIF-1α, the most important angiogenic factors in gliomas. Metronomic treatment was superior to conventional treatment with regard to the severe systemic side effect of body weight loss. The growth inhibitory effect was very similar for both low and high doses of CPT-11. These angiosuppressive effects of CPT-11 show promise for another use of CPT-11 in metronomic and scheduled angiosuppressive chemotherapy with low dose and long-term administration for malignant gliomas without systemic side effects.

S. Takano (✉) · H. Kamiyama · R. Mashiko · S. Osuka · E. Ishikawa · A. Matsumura
Department of Neurosurgery, Institute of Clinical Medicine, Graduate School of Comprehensive Human Sciences, University of Tsukuba, 1-1-1 Tennoudai, Tsukuba city, Ibaraki 305-8575, Japan
e-mail: shingo4@md.tsukuba.ac.jp

Keywords Irinotecan · Angiosuppression · Vascular endothelial growth factor · Malignant glioma · ACNU · Xenografts · Metronomic treatment

Abbreviations

IC_{50}	The concentration of drug required to inhibit cell growth by 50% compared with non-drug-treated controls
MGMT	O^6-methylguanine-DNA methyltransferase
VEGF	Vascular endothelial growth factor

Introduction

Malignant gliomas have remained a major cause of death in adults and children despite therapeutic strategies that include maximum surgical resection followed by radiochemotherapy. Although there is great promise for future strategies involving anti-angiogenic agents, chemotherapy, or vaccines, it is likely to be years before we see true therapeutic benefits from these newer modalities. Other than the nitrosoureas (BCNU, ACNU, CCNU) and temozolomide, no agents have consistently resulted in clinical benefits for patients with gliomas.

Irinotecan has shown emerging promise in the treatment of malignant gliomas following many laboratory studies and phase I and II clinical trials [1, 2]. Currently, a phase II trial of BCNU and CPT-11 in adults with newly diagnosed or recurrent malignant gliomas, and phase I and II trials of CPT-11 and temozolomide are ongoing. CPT-11 may be important to neuro-oncology for a number of reasons. CPT-11, a topoisomerase I inhibitor, utilizes a different mechanism of action compared with other glioma therapies,

particularly the alkylating agents. Preclinical and clinical data indicate that irinotecan may sensitize glioma cells to the cytotoxic actions of radiation therapy and alkylating agents. In addition, CPT-11 is among a small group of cytotoxic agents that readily cross the blood–brain barrier. However, clinical trials using weekly or three-weekly doses of irinotecan have demonstrated imaging responses in only 10–15% of patients. Recent data for CPT-11 and bevacizumab combination therapy suggests there is a synergy between irinotecan and ant-VEGF therapies, with acceptable toxicity [3]. We have demonstrated the antiangiogenic action of CPT-11 in vitro [4], including the anti-VEGF and anti-HIF (hypoxia inducible factor) effects of CPT-11 itself. Moreover, metronomic dosing regimens—either continuous infusion or frequent administration without extended rest periods—could be targeting proliferating endothelial cells in the tumor [5]. In this study, we evaluated another mechanism of action, angiosuppression, of CPT-11 using a metronomic schedule in vivo in the glioma model.

Materials and methods

Establishment of the ACNU-resistant clone: U87AR

Because U87-MG has been known to express low levels of O^6-methylguanine-DNA methyltransferase (MGMT) mRNA, which is involved in the drug resistance of tumor cells to ACNU (Mineura et al., 1996), we chose U87 MG for establishment of the ACNU-resistant clone. U87-MG was obtained from the American Type Culture Collection (Rockville, MD, USA). Cells were maintained in MEM supplemented with 10% FCS in a humidified atmosphere containing 5% CO_2 at 37°C. U87 MG was cultured in MEM supplemented with 10% FCS and 10 μM ACNU in a humidified atmosphere containing 5% CO_2 at 37°C, and the medium was changed twice a week for five weeks. Total RNA was extracted from glioma cells using the RNeasy mini kit (Qiagen, Germany) and we performed RT-PCR using the GeneAmp RNA PCR Kit (Perkin–Elmer Cetus, Norwalk, CT, USA), as described previously [6]. Briefly, 1 μg total RNA was reverse transcribed by MuLV reverse transcriptase in the presence of random hexamers, followed by the indicated number of cycles of PCR reaction (95°C for 1 min, 55°C for 1 min, and 72°C for 1 min) in the presence of 2 μM MGMT-specific primers (35 cycles), or *β*-actin-specific primers (16 cycles) as a control. The MGMT primers included the reverse primer (5′-ATCCGATGCAGTGTTACACG-3′ within exon 5) and the forward primer (5′-ACCGTTTGCGACTTGGTACT-3′ within exon 1) [7]. The *β*-actin primers included the reverse primer (5′-GGAGTTGAAGGTAGTTTCGTG-3′) spanning bases 2429–2409 and the forward primer (5′-CGGGAAATCGTGCGTGACAT-3′) spanning bases 2107–2126 [8]. The predicted sizes of the amplified MGMT and *β*-actin DNA products were 923 and 214 bp, respectively. Quantification of these RT-PCR products was performed on a computer using the public domain NIH Image program (developed at the US National Institute of Health). After repeated exposure to ACNU, we obtained U87-MG cells that exhibited high expression of MGMT mRNA, which were referred to as U87AR.

U87-MG and U87AR glioma cell proliferation with chemotherapeutic agents (ACNU and SN38: active metabolite of CPT-11) was assessed using the MTT assays described previously [9]. ACNU was provided by Sankyo (Tokyo). SN38 was provided by Daiichi Pharmaceutical (Tokyo). MGMT expression was markedly enhanced in U87AR compared with U87-MG (data not shown). The calculated IC_{50} with ACNU was 80 μM for U87-MG and 988 μM for U87AR. In contrast, the IC_{50} with SN38 was 70 nM for U87-MG and 20 nM for U87AR. U87AR is ten times more resistant than U87-MG to ACNU. CPT-11 similarly inhibited both U87AR and U87-MG proliferation (data not shown).

U87AR SCID mouse subcutaneous model

After the implantation of 1×10^5 U87AR cells in the flank of six-week-old male SCID mice (Japan Clea, Japan), U87AR tumor tissue fragments were removed and then reimplanted into another SCID mouse flank. Harvested tumor fragments 1 mm^3 in size were simultaneously implanted into the flank of another SCID mouse. When the resulting tumors were palpable, the mice were allocated to each of the treatment groups. In the first set of studies, CPT-11 was administered to mice in a conventional schedule on days 11–15 and 18–22 via intraperitoneal (i.p.) injection at 10 (low dose) and 40 (high dose) mg/kg in 10% dimethylsulfoxide (DMSO) in 0.9% saline. The mice were divided into three groups (six per group), given CPT-11 low dose, CPT-11 high dose, or saline. Body weight and xenograft tumor dimensions were recorded every each day. In the second set of studies, CPT-11 was administered to the mice in a metronomic schedule on days 1–21 daily via i.p. injection at 1 (low dose) and 4 (high dose) mg/kg. The mice were divided into three groups (eight per group), and were treated with metronomic-CPT-11 low dose, metronomic-CPT-11 high dose, or saline. Body weight and xenograft tumor dimensions were recorded on each day. In the second experiment, 21 days after the implant, the tumor tissues were removed. In order to evaluate the hypoxic area in tumor sections, pimonidazole hydrochloride (Hypoxyprobe-1, Chemicon Temecula, CA, USA) was administered at 120 mg/kg just before sacrifice. A portion of the tissues

was immediately fixed in 10% phosphate-buffered formalin for 48 h, paraffin embedded, and used for routine pathological diagnosis and immunohistochemistry. Other portions of the tissues were immediately frozen in liquid nitrogen and stored at −70°C. In the third set of studies, half of the animals treated by the metronomic schedule resumed the treatment after seven days cessation of treatment. The second cycle of metronomic administration occurred daily on days 29–50 via i.p. injection of CPT-11. The xenograft tumor dimensions were recorded every day. The protocols were in adherence with institutional guidelines for animal welfare and experimental conduct. CPT-11 was provided by Daiichi Pharmaceutical Company (Tokyo, Japan).

Antibodies and immunohistochemistry

The Dako LSAB kit for mouse and rabbit primary antibody (Dako, Glostrup, Denmark) was used [9]. Tissue sections were deparaffined and incubated with 10% normal goat serum in PBS for 20 min. The sections were then incubated with a polyclonal anti-VEGF antibody, A-20 (Santa Cruz Biotech, CA, USA) at a dilution of 1:100 (1 μg/ml IgG), a monoclonal MIB-1 antibody (Immunotech), and anti-HIF-1α antibody (Chemicon) at a dilution of 1:100 in PBS overnight at 4°C, and a monoclonal anti-mouse CD31 antibody (BD Pharmingen) at a dilution of 1:50 (10 μg/ml) and anti-pimonidazole antibody (Chemicon) at a dilution of 1:20 in PBS for 60 min at room temperature. Chromatographically purified mouse IgG and rabbit IgG (Dako) at the same IgG concentration were used as negative controls. Sections were incubated with biotin-conjugated goat anti-mouse or anti-rabbit immunoglobulin for 10 min, followed by washing in PBS for 10 min. The sections were then incubated with peroxidase-conjugated streptavidin solution for 5 min, followed by washing in PBS for 5 min. Sections were then stained with freshly prepared aminoethylcarbazole solution for 10 min, followed by washing for 5 min in tap water. The sections were then counterstained with hematoxylin and mounted with aqueous mounting media. The intracellular VEGF immunostaining was assessed for tumor cells using a semiquantitative scale (−, not detected; +, moderate; ++, strong). Nuclei positive for MIB-1 were determined by counting at least 1000 tumor cells in a homogeneously stained area.

Tumor vascular density

Vascular density was scored using the vasoproliferative component of the microscopic angiogenesis grading system (MAGS) that has been used to quantify angiogenesis in a variety of tumors [10]. The number of vessels in a 200× field (0.31 mm^2) was measured in microvessel "hot spots" (i.e., microscopic areas containing the most dense collections of microvessels, identified initially under low power magnification) with the use of an Olympus microscope, AHBT3 (Olympus, Tokyo, Japan) on CD34-stained tissue sections. Vascular density was defined by averaging the number of vessels in the three most vascularized areas.

Measurement of VEGF and HIF-1α levels in tumor extracts

Tumor extracts were prepared by homogenizing the tumors in a buffer [10]. VEGF levels were measured in tumor extract supernatants by Quantikine human VEGF immunoassay (R&D systems, Minneapolis, MN, USA). VEGF levels were normalized to total extract protein concentration as measured by DC protein assay and expressed as pg VEGF/mg total extract protein.

Total RNA from frozen tumor samples was collected using the RNeasy mini kit (Qiagen, Maryland, MD, USA). Total RNA of 1 μg/μl or less was used to perform RT-PCR using the GeneAmp RNA PCR kit (Applied Biosystems, Foster, CA, USA). The RT-PCR conditions were: 30 s at 94°C, 30 s at 55°C, 30 s at 72°C. To visualize mRNA for human VEGF, HIF-1α and β-actin, RT-PCR was performed and the PCR products were visualized on agarose gels. The mRNA expression was then quantified by densitometry. The VEGF primers consisted of the reverse primer (5′-CC TGGTGAGAGATCTGGTTC-3′) and the forward primer (5′-TCGGGCCTCCGAAACCATGA-3′) [11]. The HIF-1α primers included the reverse primer (5′-CCCTGCAG TAGGTTTCTGCT-3′) and the forward primer (5′-CTCA AAGTCGGACAGCCTCA-3′) [12].

Statistical analyses

Vascular density, MIB-1 positivities, tumor volumes, VEGF concentration, and densitometric measurements are expressed as the mean ± SD. Statistically significant differences between the groups were determined using one-way analysis of variance and Tukey's test. All P-values are two-sided; values were considered statistically significant for $P < 0.05$.

Results

CPT-11 (conventional treatment) inhibits U87AR glioma growth but with systemic toxicity

CPT-11 at low and high doses in conventional treatment significantly inhibited U87AR subcutaneous glioma growth more than 15 days after tumor implantation (Fig. 1a). Median survival time for each treatment was 7.5 weeks

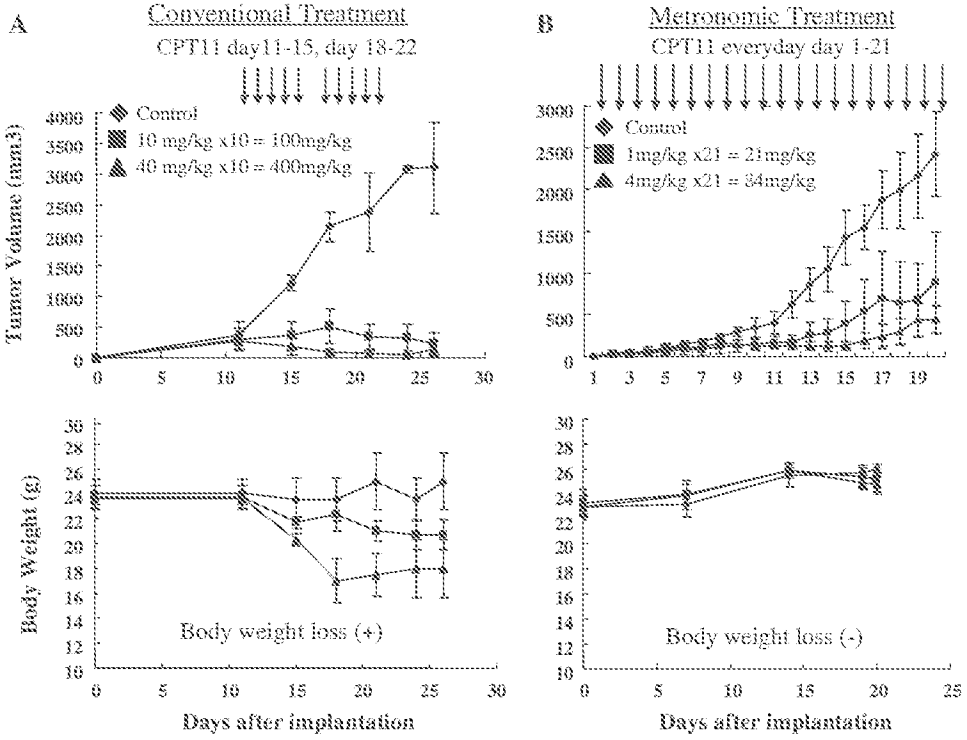

Fig. 1 The effect of CPT-11 on the growth of subcutaneous xenografts of U87 MG human malignant glioma cells in SCID mice. Mice were implanted in the flank with a tumor fragment. When the resulting tumors were palpable, mice were allocated to treatment groups of five animals each. a Conventional treatment. CPT-11 (low: 10 mg/kg, high: 40 mg/kg) was administered to the mice on days 11–15 and 18–22 via intraperitoneal injection. b Metronomic treatment. CPT-11 (low: 1 mg/kg, high: 4 mg/kg) was administered to mice on days 1–21 via intraperitoneal injection. Body weight and xenografts tumor dimensions were recorded twice weekly. The results are presented as means ± SD. *$P < 0.01$

(control), 10.6 weeks (CPT-11 low dose), and 11.5 weeks (CPT-11 high dose). The effect against growth inhibition was very similar between the low and high doses of CPT-11 treatments. However, the body weights of the mice treated with CPT-11 were significantly lower 18 days after treatment compared with control mice, suggesting that conventional CPT-11 treatment has systemic side effects even at a low doses.

CPT-11 (metronomic treatment) inhibits U87AR glioma growth without systemic toxicity

Metronomic scheduling of CPT-11 inhibited U87AR glioma growth in a dose-dependent manner (Fig. 1b). The total dose of CPT-11 administered was 21 and 84 mg/kg with the low dose and high dose metronomic schedules, respectively, i.e., one fifth of the dose with the conventional schedule. CPT-11 treatment significantly prolonged the survival of glioma-bearing mice (data not shown). The body weights of the mice treated with CPT-11 by the metronomic schedule were very similar to those of control mice, suggesting that metronomic CPT-11 treatment had no systemic side effects.

CPT-11 (metronomic schedule) inhibits U87AR angiogenesis and hypoxia

Metronomic CPT-11 treatment significantly reduced HIF-1α mRNA expression (Fig. 2). VEGF165 mRNA expression was lower than for controls, but was not significantly different. The U87AR proliferation rate was not different between the controls and the CPT-11 treatment groups (Fig. 3a). However, the VEGF protein level was reduced in a dose-dependent manner after metronomic CPT-11 treatment (Fig. 3b). Tumor angiogenesis was evaluated by vessel number and vessel area in the tissue sections. Metronomic CPT-11 treatment significantly reduced vessel number and area (Fig. 4).

Finally, HIF-1α expression and hypoxic area were evaluated by immunohistochemistry. In the control groups, HIF-1α expression was observed strongly in the tumor cells around the site of necrosis. Metronomic CPT-11 treatment resulted in reduced necrosis and reduced HIF-1α expression (Fig. 5a–c). The hypoxic areas in tissue sections, which were positive for pimonidazole, were strongly observed around the necrosis in the control group. However, the pimonidazole-positive area was reduced in the metronomic CPT-11 treatment groups, at both low and high doses (Fig. 5d–f).

CPT-11 (metronomic schedule) inhibition is cytostatic and exhibits resistance

Re-challenge of metronomic CPT-11 treatment occurred seven days after the discontinuation of treatment. The tumor started to grow rapidly after the discontinuation of the treatment. The inhibitory effect on tumor growth was minimized by re-challenge metronomic treatment (Fig. 6).

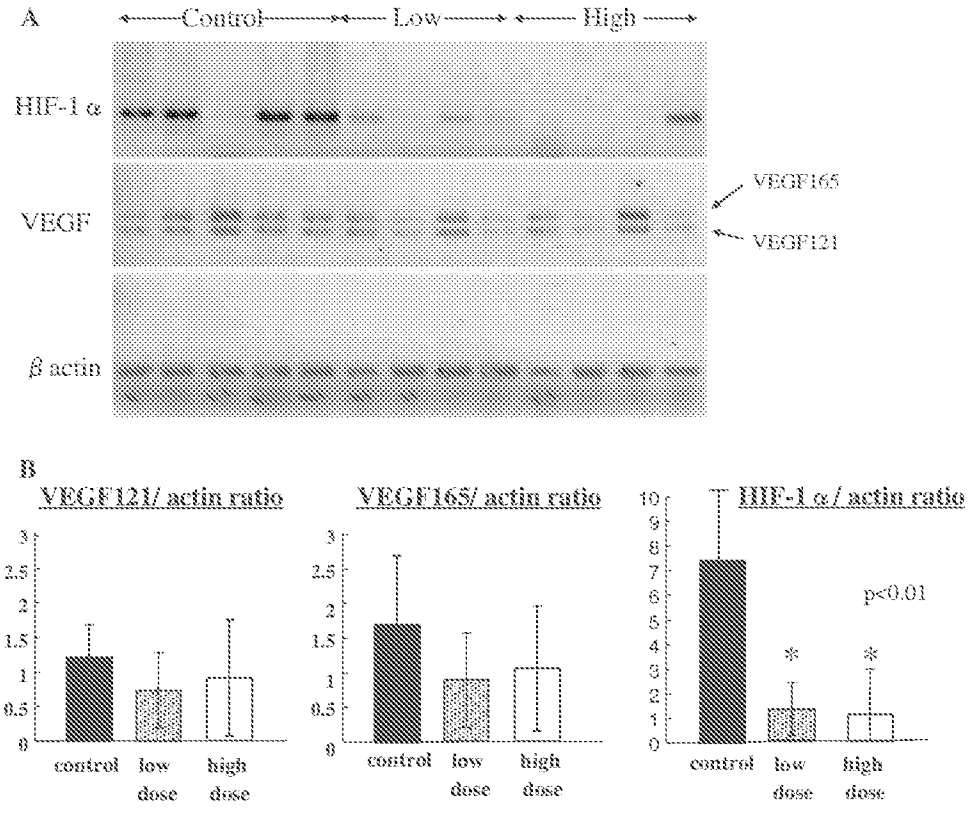

Fig. 2 HIF-1α and VEGF mRNA expression of U87 subcutaneous tumor tissue treated by the metronomic schedule. **a** HIF-1α expression was strongly observed in four of eight control tumor tissues. HIF-1α expression was weak in tumor tissues with low and high dose metronomic treatment. **b** Semiquantification of mRNA expression using the Fluorimager. HIF-1α/actin ratios were significantly lower in the low and high-dose metronomic-treated group than in the control group. $*P < 0.01$

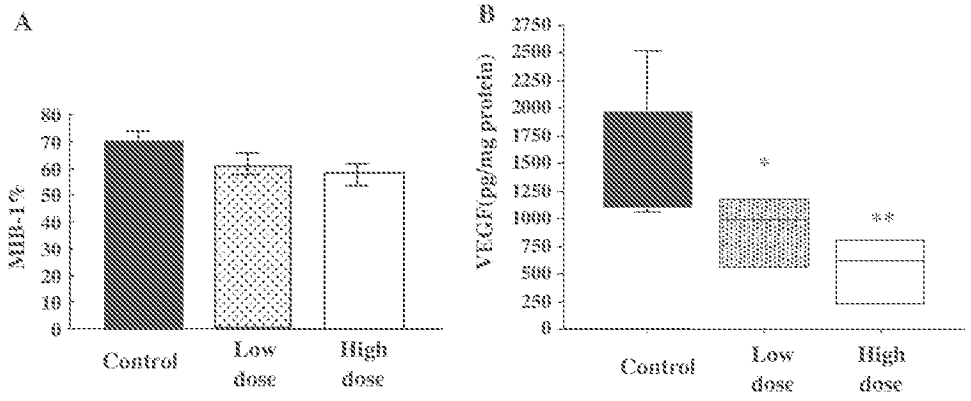

Fig. 3 MIB-1 positivities and VEGF concentration measured by ELISA. **a** MIB-1 positivities were similar for control and CPT-11 treatment groups. **b** VEGF concentrations in tumor tissues were significantly lower in low and high dose metronomic CPT-11 compared with control. $**P < 0.05$, $*P < 0.001$

Discussion

We have previously demonstrated that SN-38, an active metabolite of CPT-11, selectively inhibited endothelial cell proliferation and significantly reduced both HIF-1α and VEGF expression in glioma cells in a dose and time-dependent manner [4]. The study clearly showed that CPT-11 had a direct anti-angiogenic effect on endothelial cells and indirectly on glioma cells via down-regulation of HIF1α and VEGF. In this study we demonstrated the effect of metronomic treatment with CPT-11 on glioma growth and angiogenesis. The most striking advantage of metronomic CPT-11 treatment compared with conventional high-dose intermittent usage of CPT-11 is that it has no systemic toxicity, such as loss of body weight. Another striking effect was inhibition of glioma angiogenesis by down-regulation of HIF-1α and VEGF, resulting in reduced vessel densities and areas in the treated groups. However, the limited effect of the re-challenge treatment suggests resistance to angiosuppression for solid tumors, including gliomas. Furthermore, CPT-11 had a dramatic growth-inhibitory effect in the ACNU-resistant glioma clone. Because ACNU and temozolomide are commonly used in Japan as alkylating agents for malignant gliomas [13–15], the finding that CPT-11 is effective for the ACNU-resistant clone is clinically useful with regard to subsequent use of chemotherapy for recurrent cases.

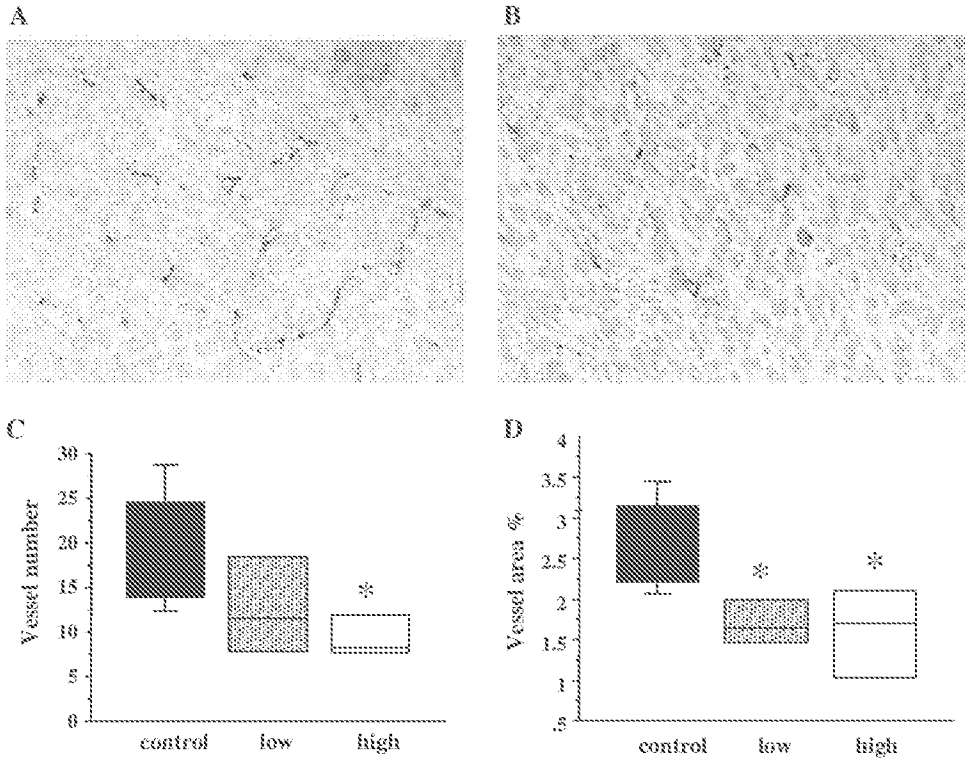

Fig. 4 Angiosuppressive effect of CPT-11. Immunohistochemical detection of tumor vessels stained by CD34. **a** Control, **b** high-dose metronomic treatment. Metronomic CPT-11 treatment significantly reduced the vessel number (**c**) and area (**d**)

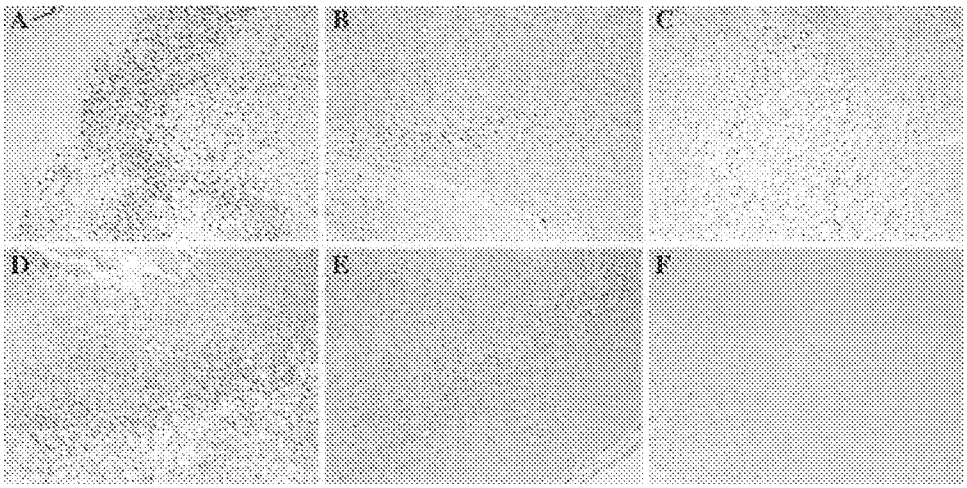

Fig. 5 Immunohistochemical detection of HIF-1α expression (**a**, **b**, **c**) and hypoxic area (**d**, **e**, **f**). In the control groups, strong HIF-1α expression was observed in the tumor cells around the necrosis (**a**). Metronomic CPT-11 treatment resulted in a decrease of the necrotic area and reduced expression of HIF-1α (**b** metronomic low dose, **c** metronomic high dose). Hypoxic areas in tissue sections that were positive for pimonidazole were clearly observed around the necrosis in the control group (**d**). However, the pimonidazole-positive area was reduced in the metronomic CPT-11 treatment groups at both low (**e**) and high (**f**) dose

Antiangiogenic activity of metronomic CPT-11 treatment

Most anticancer drugs cause DNA damage and inhibit tumor cell proliferation. They are usually administered at high doses to kill as many tumor cells as possible. However, standard chemotherapeutic drugs, for example vincristine bleomycin, adriamycin, etoposide, 5-fluorouracil, carboplatin, paclitaxel, and cyclophosphamide, can target angiogenesis when the dose and frequency of administration are optimized. Among these chemotherapeutic agents, CPT-11 was more potent in inhibiting endothelial cell tube formation in vitro [4]. Therefore, we selected CPT-11 as a candidate metronomic agent for gliomas.

The antiangiogenic properties of the camptothecins; 9-AC, topotecan, gimatecan, and CPT-11 have been

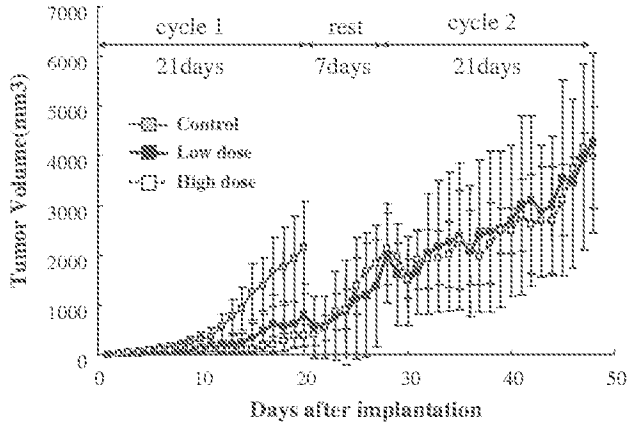

Fig. 6 CPT-11 metronomic treatment was cytostatic. The tumor growth was inhibited by the first metronomic treatment (cycle 1). The tumor started to grow rapidly during the discontinuation of the treatment (rest). The inhibitory effect on tumor growth was minimized by re-challenge metronomic treatment (cycle 2)

demonstrated in both in-vitro and in-vivo assays [16–22]. Although the precise mechanism by which camptothecins affect angiogenesis remains unclear, these drugs may be valuable therapeutic agents for treatment of angiogenic tumors.

Indeed, preclinical studies have indicated the ability of a number of established cytotoxic drugs, for example cyclophosphamide and vinblastine, to strongly inhibit the growth of sensitive and resistant tumors when administered according to an "anti-angiogenic schedule", i.e., continuous low-dose scheduling [23–25], and many antitumor chemotherapeutic agents, including CPT-11, have been tested clinically for their antiangiogenic potential in systemic cancer [26–28].

Continuous low-dose scheduling has been described as the most appropriate means of exploiting the antiangiogenic potential of cytotoxic drugs [5, 29]. Metronomic chemotherapy has been used experimentally [30] and applied clinically for glioblastoma. Tuettenberg et al. [31] demonstrated that metronomic temozolomide in combination with the COX-2 inhibitor rofecoxib was feasible, safe, and maintained a good quality of life for 13 patients with glioblastoma, especially those with tumors characterized by high angiogenic activity. Furthermore, Kong et al. [32] demonstrated that metronomic temozolomide treatment was effective for patients with recurrent temozolomide-refractory glioblastoma. We demonstrated that metronomic CPT-11 treatment reduced VEGF protein expression, which is the most potent and important angiogenic factor of gliomas and brain tumor stem cells [10, 33, 34]. HIF-1α mRNA expression was also strongly inhibited, even with low-dose metronomic CPT-11 treatment. In tissue sections, HIF-1α expression was reduced, and was associated with diminished necrosis and hypoxic areas detected by pimonidazole staining. The tumor cells within these hypoxic areas are likely to be important targets, because they are resistant to chemotherapy and radiation therapy. Anti-angiogenic treatment, for example metronomic CPT-11 treatment may overcome this problem, because of reduction of the hypoxic area. Metronomic CPT-11 treatment reduced the expression of VEGF protein. One suggested mechanism of CPT-11 inhibition of VEGF expression is down-regulation of HIF-1α mRNA expression, i.e., directly upstream of the VEGF pathway [35]. Metronomic CPT-11 treatment reduced expression of VEGF protein, but not VEGF mRNA, in tumor tissues. The recently identified HIF-independent regulation of VEGF by the transcriptional coactivator PGC-1α may be related to the down regulation of VEGF protein [36]. One important mechanism of the anti-tumoral effect of anti-angiogenesis agents is normalization of tumor vasculature, resulting in reduction of necrosis and of the hypoxic area in the tumor [37]. By contrast, overdose of anti-angiogenic agents could result excessive vascular regression associated with increased necrosis and hypoxic area. The therapeutic window of anti-angiogenic agents including CPT-11 is narrow and the administration schedule and the dose of anti-angiogenic agents is very important.

The recent combination therapy with CPT-11 and the angiogenesis inhibitor, TNP470 and thrombospondin-1 shows promise in future developments for treatment of malignant gliomas as an alternative angiosuppressive treatment [38]. Moreover, dramatic recent advances in the treatment for malignant gliomas with bevacizumab (VEGF neutralizing antibody) combined with CPT-11 treatment [3] have suggested the usefulness of CPT-11 as an anti-angiogenic, cytostatic agent, irrespective of its cytotoxic anti-tumor effect. Taken together, these results raise the possibility of the novel clinical application of CPT-11 to target hypoxia-inducible factor and VEGF.

Resistance to anti-angiogenesis treatment

In our study, the growth-inhibitory effect of re-challenged metronomic CPT-11 treatment was limited. The lack of effectiveness on the re-growing phase is similar to that in a previous study [39]. There are three possible explanations of this finding:

1. the metronomic treatment is not effective for relatively large tumors, as demonstrated with other antiangiogenesis strategies;
2. the resistance to metronomic treatment appeared with the first treatment; or
3. the targeted tumor endothelial cells acquired resistance to CPT-11.

The timing of the anti-angiogenic treatment is important. Several clinical studies with metronomic chemotherapy

have not been effective for recurrent glioblastomas. Metronomic chemotherapy with methotrexate and cyclophosphamide was ineffective in relapsed, heavily-pretreated glioblastoma [40]. Although there were some responders, oral metronomic regimens with four drugs, etoposide, cyclophosphamide, thalidomide, and celecoxib did not significantly improve overall survival in a heavily-pretreated group of malignant glioma patients who were generally ineligible for conventional protocols [41]. Although metronomic chemotherapy may not be useful in patients with advanced disease, further studies using more potent angiogenic agents in patients with less advanced disease may be warranted. The mechanisms of resistance include revascularization as a consequence of upregulation of alternative pro-angiogenic signals; protection of the tumor vasculature either by recruiting pro-angiogenic inflammatory cells or increased protective coverage by pericytes; and accentuated invasiveness of tumor cells into local tissues to co-opt the normal vasculature [42, 43]. Tumor endothelial cells are genetically distinct from normal endothelial cells. Tumor endothelial cell clones can acquire resistance to the chemotherapeutic agent used. To overcome resistance to antiangiogenesis treatment, the HIF regulatory network holds promise as a target, as with metronomic CPT-11 treatment, given its global effects on angiogenesis, invasion, and stress-adaptive cell physiology.

In summary, metronomic CPT-11 treatment inhibited human glioma growth in vivo even in the ACNU-resistant clone. Metronomic CPT-11 treatment had an anti-angiogenic effect, inhibited HIF-1α and VEGF expression, and reduced the area of the hypoxic lesion. Clinically, CPT-11 may be a useful chemotherapeutic agent especially for ACNU-treated, recurrent malignant gliomas, in part through its angiosuppressive effect. In combination with strategies that exhibit resistance to antiangiogenic treatment, metronomic CPT-11 treatment presents an exciting future opportunity for improving and sustaining the benefits of malignant glioma therapy.

Acknowledgements We gratefully acknowledge Yoshiko Tsukada and Makiko Miyakawa for their excellent technical assistance. This study was supported by a Grant-in-Aid for Scientific Research from the Japan Society for the Promotion of Science and by a grant provided by the Tsukuba Advanced Research Alliance, Japan Brain Foundation, The Japanese Foundation for Research and Promotion of Endoscopy, and the Japanese Foundation for Multidisciplinary Treatment of Cancer. Animal experiments were carried out in a humane manner after receiving approval from the Institutional Animal Experimental Committee of the University of Tsukuba and in accordance with the University's Regulation for Animal Experiments.

References

1. Buckner JC, Reid JM, Wright K, Kaufmann SH, Erlichman C, Ames M, Cha S, O'Fallon JR, Schaaf LJ, Miller LL (2003) Irinotecan in the treatment of glioma patients. Current and future studies of the north central cancer treatment group. Cancer 97 (9 suppl):2352–2358
2. Vredenburgh JJ, Desjardins A, Reardon DA, Friedman HS (2009) Experience with irinotecan for the treatment of malignant glioma. Neuro-Oncology 11:80–91
3. Vredenburgh JJ, Desjardins A, Herndon JE II, Marcello J, Reardon DA, Quinn JA, Rich JN, Sathornsumetee S, Gururangan S, Sampson J, Wagner M, Bailey L, Bigner DD, Friedman AH, Friedman HS (2007) Bevacizumab plus irinotecan in recurrent glioblastoma multiforme. J Clin Oncol 25:4722–4729
4. Kamiyama H, Takano S, Tsuboi K, Matsumura A (2005) Anti-angiogenic effects of SN38 (active metabolite of irinotecan): inhibition of hypoxia-inducible factor 1 (HIF-1α)/vascular endothelial growth factor (VEGF) expression of Glioma and growth of endothelial cells. J Cancer Res Clin Oncol 131:205–213
5. Hanahan D, Bergers G, Bergsland E (2000) Less is more, regularly: metronomic dosing of cytotoxic drugs can target tumor angiogenesis in mice. J Clin Invest 105:1045–1047
6. Takano S, Tsuboi K, Matsumura A, Tomono Y, Mishai Y, Nose T (2000) Expression of the angiogenic factor thymidine phosphorylase in human astrocytic tumors. J Cancer Res Clin Oncol 126:145–152
7. Mineura K, Yanagisawa T, Watanabe K, Kowada M, Yasui N (1996) Human brain tumor O6-methylguanine-DNA methyltransferase mRNA and its significance as an indicator of selective chloroethylnitrosourea chemotherapy. Int J Cancer 69:420–425
8. Ng SY, Gunning P, Eddy R, Ponte P, Leavitt J, Shows T, Kedes L (1985) Evolution of the functional human beta-actin gene and its multi-pseudogene family: conservation of noncoding regions and chromosomal dispersion of pseudogenes. Mol Cell Biol 5:2720–2732
9. Takano S, Tsuboi K, Matsumura A, Nose T (2003) Anti-vascular endothelial growth factor antibody and nimustine as combined therapy: effects on tumor growth and angiogenesis in human glioblastoma xenografts. Neuro-Oncology 5:1–7
10. Takano S, Yoshii Y, Kondo S, Maruno T, Shirai S, Nose T (1996) Concentration of vascular endothelial growth factor in the serum and tumor tissue of brain tumor patients. Cancer Res 56: 2185–2190
11. Weindel K, Marme D, Weich HA (1992) AIDS-associated Kaposi's sarcoma cells in culture express vascular endothelial growth factor. Biochem Biophys Res Commun 183:1167–1174
12. Nakayama K, Kanzaki S, Hata K, Katabuchi H, Okamura H, Miyazaki K, Fukumoto M, Takebayashi Y (2002) Hypoxia-inducible factor 1 alpha(HIF-1α) gene expression in human ovarian carcinoma. Cancer Lett 176:215–223
13. Nagane M, Nozue K, Shimizu S, Waha A, Miyazaki H, Kurita H, Homori M, Fujioka Y, Shiokawa Y (2009) Prolonged and severe thrombocytopenia with pancytopenia induced by radiation-combined temozolomide therapy in a patient with newly diagnosed glioblastoma-analysis of O6-methylguanine-DNA methyltransferase status. J Neurooncol 92:227–232
14. Takakura K, Abe H, Tanaka R, Kitamura K, Miwa T, Takeuchi K, Yamamoto S, Kageyama N, Handa H, Mogami H, Nishimoto A, Uozumi T, Matsutani M, Nomura K (1986) Effects of ACNU and radiotherapy on malignant glioma. J Neurosurg 64:53–57
15. Yoshida J, Kajita Y, Wakabayashi T (1994) Long-term follow-up results of 175 patients with malignant glioma: importance of radical tumor resection and postoperative adjuvant therapy with interferon, ACNU and radiation. Acta Neurochir (Wien) 127:55–57
16. Clements MK, Jones CB, Cumming M, Daoud SS (1999) Anti-angiogenic potential of camptothecin and topotecan. Cancer Chemother Pharmacol 44:411–416
17. McCrudden KW, Yokoi A, Thosani A, Soffer SZ, Kim ES, Huang J, Manley C, O'Toole K, Yamashiro DJ, Kandel JJ,

Middlesworth W (2002) Topotecan is anti-angiogenic in experimental hepatoblastoma. J Pediatr Surg 37:857–861
18. Nakashio A, Fujita N, Tsuno T (2002) Topotecan inhibits VEGF- and bFGF-induced vascular endothelial cell migration via downregulation of the PI3 K-Akt signaling pathway. Int J Cancer 98:36–41
19. O'Leary JJ, Shapiro RL, Ren CJ, Chuang N, Cohen HW, Potmesil M (1999) Antiangiogenic effects of camptothecin analogues 9-amino-20(S)-camptothecin, topotecan, and CPT-11 studied in the mouse cornea model. Clin Cancer Res 5:181–187
20. Petrangolini G, Pratesi G, De Cesare M, Supino R, Pisano C, Marcellini M, Giordano V, Laccabue D, Lanzi C, Zunino F (2003) Antiangiogenic effects of the novel camptothecin ST1481 (Gimatecan) in human tumor xenografts. Mol Cancer Res 1:863–870
21. Soffer SZ, Kim E, Moore JT, Huang J, Yokoi A, Manley C, O'Toole K, Middlesworth W, Stolar C, Yamashiro D, Kandel J (2001) Novel use of an established agent: topotecan is antiangiogenic in experimental Wilms tumor. J Pediatr Surg 36:1781–1784
22. Xiao D, Tan W, Li M, Ding J (2001) Antiangiogenic potential of 10-hydroxycamptothecin. Life Sci 69:1619–1628
23. Browder T, Butterfield CE, Kraling BM, Shi B, Marshall B, O'Reilly MS, Folkman J (2000) Antiangiogenic scheduling of chemotherapy improves efficacy against experimental drug-resistant cancer. Cancer Res 60:1878–1886
24. Klement G, Baruchel S, Rak J, Man S, Clark K, Hicklin DJ, Bohlem P, Kerbel RS (2000) Continuous low-dose therapy with vinblastin and VEGF receptor-2 antibody induces sustained tumor regression without overt toxicity. J Clin Invest 105:R15–R24
25. Man S, Bocci G, Francia Gm, Green Sk, Jothy S, Hanahan D, Bohlen P, Hicklin DJ, Bergeres G, Kerbel RS (2002) Antitumor effects in mice of low-dose (metronomic) cyclophosphamide administered continuously through the drinking water. Cancer Res 62:2731–2735
26. Bocci G, Falcone A, Fioravanti A, Orlandi P, Di Paolo A, Fanelli G, Viacava P, Naccarato AG, Kerbel RS, Danesi R, Del Tacca M, Allegrini G (2008) Antiangiogenic and anticolorectal cancer effects of metronomic irinotecan chemotherapy alone and in combination with semaxinib. Br J Cancer 98:1619–1629
27. Ogata Y, Mori S, Ishibashi N, Akagi Y, Ushijima M, Murakami H, Fukushima T, Shirouzu K (2007) Metronomic chemotherapy using weekly low-dosage CPT-11 and UFT as postoperative adjuvant therapy in colorectal cancer at high risk to recurrence. J Exp Clin Cancer Res 26:475–482
28. Shirner M (2000) Antiangiogenic chemotherapeutic agents. Cancer Metastasis Rev 19:67–73
29. Gately S, Kerbel R (2001) Antiangiogenic scheduling of lower dose cancer chemotherapy. Cancer J 7:427–436
30. Bello L, Carrabba G, Giussani C, Lucini V, Cerutti F, Scaglione F, Landre J, Pluderi M, Tomei G, Villani R, Carroll RS, Black PM, Bikfalvi A (2001) Low-dose chemotherapy combined with an antiangiogenic drug reduces human Glioma growth in vivo. Cancer Res 61:7501–7506
31. Tuettenberg J, Grobholz R, Korn T, Wenz F, Erber R, Vajkozy P (2005) Continuous low-dose chemotherapy plus inhibition of cyclooxygenase-2 as an antiangiogenic therapy of glioblastoma multiforme. J Cancer Res Clin Oncol 131:31–40
32. Kong DS, Lee JI, Kim WS, Suh MJ, Lim DH, Kim ST, Park K, Kim JH, Eoh W, Nam DH (2006) A pilot study of metronomic temozolomide treatment in patients with recurrent temozolomide-refractory glioblastoma. Oncol Rep 16:1117–1121
33. Folkins C, Man S, Xu P, Shaked Y, Hicklin DJ, Kerbel RS (2007) Anticancer therapies combining antiangiogenic and tumor cell cytotoxic effects reduce the tumor stem-like cell fraction in glioma xenograft tumors. Cancer Res 67:3560–3564
34. Gilbertson RJ, Rich JN (2007) Making a tumour's bed: glioblastoma stem cells and the vascular niche. Nat Rev Cancer 7:733–736
35 Rapisarda A, Uranchimeg B, Sordet O, Pommier Y, Shoemaker RH, Melillo G (2004) Topoisomerase I-mediated inhibition of hypoxia-inducible factor 1: mechanism and therapeutic implications. Cancer Res 64:1475–1482
36. Arany Z, Foo SY, Ma Y, Ruas JL, Bommi-Reddy A, Girnum G, Cooper M, Laznik D, Chinsomboon J, Rangwala SM, Baek KH, Rosenzweig A, Spiegelman BM (2008) HIF-independent regulation of VEGF and angiogenesis by the transcriptional coactivator PGC-1α. Nature 451:1008–1012
37. Jain RK (2005) Normalization of tumor vasculature: an emerging concept in antiangiogenic therapy. Science 307:58–62
38 Allegrini G, Goulette FA, Darnowski JW, Calabresi P (2004) Thrombospondin-1 plus irinotecan: a novel antiangiogenic-chemotherapeutic combination that inhibits the growth of advanced human colon tumor xenografts in mice. Cancer Chemother Pharmacol 53:261–266
39 Kaneko S, Ishibashi M, Kaneko M (2008) Vascular endothelial growth factor expression is closely related to irinotecan-mediated inhibition of tumor growth and angiogenesis in neuroblastoma xenografts. Cancer Sci 99:1209–1217
40. Herrlinger U, Rieger J, Steinbach JP, Nagele T, Dichgans J, Weller M (2005) UKT-04 trial of continuous metronomic low-dose chemotherapy with methotrexate and cyclophosphamide for recurrent glioblastoma. J Neuro-oncol 71:295–299
41. Kesari S, Schiff D, Doherty L, Gigas DC, Batchelor TT, Muzikansky A, O'Neill A, Drappatz J, Chen-Plotkin AS, Ramakrishna N, Weiss SE, Levy B, Bradshaw J, Kracher J, Laforme A, Black PM, Folkman J, Kieran M, Wen PY (2007) Phase II study of metronomic chemotherapy for recurrent malignant gliomas in adults. Neuro-Oncology 9:354–363
42. Bergers G, Hanahan D (2008) Modes of resistance to antiangiogenic therapy. Nat Rev Cancer 8:592–603
43 Jain RK, Duda DG, Clark JW, Loeffler JS (2006) Lessons from phase III clinical trials on anti-VEGF therapy for cancer. Nat Clin Pract Oncol 3:24–40

[CANCER RESEARCH 60, 3389–3393, July 1, 2000]

Advances in Brief

Liposomal Encapsulation of Topotecan Enhances Anticancer Efficacy in Murine and Human Xenograft Models[1]

Paul Tardi, Edward Choice, Dana Masin, Thomas Redelmeier, Marcel Bally, and Thomas D. Madden[2]

Inex Pharmaceuticals Corporation, Burnaby, British Columbia, V5J 5J8 Canada [T. D. M.]; Department of Advanced Therapeutics, British Columbia Cancer Agency [P. T., E. C., D. M., M. B.], Vancouver, British Columbia, V5Z 4E3 Canada; and Northern Lipids Inc., Jack Bell Research Centre, Vancouver, British Columbia, V6H 3Z6 Canada [T. R.]

Abstract

Topotecan was encapsulated in sphingomyelin/cholesterol liposomes using an ionophore-generated proton gradient. After i.v. injection, liposomal topotecan was eliminated from the plasma much more slowly than free drug, resulting in a 400-fold increase in plasma area under the curve. Further, high-performance liquid chromatography analysis of plasma samples demonstrated that topotecan was protected from hydrolysis within the liposomal carrier with >80% of the drug remaining as the active, lactone species up to 24 h. The improved pharmacokinetics observed with liposomal topotecan correlated with increased efficacy in both murine and human tumor models. In the L1210 ascitic tumor model, optimal doses of liposomal topotecan resulted in a 60-day survival rate of 60–80%, whereas in a L1210 liver metastasis model, 100% long-term survival (>60 days) was achieved. In contrast, long-term survivors were rarely seen after treatment with free topotecan. Further, in a human breast carcinoma model (MDA 435/LCC6), liposomal topotecan provided greatly improved increase in life span relative to the free drug. These results suggest that liposomal encapsulation can significantly enhance the therapeutic activity of topotecan.

Introduction

Topotecan is a water-soluble analogue of camptothecin that specifically inhibits the activity of topoisomerase I by stabilizing the topoisomerase I-DNA complex, resulting in lethal DNA strand breaks (1). As with all camptothecins, however, topotecan undergoes a pH-dependent hydrolysis of the lactone ring to form a relatively inactive carboxylate in aqueous solution. This rapid conversion is also observed in patients after systemic injection of the drug (2). A potential solution to this problem is to encapsulate topotecan within a liposome. Liposomes accumulate preferentially at tumor sites as a result of their ability to extravasate through "pores" or "defects" in the capillary endothelium. These "pores" appear to be a consequence of the rapid angiogenesis occurring in tumors and are generally not present in normal tissues or organs (3). Liposomes have previously been used as carriers for anticancer drugs, and they have been shown to reduce side effects, such as anthracycline-induced cardiomyopathy (4). Liposomes can also provide slow release of an encapsulated drug, resulting in sustained exposure to tumor cells and enhanced efficacy (5–7). In the case of camptothecins, liposomes could additionally provide protection against drug hydrolysis. Initial studies confirmed that insertion of camptothecins within a lipid bilayer conferred protection of the lactone species (8). For therapeutic purposes, however, this approach is limited by the relatively low drug concentrations that can be inserted into a liposomal membrane and the rapid exchange of hydrophobic drugs that occurs from liposomes to other hydrophobic binding sites after i.v. administration (9, 10). In the present work, therefore, we have encapsulated topotecan in the aqueous interior of the liposome using an ionophore-induced proton gradient. This approach provides efficient loading at high drug:lipid ratios, avoids drug exchange from the carrier, and provides an acidic environment stabilizing the lactone species. The pharmacokinetic properties and anticancer efficacy of this liposomal formulation are compared to free topotecan in the present work.

Materials and Methods

Lipids and Chemicals. Topotecan (Hycamtin, SmithKline Beecham) was purchased from the British Columbia Cancer Agency Pharmacy. Egg sphingomyelin was supplied by Northern Lipids Incorporated (Vancouver, British Columbia, Canada). Cholesterol and the divalent cation ionophore A23187 were obtained from the Sigma Chemical Company (St. Louis, MO). Tritiated [^{3}H]cholesteryl hexadecyl ether (NEN, Boston, MA) was used as a liposome marker. All other chemicals used in these studies were analytical or HPLC[3] grade.

Preparation of Liposomes. Large unilamellar vesicles consisting of egg sphingomyelin and cholesterol (55:45 mole percent) were prepared as previously described by Hope *et al.* (11). Briefly, lipids were dissolved in benzene/methanol (95:5 v/v) in the presence of [^{3}H]cholesteryl hexadecyl ether (98,000 dpm/μmol), frozen in liquid nitrogen, and lyophilized under vacuum for 5 h. The dried lipid films were hydrated in 300 mM manganese sulfate, freeze-thawed five times (12), and size-reduced using high pressure extrusion through two-stacked polycarbonate filters of 80 nm in pore size (Poretics, AMD Manufacturing Inc., Mississauga, Ontario, Canada). The vesicle diameter was typically in the range of 130 ± 20 nm based on quasi-elastic light scattering (Nicomp Particle Sizer Model 270, Santa Barbara, CA). The external buffer of the carrier system was exchanged by dialyzing at 4°C for 48 h against 100 volumes of 300 mM sucrose with buffer changes at 18 and 36 h.

Topotecan Encapsulation. Topotecan was encapsulated into the liposomes using an ionophore-mediated proton gradient (13). Drug uptake was performed at 5 mM topotecan and 40 mM lipid in a solution containing 300 mM sucrose, 30 mM EDTA, and 20 mM 2-morpholineethanesulfonic acid (pH 6.0). The divalent cation ionophore A23187 (7 μM final concentration) was first added to the liposomes, and the mixture was incubated at 65°C for 15 min to facilitate A23187 incorporation into the bilayer. Subsequently, topotecan and EDTA were added, and the mixture was incubated at 65°C for 1 h. The extent of encapsulation was determined by passing an aliquot of the sample down a Sephadex G-50 spin column (14) and measuring lipid and topotecan concentration in the eluent. Unencapsulated topotecan and A23187 were removed from the preparation by dialyzing the sample at 4°C for 48 h against 100 volumes of 300 mM sucrose. The efficiency of topotecan loading typically ranged between 90 and 100%.

Pharmacokinetic Studies in BALB/c Mice. Free topotecan (10 mg/kg) and liposomal topotecan (125 mg/kg lipid, 10 mg/kg topotecan) were injected i.v. into female BALB/c mice, and the plasma elimination of both the lipid carrier and the drug were determined over a 24-h time course. Quantitation of

Received 2/25/00; accepted 5/8/00.

The costs of publication of this article were defrayed in part by the payment of page charges. This article must therefore be hereby marked *advertisement* in accordance with 18 U.S.C. Section 1734 solely to indicate this fact.

[1] Supported by Inex Pharmaceuticals Corporation. Additional funding was by the Medical Research Council of Canada (to M. B.) and the National Cancer Institute of Canada (to T. D. M.).

[2] To whom requests for reprints should be addressed, at Inex Pharmaceuticals Corporation, 100-8900 Glenlyon Parkway, Glenlyon Business Park, Burnaby, British Columbia, Canada V5J 5J8.

[3] The abbreviations used are: HPLC, high-performance liquid chromatography; ILS, increase in life span; RES, reticuloendothelial system.

the liposomal carrier in plasma was based on liquid scintillation counting of the nonexchangeable, nonmetabolizable marker [^{3}H]cholesteryl hexadecyl ether (15). Total topotecan was determined using fluorescence spectroscopy as described in analytical methods.

Tumor Models. In the L1210 tumor model, female BDF-1 mice weighing 18–20 g were obtained from Charles River Breeding Laboratories. The L1210 cell line was obtained from the National Cancer Institute tumor cell repository and was maintained by serial passage of ascites fluid. Mice in groups of four or five were inoculated on day 0 with 1×10^4 cells i.v. or 1×10^5 cells i.p. In the MDA435/LCC6 tumor model, female SCID/RAG-2 mice weighing 18–20 g were bred by the British Columbia Cancer Agency Joint Animal Facility through a licensing agreement with Taconic (Germantown, NY). The MDA435/LCC6 cell line was kindly provided by Dr. Robert Clarke of the Vincent Lombardi Cancer Center. The cell line has been previously characterized (16) and was maintained by serial passage of ascites fluid. Groups of four mice were inoculated i.p. with 1×10^6 cells on day 0. Treatments in all tumor models were initiated as a single i.v. dose on day 1 or multiple dosing on days 1, 5, and 9. For the treatment groups, drug dosage was adjusted for average body weight for each group. Control animals received injections of sterile saline. Mice were weighed on the day of tumor injection, and weights were recorded daily until the first death within each group. Survival times were recorded as days after tumor cell injection. Because death cannot be used as an end point, mice were evaluated twice daily by trained animal health technicians and sacrificed at the first sign of distress.

Analytical Methods. Topotecan was quantified using two different methods. In the blood clearance studies, total topotecan was quantified using fluorescence spectroscopy. Briefly, plasma proteins were precipitated by the addition of 200 μl of methanol to 50 μl of plasma, and the sample was centrifuged in an Eppendorf microcentrifuge for 10 min at 3500 rpm. Topotecan was quantified using a Perkin-Elmer LS50 fluorescence spectrometer (Norfolk, CT) set at an excitation wavelength of 380 nm (2.5-nm slit width) and emission wavelength of 518 nm (2.5-nm slit width).

Quantitation of the lactone and carboxylate forms of topotecan was performed by HPLC analysis (17). Briefly, topotecan was extracted from 50 μl of plasma by diluting the sample in ice-cold methanol (final concentration 80% methanol) to precipitate plasma proteins and solubilize the liposomes. The methanolic solution was stored at −30°C until analysis. These conditions were found to stabilize the lactone species of the drug for several days. Just before HPLC analysis, the samples were diluted with an equal volume of refrigerated water. Standard curves for the two species of the drug were generated by dissolving the drug in either 40% methanol:60% 10 mM citrate buffer (pH 3) for the lactone species or 40% methanol:60% 10 mM borate buffer (pH 9) for the carboxylate species. HPLC analysis used a Waters Novo-pak column (150 × 3.9 mm) with a run time of 15 min at a flow rate of 1 ml/min. A two solvent mobile phase system consisted of mobile phase A (0.6% acetic acid, 1.5% triethylamine in HPLC grade water) and mobile phase B (0.6% acetic acid, 1.5% triethylamine in 47.9% HPLC grade water and 50% acetonitrile). The elution gradient consisted of a mixture of A:B in the following ratios: 78%:22% for minutes 0–4, 50%:50% for minutes 4–8, followed by 78%:22% for minutes 8–15. Under the HPLC conditions outlined above, the carboxylate species of topotecan elutes at 3 min and the lactone species elutes at 7 min.

Results

Liposomal Encapsulation of Topotecan. Topotecan was encapsulated into vesicles composed of sphingomyelin and cholesterol. These lipid components were selected based on their chemical stability and ability to provide slow, sustained drug leakage (5). Efficient drug loading was achieved using a manganese ion gradient to drive formation of a pH gradient (13). In this study, topotecan was loaded into vesicles at a drug:lipid ratio of 1:8 (mole ratio), and trapping efficiencies of 90–100% were achieved over a 1-h incubation at 60–65°C. No drug leakage was seen on storage of liposomal topotecan at 4°C for 3 weeks.

Pharmacokinetics of Liposomal Topotecan. Pharmacokinetic studies examined plasma elimination rates for both topotecan and the liposomal carrier. After i.v. injection in BALB/c mice, sphingomyelin/cholesterol liposomes show extended blood circulation times (Fig. 1*A*). Carrier elimination rates are similar for topotecan-loaded liposomes, mock-loaded liposomes, and empty liposomes, with 15–20% of the injected doses remaining in the circulation at 24 h. This is comparable to circulation lifetimes reported for liposomal systems that contain polyethylene glycol-conjugated lipids (18). In contrast to free topotecan, which is rapidly eliminated from the plasma, liposomal topotecan shows an extended circulation lifetime, with 23% of the injected dose remaining in the circulation at 4 h (Fig. 1*B*). Over 24 h, a 400-fold increase in plasma area under the curve is observed for liposomal topotecan compared to the free drug. From the carrier and drug pharmacokinetic data, it is also possible to calculate the rate of topotecan release from circulating liposomes. As shown in Fig. 1*C*, sphingomyelin/cholesterol carriers provide sustained drug release over about 24 h.

Topotecan is reversibly hydrolyzed from a closed-ring lactone to an open-ring carboxylate in aqueous solution. The rate of hydrolysis is pH-dependent, with the carboxylate form being favored at physiological pH (19). Because the lactone form is the active species, we quantified the relative proportions of lactone and carboxylate after the systemic injection of free and liposomal drug. After injection of free topotecan, ~50% of the drug recovered from the plasma is the active

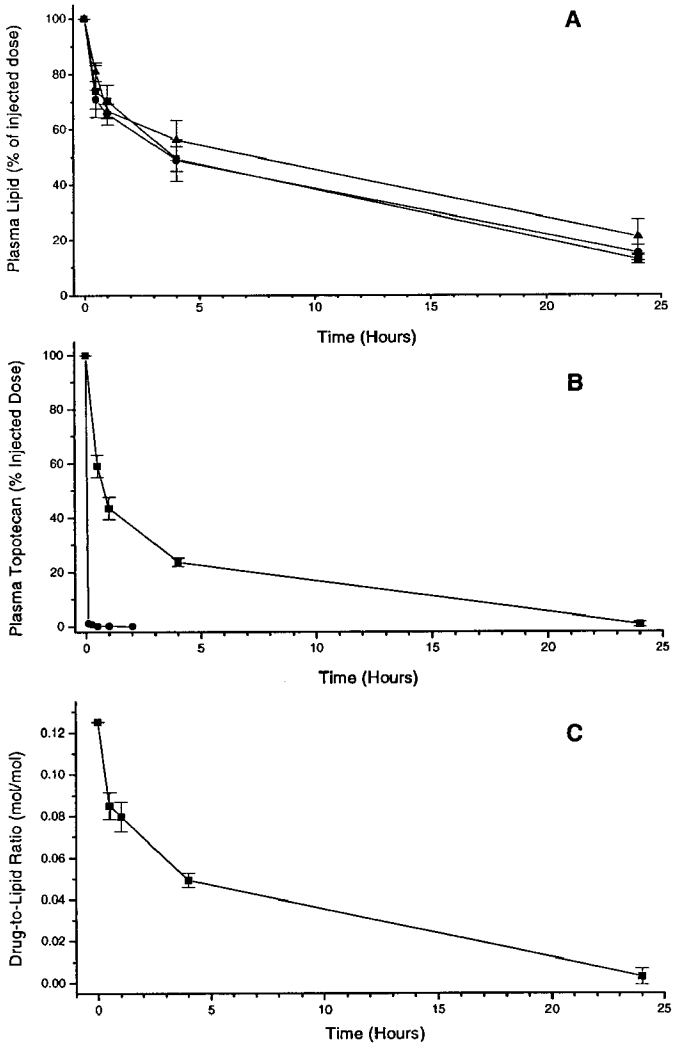

Fig. 1. Plasma elimination of free and liposomal topotecan. *A*, mice were injected i.v. with liposomal topotecan (▲), mock-loaded liposomes (●), or empty liposomes (■). At various times, plasma was collected and liposomal lipid levels were determined ("Materials and Methods"). *B*, plasma levels of topotecan were determined at various times after injection of free drug (●) or liposomal topotecan (■). *C*, topotecan release rate from circulating liposomes calculated from data presented in *A* and *B*.

lactone form after 5 min (Table 1). The distribution between lactone and carboxylate changes very little by the 15-min time point. In contrast, liposomal topotecan is protected as the lactone species. Up to 4 h after injection, >95% of the topotecan recovered from plasma was in the active lactone form. At 24 h after injection, the lactone content had decreased to 84%, but the total plasma concentration was still twice the levels detected at 5 min after injection of the free drug. In conclusion, liposomal topotecan was found to selectively maintain the drug in the active lactone form as well as substantially enhance plasma concentrations. To determine if these pharmacokinetic benefits would translate into enhanced efficacy, liposomal topotecan was compared to free drug in L1210 and MDA435/LCC6 tumor models.

Antitumor Efficacy of Liposomal Topotecan. In an L1210 ascites tumor model, mice were inoculated on day 0, and topotecan (free or liposomal) was administered either as a single dose on day 1 or in multiple doses on days 1, 5, and 9. Free topotecan was well tolerated at the doses given, with little change in animal weights after treatment. In the case of the liposomal topotecan, weight loss was observed in the multiple dosing schedule at 8 mg/kg, and one drug-related death was seen in this group. In general, liposomal topotecan caused more weight loss than the equivalent dose of free drug. In subsequent studies, therefore, liposomal topotecan was administered at 50% of the doses used for free drug. In all treatment groups tested, the liposomal form of the drug showed superior activity to free drug. In the single dosing regimen, 10 mg/kg free drug resulted in a median survival time of 10.5 days compared to liposomal topotecan of 25 days. Median survival times could not be determined for the remaining liposomal topotecan groups because of the high incidence of long-term survivors (>60 days). All mice surviving at 60 days were reinjected i.p. with 1×10^5 L1210 cells. The subsequent survival time of the reinjected mice ranged from 8–11 days.

In the second L1210 model, cells were injected i.v., resulting in tumor seeding primarily to the liver. Again, both single and multidose schedules were examined. As observed in the ascites model, liposomal topotecan showed superior activity to the free drug, even at half the free drug dosage (Fig. 2*B*; Table 2). In the groups treated with free drug, no long-term survivors (>60 days) were observed, whereas all mice receiving liposomal topotecan survived beyond 60 days regardless of treatment protocol. At autopsy on day 61, no tumors were found in any of the liposomal topotecan-treated animals.

The efficacy of liposomal and free topotecan was also examined in a breast cancer tumor model (16). The human breast cancer cell line MDA435/LCC6 was injected i.p. into SCID mice on day 0, and treatment with drug began as a single dose on day 1 or in multiple doses on days 1, 5, and 9. Free topotecan administered in single or multiple doses had little effect on improving mice survival. The most efficacious dose of free drug was observed at 20 mg/kg (day 1) where a 21% ILS was achieved (Table 2). In contrast, liposomal topotecan improved on this result >2-fold with a single 5-mg/kg dose (54% ILS) and 5-fold with multiple doses of 2 mg/kg (117% ILS). As observed in the L1210 tumor models, higher doses of liposomal topotecan resulted in animal weight loss and were not pursued.

Table 1 *Analysis of plasma topotecan after injection of free or liposomal drug*

	Plasma concentration (μg/ml)			Topotecan (% of total)	
Time	Lactone	Carboxylate	Total	Lactone	Carboxylate
Free topotecan					
5 min	1.5	1.6	3.1	48	52
15 min	1.4	1.0	2.4	58	42
Liposomal topotecan					
30 min	56.5	2.0	58.5	97	3
1 h	54.4	2.7	57.1	95	5
4 h	35.0	2.0	37	95	5
16 h	17.1	1.4	18.5	92	8
24 h	5.35	0.9	6.4	84	16

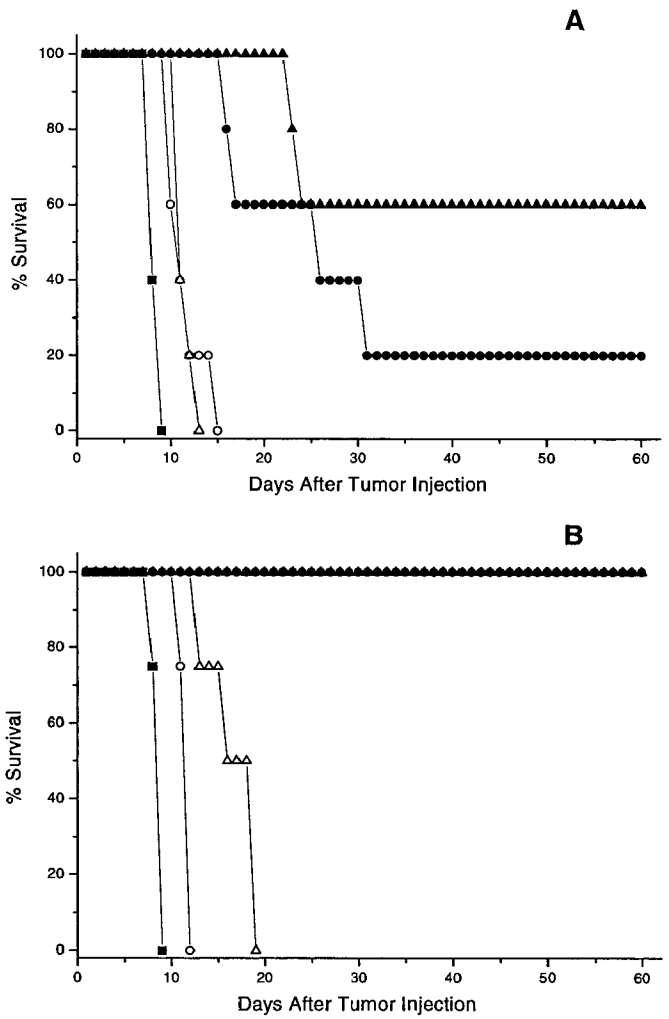

Fig. 2. Antitumor efficacy of free and liposomal topotecan in L1210 tumor models. Mouse survival after i.p. injection (*A*) or i.v. injection (*B*) of L1210 tumor cells on day 0. Single injections of free or liposomal topotecan were administered i.v. on day 1. *A*, groups shown are control, untreated animals (■); free topotecan, 10 mg/kg (○); free topotecan, 20 mg/kg (△); liposomal topotecan, 10 mg/kg (●); and liposomal topotecan, 20 mg/kg (▲). *B*, groups shown are control, untreated animals (■); free topotecan, 10 mg/kg (○); free topotecan, 20 mg/kg (△); liposomal topotecan, 5 mg/kg (●); and liposomal topotecan, 10 mg/kg (▲).

Discussion

It has been shown previously that liposomes can reduce the toxicity of anticancer drugs while maintaining or enhancing efficacy (20, 21). These benefits derive from the altered pharmacokinetics and biodistribution afforded by the liposomal carrier. In the case of camptothecins, an additional benefit can be achieved by protection of the active lactone species. An earlier study by Burke and Gao (22) showed that large (500-nm diameter) multilamellar vesicles with an acidic interior could stabilize topotecan as the lactone form. Unfortunately, multilamellar vesicles have limited value as drug carriers because of their rapid clearance from the circulation (18). We therefore examined the application of highly stable sphingomyelin/cholesterol liposomes of ~100 nm in diameter. Defects in the capillary endothelium of tumor vasculature are typically in the size range of 200–600 nm (3), and therefore, liposomes of 100 nm in diameter can efficiently extravasate and accumulate within the tumor interstitial space (23). This tumor accumulation is enhanced for systems that

Table 2 *Antitumor efficacy of free and liposomal topotecan*

Formulation	Drug dose (mg/kg)	Dosage administration day	Long-term survivors (>60 days)	Median survival time (days)[a]	ILS[b]
L1210 ascitic tumor model					
Saline	NA	1	0/5	8	
Free topotecan	10	1	0/5	10.5	31%
Free topotecan	20	1	0/5	11	38%
Free topotecan	4	1, 5, 9	0/5	11	38%
Free topotecan	8	1, 5, 9	1/5	15	88%
Liposomal topotecan	10	1	1/5	25	212%
Liposomal topotecan	20	1	3/5	NA[c]	ND
Liposomal topotecan	4	1, 5, 9	4/5	NA	ND
Liposomal topotecan	8	1, 5, 9	4/5	NA	ND
L1210 liver metastasis model					
Saline	NA	1	0/4	9	
Free topotecan	10	1	0/4	12	33%
Free topotecan	20	1	0/4	19	111%
Free topotecan	4	1, 5, 9	0/4	14	56%
Free topotecan	8	1, 5, 9	0/4	16.5	83%
Liposomal topotecan	5	1	4/4	NA	ND
Liposomal topotecan	10	1	4/4	NA	ND
Liposomal topotecan	2	1, 5, 9	4/4	NA	ND
Liposomal topotecan	4	1, 5, 9	4/4	NA	ND
MDA435/LCC6 human breast carcinoma model					
Saline	NA	1	0/4	24	
Free topotecan	10	1	0/4	18	−25%
Free topotecan	20	1	0/4	29	21%
Free topotecan	4	1, 5, 9	0/4	20.5	−15%
Free topotecan	8	1, 5, 9	0/4	28.5	19%
Liposomal topotecan	5	1	0/4	37	54%
Liposomal topotecan	2	1, 5, 9	0/4	52	117%

[a] Median survival time is not applicable for groups in which the majority of animals were long-term survivors.
[b] ILS was not determined for groups in which the majority of animals were long-term survivors.
[c] NA, not applicable; ND, not determined.

display a long circulation lifetime and, as we show here, sphingomyelin/cholesterol liposomes exhibit this property. The blood residency lifetimes we observe are comparable to those of liposomes possessing polyethylene glycol-conjugated lipids (termed Stealth liposomes). This is the result of two main factors. First, the sphingomyelin/cholesterol bilayer is highly rigid and therefore protein binding to the surface is minimized. This reduces the rate of opsonin-induced carrier clearance (24). Second, liposome clearance rates are influenced by lipid dose because RES clearance mechanisms are partly saturable (18). The drug:lipid ratio selected for liposomal topotecan provides a lipid dose that avoids rapid carrier clearance by the RES.

An interesting aspect of the present work is that we observe similar plasma elimination rates for topotecan-loaded liposomes and mock-loaded or empty carriers. This result is in contrast to the decreased elimination rates seen for liposomal doxorubicin compared to empty carriers (25). In the case of liposomal doxorubicin, drug-induced inhibition of RES activity is believed to account for the slower clearance of drug-loaded carriers. This inhibition, or "RES blockade," is believed to reflect cytotoxicity against phagocytic cells responsible for clearance. Because this phenomenon is not observed for liposomal topotecan, it may suggest that topotecan is not inhibiting the nondividing RES cell population. This result supports previously published *in vitro* studies showing that in the absence of DNA replication, the reversibly stabilized topoisomerase I-DNA complex has minimal effect on cell survival (26). The absence of nonspecific cell toxicities could prove to be an advantage associated with the use of liposomal topotecan over other liposomal drugs, such as doxorubicin and vincristine.

In addition to increasing topotecan delivery to tumor sites, sphingomyelin/cholesterol liposomes provide sustained drug release over about 24 h. In view of the fact that topotecan activity is cell-cycle-dependent, increasing tumor cell exposure time should increase tumor cell killing dramatically. Previous studies attempting to increase the therapeutic activity of the free drug have met limited success. In a Phase I clinical trial, continuous infusion of free topotecan increased tumor exposure time, but the conversion to the inactive carboxylate form was so rapid that tolerable doses were often too low to provide any antineoplastic effect (27). This problem is overcome in the present work by using an ionophore-generated ion gradient to create an acidic carrier interior. This protected topotecan as the lactone species for an extended period ensuring that drug released at the tumor site is in the active form.

Initial animal studies evaluated the toxicity and efficacy of liposomal topotecan in the murine L1210 leukemia model. This model has previously been used in several studies that characterized topotecan activity *in vivo* (2, 28, 29). Higher drug toxicity, evidenced by weight loss, was seen for liposomal topotecan relative to free drug. This result is not surprising in view of the considerable increase in plasma area under the curve (400-fold) observed for the liposomal formulation and the previously reported correlation of plasma topotecan levels with toxicity (2). Further, a much greater proportion of the drug is preserved as the lactone species when administered in the liposomal carrier. It should be noted that no toxicity (weight loss) was observed in mice administered empty (mock loaded) liposomes at an equivalent lipid dose to that of the highest liposomal topotecan dose. In the L1210 ascites model, liposomal topotecan was much more efficacious than free drug using either a single dose or multidose schedule. Long-term survivors were seen in all liposomal topotecan-treated groups, whereas only one 60-day survivor was achieved in any of the free drug groups. The comparative activities of free and liposomal topotecan were even more pronounced in the L1210 liver metastasis model. All groups treated with liposomal topotecan showed 100% long-term survival with no evidence of tumor at autopsy, even at half the dose of free drug. No long-term survivors were seen in groups treated with free drug. This remarkable improvement in efficacy may be partially related to the fact that liposomes accumulate in the organs of the RES. Because these organs include the liver, the primary site of tumor seeding after i.v. inoculation of L1210 cells, topotecan delivery

to the site may be further enhanced over that achieved with the ascitic tumor model. Finally, in a human breast tumor model MDA435/LCC6, improvements in the therapeutic activity of topotecan were also observed for the liposomal formulation. In this model, free drug showed no significant ILS, whereas liposomal topotecan showed significant activity. The combined results from these tumor models indicate that the therapeutic activity of topotecan can be significantly improved by encapsulating the drug within an appropriate liposomal carrier.

Topotecan is a very promising anticancer drug that has shown clinical activity against small cell and non-small cell lung cancer, ovarian cancer, refractory leukemias/myelodysplastic syndromes, and in childhood sarcomas (30). As for camptothecins in general, conversion of the drug from the active lactone to an inactive carboxylate occurs rapidly *in vivo*. By encapsulating topotecan within a liposome, we selectively retained the drug in the active lactone form, increased delivery to tumor sites, and provided sustained drug release and hence tumor exposure. These pharmacokinetic changes significantly enhanced the activity of topotecan against both murine and human tumor models. These findings warrant the further development of liposomal topotecan for potential clinical investigation.

References

1. D'Arpa, P., and Liu, L. F. Topoisomerase-targeted anticancer drugs. Biochim. Biophys. Acta, *989:* 163–177, 1989.
2. Grochow, L. B., Rowinsky, E. K., Johnson, R., Ludeman, S., Kaufmann, S. H., McCabe, F. L., Smith, B. R., Hurowitz, L., DeLisa, A., Donehower, R. C., and Noe, D. A. Pharmacokinetics and pharmacodynamics of topotecan in patients with advanced cancer. Drug Metab. Dispos., *20:* 706–713, 1992.
3. Yuan, F., Dellian, M., Fukumura, D., Leunig, M., Berk, D. A., Torchilin, V. P., and Jain, R. K. Vascular permeability in a human tumor xenograft: molecular size dependence and cutoff size. Cancer Res., *55:* 3752–3756, 1995.
4. Gabizon, A., Goren, D., Cohen, R., and Barenholz, Y. Development of liposomal anthracyclines: from basics to clinical applications. J. Control Release, *53:* 275–279, 1998.
5. Webb, M. S. Harasym, T. O., Masin, D., Bally, M. B., and Mayer, L. D. Sphingomyelin-cholesterol liposomes significantly enhance the pharmacokinetics and therapeutic properties of vincristine in murine and human tumor models. Br. J. Cancer, *72:* 896–904, 1995.
6. Chang, C. W., Barber, L., Ouyang, C., Masin, D., Bally, M. B., and Madden, T. D. Plasma clearance, biodistribution and therapeutic properties of mitoxantrone encapsulated in conventional and sterically stabilized liposomes after intravenous administration in BDF1 mice. Br. J. Cancer, *75:* 169–177, 1997.
7. Lim, H., Masin, D., Madden, T. D., and Bally, M. B. Influence of drug release characteristics on the therapeutic activity of liposomal mitoxantrone. J. Pharmacol. Exp. Ther., *281:* 566–573, 1997.
8. Burke, T. G., Mishra, A. K., Wani, M. C., and Wall, M. E. Lipid bilayer partitioning and stability of camptothecin drugs. Biochemistry, *32:* 5352–5364, 1993.
9. Ouyang, C., Choice, E., Holland, J., Meloche, M., and Madden, T. D. Liposomal cyclosporine: characterization of drug incorporation and interbilayer exchange. Transplantation, *60:* 999–1006, 1995.
10. Choice, E., Masin, D., Bally, M. B., Meloche, M., and Madden, T. D. Liposomal cyclosporine: comparison of drug and lipid carrier pharmacokinetics and biodistribution. Transplantation, *60:* 1006–1011, 1995.
11. Hope, M. J., Bally, M. B., Webb, G., and Cullis, P. R. Production of large unilamellar vesicles by a rapid extrusion procedure. Characterization of size distribution, trapped volume and ability to maintain a membrane potential. Biochim. Biophys. Acta, *812:* 55–65, 1985.
12. Mayer, L. D., Hope, M. J., Cullis, P. R., and Janoff, A. S. Solute distributions and trapping efficiencies observed in freeze-thawed multilamellar vesicles. Biochim. Biophys. Acta, *817:* 193–196, 1986.
13. Fenske, D. B., Wong, K. F., Maurer, E., Maurer, N., Leenhouts, J. M., Boman, N., Amankwa, L., and Cullis, P. R. Ionophore-mediated uptake of ciprofloxacin and vincristine into large unilamellar vesicles exhibiting transmembrane ion gradients. Biochim. Biophys. Acta, *1414:* 188–204, 1998.
14. Pick, U. Liposomes with a large trapping capacity prepared by freezing and thawing sonicated phospholipid mixtures. Arch. Biochem. Biophys., *212:* 186–194, 1981.
15. Stein, Y., Halperin, G., and Stein, O. Biological stability of [^{3}H]cholesteryl oleyl ether in cultured fibroblasts and intact rat. FEBS Lett., *111:* 104–106, 1980.
16. Leonessa, F., Green, D., Licht, T., Wright, A., Wingate-Legette, K., Lippman, J., Gottesman, M. M., and Clarke, R. MDA435/LCC6 and MDA435/LCC6MDR1: ascites models of human breast cancer. Br. J. Cancer, *73:* 154–161, 1996.
17. Warner, D. L., and Burke, T. G. Simple and versatile high-performance chromatographic method for the simultaneous quantitation of the lactone and carboxylate forms of camptothecin anticancer drugs. J. Chromatogr. B, *691:* 161–171, 1997.
18. Allen, T. M., and Stuart, D. D. Liposome pharmacokinetics: classical, sterically stabilized, cationic liposomes and immunoliposomes. *In:* A. S. Janoff (ed.), Liposomes: Rational Design, pp. 63–87. New York: Marcel Dekkar, 1999.
19. Mi, Z., and Burke, T. G. Differential interactions of camptothecin lactone and carboxylate forms with human blood components. Biochemistry, *33:* 10325–10336, 1994.
20. Mayer, L. D., Cullis, P. R., and Bally, M. B. Designing therapeutically optimized liposomal anticancer delivery systems: lessons from conventional liposomes. *In:* D. Lasic and D. Papahadjopoulos (eds.), Medical Applications of Liposomes, pp. 231–257. Amsterdam: Elsevier Science, 1998.
21. Boman, N. L., Bally, M. B., Cullis, P. R., Mayer, L. D., and Webb, M. S. Encapsulation of vincristine in liposomes reduces toxicity and improves antitumor efficacy. J. Liposome Res., *5:* 523–541, 1995.
22. Burke, T. G., and Gao, X. Stabilization of topotecan in low pH liposomes composed of distearoylphosphatidylcholine. J. Pharm. Sci., *83:* 967–969, 1994.
23. Yuan, F., Leunig, M., Huang, S. K., Berk, D., Papahadjopoulos, D., and Jain, R. K. Micro-vascular and interstitial penetration of sterically stabilized (Stealth) liposomes in a human tumor xenograft. Cancer Res., *54:* 3352–3356, 1994.
24. Chonn, A., Semple, S. C., and Cullis, P. R. Separation of large unilamellar liposomes from blood components by a spin column procedure: towards identifying plasma proteins which mediate liposome clearance *in vivo*. Biochim. Biophys. Acta, *1070:* 215–222, 1991.
25. Bally, M. B., Nayar, R., Masin, D., Hope, M. J., Cullis, P. R., and Mayer, L. D. Liposomes with entrapped doxorubicin exhibit extended blood residency times. Biochim. Biophys. Acta, *1023:* 133–139, 1990.
26. Horwitz, S. B., and Horwitz, M. S. Effects of camptothecin on the breakage and repair of DNA during the cell cycle. Cancer Res., *33:* 2834–2836, 1973.
27. Recondo, G., Abbruzzese, J., Newman, B., Newman, R., Kuhn, J., von Hoff, D., Gartiez, D., and Raber, M. A Phase I trial of topotecan (TOPO) administered by a 24 hour infusion. Proc. Am. Assoc. Cancer Res., *32:* 206, 1991.
28. Slichenmyer, W. J., Rowinsky, E. K., Donehower, R. C., and Kaufmann, S. H. The current status of camptothecin analogues as antitumor agents. J. Natl. Cancer Inst., *85:* 271–291, 1993.
29. McCabe, F. L., and Johnson, R. K. Comparative activity of oral and parenteral topotecan in murine tumor models: efficacy of oral topotecan. Cancer Invest., *12:* 308–313, 1994.
30. Kollmannsberger, C., Mross, K., Jakob, A., Kanz, L., and Bokemeyer, C. Topotecan—a novel topoisomerase I inhibitor: pharmacology and clinical experience. Oncology, *56:* 1–12, 1999.

Available online at www.sciencedirect.com
ScienceDirect
Biochimica et Biophysica Acta 1768 (2007) 678–687
www.elsevier.com/locate/bbamem

Coencapsulation of irinotecan and floxuridine into low cholesterol-containing liposomes that coordinate drug release in vivo

Paul G. Tardi [a,*], Ryan C. Gallagher [a], Sharon Johnstone [a], Natashia Harasym [a], Murray Webb [b], Marcel B. Bally [b], Lawrence D. Mayer [a]

[a] *Celator Pharmaceuticals Corp., 1779 West 75th Avenue, Vancouver, BC, Canada V6P 6P2*
[b] *Department of Advanced Therapeutics, British Columbia Cancer Agency, 600 West 10th Avenue, Vancouver, BC, Canada V5Z 4E6*

Received 7 September 2006; received in revised form 23 November 2006; accepted 30 November 2006
Available online 6 December 2006

Abstract

A liposomal delivery system that coordinates the release of irinotecan and floxuridine in vivo has been developed. The encapsulation of floxuridine was achieved through passive entrapment while irinotecan was actively loaded using a novel copper gluconate/triethanolamine based procedure. Coordinating the release rates of both drugs was achieved by altering the cholesterol content of distearoylphosphatidylcholine (DSPC)/distearoylphosphatidylglycerol (DSPG) based formulations. The liposomal retention of floxuridine in plasma after intravenous injection was dramatically improved by decreasing the cholesterol content of the formulation below 20 mol%. In the case of irinotecan, the opposite trend was observed where increasing cholesterol content enhanced drug retention. Liposomes composed of DSPC/DSPG/Chol (7:2:1, mole ratio) containing co-encapsulated irinotecan and floxuridine at a 1:1 molar ratio exhibited matched leakage rates for the two agents so that the 1:1 ratio was maintained after intravenous administration to mice. The encapsulation of irinotecan was optimal when copper gluconate/triethanolamine (pH 7.4) was used as the intraliposomal buffer. The efficiency of irinotecan loading was approximately 80% with a starting drug to lipid molar ratio of 0.1/1. Leakage of floxuridine from the liposomes during irinotecan loading at 50 °C complicated the ability to readily achieve the target 1:1 irinotecan/floxuridine ratio inside the formulation. As a result, a procedure for the simultaneous encapsulation of irinotecan and floxuridine was developed. This co-encapsulation method has the advantage over sequential loading in that extrusion can be performed in the absence of chemotherapeutic agents and the drug/drug ratios in the final formulation can be more precisely controlled.

Keywords: Liposomes, Irinotecan, Floxuridine; Coordinated release, Metal loading

1. Introduction

Liposomes have been used extensively to improve the therapeutic index of a variety of drugs by ameliorating toxicity and/or increasing the therapeutic potency of the encapsulated agent [1,2]. This is perhaps best exemplified in the delivery of anticancer drugs where it has been well documented both preclinically and clinically that small (approximately 100 nm) liposomes reduce exposure of entrapped drugs to susceptible healthy tissues while preferentially accumulating in sites of tumor growth due to enhanced permeability and retention (EPR) effects associated with solid tumors [3–6]. This in turn has often resulted in improvements of the overall therapeutic activity of the drug and has led to the regulatory approval of several liposome-based anticancer products [7,8]. Interestingly, very little work has been undertaken to deliver drug combinations in liposomes. This is likely the result of difficulties associated with the efficient and stable encapsulation of two chemotherapeutics inside a single liposome as well as challenges in controlling the release of chemically disparate drugs with one liposome composition.

Our interest in developing liposome formulations containing co-encapsulated anticancer drug combinations stems from the fact that virtually all curative cancer treatment regimens utilize drug combinations. We hypothesized that enhanced antitumor activity may be achieved by simultaneously delivering and

* Corresponding author. Tel.: +1 604 675 2105; fax: +1 604 708 5883.
E-mail address: ptardi@celatorpharma.com (P.G. Tardi).

0005-2736/$ - see front matter © 2006 Elsevier B.V. All rights reserved.
doi:10.1016/j.bbamem.2006.11.014

exposing anticancer drug combinations to tumor cells in vivo, since tumor cells would be less able to develop compensatory resistance mechanisms compared to single or sequentially administered agents. This approach became of even greater importance when we recently observed that the antitumor activity of drug combinations can be dramatically dependent on the molecular ratio of the combined drugs [9]. Specifically, some ratios of a drug combination can be synergistic whereas other ratios of the same drugs can be additive or even antagonistic [10]. This highlighted the need to control drug ratios being exposed to tumor cells after systemic administration since the uncontrolled and dissimilar pharmacokinetics of individual drugs utilized in conventional drug "cocktails" no doubt results in exposure to sub-optimal drug ratios with a concomitant loss in therapeutic activity. Further, although an increasing number of individual liposomal anticancer drugs are being developed, the pharmacokinetics of currently available formulations vary greatly which would hinder attempts to coordinate the exposure of different drugs using existing liposome formulations [11,12]. In addition, combining multiple liposome-based anticancer drugs poses potential difficulties due to high lipid doses which have been shown in humans to lead to infusion-related adverse events [13,14].

In view of the above considerations, we undertook a series of studies aimed at developing single liposome formulations that are able to stably co-encapsulate drug combinations and coordinate the release of the two agents after intravenous (i.v.) injection. In this report we describe the co-encapsulation of irinotecan and floxuridine. This drug combination was selected based on the fact that irinotecan and fluoropyrimidine (typically 5-fluorouracil, 5-FU) combination treatment is standard of care for metastatic colorectal cancer. The focus on floxuridine rather than 5-FU was based on the superior encapsulation and retention properties of floxuridine compared to 5-FU [15] and the fact that trials conducted in the 1960s established the clinical equivalency of these two fluoropyrimidines [16,17]. We have shown in previous studies that a 1:1 molar ratio of these drugs optimizes drug synergy in a panel of gastrointestinal tumor lines [9]. We describe here the identification of liposome encapsulation techniques and lipid compositions that result in stable drug entrapment and drug release rates that maintain irinotecan and floxuridine at a 1:1 molar ratio after i.v. administration.

2. Materials and methods

2.1. Lipids, drugs and chemicals

Distearoylphosphatidylglycerol (DSPG), distearoylphosphatidylcholine (DSPC) and cholesterol were obtained from Avanti Polar Lipids (Alabaster, AL, USA). Irinotecan hydrochloride trihydrate (Camptosar) is a product of Pharmacia and Upjohn Company (Kalamazoo, MI, USA) and was obtained from the pharmacy of the British Columbia Cancer Agency. It was also obtained as a dry powder from SciroPharm Taiwan, Ltd. (Taipei, Taiwan). Floxuridine was obtained from the Zhejiang Hisun Pharmaceutical Company (Taizhou City, China). Radiolabelled [^{3}H]floxuridine was obtained from Moravek Biochemicals (Brea, CA, USA). Cholesterol hexadecyl ether (CHE) radiolabelled with [^{3}H] or [^{14}C] was obtained from NEN Life Science Products (Oakville, ON, Canada). All other chemicals were purchased from Sigma Chemical Company (St. Louis, MO, USA).

2.2. Preparation of liposomes

Based on the appropriate molar composition, DSPC and DSPG were dissolved in chloroform/methanol/water (5/1/.1) at 50 mg/ml and combined with cholesterol dissolved in chloroform. Where appropriate, cholesteryl hexadecyl ether [^{14}C]CHE or [^{3}H]CHE was added as a non-exchangeable, non-metabolizable lipid marker [18]. The solvent was removed under a stream of nitrogen gas and the lipid films placed under high vacuum overnight. Typically, the lipid films were rehydrated at 70 °C with 100 mM copper gluconate, 220 mM triethanolamine (TEA), pH 7.4. The pH of the copper gluconate solution was adjusted by varying the TEA content and not through the addition of sodium hydroxide. In experiments involving the sequential loading of floxuridine and irinotecan, the floxuridine was passively trapped in the liposomes by adding 122 mM floxuridine plus [^{3}H]floxuridine as a tracer to the copper gluconate buffer. The newly formed multilamellar vesicles (MLVs) were passed 10 times through an extruding apparatus (Northern Lipids) containing two stacked 100 nm polycarbonate filters. The mean diameter and size distribution of each liposome preparation, analyzed by a NICOMP Model 270 Submicron particle sizer (Pacific Scientific, Santa Barbara, CA, USA) operating at 632.8 nm, was typically 110±20 nm. Following extrusion the external liposomal buffer was exchanged for 300 mM sucrose, 20 mM HEPES, 30 mM EDTA, pH 7.4 (SHE) using tangential flow chromatography.

2.3. Time course of irinotecan encapsulation

The following conditions were used to examine irinotecan encapsulation into liposomes containing various metal salts, copper gluconate at different pH and irinotecan to lipid ratios. Irinotecan (Camptosar) and liposomes were heated separately at 50 °C for 1 min and then combined at $t=0$ by adding the lipid to the drug while vortexing. The final lipid concentration was diluted to 30 mM using SHE buffer. Aliquots of 100 μl were removed at various time points and applied to 1 ml Sephadex G-50 spin columns. The columns were prepared by adding glass wool to a 1 ml syringe and Sephadex G-50 beads hydrated in HEPES buffered saline (HBS; 20 mM HEPES, 150 mM NaCl, pH 7.4). The columns were packed by spinning at 500 × g for 2 min. Following addition of the sample to the column, the liposome fraction was collected in the void volume by centrifuging at 650 × g for 1 min. Aliquots of the spin column eluant and the pre-column solution were taken and analyzed by liquid scintillation counting to determine the lipid concentration at each time point. The irinotecan concentration in each liposomal fraction was determined using a UV based assay. Briefly, a 100 μl aliquot of each liposomal sample (or smaller volume adjusted to 100 μl with distilled water) was solubilized in 100 μl of 10% Triton X-100 plus 800 μl of 50 mM citrate/trisodium citrate, 15 mM EDTA, pH 5.5 and heated in boiling water until the cloud point was reached. The samples were cooled to room temperature and the absorbance at 370 nm measured and compared to a standard curve. For mouse studies utilizing irinotecan containing formulations, the unencapsulated irinotecan and EDTA was removed by replacing the external buffer with SH buffer (300 mM sucrose, 20 mM HEPES, pH 7.4) using tangential flow chromatography.

2.4. Simultaneous encapsulation of irinotecan and floxuridine

A lipid film composed of DSPC/DSPG/Chol (7:2:1, mol/mol/mol) was prepared as previously described in Section 2.2 containing [^{14}C]CHE as the lipid marker. The film was hydrated with 100 mM copper gluconate, 220 mM TEA, pH 7.4 at 70 °C and the resulting MLVs were extruded at 70 °C through two stacked 100 nm filters for a total of ten passes. The liposomes were subsequently exchanged for SHE using tangential flow chromatography and concentrated to 60 mg/ml. To prepare a drug solution containing floxuridine and irinotecan, ^{3}H-floxuridine was first added to a test tube and dried under a stream of nitrogen. Subsequently, floxuridine and irinotecan were added to the same tube as a powder and hydrated with SHE buffer. The pH of the drug solution was adjusted to 7.4 with NaOH. The amount of irinotecan in the loading solution was based on a 0.12 drug to lipid molar ratio. The final floxuridine concentration was adjusted so that a concentration of 122 mM would be achieved after its addition to the liposome solution. The drug solution and the liposomes were incubated separately at 50 °C for approximately 5 min to equilibrate the temperature. The

two solutions were then combined and 100 μL aliquots were removed at various time points and applied to a Sephadex G-50 spin column as previously described. The drug to lipid ratio for floxuridine, from the eluted column sample, was determined using dual label liquid scintillation counting. The irinotecan concentration was determined by measuring the irinotecan absorbance at 370 nm as previously described.

2.5. Mice

Female Balb/c mice (6–8 weeks), 20–22 g breeders were purchased from Charles River Laboratories (St. Constant, PQ, Canada) and bred in house. Mice were housed in microisolator cages and given free access to water and food. The animals were maintained according to the procedures established at the BC Cancer Agency Joint Animal Facility. All animal studies were approved by the University of British Columbia Animal Care Committee in accordance with the guidelines established by the Canadian Council of Animal Care.

2.6. Plasma elimination of liposomes

To determine the retention of irinotecan and floxuridine in various liposomal formulations in vivo, plasma elimination studies were performed. Radiolabelled liposomes containing floxuridine and/or irinotecan were administered at the appropriate concentration intravenously into the lateral tail vein of mice. At 1, 4 and 24 h after administration, mice were asphyxiated with CO_2 and the blood collected by cardiac puncture and placed into EDTA coated microtainer tubes. The blood was centrifuged at 900×*g* for 10 min at 4 °C to isolate the plasma fraction. Liposomes and floxuridine concentrations were determined by liquid scintillation counting while irinotecan concentrations were determined by HPLC.

2.7. Irinotecan quantitation using HPLC

To determine the $T=0$ irinotecan concentration in the liposome sample prior to injection, the liposomes were diluted 1:100 in saline. Subsequently, a 100 μL aliquot of the diluted liposome sample was mixed with internal standard (camptothecin), followed by adding 600 μL acidified methanol (pH 2.0). For determination of irinotecan HCl in plasma, 10 μL (1-h and 4-h time points) or 20 μL (24-h time points) mouse plasma was mixed with 10 μL internal standard (camptothecin) followed by adding 600 μL acidified methanol (pH 2.0). Samples were then vortexed vigorously and stored in −70 °C freezer for 1 h. After cooling, the samples were centrifuged for 10 min at 1500×*g* and the supernatant was analyzed for irinotecan HCl using HPLC. The chromatographic system consisted of a Waters Alliance 2695 system and 2475 fluorescence detector. Waters Symmetry reverse phase C18 column (4.6×250 mm, 5μ) protected by a Symmetry Sentry guard column (3.9×20 mm, 5μ) was used for chromatographic separation. The analytical column was maintained at a temperature of 30 °C. The mobile phase was composed of acetonitrile –75 mM ammonium acetate containing 7.5 mM tetrabutylammonium bromide (24:76, v/v), with pH adjusted to 6.4 using glacial acetic acid. The mobile phase was delivered isocratically at a flow rate of 1.5 mL/min. Column elute was monitored fluorimetrically at excitation wavelength of 362 nm and emission wavelength of 425 nm. Detection and integration of chromatographic peaks was performed by Waters Empower software. Irinotecan HCl concentration was calculated using a calibration curve (linear range 2–100 μg/mL).

3. Results

3.1. Irinotecan encapsulation into transition metal containing liposomes

Based on the structure of irinotecan and the documented ability of transition metals to interact with drugs [19], we hypothesized that the presence of a free hydroxyl on the E-ring adjacent to the lactone group could be a candidate for the formation of a coordination complex with metal ions [20,21], thus enabling active loading of the irinotecan into preformed liposomes containing a metal salt solution. To determine if irinotecan could be encapsulated into liposomes using transition metals, DSPC/Chol (55:45 mol/mol) liposomes were prepared containing 300 mM sulfate salts of manganese, zinc, copper, nickel or cobalt. The liposomes were incubated with irinotecan at 50 °C using a drug to lipid ratio of 0.1:1 (mol/mol) for 1 h. This temperature was selected based on the fact that temperatures ≤40 °C provided very slow irinotecan encapsulation rates (data not shown). At various time points, aliquots were removed and the encapsulated drug to lipid ratio was determined (Fig. 1). Less than 10% encapsulation was observed under these conditions for all metals except zinc and copper which rapidly accumulated irinotecan. Zinc encapsulation was less efficient than copper with a maximum irinotecan to lipid ratio of 0.075:1 (mol/mol) and showed a gradual decrease in trapped irinotecan over the 60-min time course. Irinotecan encapsulation into copper containing liposomes was very effective with >95% encapsulation efficiency at all time points tested. It should be noted that although evidence of transition metal–fluoropyrimidine interactions have been reported [22], attempts to actively encapsulate floxuridine into metal containing liposomes in a manner similar to irinotecan were unsuccessful (data not shown).

Numerous copper salts (chloride, sulfate, nitrate, gluconate and tartrate) are commercially available, however, only the sulfate and gluconate forms were found to be sufficiently soluble and stable to promote efficient irinotecan encapsulation described here. When dissolved in water, both the sulfate and gluconate forms of copper are acidic with a pH of approximately 4. Since it was desirable to have an internal liposomal pH near neutrality, the copper solutions were adjusted to pH 7.4. When copper sulfate was pH adjusted with sodium hydroxide, however, a significant copper oxide

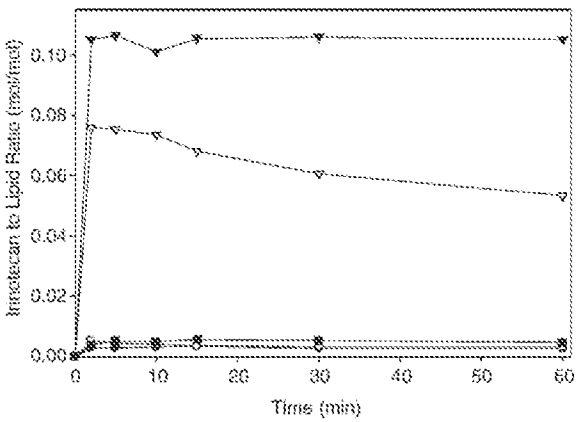

Fig. 1. Irinotecan encapsulation into DSPC/Chol (55:45, mol%) liposomes using various metal salts. Liposomes radiolabelled with [^{3}H]CHE were extruded in the presence of various unbuffered metal salt solutions and subsequently exchanged into SHE buffer (pH 7.4). The liposomes were incubated at 50 °C in the presence of irinotecan at a 0.1/1 molar drug to lipid ratio. At various time points aliquots were removed and assayed for drug encapsulation as outlined in Section 2.3. The following metal solutions, $CuSO_4$ (▼); $ZnSO_4$ (▽); $MnSO_4$ (■); $CoSO_4$ (●) and $NiSO_4$ (○) were all prepared at a concentration of 300 mM and were not pH adjusted (representative data shown).

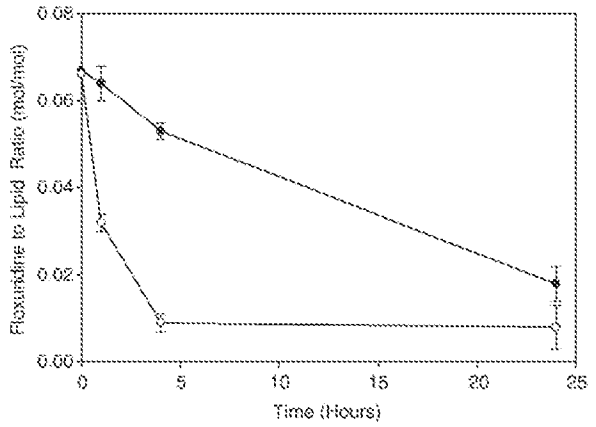

Fig. 2. The influence of liposome composition on the retention of floxuridine in vivo. Liposomes composed of either DSPC/DSPG (8:2 molar ratio, ●) or DSPC/Chol (55: 45 molar ratio, ○) were radiolabelled with [^{14}C]CHE were extruded in the presence of a 100 mM solution of [^{3}H]floxuridine dissolved in HBS (pH 7.4). The unencapsulated floxuridine was exchanged for saline using tangential flow chromatography. The liposomes were injected into the tail vein of female Balb/c mice at a floxuridine dose of 5 mg/kg. Blood was collected via cardiac puncture at 1, 4 and 24 h after injection (3 mice per time point). Lipid and floxuridine recovery was determined by liquid scintillation counting.

precipitate formed immediately after mixing. The biological buffer triethanolamine (TEA) was found to be the most compatible buffer for both copper sulfate and copper gluconate pH adjustment. When pH 7.4 solutions of copper gluconate and copper sulfate were compared for their ability to encapsulate irinotecan, the copper gluconate solution was found to be superior in total capacity, percent encapsulation and drug retention (data not shown). As a result, all subsequent formulation studies focused on copper gluconate buffered with TEA. It should be noted that stable liposome formulations containing gluconate salts of the other transition metals buffered to physiological pH could not be prepared due to instability of the salt solution which lead to significant precipitation (data not shown).

3.2. Floxuridine encapsulation and retention in liposomes

Since floxuridine could not be actively loaded into liposomes via metal complexation, the drug was passively encapsulated into liposomes by hydrating lipid films in the presence of floxuridine solutions. A previous study reported that the trapping efficiency of floxuridine can be increased when trapped in negatively charged liposomes [15]. Also, recent studies have shown that cholesterol-free liposomes can enhance the retention properties of certain drugs [23]. Taken together, this information led us to investigate the in vivo drug retention properties of cholesterol-free, negatively charged liposomes composed of DSPC/DSPG (80:20, mol/mol) compared to DSPC/Chol (55:45, mol/mol) formulations. As shown in Fig. 2, the retention of floxuridine (reflected by maintenance of the encapsulated drug to lipid ratio) inside liposomes after i.v. injection to mice was found to be superior in the cholesterol free formulation. The half life for the release of floxuridine from the liposomes increased from approximately 1 h for DSPC/Chol (55:45, mol/mol) liposomes to approximately 16 h for the DSPC/DSPG (80:20, mol/mol) formulation. Based on the superior floxuridine retention properties and circulation lifetimes, the DSPC/DSPG formulation was studied as a potential delivery system for the drug combination of irinotecan and floxuridine.

3.3. Co-formulation of irinotecan and floxuridine

Initial studies on the co-formulation of irinotecan and floxuridine focused on the hydration of lipid films with solutions of copper gluconate/TEA that contained floxuridine. However, irinotecan encapsulation was not affected by the presence or absence of floxuridine within the liposomes. As a result, the optimization of irinotecan loading was determined in the absence of entrapped floxuridine. The liposomes hydrated from lipid films were extruded and the unencapsulated copper was removed by tangential flow dialysis. The conditions that were found to impact the subsequent encapsulation of irinotecan to the greatest degree were pH and temperature. To determine the optimal pH for irinotecan loading, liposomes were prepared with matching internal and external buffer pH. The time course for irinotecan loading into liposomes at 50 °C is presented in Fig. 3. Maximum irinotecan encapsulation leading to a final drug to lipid ratio of approximately 0.8:1 (mol/mol) was achieved with buffers at pH 7.0 and 7.5. This reflected an encapsulation efficiency of 80% based on the starting irinotecan to lipid ratio of 0.1:1 (mol/mol). The rate of irinotecan accumulation inside the copper containing liposomes was most rapid at pH 7.5 where uptake levels were 85% of maximum within 5 min. Decreasing the pH to 6.5 or 6.0 resulted in decreased rates of irinotecan accumulation and liposome uptake levels after incubating for 60 min were 0.061 and 0.039 μmole drug/μmol lipid, respectively. Due to the similar

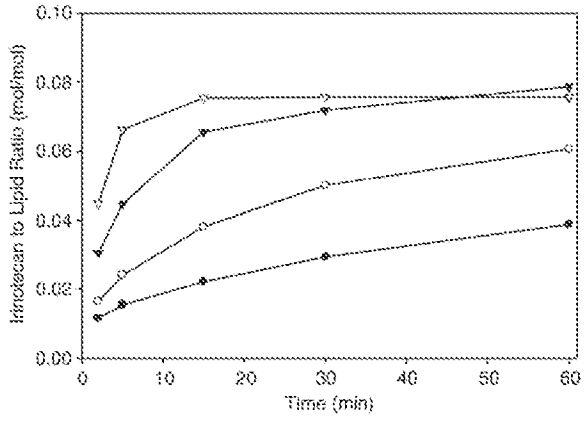

Fig. 3. The effect of pH on irinotecan encapsulation. Liposomes composed of DSPC/DSPG (80:20 molar ratio) were radiolabelled with [^{3}H]CHE and extruded in the presence of 100 mM copper gluconate that was pH adjusted with TEA to pH 7.5 (▽); pH 7 (▼), pH 6.5 (○) or pH 6 (●). The external liposomal solution was replaced with 150 mM NaCl, 10 mM HEPES and 10 mM MES which was pH adjusted to match the internal liposomal pH. Irinotecan was incubated with the liposomes at 50 °C and at various times aliquots were removed and passed through a spin column to determine the extent of irinotecan encapsulation. The irinotecan to lipid ratio was determined as described previously in Section 2.3 (representative data shown).

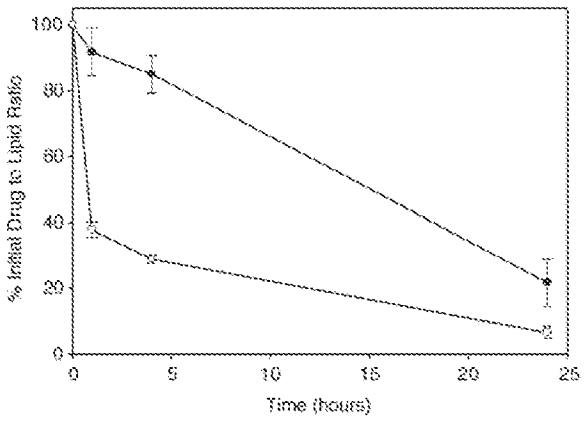

Fig. 4. The in vivo retention of floxuridine and irinotecan coformulated in DSPC/DSPG (80:20 molar ratio) liposomes. Liposomes were radiolabelled with [^{14}C]CHE and extruded in the presence of 100 mM copper gluconate/TEA pH 7.4 containing [^{3}H] labelled floxuridine. The external buffer was exchanged for SHE (pH 7.4) and loaded with irinotecan at a drug to lipid molar ratio of 0.1/1. The unencapsulated irinotecan and EDTA was removed by exchanging into SH buffer using tangential flow chromatography. Mice were injected via the tail vein at a lipid dose of 200 μmol/kg (16 μmol/kg of irinotecan and floxuridine). Blood was recovered at 1, 4 and 24 h after injection and centrifuged to isolate plasma (3 mice per time point). Lipid and floxuridine (●) levels were determined by liquid scintillation counting while irinotecan (○) concentrations were determined by HPLC analysis.

irinotecan loading properties at pH 7 and 7.5, the physiological pH of 7.4 was chosen for all subsequent studies.

Liposomes composed of DSPC/DSPG (80:20, mol/mol), containing both floxuridine and irinotecan at a molar drug ratio of 1:1 (drug to lipid molar ratios of approximately 0.08:1), were administered i.v. into mice to determine if this formulation could coordinate drug release after injection. The drug to lipid ratio for both drugs was monitored in the plasma over 24 h as an indicator of drug release from the liposomes in the circulation. As shown in Fig. 4, the retention of floxuridine in this cholesterol-free formulation was far greater than that observed for irinotecan. The floxuridine drug to lipid ratio decreased linearly over time with a half life of approximately 14 h and 22% of the original drug to lipid ratio remained after 24 h. In contrast, the retention of irinotecan was poor with greater than 60% drug leakage within the first hour after injection and the plasma irinotecan to lipid ratio at 24 h was only 5% of the starting drug to lipid ratio. This large difference in drug release rates lead to circulating irinotecan/floxuridine ratios that rapidly deviated from the desired 1:1 ratio. It should be noted that the rates of irinotecan and floxuridine release when co-formulated inside the same liposome were similar to those obtained for each respective drug encapsulated individually inside the liposomes (data not shown).

In order to better coordinate the release of irinotecan and floxuridine co-formulated inside 100 nm liposomes, an iterative variation of lipid composition was performed. Since cholesterol content was shown to have a dramatic impact on the retention of floxuridine (Fig. 2), we reasoned that it may also play a role in the retention of irinotecan. Various liposome formulations containing cholesterol at levels ranging from 0 to 15% were tested for drug retention in vivo. At 1, 4 and 24 h after injection, blood was collected and the plasma was analyzed for irinotecan, floxuridine and lipid levels. Irinotecan to lipid ratios were found to be significantly affected by cholesterol content (Fig. 5, top panel). In the formulations containing 0 or 5% cholesterol, rapid leakage of irinotecan is observed. One hour after injection of these formulations, the circulating liposomes retained only 38%

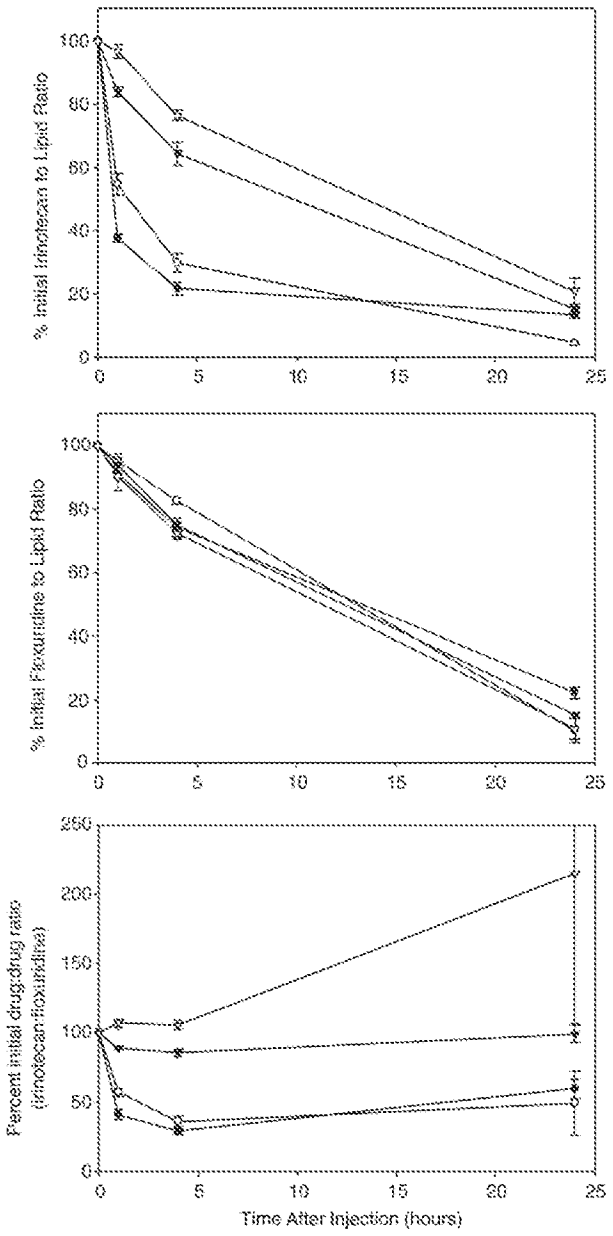

Fig. 5. The in vivo retention of floxuridine and irinotecan coformulated in various liposomal formulations. Liposomes composed of DSPC/Chol/DSPG (65:15:20 molar ratio); ▽, DSPC/Chol/DSPG (70:10:20 molar ratio); ▼, DSPC/Chol/DSPG (75.5:20 molar ratio); ○, and DSPC/DSPG (80:20 molar ratio); ● were radiolabelled with [^{14}C]CHE and coformulated with irinotecan and floxuridine as previously described. Samples were injected into the tail vein of mice at a lipid dose of 370 μmoles/kg (37 μmoles/kg irinotecan and floxuridine). At 1, 4 and 24 h after injection blood was collected and assayed for lipid, irinotecan and floxuridine levels (3 mice per time point). Changes to irinotecan to lipid levels with time are monitored in the upper panel while the middle panel plots the floxuridine to lipid levels from the same formulation. The lower panel charts changes in the drug: drug molar ratio in the various liposomal formulations over time.

and 55% of the initial encapsulated irinotecan, respectively. When the cholesterol content was increased to 10 and 15 mol%, we observed 84 and 97% of initial irinotecan to lipid ratios in the plasma after 1 h. The small increase in cholesterol content from 5 to 10 mol% increased the irinotecan half life by approximately 6.5-fold from 1.5 h to 10 h. This large dependency of irinotecan retention in vivo on cholesterol content was not observed at liposome cholesterol levels above 10 mol%. The sensitivity of irinotecan retention in the 10 mol% cholesterol range was subsequently investigated with formulations containing 7.5, 10 and 12.5 mol% cholesterol. Analysis of irinotecan release rates over 24 h found no significant differences between these three formulations (data not shown). As a result it appears that irinotecan retention is not correlated with cholesterol content in a linear fashion but requires a minimum threshold level. In addition, it should be noted that irinotecan can exist in an open ring carboxylate or closed ring lactone form. Only the lactone form of the drug is biologically active and was found to be the predominant form (>90%) in all the liposomal formulations tested.

The release of floxuridine from DSPC/DSPG-based liposomes as a function of cholesterol content was monitored and the results are presented in Fig. 5 (middle panel). Unlike irinotecan, floxuridine retention was not significantly influenced by cholesterol content between 0 and 15 mol%. The drug to lipid half life for floxuridine ranged from a high of approximately 13 h in the cholesterol free formulation to a low of approximately 11 h in the 15 mol% formulation. This was somewhat surprising since the results shown in Fig. 2 suggest that floxuridine leakage is dramatically enhanced in the presence of 45 mol% cholesterol. The fact that little difference was observed between 0 and 15 mol% cholesterol suggests that, similar to irinotecan leakage, there appears to be a threshold amount of cholesterol that is required before large changes in drug release are observed. When the encapsulated irinotecan to floxuridine molar ratio was plotted (Fig. 5, lower panel) for the 0 and 5 mol% formulations, the starting drug to drug molar ratio was observed to drop from 1:1 to 1:2 within 1 h. The initial drop in the molar drug ratio is the result of rapid leakage of irinotecan from these formulations. Following the initial drop at 1 h, the molar drug ratio is maintained out to 24 h. In the formulation containing 15 mol% cholesterol, the opposite trend was observed where the drug to drug ratio increases as a result of enhanced irinotecan retention relative to floxuridine. The synergistic 1:1 molar drug ratio was optimally maintained in the formulation containing 10 mol% cholesterol for which the release rates of both agents was matched.

3.4. Optimization of drug encapsulation

The studies described thus far have demonstrated that irinotecan and floxuridine can be stably co-encapsulated at a 1:1 molar ratio inside DSPC/DSPG/Chol (70:20:10, mol/mol) liposomes containing copper gluconate/TEA pH 7.4 and that these liposomes coordinate the release of the two drugs, thereby maintaining the irinotecan/floxuridine ratio for extended times after i.v. administration. In an attempt to increase the liposomal drug capacity, copper gluconate/TEA pH 7.4 containing liposomes were incubated at elevated starting irinotecan to lipid ratios to determine the maximum amount of drug that could be loaded into these formulations. Irinotecan encapsulation was not affected by the presence or absence of floxuridine within the liposomes, therefore irinotecan loading was determined in the absence of entrapped drug. At a starting drug to lipid ratio of 0.1:1, approximately 80% drug encapsulation is observed (Fig. 6). A similar encapsulation efficiency was observed at a starting irinotecan to lipid molar ratio of 0.2:1 where the final encapsulated drug to lipid ratio was approximately 0.15:1. However, when the starting irinotecan to lipid ratio was elevated to 0.3:1 the encapsulated irinotecan to lipid ratio increased only to 0.18:1, reflecting a decrease in encapsulation efficiency to approximately 60%. As a result, incubating the liposomes with irinotecan at a 0.2:1 ratio provided the highest drug to lipid ratio in the final formulation (0.14–0.15/1) without significantly decreasing the irinotecan loading efficiency.

Floxuridine levels were also increased in the liposome formulations in order to compensate for the increase in irinotecan to lipid ratio and maintain the 1:1 molar drug ratio inside the liposomes. This was achieved by extruding the liposomes in the presence of elevated floxuridine concentrations. However, floxuridine leakage during irinotecan encapsulation at 50 °C when the higher drug to lipid ratios were utilized caused significant difficulty in controlling final irinotecan to floxuridine ratios in the liposomes. This effect is reflected in Fig. 7 which presents the encapsulated floxuridine to lipid ratio over time for liposomes incubated at temperatures ranging from 40 °C to 60 °C. Floxuridine release from DSPC/DSPG/Chol (70:20:10, mol/mol) liposomes at 40 °C and 45 °C was < 10% over 20 mn, however under these conditions, irinotecan encapsulation was <50% (data not shown). In contrast, >90% floxuridine release was observed within 5 min when the liposomes were incubated at ≥55 °C. The rapid drug release at this temperature occurred as a result of the liposomal membrane

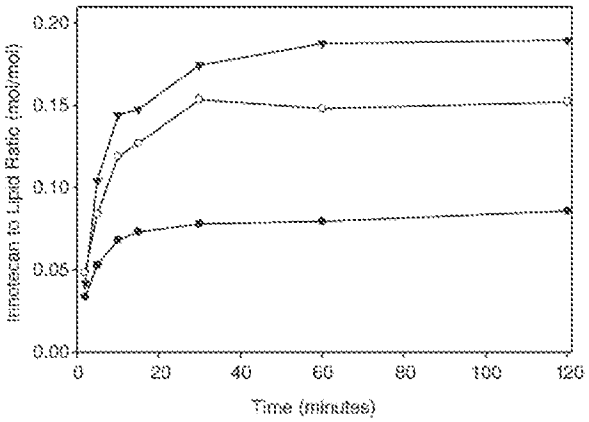

Fig. 6. The extent of irinotecan encapsulation at various starting drug to lipid ratios. Liposomes composed of DSPC/Chol/DSPG (70:10:20 molar ratio) were radiolabelled with [^{3}H]CHE and incubated with irinotecan at drug to lipid molar ratios of 0.1:1 (◆), 0.2:1 (○) and 0.3 :1 (▼). The reaction was carried out at 50 °C for various times and assayed for drug encapsulation as previously described (representative data shown).

converting from a gel state to a liquid–crystalline state with a phase transition temperature (T_m) of 54.5 °C as measured using differential scanning calorimetry (data not shown). By decreasing the loading temperature to 50 °C, approximately 10% drug leakage was observed after 10 min, at which time irinotecan loading achieved maximum levels (see Fig. 3).

3.5. Simultaneous drug loading

In view of the difficulties associated with reproducibly achieving target irinotecan/floxuridine ratios inside DSPC/DSPG/Chol (70:20:10, mol/mol) liposomes with descending floxuridine entrapment due to leakage during irinotecan encapsulation, we examined alternative entrapment procedures whereby the two drugs could be simultaneously loaded subsequent to liposome formation and extrusion. We reasoned that if floxuridine could leak from liposomes when incubated at 50 °C, it should also be possible for the drug to load into preformed liposomes by following its concentration gradient and equilibrating across the liposome bilayer during irinotecan encapsulation. This approach relied on the ability of floxuridine and irinotecan to permeate the membrane under conditions where copper remained inside the liposomes. Liposomes were extruded in the presence of copper gluconate/TEA (pH 7.4) in the absence of floxuridine and then buffer exchanged to remove unencapsulated copper. Just prior to liposome loading, a single drug solution containing irinotecan and floxuridine was prepared. As shown in Fig. 8, floxuridine passively accumulated into liposomes simultaneously with irinotecan active encapsulation without compromising the integrity of irinotecan loading. The similar kinetics of liposome accumulation for floxuridine and irinotecan facilitated the ability to precisely control the drug/drug ratios in the final formulation and reliably achieve the target 1:1 molar ratio. It should be noted that the pharmacokinetics and drug release properties of this formulation did not differ from those observed with liposome formulations in which floxuridine and irinotecan were sequentially loaded (see Fig. 5).

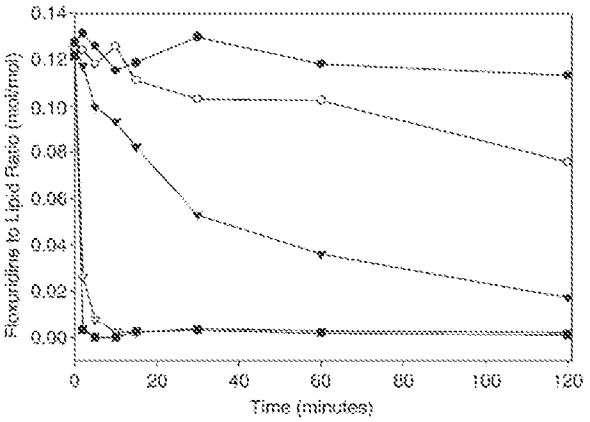

Fig. 7. The extent of floxuridine leakage from DSPC/Chol/DSPG (70:10:20 molar ratio) liposomes at various temperatures. Liposomes labelled with [^{14}C]CHE were extruded in the presence of 122 mM [^{3}H]floxuridine in HBS pH 7.4 and subsequently buffer exchanged to remove unencapsulated drug. To monitor the leakage rates of floxuridine from the formulation at a range of temperatures, the liposomes were incubated at 40 °C (◆), 45 °C (○), 50 °C (▼), 55 °C (▽) and 60 °C (■) for 2 h. At various time points, aliquots were removed and passed though a Sephadex G-50 spin column and assayed for lipid and floxuridine content using liquid scintillation counting (representative data shown).

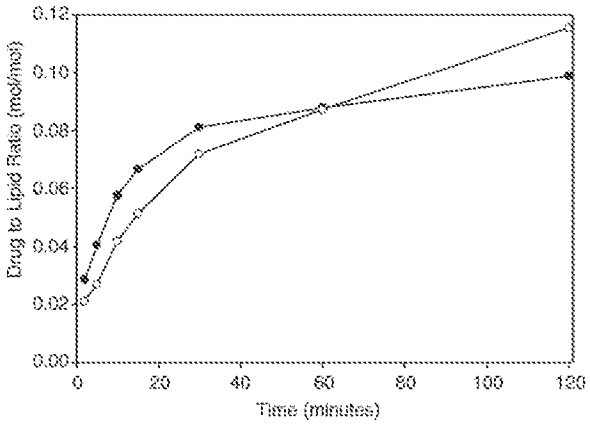

Fig. 8. The drug to lipid ratio of irinotecan and floxuridine during simultaneous drug loading. Liposomes composed of DSPC/Chol/DSPG (70:10:20 molar ratio) were radiolabelled with [^{14}C]CHE and incubated at 50 °C with [^{3}H] floxuridine and irinotecan as outlined in Section 2.4. At various time points aliquots were removed and passed through a Sephadex G-50 spin column to determine the irinotecan to lipid ratio (◆) and the floxuridine to lipid ratio (○) (representative data shown).

4. Discussion

The use of drug combinations has been standard of care in the treatment of cancer for many years. Given this and the expanded use of liposomal delivery vehicles for cancer chemotherapy, it is somewhat surprising that very little research has focused on the development of liposomal drug combinations, either in separate liposomes or co-encapsulated in the same liposome. This may be related to expectations that the activity of liposomal drug combinations would simply be the sum of the individual liposomal drug components. In fact, the limited examples where liposomal drug combinations have been investigated resulted in therapeutic activity that was less than predicted for additivity [24,25]. Such adverse outcomes could have resulted from unfavorable pharmacological interactions such as restricted delivery of encapsulated drugs to tumor sites, counteractive drug activities or altered drug release rates.

We have recently identified a new and potentially important application for liposome delivery of drug combinations. This application arose from in vitro observations in cytotoxicity assays where the degree of drug synergy or antagonism has been shown to be dependent on the ratio of drugs in the combination [9]. The implications of this observation are that unless drug combinations are maintained in a synergistic range after administration in vivo, therapeutic activity will be compromised. Clearly, such control of systemic drug ratios after injection of unencapsulated drug cocktails is difficult, if not impossible, to achieve. Our approach to this problem is therefore to: (1) identify the optimum drug/drug ratio in a range of in vitro tumor cell lines, (2) develop liposomes that can co-

encapsulate the desired drug/drug ratio and (3) maintain the drug/drug ratio in the synergistic range after administration so it can be exposed to tumor cells in vivo. One of the first drug combinations we applied this approach to was irinotecan and floxuridine, which are commonly used in the treatment of colorectal cancer [26–28]. This drug combination exhibited drug ratio-dependent synergy when examined in vitro where a 1:1 molar ratio was shown to be optimal over a broad range of tumor cell lines [9,29]. Consequently, we focused efforts to generate liposome formulations that could both encapsulate and maintain this drug combination at a 1:1 ratio.

In practical terms, the most challenging hurdle to achieving coordinated pharmacokinetics of drug combinations co-encapsulated in liposomes is the development of a single formulation that can simultaneously, yet independently control the release of two drugs that exhibit very differing physico-chemical properties, as is the case with irinotecan and floxuridine. Considering the significant differences in solubility properties of irinotecan and floxuridine, we contemplated establishing formulation conditions that would differentially control the entrapment and retention of these two drugs. As a very water-soluble compound (>400 mg/ml), floxuridine can be readily entrapped passively during liposome production and its release from liposomes will be predominately controlled by lipid permeability properties. In comparison, irinotecan can be actively entrapped inside liposomes with high efficiency using transmembrane pH gradients [30]. However, the use of pH gradients can be problematic due to the instability of phospholipids exposed to the acidic liposome interior which can lead to altered drug retention properties [31]. We therefore examined the use of encapsulated transition metals to actively load irinotecan without the use of pH gradients.

The rationale for utilizing encapsulated transition metals to actively load and retain irinotecan was based on the more than 40 years of evidence documenting interactions between transition metals and drugs [19]. We observed that only copper and zinc were able to promote the efficient encapsulation of irinotecan when high concentrations of liposome encapsulated unbuffered metal sulfates were utilized. The other metal sulfates tested (Ni, Mn, Co) provided little or no encapsulation under the conditions utilized even though $MnSO_4$ was previously reported to promote the encapsulation of doxorubicin into liposomes [32]. The pH of these unbuffered metal solutions ranged from a low of 3.3 for $MnSO_4$ to a high of 5.5 for $CoSO_4$. Based on this information and the loading curves, there appeared to be no correlation between the pH of the encapsulated salt solution and the extent of drug encapsulation. The lack of irinotecan uptake in the presence of $MnSO_4$ observed here contrasts the results obtained previously with another weak base camptothecin, topotecan, where liposomes containing this metal and the ionophore A23187 actively accumulated the drug [33]. This difference is related to the fact that in the presence of the ionophore, a transmembrane pH gradient (inside acidic) is generated which drives drug uptake. The fact that irinotecan does not load into the $MnSO_4$ without an ionophore indicates that the encapsulation observed here is not due to a pH gradient, but rather is related to selective interactions between irinotecan and the transition metals copper and zinc. The strength of the irinotecan interaction, correlates with the stability constants commonly observed with metal complexes [34]. Specific interactions between copper and the anthracyclines have been previously reported [35,36].

We were also able to achieve efficient loading using liposomes containing copper gluconate buffered to physiological pH with TEA, thereby alleviating potential difficulties with lipid degradation at acidic pH. When the influence of internal and external pH on the encapsulation of irinotecan was investigated, significantly lower irinotecan encapsulation was observed with decreasing pH. This may be the result of a decreased irinotecan permeability at lower pH due to a larger fraction of protonated amine, decreased interactions between irinotecan and copper gluconate/TEA or a combination of both. The mechanism responsible for this decrease has not been fully elucidated at this time. When the starting drug to lipid ratio was increased to 0.3:1, irinotecan encapsulation reached a maximum drug to lipid ratio of 0.18:1. This saturation effect suggests a stoichiometric relationship between irinotecan and copper gluconate/TEA. Further investigations are underway to fully characterize the nature of the interaction between irinotecan and copper gluconate/TEA inside liposomes. It is important to note that preliminary evidence for this buffer system indicates that TEA plays a major role in mediating the encapsulation and retention of irinotecan in contrast to the case of unbuffered copper sulfate where evidence for a direct irinotecan–copper interaction was obtained [37]. The copper gluconate/TEA irinotecan loading process described here provided an encapsulation system that was more amenable to pharmaceutical applications and was therefore utilized in an iterative optimization process to coordinate the release of irinotecan and floxuridine in vivo. This copper based formulation of irinotecan and floxuridine has been evaluated in dog toxicological studies and no evidence of copper toxicity was detected.

When floxuridine and irinotecan encapsulated in liposomes were administered i.v. to mice, surprising trends were observed in drug pharmacokinetics as a function of lipid composition. Historically, liposomes composed of saturated phospholipids and high cholesterol content (>33 mol%) have provided maximum drug retention in vivo for a wide range of drugs [38,39]. More recently, we demonstrated that for some drugs, low cholesterol-containing gel phase liposomes can reduce in vivo drug release compared to cholesterol-enriched systems [23]. In the studies here we observed a rather striking dependence of irinotecan and floxuridine leakage from DSPC-based liposomes in that the relationship between drug release and cholesterol content in the liposome was diametrically opposed for the two drugs. Whereas cholesterol-free DSPC/DSPG liposomes displayed optimal floxuridine retention, irinotecan was rapidly released from these systems. By titrating the cholesterol content in DSPC/DSPG liposomes containing floxuridine/irinotecan at a 1:1 ratio and assessing the plasma drug release properties after i.v. injection, we were able to identify that liposomes composed of DSPC/DSPG/Chol at a 70:20:10 molar ratio (DSPC: this is to coordinate the

pharmacokinetics of the two agents such that the circulating drug/drug ratio was maintained at approximately 1:1 for up to 24 h. The fact that the circulating drug to lipid ratios for both irinotecan and floxuridine decrease at the same rate over time indicates that both drugs are bioavailable and are being exposed systemically at the 1:1 ratio.

When liposomes were passively encapsulated with floxuridine and subsequently loaded with irinotecan, the temperature of loading had a dramatic impact on the drug content of the final formulation. In the cholesterol-free and low cholesterol formulations, irinotecan encapsulation was almost immediate at 60 °C. Unfortunately, this temperature resulted in over 90% floxuridine leakage within 2 min. This rapid leakage is likely the result of heating the liposomes above their transition temperature of 55 °C. Since these liposomes contain very little cholesterol, bilayer fluidity at these temperatures prevents adequate retention of floxuridine. Complete retention of floxuridine could be achieved at 40 °C, however, the encapsulation of irinotecan at this temperature was observed to be very poor. Consequently, a temperature of 50 °C was identified at which irinotecan could be encapsulated with high efficiency with manageable loss of floxuridine such that the target 1:1 drug ratio could be achieved. Although this was achievable in formulation batches less than 10 mL, it was not possible to achieve the desired accuracy and reproducibility in larger volumes.

In order to resolve this problem, an alternative loading scheme was developed based on the observed leakage of floxuridine at 50 °C. The high permeability of floxuridine near the phase transition temperature of the formulation allowed for the passive loading of floxuridine during irinotecan encapsulation. Analysis of the drug loading curves in Fig. 8 for the two drugs revealed very similar kinetics. This is somewhat surprising since the mechanisms driving the encapsulation of floxuridine and irinotecan are quite different and the two drugs display very different drug release dependence on cholesterol content. This method, however, has allowed us to control the encapsulated drug/drug molar ratio over a wide range of time. This unique dual loading method has the advantage over sequential loading in that the liposomes are prepared and extruded in the absence of chemotherapeutics and the final drug/drug ratio in the formulation can be tightly controlled.

This report describes one of the first attempts to co-formulate drug combinations in a manner that coordinates the pharmacokinetics of the different drugs after i.v. administration. By combining copper gluconate/TEA-based drug encapsulation and low-cholesterol containing gel phase liposomes, we were able to encapsulate and maintain irinotecan and floxuridine at a fixed, synergistic molar ratio of 1:1. We believe that maintaining this ratio will be critical to maximizing the therapeutic activity of this drug combination, based on results in tumor models [9,29]. As more cancer therapies utilize a greater number of agents, it will become increasingly important to avoid antagonistic drug interactions in order to maximize therapeutic activity. Since the pharmacokinetics of the individual drugs in conventional combination treatments cannot be controlled, formulating multiple drugs into delivery vehicles that can coordinate their pharmacokinetics is a viable approach to optimize the therapeutic activity of multiple agent combinations.

References

[1] N.L. Boman, P.R. Cullis, L.D. Mayer, M.B. Bally, M.S. Webb, Liposomal vincristine: the central role of drug retention in defining therapeutically optimized anticancer formulations, In: M.C. Woodle, G. Storm (Eds.), Long-Circulating Liposomes: Old Drugs, New Therapeutics, Landes Bioscience, Austin, TX, 1998, pp. 29–49.

[2] J.W. Park, Liposome-based drug delivery in breast cancer treatment, Breast Cancer Res. 4 (2002) 95–99.

[3] L.D. Mayer, P.R. Cullis, M.B. Bally, Designing therapeutically optimized liposomal anticancer delivery systems: lessons from conventional liposomes, In: D. Lasic, D. Papahadjopoulos (Eds.), Medical Applications of Liposomes, Elsevier Science B.V., Amsterdam, 1998, pp. 231–257.

[4] A. Gabizon, D. Papahadjopoulos, Liposome formulations with prolonged circulation time in blood and enhanced uptake by tumors, Proc. Natl. Acad. Sci. U. S. A. 85 (1988) 6949–6953.

[5] F. Yuan, M. Leunig, S.K. Huang, D.A. Berk, D. Papahadjopoulos, R.K. Jain, Microvascular permeability and interstitial penetration of sterically stabilized (Stealth) liposomes in a human tumor xenograft, Cancer Res. 54 (1994) 3352–3356.

[6] A.A. Gabizon, Stealth liposomes and tumor targeting: one step further in the quest for the magic bullet, Clin. Cancer Res. 7 (2001) 223–225.

[7] D.N. Waterhouse, P.G. Tardi, L.D. Mayer, M.B. Bally, A comparison of liposomal formulations of doxorubicin with drug administered in free form: changing toxicity profiles, Drug Safety 24 (2001) 903–920.

[8] T.M. Allen, P.R. Cullis, Drug delivery systems: entering the mainstream, Science 303 (2004) 1818–1822.

[9] L.D. Mayer, T.O. Harasym, P.G. Tardi, N.L. Harasym, C.R. Shew, S.A. Johnstone, E.C. Ramsay, M.B. Bally, A.S. Janoff, Ratiometric dosing of anticancer drug combinations: controlling drug ratios after systemic administration regulates therapeutic activity in tumor-bearing mice, Mol. Cancer Ther. 5 (7) (2006) 1854–1863.

[10] T.O. Harasym, P.G. Tardi, S.A. Johnstone, M.B. Bally, A.S. Janoff, L.D. Mayer, Fixed drug ratio liposome formulations of combination cancer therapeutics, In: G. Gregoriadis (Ed.), Liposome Technology, 3rd Edition, Volume III: Interactions of Liposomes with the Biological Milieu, 2006, pp. 25–48.

[11] R. Krishna, M.S. Webb, G. St Onge, L.D. Mayer, Liposomal and non-liposomal drug pharmacokinetics after administration of liposome-encapsulated vincristine and their contribution to drug tissue distribution properties, J. Pharacol. Exp. Ther. 298 (2001) 1206–1212.

[12] A. Gabizon, D. Goren, R. Cohen, Y. Barenholz, Development of liposomal anthracyclines: from basics to clinical applications, J. Control. Release 53 (1998) 275–279.

[13] L. Cattel, M. Ceruti, F. Dosio, From conventional to stealth liposomes, a new frontier in cancer chemotherapy, Tumori 89 (2003) 237–249.

[14] J.R. Wingard, M.H. White, E. Anaissie, J. Raffalli, J. Goodman, A. Arrieta, the L Amph/ABLC Collaborative Study Group, A randomized, double-blind comparative trial evaluating the safety of liposomal Amphotericin B versus Amphotericin B lipid complex in the empirical treatment of febrile neutropenia, Clin. Infect. Dis. 31 (2000) 1155–1163.

[15] S.P. Simmons, P.A. Kramer, Liposomal entrapment of floxuridine, J. Pharm. Sci. 66 (1977) 984–986.

[16] C.W. Young, R.R. Ellison, R.D. Sullivan, S.N. Levick, R. Kaufman, E. Miller, J. Woldow, G. Escher, M.C. Li, D.A. Karnofsky, J.H. Burchenal, The clinical evaluation of 5-fluorouracil and 5-fluoro-2′-deoxyuridine in solid tumors in adults, Cancer Chemother. Rep. 6 (1960) 17–20.

[17] R.J. Reitemeier, C.G. Moertel, R.G. Hahn, Comparison of 5-fluorouracil (NSC-19893) and 2′-deoxy-5-fluorouridine (NSC-27640) in treatment of patients with advanced adenocarcinoma of colon or rectum, Cancer Chemother. Rep. 44 (1965) 39–43.

[18] J.T. Derksen, H.W. Morselt, G.L. Scherphof, Processing of different liposome markers after in vitro uptake of immunoglobulin-coated liposomes by rat liver macrophages, Biochim. Biophys. Acta 931 (1987) 33–40.

[19] W.O. Foye, Role of metal-binding in the biological activities of drugs, J. Pharm. Sci. 50 (1961) 93–103.
[20] J. Kuwahara, T. Suzuki, K. Funakoshi, Y. Sugiura, Photosensitive DNA cleavage and phage inactivation by copper(II)-camptothecin, Biochemistry 25 (1986) 1216–1221.
[21] J. Kuwahara, T. Suzuki, Y. Sugiura, Studies on antitumor drugs targeting DNA: photosensitive DNA cleavage of copper-camptothecin, Nucleic Acids Symp. Ser. 16 (1985) 201–204.
[22] U.P. Singh, R. Ghose, A.K. Ghose, A. Sodhi, S.M. Singh, R.K. Singh, The effect of histidine on the structure and antitumor activity of metal-5-halouracil complexes, J. Inorg. Biochem. 37 (1989) 325–339.
[23] N. Dos Santos, L.D. Mayer, S.A. Abraham, R.C. Gallagher, K.A.K. Cox, P.G. Tardi, M.B. Bally, Improved retention of idarubicin after intravenous injection obtained for cholesterol-free liposomes, Biochim. Biophys. Acta 1561 (2002) 188–201.
[24] S.A. Abraham, C. McKenzie, D. Masin, R. Ng, T.O. Harasym, L.D. Mayer, M.B. Bally, In vitro and in vivo characterization of doxorubicin and vincristine coencapsulated within liposomes through use of transition metal ion complexation and pH gradient loading, Clin. Cancer Res. 10 (2004) 728–738.
[25] J. Vaage, D. Donovan, E. Mayhew, P. Uster, M. Woodle, Therapy of mouse mammary carcinomas with vincristine and doxorubicin encapsulated in sterically stabilized liposomes, Int. J. Cancer 54 (1993) 959–964.
[26] N. Kemeny, M. Gonen, D. Sullivan, L. Schwartz, F. Benedetti, L. Saltz, J. Stockman, Y. Fong, W. Jarnagin, J. Bertino, W. Tong, P. Paty, Phase I study of hepatic arterial infusion of floxuridine and dexamethasone with systemic irinotecan for unresectable hepatic metastases from colorectal cancer, J. Clin. Oncol. 19 (2001) 2687–2695.
[27] D.A. Litvak, T.F. Wood, G.J. Tsioulias, M. Chung, S.P. Chawla, L.J. Foshag, D.L. Morton, K.P. Ramming, A.J. Bilchik, Systemic irinotecan and regional floxuridine after hepatic cytoreduction in 185 patients with unresectable colorectal cancer metastases, Ann. Surg. Oncol. 9 (2002) 148–155.
[28] N. Kemeny, W. Jarnagin, M. Gonen, J. Stockman, L. Blumgart, D. Sperber, A. Hummer, Y. Fong, Phase I/II study of hepatic arterial therapy with floxuridine and dexamethasone in combination with intravenous irinotecan as adjuvant treatment after resection of hepatic metastases from colorectal cancer, J. Clin. Oncol. 21 (2003) 3303–3309.
[29] L.D. Mayer, T. Harasym, N. Harasym, P. Tardi, Y. Shu, C. Suragh, E.M. Simms, M.B. Bally, A pharmaceutical approach to achieve synergy in vivo: a fixed ratio formulation of irinotecan and floxuridine for treatment of colorectal cancer, Proc. Am. Assoc. Cancer Res. 45 (2004) 126.
[30] C.L. Messerer, E.C. Ramsay, D. Waterhouse, R. Ng, E.M. Simms, N. Harasym, P. Tardi, L.D. Mayer, M.B. Bally, Liposomal irinotecan: formulation development and therapeutic assessment in murine xenograft models of colorectal cancer, Clin. Cancer Res. 10 (2004) 6638–6649.
[31] M. Grit, D.J.A. Crommelin, Chemical stability of liposomes: implications for their physical stability, Chem. Phys. Lipids 64 (1993) 3–18.
[32] B.C. Cheung, T.H. Sun, J.M. Leenhouts, P.R. Cullis, Loading of doxorubicin into liposomes by forming Mn^{2+} drug complexes, Biochim. Biophys. Acta 1414 (1998) 205–216.
[33] P. Tardi, E. Choice, D. Masin, T. Redelmeier, M. Bally, T.D. Madden, Liposomal encapsulation of topotecan enhances anticancer efficacy in murine and human xenograft models, Cancer Res. 60 (2000) 3389–3393.
[34] T.E. Furia, Sequestrants in food, In: T.E. Furia (Ed.), CRC Handbook of Food Additives, 2nd ed., CRC Press, West Palm Beach, FL, 1972, pp. 271–294.
[35] F.T. Greenaway, J.C. Dabrowiak, The binding of copper ions to daunomycin and adriamycin, J. Inorg. Biochem. 16 (1982) 91–107.
[36] P.K. Dutta, J.A. Hutt, Resonance raman spectroscopic studies of adriamycin and copper (II)-adriamycin and copper (II)–adriamycin–DNA complexes, Biochemistry 25 (1986) 691–695.
[37] A. Dicko, P. Tardi, L. Mayer, Spectroscopic characterization of irinotecan encapsulation in copper gluconate/triethanolamine containing liposomes, (submitted for publication) to Int. J. Pharm.
[38] C. Kirby, J. Clarke, G. Gregoriadis, Effect of the cholesterol content of small unilamellar liposomes on their stability in vivo and in vitro, Biochem. J. 186 (1980) 591–598.
[39] I. Ogihara-Umeda, S. Kojima, Cholesterol enhances the delivery of liposome-encapsulated gallium-67 to tumors, Eur. J. Nucl. Med. 15 (1989) 612–617.

J. vet. Pharmacol. Therap. **27**, 427–439, 2004. REVIEW

Plasma terminal half-life

P. L. TOUTAIN &
A. BOUSQUET-MÉLOU

UMR 181 Physiopathologie et Toxicologie Expérimentales INRA/ENVT, Ecole Nationale Vétérinaire de Toulouse, Toulouse cedex 03, France

Toutain, P. L., Bousquet-Mélou, A. Plasma terminal half-life. *J. vet. Pharmacol. Therap.* **27**, 427–439.

Terminal plasma half-life is the time required to divide the plasma concentration by two after reaching pseudo-equilibrium, and not the time required to eliminate half the administered dose. When the process of absorption is not a limiting factor, half-life is a hybrid parameter controlled by plasma clearance and extent of distribution. In contrast, when the process of absorption is a limiting factor, the terminal half-life reflects rate and extent of absorption and not the elimination process (flip-flop pharmacokinetics). The terminal half-life is especially relevant to multiple dosing regimens, because it controls the degree of drug accumulation, concentration fluctuations and the time taken to reach equilibrium.

P. L. Toutain, UMR 181 Physiopathologie et Toxicologie Expérimentales INRA/ENVT, Ecole Nationale Vétérinaire de Toulouse, 23, chemin des Capelles, 31076 Toulouse cedex 03, France. E-mail: pl.toutain@envt.fr

INTRODUCTION

The plasma half-life (half-life of elimination or half-life of the terminal phase) is the most frequently reported of all pharmacokinetic parameters. It has the apparent advantage of being a familiar term, immediately comprehensible because it is expressed in units of time. This is not the case for body clearance (the most important pharmacokinetic parameter), which is more difficult to conceive because it has the units of flow.

The half-life is (apparently) easy to compute and it is often the only reported pharmacokinetic parameter in some *in vitro* or *in vivo* assays. In some circumstances, it is generally the only parameter which can be computed, e.g. for a drug metabolite or any analyte disposition when the dose is unknown.

Actually, plasma half-life is very often wholly misunderstood and many non-kineticists continue to mistakenly believe that it represents the time required to eliminate half the administered dose of a drug.

In this review, we will re-state the definition of terminal half-life and qualify its pharmacokinetic meaning, which can be very different after intravenous (i.v.) and extra-vascular administration. The clinical relevance of terminal half-life will also be discussed together with its value in the rational selection of dosage interval. Finally, some technical issues concerning its estimation (sampling time and level of quantification of the analytical technique) will be addressed.

In this review, the term 'terminal half-life' is preferred to 'elimination half-life', because it does not prejudge the mechanism controlling plasma concentration decay.

DEFINITION OF TERMINAL HALF-LIFE

Following i.v. administration, the terminal half-life is the time required for plasma/blood concentration to decrease by 50% after pseudo-equilibrium of distribution has been reached; then, terminal half-life is computed when the decrease in drug plasma concentration is due only to drug elimination, and the term 'elimination half-life' is applicable. Therefore, it is not the time necessary for the amount of the *administered drug* to fall by one half.

The decay of a drug following first-order pharmacokinetics being exponential, the terminal half-life is obtained from Eqn 1:

$$t_{1/2} = \frac{0.693}{\lambda_z} \quad (1)$$

where 0.693 is the natural logarithm of 2 and λ_z, the slope of the terminal phase.

Figure 1 shows two drugs having the same terminal half-life but with very different clearances. In order to express the overall persistence of a drug in the body using a time parameter, then the mean residence time (*MRT*), and not the terminal plasma half-life, should be selected.

The confusion in the definition of half-life is historical. In the early stages of pharmacokinetics, analytical performances were poor and many drug dispositions were described by a single mono-exponential phase. In this situation, and only in this situation, the half-life is also the time it takes to eliminate half the administered dose of the drug. It is also relevant to note that when the pseudo-equilibrium has been reached, the disposition curve becomes mono-exponential and here also, the terminal half-time becomes the time taken to eliminate half the *remaining fraction* (not half the administered dose).

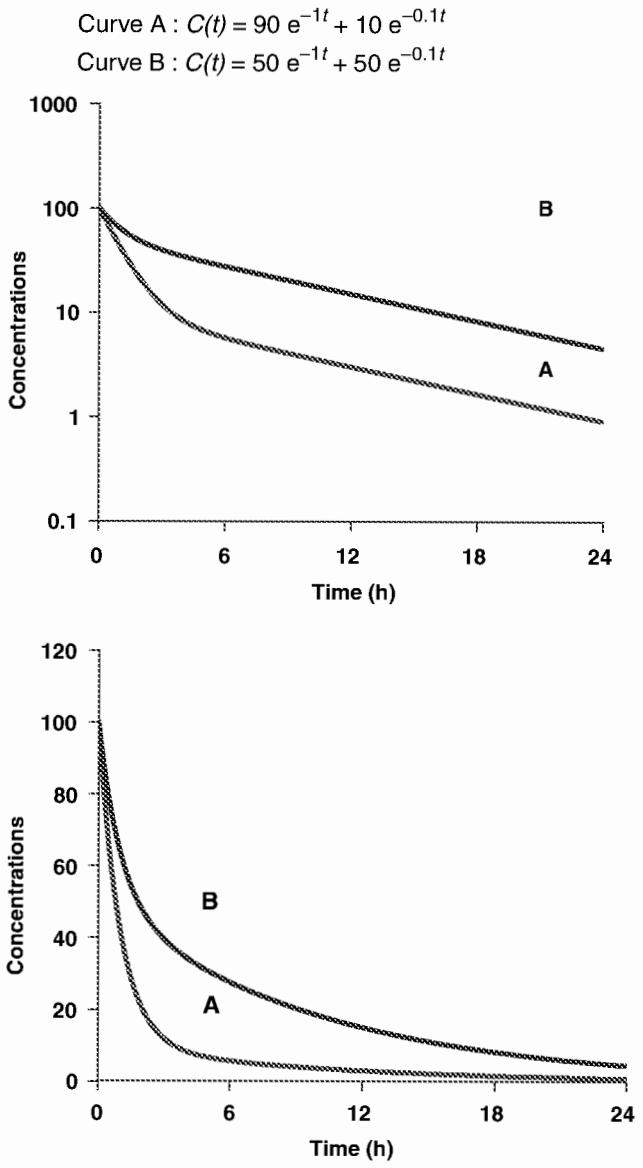

Fig. 1. Terminal half-life is the time required for the plasma concentration to fall by 50% during the terminal phase, and not the time required to eliminate half the administered dose. The figure shows two drugs (A and B) having exactly the same terminal half-life (6.93 h) (see top figure semi-logarithmic plot), but for which the time required to eliminate half the administered dose is very different (6 h for drug B and 2 h for drug A) (see bottom figure arithmetic plot). This difference is due to the fact that drug B has a lower clearance than drug A (0.182 mL/kg/h vs. 0.526 mL/kg/h), and a lower V_{area} (1.82 mL/kg vs. 5.26 mL/kg). It is only when the pseudo-equilibrium state has been reached (e.g. 12 h after drug administration), that the time required to eliminate half the *remaining* amount of drug in the body becomes equal to the terminal half-life.

PHARMACOKINETIC MEANING OF HALF-LIFE

It is sometimes difficult for a non-pharmacokineticist to understand the difference between information conveyed by plasma clearance and terminal half-life. Table 1 gives an example of antibiotics having the same clearance in dog but very different terminal half-lives. The plasma clearance expresses only the ability of the body to eliminate the drug (see Toutain & Bousquet-Mélou, 2004a). In contrast, terminal half-life expresses the overall rate of the actual drug elimination process during the terminal phase; this overall rate of elimination depends not only on drug clearance but also on the extent of drug distribution.

Figure 2 provides a pictorial representation of the influence of clearance and distribution on terminal half-life. More formally, Eqn 2 expresses the dependency of the terminal half-life on the volume of distribution and clearance:

$$t_{1/2} = \frac{0.632 \times \text{Volume of distribution}}{\text{Plasma clearance}} \qquad (2)$$

Equation 2 indicates that a long terminal half-life can be associated to a large volume of distribution (V_d) or/and attributable to a small plasma clearance. During the terminal phase, the drug will be eliminated only if it is presented to the clearing organs, regardless of the capacity level of these clearing organs to eliminate the drug. In mammals, the two most important clearing organs are the liver and kidney. In the framework of compartmental models, both are located in the central compartment and if the drug is present mainly in a peripheral compartment, the efficiency of the overall clearance process of drug elimination will be low and terminal half-life will be long.

HOW TO USE TERMINAL SLOPE TO EXPRESS THE EFFICIENCY OF DRUG ELIMINATION

A simple way to express the efficiency of drug elimination is to consider the numerical value of the slope (λ_z) of the terminal phase. For instance, the terminal half-life of phenylbutazone in cattle following i.v. administration is about 48 h, which corresponds to a terminal slope of 0.0144/h (Toutain *et al.*, 1980), a figure not easy to conceptualize. However, if this rate constant is multiplied by 100, it will mean that during the terminal phase of elimination, about 1.44% of the residual

Table 1. Terminal half-life vs. plasma clearance for different antibiotics in the dog

Parameters	Benzyl penicillin	Gentamicin	Oxytetracycline	Tylosin
Plasma clearance (mL/kg/min)	3.5	3.1	4.0	22
Terminal half-life (min)	30	75	360	54

Note that for three antibiotics (penicillin, gentamicin and oxytetracycline) the plasma clearances are very similar but the terminal half-lives are very different, indicating that terminal half-life and plasma clearance do not convey the same information. The terminal half-life is also influenced by the extent of drug distribution, so that, for almost the same plasma clearance, oxytetracycline having the largest volume of distribution also has the longest half-life.

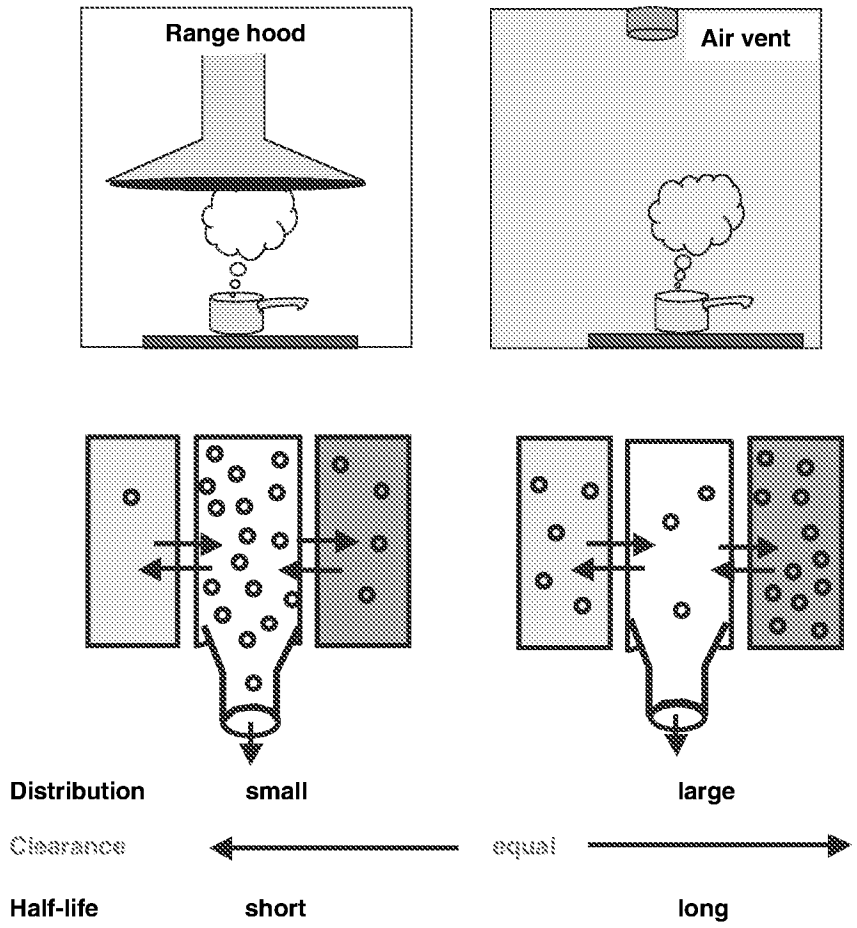

Fig. 2. Top: A pictorial explanation of the hybrid characteristic of a half-life. Imagine that we have to boil water (drug) in a kitchen (the body). In a modern kitchen (left), the boiling kettle is placed just under an efficient range hood (high clearance) and the steam produced (the dose) is quickly eliminated from the kitchen (with a short half-life) because the volume in which the steam is scattered (volume of distribution of the steam) is small. In a less ideal situation, there is no kitchen range hood but an air vent having exactly the same intrinsic capacity as the range hood (the same clearance). In this situation, the time required to eliminate the same amount of steam (the same dose) will be longer (longer half-life), because the steam disperses all over the kitchen (has a larger volume of distribution). Bottom: a compartmental view of the preceding system.

amount of phenylbutazone is eliminated per hour. This approximation is relatively accurate if λ_z is expressed with an appropriate time unit in order to obtain a low numerical value of λ_z (e.g. lower than 0.02).

PLASMA HALF-LIFE AND OTHER TIME PARAMETERS USED IN PHARMACOKINETICS ARE HYBRID PARAMETERS

Plasma half-life is a dependent parameter in contrast to plasma clearance and volume of distribution, which are said to be independent parameters, because they have a primary physiological basis and they are not determined by a combination of other basic pharmacokinetic parameters (at least at the macroscopic level). In pharmacokinetics, all time parameters (derived from rate constants) are hybrid (composite) parameters (Fig. 3), and terminal half-life is the most hybrid of all pharmacokinetic parameters, i.e. it is influenced by many other kinetic parameters (Fig. 4). Figure 5 explains the dependence of terminal half-life on the different microconstants for a bi-compartmental model.

The dependency of time parameters (rate constants) on clearance and volume of distribution should be recognized to avoid misinterpretation. A classical equation in compartmental analysis used to compute clearance is (Eqn 3):

$$Cl = K_{10}\mathrm{V_c} \tag{3}$$

where K_{10} is the rate constant of drug elimination from the central compartment of volume V_c (see Fig. 3).

This equation should not be used to interpret plasma clearance (e.g. to say that plasma clearance is low because K_{10} is small); rather the following relationship holds (Eqn 4):

$$K_{10} = \frac{Cl}{\mathrm{V_c}} \tag{4}$$

so that K_{10} can be explained in terms of Cl and $\mathrm{V_c}$, which in turn can be explained in terms of blood flow, binding to plasma proteins and so on.

The consequence of the hybrid character of terminal half-life is that half-life is a poor parameter to evaluate the influence of physiological factors (age, sex, etc.) or of pathology (renal failure, etc.) in drug disposition. For instance, the pharmacokinetics of gentamicin was investigated in horse before and after occurrence of nephrotoxicity. It was shown that body clearance was reduced by 40%, indicating impairment of the body capacity to eliminate gentamicin but with the terminal half-life remaining unchanged (192 min vs. 204 min). This was because of the fact that the

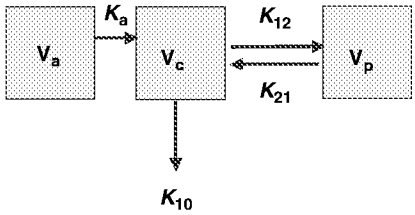

K_{12} = distribution clearance / V_c
K_{10} = plasma clearance / V_c
K_{21} = distribution clearance / V_p
MRT = steady-state volume of distribution / plasma clearance
$MTT_C = V_c$ / (plasma clearance and distribution clearance)
K_a = absorption clearance / V_a
$t_{1/2} = 0.693\ V_{area}$ / plasma clearance

Fig. 3. Physiological primary determinants of the main time parameters in pharmacokinetics. The time parameters such as half-life ($t_{1/2}$), mean residence time (*MRT*), mean transit time (*MTT*) in the central compartment, and rate constants (K_a, K_{12}, K_{21}, K_{10},...) are called hybrid parameters because they are actually a combination of parameters having a direct physiological meaning. All the rate constants can be interpreted in terms of ratio of a solute conductance term (clearance of absorption, clearance of distribution, clearance for elimination, etc.) and as capacitance terms (a volume of distribution) such as V_a: volume of the site of administration, V_c: volume of the central compartment, V_p: volume of the peripheral compartment, V_{ss}: steady-state volume of distribution, V_{area}: volume of distribution by area method. For rate constants like the rate constant of absorption (K_a), it is seldom possible to evaluate separately the two physiological determinants (clearance of absorption and volume of the site of administration), unless it is possible to sample the administration site (e.g. udder after an intra-mammary administration) (see Chiou, 1995 for the application of the clearance concept to absorption). *MRT*: mean residence time of the system, MTT_C: mean transit time in the central compartment, i.e. the average interval of time spent by a drug molecule from its entry into the central compartment to its next exit; $t_{1/2}$: terminal half-life.

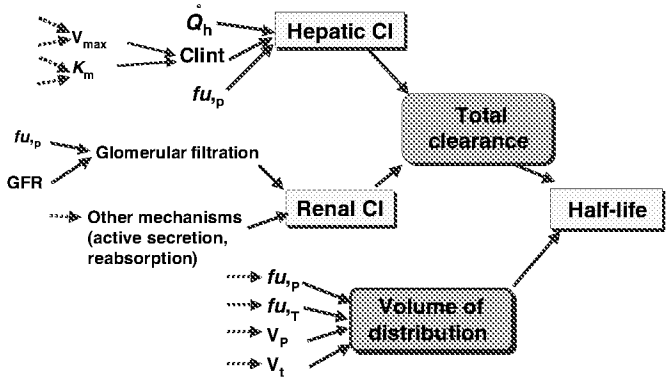

Fig. 4. Physiological factors influencing the terminal half-life ($t_{1/2}$) and giving it the status of a hybrid parameter. The value of $t_{1/2}$ is linked to that of clearance and volume of distribution. In turn, plasma clearance is the sum of different organs clearances (e.g. hepatic and renal clearances) themselves depending on many factors, including (for hepatic clearance) hepatic blood flow ($\dot{Q}h$), intrinsic hepatic clearance (Clint), free fraction in plasma (fu_P). Intrinsic hepatic clearance reflects maximum metabolism capacity (V_{max}), and the Michaelis Menten constant which is linked to drug affinity for the metabolic enzymatic system (K_M). Many factors also influence renal clearance. In addition, $t_{1/2}$ is influenced by the extent of drug distribution, which in turn depends on the drug affinity for circulating proteins (fu_P), for tissues (fu_T), on the volume of plasma (V_P) and tissues (V_T) etc.

volume of distribution was reduced in the same proportion as clearance (Riviere *et al.*, 1983).

WHY CALCULATE A TERMINAL HALF-LIFE

Terminal half-life is an index of drug persistence in the body during the terminal phase. The main clinical application of terminal half-life is to select an appropriate length for the dosing interval in circumstances of multiple dose administration. Indeed, terminal half-life allows prediction of drug accumulation and the time to reach steady-state equilibrium. This explains why the consequence of the value of terminal half-life is not the same for drugs having a short terminal half-life vs. a long terminal half-life. The impact of the value of half-life also differs for drugs requiring only a single dose administration vs. those requiring a multiple dose regimen.

For drugs having a short terminal half-life, it is important to maintain the plasma therapeutic concentration, and this will require dosage forms with a low input rate in order to obtain a flip-flop condition (*vide infra*). In contrast, if terminal half-life is long and the drug is to be administered repeatedly, questions of

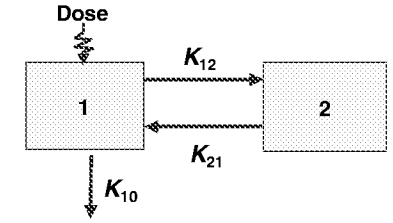

$$t_{1/2} = \frac{0.693}{1/2\left[(K_{12}+K_{21}+K_{10}) - \sqrt{(K_{12}+K_{21}+K_{10})^2 - 4K_{21}K_{10}}\right]}$$

$$t_{1/2} = \frac{0.693}{\lambda_2}$$

Fig. 5. The terminal half-life for a bi-compartmental model. The terminal half-life reflects both capacity of elimination (K_{10}), and processes of distribution (K_{12}) and redistribution (K_{21}). The numerical value of $t_{1/2}$ is a combination of K_{10}, K_{12} and K_{21}.

drug accumulation and delay in the time to reach steady-state conditions arise.

TERMINAL HALF-LIFE AND REPEATED ADMINISTRATION

Terminal plasma half-life is an important determinant of drug concentration–time profiles following repeated drug adminis-

tration, which are characterized by an initial accumulation phase, followed by a steady-state with fluctuations of concentration during the inter-dosing interval. Plasma half-life can be used to predict these different factors (*vide infra*). For simplification, the calculations presented in the following sections were performed assuming a mono-compartmental disposition of the drug.

Drug accumulation for drugs having a monophasic disposition

The terminal half-life can be used to predict drug accumulation. This is straightforward for a drug which obeys monophasic decay (mono-compartmental model), where it can easily be demonstrated that the accumulation ratio (R) is equal to (Eqn 5):

$$R = \frac{1}{\left[1 - e^{-\left(\frac{0.693}{\text{Terminal half-life}} \times \text{Dosing interval}\right)}\right]} = \frac{1}{\left[1 - (0.5)^{\tau/t_{1/2}}\right]} \quad (5)$$

where R is the index which corresponds to the ratio of AUC at steady state (i.e. AUC over the dosage interval) on the AUC following the first dosing interval, τ is the dosing interval and $t_{1/2}$, the terminal half-life (Fig. 6). Inspection of Eqn 5 indicates that there are two determinants of drug accumulation during multiple dosing: the first one is the terminal half-life, which is a drug property and the second one is the dosing interval, which is a clinician's decision. Thus, the accumulation ratio can be controlled by clinicians when selecting the dosing interval. If the dosing interval (i.e. τ) is equal to $t_{1/2}$, the accumulation ratio will be of 2. Table 2 presents the values of R for different values of the ratio $\tau/t_{1/2}$ assuming administration of a fixed dose.

Many veterinary drugs have terminal half-lives shorter than 12 h. When these drugs are given once daily (τ = 24 h), their accumulation ratios are less than 1.3. In consequence, the concentrations at equilibrium will not be more than 30% greater than plasma concentrations obtained following the first administration. From a practical clinical point of view, problems associated with accumulation are likely to be minimal for drugs exhibiting plasma half-lives shorter than 12 h.

The time to reach steady-state conditions

In contrast to the accumulation ratio, the time to reach the steady state is not influenced by the dosing interval but is only a function of terminal half-life. Figure 7 presents plasma concentration–time profiles of the same drug obtained with three different dosage regimens but with the same daily dosage (repeated administration of the dose 100 once daily, τ = 24 h; repeated administration of the dose 50 BID, τ = 12 h; i.v. infusion at the rate of 100/24 h). For the three dosage regimens, the same average concentration (C_{ss}) is obtained at steady-state (because C_{ss} depends only on drug entry, Dose/τ, and drug clearance), and the time required to reach this concentration is the same. Practically speaking, steady state is obtained after a delay of 3–5 times the half-life. Thus, for any drug having a terminal half-life of 12 h or less, the steady state will be reached after the second or third daily administration. For drugs exhibiting longer half-lives (more than 24 h), the delay before reaching therapeutic concentrations can be so long that initial administration of a loading dose is required.

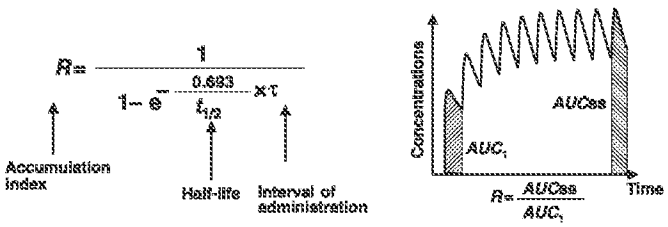

Fig. 6. Terminal half-life and drug accumulation during a multiple dosing regimen. After the first drug administration, the entire administered drug is not eliminated at the time of the second administration, and plasma concentration will be higher during the second dosing interval than after the first administration (superposition principle). With the repetition of dosing (at the same dose rate), plasma concentrations increase progressively until reaching a plateau, i.e. steady-state conditions. Under steady-state conditions, the amount of administered drug exactly compensates for the amount of eliminated drug over the dosing interval (noted τ). An accumulation index can be defined as the ratio of the average amount of drug in the body under steady-state conditions to the average amount of drug in the body after the first administration, thus,

$$R = \frac{\text{Amount (average) in steady-state condition}}{\text{Amount (average) after the first dose}}$$

R is estimated by the ratio of the two corresponding areas under the curve (AUC) (hatched area) with $R = AUC_{ss}/AUC_1$. For a mono-compartmental model or if drug is administered in the post-absorption phase for a multi-compartmental model, R is given by a simple mathematical expression having two parameters: terminal half-life and τ. Therefore, drug accumulation is not an intrinsic drug property but rather a variable which relies on both the drug property ($t_{1/2}$) and a clinical decision (the dosing interval).

Table 2. Accumulation index (R) and peak/trough concentration ratio (P/T ratio) at steady-state for different values of the ratio of the dosage interval (τ) and the terminal half-life ($t_{1/2}$)

$\tau/t_{1/2}$	0.125	0.25	0.5	1	2	4
R	12	6	3	2	1.3	1.07
P/T ratio	1.09	1.2	1.4	2	4	16

R and P/T ratios are defined by Eqns 5 and 6, respectively, in the text. The calculation assumes administration of a fixed dose.

Fluctuations of plasma concentrations at steady-state

Plasma concentration–time profiles at steady state are characterized by a succession of peak and trough concentrations. These fluctuations within a dosing interval are controlled by both τ and $t_{1/2}$, as indicated by the Peak–Trough concentration ratio (P/T ratio) presented in the following equation:

$$\frac{P}{T}\ \text{ratio} = \frac{C_{\max,ss}}{C_{\min,ss}} = 2^{\tau/t_{1/2}} \quad (6)$$

where $C_{max,\ ss}$ and $C_{min,\ ss}$ are the steady-state peak and trough concentrations, respectively.

The influence of modifying the $\tau/t_{1/2}$ ratio on the Peak-Trough ratio is presented in Table 2 and illustrated in Fig. 7. Practically speaking, for a given drug, to divide the daily dose is associated with a reduction of the amplitude of fluctuations at steady state, which usually represents an increase of safety for drugs exhibiting a narrow therapeutic window. However, this is not always the case, particularly when total exposure of the target tissue to the drug relies more closely on toxicity than the peak plasma concentration. This is the case for the nephrotoxicity of aminoglycoside which is lesser for a SID than a BID dosing rate because for a SID dosing rate, the total kidney exposure will be less important than for a BID due to saturation of aminoglycoside kidney capture for high amynoglycoside concentrations.

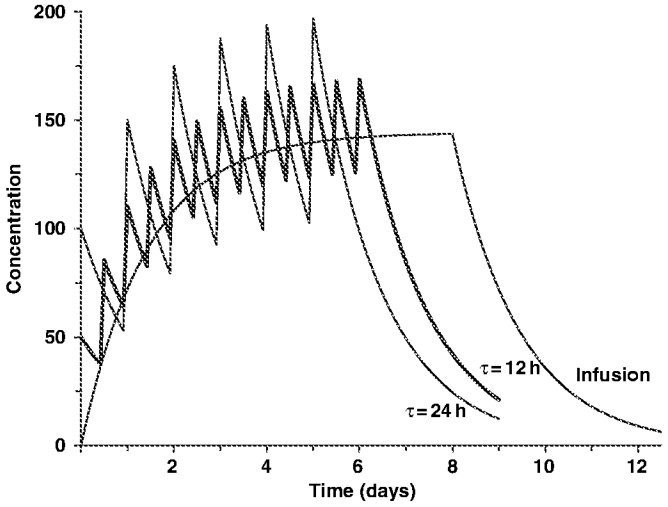

Fig. 7. Terminal half-life and the time required to reach steady-state conditions. For a multiple dosing regimen (or for an i.v. infusion), the time required to reach steady state (plateau) is a genuine drug property governed only by the terminal half-life. This figure illustrates two dosing regimens; the same total daily dose is administered but with two dosing intervals (12 and 24 h) for a drug having a terminal half-life of 48 h. Visual inspection shows that the plateau is reached after about 8–10 days regardless of the dosing interval (i.e. 3–5 times the terminal half-life); it should be noted that the accumulation ratios (as defined by Eqn 5 and illustrated in Fig. 6) are however different (3.414 and 6.286 for the dosing intervals of 24 and 12 h, respectively). From a clinical perspective, it should be noted that the average amount of drug at steady state (or the average plasma concentration) is the same for the two dosing strategies, the only relevant difference being the degree of plasma concentration excursion (i.e. the extent of the difference between peak and trough plasma concentrations).

ACCUMULATION AND TIME TO REACH STEADY-STATE CONDITIONS FOR DRUGS HAVING A MULTIPHASIC DISPOSITION

When drug disposition displays a multiphasic profile, the situation becomes more complicated because there are several half-lives corresponding to the different distribution phases preceding the terminal half-life of elimination. Each half-life is, to some degree, a function of distribution, redistribution, and elimination. Practically speaking, terminal $t_{1/2}$ controls drug accumulation when at least 50% of the drug is eliminated during the terminal decay phase. When this is not the case, the terminal phase can be irrelevant. Figure 8 illustrates the pharmacokinetics of two drugs obeying a bi-compartmental model and also having the same initial and terminal half-lives, but for which the degree of drug accumulation differs because the contribution of the terminal phase to drug elimination is different. To predict the degree of drug accumulation for a drug having a multiphasic disposition, the most straightforward approach involves under-

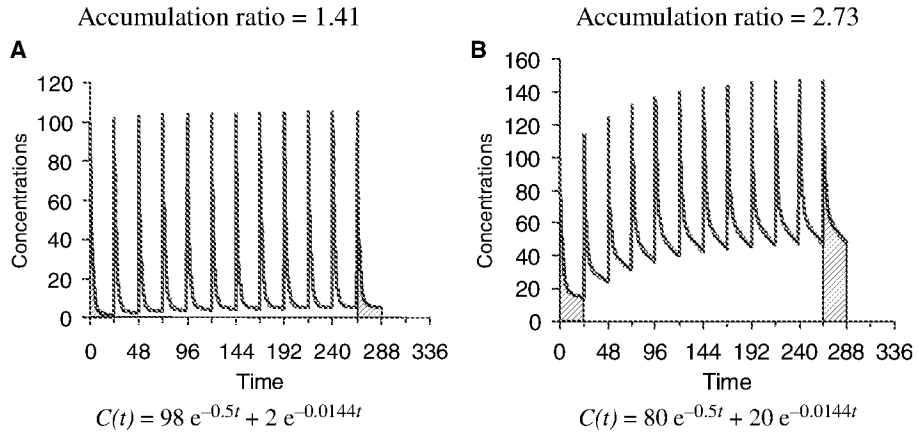

Fig. 8. Half-life and time to reach steady-state conditions and the extent of accumulation for two drugs obeying a bi-compartmental model and having the same terminal half-life (48 h), but which differ regarding the fraction of the dose which remains to be eliminated during the terminal phase (low for drug A and high for drug B). Visual inspection shows that apparent steady state is reached more rapidly when most of the drug is eliminated during the distribution phase (drug A) than when most of the drug is eliminated during the terminal phase (drug B). Practically speaking, $t_{1/2}\lambda_z$ controls drug accumulation only if at least 50% of the drug is eliminated during the terminal phase. The equations used for simulation are given under the figures.

standing that, under equilibrium conditions, the *AUC* over the dosing interval is equal to the total *AUC* (i.e. from 0 to ∞) after a single dose administration. On the other hand, if doses are administered in the post-distributive phase (i.e. when the decay is again monoexponential), Eqn 5 is also applicable, if most of the drug is eliminated during the elimination phase.

ACCUMULATION AND DELAY TO REACH STEADY STATE IN PERIPHERAL COMPARTMENTS

Most drugs display multiphasic pharmacokinetic profiles, which suggests the existence of both a central and several peripheral compartments. For these drugs, it is relevant to examine the degree of drug accumulation, not only in plasma but also in the peripheral compartment (possible location of the biophase, level of drug residues, etc.). Figure 9 illustrates the example of a hypothetical drug obeying a tri-compartmental model and having a terminal half-life of 48 h. The drug is administered once daily. Figure 9 shows that drug accumulation in the shallow and deep compartments is very different. In the deep compartment, drug accumulation is large and progressive. In contrast, in the shallow compartment, a pseudo-plateau is reached much sooner. If the site of action is in rapid equilibrium with plasma, pharmacological (or toxicological) effects can be immediately equivalent to those characterizing the steady-state conditions. In contrast, if the effect site is in the deep compartment, there is a time development of effects, which progressively increases with successive drug administrations. This example illustrates the general rule that delay to reach steady-state conditions in the deepest tissue compartment is controlled by the terminal half-life, and that the rate of accumulation is associated with the rate constant of redistribution from the deep compartment to the central compartment when this rate constant is a major determinant of the terminal half-life.

TERMINAL HALF-LIFE AND THE RATIONAL SELECTION OF A DOSING INTERVAL

The dosing interval is often selected for practical convenience (SID, BID, etc.). For many drugs and formulations it is necessary to control not only the dose but also the dosing interval, in order to optimize efficacy and/or to minimize side-effects. The relationship between terminal half-life and dosing interval determines the amplitude of fluctuations in drug plasma concentrations during the dosing intervals (Fig. 7). If the dosing interval is large relative to terminal half-life, there will be wide fluctuations in concentrations with possible side-effects (C_{max} too high), or lack of efficacy (C_{min} too low). The particular drugs for such considerations are those having a narrow therapeutic index (anti-arrhythmic, anti-epileptic, etc.), a poor selectivity (Cox1 vs. Cox2 inhibitory effect for NSAID), or which should be maintained above some threshold value (anti-arrhythmic drugs, time-dependent antibiotics, etc.).

In the case of digoxin in the dog, it has been proposed that plasma concentrations should exceed 2 ng/mL for therapeutic effects and that the probability of adverse effects increase when concentrations exceed 2.5 ng/mL. Therefore, an appropriate dosage regimen must guarantee that digoxin plasma concentrations fluctuate within this narrow therapeutic window. First, the daily dose can be selected to obtain an average steady-state concentration within the therapeutic window [see the relation between dose, clearance and average steady-state concentration (Toutain & Bousquet-Mélou, 2004a)]. Secondly, calculating the ratio of the upper and lower required concentrations (2.5/2) we obtain the value 1.25, which can be compared to the fluctuations of digoxin plasma concentrations at steady-state given by the *P*/*T* ratio (Eqn 6). This *P*/*T* ratio must be smaller than 1.25, and using Eqn 6 or Table 2, it can be calculated that this fluctuation is obtained for a $\tau/t_{1/2}$ ratio of 0.25. Finally, because digoxin $t_{1/2}$ in dog being 40–48 h, the corresponding dosing interval is 10–12 h. This is the reason why the dosage

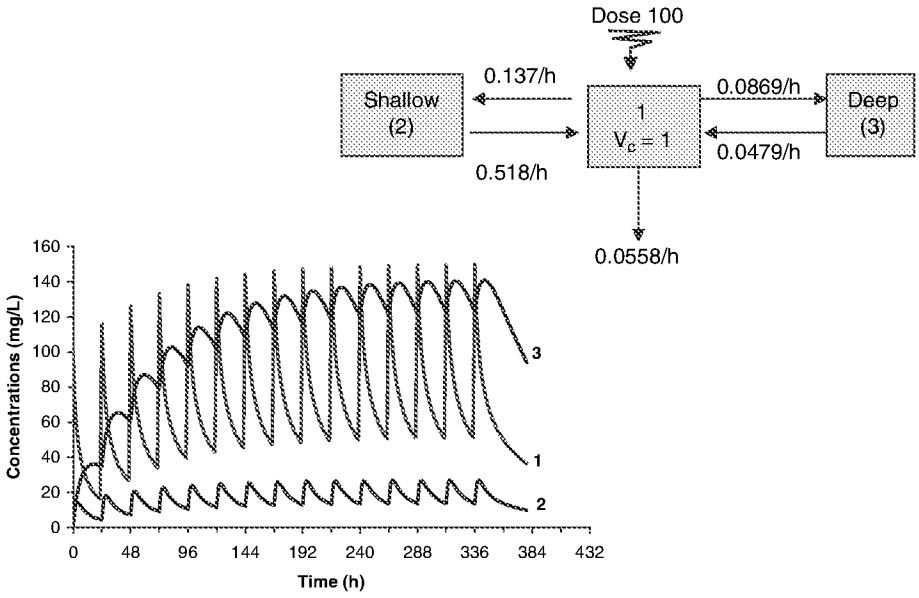

Fig. 9. Terminal half-life and accumulation of drug in peripheral compartment vs. central compartment. A tri-compartmental model was simulated to show that the degree of drug accumulation for daily administration of a fixed dose can be very different in central (1), shallow (2) and deep (3) peripheral compartments. This can be of clinical relevance with regard to location of the biophase. If the biophase is located in a shallow (2) compartment, the 'steady-state' condition for efficacy is obtained almost immediately, whereas when the biophase is in the deep (3) compartment, the effect would develop progressively over several days. This situation can also apply to residues in edible tissues.

regimen of digoxin requires the daily dose to be divided in two (half in the morning and half in the evening).

The extent of fluctuation can be easily predicted using the steady-state volume of distribution (V_{ss}) (Toutain & Bousquet-Mélou, 2004b). It should also be realized that the biophase is generally outside the plasma compartment and the effects can be indirectly related to plasma concentration. In this case, the best strategy for designing an appropriate dosage interval is to simulate the effects using a PK/PD approach.

THE TERMINAL HALF-LIFE AND THE REQUIREMENT FOR A LOADING DOSE

The terminal half-life can be used to predict the time taken to reach steady state, and the necessity or not of administering a loading dose (Toutain & Bousquet-Mélou, 2004b). The loading dose (LD) can also be predicted from the maintenance dose using Eqn 7:

$$\text{LD} = \text{Maintenance dose} \times R \qquad (7)$$

where R is the accumulation factor as defined above. Equation 7 assumes that each dose is administered in the post-absorption–post-distribution phase of each previous dose. The accumulation factor method produces a similar loading dose as the volume method (i.e. $\text{LD} = V_{ss}C_{ss}$), when most of the drug is eliminated during the terminal phase.

TERMINAL HALF-LIFE FOR AN EXTRA-VASCULAR ROUTE OF ADMINISTRATION AND THE FLIP-FLOP PHENOMENON

After an extra-vascular (EV) drug administration, the terminal half-life can be more prolonged than after an i.v. administration. This is frequently the case in veterinary medicine where many long-acting formulations, obtained using slow sustained release dosage forms, subdermal implants and vaginal sponges are marketed to provide a prolonged duration of action by maintaining plasma concentration above a minimal therapeutic concentration.

Similarly, some active principles (e.g. penicillin G) are or have been marketed as repository salt preparations (e.g. procaine penicillin G and benzathine penicillin G), or as water insoluble esters (e.g. corticoids) to obtain a prolonged duration of action (Fig. 10). Alternatively, an antibiotic, e.g. oxytetracycline may be solubilized in organic solvents in a series of concentrations (5, 10, 20 and 30%). After intramuscularly injection the active principle precipitates in increasing amounts at the injection site to provide increasing values of the terminal half-life. The route of administration for a given formulation can also be responsible for the flip-flop phenomenon. For instance, methylprednisolone acetate is poorly water soluble and it is a long acting formulation when administered by the i.m. route, but a short acting formulation when administered orally because the acetate ester is hydrolyzed in the digestive tract before intestinal drug absorption.

For all the aforementioned formulations, dosage forms, etc. the terminal half-life no longer reflects the drug elimination rate (as after an i.v. administration), but rather the absorption rate. The term flip-flop is used to describe this phenomenon, and a flip-flop exists when the rate of absorption is the rate limiting step in the sequential processes of drug absorption and elimination. In other words, a drug cannot be eliminated before it has been absorbed.

The consequence of flip-flop is that the terminal half-life is actually a half-life of absorption (or more exactly, as will be seen later, a half-life of drug disappearance from the administration site).

It is essential to recognize when the flip-flop mechanism occurs in order to avoid erroneous physiological interpretations. In a flip-flop situation, the terminal slope is no longer controlled by clearance and volume of distribution (Eqn 2) but instead by the bioavailability factor (rate and also extent of absorption)

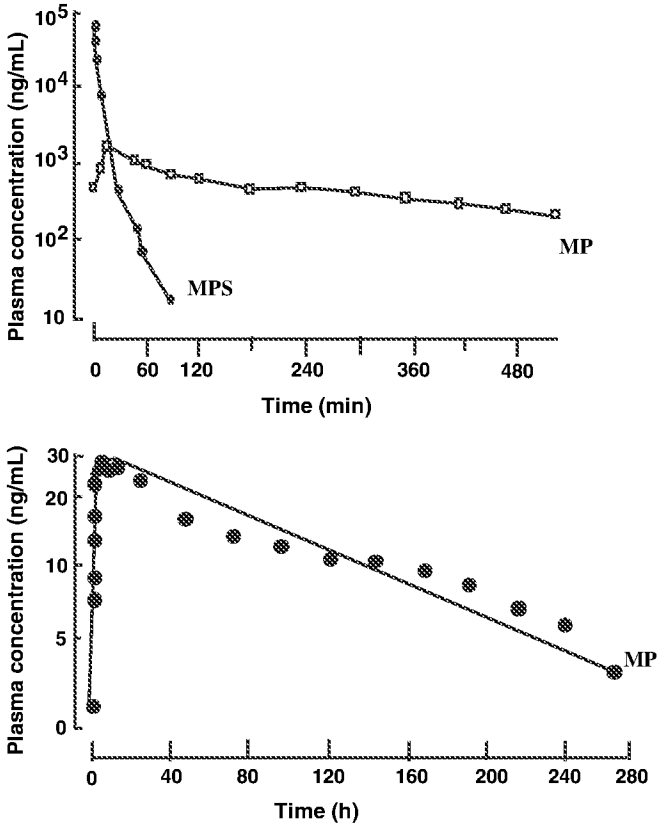

Fig. 10. Flip-flop and half-life of methylprednisolone in dogs. Top: methylprednisolone sodium succinate (MPS), a hydrosoluble pro-drug of methylprednisolone (MP), has been administered i.v. to dogs at a dose rate of 4 mg/kg (as MP). MPS was rapidly transformed into MP and the terminal half-life of MP, the active metabolite of MPS was 1.6–2.64 h. Bottom: methylprednisolone acetate, a non-hydrosoluble pro-drug of MP was administered by the intramuscular route at the same dose rate of 4 mg/kg (as MP). Now, the terminal half-life was 70 h, i.e. much longer than after the i.v. MPS administration, reflecting the very slow process of drug absorption from muscle. This example shows that the same active principle may behave very differently according to the selected formulation for administration (Toutain *et al.*, 1986).

(*vide infra*). Similarly, recognizing the occurrence of flip-flop avoids incorrectly calculation of some parameters such as Varea (Toutain & Bousquet-Mélou, 2004b). The best way to detect a flip-flop situation is to compare with a cross-over design i.v. and EV kinetics (Fig. 11). One of the major requirements for rational drug development is that the pharmacokinetics of any new chemical entity should be investigated by the i.v. route (to determine half-life of the substance itself), regardless of the expected route of administration for the final marketed formulation.

Ignoring the flip-flop phenomenon is the most frequent mistake in veterinary pharmacological papers, especially for some classes of drugs (avermectins and milbemycins) for which i.v. pharmacokinetic parameters are never (or seldom) reported for comparison with those obtained for the recommended route of administration.

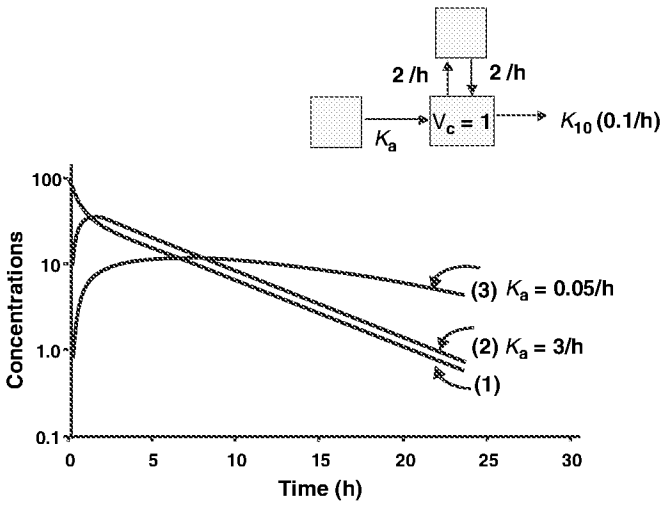

Fig. 11. Terminal half-life and the flip-flop phenomenon. The pharmacokinetic disposition of a hypothetical drug having a terminal half-life of 7 h was simulated for an i.v. (1) administration, and for an extravascular administration with a rapid rate of absorption (K_a = 3/h) (2) or a slow rate of absorption (K_a = 0.05/h) (3). The parameters used for simulation were $K_{12} = K_{21}$ = 2/h and K_{10} = 0.1/h. For the rapid rate constant of absorption (2) the slope of the terminal phase is parallel to that of the i.v. disposition curve and represents a rate of drug elimination (i.e. it is controlled by drug clearance and extent of distribution). In contrast, for a slow rate constant of absorption (3), the slope of the terminal phase is no longer parallel to that of the i.v. administration, reflecting the actual rate limiting step which is now related to drug absorption.

THE FLIP-FLOP PHENOMENON AND INTERPRETATION OF THE TERMINAL PHASE IN TERMS OF BIOAVAILABILITY FACTORS

It is frequently not understood that the so-called half-life of absorption (reported as $t_{1/2}$ K_a) is not actually a true half-life of absorption (with or without presence of a flip-flop) but rather the half-time of disappearance of the drug from the site of administration (Garrett, 1994; Rescigno, 1994) (Fig. 12). Actually, K_a is the rate constant of drug disappearance from the injection site and it can be viewed as the sum of two rate constants, namely K_{a1} and K_{a2}. K_{a1} is the rate constant of transfer from the site of administration to the central compartment and reflects the physiological absorption process, whereas K_{a2} can be viewed as the rate constant expressing the drug 'leakage', i.e. the fraction which is not bioavailable. Therefore, the bioavailability (from 0 to 1) is given by Eqn 8:

$$F = \frac{K_{a1}}{K_{a1} + K_{a2}} \tag{8}$$

Now consider the classical equation for an EV administration (mono-compartmental model) (Eqn 9):

$$C(t) = \frac{F \times \text{Dose} \times K_a}{V_c(K_a - K_{10})}\left[e^{-K_{10}t} - e^{-K_a t}\right] \tag{9}$$

where K_{10} is the first-order rate constant of drug elimination, V_c is the volume of distribution, and K_a is the so-called rate constant of absorption. As $K_a = K_{a1} + K_{a2}$, Eqn 9 can be parameterized as (Eqn 10):

$$C(t) = \frac{F \times \text{Dose} \times (K_{a1} + K_{a2})}{V_c(K_{a1} + K_{a2} - K_{10})}\left[e^{-K_{10}t} - e^{-(K_{a1}+K_{a2})t}\right] \tag{10}$$

Combining Eqns 10 and 8 (Eqn 11):

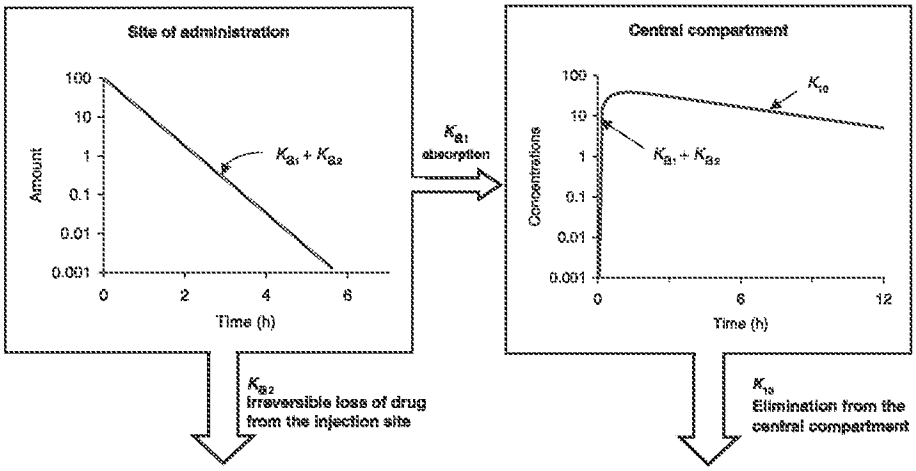

Fig. 12. The so-called half-life of absorption vs. the process of drug absorption. This figure corresponds to a drug obeying a mono-compartmental model with a phase of absorption. The reported half-life of absorption ($t_{1/2}$ K_a) does not reflect solely the process of drug absorption (here represented by K_{a1}, the first-order rate constant of drug transfer from the injection site to the central compartment) but the sum of K_{a1} and K_{a2}, K_{a2} being the rate constant reflecting the irreversible loss of drug at the administration site. $t_{1/2}$ K_a reflects simply drug absorption only if K_{a2} = 0, i.e. if the bioavailability is total. Here $K_{a1} + K_{a2} >> K_{10}$ and so no flip-flop phenomenon is observed.

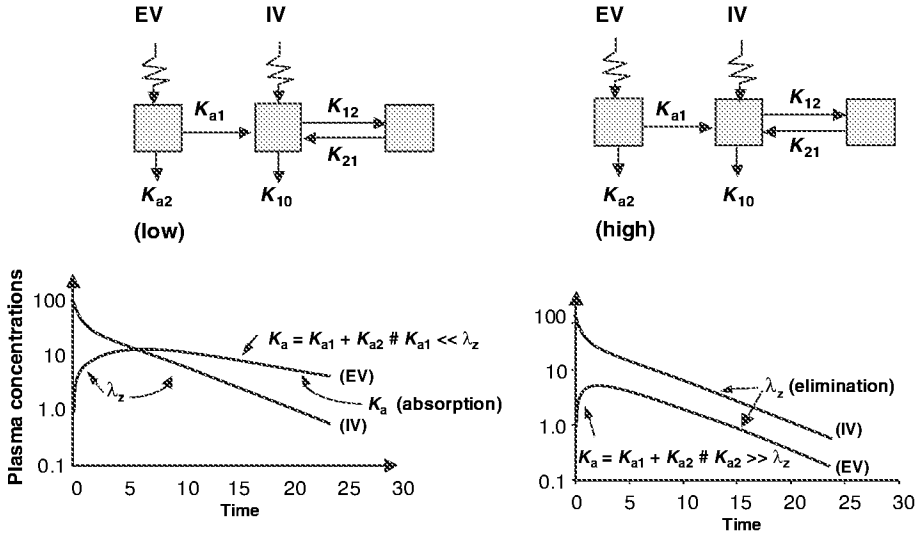

Fig. 13. Terminal half-life and the flip-flop case. This figure illustrates the influence of bioavailability on the slope of the terminal phase. Left: a hypothetical drug formulation administered by the extra-vascular route (EV) is absorbed according to a slow process (K_{a1}), leading to a flip-flop. Right: for the same drug and the same physiological process of absorption (the same K_{a1}), the slope of the terminal phase can be dramatically decreased if bioavailability becomes low due to a source of drug leakage (represented here by K_{a2}); if the sum of K_{a1} and K_{a2} is higher than the terminal slope (λ_z) following i.v. administration, the terminal phase will represent in fact the process of drug elimination. Without an i.v. study, the interpretation of the left vs. right curves can be totally misleading (i.e. one can consider the right curve as being a formulation having a rapid absorption, whereas it is only a formulation with a low bioavailability).

$$C(t) = \frac{K_{a1} \times \text{Dose}}{V_c(K_{a1} + K_{a2} - K_{10})}\left[e^{-K_{10}t} - e^{-(K_{a1}+K_{a2})t}\right] \qquad (11)$$

Equation 11 allows consideration of two opposite situations. The first is when $K_{10} \ll K_{a1} + K_{a2}$. This is the classical situation and when the time becomes large, $e^{-(K_{a1} + K_{a2})t}$ approaches 0 and Eqn 10 becomes (Eqn 12):

$$C(t) = \frac{K_{a1} \times \text{Dose}}{V_c(K_{a1} + K_{a2} - K_{10})}e^{-K_{10}t} \qquad (12)$$

Here the terminal slope is K_{10} and it reflects the process of drug elimination, and the initial phase has a slope of $K_{a1} + K_{a2}$.

The second circumstance occurs when $K_{10} \gg K_{a1} + K_{a2}$, Eqn 11 becomes (Eqn 13):

$$C(t) = \frac{K_{a1} \times \text{Dose}}{V_c[K_{10} - (K_{a1} + K_{a2})]}e^{-(K_{a1}+K_{a2})t} \qquad (13)$$

Now, the terminal slope reflects $K_{a1} + K_{a2}$, i.e. both drug absorption (K_{a1}) and drug leakage (K_{a2}), whereas the initial phase reflects K_{10}, thus justifying the term flip-flop.

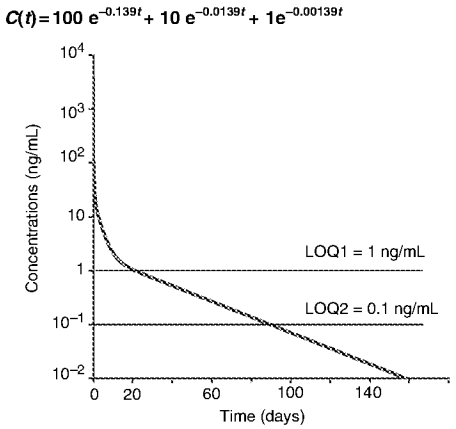

Bias in the estimation of PK parameters with respect to the LOQ

Time (h), Dose = 100 µg/kg

	LOQ (ng/mL)		
	1	0.1	Ratio
Clearance (L/kg/h)	0.0695	0.0463	1/0.66
V_{ss} (L/kg)	2.75	12.3	1/4.47
MRT (h)	39.6	266	1/6.7
V_{area} (L/kg)	5.0	33.3	1/6.6
$t_{1/2}$ (h)	49.85	498.5	1/10

Fig. 14. Terminal half-life and level of quantification of the analytical technique. The reported terminal half-life (and also the other pharmacokinetic parameters) is influenced by the performance of the analytical technique, and especially by the level of quantification (LOQ). A curve was simulated with the equation given in the figure (time in hours and concentrations in ng/mL), and the pharmacokinetic parameters (clearance, volume of distribution, half-life) were computed from results obtained with analytical techniques having a LOQ of either 1 (LOQ1) or 0.1 ng/mL (LOQ2). It is clear that the calculated terminal half-life is very sensitive to the LOQ (50 h vs. 500 h), whereas clearance is least affected (the most robust) parameter with respect to the LOQ (0.0695 vs. 0.0464 L/kg/h), as indicated by the quoted ratios.

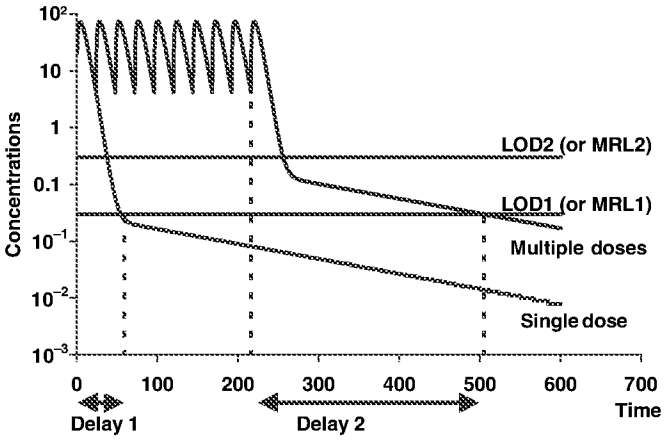

Fig. 15. Significance of a very late terminal phase for doping control or for withdrawal time. Doping (medication) controls are generally carried out with analytical techniques having a low level of detection (LOD1), i.e. they are able to detect urine or plasma concentrations having no therapeutic impact but requiring a more or less prolonged delay after a drug treatment. This delay, required to achieve a 'negative' finding, can be much more prolonged after a multiple dosing regimen (delay 2) than after a single dose administration (delay 1). This is because a very late terminal phase (not detected after a single administration) gives concentrations above the LOD1 after a multiple dose administration due to accumulation specially linked to this very late phase. In contrast, with a higher LOD (LOD2) the delay to become 'negative' after a single dose or a multiple dose administration will be similar. The same phenomenon may explain that the withdrawal period, dictated by the time to fall below the MRL can be very different after a single and a multiple dose administration with regard to the value of MRL (MRL1 vs. MRL2). It is noteworthy that in this example, there is no therapeutically relevant accumulation in plasma concentration during the treatment itself but it is only the remnant amount of drug during the terminal phase which is consistently higher after a repeated dosing regimen. This situation is observed with phenylbutazone but not with meloxicam in horse.

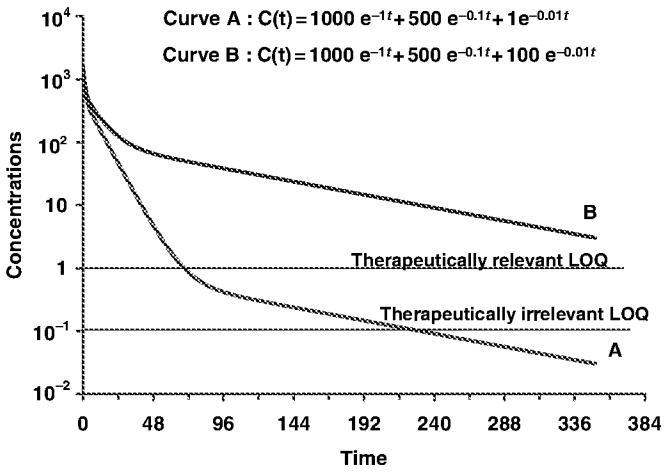

Fig. 16. Clinical meaning of a terminal phase. The continual improvement of analytical techniques can lead to the detection of a very late terminal phase (e.g. for ivermectin) without clinical meaning. The questions are (a) when to stop sampling and (b) what is the appropriate level of quantification (LOQ) for an analytical technique. If the pharmacokinetic study is performed to address the question of drug efficacy, the range of efficacious concentrations should be considered. If there is evidence that the total exposure (as evaluated by the area under the plasma concentration time curve or *AUC*) is relevant in terms of drug efficacy, the different *AUC* associated with the different phases can be determined by integrating the equation describing drug disposition (i.e. for a tri-exponential curve $AUC_1 = Y_1/\lambda_1$, $AUC_2 = Y_2/\lambda_2$ and $AUC_3 = Y_3/\lambda_3$) with Y_1, Y_2, Y_3: the intercepts, and λ_1,λ_2, and λ_3: the slopes of the different phases. Two curves (drug A and drug B) were simulated with exactly the same terminal slopes (0.01/h) but with different intercepts [low ($Y_3 = 1$) for drug A and high ($Y_3 = 100$) for drug B]. By integrating the equation describing these 2 curves respectively, it can be computed that the terminal phase (half-time of 69.3 h) accounts for only 1.6% of the total exposure (*AUC*) for drug A, whereas for drug B, the corresponding value is of 62.5%. For drug B, it is likely to be necessary to determine the last terminal phase (i.e. to carry out the study with an analytical technique having a LOQ of about 1), whereas for drug A, the last terminal phase can be considered as a very late terminal phase without clinical meaning, and it is not necessary to improve the analytical technique, i.e. to have a LOQ < 1 to detect the late terminal phase. However, this very late terminal phase may be very significant in terms of residues (e.g. for aminoglycosides).

The practical consequence is that for a slowly absorbed drug (low K_{a1}), some formulations can lead to a flip-flop phenomenon because K_{a2} is low or null (good bioavailability), whereas some other formulations do not display a flip-flop phenomenon, not because they are rapidly absorbed but because K_{a2} is large, because their bioavailability is low (Fig. 13).

More generally, interpretation of the terminal slope in presence of a flip-flop system should be undertaken in terms of K_{a1} and K_{a2}, i.e. in terms of bioavailability factors and not in terms of clearance and volume of distribution.

A RELEVANT TERMINAL HALF-LIFE AND THE MEANING OF A VERY LATE TERMINAL HALF-LIFE

Terminal half-life is the parameter most sensitive to performance of the analytical technique, especially the level of quantification (LOQ). Figure 14 shows, for a hypothetical drug, values of terminal half-life for different levels of LOQ. Using the same equation, different kinetic parameters were calculated for a LOQ of 1 or 0.1 ng/mL. It can be seen that the body clearance is the most robust pharmacokinetic parameter, the ratio between the values obtained with LOQ of 1 and 0.1 being of 1.51, whereas the terminal half-life was 10 times longer for a LOQ of 0.1.

Twenty years ago, we published pharmacokinetic parameters for dexamethasone (DXM) in horses using a HPLC technique with a LOQ of 2–3 ng/mL. We reported a plasma clearance of 12.8 mL/kg/min and a short terminal half-life of 53 min (Toutain *et al.*, 1984). More recently, Cunningham *et al.* (1996), using an improved analytical technique (LOQ = 200 pg/mL) reported that the plasma clearance of DXM in horse was 8 mL/kg/min, i.e. not markedly different from that in our earlier study, whereas the reported terminal half-life was three times longer (158 min) because a supplementary phase was detected.

The steady improvement in sensitivity of analytical techniques raises the question of relevance of detection of a

supplementary very late terminal phase. The importance of any terminal half-life depends on its biological relevance (contribution to clinical efficacy, persistence of residues in food producing species, persistence of doping agents in the horse, required duration of a washout for a cross-over design, etc.). The case of aminoglycosides may be cited. The terminal phase of clinical relevance is relatively short (2 h) but, using a sensitive analytical technique, a supplementary phase can be detected having a half-life of approximately 24 h. This phase does not contribute to the antibiotic efficacy but reflects persistence of drug residues, this terminal phase being controlled by the redistribution rate constant from tissue to plasma. Aminoglycosides achieve particularly high and persistent concentrations in the kidney, so that concentrations in plasma decline with hours or days, whilst concentrations in renal tissue can exceed the MRL (maximum residue limit) for weeks or months. A similar find of binding to kidney has been described for polymyxins.

When estimating an acceptable daily intake (ADI) for a residue, it is assumed that 'residues' are ingested daily for life. Therefore, a very late terminal phase without any toxic or even therapeutic significance for the treated animal may become theoretically significant in terms of drug accumulation from the regulatory perspective of whole-life repeated dosing.

The presence of a very late terminal half-life can also create difficulties for a cross-over design when trying to avoid a carry-over effect (residual effect from the first period impacting on the second). The washout period should be long enough to guarantee that most of the drug has been cleared.

For doping control in relation to equine and canine competitive sports, a very late terminal phase, not detected in plasma, may be easily measured in urine when the urine-to-plasma concentration ratio is large. This may require a long withdrawal period to reach regulatory limits. In addition, this very late phase may be a cause of accumulation during a multiple dosing regimen. In consequence, the withdrawal period for doping control can be much longer after the cessation of a multiple dosing regimen than after a single-dose administration (Fig. 15). A similar phenomenon may occur during withdrawal periods for edible tissues in food producing animals. The time point at which the concentration of residues in all tissues falls below the respective maximum residue limit may be significantly longer after a multiple administration than after a single dose.

A practical approach to determine (a) if a terminal half-life has a therapeutic meaning and (b) what is the appropriate LOQ for an analytical technique, is to compute the *AUC* associated with each phase (Fig. 16) by integrating an equation describing the drug pharmacokinetics. For example, for gentamicin, the plasma pharmacokinetics can be described by a tri-exponential equation, the two first phases representing 98% of the total *AUC* indicating that the last phase (2% of *AUC*) does not significantly contribute to the overall drug exposure and can be discounted when discussing drug efficacy.

SOME CONSIDERATIONS FOR THE ESTIMATION OF TERMINAL HALF-LIFE

It is not within the scope of the present article to explain how to effectively estimate pharmacokinetic parameters such as terminal half-life, but some technical points deserve mention. First, the accurate estimation of a slope requires sampling times over at least three times the expected half-life. In other words, it can be very misleading to estimate a half-life of 24 h with sampling data for 12 or 24 h.

Raw data

Time (h)	Concentrations (μg/mL)
0.0333	240
0.0833	150
0.167	100
0.25	85
0.5	60
0.75	45
1	35
1.5	25
2	21
2.5	15
3	14
4	9
5	7
6	5
8	3.5
10	2.5
12	1.8

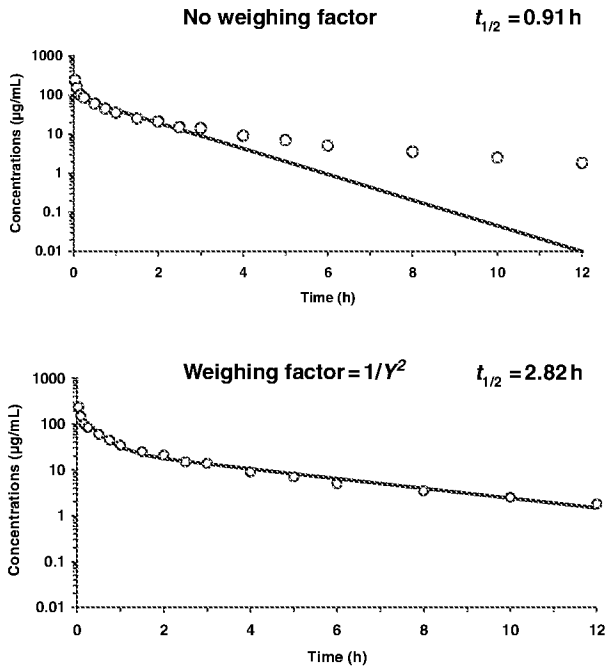

Fig. 17. Influence of weighing factor on the calculated values of terminal half-life. Raw data were fitted using a bi-compartmental model (WinNonlin 4.0.1; Pharsight Corp., Mountain View, CA, USA), without (top) or with (bottom) a weighing factor ($1/Y^2$), Y being the observed concentration. Visual inspection reveals a serious misfit when no weighing factor is used.

Another point which can strongly influence half-life estimation is the use (or not) of an appropriate weighting factor when fitting data using non-linear regression analysis. It is acknowledged that one of the main factors of variation in half-lives reported in the literature derives not from biological factors but from the selection of the weighting scheme. As an example, Fig. 17 provides raw data for which fitting with or without a weighting factor leads to very different terminal half-lives.

More generally, if a terminal half-life is first roughly approximated by visual inspection, computer programs using non-linear regression and an appropriate weighting scheme can then improve the isolation and estimation of terminal half-life.

After computation, of half-life for each individual animal, the results are generally reported as mean ± SD or SE. For terminal half-life, it is recommended that harmonic mean is used rather than arithmetic mean, and it is appropriate to compute standard error using a jackknife technique (Lam *et al.*, 1985).

CONCLUSION

Terminal half-life is the most frequently reported pharmacokinetic parameter, but it is commonly misinterpreted. It is the least robustly estimated and its interpretation can be totally flawed if a flip-flop situation is not recognized. The clinical utility of terminal half-life is mainly to select an appropriate dosage regimen interval.

REFERENCES

Chiou, W.L. (1995) We may not measure the correct intestinal wall permeability coefficient of drugs: alternative absorptive clearance concept. *Journal of Pharmacokinetics and Biopharmaceutics*, **23**, 323–331.

Cunningham, F.E., Rogers, S., Fischer, J.H. & Jensen, R.C. (1996) The pharmacokinetics of dexamethasone in the thoroughbred racehorse. *Journal of Veterinary Pharmacology and Therapeutics*, **19**, 68–71.

Garrett, E.R. (1994) The Bateman function revisited: a critical reevaluation of the quantitative expressions to characterize concentrations in the one compartment body model as a function of time with first-order invasion and first-order elimination. *Journal of Pharmacokinetics and Biopharmaceutics*, **22**, 103–128.

Lam, F.C., Hung, C.T. & Perrier, D.G. (1985) Estimation of variance for harmonic mean half-lives. *Journal of Pharmaceutical Sciences*, 74, 229–231.

Rescigno, A. (1994) Brief retrospectives in pharmacokinetics. On absorption rate and fraction absorbed. *Journal of Pharmacokinetics and Biopharmaceutics*, **22**, 255–257, (see Discussion on p. 253).

Riviere, J.E., Coppoc, G.L., Hinsman, E.J., Carlton, W.W. & Traver, D.S. (1983) Species dependent gentamicin pharmacokinetics and nephrotoxicity in the young horse. *Fundamental and Applied Toxicology*, **3**, 448–457.

Toutain, P.L. & Bousquet-Mélou A. (2004a) Plasma clearance. *Journal of Veterinary Pharmacology and Therapeutics*, **27**, 415–425.

Toutain, P.L. & Bousquet-Mélou A. (2004b) Volumes of distribution. *Journal of Veterinary Pharmacology and Therapeutics*, **27**, 441–453.

Toutain, P.L., Alvinerie, M. & Ruckebusch, Y. (1980) Pharmacokinetics and residue levels of phenylbutazone in the cow. *Annales de Recherches Vetetrinaires*, 11, 391–397.

Toutain, P.L., Brandon, R.A., de Pomyers, H., Alvinerie, M. & Baggot, J.D. (1984) Dexamethasone and prednisolone in the horse: pharmacokinetics and action on the adrenal gland. *American Journal of Veterinary Research*, **45**, 1750–1756.

Toutain, P.L., Koritz, G.D., Fayolle, P.M. & Alvinerie, M. (1986) Pharmacokinetics of methylprednisolone, methylprednisolone sodium succinate, and methylprednisolone acetate in dogs. *Journal of Pharmaceutical Sciences*, **75**, 251–255.

UNITED STATES PATENT AND TRADEMARK OFFICE

UNITED STATES DEPARTMENT OF COMMERCE
United States Patent and Trademark Office
Address: COMMISSIONER FOR PATENTS
P.O. Box 1450
Alexandria, Virginia 22313-1450
www.uspto.gov

APPLICATION NO.	FILING DATE	FIRST NAMED INVENTOR	ATTORNEY DOCKET NO.	CONFIRMATION NO.
15/664,976	07/31/2017	Keelung Hong	263266-416123	4323

153749 7590 11/04/2019

McNeill Baur PLLC/Ipsen
Ipsen Bioscience, Inc.
125 Cambridge Park Drive
Suite 301
Cambridge, MA 02140

EXAMINER	
SHOMER, ISAAC	

ART UNIT	PAPER NUMBER
1612	

NOTIFICATION DATE	DELIVERY MODE
11/04/2019	ELECTRONIC

Please find below and/or attached an Office communication concerning this application or proceeding.

The time period for reply, if any, is set in the attached communication.

Notice of the Office communication was sent electronically on above-indicated "Notification Date" to the following e-mail address(es):

docketing@mcneillbaur.com
eofficeaction@appcoll.com
patents.us@ipsen.com

Office Action Summary	Application No. 15/664,976	Applicant(s) Hong et al.	
	Examiner ISAAC SHOMER	Art Unit 1612	AIA (FITF) Status No

-- The MAILING DATE of this communication appears on the cover sheet with the correspondence address --

Period for Reply

A SHORTENED STATUTORY PERIOD FOR REPLY IS SET TO EXPIRE 3 MONTHS FROM THE MAILING DATE OF THIS COMMUNICATION.

- Extensions of time may be available under the provisions of 37 CFR 1.136(a). In no event, however, may a reply be timely filed after SIX (6) MONTHS from the mailing date of this communication.
- If NO period for reply is specified above, the maximum statutory period will apply and will expire SIX (6) MONTHS from the mailing date of this communication.
- Failure to reply within the set or extended period for reply will, by statute, cause the application to become ABANDONED (35 U.S.C. § 133). Any reply received by the Office later than three months after the mailing date of this communication, even if timely filed, may reduce any earned patent term adjustment. See 37 CFR 1.704(b).

Status

1)☑ Responsive to communication(s) filed on 21 October 2019.

☐ A declaration(s)/affidavit(s) under **37 CFR 1.130(b)** was/were filed on _____.

2a)☐ This action is **FINAL.** 2b) ☑ This action is non-final.

3)☐ An election was made by the applicant in response to a restriction requirement set forth during the interview on _____; the restriction requirement and election have been incorporated into this action.

4)☐ Since this application is in condition for allowance except for formal matters, prosecution as to the merits is closed in accordance with the practice under *Ex parte Quayle*, 1935 C.D. 11, 453 O.G. 213.

Disposition of Claims*

5) ☑ Claim(s) 173-175 and 177-184 is/are pending in the application.

5a) Of the above claim(s) _____ is/are withdrawn from consideration.

6) ☐ Claim(s) _____ is/are allowed.

7) ☑ Claim(s) 173-175 and 177-184 is/are rejected.

8) ☐ Claim(s) _____ is/are objected to.

9) ☐ Claim(s) _____ are subject to restriction and/or election requirement

* If any claims have been determined allowable, you may be eligible to benefit from the **Patent Prosecution Highway** program at a participating intellectual property office for the corresponding application. For more information, please see http://www.uspto.gov/patents/init_events/pph/index.jsp or send an inquiry to **PPHfeedback@uspto.gov.**

Application Papers

10)☐ The specification is objected to by the Examiner.

11)☐ The drawing(s) filed on _____ is/are: a)☐ accepted or b)☐ objected to by the Examiner.

Applicant may not request that any objection to the drawing(s) be held in abeyance. See 37 CFR 1.85(a).

Replacement drawing sheet(s) including the correction is required if the drawing(s) is objected to. See 37 CFR 1.121(d).

Priority under 35 U.S.C. § 119

12)☐ Acknowledgment is made of a claim for foreign priority under 35 U.S.C. § 119(a)-(d) or (f).

Certified copies:

a)☐ All b)☐ Some** c)☐ None of the:

1.☐ Certified copies of the priority documents have been received.

2.☐ Certified copies of the priority documents have been received in Application No. _____.

3.☐ Copies of the certified copies of the priority documents have been received in this National Stage application from the International Bureau (PCT Rule 17.2(a)).

** See the attached detailed Office action for a list of the certified copies not received.

Attachment(s)

1) ☑ Notice of References Cited (PTO-892)

2) ☑ Information Disclosure Statement(s) (PTO/SB/08a and/or PTO/SB/08b) Paper No(s)/Mail Date _____.

3) ☐ Interview Summary (PTO-413) Paper No(s)/Mail Date _____.

4) ☐ Other: _____.

DETAILED ACTION

Applicants' arguments, filed 21 October 2019, have been fully considered. Rejections and/or objections not reiterated from previous office actions are hereby withdrawn. The following rejections and/or objections are either reiterated or newly applied. They constitute the complete set presently being applied to the instant application.

The present application is being examined under the pre-AIA first to invent provisions.

New claim 183 appears to be supported as of page 121, paragraph 0290. New claim 184 appears to be supported as of at least page 52, paragraph 0148.

Reopening of Prosecution

This office action is made NON-FINAL because the office action includes a newly provided double patenting rejection that was not necessitated by amendment.

Withdrawn Rejection

The previously applied prior art rejection over Chou et al. (Journal of Bioscience and Bioengineering, Vol. 95 No. 4, 2003, pages 405-408) in view of Schlessinger et al. (US Patent 5,783,568), which was previously presented in the office action on 21 May 2019, has been withdrawn.

Chou et al. (hereafter referred to as Chou) is drawn to liposomal irinotecan, as of Chou, page 405, title and abstract.

Schlessinger et al. (hereafter referred to as Schlessinger) is drawn to treatment of cancer or other proliferative diseases. Schlessinger teaches administration of a salt of sucrose octasulfate for treating cancer or abnormal angiogenic cell proliferation, as of Schlessinger, column 27 line 19 to column 28 line 2.

Nevertheless, the above rejection does not apply to the currently pending claims. This is because there is insufficient evidence for the examiner to make the determination that the requirements regarding stability during storage would have been met by the prior art. The fact that a certain result or characteristic (the recited stability during storage) may occur or be present in the prior art is not sufficient to establish the inherency of that result or characteristic. See MPEP 2112(IV). In addition, there does not appear to be a reasonable expectation that the composition of the prior art could have been successfully optimized to have the storage stability recited by the currently pending claims.

Additionally, inherency must be based upon what is necessarily present in the prior art, not what would have resulted from optimization of conditions. See MPEP 2112(IV). It is the examiner's position that a liposome comprising both sucrose octasulfate and irinotecan is not necessarily present in the prior art. Even if, purely *en arguendo*, it would have been prima facie obvious for the skilled artisan to have made such a composition, inherency cannot be based upon such a composition since it is not necessarily present in the prior art.

Non-Statutory Double Patenting

The nonstatutory double patenting rejection is based on a judicially created doctrine grounded in public policy (a policy reflected in the statute) so as to prevent the unjustified or improper timewise extension of the "right to exclude" granted by a patent and to prevent possible harassment by multiple assignees. A nonstatutory double patenting rejection is appropriate where the conflicting claims are not identical, but at least one examined application claim is not patentably distinct from the reference claim(s) because the examined application claim is either anticipated by, or would have been obvious over, the reference claim(s). See, e.g., *In re Berg*, 140 F.3d 1428, 46 USPQ2d 1226 (Fed. Cir. 1998); *In re Goodman*, 11 F.3d 1046, 29 USPQ2d 2010 (Fed. Cir. 1993); *In re Longi*, 759 F.2d 887, 225 USPQ 645 (Fed. Cir. 1985); *In re Van Ornum*, 686 F.2d 937, 214 USPQ 761 (CCPA 1982); *In re Vogel*, 422 F.2d 438, 164 USPQ 619 (CCPA 1970); *In re Thorington*, 418 F.2d 528, 163 USPQ 644 (CCPA 1969).

A timely filed terminal disclaimer in compliance with 37 CFR 1.321(c) or 1.321(d) may be used to overcome an actual or provisional rejection based on nonstatutory double patenting provided the reference application or patent either is shown to be commonly owned with the examined application, or claims an invention made as a result of activities undertaken within the scope of a joint research agreement. See MPEP § 717.02 for applications subject to examination under the first inventor to file provisions of the AIA as explained in MPEP § 2159. See MPEP §§ 706.02(l)(1) - 706.02(l)(3) for applications not subject to examination under the first inventor to file provisions of the AIA. A terminal disclaimer must be signed in compliance with 37 CFR 1.321(b).

The USPTO Internet website contains terminal disclaimer forms which may be used. Please visit www.uspto.gov/patent/patents-forms. The filing date of the application in which the form is filed determines what form (e.g., PTO/SB/25, PTO/SB/26, PTO/AIA/25, or PTO/AIA/26) should be used. A web-based eTerminal Disclaimer may be filled out completely online using web-screens. An eTerminal Disclaimer that meets all requirements is auto-processed and approved immediately upon submission. For more information about eTerminal Disclaimers, refer to www.uspto.gov/patents/process/file/efs/guidance/eTD-info-I.jsp.

Claims 173-175 and 177-184 are rejected on the ground of nonstatutory double patenting as being unpatentable over claims 1-31 of U.S. Patent No. 10,456,360. Although the claims at issue are not identical, they are not patentably distinct from each other because of the following reasons:

Instant claim 173 is drawn to unilamellar liposomes comprising irinotecan with sucrose octasulfate, in which 90% of the irinotecan remains encapsulated after storage over 6 months at from 2°C to 8°C.

Conflicting claim 1 is drawn to a storage stabilized liposomal composition comprising irinotecan sucrose octasulfate. Claim 1 recites that the composition is stabilized to have less than 20 mol% of the total phospholipids degrade to lysophosphatidylcholine during the first 6 months of storage at 2°C to 8°C. Conflicting claim 6 recites that 98% of the irinotecan remains encapsulated after 6 months of storage at 2°C to 8°C.

The instant and conflicting claims differ because the conflicting claims recite a number of limitations not recited by the instant claims, such as a specific concentration of sucrose octasulfate and a specific pH range. Nevertheless, the subject matter of the conflicting claims is within the scope of that of the instant claims. As such, the subject matter of the conflicting claims effectively anticipates that of the instant claims, resulting in a prima facie case of anticipatory-type non-statutory double patenting.

Note Regarding Reference Date: The examiner notes that the instant application has an earlier effective filing date than the U.S. Patent No. 10,456,360. However, this feature does not negate the propriety of the applied double patenting rejection.

Terminal Disclaimers

The terminal disclaimer filed on 8 March 2019 disclaiming the terminal portion of any patent granted on this application which would extend beyond the expiration date of

US Patent 8,147,867

US Patent 8,329,213

US Patent 8,703,181

US Patent 8,992,970

US Patent 8,658,203

US Patent 9,717,723

US Patent 9,782,349

US Patent 9,737,528

US Patent 9,724,303 and

US Patent 9,703,891

has been reviewed and is accepted. The terminal disclaimer has been recorded.

The terminal disclaimer filed on 8 March 2019 disclaiming the terminal portion of any patent granted on this application which would extend beyond the expiration date of

US application 15/227,561

US application 15/227,631

US application 15/896,389; and

US application 15/896,436

has been reviewed and is accepted. The terminal disclaimer has been recorded.

Conclusion

No claim is allowed.

Any inquiry concerning this communication or earlier communications from the examiner should be directed to ISAAC SHOMER whose telephone number is (571)270-7671. The examiner can normally be reached on 7:30 AM to 5:00 PM Monday Through Friday.

Examiner interviews are available via telephone, in-person, and video conferencing using a USPTO supplied web-based collaboration tool. To schedule an

interview, applicant is encouraged to use the USPTO Automated Interview Request (AIR) at http://www.uspto.gov/interviewpractice.

If attempts to reach the examiner by telephone are unsuccessful, the examiner's supervisor, Frederick F Krass can be reached on (571)272-0580. The fax phone number for the organization where this application or proceeding is assigned is 571-273-8300.

Information regarding the status of an application may be obtained from the Patent Application Information Retrieval (PAIR) system. Status information for published applications may be obtained from either Private PAIR or Public PAIR. Status information for unpublished applications is available through Private PAIR only. For more information about the PAIR system, see https://ppair-my.uspto.gov/pair/PrivatePair. Should you have questions on access to the Private PAIR system, contact the Electronic Business Center (EBC) at 866-217-9197 (toll-free). If you would like assistance from a USPTO Customer Service Representative or access to the automated information system, call 800-786-9199 (IN USA OR CANADA) or 571-272-1000.

ISAAC . SHOMER
Primary Examiner
Art Unit 1612

/ISAAC SHOMER/
Primary Examiner, Art Unit 1612

UNITED STATES PATENT AND TRADEMARK OFFICE

UNITED STATES DEPARTMENT OF COMMERCE
United States Patent and Trademark Office
Address: COMMISSIONER FOR PATENTS
P.O. Box 1450
Alexandria, Virginia 22313-1450
www.uspto.gov

APPLICATION NO.	FILING DATE	FIRST NAMED INVENTOR	ATTORNEY DOCKET NO.	CONFIRMATION NO.
15/664,976	07/31/2017	Keelung Hong	263266-416123	4323

153749 7590 05/18/2020

McNeill Baur PLLC/Ipsen
Ipsen Bioscience, Inc.
125 Cambridge Park Drive
Suite 301
Cambridge, MA 02140

EXAMINER	
SHOMER, ISAAC	

ART UNIT	PAPER NUMBER
1612	

NOTIFICATION DATE	DELIVERY MODE
05/18/2020	ELECTRONIC

Please find below and/or attached an Office communication concerning this application or proceeding.

The time period for reply, if any, is set in the attached communication.

Notice of the Office communication was sent electronically on above-indicated "Notification Date" to the following e-mail address(es):

docketing@mcneillbaur.com
eofficeaction@appcoll.com
patents.us@ipsen.com

Office Action Summary	Application No. 15/664,976	Applicant(s) Hong et al.	
	Examiner ISAAC SHOMER	Art Unit 1612	AIA (FITF) Status No

-- The MAILING DATE of this communication appears on the cover sheet with the correspondence address --

Period for Reply

A SHORTENED STATUTORY PERIOD FOR REPLY IS SET TO EXPIRE 3 MONTHS FROM THE MAILING DATE OF THIS COMMUNICATION.

- Extensions of time may be available under the provisions of 37 CFR 1.136(a). In no event, however, may a reply be timely filed after SIX (6) MONTHS from the mailing date of this communication.
- If NO period for reply is specified above, the maximum statutory period will apply and will expire SIX (6) MONTHS from the mailing date of this communication.
- Failure to reply within the set or extended period for reply will, by statute, cause the application to become ABANDONED (35 U.S.C. § 133). Any reply received by the Office later than three months after the mailing date of this communication, even if timely filed, may reduce any earned patent term adjustment. See 37 CFR 1.704(b).

Status

1)☑ Responsive to communication(s) filed on 01 May 2020.

☐ A declaration(s)/affidavit(s) under **37 CFR 1.130(b)** was/were filed on _____.

2a)☑ This action is **FINAL.** 2b) ☐ This action is non-final.

3)☐ An election was made by the applicant in response to a restriction requirement set forth during the interview on _____; the restriction requirement and election have been incorporated into this action.

4)☐ Since this application is in condition for allowance except for formal matters, prosecution as to the merits is closed in accordance with the practice under *Ex parte Quayle*, 1935 C.D. 11, 453 O.G. 213.

Disposition of Claims*

5) ☑ Claim(s) 185-192 is/are pending in the application.

5a) Of the above claim(s) _____ is/are withdrawn from consideration.

6) ☐ Claim(s) _____ is/are allowed.

7) ☑ Claim(s) 185-192 is/are rejected.

8) ☐ Claim(s) _____ is/are objected to.

9) ☐ Claim(s) _____ are subject to restriction and/or election requirement

* If any claims have been determined allowable, you may be eligible to benefit from the **Patent Prosecution Highway** program at a participating intellectual property office for the corresponding application. For more information, please see http://www.uspto.gov/patents/init_events/pph/index.jsp or send an inquiry to **PPHfeedback@uspto.gov.**

Application Papers

10)☐ The specification is objected to by the Examiner.

11)☐ The drawing(s) filed on _____ is/are: a)☐ accepted or b)☐ objected to by the Examiner.

Applicant may not request that any objection to the drawing(s) be held in abeyance. See 37 CFR 1.85(a).

Replacement drawing sheet(s) including the correction is required if the drawing(s) is objected to. See 37 CFR 1.121(d).

Priority under 35 U.S.C. § 119

12)☐ Acknowledgment is made of a claim for foreign priority under 35 U.S.C. § 119(a)-(d) or (f).

Certified copies:

a)☐ All b)☐ Some** c)☐ None of the:

1.☐ Certified copies of the priority documents have been received.

2.☐ Certified copies of the priority documents have been received in Application No. _____.

3.☐ Copies of the certified copies of the priority documents have been received in this National Stage application from the International Bureau (PCT Rule 17.2(a)).

** See the attached detailed Office action for a list of the certified copies not received.

Attachment(s)

1) ☑ Notice of References Cited (PTO-892)

2) ☑ Information Disclosure Statement(s) (PTO/SB/08a and/or PTO/SB/08b) Paper No(s)/Mail Date _____.

3) ☐ Interview Summary (PTO-413) Paper No(s)/Mail Date _____.

4) ☐ Other: _____.

DETAILED ACTION

Applicants' arguments, filed 1 May 2020, have been fully considered. Rejections and/or objections not reiterated from previous office actions are hereby withdrawn. The following rejections and/or objections are either reiterated or newly applied. They constitute the complete set presently being applied to the instant application.

The present application is being examined under the pre-AIA first to invent provisions.

Claim Rejections - 35 USC § 103 – Obviousness

The following is a quotation of pre-AIA 35 U.S.C. 103(a) which forms the basis for all obviousness rejections set forth in this Office action:

> (a) A patent may not be obtained though the invention is not identically disclosed or described as set forth in section 102, if the differences between the subject matter sought to be patented and the prior art are such that the subject matter as a whole would have been obvious at the time the invention was made to a person having ordinary skill in the art to which said subject matter pertains. Patentability shall not be negatived by the manner in which the invention was made.

The factual inquiries set forth in *Graham v. John Deere Co.*, 383 U.S. 1, 148 USPQ 459 (1966), that are applied for establishing a background for determining obviousness under pre-AIA 35 U.S.C. 103(a) are summarized as follows:

1. Determining the scope and contents of the prior art.

2. Ascertaining the differences between the prior art and the claims at issue.

3. Resolving the level of ordinary skill in the pertinent art.

4. Considering objective evidence present in the application indicating obviousness or nonobviousness.

This application currently names joint inventors. In considering patentability of the claims under pre-AIA 35 U.S.C. 103(a), the examiner presumes that the subject matter of the various claims was commonly owned at the time any inventions covered therein were made absent any evidence to the contrary. Applicant is advised of the obligation under 37 CFR 1.56 to point out the inventor and invention dates of each claim that was not commonly owned at the time a later invention was made in order for the examiner to consider the applicability of pre-AIA 35 U.S.C. 103(c) and potential pre-AIA 35 U.S.C. 102(e), (f) or (g) prior art under pre-AIA 35 U.S.C. 103(a).

Claims 185-189 and 192 is/are rejected under pre-AIA 35 U.S.C. 103(a) as being unpatentable over Chou et al. (Journal of Bioscience and Bioengineering, Vol. 95, No. 4, 2003, pages 405-408) in view of Vucenik et al. (The Journal of Nutrition, Volume 133, Issue 11, November 2003, Pages 3778S–3784S).

Chou et al. (hereafter referred to as Chou) is drawn to a liposome comprising irinotecan, as of Chou, page 405, title and abstract. This liposome for the treatment of cancer, as of Chou, page 405, left column, first paragraph below abstract, which teaches antitumor activity of irinotecan. Chou teaches lipids such as phosphatidylcholines, as of Chou, page 405, title and abstract.

Chou does not teach inositol hexaphosphate.

Vucenik et al. (hereafter referred to as Vucenik) is drawn to cancer inhibition by inositol hexaphosphate, as of Vucenik, page 3778S, title and abstract. Vucenik provides teachings regarding anticancer action of inositol hexaposphate (abbreviated as IP_6, as of Vucenik, page 3779S, right column, and onto page 3780S.

Vucenik does not teach irinotecan.

It would have been prima facie obvious for one of ordinary skill in the art to have combined inositol hexaphosphate, as of Vucenik, with the liposome of Chou. Both inositol hexaphosphate and the liposome of Chou are useful for treating cancer. As such, the skilled artisan would have been motivated to have combined inositol hexaphosphate, as of Vucenik, with the liposome of Chou, to have predictably treated cancer with a reasonable expectation of success. Combining prior art elements (e.g. the liposome of Chou and the inositol hexaphosphate of Vucenik) according to known methods to achieve predictable results (treatment of cancer) is prima facie obvious. See MPEP 2143, Exemplary Rationale A. Additionally, it is prima facie obvious to combine two compositions (e.g. the liposome comprising irinotecan, as of Chou, with inositol hexaphosphate, as of Vucenik) each of which is taught by the prior art to be useful for the same purpose (treating cancer), in order to form a third composition to be used for the very same purpose. The idea of combining them flows logically from their having been individually taught in the prior art. See MPEP 2144.06(I).

As to claim 185, the claim requires about 0.15 to about 1.5 moles of irinotecan per moles of liposome lipid. Chou also teaches a loading amount of 0.254 mg drug per mg lipid, as of Chou, page 407, right column, last full paragraph. The units of this concentration differ from the recited units. Nevertheless, the examiner has performed a calculation below to estimate the concentration of irinotecan in Chou in mg of irinotecan per mmol of total phospholipids. As best understood by the examiner, and assuming molecular weight of liposome lipids of 790 Daltons (which is a molecular weight of

DSPC) and 587 Daltons for irinotecan this is a concentration of about 0.342 mmol irinotecan per mmol lipid, as of the calculation below.

$$\frac{0.254\ mg\ irinotecan}{1\ mg\ lipid} \times \frac{1\ mmol\ irinotecan}{587\ mg\ irinotecan} \times \frac{790\ mg\ lipid}{1\ mmol\ lipid} = 0.342\ \frac{mmol\ irinotean}{mmol\ lipid}$$

This concentration is within the range of about 0.15 to about 1.5 moles of irinotecan per moles of lipid, and as such, reads on the claimed requirements.

In the alternative, as to claim 185, even if, purely *en arguendo*, the above calculation is not correct, the skilled artisan would have been motivated to have optimized the amount of irinotecan to have been within the claimed range. Where the general conditions of a claim are disclosed in the prior art, it is not inventive to discover the optimum or workable ranges by routine experimentation. See MPEP 2144.05(II)(A). In this case, the general conditions of an irinotecan containing liposome is taught by the prior art. As such, it would not have been inventive to have discovered the optimum or workable range of irinotecan concentration by routine experimentation.

As to claim 186, the liposome of Chou comprises distearoyl phosphatidylcholine (DSPC) and cholesterol, as of Chou, page 405, abstract. DSPC is a zwitterionic phospholipid which is neutrally charged as the positive and negative charges cancel each other out.

As to claim 187, Chou teaches the following ratios of DSPC to cholesterol, as of Chou, page 406, right column, figure 1, reproduced below.

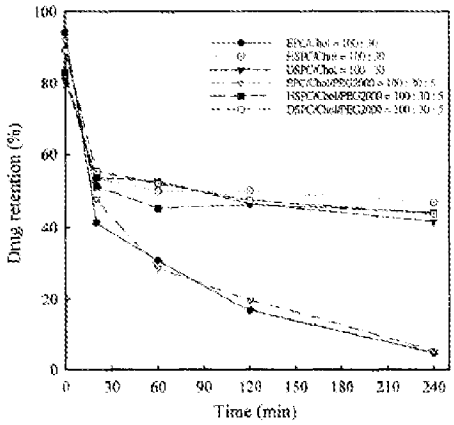

FIG. 1. Drug retention percentage against time for liposomes of different compositions. The standard deviations for these samples were typically <5%. Each data point represents the average of three or more determinations.

As best understood by the examiner, the above ratios are molar ratios. While the above ratios differ from the instantly claimed ratios, it would have been prima facie obvious for the skilled artisan to have optimized the ratio of DSPC to cholesterol to have been within the claimed range. Where the general conditions of a claim are disclosed in the prior art, it is not inventive to discover the optimum or workable ranges by routine experimentation. See MPEP 2144.05(II)(A). In this case, the general conditions of an irinotecan containing liposome comprising phosphatidylcholine and cholesterol is taught by the prior art. As such, it would not have been inventive to have discovered the optimum or workable range of phosphatidyhlcholine to cholesterol by routine experimentation.

As to claim 188, Chou teaches a polyethylene glycol phosphatidylethanolamine, as of Chou, page 405, abstract.

As to claim 189, Chou teaches that the molecular weight of the polyethylene glycol portion of the polyethylene glycol phosphatidylethanolamine is 2000 Daltons, as of Chou, page 405, abstract.

As to claim 192, Chou teaches the following particle sizes of between about 80 nm and about 140 nm, as of Chou, page 407, left column, figure 2, reproduced below.

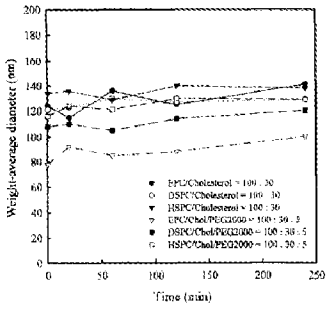

FIG. 2. Particle size (weight-averaged diameter) of liposomes of different compositions versus time. The standard deviations for these samples were typically ±15 nm. Each data point represents the average of three or more determinations.

This particle size overlaps with the claimed particle size value. While the prior art does not disclose the exact claimed values, but does overlap: in such instances even a slight overlap in range establishes a *prima facie* case of obviousness. See MPEP 2144.05(I).

Claims 190-191 is/are rejected under pre-AIA 35 U.S.C. 103(a) as being unpatentable over Chou et al. (Journal of Bioscience and Bioengineering, Vol. 95, No. 4, 2003, pages 405-408) in view of Vucenik et al. (The Journal of Nutrition, Volume 133, Issue 11, November 2003, Pages 3778S–3784S), the combination further in view of Uster et al. (FEBS Letters, Vol. 386, 1996, pages 243-246).

Chou is drawn to an irinotecan liposome for treating cancer. Vucenik is drawn to inositol hexaphosphate for treating cancer. See the rejection above over the combination of Chou in view of Vucenik. One of the lipids in the liposome is DSPE-PEG, as taught by Chou.

Chou does not specify that the PEG in DSPE-PEG is methoxy-terminated.

Uster et al. (hereafter referred to as Uster) is drawn to poly(ethylene glycol) derivatized phospholipid being placed into pre-formed liposomes, as of Uster, page 243, title and abstract. The pegylated lipid of Uster was made by attaching methoxypoly(ethylene glycol) via the carbamate linakte to the amino head group of 1,2-distearoyl-*sn*-glycero-3-phosphoethanolamine to make DSPE-PEG, as of Uster, page 243, right column, section 2.1.

Uster does not teach irinotecan.

It would have been prima facie obvious for one of ordinary skill in the art to have used a methoxy-terminated PEG to have formed the DSPE-PEG of Chou. Chou teaches using DSPE-PEG in a liposome, but is silent as to the end-group of the DSPE-PEG. As Uster teaches that a methoxy group is a known terminus of PEG to be used in DSPE-PEG in a liposome, the skilled artisan would have been motivated to have used methoxy terminated PEG, as of Ulster, to have predictably formed the DSPE-PEG of Chou with a reasonable expectation of success.

As to claims 190-191, Chou teaches DSPC, cholesterol, and DSPE-PEG, wherein PEG has a molecular weight of 2000 Daltons. Uster suggests that the PEG be methoxy-terminated. While none of the references appear to teach the required ratio of these components, it would have been prima facie obvious for the skilled artisan to have optimized the amounts of each component to have achieved the claimed invention. Where the general conditions of a claim are disclosed in the prior art, it is not inventive to discover the optimum or workable ranges by routine experimentation. See MPEP 2144.05(II)(A). In this case, the general conditions of an irinotecan containing liposome comprising phosphatidylcholine, cholesterol, and DSPE-PEG is taught by the prior art.

As such, it would not have been inventive to have discovered the optimum or workable range of phosphatidyhlcholine to cholesterol to DSPE-PEG by routine experimentation.

Conclusion

No claim is allowed.

Applicant's amendment necessitated the new ground(s) of rejection presented in this Office action. Accordingly, **THIS ACTION IS MADE FINAL**. See MPEP § 706.07(a). Applicant is reminded of the extension of time policy as set forth in 37 CFR 1.136(a).

A shortened statutory period for reply to this final action is set to expire THREE MONTHS from the mailing date of this action. In the event a first reply is filed within TWO MONTHS of the mailing date of this final action and the advisory action is not mailed until after the end of the THREE-MONTH shortened statutory period, then the shortened statutory period will expire on the date the advisory action is mailed, and any extension fee pursuant to 37 CFR 1.136(a) will be calculated from the mailing date of the advisory action. In no event, however, will the statutory period for reply expire later than SIX MONTHS from the date of this final action.

Any inquiry concerning this communication or earlier communications from the examiner should be directed to ISAAC SHOMER whose telephone number is (571)270-7671. The examiner can normally be reached on 7:30 AM to 5:00 PM Monday Through Friday.

Examiner interviews are available via telephone, in-person, and video conferencing using a USPTO supplied web-based collaboration tool. To schedule an interview, applicant is encouraged to use the USPTO Automated Interview Request (AIR) at http://www.uspto.gov/interviewpractice.

If attempts to reach the examiner by telephone are unsuccessful, the examiner's supervisor, Frederick F Krass can be reached on (571)272-0580. The fax phone number for the organization where this application or proceeding is assigned is 571-273-8300.

Information regarding the status of an application may be obtained from the Patent Application Information Retrieval (PAIR) system. Status information for published applications may be obtained from either Private PAIR or Public PAIR. Status information for unpublished applications is available through Private PAIR only. For more information about the PAIR system, see https://ppair-my.uspto.gov/pair/PrivatePair. Should you have questions on access to the Private PAIR system, contact the Electronic Business Center (EBC) at 866-217-9197 (toll-free). If you would like assistance from a USPTO Customer Service Representative or access to the automated information system, call 800-786-9199 (IN USA OR CANADA) or 571-272-1000.

ISAAC . SHOMER
Primary Examiner
Art Unit 1612

/ISAAC SHOMER/
Primary Examiner, Art Unit 1612

UNITED STATES PATENT AND TRADEMARK OFFICE

UNITED STATES DEPARTMENT OF COMMERCE
United States Patent and Trademark Office
Address: COMMISSIONER FOR PATENTS
P.O. Box 1450
Alexandria, Virginia 22313-1450
www.uspto.gov

NOTICE OF ALLOWANCE AND FEE(S) DUE

153749 7590 10/13/2020

McNeill Baur PLLC/Ipsen
Ipsen Bioscience, Inc.
125 Cambridge Park Drive
Suite 301
Cambridge, MA 02140

EXAMINER
SHOMER, ISAAC

ART UNIT	PAPER NUMBER
1612	

DATE MAILED: 10/13/2020

APPLICATION NO.	FILING DATE	FIRST NAMED INVENTOR	ATTORNEY DOCKET NO.	CONFIRMATION NO.
15/664,976	07/31/2017	Keelung Hong	263266-416123	4323

TITLE OF INVENTION: Liposomes Useful for Drug Delivery

APPLN. TYPE	ENTITY STATUS	ISSUE FEE DUE	PUBLICATION FEE DUE	PREV. PAID ISSUE FEE	TOTAL FEE(S) DUE	DATE DUE
nonprovisional	UNDISCOUNTED	$1200	$0.00	$0.00	$1200	01/13/2021

THE APPLICATION IDENTIFIED ABOVE HAS BEEN EXAMINED AND IS ALLOWED FOR ISSUANCE AS A PATENT. PROSECUTION ON THE MERITS IS CLOSED. THIS NOTICE OF ALLOWANCE IS NOT A GRANT OF PATENT RIGHTS. THIS APPLICATION IS SUBJECT TO WITHDRAWAL FROM ISSUE AT THE INITIATIVE OF THE OFFICE OR UPON PETITION BY THE APPLICANT. SEE 37 CFR 1.313 AND MPEP 1308.

THE ISSUE FEE AND PUBLICATION FEE (IF REQUIRED) MUST BE PAID WITHIN THREE MONTHS FROM THE MAILING DATE OF THIS NOTICE OR THIS APPLICATION SHALL BE REGARDED AS ABANDONED. THIS STATUTORY PERIOD CANNOT BE EXTENDED. SEE 35 U.S.C. 151. THE ISSUE FEE DUE INDICATED ABOVE DOES NOT REFLECT A CREDIT FOR ANY PREVIOUSLY PAID ISSUE FEE IN THIS APPLICATION. IF AN ISSUE FEE HAS PREVIOUSLY BEEN PAID IN THIS APPLICATION (AS SHOWN ABOVE), THE RETURN OF PART B OF THIS FORM WILL BE CONSIDERED A REQUEST TO REAPPLY THE PREVIOUSLY PAID ISSUE FEE TOWARD THE ISSUE FEE NOW DUE.

HOW TO REPLY TO THIS NOTICE:

I. Review the ENTITY STATUS shown above. If the ENTITY STATUS is shown as SMALL or MICRO, verify whether entitlement to that entity status still applies.

If the ENTITY STATUS is the same as shown above, pay the TOTAL FEE(S) DUE shown above.

If the ENTITY STATUS is changed from that shown above, on PART B - FEE(S) TRANSMITTAL, complete section number 5 titled "Change in Entity Status (from status indicated above)".

For purposes of this notice, small entity fees are 1/2 the amount of undiscounted fees, and micro entity fees are 1/2 the amount of small entity fees.

II. PART B - FEE(S) TRANSMITTAL, or its equivalent, must be completed and returned to the United States Patent and Trademark Office (USPTO) with your ISSUE FEE and PUBLICATION FEE (if required). If you are charging the fee(s) to your deposit account, section "4b" of Part B - Fee(s) Transmittal should be completed and an extra copy of the form should be submitted. If an equivalent of Part B is filed, a request to reapply a previously paid issue fee must be clearly made, and delays in processing may occur due to the difficulty in recognizing the paper as an equivalent of Part B.

III. All communications regarding this application must give the application number. Please direct all communications prior to issuance to Mail Stop ISSUE FEE unless advised to the contrary.

IMPORTANT REMINDER: Maintenance fees are due in utility patents issuing on applications filed on or after Dec. 12, 1980. It is patentee's responsibility to ensure timely payment of maintenance fees when due. More information is available at www.uspto.gov/PatentMaintenanceFees.

PART B - FEE(S) TRANSMITTAL

Complete and send this form, together with applicable fee(s), by mail or fax, or via EFS-Web.

By mail, send to: Mail Stop ISSUE FEE
Commissioner for Patents
P.O. Box 1450
Alexandria, Virginia 22313-1450

By fax, send to: (571)-273-2885

INSTRUCTIONS: This form should be used for transmitting the ISSUE FEE and PUBLICATION FEE (if required). Blocks 1 through 5 should be completed where appropriate. All further correspondence including the Patent, advance orders and notification of maintenance fees will be mailed to the current correspondence address as indicated unless corrected below or directed otherwise in Block 1, by (a) specifying a new correspondence address; and/or (b) indicating a separate "FEE ADDRESS" for maintenance fee notifications.

CURRENT CORRESPONDENCE ADDRESS (Note: Use Block 1 for any change of address)

153749 7590 10/13/2020

McNeill Baur PLLC/Ipsen
Ipsen Bioscience, Inc.
125 Cambridge Park Drive
Suite 301
Cambridge, MA 02140

Note: A certificate of mailing can only be used for domestic mailings of the Fee(s) Transmittal. This certificate cannot be used for any other accompanying papers. Each additional paper, such as an assignment or formal drawing, must have its own certificate of mailing or transmission.

Certificate of Mailing or Transmission

I hereby certify that this Fee(s) Transmittal is being deposited with the United States Postal Service with sufficient postage for first class mail in an envelope addressed to the Mail Stop ISSUE FEE address above, or being transmitted to the USPTO via EFS-Web or by facsimile to (571) 273-2885, on the date below.

(Typed or printed name)
(Signature)
(Date)

APPLICATION NO.	FILING DATE	FIRST NAMED INVENTOR	ATTORNEY DOCKET NO.	CONFIRMATION NO.
15/664,976	07/31/2017	Keelung Hong	263266-416123	4323

TITLE OF INVENTION: Liposomes Useful for Drug Delivery

APPLN. TYPE	ENTITY STATUS	ISSUE FEE DUE	PUBLICATION FEE DUE	PREV. PAID ISSUE FEE	TOTAL FEE(S) DUE	DATE DUE
nonprovisional	UNDISCOUNTED	$1200	$0.00	$0.00	$1200	01/13/2021

EXAMINER	ART UNIT	CLASS-SUBCLASS
SHOMER, ISAAC	1612	424-450000

1. Change of correspondence address or indication of "Fee Address" (37 CFR 1.363).

❑ Change of correspondence address (or Change of Correspondence Address form PTO/SB/122) attached.

❑ "Fee Address" indication (or "Fee Address" Indication form PTO/SB/47; Rev 03-09 or more recent) attached. **Use of a Customer Number is required.**

2. For printing on the patent front page, list
(1) The names of up to 3 registered patent attorneys or agents OR, alternatively,
(2) The name of a single firm (having as a member a registered attorney or agent) and the names of up to 2 registered patent attorneys or agents. If no name is listed, no name will be printed.

1 _____
2 _____
3 _____

3. ASSIGNEE NAME AND RESIDENCE DATA TO BE PRINTED ON THE PATENT (print or type)

PLEASE NOTE: Unless an assignee is identified below, no assignee data will appear on the patent. If an assignee is identified below, the document must have been previously recorded, or filed for recordation, as set forth in 37 CFR 3.11 and 37 CFR 3.81(a). Completion of this form is NOT a substitute for filing an assignment.

(A) NAME OF ASSIGNEE (B) RESIDENCE: (CITY and STATE OR COUNTRY)

Please check the appropriate assignee category or categories (will not be printed on the patent) : ❑ Individual ❑ Corporation or other private group entity ❑ Government

4a. Fees submitted: ❑ Issue Fee ❑ Publication Fee (if required) ❑ Advance Order - # of Copies _____

4b. Method of Payment: *(Please first reapply any previously paid fee shown above)*

❑ Electronic Payment via EFS-Web ❑ Enclosed check ❑ Non-electronic payment by credit card (Attach form PTO-2038)

❑ The Director is hereby authorized to charge the required fee(s), any deficiency, or credit any overpayment to Deposit Account No. _____

5. **Change in Entity Status** (from status indicated above)

❑ Applicant certifying micro entity status. See 37 CFR 1.29

❑ Applicant asserting small entity status. See 37 CFR 1.27

❑ Applicant changing to regular undiscounted fee status.

NOTE: Absent a valid certification of Micro Entity Status (see forms PTO/SB/15A and 15B), issue fee payment in the micro entity amount will not be accepted at the risk of application abandonment.
NOTE: If the application was previously under micro entity status, checking this box will be taken to be a notification of loss of entitlement to micro entity status.
NOTE: Checking this box will be taken to be a notification of loss of entitlement to small or micro entity status, as applicable.

NOTE: This form must be signed in accordance with 37 CFR 1.31 and 1.33. See 37 CFR 1.4 for signature requirements and certifications.

Authorized Signature _____ Date _____

Typed or printed name _____ Registration No. _____

UNITED STATES PATENT AND TRADEMARK OFFICE

UNITED STATES DEPARTMENT OF COMMERCE
United States Patent and Trademark Office
Address: COMMISSIONER FOR PATENTS
P.O. Box 1450
Alexandria, Virginia 22313-1450
www.uspto.gov

APPLICATION NO.	FILING DATE	FIRST NAMED INVENTOR	ATTORNEY DOCKET NO.	CONFIRMATION NO.
15/664,976	07/31/2017	Keelung Hong	263266-416123	4323

153749 7590 10/13/2020

McNeill Baur PLLC/Ipsen
Ipsen Bioscience, Inc.
125 Cambridge Park Drive
Suite 301
Cambridge, MA 02140

EXAMINER	
SHOMER, ISAAC	
ART UNIT	PAPER NUMBER
1612	

DATE MAILED: 10/13/2020

Determination of Patent Term Adjustment under 35 U.S.C. 154 (b)
(Applications filed on or after May 29, 2000)

The Office has discontinued providing a Patent Term Adjustment (PTA) calculation with the Notice of Allowance.

Section 1(h)(2) of the AIA Technical Corrections Act amended 35 U.S.C. 154(b)(3)(B)(i) to eliminate the requirement that the Office provide a patent term adjustment determination with the notice of allowance. See Revisions to Patent Term Adjustment, 78 Fed. Reg. 19416, 19417 (Apr. 1, 2013). Therefore, the Office is no longer providing an initial patent term adjustment determination with the notice of allowance. The Office will continue to provide a patent term adjustment determination with the Issue Notification Letter that is mailed to applicant approximately three weeks prior to the issue date of the patent, and will include the patent term adjustment on the patent. Any request for reconsideration of the patent term adjustment determination (or reinstatement of patent term adjustment) should follow the process outlined in 37 CFR 1.705.

Any questions regarding the Patent Term Extension or Adjustment determination should be directed to the Office of Patent Legal Administration at (571)-272-7702. Questions relating to issue and publication fee payments should be directed to the Customer Service Center of the Office of Patent Publication at 1-(888)-786-0101 or (571)-272-4200.

OMB Clearance and PRA Burden Statement for PTOL-85 Part B

The Paperwork Reduction Act (PRA) of 1995 requires Federal agencies to obtain Office of Management and Budget approval before requesting most types of information from the public. When OMB approves an agency request to collect information from the public, OMB (i) provides a valid OMB Control Number and expiration date for the agency to display on the instrument that will be used to collect the information and (ii) requires the agency to inform the public about the OMB Control Number's legal significance in accordance with 5 CFR 1320.5(b).

The information collected by PTOL-85 Part B is required by 37 CFR 1.311. The information is required to obtain or retain a benefit by the public which is to file (and by the USPTO to process) an application. Confidentiality is governed by 35 U.S.C. 122 and 37 CFR 1.14. This collection is estimated to take 30 minutes to complete, including gathering, preparing, and submitting the completed application form to the USPTO. Time will vary depending upon the individual case. Any comments on the amount of time you require to complete this form and/or suggestions for reducing this burden, should be sent to the Chief Information Officer, U.S. Patent and Trademark Office, U.S. Department of Commerce, P.O. Box 1450, Alexandria, Virginia 22313-1450. DO NOT SEND FEES OR COMPLETED FORMS TO THIS ADDRESS. SEND TO: Commissioner for Patents, P.O. Box 1450, Alexandria, Virginia 22313-1450. Under the Paperwork Reduction Act of 1995, no persons are required to respond to a collection of information unless it displays a valid OMB control number.

Privacy Act Statement

The Privacy Act of 1974 (P.L. 93-579) requires that you be given certain information in connection with your submission of the attached form related to a patent application or patent. Accordingly, pursuant to the requirements of the Act, please be advised that: (1) the general authority for the collection of this information is 35 U.S.C. 2(b)(2); (2) furnishing of the information solicited is voluntary; and (3) the principal purpose for which the information is used by the U.S. Patent and Trademark Office is to process and/or examine your submission related to a patent application or patent. If you do not furnish the requested information, the U.S. Patent and Trademark Office may not be able to process and/or examine your submission, which may result in termination of proceedings or abandonment of the application or expiration of the patent.

The information provided by you in this form will be subject to the following routine uses:

1. The information on this form will be treated confidentially to the extent allowed under the Freedom of Information Act (5 U.S.C. 552) and the Privacy Act (5 U.S.C 552a). Records from this system of records may be disclosed to the Department of Justice to determine whether disclosure of these records is required by the Freedom of Information Act.
2. A record from this system of records may be disclosed, as a routine use, in the course of presenting evidence to a court, magistrate, or administrative tribunal, including disclosures to opposing counsel in the course of settlement negotiations.
3. A record in this system of records may be disclosed, as a routine use, to a Member of Congress submitting a request involving an individual, to whom the record pertains, when the individual has requested assistance from the Member with respect to the subject matter of the record.
4. A record in this system of records may be disclosed, as a routine use, to a contractor of the Agency having need for the information in order to perform a contract. Recipients of information shall be required to comply with the requirements of the Privacy Act of 1974, as amended, pursuant to 5 U.S.C. 552a(m).
5. A record related to an International Application filed under the Patent Cooperation Treaty in this system of records may be disclosed, as a routine use, to the International Bureau of the World Intellectual Property Organization, pursuant to the Patent Cooperation Treaty.
6. A record in this system of records may be disclosed, as a routine use, to another federal agency for purposes of National Security review (35 U.S.C. 181) and for review pursuant to the Atomic Energy Act (42 U.S.C. 218(c)).
7. A record from this system of records may be disclosed, as a routine use, to the Administrator, General Services, or his/her designee, during an inspection of records conducted by GSA as part of that agency's responsibility to recommend improvements in records management practices and programs, under authority of 44 U.S.C. 2904 and 2906. Such disclosure shall be made in accordance with the GSA regulations governing inspection of records for this purpose, and any other relevant (i.e., GSA or Commerce) directive. Such disclosure shall not be used to make determinations about individuals.
8. A record from this system of records may be disclosed, as a routine use, to the public after either publication of the application pursuant to 35 U.S.C. 122(b) or issuance of a patent pursuant to 35 U.S.C. 151. Further, a record may be disclosed, subject to the limitations of 37 CFR 1.14, as a routine use, to the public if the record was filed in an application which became abandoned or in which the proceedings were terminated and which application is referenced by either a published application, an application open to public inspection or an issued patent.
9. A record from this system of records may be disclosed, as a routine use, to a Federal, State, or local law enforcement agency, if the USPTO becomes aware of a violation or potential violation of law or regulation.

Notice of Allowability	Application No. 15/664,976	Applicant(s) Hong et al.	
	Examiner ISAAC SHOMER	Art Unit 1612	AIA (FITF) Status No

-- The MAILING DATE of this communication appears on the cover sheet with the correspondence address--

All claims being allowable, PROSECUTION ON THE MERITS IS (OR REMAINS) CLOSED in this application. If not included herewith (or previously mailed), a Notice of Allowance (PTOL-85) or other appropriate communication will be mailed in due course. **THIS NOTICE OF ALLOWABILITY IS NOT A GRANT OF PATENT RIGHTS.** This application is subject to withdrawal from issue at the initiative of the Office or upon petition by the applicant. See 37 CFR 1.313 and MPEP 1308.

1. ☑ This communication is responsive to RCE on 18 September 2020.
   ☐ A declaration(s)/affidavit(s) under **37 CFR 1.130(b)** was/were filed on _____.

2. ☐ An election was made by the applicant in response to a restriction requirement set forth during the interview on _____; the restriction requirement and election have been incorporated into this action.

3. ☑ The allowed claim(s) is/are 185-192 . As a result of the allowed claim(s), you may be eligible to benefit from the **Patent Prosecution Highway** program at a participating intellectual property office for the corresponding application. For more information , please see **http://www.uspto.gov/patents/init_events/pph/index.jsp** or send an inquiry to **PPHfeedback@uspto.gov.**

4. ☐ Acknowledgment is made of a claim for foreign priority under 35 U.S.C. § 119(a)-(d) or (f).

   Certified copies:

   a) ☐ All b) ☐ Some *c) ☐ None of the:

   1. ☐ Certified copies of the priority documents have been received.
   2. ☐ Certified copies of the priority documents have been received in Application No. _____ .
   3. ☐ Copies of the certified copies of the priority documents have been received in this national stage application from the International Bureau (PCT Rule 17.2(a)).

   * Certified copies not received: _____ .

Applicant has THREE MONTHS FROM THE "MAILING DATE" of this communication to file a reply complying with the requirements noted below. Failure to timely comply will result in ABANDONMENT of this application.
THIS THREE-MONTH PERIOD IS NOT EXTENDABLE.

5. ☐ CORRECTED DRAWINGS (as "replacement sheets") must be submitted.
   ☐ including changes required by the attached Examiner's Amendment / Comment or in the Office action of Paper No./Mail Date _____ .

   Identifying indicia such as the application number (see 37 CFR 1.84(c)) should be written on the drawings in the front (not the back) of each sheet. Replacement sheet(s) should be labeled as such in the header according to 37 CFR 1.121(d).

6. ☐ DEPOSIT OF and/or INFORMATION about the deposit of BIOLOGICAL MATERIAL must be submitted. Note the attached Examiner's comment regarding REQUIREMENT FOR THE DEPOSIT OF BIOLOGICAL MATERIAL.

Attachment(s)

1. ☑ Notice of References Cited (PTO-892)
2. ☑ Information Disclosure Statements (PTO/SB/08), Paper No./Mail Date _____.
3. ☐ Examiner's Comment Regarding Requirement for Deposit of Biological Material _____.
4. ☐ Interview Summary (PTO-413), Paper No./Mail Date. _____.
5. ☐ Examiner's Amendment/Comment
6. ☑ Examiner's Statement of Reasons for Allowance
7. ☐ Other _____.

/ISAAC SHOMER/
Primary Examiner, Art Unit 1612

REASONS FOR ALLOWANCE

The following is an examiner's statement of reasons for allowance:

As an initial matter, the claim amendments of claim 185 on 18 September 2020 are adequately supported in view of the instant specification at page 34, end of paragraph 0109. With regard to claim 192, which was previously newly added in the claim set on 1 May 2020, the recited size, as measured by quasi-elastic light scattering, is disclosed on page 116, paragraph 0280 of the instant specification. While this paragraph of the instant specification does not specifically disclose that the Gaussian model is used, this is disclosed elsewhere in the instant application, including but not limited to page 87, paragraph 0221. This is understood by the examiner to adequately support claim 192.

As close prior art, the examiner cites Chou et al. (Journal of Bioscience and Bioengineering, Vol. 95, No. 4, 2003, pages 405-408), which was cited earlier in the prosecution history of the instant application. Chou et al. (hereafter referred to as Chou) is drawn to a liposome comprising irinotecan, as of Chou, page 405, title and abstract. This liposome for the treatment of cancer, as of Chou, page 405, left column, first paragraph below abstract, which teaches antitumor activity of irinotecan. Chou teaches lipids such as phosphatidylcholines, as of Chou, page 405, title and abstract.

Chou differs from the claimed invention for at least the following reasons.

(a) First, Chou does not teach inositol hexaphosphate.

(b) Secondly, Chou does not teach that the concentration of encapsulated irinotecan in milimoles of irinotecan per gram of total liposome lipids is between 0.8 and

1.3. In contrast, the concentration of encapsulated irinotecan that is taught by prior art reference Chou is lower than what is required by the instant claims.

In view of at least these differences, the examiner takes the position that the instant claims are not prima facie obvious over Chou, either by itself or in view of another reference. The examiner presents the following reasoning below in support of this position.

Chou teaches a maximum concentration of encapsulated drug of 0.254 milligrams of drug per milligram of lipid, as of Chou, page 407, right column, end of last full paragraph. The drug referred to by Chou at this portion in the text of Chou appears to be irinotecan. The examiner has provided the following calculation to convert this value into millimoles of irinotecan per gram of total liposome lipids, which are the units recited by instant claim 185 – this calculation is based upon an irinotecan molecular weight of 586.673 Daltons[1].

$$\left(\frac{0.254\ mg\ irinotecan}{1\ mg\ lipid}\right) \times \left(\frac{1000\ mg\ lipid}{1\ gram\ lipid}\right) \times \left(\frac{1\ mmol\ irinotecan}{586.673\ g\ irinotecan}\right) \approx 0.433 \frac{mmol}{gram}$$

In view of the above calculation, Chou appears to teach a maximum amount of encapsulated irinotecan of 0.433 mmol of irinotecan per gram of liposome lipid. As such, the minimum amount of irinotecan encapsulated by the claimed liposome of 0.8 mmol irinotecan per gram of liposome lipid is almost twice the maximum amount of irinotecan encapsulated in a liposome by Chou.

[1] In the above calculation, the examiner used the molecular weight of free irinotecan to perform the calculation. If, purely *en arguendo*, the examiner erred in estimating the molecular weight of irinotecan by failing to account for the counter-ion of irinotecan or waters of hydration of irinotecan, this would have resulted in a higher apparent molecular weight of irinotecan and therefore a lower concentration of irinotecan in terms of millimoles of irinotecan per gram of liposome lipids. If this were the case, the concentration of irinotecan in terms of millimoles per gram would be lower, which would further strengthen the examiner's position.

The examiner takes the position that the increase in the amount of encapsulated irinotecan in the claimed invention as compared with the prior art is not a matter of routine optimization. This is because increasing the amount of irinotecan encapsulated in a liposome is not a matter of simply increasing the concentration of irinotecan, at least because successfully encapsulating[2] drug in a liposome is difficult. The difficulty of encapsulation of irinotecan is evidenced by Chou, at least in view of the fact that Chou needs to use a pH gradient comprising ammonium ions to load irinotecan into the liposome, as of Chou, page 405. Additionally, Chou appears to experience problems with drug leakage, as of Chou, page 406, right column, first full paragraph, which indicates that successfully encapsulating drug into a liposome and having it remain in the liposome is difficult.

Also, that a fairly specific protocol is needed to achieve drug encapsulation is evident through the instant specification. See the instant specification at page 32, paragraph 0108 at the bottom of the page and onto page 33, which appears to indicate that incubating the active agent with the liposome at a specific temperature above the phase transition of the lipids and with a specific ionic strength is needed to encapsulate the active agent.

As such, in view of the apparent difficulty of encapsulating irinotecan in a liposome, there would have been no reasonable expectation that the entrapped concentration of irinotecan could have successfully been increased from 0.433 mmol irinotecan per gram of liposome lipids, as in the prior art, to the range of between 0.8

[2] As best understood by the examiner, the word “encapsulating” has the same meaning as the word “entrapping”, as used in instant claim 185. See the instant specification on page 1, last line, and page 2, first two lines in paragraph 0003.

and 1.3 mmol irinotecan per gram of liposome lipids, as required by the instantly claimed invention. Obvious requires a reasonable expectation of success; however, in this case, the reasonable expectation of success appear to be lacking. See MPEP 2143.02.

In order to further explain this point, the examiner notes MPEP 2144.05(II)(A). A portion of text from this section of the MPEP is reproduced below.

> Generally, differences in concentration or temperature will not support the patentability of subject matter encompassed by the prior art unless there is evidence indicating such concentration or temperature is critical. "[W]here the general conditions of a claim are disclosed in the prior art, it is not inventive to discover the optimum or workable ranges by routine experimentation." In re Aller, 220 F.2d 454, 456, 105 USPQ 233, 235 (CCPA 1955) (Claimed process which was performed at a temperature between 40°C and 80°C and an acid concentration between 25% and 70% was held to be prima facie obvious over a reference process which differed from the claims only in that the reference process was performed at a temperature of 100°C and an acid concentration of 10%.);

The instantly claimed invention differs from the cited case because in the cited case, the amount of acid could have been increased from 10%, as in the prior art in the cited case, to 25-70%, as in the claimed invention in the cited case, simply by adding more acid. In contrast, in the instant application, adding more irinotecan to a liposome preparation would not have been expected to have been sufficient to have resulted in greater encapsulation of irinotecan in a liposome due to the difficulty of encapsulating irinotecan in a liposome. As such, while there would have been a reasonable expectation that acid concentration could have successfully been increased to achieve the claimed range in the cited case, there would have been no reasonable expectation

that the concentration of encapsulated irinotecan could have been successfully increased to achieve the claimed amounts in the instantly claimed invention.

The claimed invention also differs from the prior art of Chou in that the claimed invention recites inositol hexaphosphate, which is not taught by Chou. The examiner notes that an anti-cancer use of inositol hexaphosphate is taught by the prior art, specifically as of the Vucenik reference cited on page 3 of the prior office action on 18 May 2020. Nevertheless, Vucenik does not appear to teach encapsulation of inositol hexaphosphate in liposomes. Furthermore, Vucenik does not teach that, had inositol hexaphosphate been encapsulated in liposomes with irinotecan, the concentration of encapsulated irinotecan could have been increased as compared with the concentration of irinotecan encapsulated in a liposome lacking inositol hexaphosphate. As such, there would have been no reasonable expectation that the combination of Chou and Vucenik would have been successfully capable of encapsulating or entrapping between 0.8 and 1.3 millimoles of irinotecan per gram of total liposome lipids.

As additional relevant art, the examiner cites two post-filing date references published well after the earliest effective filing date of the instant application. These references are Hattori et al. (Journal of Controlled Release, Vol. 136, 2009, pages 30-37) and Wei et al. (Asian Journal of Pharmaceutical Sciences, Vol. 8, 2013, pages 303-311). Both references are drawn to liposomes comprising irinotecan, as of the titles and abstracts of both references. Hattori combines irinotecan with phytic acid, as of the title of Hattori, wherein phytic acid is a synonym for inositol hexaphosphate. Wei combines irinotecan with ammonium phytate, as of page 304, right column, section 2.3, wherein

"ammonium phytate" is understood to refer to the ammonium salt of the conjugate base of phytic acid, wherein phytic acid is inositol hexaphsophate.

Any comments considered necessary by applicant must be submitted no later than the payment of the issue fee and, to avoid processing delays, should preferably accompany the issue fee. Such submissions should be clearly labeled "Comments on Statement of Reasons for Allowance."

Terminal Disclaimers

The terminal disclaimer filed on 8 March 2019 disclaiming the terminal portion of any patent granted on this application which would extend beyond the expiration date of

US Patent 8,147,867

US Patent 8,329,213

US Patent 8,703,181

US Patent 8,992,970

US Patent 8,658,203

US Patent 9,717,723

US Patent 9,782,349

US Patent 9,737,528

US Patent 9,724,303 and

US Patent 9,703,891

has been reviewed and is accepted. The terminal disclaimer has been recorded.

The terminal disclaimer filed on 8 March 2019 disclaiming the terminal portion of any patent granted on this application which would extend beyond the expiration date of

US application 15/227,561

US application 15/227,631

US application 15/896,389 (now US Patent 10,722,508); and

US application 15/896,436

has been reviewed and is accepted. The terminal disclaimer has been recorded.

Conclusion

Any inquiry concerning this communication or earlier communications from the examiner should be directed to ISAAC SHOMER whose telephone number is (571)270-7671. The examiner can normally be reached on 7:30 AM to 5:00 PM Monday Through Friday.

Examiner interviews are available via telephone, in-person, and video conferencing using a USPTO supplied web-based collaboration tool. To schedule an interview, applicant is encouraged to use the USPTO Automated Interview Request (AIR) at http://www.uspto.gov/interviewpractice.

If attempts to reach the examiner by telephone are unsuccessful, the examiner's supervisor, Frederick F Krass can be reached on (571)272-0580. The fax phone number for the organization where this application or proceeding is assigned is 571-273-8300.

Information regarding the status of an application may be obtained from the Patent Application Information Retrieval (PAIR) system. Status information for published applications may be obtained from either Private PAIR or Public PAIR. Status information for unpublished applications is available through Private PAIR only. For more information about the PAIR system, see https://ppair-my.uspto.gov/pair/PrivatePair. Should you have questions on access to the Private PAIR system, contact the Electronic Business Center (EBC) at 866-217-9197 (toll-free). If you would like assistance from a USPTO Customer Service Representative or access to the automated information system, call 800-786-9199 (IN USA OR CANADA) or 571-272-1000.

ISAAC . SHOMER
Primary Examiner
Art Unit 1612

/ISAAC SHOMER/
Primary Examiner, Art Unit 1612

UNITED STATES PATENT AND TRADEMARK OFFICE

UNITED STATES DEPARTMENT OF COMMERCE
United States Patent and Trademark Office
Address: COMMISSIONER FOR PATENTS
P.O. Box 1450
Alexandria, Virginia 22313-1450
www.uspto.gov

APPLICATION NO.	FILING DATE	FIRST NAMED INVENTOR	ATTORNEY DOCKET NO.	CONFIRMATION NO.
15/809,815	11/10/2017	Eliel Bayever	263266-421428	5137

153749 7590 02/27/2020

McNeill Baur PLLC/Ipsen
Ipsen Bioscience, Inc.
125 Cambridge Park Drive
Suite 301
Cambridge, MA 02140

EXAMINER	
RONEY, CELESTE A	

ART UNIT	PAPER NUMBER
1612	

NOTIFICATION DATE	DELIVERY MODE
02/27/2020	ELECTRONIC

Please find below and/or attached an Office communication concerning this application or proceeding.

The time period for reply, if any, is set in the attached communication.

Notice of the Office communication was sent electronically on above-indicated "Notification Date" to the following e-mail address(es):

docketing@mcneillbaur.com
eofficeaction@appcoll.com
patents.us@ipsen.com

Office Action Summary	Application No. 15/809,815	Applicant(s) Bayever et al.	
	Examiner CELESTE A RONEY	Art Unit 1612	AIA (FITF) Status Yes

-- The MAILING DATE of this communication appears on the cover sheet with the correspondence address --

Period for Reply

A SHORTENED STATUTORY PERIOD FOR REPLY IS SET TO EXPIRE 3 MONTHS FROM THE MAILING DATE OF THIS COMMUNICATION.

- Extensions of time may be available under the provisions of 37 CFR 1.136(a). In no event, however, may a reply be timely filed after SIX (6) MONTHS from the mailing date of this communication.
- If NO period for reply is specified above, the maximum statutory period will apply and will expire SIX (6) MONTHS from the mailing date of this communication.
- Failure to reply within the set or extended period for reply will, by statute, cause the application to become ABANDONED (35 U.S.C. § 133). Any reply received by the Office later than three months after the mailing date of this communication, even if timely filed, may reduce any earned patent term adjustment. See 37 CFR 1.704(b).

Status

1)☑ Responsive to communication(s) filed on 07 January 2020.

☐ A declaration(s)/affidavit(s) under **37 CFR 1.130(b)** was/were filed on _____.

2a)☑ This action is **FINAL.** 2b) ☐ This action is non-final.

3)☐ An election was made by the applicant in response to a restriction requirement set forth during the interview on _____; the restriction requirement and election have been incorporated into this action.

4)☐ Since this application is in condition for allowance except for formal matters, prosecution as to the merits is closed in accordance with the practice under *Ex parte Quayle*, 1935 C.D. 11, 453 O.G. 213.

Disposition of Claims*

5) ☑ Claim(s) 1,4-15,18-19 and 21-23 is/are pending in the application.

5a) Of the above claim(s) _____ is/are withdrawn from consideration.

6) ☐ Claim(s) _____ is/are allowed.

7) ☑ Claim(s) 1,4-15,18-19 and 21-23 is/are rejected.

8) ☐ Claim(s) _____ is/are objected to.

9) ☐ Claim(s) _____ are subject to restriction and/or election requirement

* If any claims have been determined allowable, you may be eligible to benefit from the **Patent Prosecution Highway** program at a participating intellectual property office for the corresponding application. For more information, please see http://www.uspto.gov/patents/init_events/pph/index.jsp or send an inquiry to **PPHfeedback@uspto.gov.**

Application Papers

10)☐ The specification is objected to by the Examiner.

11)☐ The drawing(s) filed on _____ is/are: a)☐ accepted or b)☐ objected to by the Examiner.

Applicant may not request that any objection to the drawing(s) be held in abeyance. See 37 CFR 1.85(a).

Replacement drawing sheet(s) including the correction is required if the drawing(s) is objected to. See 37 CFR 1.121(d).

Priority under 35 U.S.C. § 119

12)☐ Acknowledgment is made of a claim for foreign priority under 35 U.S.C. § 119(a)-(d) or (f).

Certified copies:

a)☐ All b)☐ Some** c)☐ None of the:

1.☐ Certified copies of the priority documents have been received.

2.☐ Certified copies of the priority documents have been received in Application No. _____.

3.☐ Copies of the certified copies of the priority documents have been received in this National Stage application from the International Bureau (PCT Rule 17.2(a)).

** See the attached detailed Office action for a list of the certified copies not received.

Attachment(s)

1) ☐ Notice of References Cited (PTO-892)

2) ☑ Information Disclosure Statement(s) (PTO/SB/08a and/or PTO/SB/08b) Paper No(s)/Mail Date 1/7/2020(4); 1/9/2020 (4).

3) ☐ Interview Summary (PTO-413) Paper No(s)/Mail Date _____.

4) ☐ Other: _____.

DETAILED ACTION

Previous Rejections

Applicant's arguments, filed 01/07/2020, have been fully considered. Rejections and/or objections not reiterated from previous office actions are hereby withdrawn. The following rejections and/or objections are either reiterated or newly applied. They constitute the complete set presently being applied to the instant application.

Claim Rejections - 35 USC § 103 - Obviousness

The following is a quotation of 35 U.S.C. 103 which forms the basis for all obviousness rejections set forth in this Office action:

> A patent for a claimed invention may not be obtained, notwithstanding that the claimed invention is not identically disclosed as set forth in section 102, if the differences between the claimed invention and the prior art are such that the claimed invention as a whole would have been obvious before the effective filing date of the claimed invention to a person having ordinary skill in the art to which the claimed invention pertains. Patentability shall not be negated by the manner in which the invention was made.

Claims 1, 5-8, 10 and 19 are rejected under 35 U.S.C. 103 as being unpatentable over Bayever et al (WO 2013/188586), in view of Conroy et al (NEJM, 34(19), 2011, 1817) and further in view of Melis et al (The Society for Surgery of the Alimentary Tract, 2011; http://meetings.ssat.com/abstracts/11ddw/P57.cgi).

Bayever et al disclosed a method for treatment of pancreatic cancer in a patient (e.g., a human, at page 3, 1st paragraph), comprising co-administering to the patient active agents, at a dose of 60 mg/m^2 (e.g., liposomal irinotecan). Bayever further disclosed 5-fluorouracil at a dose of 2400 mg/m^2 and leucovorin (*l* form administered at 200 mg/m^2 or the *l*+*d* racemic form administered at 400 mg/m^2). The method comprised

at least one cycle of administration, wherein the cycle was a period of two weeks (page 3, last full paragraph).

In one embodiment, Bayever's population was patients undergoing treatment for metastatic adenocarcinoma pancreatic cancer (e.g. a patient who has not previously received an antineoplastic agent) (page 12, section V, last embodiment, and claim 10).

Bayever did not disclose oxaliplatin, as recited in claim 9.

Conroy disclosed FOLFIRINOX (oxaliplatin; irinotecan; leucovorin and fluorouracil) treatment of patients having metastatic pancreatic cancer (title and the methods section of the abstract). Conroy disclosed that oxaliplatin has clinical activity against pancreatic cancer only when combined with fluorouracil, and that oxaliplatin and irinotecan have been shown to have synergistic activity *in vitro* (page 1818, left column, second paragraph).

Conroy did not disclose that the irinotecan was liposomal irinotecan.

Since Bayever disclosed treating metastatic pancreatic carcinoma with 5-fluorouracil and irinotecan, it would have been prima facie obvious to one of ordinary skill in the art to include oxaliplatin within Bayever's methods of treatment. An ordinarily skilled artisan would have been motivated because oxaliplatin has clinical activity against pancreatic cancer when combined with fluorouracil, and because oxaliplatin and irinotecan have synergistic activity *in vitro*, as taught by Conroy (Conroy, page 1818, left column, second paragraph).

Regarding the claims 1 and 19 limitation of 60 mg/m^2 oxaliplatin, the combination of Bayever (e.g., Bayever taught 85 mg/m^2 oxlaplatin at the abstract), though not silent the claimed amount of oxaliplatin, does not specifically teach 60 mg/m^2 oxaliplatin.

However, Melis taught [abstract] that a dosage of 60 mg/m^2 oxaliplatin was well tolerated in advanced pancreatic adenocarcinoma patients.

As such, oxlaplatin, and its amount, is recognized to have different effects (treatment of advanced pancreatic adenocarcinoma) with changing amounts used. Thus, the general condition (the dosage) is known and the amount of this ingredient is recognized to be result effective. Therefore, result effective variables can be optimized by routine experimentation, and it would have been prima facie obvious to optimize the dosage of the oxaliplatin present in the combined composition of Bayever and Conroy, as taught by Melis.

The combination of Bayever, Conroy and Melis reads on claims 1 and 19.

Claims 5-6 and 8 are rendered prima facie obvious because Bayever disclosed that 5-fluorouracil was administered intravenously over 46 hours, liposomal irinotecan was administered intravenously over 90 minutes, and that leucovorin was administered prior to 5-FU (page 12, section IV).

Claim 7 is rendered prima facie obvious because Bayever disclosed that active agents were administered on day one of a two-week cycle, where cycles comprised at least one administration. For example, Bayever's method overlaps that which is instantly recited (e.g. administration on days 1 and 15 of a 28-day cycle), because administration on day 1 of at least one 2-week cycle can also be administration on days 1 and 15 of a 28 day cycle (e.g. two 2-week cycles). In the case where the claimed ranges

"overlap or lie inside ranges disclosed by the prior art", a prima facie case of obviousness exists. MPEP 2144.05 A.

Claim 10 is rendered prima facie obvious because Bayever disclosed irinotecan sucrose octasulfate liposomal irinotecan, where the irinotecan was entrapped within the liposome, at page 4, and the last paragraph.

Response to Arguments

Applicant's arguments filed 01/07/2020 have been fully considered but they are not persuasive.

Applicants argued that neither Bayever, Conroy, nor Melis teach or suggests (solely or in combination) the claimed methods of treating a patient with metastatic adenocarcinoma of the pancreas who has not previously been treated with an antineoplastic agent (claim 1) or gemcitabine (claim 19), comprising co-administering to the patient 60 mg/m^2 liposomal irinotecan, 60 mg/m^2 oxaliplatin, leucovorin (200 mg/m^2 l-form or 400 mg/m^2 l+d form), and 2,400 mg/m^2 5-fluorouracil once every two weeks.

The Examiner disagrees that the combined prior art does not teach the claimed invention (claims 1 and 19). The combination of Bayever, Conroy and Melis reads on claims 1 and 19, the discussion of which was presented above.

Applicants argued that the Examiner has failed to establish a prima facie case of obviousness of the claimed methods, over the rejection of Melis.

The Examiner disagrees that a prima facie case of obviousness over Melis was not presented. Melis was relied upon to show that the dosage of oxaliplatin is a result effective variable. Result effective variables can be optimized by routine experimentation,

and it would have been prima facie obvious to optimize the dosage of the oxaliplatin present in the combined composition of Bayever and Conroy, as taught by Melis.

Regarding Melis, the Applicants argued that (1) the Melis Study involved patients with locally advanced pancreatic cancer and excluded patients with metastatic disease; (2) in contrast to the "once every two weeks" coadministration schedule recited in the pending claims, the Melis Study involved weekly administration of 60 mg/m^2 oxaliplatin; (3) the Melis study included continuous infusion of 200 mg/m^2 5-fluorouracil compared to the claimed coadministration of 2,400 mg/m2 5-fluorouracil once every two weeks; (4) the Melis treatment regime did not result in improved outcomes compared to other combination therapies for locally advanced pancreatic cancer and (5) "those who remained unresectable for cure but did not progress received a treatment regime involving a higher 85 mg/m^2 oxaliplatin dose every two weeks.

The Examiner responds that Melis was relied upon to show that the dosage of oxaliplatin is a result effective variable that can be optimized by routine experimentation (discussed above). Furthermore, cannot show nonobviousness by attacking references individually where the rejections are based on combinations of references. See *In re Keller*, 642 F.2d 413, 208 USPQ 871 (CCPA 1981); *In re Merck & Co.,* 800 F.2d 1091, 231 USPQ 375 (Fed. Cir. 1986); & MPEP 2145(IV)].

In response to Applicant's argument that the Examiner's conclusion of obviousness is based upon improper hindsight reasoning, it must be recognized that any judgment on obviousness is in a sense necessarily a reconstruction based upon hindsight reasoning. But so long as it takes into account only knowledge which was within the level of ordinary skill at the time the claimed invention was made, and does not include knowledge gleaned

only from the applicant's disclosure, such a reconstruction is proper. See *In re McLaughlin*, 443 F.2d 1392, 170 USPQ 209 (CCPA 1971).

Applicants argued that the Examiner failed to account for the many factors, such as patient population, disease severity, drug combination, dose, dosing schedule, drug interactions and toxicities that affect tolerability and efficacy of a cancer treatment method.

The Examiner responds that the skilled artisan would be led by Bayever's guidance of study design and patient selection [pages 25-31], at the discretion of the investigator, to account for factors affecting tolerability and efficacy of the protocol.

Applicant reiterated that the skilled artisan would not be motivated to combine Melis with Bayever and Conroy, to which the Examiner disagrees. The combination of Bayever and Conroy taught oxaliplatin, though not specific to the instantly claimed amount. Melis was presented to show that the dosage of oxaliplatin could be optimized without undue experimentation, and with a reasonable expectation of success (discussed above).

Applicants argued that Melis excluded patients with metastatic disease, to which the Examiner responds that the rejection was based upon the combination of the prior art. Bayever taught patients undergoing treatment for metastatic cancer.

Claims 4, 9, 18 and 23 are rejected under 35 U.S.C. 103 as being unpatentable over Bayever et al (WO 2013/188586), in view of Conroy et al (NEJM, 34(19), 2011,1817) further in view of Melis et al (The Society for Surgery of the Alimentary Tract, 2011; http://meetings.ssat.com/abstracts/11ddw/P57.cgi) and further in view of Fleming et al

(http://www.oncologynurseadvisor.com/advisor-forum/importance-of-sequence-in-chemotherapy-administration/article/378072/).

The 35 U.S.C. 103 rejection over Bayever, in view of Conroy and Melis, has been discussed above.

Additionally, Bayever disclosed that prior to each administration of liposomal irinotecan, the patient was pre-medicated with dexamethasone (e.g. corticosteroid) and another anti-emetic (page 4, fourth embodiment from the top of the page).

Further, Conroy disclosed that a second active agent was given two hours after a first active agent (e.g., leucovorin was given two hours after oxaliplatin) (page 1819, 1st paragraph of the section entitled Treatment).

However, the combination of Bayever and Conroy did not specifically disclose oxaliplatin administration after liposomal irinotecan, as recited in claims 4, 18 and 23; liposomal irinotecan administration, followed by oxaliplatin administration, followed by leucovorin administration, followed by 5-fluorouracil administration, as recited in claim 9.

Fleming disclosed that the sequence of various chemotherapy drugs in general does not matter, as the half-life of each drug makes it impossible to determine what drug is at what level at any particular time, based on individual patient pharmacodynamics (last sentence of the first paragraph).

Since the combination of Bayever and Conroy disclosed administration of oxaliplatin, liposomal irinotecan, leucovorin and 5-fluorouracil, it would have been prima facie obvious to one of ordinary skill in the art to have varied the order of administration of the combined methods of Bayever and Conroy, such that the order of

administration was liposomal irinotecan, followed by oxaliplatin, followed by leucovorin, followed by 5-fluorouracil administration.

An ordinarily skilled artisan would have been motivated because the sequence of various chemotherapy drugs in general does not matter, as the half-life of each drug makes it impossible to determine what drug is at what level at any particular time, based on individual patient pharmacodynamics, as taught by Fleming (Fleming, last sentence of the first paragraph).

Response to Arguments

Applicant's arguments filed 01/07/2020 have been fully considered but they are not persuasive.

The Applicants reiterated the above arguments regarding a failing to show a prima facie case of obviousness and hindsight reasoning, to which the Examiner disagrees. A prima facie case of obviousness to combine each of the prior art was previously discussed. The Examiner disagrees that hindsight reasoning was used in the rejection of the claims, as discussed above. A motivation to combine the prior art (discussed above) was used in the rejection of the claims.

Claims 11-15 and 21-22 are rejected under 35 U.S.C. 103 as being unpatentable over Bayever et al (WO 2013/188586), in view of Conroy et al (NEJM, 34(19), 2011, 1817), further in view of Melis et al (The Society for Surgery of the Alimentary Tract, 2011; http://meetings.ssat.com/abstracts/11ddw/P57.cgi) and as evidenced by Bayever et al (WO 2016/094402).

The 35 U.S.C. 103 rejection over Bayever (2013), in view of Conroy and Melis, has been discussed above.

Although, Bayever (2013) disclosed MM-398 liposome (at page 4, last paragraph and as discussed above), Bayever was not specific as to the ingredients of the liposome, as recited in claims 11-12 and 21-22.

However, Bayever (2016) evidenced that MM-398 contained irinotecan sucrose octasulfate, DSPC, cholesterol and MPEG-2000-DSPE (page 30, section describing the drug product).

Thus, it is reasonable to assume that Bayever's (2013) MM-398 contained irinotecan, DSPC, cholesterol and MPEG-2000-DSPE, as evidenced by Bayever's (2016) disclosure of the liposomal constituents of MM-398.

Claims 13-15 and 21-22 are rendered prima facie obvious because Bayever disclosed that 5-fluorouracil was administered intravenously over 46 hours, liposomal irinotecan was administered intravenously over 90 minutes; liposomal irinotecan was administered prior to leucovorin; leucovorin was administered prior to 5-FU (page 12, section IV). Further, Bayever disclosed that active agents were administered on day one of a two-week cycle, where cycles comprised at least one administration.

For example, Bayever's method overlaps that which is instantly recited (e.g. administration on days 1 and 15 of a 28-day cycle) because administration on day 1 of at least one 2-week cycle can also be administration on days 1 and 15 of a 28-day cycle (e.g. two 2-week cycles). A prima facie case of obviousness exists because of overlap, as discussed above.

Response to Arguments

Applicant's arguments filed 01/07/2020 have been fully considered but they are not persuasive.

The Applicants reiterated the above arguments regarding a failing to show a prima facie case of obviousness and hindsight reasoning, to which the Examiner disagrees. A prima facie case of obviousness to combine each of the prior art was previously discussed. The Examiner disagrees that hindsight reasoning was used in the rejection of the claims, as discussed above. A motivation to combine the prior art (discussed above) was used in the rejection of the claims.

Nonstatutory Double Patenting

A nonstatutory double patenting rejection is appropriate where the conflicting claims are not identical, but at least one examined application claim is not patentably distinct from the reference claim(s) because the examined application claim is either anticipated by, or would have been obvious over, the reference claim(s). See, e.g., *In re Berg*, 140 F.3d 1428, 46 USPQ2d 1226 (Fed. Cir. 1998); *In re Goodman*, 11 F.3d 1046, 29 USPQ2d 2010 (Fed. Cir. 1993); *In re Longi*, 759 F.2d 887, 225 USPQ 645 (Fed. Cir. 1985); *In re Van Ornum*, 686 F.2d 937, 214 USPQ 761 (CCPA 1982); *In re Vogel*, 422 F.2d 438, 164 USPQ 619 (CCPA 1970); *In re Thorington*, 418 F.2d 528, 163 USPQ 644 (CCPA 1969).

A timely filed terminal disclaimer in compliance with 37 CFR 1.321(c) or 1.321(d) may be used to overcome an actual or provisional rejection based on nonstatutory double patenting provided the reference application or patent either is shown to be commonly

owned with the examined application, or claims an invention made as a result of activities undertaken within the scope of a joint research agreement. See MPEP § 717.02 for applications subject to examination under the first inventor to file provisions of the AIA as explained in MPEP § 2159. See MPEP §§ 706.02(l)(1) - 706.02(l)(3) for applications not subject to examination under the first inventor to file provisions of the AIA. A terminal disclaimer must be signed in compliance with 37 CFR 1.321(b).

The USPTO Internet website contains terminal disclaimer forms which may be used. Please visit www.uspto.gov/patent/patents-forms. The filing date of the application in which the form is filed determines what form (e.g., PTO/SB/25, PTO/SB/26, PTO/AIA/25, or PTO/AIA/26) should be used. A web-based eTerminal Disclaimer may be filled out completely online using web-screens. An eTerminal Disclaimer that meets all requirements is auto-processed and approved immediately upon submission. For more information about eTerminal Disclaimers, refer to www.uspto.gov/patents/process/file/efs/guidance/eTD-info-I.jsp.

Claims 1, 4-15, 18-19 and 21-23 are rejected on the ground of nonstatutory double patenting as being unpatentable over claims 1-18 of U.S. Patent No. 9,492,442, in view of Conroy et al (NEJM, 34(19), 2011, 1817) and further in view of Melis et al (The Society for Surgery of the Alimentary Tract, 2011; http://meetings.ssat.com/abstracts/11ddw/P57.cgi)

Although the claims at issue are not identical, they are not patentably distinct from each other. The issued claims recite all of the features instantly recited for the method of

treatment except for the administration of oxaliplatin. The instant claims require oxaliplatin, and such an ingredient is not recited by the issued claims.

Conroy disclosed FOLFIRINOX (oxaliplatin; irinotecan; leucovorin and fluorouracil) treatment of patients having metastatic pancreatic cancer (title and the methods section of the abstract). Conroy disclosed that oxaliplatin has clinical activity against pancreatic cancer only when combined with fluorouracil, and that oxaliplatin and irinotecan have been shown to have synergistic activity *in vitro* (page 1818, left column, second paragraph).

Melis taught [abstract] that a dosage of 60 mg/m^2 oxaliplatin was well tolerated in advanced pancreatic adenocarcinoma patients.

Thus, it would have been prima facie obvious to use oxaliplatin in the issued method, because oxaliplatin has clinical activity against pancreatic cancer only when combined with fluorouracil, and because oxaliplatin and irinotecan have been shown to have synergistic activity *in vitro*. It would have been prima facie obvious to use oxaliplatin at 60 mg/m^2 because the said dosage is well tolerated in advanced pancreatic adenocarcinoma patients.

Response to Arguments

Applicant's arguments filed 01/07/2020 have been fully considered but they are not persuasive.

The Applicants reiterated the above arguments regarding a failing to show a prima facie case of obviousness, to which the Examiner disagrees. A prima facie case of obviousness to combine each of the prior art was previously discussed.

Conclusion

THIS ACTION IS MADE FINAL. Applicant is reminded of the extension of time policy as set forth in 37 CFR 1.136(a).

A shortened statutory period for reply to this final action is set to expire THREE MONTHS from the mailing date of this action. In the event a first reply is filed within TWO MONTHS of the mailing date of this final action and the advisory action is not mailed until after the end of the THREE-MONTH shortened statutory period, then the shortened statutory period will expire on the date the advisory action is mailed, and any extension fee pursuant to 37 CFR 1.136(a) will be calculated from the mailing date of the advisory action. In no event, however, will the statutory period for reply expire later than SIX MONTHS from the mailing date of this final action.

Any inquiry concerning this communication or earlier communications from the examiner should be directed to CELESTE A RONEY whose telephone number is (571)272-5192. The examiner can normally be reached on Monday-Thursday; 7 AM-5 PM.

Examiner interviews are available via telephone, in-person, and video conferencing using a USPTO supplied web-based collaboration tool. To schedule an interview, applicant is encouraged to use the USPTO Automated Interview Request (AIR) at http://www.uspto.gov/interviewpractice.

If attempts to reach the examiner by telephone are unsuccessful, the examiner's supervisor, Frederick Krass can be reached on 571-272-0580. The fax phone number for the organization where this application or proceeding is assigned is 571-273-8300.

Information regarding the status of an application may be obtained from the Patent Application Information Retrieval (PAIR) system. Status information for published applications may be obtained from either Private PAIR or Public PAIR. Status information for unpublished applications is available through Private PAIR only. For more information about the PAIR system, see https://ppair-my.uspto.gov/pair/PrivatePair. Should you have questions on access to the Private PAIR system, contact the Electronic Business Center (EBC) at 866-217-9197 (toll-free). If you would like assistance from a USPTO Customer Service Representative or access to the automated information system, call 800-786-9199 (IN USA OR CANADA) or 571-272-1000.

/CELESTE A RONEY/
Primary Examiner, Art Unit 1612

UNITED STATES PATENT AND TRADEMARK OFFICE

UNITED STATES DEPARTMENT OF COMMERCE
United States Patent and Trademark Office
Address: COMMISSIONER FOR PATENTS
P.O. Box 1450
Alexandria, Virginia 22313-1450
www.uspto.gov

APPLICATION NO.	FILING DATE	FIRST NAMED INVENTOR	ATTORNEY DOCKET NO.	CONFIRMATION NO.
15/896,389	02/14/2018	Keelung Hong	263266-426640	3157

153749 7590 01/31/2020

McNeill Baur PLLC/Ipsen
Ipsen Bioscience, Inc.
125 Cambridge Park Drive
Suite 301
Cambridge, MA 02140

EXAMINER	
SHOMER, ISAAC	

ART UNIT	PAPER NUMBER
1612	

NOTIFICATION DATE	DELIVERY MODE
01/31/2020	ELECTRONIC

Please find below and/or attached an Office communication concerning this application or proceeding.

The time period for reply, if any, is set in the attached communication.

Notice of the Office communication was sent electronically on above-indicated "Notification Date" to the following e-mail address(es):

docketing@mcneillbaur.com
eofficeaction@appcoll.com
patents.us@ipsen.com

Office Action Summary	Application No. 15/896,389	Applicant(s) Hong et al.	
	Examiner ISAAC SHOMER	Art Unit 1612	AIA (FITF) Status No

-- The MAILING DATE of this communication appears on the cover sheet with the correspondence address --

Period for Reply

A SHORTENED STATUTORY PERIOD FOR REPLY IS SET TO EXPIRE 3 MONTHS FROM THE MAILING DATE OF THIS COMMUNICATION.

- Extensions of time may be available under the provisions of 37 CFR 1.136(a). In no event, however, may a reply be timely filed after SIX (6) MONTHS from the mailing date of this communication.
- If NO period for reply is specified above, the maximum statutory period will apply and will expire SIX (6) MONTHS from the mailing date of this communication.
- Failure to reply within the set or extended period for reply will, by statute, cause the application to become ABANDONED (35 U.S.C. § 133). Any reply received by the Office later than three months after the mailing date of this communication, even if timely filed, may reduce any earned patent term adjustment. See 37 CFR 1.704(b).

Status

1)☑ Responsive to communication(s) filed on 17 January 2020.

☐ A declaration(s)/affidavit(s) under **37 CFR 1.130(b)** was/were filed on _____.

2a)☑ This action is **FINAL.** 2b) ☐ This action is non-final.

3)☐ An election was made by the applicant in response to a restriction requirement set forth during the interview on _____; the restriction requirement and election have been incorporated into this action.

4)☐ Since this application is in condition for allowance except for formal matters, prosecution as to the merits is closed in accordance with the practice under *Ex parte Quayle*, 1935 C.D. 11, 453 O.G. 213.

Disposition of Claims*

5) ☑ Claim(s) 58-72 is/are pending in the application.

5a) Of the above claim(s) _____ is/are withdrawn from consideration.

6) ☐ Claim(s) _____ is/are allowed.

7) ☑ Claim(s) 58-72 is/are rejected.

8) ☐ Claim(s) _____ is/are objected to.

9) ☐ Claim(s) _____ are subject to restriction and/or election requirement

* If any claims have been determined allowable, you may be eligible to benefit from the **Patent Prosecution Highway** program at a participating intellectual property office for the corresponding application. For more information, please see http://www.uspto.gov/patents/init_events/pph/index.jsp or send an inquiry to **PPHfeedback@uspto.gov.**

Application Papers

10)☐ The specification is objected to by the Examiner.

11)☐ The drawing(s) filed on _____ is/are: a)☐ accepted or b)☐ objected to by the Examiner.

Applicant may not request that any objection to the drawing(s) be held in abeyance. See 37 CFR 1.85(a).

Replacement drawing sheet(s) including the correction is required if the drawing(s) is objected to. See 37 CFR 1.121(d).

Priority under 35 U.S.C. § 119

12)☐ Acknowledgment is made of a claim for foreign priority under 35 U.S.C. § 119(a)-(d) or (f).

Certified copies:

a)☐ All b)☐ Some** c)☐ None of the:

1.☐ Certified copies of the priority documents have been received.

2.☐ Certified copies of the priority documents have been received in Application No. _____.

3.☐ Copies of the certified copies of the priority documents have been received in this National Stage application from the International Bureau (PCT Rule 17.2(a)).

** See the attached detailed Office action for a list of the certified copies not received.

Attachment(s)

1) ☑ Notice of References Cited (PTO-892)

2) ☑ Information Disclosure Statement(s) (PTO/SB/08a and/or PTO/SB/08b) Paper No(s)/Mail Date _____.

3) ☐ Interview Summary (PTO-413) Paper No(s)/Mail Date _____.

4) ☐ Other: _____.

DETAILED ACTION

Applicants' arguments, filed 17 January 2020, have been fully considered. Rejections and/or objections not reiterated from previous office actions are hereby withdrawn. The following rejections and/or objections are either reiterated or newly applied. They constitute the complete set presently being applied to the instant application.

The present application is being examined under the pre-AIA first to invent provisions.

Claim Rejections - 35 USC § 112(a) – New Matter

The following is a quotation of the first paragraph of 35 U.S.C. 112(a):

> (a) IN GENERAL.—The specification shall contain a written description of the invention, and of the manner and process of making and using it, in such full, clear, concise, and exact terms as to enable any person skilled in the art to which it pertains, or with which it is most nearly connected, to make and use the same, and shall set forth the best mode contemplated by the inventor or joint inventor of carrying out the invention.

The following is a quotation of the first paragraph of pre-AIA 35 U.S.C. 112:

> The specification shall contain a written description of the invention, and of the manner and process of making and using it, in such full, clear, concise, and exact terms as to enable any person skilled in the art to which it pertains, or with which it is most nearly connected, to make and use the same, and shall set forth the best mode contemplated by the inventor of carrying out his invention.

Claims 63-67 are rejected under 35 U.S.C. 112(a) or 35 U.S.C. 112 (pre-AIA), first paragraph, as failing to comply with the written description requirement. The claim(s) contains subject matter which was not described in the specification in such a way as to reasonably convey to one skilled in the relevant art that the inventor or a joint

inventor, or for pre-AIA the inventor(s), at the time the application was filed, had possession of the claimed invention.

Claim 63 is a new claim reciting that the molar ratio of irinotecan per mole of liposomal lipids is from about 0.15 to about 1.5. In support of this newly added limitation, applicant cites paragraphs 0075, 0099, 0101, 0102, 0109, and Example 11 in applicant's response on 17 January 2020.

Looking to paragraph 0109 of the instant specification, this paragraph discloses ratios of at least 0.1 and preferably at least 0.2 moles of camptothecin derivative (e.g. irinotecan) per one mole of liposome lipid. This fails to provide support for the full range of 0.15 to 1.5 moles of irinotecan per mole of liposome lipids.

Claim Rejections - 35 USC § 112(d) – Failure to Limit Parent Claim

The following is a quotation of 35 U.S.C. 112(d):

> (d) REFERENCE IN DEPENDENT FORMS.—Subject to subsection (e), a claim in dependent form shall contain a reference to a claim previously set forth and then specify a further limitation of the subject matter claimed. A claim in dependent form shall be construed to incorporate by reference all the limitations of the claim to which it refers.

The following is a quotation of pre-AIA 35 U.S.C. 112, fourth paragraph:

> Subject to the following paragraph [i.e., the fifth paragraph of pre-AIA 35 U.S.C. 112], a claim in dependent form shall contain a reference to a claim previously set forth and then specify a further limitation of the subject matter claimed. A claim in dependent form shall be construed to incorporate by reference all the limitations of the claim to which it refers.

Claims 60, 65, and 70 are rejected under 35 U.S.C. 112(d) or pre-AIA 35 U.S.C. 112, 4th paragraph, as being of improper dependent form for failing to further

limit the subject matter of the claim upon which it depends, or for failing to include all the limitations of the claim upon which it depends.

Claims 60, 65, and 70 attempt to further limit the claims that they depend upon by reciting that DSPE-PEG, as of the independent claims, is anionic. However, as best understood by the examiner, DSPE-PEG is inherently anionic because DSPE-PEG comprises a phosphate group that is negatively charged, but does not comprise a positively charged group to balance the negative charge because the amine in DSPE has been reacted to form an amide in DSPE-PEG. As such, claims 60, 65, and 70 attempt to further limit the claims upon which they depend by reciting that DSPE-PEG is anionic; however, as this compound is inherently anionic, this limitation does not appear to further limit the respective chemical structure.

For the purposes of examination under prior art, claims 60, 65, and 70 will be understood by the examiner to recite the same chemical structure of DSPE-PEG recited by the claims upon which they depend.

Claim Rejections - 35 USC § 103 – Obviousness

The following is a quotation of pre-AIA 35 U.S.C. 103(a) which forms the basis for all obviousness rejections set forth in this Office action:

> (a) A patent may not be obtained though the invention is not identically disclosed or described as set forth in section 102, if the differences between the subject matter sought to be patented and the prior art are such that the subject matter as a whole would have been obvious at the time the invention was made to a person having ordinary skill in the art to which said subject matter pertains. Patentability shall not be negatived by the manner in which the invention was made.

The factual inquiries set forth in *Graham v. John Deere Co.*, 383 U.S. 1, 148 USPQ 459 (1966), that are applied for establishing a background for determining obviousness under pre-AIA 35 U.S.C. 103(a) are summarized as follows:

1. Determining the scope and contents of the prior art.

2. Ascertaining the differences between the prior art and the claims at issue.

3. Resolving the level of ordinary skill in the pertinent art.

4. Considering objective evidence present in the application indicating obviousness or nonobviousness.

This application currently names joint inventors. In considering patentability of the claims under pre-AIA 35 U.S.C. 103(a), the examiner presumes that the subject matter of the various claims was commonly owned at the time any inventions covered therein were made absent any evidence to the contrary. Applicant is advised of the obligation under 37 CFR 1.56 to point out the inventor and invention dates of each claim that was not commonly owned at the time a later invention was made in order for the examiner to consider the applicability of pre-AIA 35 U.S.C. 103(c) and potential pre-AIA 35 U.S.C. 102(e), (f) or (g) prior art under pre-AIA 35 U.S.C. 103(a).

Claims 63-67 are is/are rejected under pre-AIA 35 U.S.C. 103(a) as being unpatentable over Chou et al. (Journal of Bioscience and Bioengineering, Vol. 95, No. 4, 2003, pages 405-408) in view of Gunay et al. (Analytical Chemistry, Vol. 75, 2003, pages 3226-3231) and Uster et al. (FEBS Letters, Vol. 386, 1996, pages 243-246).

Chou et al. (hereafter referred to as Chou) is drawn to a liposome comprising irinotecan, which has antitumor activity, as of Chou, page 405, title and abstract. Said liposome includes phospholipids such as phosphatidylcholines, as of Chou, page 405, title.

Chou also teaches a loading amount of 0.254 mg drug per mg lipid, as of Chou, page 407, right column, last full paragraph. The units of this concentration differ from the recited units. Nevertheless, the examiner has performed a calculation below to estimate the concentration of irinotecan in Chou in mg of irinotecan per mmol of total phospholipids. As best understood by the examiner, and assuming molecular weight of liposome lipids of 734 Daltons (which is a molecular weight of DSPC) and 587 Daltons for irinotecan this is a concentration of

$$\frac{0.254\,mg\ irinotecan}{1\,mg\ lipid} \times \frac{1\,mmol\ irinotecan}{587\,mg\ irinotecan} \times \frac{734\,mg\ lipid}{1\,mmol\ lipid} = 0.318\ \frac{mmol\ irinotean}{mmol\ lipid}$$

This concentration is within the range of about 0.15 to about 1.5 moles of irinotecan per moles of lipid, and as such, reads on the claimed requirements.

Chou differs from the claimed invention at least because Chou does not teach sucrose octasulfate.

Gunay et al. (hereafter referred to as Gunay) is drawn to sucrose octasulfate, which is taught to be a highly sulfate carbohydrate, as of Gunay, page 3226, title and abstract. Gunay suggests sucrose octasulfate for the treatment of cancer, as of Gunay, page 3226, right column, top paragraph below title.

Gunay does not teach a liposome comprising irinotecan.

It would have been prima facie obvious for one of ordinary skill in the art to have combined sucrose octasulfate with the liposome of Chou. Chou is drawn to a liposome

comprising irinotecan, but suggests that sulfated oligosaccharides can be included, as of Chou, page 408, left column, second paragraph. As sucrose octasulfate is a sulfate oligosaccharide that has potential to treat cancer, as of Gunay, the skilled artisan would have been motivated to have included the sucrose octasulfate of Gunay in the liposome of Chou for predictable formation of a complex with irinotecan and for predictable improvement in treating cancer with a reasonable expectation of success. The skilled artisan would have been motivated to have made combination at least because Chou suggests the inclusion of a sulfated oligosaccharide.

As to claim 63, the claim recites a neutral phospholipid and cholesterol in a ratio of 3:2. Chou teaches phosphatidylcholine and cholesterol, as of Chou, page 406, right column, figure 1, reproduced below.

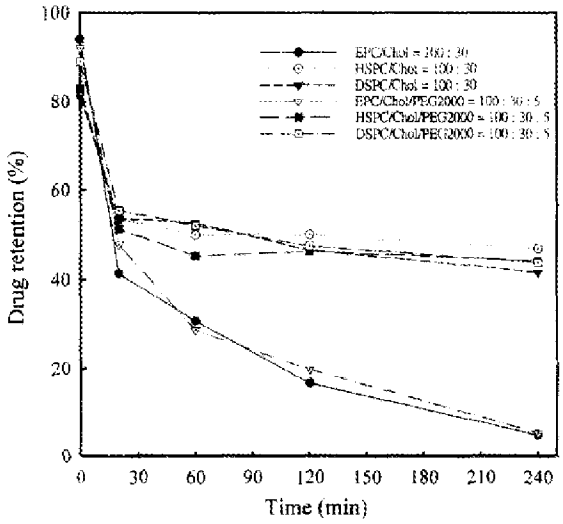

The above drawing shows the ratio of neutral phospholipid (e.g. phosphatidylcholine) to cholesterol in the above-shown liposomes appears to be 10:3 rather than 3:2. In addition, the above drawing appears to show about 3.7% pegylated lipid, which is higher than what is claimed. Nevertheless, the skilled artisan would have been motivated to have optimized this ratio in order to have achieved the claimed

subject matter. Where the general conditions of a claim are disclosed in the prior art, it is not inventive to discover the optimum or workable ranges by routine experimentation. See MPEP 2144.05(II)(A). In this case, the general conditions of a liposome comprising phosphatidylcholine, cholesterol, pegylated lipid, and irinotecan are taught by the prior art; as such, it would not have been inventive to have discovered optimum ratios of each ingredient by routine experimentation. Also, there is a motivation to optimize result-effective variables. See MPEP 2144.05(II)(B). The amount of phosphatidylcholine and cholesterol is understood to be result-effective because it would have affected the result of structurally forming the liposome. The amount of pegylated lipid is result-effective because it would have affected the result of the liposome successfully evading immune system clearance.

None of the above references teach that the polyethylene glycol (PEG) is methoxy terminated.

Uster et al. (hereafter referred to as Uster) is drawn to poly(ethylene glycol) derivatized phospholipid being placed into pre-formed liposomes, as of Uster, page 243, title and abstract. The pegylated lipid of Uster was made by attaching methoxypoly(ethylene glycol) via the carbamate linakte to the amino head group of 1,2-distearoyl-*sn*-glycero-3-phosphoethanolamine to make DSPE-PEG, as of Uster, page 243, right column, section 2.1.

Uster does not teach irinotecan.

It would have been prima facie obvious for one of ordinary skill in the art to have used a methoxy-terminated PEG to have formed the DSPE-PEG of Chou. Chou teaches using DSPE-PEG in a liposome, but is silent as to the end-group of the DSPE-

PEG. As Uster teaches that a methoxy group is a known terminus of PEG to be used in DSPE-PEG in a liposome, the skilled artisan would have been motivated to have used methoxy terminated PEG, as of Ulster, to have predictably formed the DSPE-PEG of Chou with a reasonable expectation of success.

As to claim 64, the optimization rationale applied by the examiner in the above rejection of claim 63 with regard to the amount of pegylated lipid also applies to the subject matter of claim 64.

As to claim 65, this claim is rejected for the same reason that claim 63 is rejected.

As to claim 66, Chou teaches that sulfated oligosaccharides form an insoluble complex with irinotecan, as of Chou, page 408, left column, second paragraph. This is understood to read on the required gelation or precipitation.

As to claim 67, Chou teaches a liposome size of between 80 nm and 140 nm, as of Chou, page 405, right column, last full paragraph. This overlaps with the claimed amount. While the prior art does not disclose the exact claimed values, but does overlap: in such instances even a slight overlap in range establishes a *prima facie* case of obviousness. See MPEP 2144.05(I).

No Rejection of Claims 58-62 and 68-72: Claims 58 and 68 recite that there are between 0.8 and 1.3 millimoles of irinotecan per gram of liposome lipids. Chou teaches a loading amount of 0.254 mg irinotecan per mg lipid, as of Chou, page 407, right column, last full paragraph. This can be expressed in terms of mmol of irinotecan per gram of lipid via the following calculation.

$$\frac{0.254\ mg\ irinotecan}{1\ mg\ lipid} \times \frac{1\ mmol\ irinotecan}{587\ mg\ irinotecan} \times \frac{1000\ mg\ lipid}{1\ g\ lipid} = 0.433\ \frac{mmol\ irinotean}{g\ lipid}$$

This amount is significantly less than the recited lower limit of 0.8 mmol of irinotecan per gram of liposomal lipids in instant claims 58 and 68.

The examiner notes here that, according to MPEP 2144.05(II)(A), it is generally not inventive to discover the optimum or workable ranges (e.g. of concentration) by routine experimentation. Nevertheless, it is the examiner's position that this provision of the MPEP does not apply to the instant claims. This is because the claims not only require a specific concentration of irinotecan, the claims also require that this concentration of irinotecan be entrapped by the liposome. Loading a drug such as irinotecan into a lipid matrix would not have been straightforward or predictable to one of ordinary skill in the art, and the skilled artisan would not have been able to have predictably loaded more irinotecan drug simply by increasing the concentration of irinotecan. This is because addition of more irinotecan to the mixture of reagents would not have necessarily and predictably resulted in said irinotecan being loaded in the liposome.

The difficulty of loading irinotecan into a liposome is evident as of Chou, which uses dextran sulfate and a transmembrane gradient loading to load irinotecan, as of Chou, paragraph bridging pages 405 and 406. There would have been no need for such a transmembrane gradient if the concentration of irinotecan in the product could have been increased simply by increasing the irinotecan amount in the starting material. The difficulty of loading irinotecan would have been further increased by the low water solubility of irinotecan.

As such, the claimed concentration of irinotecan, should **not** be understood as merely a concentration that could have been manipulated at will by one of ordinary skill

in the art at the time the invention was made by routine optimization. This is at least due to the lack of a reasonable expectation that the loaded concentration could have been successfully increased to the claimed amount due to the difficulty of loading irinotecan into a liposome.

Non-Statutory Double Patenting

The nonstatutory double patenting rejection is based on a judicially created doctrine grounded in public policy (a policy reflected in the statute) so as to prevent the unjustified or improper timewise extension of the "right to exclude" granted by a patent and to prevent possible harassment by multiple assignees. A nonstatutory double patenting rejection is appropriate where the conflicting claims are not identical, but at least one examined application claim is not patentably distinct from the reference claim(s) because the examined application claim is either anticipated by, or would have been obvious over, the reference claim(s). See, e.g., *In re Berg*, 140 F.3d 1428, 46 USPQ2d 1226 (Fed. Cir. 1998); *In re Goodman*, 11 F.3d 1046, 29 USPQ2d 2010 (Fed. Cir. 1993); *In re Longi*, 759 F.2d 887, 225 USPQ 645 (Fed. Cir. 1985); *In re Van Ornum*, 686 F.2d 937, 214 USPQ 761 (CCPA 1982); *In re Vogel*, 422 F.2d 438, 164 USPQ 619 (CCPA 1970); *In re Thorington*, 418 F.2d 528, 163 USPQ 644 (CCPA 1969).

A timely filed terminal disclaimer in compliance with 37 CFR 1.321(c) or 1.321(d) may be used to overcome an actual or provisional rejection based on nonstatutory double patenting provided the reference application or patent either is shown to be

commonly owned with the examined application, or claims an invention made as a result of activities undertaken within the scope of a joint research agreement. See MPEP § 717.02 for applications subject to examination under the first inventor to file provisions of the AIA as explained in MPEP § 2159. See MPEP §§ 706.02(l)(1) - 706.02(l)(3) for applications not subject to examination under the first inventor to file provisions of the AIA. A terminal disclaimer must be signed in compliance with 37 CFR 1.321(b).

The USPTO Internet website contains terminal disclaimer forms which may be used. Please visit www.uspto.gov/patent/patents-forms. The filing date of the application in which the form is filed determines what form (e.g., PTO/SB/25, PTO/SB/26, PTO/AIA/25, or PTO/AIA/26) should be used. A web-based eTerminal Disclaimer may be filled out completely online using web-screens. An eTerminal Disclaimer that meets all requirements is auto-processed and approved immediately upon submission. For more information about eTerminal Disclaimers, refer to www.uspto.gov/patents/process/file/efs/guidance/eTD-info-I.jsp.

Claims 58-72 are rejected on the ground of nonstatutory double patenting as being unpatentable over claims 1-35 of U.S. Patent No. 8,147,867 in view of Allen et al. (US 2001/0038851 A1) and Burke (US Patent 5,552,156). Although the claims at issue are not identical, they are not patentably distinct from each other because of the following reasons:

Instant claim 58 is drawn to a liposomal comprising irinotecan and sucrose octasulfate. Said liposome comprises a neutral phospholipid and cholesterol in a

specific ratio, as well as a pegylated lipid. Specific amounts of the lipids and of irinotecan are recited.

Conflicting claim 1 is drawn to a liposomal irinotecan composition comprising sucrose octasulfate and optionally a substituted ammonium compound. With regard to the lipid bilayer components, conflicting claim 29 recites lecithin and cholesterol in a 3:2 molar ratio, wherein lecithin is a neutral phospholipid (lecithin is zwitterionic and thereby neutral). Conflicting claims 31 recites N-(methoxy-poly(ethylene glycol)-distearoylphosphatidylethanolamine in an amount of 1 mol part. With regard to the amount of irinotecan, this is recited in conflicting claims 14-16.

The conflicting claims do not recite the required PEG molecular weight.

Allen et al. (hereafter referred to as Allen) is drawn to a therapeutic liposome, as of Allen, title and abstract. Said liposome comprises lipid such as DSPE that is derivatized with a hydrophilic polymer, as of Allen, paragraph 0065. Said hydrophilic polymer may be polyethylene glycol (PEG), as of Allen, paragraph 0067. Said PEG may have a molecular weight from 1000 to 5000 Daltons, as of Allen, paragraph 0067.

Allen does not appear to teach why derivitization with PEG is beneficial.

Burke is drawn to liposomal stabilization of camptothecin drugs, as of Burke, title and abstract. Burke teaches that liposomes may be coated with polyethylene glycol, which assists the particles in avoiding the reticuloendothelial system, as of Burke, column 6 lines 35-37.

Burke does not appear to teach PEG molecular weight.

It would have been prima facie obvious for one of ordinary skill in the art to have provided the PEG in the DSPE-PEG of the conflicting claims with the molecular weight

taught by Allen. The conflicting claims are drawn to a liposome comprising DSPE-PEG, as of conflicting claims 29-31. While the conflicting claims are silent as to PEG molecular weight, Allen teaches that a PEG molecular weight from 1000 to 5000 Daltons is suitable for a PEG derivatized lipid. As pegylated lipids are useful for preventing reticuloendothelial system clearance, as taught by Burke, the skilled artisan would have been motivated to have modified the molecular weight of the PEG in the DSPE-PEG of the conflicting claims to have had a molecular weight of 1000 to 5000 Daltons for predictably avoiding reticuloendothelial system clearance with a reasonable expectation of success.

As to the instant claims, instant claim 58 recites an amount of irinotecan of 0.8 to 1.3 mmol of irinotecan per gram of liposomal lipids. Instant claim 63 recites about 0.15 to about 1.5 mmol of irinotecan per gram of liposomal lipids. For example conflicting claim 15 recites about 1.76 mol of irinotecan per mol of neutral phospholipid. Assuming that the neutral phospholipid is DSPC and has a molecular weight of about 734 Daltons, this is a value of

$$\frac{1.76\ mol\ irinotecan}{1\ mol\ DSPC} \times \frac{1\ mol\ DSPC}{734\ g\ DSPC} \times \frac{1000\ mmol\ irinotecan}{1\ mol\ irinotecan} \cong \frac{2.39\ mmol\ irinotecan}{g\ DSPC}$$

The examiner notes that this value of 2.39 mmol irinotecan per gram of lipid would have been lower when measured against the total lipids as opposed to only DSPC as there are other lipids present besides DSPC. Furthermore, even if, purely *en arguendo*, the millimoles of irinotecan per mg lipid in the conflicting claims exceeds that of the instant claims, this is insufficient to overcome the prima facie case of obviousness. Where the general conditions of a claim are disclosed in the prior art (or in this case, by the conflicting claims), it is not inventive to discover the optimum or

workable ranges by routine experimentation. See MPEP 2144.05(II)(A). In this case, the general conditions of a liposome comprising irinotecan, sucrose octasulfate, and the lipids phosphatidylcholine, cholesterol, and DSPE-PEG are recited by the conflicting claims. As such, it would not have been inventive for the skilled artisan to have discovered workable ranges of amounts/concentrations of these by routine experimentation. Additionally, there is a motivation to optimize result-effective variables. See MPEP 2144.05(II)(B). Irinotecan concentration is a result-effective variable because it affects the result of treating cancer. The examiner notes that similar rationale regarding optimization may be applied to the concentration of individual lipids, including DSPE-PEG. Concentration of DSPE-PEG is a result-effective variable because it affects the result of reticuloendothlial system clearance.

Claims 58-72 are rejected on the ground of nonstatutory double patenting as being unpatentable over claim 1 of U.S. Patent No. 9,737,528 in view of Allen et al. (US 2001/0038851 A1) and Burke (US Patent 5,552,156). Although the claims at issue are not identical, they are not patentably distinct from each other because of the following reasons.

Instant claim 58 is drawn to a liposomal comprising irinotecan and sucrose octasulfate. Said liposome comprises a neutral phospholipid and cholesterol in a specific ratio, as well as a pegylated lipid. Specific amounts of the lipids and of irinotecan are recited.

Conflicting claim 1 is drawn to an injectable pharmaceutical composition comprising irinotecan sucrose octasulfate liposomes. Said liposomes comprise DSPC (a neutral zwitterionic lipid), cholesterol, and PEG-DSPE in a molar ratio of 3:2:0.015. Said composition encapsulates irinotecan in an amount of 500-550 mg irinotecan per mmol of the total liposome phospholipids.

The conflicting claims do not recite the required PEG molecular weight.

Allen et al. (hereafter referred to as Allen) is drawn to a therapeutic liposome, as of Allen, title and abstract. Said liposome comprises lipid such as DSPE that is derivatized with a hydrophilic polymer, as of Allen, paragraph 0065. Said hydrophilic polymer may be polyethylene glycol (PEG), as of Allen, paragraph 0067. Said PEG may have a molecular weight from 1000 to 5000 Daltons, as of Allen, paragraph 0067.

Allen does not appear to teach why derivitization with PEG is beneficial.

Burke is drawn to liposomal stabilization of camptothecin drugs, as of Burke, title and abstract. Burke teaches that liposomes may be coated with polyethylene glycol, which assists the particles in avoiding the reticuloendothelial system, as of Burke, column 6 lines 35-37.

Burke does not appear to teach PEG molecular weight.

It would have been prima facie obvious for one of ordinary skill in the art to have provided the PEG in the DSPE-PEG of the conflicting claims with the molecular weight taught by Allen. The conflicting claims are drawn to a liposome comprising DSPE-PEG, as of conflicting claim 1. While the conflicting claims are silent as to PEG molecular weight, Allen teaches that a PEG molecular weight from 1000 to 5000 Daltons is suitable for a PEG derivatized lipid. As pegylated lipids are useful for preventing

reticuloendothelial system clearance, as taught by Burke, the skilled artisan would have been motivated to have modified the molecular weight of the PEG in the DSPE-PEG of the conflicting claims to have had a molecular weight of 1000 to 5000 Daltons for predictably avoiding reticuloendothelial system clearance with a reasonable expectation of success.

The conflicting claims and the instant claims differ because the instant claims recite that the irinotecan is present in a concentration of between 0.8 to 1.3 millimoles of irinotecan per gram of liposomal lipids. In contrast, the conflicting claims recite 500-550 mg of irinotecan hydrochloride per mmol of the total liposome phospholipids. Nevertheless, the skilled artisan would have been motivated to have optimized the concentration of irinotecan in the composition of the conflicting claims to have achieved the concentration of irinotecan recited by the instant claims. The optimization rationale also applies to the amount of DSPE-PEG.

Claims 58-72 are rejected on the ground of nonstatutory double patenting as being unpatentable over claims 1-20 of U.S. Patent No. 9,730,891. Although the claims at issue are not identical, they are not patentably distinct from each other because of the following reasons.

Instant claim 58 is drawn to a liposomal comprising irinotecan and sucrose octasulfate. Said liposome comprises a neutral phospholipid and cholesterol in a specific ratio, as well as a pegylated lipid. Specific amounts of the lipids and of irinotecan are recited.

Conflicting claim 1 is drawn to a method of treatment comprising parenteral administration of an irinotecan liposome comprising sucrose octasulfate. Conflicting claim 12 recites that the liposome comprises DSPC, cholesterol, and PEG-2000-DSPE in a molar ratio of 3:2:0.015. Conflicting claim 12 recites 0.15 to 1.5 moles of irinotecan per moles of total lipid in the liposome.

The conflicting claims and the instant claims differ because the instant claims recite that the irinotecan is present in a concentration of between 0.8 to 1.3 millimoles of irinotecan per gram of liposomal lipids. In contrast, the conflicting claims recite 0.15 to 12.5 moles of irinotecan per mole of the total liposome phospholipids. Nevertheless, the skilled artisan would have been motivated to have optimized the concentration of irinotecan in the composition of the conflicting claims to have achieved the concentration of irinotecan recited by the instant claims. The optimization rationale also applies to the amount of DSPE-PEG.

The instant and conflicting claims differ because the instant claims are composition claims, whereas the conflicting claims are method claims. Nevertheless, the method of the conflicting claims entails administering a composition comprising sucrose octasulfate and irinotecan. The composition used in the method of the conflicting claims differs with the instantly claimed invention only in that the conflicting claims do not recite the required concentration; however, it would have been prima facie obvious for the skilled artisan to have optimized this for the reasons set forth above.

Claims 58-72 are rejected on the ground of nonstatutory double patenting as being unpatentable over claims 1-19 of U.S. Patent No. 9,717,723. Although the

claims at issue are not identical, they are not patentably distinct from each other because of at least the following reasons:

Instant claim 58 is drawn to a liposomal comprising irinotecan and sucrose octasulfate. Said liposome comprises a neutral phospholipid and cholesterol in a specific ratio, as well as a pegylated lipid. Specific amounts of the lipids and of irinotecan are recited.

Conflicting claim 1 is drawn to a method of preparing a liposomal irinotecan composition. The method entails contacting sucrose octasulfate, liposome lipids, and irinotecan, with a substituted ammonium for gradient loading, as of conflicting claim 1. Conflicting claim 18 recites that the liposome comprises DSPC, cholesterol, and methoxy-PEG(2000)-DSPE in a 3:2:0.015 mole ratio. Conflicting claim 7 recites irinotecan in an amount of 150-550 mg irinotecan per mmol of total liposome phospholipid.

The conflicting claims and the instant claims differ because the instant claims recite that the irinotecan is present in a concentration of between 0.8 to 1.3 millimoles of irinotecan per gram of liposomal lipids. In contrast, the conflicting claims recite 150-550 mg of irinotecan per mmol of the total liposome phospholipids. Nevertheless, the skilled artisan would have been motivated to have optimized the concentration of irinotecan in the composition of the conflicting claims to have achieved the concentration of irinotecan recited by the instant claims. The optimization rationale also applies to the amount of DSPE-PEG.

The instant and conflicting claims differ because the instant claims are composition claims, whereas the conflicting claims are method claims. Nevertheless,

the method of the conflicting claims is drawn to a method of making a composition comprising sucrose octasulfate and irinotecan. The composition made by the method of the conflicting claims differs with the instantly claimed invention only in that the conflicting claims do not recite the required concentration; however, it would have been prima facie obvious for the skilled artisan to have optimized this for the reasons set forth above.

Claims 58-72 are rejected on the ground of nonstatutory double patenting as being unpatentable over claims 1-14 of U.S. Patent No. 8,992,970. Although the claims at issue are not identical, they are not patentably distinct from each other because of at least the following reasons:

Instant claim 58 is drawn to a liposomal comprising irinotecan and sucrose octasulfate. Said liposome comprises a neutral phospholipid and cholesterol in a specific ratio, as well as a pegylated lipid. Specific amounts of the lipids and of irinotecan are recited.

Conflicting claim 1 is drawn to a liposomal composition comprising irinotecan, sucrose octasulfate, and a substituted ammonium compound. Conflicting claim 6 recites that the liposome lipids comprise 59.8 mol% distearoyl phosphatidylcholine, 39.9% cholesterol, and 0.3 mol% poly(Ethylene glycol) distearoyl phosphatidylethanolamine. The poly(ethylene glycol) has a molecular weight of about 2000, as of conflicting claim 7. The molar ratio of irinotecan to the totality of lipids is at least 1.0, as of conflicting claim 9.

The conflicting claims and the instant claims differ because the instant claims recite that the irinotecan is present in a concentration of between 0.8 to 1.3 millimoles of irinotecan per gram of liposomal lipids. In contrast, the conflicting claims recite at least 1.0 moles of irinotecan per moles of total lipid in the liposome. Nevertheless, the skilled artisan would have been motivated to have optimized the concentration of irinotecan in the composition of the conflicting claims to have achieved the concentration of irinotecan recited by the instant claims.

Claims 58-72 are rejected on the ground of nonstatutory double patenting as being unpatentable over claims 1-20 of U.S. Patent No. 9,724,303. Although the claims at issue are not identical, they are not patentably distinct from each other because of at least the following reasons:

Instant claim 58 is drawn to a liposomal comprising irinotecan and sucrose octasulfate. Said liposome comprises a neutral phospholipid and cholesterol in a specific ratio, as well as a pegylated lipid. Specific amounts of the lipids and of irinotecan are recited.

Conflicting claim 1 is drawn to an irinotecan liposome comprising irinotecan sucrose octasulfate encapsulated in lipid vesicles. Said irinotecan can be present in an amount of 150-550 mg of irinotecan base per mmol of total vesicle phospholipid. Conflicting claim 17 recites DSPC, cholesterol, and PEG-DSPE. Conflicting claim 8 recites a PEG molecular weight from about 250 to about 20,000 Daltons.

The conflicting claims and the instant claims differ because the instant claims recite that the irinotecan is present in a concentration of between 0.8 to 1.3 millimoles of

irinotecan per gram of liposomal lipids. In contrast, the conflicting claims recite 150-550 mg of irinotecan of irinotecan per mmol of total phospholipid in the liposome. Nevertheless, the skilled artisan would have been motivated to have optimized the concentration of irinotecan in the composition of the conflicting claims to have achieved the concentration of irinotecan recited by the instant claims. The optimization rationale also applies to the amount of the lipids that form the liposome, as well as to irinotecan.

Claims 58-72 are provisionally rejected on the ground of nonstatutory double patenting as being unpatentable over claims 173-175 and 177-184 of copending Application No. 15/664,976 (reference application). Although the claims at issue are not identical, they are not patentably distinct from each other because of at least the following reasons.

Instant claim 58 is drawn to a liposomal comprising irinotecan and sucrose octasulfate. Said liposome comprises a neutral phospholipid and cholesterol in a specific ratio, as well as a pegylated lipid. Specific amounts of the lipids and of irinotecan are recited.

Copending claim 1 is drawn to a liposome comprising irinotecan and sucrose octasulfate. Copending claim 7 recites about 0.15 to 1.5 moles of irinotecan per mole of total lipid. Copending claim 175 recites DSPC, cholesterol, and PEG(2000)-DSPE in a molar ratio of 3:2:0.015.

The copending claims and the instant claims differ because the instant claims recite that the irinotecan is present in a concentration of between 0.8 to 1.3 millimoles of

irinotecan per gram of liposomal lipids. In contrast, the copending claims recite about 0.15 to about 1.5 moles of irinotecan per moles of total lipid in the liposome. Nevertheless, the skilled artisan would have been motivated to have optimized the concentration of irinotecan in the composition of the conflicting claims to have achieved the concentration of irinotecan recited by the instant claims. This optimization rationale also applies to the concentration of PEG-DSPE.

This is a provisional nonstatutory double patenting rejection because the patentably indistinct claims have not in fact been patented.

Claims 58-72 are rejected on the ground of nonstatutory double patenting as being unpatentable over claims 1-31 of U.S. Patent No. 10,456,360. Although the claims at issue are not identical, they are not patentably distinct from each other because of the following reasons:

Instant claim 58 is drawn to a liposomal comprising irinotecan and sucrose octasulfate. Said liposome comprises a neutral phospholipid and cholesterol in a specific ratio, as well as a pegylated lipid. Specific amounts of the lipids and of irinotecan are recited.

Conflicting claim 1 is drawn to a storage stable irinotecan sucrose octasulfate liposome. Conflicting claim 12 recites that the liposome comprises 6.81 mg DSPC/mL, 2.22 mg cholesterol/mL, and 0.12 mg MPEG-2000-DSPE/mL. Conflicting claims recite 4.3 mg/mL irinotecan free base. Given a molecular weight of irinotecan of about 587 Daltons, this is an amount of

$$\frac{4.3\ mg\ irinotecan}{mL} \times \frac{1\ mmol\ irinotecan}{587\ mg\ irinotecan} \times \frac{1\ mL}{6.81+2.22+0.12\ mg\ lipid} \times \frac{1000\ mg}{1g} = \frac{0.8\ mmol\ irinotecan}{g\ lipid}$$

As such, the conflicting claims are understood to teach the required amount of irinotecan within the claim scope.

With regard to the amount of lipids, the skilled artisan would have been motivated to have optimized the amount of lipids to have achieved the claimed liposome.

Subject Matter Over Which No Double Patenting Rejection is Written

The examiner notes US Patents 9,782,349 and 8,658,203. The claims of both of these patents are drawn to liposomes comprising irinotecan sucrose octasulfate. Nevertheless, the liposomes of the claims of the '349 and '203 patents do not appear to include polyethylene glycol. Also, it is unclear as to whether the claims of the '349 and '203 patents recite the required ratio of irinotecan per gram of liposomal lipid. As such, no double patenting rejection over the '349 and '203 patents has been written.

No double patenting rejection has been written over the claims of US Patent 8,329,213. This is at least because the claims of the '213 patent, while reciting a liposome comprising irinotecan sucrose octasulfate, do not recite that the lipids comprise cholesterol. Additionally, no guidance is provided about the amount of irinotecan that can be encapsulated.

No double patenting reject is written over the claims of US Patent 8,703,181. The claims of the '181 patent are drawn to a method of delivering irinotecan to a tumor comprising administering a liposome comprising irinotecan sucrose octasulfate. However, the claims of the '181 patent, while reciting a liposome comprising irinotecan

sucrose octasulfate, do not recite that the lipids comprise cholesterol. Additionally, no guidance is provided about the amount of irinotecan that can be encapsulated.

Response to Arguments

Applicant provided arguments in applicant's response on 17 January 2020. These arguments are moot in view of the cancellation of the previously presented claims and the presentation of new claims.

Conclusion

No claim is allowed.

Applicant's amendment necessitated the new ground(s) of rejection presented in this Office action. Accordingly, **THIS ACTION IS MADE FINAL**. See MPEP § 706.07(a). Applicant is reminded of the extension of time policy as set forth in 37 CFR 1.136(a).

A shortened statutory period for reply to this final action is set to expire THREE MONTHS from the mailing date of this action. In the event a first reply is filed within TWO MONTHS of the mailing date of this final action and the advisory action is not mailed until after the end of the THREE-MONTH shortened statutory period, then the shortened statutory period will expire on the date the advisory action is mailed, and any extension fee pursuant to 37 CFR 1.136(a) will be calculated from the mailing date of

the advisory action. In no event, however, will the statutory period for reply expire later than SIX MONTHS from the date of this final action.

Any inquiry concerning this communication or earlier communications from the examiner should be directed to ISAAC SHOMER whose telephone number is (571)270-7671. The examiner can normally be reached on 7:30 AM to 5:00 PM Monday Through Friday.

Examiner interviews are available via telephone, in-person, and video conferencing using a USPTO supplied web-based collaboration tool. To schedule an interview, applicant is encouraged to use the USPTO Automated Interview Request (AIR) at http://www.uspto.gov/interviewpractice.

If attempts to reach the examiner by telephone are unsuccessful, the examiner's supervisor, Frederick F Krass can be reached on (571)272-0580. The fax phone number for the organization where this application or proceeding is assigned is 571-273-8300.

Information regarding the status of an application may be obtained from the Patent Application Information Retrieval (PAIR) system. Status information for published applications may be obtained from either Private PAIR or Public PAIR. Status information for unpublished applications is available through Private PAIR only. For more information about the PAIR system, see https://ppair-my.uspto.gov/pair/PrivatePair. Should you have questions on access to the Private PAIR system, contact the Electronic Business Center (EBC) at 866-217-9197 (toll-free). If you would like assistance from a USPTO Customer Service Representative or access

to the automated information system, call 800-786-9199 (IN USA OR CANADA) or 571-272-1000.

ISAAC . SHOMER
Primary Examiner
Art Unit 1612

/ISAAC SHOMER/
Primary Examiner, Art Unit 1612

UNITED STATES PATENT AND TRADEMARK OFFICE

UNITED STATES DEPARTMENT OF COMMERCE
United States Patent and Trademark Office
Address: COMMISSIONER FOR PATENTS
P.O. Box 1450
Alexandria, Virginia 22313-1450
www.uspto.gov

APPLICATION NO.	FILING DATE	FIRST NAMED INVENTOR	ATTORNEY DOCKET NO.	CONFIRMATION NO.
15/896,389	02/14/2018	Keelung Hong	263266-426640	3157

153749 7590 03/26/2020

McNeill Baur PLLC/Ipsen
Ipsen Bioscience, Inc.
125 Cambridge Park Drive
Suite 301
Cambridge, MA 02140

EXAMINER	
SHOMER, ISAAC	

ART UNIT	PAPER NUMBER
1612	

NOTIFICATION DATE	DELIVERY MODE
03/26/2020	ELECTRONIC

Please find below and/or attached an Office communication concerning this application or proceeding.

The time period for reply, if any, is set in the attached communication.

Notice of the Office communication was sent electronically on above-indicated "Notification Date" to the following e-mail address(es):

docketing@mcneillbaur.com
eofficeaction@appcoll.com
patents.us@ipsen.com

Applicant-Initiated Interview Summary	Application No. 15/896,389	Applicant(s) Hong et al.		
	Examiner ISAAC SHOMER	Art Unit 1612	AIA (First Inventor to File) Status No	Page 1 of 3

All participants (applicant, applicants representative, PTO personnel):

1. ISAAC SHOMER (Primary Examiner); WebEx/ Video Conference

2. Deborah Herzfeld (Attomey of Record); WebEx/ Video Conference

Date of Interview: 20 March 2020

Exhibit shown or demonstration conducted (If so, please describe): Representative of applicant showed a slide presentation summarizing various arguments made. This was presented on WebEx, and following the interview, was emailed to the examiner. This presentation is attached to this interview summary.

Claims Discussed: 58-72

Prior Art Discussed: Chou (of record)

BK Yeh, AV Eliseenkova, AN Plotnikov, D Green, J Pinnell, T Polat, A Gritle-Linde, RJ Lindhart, and M Mohammadi. "Structural Basis for Activation of Fibroblast Growth Factor Signaling by Sucrose Octasulfate." Molecular and Cellular Biology, Vol. 22 No. 20, October 2002, pages 7184-7192.

Y Sadzuka, S Hirotsu, and S Hirota. "Effective Irinotecan (CPT-11)-containing Liposomes: Intraliposomal Conversion to the Active Metabolite SN-38." Japanese Journal of Cancer Research, Vol. 90, February 1999, pages 226-232.

Brief Description of the main topic(s) of discussion: Representative of applicant cited Yeh reference which teaches that sucrose octasulfate causes issues like cell proliferation and neovascularization. Examiner provisionally agreed that the skilled artisan would have expected cell proliferation and neovascularization to have made cancer worse, and as such, would not have been motivated to have used sucrose octasulfate in a composition to treat cancer.

Issues Discussed:

Item(s) under 35 U.S.C. 112:
A) New Matter: With regard to the new matter rejection, representative of applicant took the position that the instant specification, on page 34, paragraph 0109, discloses the following:

"In terms of molar ratio, the entity-to-lipid ratio according to the present invention is at least from about 0.02, to about 5, preferably at least 0.1 to about 2, and more preferably, from about 0.15 to about 1.5 moles of the drug per mole of the liposome lipid."

Representative of applicant alleges that this provides adequate support for claims 63-67, and as such, the rejection of claims 63-67 is incorrect. The examiner notes that the term "entity" refers to a drug which may be a camptothecin derivative. As such, the examiner appears to agree with applicant's position that the above-cited text provides adequate support for claims 63-67 and that the new matter rejection of this claim was not proper."

112(d) Rejection: With regard to the 112(d) rejection, representative of applicant verbally appeared to agree with the examiner's rejection and verbally expressed an intention to cancel the claims rejected under 35 U.S.C. 112(d).

Item(s) under 35 U.S.C. 103:
Calculation: Representative of applicant took the position that the examiner made some mistakes in the calculation on page 6 of the previous office action on 31 January 2020. First, representative of applicant took the position that the molecular weight of DSPC is 790 mg/mmol, not 734 mg/mmol, as used by the examiner. The examiner agreed with applicant's position that this value was in error. Representative of applicant also argued that the molecular weight of irinotecan used by the examiner was incorrect, and the molecular weight that should have been used was that for irinotecan hydrochloride trihydrate. The examiner did not take a position on this. Also discussed was the impact of non-phospholipid lipids and their impact on the calculation. Regardless, the examiner took the position that, regardless of any errors made by the examiner in the calculation, the examiner is unaware of how this has a bearing on the propriety of the applied rejection.

Sucrose Octasulfate: Representative of applicant cited the Yeh reference which is alleged to teach that sucrose octasulfate causes neovascularization, neoangiogenesis, and cell proliferation. This appears to be taught as of Yeh, page 7184, right column, second to last paragraph. The examiner agrees that neovascularization, neoangiogenesis and cell proliferation would have made cancer worse. This is because cancer is drawn to overproliferation of cells, and causing additional cell proliferation and/or providing blood to said proliferation of cells (e.g. by neovascularization) would have worsened said cell proliferation. As such, examiner agrees that the skilled artisan would not have been motivated to have used sucrose octasulfate in a composition for cancer treatment.

Percentage of Pegylated Lipid: Applicant argues that the percentage of DSPE-PEG in the instant application is from about 0.1-1 mol% whereas Chou teaches about 3.7 mol%. Representative of applicant argued that the skilled artisan would not have been motivated to have optimized the amount of DSPE-PEG to have been in the claimed range. The examiner disagreed. No agreement was reached on this issue.

Other:
In order to expedite prosecution, examiner will send a copy of the interview summary by email to representative of applicant upon finishing writing the interview summary. This will enable representative of applicant to have the interview summary earlier, so that representative of applicant can better decide how to write the next response based upon what is written in the interview summary.

Attachment(s): Agenda, Other Attachment
{PTO-892 with references, email record}

/ISAAC SHOMER/ Primary Examiner, Art Unit 1612	

Applicant is reminded that a complete written statement as to the substance of the interview must be made of record in the application file. It is the applicants responsibility to provide the written statement, unless the interview was initiated by the Examiner and the Examiner has indicated that a written summary will be provided. See MPEP 713.04
Please further see:
MPEP 713.04
Title 37 Code of Federal Regulations (CFR) § 1.133 Interviews, paragraph (b)
37 CFR § 1.2 Business to be transacted in writing

Applicant recordation instructions: The formal written reply to the last Office action must include the substance of the interview. (See MPEP section 713.04). If a reply to the last Office action has already been filed, applicant is given a non-extendable period of the longer of one month or thirty days from this interview date, or the mailing date of this interview summary form, whichever is later, to file a statement of the substance of the interview.

Examiner recordation instructions: Examiners must summarize the substance of any interview of record. A complete and proper recordation of the substance of an interview should include the items listed in MPEP 713.04 for complete and proper recordation including the identification of the general thrust of each argument or issue discussed, a general indication of any other pertinent matters discussed regarding patentability and the general results or outcome of the interview, to include an indication as to whether or not agreement was reached on the issues raised.

Notice of References Cited	Application/Control No. 15/896,389	Applicant(s)/Patent Under Reexamination Hong et al.	
	Examiner ISAAC SHOMER	Art Unit 1612	Page 1 of 1

U.S. PATENT DOCUMENTS

*		Document Number Country Code-Number-Kind Code	Date MM-YYYY	Name	CPC Classification	US Classification
	A					
	B					
	C					
	D					
	E					
	F					
	G					
	H					
	I					
	J					
	K					
	L					
	M					

FOREIGN PATENT DOCUMENTS

*		Document Number Country Code-Number-Kind Code	Date MM-YYYY	Country	Name	CPC Classification
	N					
	O					
	P					
	Q					
	R					
	S					
	T					

NON-PATENT DOCUMENTS

*		Include as applicable: Author, Title Date, Publisher, Edition or Volume, Pertinent Pages)
	U	Y Sadzuka, S Hirotsu, and S Hirota. "Effective Irinotecan (CPT-11)-containing Liposomes: Intraliposomal Conversion to the Active Metabolite SN-38." Japanese Journal of Cancer Research, Vol. 90, February 1999, pages 226-232. (Year: 1999)
	V	BK Yeh, AV Eliseenkova, AN Plotnikov, D Green, J Pinnell, T Polat, A Gritle-Linde, RJ Lindhart, and M Mohammadi. "Structural Basis for Activation of Fibroblast Growth Factor Signaling by Sucrose Octasulfate." Molecular and Cellular Biology, Vol. 22 No. 20, October 2002, pages 7184-7192. (Year: 2002)
	W	
	X	

*A copy of this reference is not being furnished with this Office action. (See MPEP § 707.05(a).)
Dates in MM-YYYY format are publication dates. Classifications may be US or foreign.

Interview for US 15/896,389

Examiner Shomer

Deb Herzfeld/McNeill Baur

March 20, 2020

MCNEILL|BAUR
Intellectual Property Law

Agenda Outline

- Status of Claims
- § 112(a)
- § 112(d)
- § 103(a)
- ODP

Status of the Claims

Claims 58-72 are pending

- Claims 63-67 rejected under § 112(a)
- Claims 60, 65, and 70 rejected under § 112(d)
- Claims 63-67 rejected under § 103(a)
- Claims 58-72 rejected under ODP
  - Request to hold in abeyance until patentable subject matter agreed upon

Claims 63-67 rejected under § 112(a)

Claim 63: A liposome composition comprising neutral phospholipid and cholesterol in a mole ratio of 3:2, and N-(methoxy-poly(ethylene glycol) (PEG molecular weight from 500 to 5,000)-oxycarbonyl)-distearoylphosphatidylethanolamine present in an amount between 0.1 and 1 mol % with respect to liposomal lipids;

the liposomes in the composition entrapping irinotecan and sucrose octasulfate, wherein **the moles of irinotecan per mole of liposomal lipids is from about 0.15 to about 1.5**. (emphasis added)

- The Office alleges that paragraph [0109] of the specification "fails to provide support for the full range of 0.15 to 1.5 moles of irinotecan per mole of liposome lipids." Final Office Action ("FOA") at pg. 3

- Applicant traverses

Claims 63-67 rejected under § 112(a)

The essential objective question to be addressed when considering the written description requirement is "does the description clearly allow persons of ordinary skill in the art to recognize that he or she invented what is claimed." MPEP § 2163.02 (citing *In re Gosteli*, 872 F.2d 1008, 1012, 10 USPQ2d 1614, 1618 (Fed. Cir. 1989)).

- Paragraph [0109] of the specification literally states the claimed range "In terms of molar ratio, the entity-to-lipid ratio according to the present invention is at least from about 0.02, to about 5, preferably at least 0.1 to about 2, and more preferably, **from about 0.15 to about 1.5 moles of the drug per mole of the liposome lipid**." (emphasis added)

- The Office "has the initial burden of presenting by a preponderance of evidence why a person skilled in the art would not recognize in an applicant's disclosure a description of the invention defined by the claims." MPEP § 2163.04 (citing *In re Wertheim*, 541 F.2d 257, 263, 191 USPQ 90, 97 (CCPA 1976)).

Claims 60, 65, and 70 rejected under § 112(d)

Claim 60: The liposome composition of claim 59, wherein the N-(methoxy-poly(ethylene glycol)(PEG molecular weight from 500 to 5,000)-oxycarbonyl)-distearoylphosphatidylethanolamine is **anionic** N-(methoxy-poly(ethylene glycol) (PEG molecular weight 2000)-oxycarbonyl)-distearoylphosphatidylethanolamine. (emphasis added)

- The Office alleges the limitation "anionic" of claims 60, 65, and 70 "does not appear to further limit the respective chemical structure" because "DSPE-PEG is inherently anionic." FOA at pg. 4

- Applicant agrees to cancel claims 60, 65, and 70 as it is agreed by the Office that DSPE-PEG is, in fact, anionic

Claims 63-67 rejected under § 103(a)

Claim 63: A liposome composition comprising neutral phospholipid and cholesterol in a mole ratio of 3:2, and N-(methoxy-poly(ethylene glycol) (PEG molecular weight from 500 to 5,000)-oxycarbonyl)-distearoylphosphatidylethanolamine present in an amount between 0.1 and 1 mol % with respect to liposomal lipids;

the liposomes in the composition entrapping irinotecan and sucrose octasulfate, wherein the moles of irinotecan per mole of liposomal lipids is from about 0.15 to about 1.5.

- The Office alleges that claims 63-67 are "unpatentable over" Chou et al. (Journal of Bioscience and Bioengineering, Vol. 95, No. 4, 2003, pages 405-408) ("**Chou**") in view of Gunay et al. (Analytical Chemistry, Vol. 75, 2003, pages 3226-3231) ("**Gunay**") and Uster et al. (FEBS Letters, Vol. 386, 1996, pages 243-246) ("**Uster**"). FOA at pgs. 4-6

- Applicant traverses

Claims 63-67 rejected under § 103(a)
Teachings of Chou

Claim 63: A liposome composition comprising neutral phospholipid and cholesterol in a mole ratio of 3:2, and N-(methoxy-poly(ethylene glycol) (PEG molecular weight from 500 to 5,000)-oxycarbonyl)-distearoylphosphatidylethanolamine present in an amount between 0.1 and 1 **mol % with respect to liposomal lipids**;
the liposomes in the composition entrapping irinotecan and sucrose octasulfate, wherein the **moles of irinotecan per mole of liposomal lipids** is from about 0.15 to about 1.5. (emphasis added)

- The Office alleges (at FOA pg. 6) that:
  1) Chou "is drawn to a liposome comprising irinotecan, which has antitumor activity. … Said liposome includes phospholipids such as phosphatidylcholines."
  2) "Chou also teaches a loading amount of 0.254 mg drug per mg lipid, as of Chou, page 407, right column, last full paragraph."
  3) "Chou differs from the claimed invention at least because Chou does not teach sucrose octasulfate."

- Applicant traverses the rejection

Claims 63-67 rejected under § 103(a)
Teachings of Chou

The Office states "Chou also teaches a loading amount of 0.254 mg drug per mg lipid, as of Chou, page 407, right column, last full paragraph. **The units of this concentration differ from the recited units. Nevertheless, the examiner has performed a calculation below to estimate the concentration of irinotecan in Chou in mg of irinotecan per mmol of total phospholipids**." (emphasis added)

The Office provides the following calculation "assuming molecular weight of liposome lipids of 734 Daltons (which is a molecular weight of DSPC) and 587 Daltons for irinotecan this is a concentration of:

$$\frac{0.254\ mg\ irinotecan}{1\ mg\ lipid} \times \frac{1\ mmol\ irinotecan}{587\ mg\ irinotecan} \times \frac{734\ mg\ lipid}{1\ mmol\ lipid} = 0.318\ \frac{mmol\ irinotean}{mmol\ lipid}$$

- Applicant respectfully disagrees with assumptions made in the Examiner's calculations

Claims 63-67 rejected under § 103(a)
Teachings of Chou

Chou would not motivate POSITA to arrive at the presently claimed DSPE-PEG2000 content

- Chou teaches (at page 408; left col., 1st paragraph) that:
  - "[a]dding 5 mol% DSPE-PEG2000 increased the uptake of the drug into liposomes.".
    - The Examiner notes that 5 mol % DSPE-PEG2000 is actually 3.7% of all lipids (FOA at pg. 8, which is still outside claimed range of "between 0.1 and 1 mol %"
  - "Furthermore, an appropriate proportion of DSPE-PEG is commonly added to liposomes to prevent mononuclear phagocytic system uptake *in vivo*."

- POSITA would have concluded from Chou that higher mol% of DSPE-PEG2000 leads to
  - higher drug loading and
  - improved duration of liposome circulation

Thus, POSITA would not be motivated to lower DSPE-PEG2000 amount to the presently claimed range based on Chou's teaching of the relationship between DSPE-PEG2000 and drug loading

Claims 63-67 rejected under § 103(a)
Teachings of Chou in view of Gunay

The Office alleges (FOA pg. 6) (emphasis added) :

- "Chou differs from the claimed invention at least because Chou does not teach sucrose octasulfate."
- Gunay "is drawn to sucrose octasulfate, which is taught to be a highly sulfate carbohydrate, as of Gunay, page 3226, title and abstract. **Gunay suggests sucrose octasulfate for the treatment of cancer,** as of Gunay, page 3226, right column, top paragraph below title."

- The Office concludes "It would have been prima facie obvious for one of ordinary skill in the art to have combined sucrose octasulfate with the liposome of Chou. Chou is drawn to a liposome comprising irinotecan**, but suggests that sulfated oligosaccharides can be included,** as of Chou, page 408, left column, second paragraph. … The skilled artisan would have been motivated to have made combination at least because Chou **suggests the inclusion of a sulfated oligosaccharide**.

- Applicant traverses for multiple reasons, as will be discussed on the following slides

Teachings of Chou: General Oligosaccharide Teaching

Chou states, but does not provide data proof, of possible insoluble complex between irinotecan and sulfated oligosaccharides: "…it was also found that sulfated **oligo**saccharides **can** form an insoluble complex with irinotecan **(data not shown).**" (Chou at page 408; left col., 2nd paragraph) (emphasis added)

- no specific sulfated oligosaccharides named
- no information on conditions provided
- no motivation in Chou to move from oligosaccharides to a specific disaccharide

- Proper support for a §103 rejection in the chemical arts requires the prior art to supply a reason or motivation to make the claimed compositions. *See* MPEP § 2143 (I)(B) Example 8 (citing *Aventis Pharma. Deutschland GmbH v. Lupin Ltd.*, 84 USPQ 2d 1197, 1204 (Fed. Cir. 2007))

Claims 63-67 rejected under § 103(a)
Teachings of Chou in view of Gunay

The Office alleges (FOA pg. 6) (emphasis added) :

- Gunay "is drawn to sucrose octasulfate, which is taught to be a highly sulfate carbohydrate, as of Gunay, page 3226, title and abstract. **Gunay suggests sucrose octasulfate for the treatment of cancer,** as of Gunay, page 3226, right column, top paragraph below title."

- Despite the lack of motivation within Chou to select general oligosaccharide teaching as starting point for change, the Office concludes "It would have been prima facie obvious for one of ordinary skill in the art to have combined sucrose octasulfate with the liposome of Chou. … As sucrose octasulfate is a **sulfate oligosaccharide that has potential to treat cancer, as of Gunay**."

- Applicant traverses for multiple reasons, as will be discussed on the following slides

The Teachings of Gunay

- Gunay teaches mass spec analysis of SOS, as indicated by the title
  - "Evaluation of Counterions for Electrospray Ionization Mass Spectral Analysis of A Highly Sulfated Carbohydrate, Sucrose Octasulfate"

- Gunay's "suggestion" of SOS for cancer is a broad, misleading statement taken out of context.
- Gunay states: "The crystallization of the sodium salt of SOS within the signal transduction complex[10] and demonstration of its modest oral bioavailability[6] has suggested new and important application for SOS and its analogues in wound healing and in the treatment of cancer.[10]"

- Reference 10 is Yeh, which (as previously acknowledged by the Office) does not teach SOS as an anti-cancer agent
  - The Examiner's reliance on Gunay's misstated summary of Yeh is improper.
  - A prior art reference must be considered in its entirety, i.e., as a whole, including portions that would lead away from the claimed invention. See MPEP § 2141.02(VI) (citing *W.L. Gore & Assoc., Inc. v. Garlock, Inc.*, 721 F.2d 1540, 220 USPQ 303 (Fed. Cir. 1983))

The Teachings of Yeh (cited in Gunay)

Yeh teaches:

- "SOS has been shown to mimic heparin action in supporting FGF-induced **neoangiogenesis** and **cell proliferation** in vitro (2, 11, 23, 29, 45, 49)." Yeh at 7184, 2nd col (emphasis added).

- "In adult organisms, FGFs are thought to be involved in physiological angiogenesis and wound healing as well as in **pathological angiogenesis,** such as in **tumor neovascularization** and diabetic retinopathy (3, 13, 16)." Yeh at 7190, 2nd col (emphasis added).

- Accordingly, the substance of Yeh (cited in Gunay), teaches away from the combination of Chou and Gunay

Claims 63-67 rejected under § 103(a)
Teachings of Chou in view of Gunay and Uster

The Office alleges (FOA pg. 8):

- "None of [Chou and Gunay] teach that the polyethylene glycol (PEG) is methoxy terminated."
- Uster "is drawn to poly(ethylene glycol) derivatized phospholipid being placed into pre-formed liposomes, as of Uster, page 243, title and abstract. The pegylated lipid of Uster was made by attaching methoxypoly(ethylene glycol) via the carbamate linkage to the amino head group of 1,2-distearoyl-sn-glycero-3-phosphoethanolamine to make DSPE-PEG, as of Uster, page 243, right column, section 2.1."

- The Office concludes "As Uster teaches that a methoxy group is a known terminus of PEG to be used in DSPE-PEG in a liposome, the skilled artisan would have been motivated to have used methoxy terminated PEG, as of Uster, to have predictably formed the DSPE-PEG of Chou with a reasonable expectation of success."

- Applicant traverses as Uster cannot cure the deficiencies of Chou and Gunay discussed herein

Conclusion

- Claims 63-67 are patentable under § 112(a)
- Claims 63-67 are patentable under § 103(a)
- Claims 58-72 rejected under ODP
  - Request to hold in abeyance until patentable subject matter agreed upon

UNITED STATES PATENT AND TRADEMARK OFFICE

UNITED STATES DEPARTMENT OF COMMERCE
United States Patent and Trademark Office
Address: COMMISSIONER FOR PATENTS
P.O. Box 1450
Alexandria, Virginia 22313-1450
www.uspto.gov

APPLICATION NO.	FILING DATE	FIRST NAMED INVENTOR	ATTORNEY DOCKET NO.	CONFIRMATION NO.
15/896,389	02/14/2018	Keelung Hong	263266-426640	3157

153749 7590 04/09/2020

McNeill Baur PLLC/Ipsen
Ipsen Bioscience, Inc.
125 Cambridge Park Drive
Suite 301
Cambridge, MA 02140

EXAMINER	
SHOMER, ISAAC	

ART UNIT	PAPER NUMBER
1612	

NOTIFICATION DATE	DELIVERY MODE
04/09/2020	ELECTRONIC

Please find below and/or attached an Office communication concerning this application or proceeding.

The time period for reply, if any, is set in the attached communication.

Notice of the Office communication was sent electronically on above-indicated "Notification Date" to the following e-mail address(es):

docketing@mcneillbaur.com
eofficeaction@appcoll.com
patents.us@ipsen.com

Advisory Action Before the Filing of an Appeal Brief	**Application No.** 15/896,389	**Applicant(s)** Hong et al.	
	Examiner ISAAC SHOMER	**Art Unit** 1612	**AIA (FITF) Status** No

--The MAILING DATE of this communication appears on the cover sheet with the correspondence address --

THE REPLY FILED 31 March 2020 FAILS TO PLACE THIS APPLICATION IN CONDITION FOR ALLOWANCE.

NO NOTICE OF APPEAL FILED

1. ☑ The reply was filed after a final rejection. No Notice of Appeal has been filed. To avoid abandonment of this application, applicant must timely file one of the following replies: (1) an amendment, affidavit, or other evidence, which places the application in condition for allowance; (2) a Notice of Appeal (with appeal fee) in compliance with 37 CFR 41.31; or (3) a Request for Continued Examination (RCE) in compliance with 37 CFR 1.114 if this is a utility or plant application. Note that RCEs are not permitted in design applications. The reply must be filed within one of the following time periods:
   a) ☐ The period for reply expires ____ months from the mailing date of the final rejection.
   b) ☑ The period for reply expires on: (1) the mailing date of this Advisory Action; or (2) the date set forth in the final rejection, whichever is later. In no event, however, will the statutory period for reply expire later than SIX MONTHS from the mailing date of the final rejection.
   c) ☐ A prior Advisory Action was mailed more than 3 months after the mailing date of the final rejection in response to a first after-final reply filed within 2 months of the mailing date of the final rejection.The current period for reply expires ____ months from the mailing date of *the prior Advisory Action* or SIX MONTHS from the mailing date of the final rejection, whichever is earlier.

   Examiner Note: If box 1 is checked, check either box (a), (b) or (c). ONLY CHECK BOX (b) WHEN THIS ADVISORY ACTION IS THE FIRST RESPONSE TO APPLICANTS FIRST AFTER-FINAL REPLY WHICH WAS FILED WITHIN TWO MONTHS OF THE FINAL REJECTION. ONLY CHECK BOX (c) IN THE LIMITED SITUATION SET FORTH UNDER BOX (c). See MPEP 706.07(f).

Extensions of time may be obtained under 37 CFR 1.136(a). The date on which the petition under 37 CFR 1.136(a) and the appropriate extension fee have been filed is the date for purposes of determining the period of extension and the corresponding amount of the fee. The appropriate extension fee under 37 CFR 1.17(a) is calculated from: (1) the expiration date of the shortened statutory period for reply originally set in the final Office action; or (2) as set forth in (b) or (c) above, if checked. Any reply received by the Office later than three months after the mailing date of the final rejection, even if timely filed, may reduce any earned patent term adjustment. See 37 CFR 1.704(b).

NOTICE OF APPEAL

2. ☐ The Notice of Appeal was filed on _____. A brief in compliance with 37 CFR 41.37 must be filed within two months of the date of filing the Notice of Appeal (37 CFR 41.37(a)), or any extension thereof (37 CFR 41.37(e)), to avoid dismissal of the appeal. Since a Notice of Appeal has been filed, any reply must be filed within the time period set forth in 37CFR 41.37(a).

AMENDMENTS

3. ☐ The proposed amendments filed after a final rejection, but prior to the date of filing a brief, will not be entered because
   a) ☐ They raise new issues that would require further consideration and/or search (see NOTE below);
   b) ☐ They raise the issue of new matter (see NOTE below);
   c) ☐ They are not deemed to place the application in better form for appeal by materially reducing or simplifying the issues for appeal; and/or
   d) ☐ They present additional claims without canceling a corresponding number of finally rejected claims.

   NOTE: _____ (See 37CFR 1.116 and 41.33(a)).
4. ☐ The amendments are not in compliance with 37CFR 1.121. See attached Notice of Non-Compliant Amendment (PTOL-324).
5. ☑ Applicants reply has overcome the following rejection(s): See Continuation Sheet
6. ☐ Newly proposed or amended claim(s) _____ would be allowable if submitted in a separate, timely filed amendment canceling the non-allowable claim(s).
7. ☑ For purposes of appeal, the proposed amendment(s):(a) ☐ will not be entered, or (b) ☑ will be entered, and an explanation of how the new or amended claims would be rejected is provided below or appended.

AFFIDAVIT OR OTHER EVIDENCE

8. ☐ A declaration(s)/affidavit(s) under **37 CFR 1.130(b)** was/were filed on _____
9. ☐ The affidavit or other evidence filed after final action, but before or on the date of filing a Notice of Appeal will not be entered because applicant failed to provide a showing of good and sufficient reasons why the affidavit or other evidence is necessary and was not earlier presented. See 37 CFR 1.116(e).
10. ☐ The affidavit or other evidence filed after the date of filing the Notice of Appeal, but prior to the date of filing a brief, will not be entered because the affidavit or other evidence failed to overcome all rejections under appeal and/or appellant fails to provide a showing of good and sufficient reasons why it is necessary and was not earlier presented. See 37 CFR 41.33(d)(1).
11. ☐ The affidavit or other evidence is entered. An explanation of the status of the claims after entry is below or attached.

REQUEST FOR RECONSIDERATION/OTHER

12. ☑ The request for reconsideration has been considered but does NOT place the application in condition for allowance because: Applicant did not provide substantive arguments regarding the double patenting rejections. As such, these rejections have been maintained..
13. ☐ Note the attached Information *Disclosure Statement*(s). (PTO/SB/08) Paper No(s). _____
14. ☐ Other: _____.

STATUS OF CLAIMS

15. The status of the claim(s) is (or will be) as follows:
    Claim(s) allowed:_____.
    Claim(s) objected to:_____.
    Claim(s) rejected:58-59,61-64,66-69 and 71-72.
    Claim(s) withdrawn from consideration:_____.

/ISAAC SHOMER/ Primary Examiner, Art Unit 1612	

Continuation of AMENDMENTS 5. Applicant's reply has overcome the following rejection(s): 112(a), 112(d) and 103 rejections. With regard to the now-withdrawn 103 rejection, the examiner additionally notes here that, to the extent that Gunay teaches benefits of sucrose octasulfate, those benefits are in regard to oral administration, specifically oral bioavailability. However, the skilled artisan would have been unlikely to have been motivated to have administered the composition of Chou orally because the liposome of Chou would have been unlikely to have survived the stomach environment. In contrast, the skilled artisan would have been motivated to have administered the irinotecan liposome of Chou parenterally (e.g. via injection or infusion), as this is how chemotherapy is normally administered.
Gunay teaches sucrose octasulfate for improving oral bioavailability, as of Gunay, page 3226, right column, top paragraph. There would be no motivation for combining a molecule with high oral bioavailability with the composition of Chou, which would not appear to be intended for oral administration.

UNITED STATES PATENT AND TRADEMARK OFFICE

UNITED STATES DEPARTMENT OF COMMERCE
United States Patent and Trademark Office
Address: COMMISSIONER FOR PATENTS
P.O. Box 1450
Alexandria, Virginia 22313-1450
www.uspto.gov

NOTICE OF ALLOWANCE AND FEE(S) DUE

153749 7590 06/05/2020

McNeill Baur PLLC/Ipsen
Ipsen Bioscience, Inc.
125 Cambridge Park Drive
Suite 301
Cambridge, MA 02140

EXAMINER
SHOMER, ISAAC

ART UNIT	PAPER NUMBER
1612	

DATE MAILED: 06/05/2020

APPLICATION NO.	FILING DATE	FIRST NAMED INVENTOR	ATTORNEY DOCKET NO.	CONFIRMATION NO.
15/896,389	02/14/2018	Keelung Hong	263266-426640	3157

TITLE OF INVENTION: LIPOSOMES USEFUL FOR DRUG DELIVERY

APPLN. TYPE	ENTITY STATUS	ISSUE FEE DUE	PUBLICATION FEE DUE	PREV. PAID ISSUE FEE	TOTAL FEE(S) DUE	DATE DUE
nonprovisional	UNDISCOUNTED	$1000	$0.00	$0.00	$1000	09/08/2020

THE APPLICATION IDENTIFIED ABOVE HAS BEEN EXAMINED AND IS ALLOWED FOR ISSUANCE AS A PATENT. PROSECUTION ON THE MERITS IS CLOSED. THIS NOTICE OF ALLOWANCE IS NOT A GRANT OF PATENT RIGHTS. THIS APPLICATION IS SUBJECT TO WITHDRAWAL FROM ISSUE AT THE INITIATIVE OF THE OFFICE OR UPON PETITION BY THE APPLICANT. SEE 37 CFR 1.313 AND MPEP 1308.

THE ISSUE FEE AND PUBLICATION FEE (IF REQUIRED) MUST BE PAID WITHIN THREE MONTHS FROM THE MAILING DATE OF THIS NOTICE OR THIS APPLICATION SHALL BE REGARDED AS ABANDONED. THIS STATUTORY PERIOD CANNOT BE EXTENDED. SEE 35 U.S.C. 151. THE ISSUE FEE DUE INDICATED ABOVE DOES NOT REFLECT A CREDIT FOR ANY PREVIOUSLY PAID ISSUE FEE IN THIS APPLICATION. IF AN ISSUE FEE HAS PREVIOUSLY BEEN PAID IN THIS APPLICATION (AS SHOWN ABOVE), THE RETURN OF PART B OF THIS FORM WILL BE CONSIDERED A REQUEST TO REAPPLY THE PREVIOUSLY PAID ISSUE FEE TOWARD THE ISSUE FEE NOW DUE.

HOW TO REPLY TO THIS NOTICE:

I. Review the ENTITY STATUS shown above. If the ENTITY STATUS is shown as SMALL or MICRO, verify whether entitlement to that entity status still applies.

If the ENTITY STATUS is the same as shown above, pay the TOTAL FEE(S) DUE shown above.

If the ENTITY STATUS is changed from that shown above, on PART B - FEE(S) TRANSMITTAL, complete section number 5 titled "Change in Entity Status (from status indicated above)".

For purposes of this notice, small entity fees are 1/2 the amount of undiscounted fees, and micro entity fees are 1/2 the amount of small entity fees.

II. PART B - FEE(S) TRANSMITTAL, or its equivalent, must be completed and returned to the United States Patent and Trademark Office (USPTO) with your ISSUE FEE and PUBLICATION FEE (if required). If you are charging the fee(s) to your deposit account, section "4b" of Part B - Fee(s) Transmittal should be completed and an extra copy of the form should be submitted. If an equivalent of Part B is filed, a request to reapply a previously paid issue fee must be clearly made, and delays in processing may occur due to the difficulty in recognizing the paper as an equivalent of Part B.

III. All communications regarding this application must give the application number. Please direct all communications prior to issuance to Mail Stop ISSUE FEE unless advised to the contrary.

IMPORTANT REMINDER: Maintenance fees are due in utility patents issuing on applications filed on or after Dec. 12, 1980. It is patentee's responsibility to ensure timely payment of maintenance fees when due. More information is available at www.uspto.gov/PatentMaintenanceFees.

PART B - FEE(S) TRANSMITTAL

Complete and send this form, together with applicable fee(s), by mail or fax, or via EFS-Web.

By mail, send to: Mail Stop ISSUE FEE
Commissioner for Patents
P.O. Box 1450
Alexandria, Virginia 22313-1450

By fax, send to: (571)-273-2885

INSTRUCTIONS: This form should be used for transmitting the ISSUE FEE and PUBLICATION FEE (if required). Blocks 1 through 5 should be completed where appropriate. All further correspondence including the Patent, advance orders and notification of maintenance fees will be mailed to the current correspondence address as indicated unless corrected below or directed otherwise in Block 1, by (a) specifying a new correspondence address; and/or (b) indicating a separate "FEE ADDRESS" for maintenance fee notifications.

CURRENT CORRESPONDENCE ADDRESS (Note: Use Block 1 for any change of address)

153749 7590 06/05/2020

McNeill Baur PLLC/Ipsen
Ipsen Bioscience, Inc.
125 Cambridge Park Drive
Suite 301
Cambridge, MA 02140

Note: A certificate of mailing can only be used for domestic mailings of the Fee(s) Transmittal. This certificate cannot be used for any other accompanying papers. Each additional paper, such as an assignment or formal drawing, must have its own certificate of mailing or transmission.

Certificate of Mailing or Transmission

I hereby certify that this Fee(s) Transmittal is being deposited with the United States Postal Service with sufficient postage for first class mail in an envelope addressed to the Mail Stop ISSUE FEE address above, or being transmitted to the USPTO via EFS-Web or by facsimile to (571) 273-2885, on the date below.

(Typed or printed name)
(Signature)
(Date)

APPLICATION NO.	FILING DATE	FIRST NAMED INVENTOR	ATTORNEY DOCKET NO.	CONFIRMATION NO.
15/896,389	02/14/2018	Keelung Hong	263266-426640	3157

TITLE OF INVENTION: LIPOSOMES USEFUL FOR DRUG DELIVERY

APPLN. TYPE	ENTITY STATUS	ISSUE FEE DUE	PUBLICATION FEE DUE	PREV. PAID ISSUE FEE	TOTAL FEE(S) DUE	DATE DUE
nonprovisional	UNDISCOUNTED	$1000	$0.00	$0.00	$1000	09/08/2020

EXAMINER	ART UNIT	CLASS-SUBCLASS
SHOMER, ISAAC	1612	424-450000

1. Change of correspondence address or indication of "Fee Address" (37 CFR 1.363).

❑ Change of correspondence address (or Change of Correspondence Address form PTO/SB/122) attached.

❑ "Fee Address" indication (or "Fee Address" Indication form PTO/SB/47; Rev 03-09 or more recent) attached. **Use of a Customer Number is required.**

2. For printing on the patent front page, list
(1) The names of up to 3 registered patent attorneys or agents OR, alternatively,
(2) The name of a single firm (having as a member a registered attorney or agent) and the names of up to 2 registered patent attorneys or agents. If no name is listed, no name will be printed.

1 _____
2 _____
3 _____

3. ASSIGNEE NAME AND RESIDENCE DATA TO BE PRINTED ON THE PATENT (print or type)

PLEASE NOTE: Unless an assignee is identified below, no assignee data will appear on the patent. If an assignee is identified below, the document must have been previously recorded, or filed for recordation, as set forth in 37 CFR 3.11 and 37 CFR 3.81(a). Completion of this form is NOT a substitute for filing an assignment.

(A) NAME OF ASSIGNEE (B) RESIDENCE: (CITY and STATE OR COUNTRY)

Please check the appropriate assignee category or categories (will not be printed on the patent) : ❑ Individual ❑ Corporation or other private group entity ❑ Government

4a. Fees submitted: ❑ Issue Fee ❑ Publication Fee (if required) ❑ Advance Order - # of Copies _____

4b. Method of Payment: *(Please first reapply any previously paid fee shown above)*

❑ Electronic Payment via EFS-Web ❑ Enclosed check ❑ Non-electronic payment by credit card (Attach form PTO-2038)

❑ The Director is hereby authorized to charge the required fee(s), any deficiency, or credit any overpayment to Deposit Account No. _____

5. **Change in Entity Status** (from status indicated above)

❑ Applicant certifying micro entity status. See 37 CFR 1.29

❑ Applicant asserting small entity status. See 37 CFR 1.27

❑ Applicant changing to regular undiscounted fee status.

NOTE: Absent a valid certification of Micro Entity Status (see forms PTO/SB/15A and 15B), issue fee payment in the micro entity amount will not be accepted at the risk of application abandonment.
NOTE: If the application was previously under micro entity status, checking this box will be taken to be a notification of loss of entitlement to micro entity status.
NOTE: Checking this box will be taken to be a notification of loss of entitlement to small or micro entity status, as applicable.

NOTE: This form must be signed in accordance with 37 CFR 1.31 and 1.33. See 37 CFR 1.4 for signature requirements and certifications.

Authorized Signature _____ Date _____

Typed or printed name _____ Registration No. _____

UNITED STATES PATENT AND TRADEMARK OFFICE

UNITED STATES DEPARTMENT OF COMMERCE
United States Patent and Trademark Office
Address: COMMISSIONER FOR PATENTS
P.O. Box 1450
Alexandria, Virginia 22313-1450
www.uspto.gov

APPLICATION NO.	FILING DATE	FIRST NAMED INVENTOR	ATTORNEY DOCKET NO.	CONFIRMATION NO.
15/896,389	02/14/2018	Keelung Hong	263266-426640	3157

153749 7590 06/05/2020

McNeill Baur PLLC/Ipsen
Ipsen Bioscience, Inc.
125 Cambridge Park Drive
Suite 301
Cambridge, MA 02140

EXAMINER	
SHOMER, ISAAC	

ART UNIT	PAPER NUMBER
1612	

DATE MAILED: 06/05/2020

Determination of Patent Term Adjustment under 35 U.S.C. 154 (b)
(Applications filed on or after May 29, 2000)

The Office has discontinued providing a Patent Term Adjustment (PTA) calculation with the Notice of Allowance.

Section 1(h)(2) of the AIA Technical Corrections Act amended 35 U.S.C. 154(b)(3)(B)(i) to eliminate the requirement that the Office provide a patent term adjustment determination with the notice of allowance. See Revisions to Patent Term Adjustment, 78 Fed. Reg. 19416, 19417 (Apr. 1, 2013). Therefore, the Office is no longer providing an initial patent term adjustment determination with the notice of allowance. The Office will continue to provide a patent term adjustment determination with the Issue Notification Letter that is mailed to applicant approximately three weeks prior to the issue date of the patent, and will include the patent term adjustment on the patent. Any request for reconsideration of the patent term adjustment determination (or reinstatement of patent term adjustment) should follow the process outlined in 37 CFR 1.705.

Any questions regarding the Patent Term Extension or Adjustment determination should be directed to the Office of Patent Legal Administration at (571)-272-7702. Questions relating to issue and publication fee payments should be directed to the Customer Service Center of the Office of Patent Publication at 1-(888)-786-0101 or (571)-272-4200.

OMB Clearance and PRA Burden Statement for PTOL-85 Part B

The Paperwork Reduction Act (PRA) of 1995 requires Federal agencies to obtain Office of Management and Budget approval before requesting most types of information from the public. When OMB approves an agency request to collect information from the public, OMB (i) provides a valid OMB Control Number and expiration date for the agency to display on the instrument that will be used to collect the information and (ii) requires the agency to inform the public about the OMB Control Number's legal significance in accordance with 5 CFR 1320.5(b).

The information collected by PTOL-85 Part B is required by 37 CFR 1.311. The information is required to obtain or retain a benefit by the public which is to file (and by the USPTO to process) an application. Confidentiality is governed by 35 U.S.C. 122 and 37 CFR 1.14. This collection is estimated to take 30 minutes to complete, including gathering, preparing, and submitting the completed application form to the USPTO. Time will vary depending upon the individual case. Any comments on the amount of time you require to complete this form and/or suggestions for reducing this burden, should be sent to the Chief Information Officer, U.S. Patent and Trademark Office, U.S. Department of Commerce, P.O. Box 1450, Alexandria, Virginia 22313-1450. DO NOT SEND FEES OR COMPLETED FORMS TO THIS ADDRESS. SEND TO: Commissioner for Patents, P.O. Box 1450, Alexandria, Virginia 22313-1450. Under the Paperwork Reduction Act of 1995, no persons are required to respond to a collection of information unless it displays a valid OMB control number.

Privacy Act Statement

The Privacy Act of 1974 (P.L. 93-579) requires that you be given certain information in connection with your submission of the attached form related to a patent application or patent. Accordingly, pursuant to the requirements of the Act, please be advised that: (1) the general authority for the collection of this information is 35 U.S.C. 2(b)(2); (2) furnishing of the information solicited is voluntary; and (3) the principal purpose for which the information is used by the U.S. Patent and Trademark Office is to process and/or examine your submission related to a patent application or patent. If you do not furnish the requested information, the U.S. Patent and Trademark Office may not be able to process and/or examine your submission, which may result in termination of proceedings or abandonment of the application or expiration of the patent.

The information provided by you in this form will be subject to the following routine uses:

1. The information on this form will be treated confidentially to the extent allowed under the Freedom of Information Act (5 U.S.C. 552) and the Privacy Act (5 U.S.C 552a). Records from this system of records may be disclosed to the Department of Justice to determine whether disclosure of these records is required by the Freedom of Information Act.
2. A record from this system of records may be disclosed, as a routine use, in the course of presenting evidence to a court, magistrate, or administrative tribunal, including disclosures to opposing counsel in the course of settlement negotiations.
3. A record in this system of records may be disclosed, as a routine use, to a Member of Congress submitting a request involving an individual, to whom the record pertains, when the individual has requested assistance from the Member with respect to the subject matter of the record.
4. A record in this system of records may be disclosed, as a routine use, to a contractor of the Agency having need for the information in order to perform a contract. Recipients of information shall be required to comply with the requirements of the Privacy Act of 1974, as amended, pursuant to 5 U.S.C. 552a(m).
5. A record related to an International Application filed under the Patent Cooperation Treaty in this system of records may be disclosed, as a routine use, to the International Bureau of the World Intellectual Property Organization, pursuant to the Patent Cooperation Treaty.
6. A record in this system of records may be disclosed, as a routine use, to another federal agency for purposes of National Security review (35 U.S.C. 181) and for review pursuant to the Atomic Energy Act (42 U.S.C. 218(c)).
7. A record from this system of records may be disclosed, as a routine use, to the Administrator, General Services, or his/her designee, during an inspection of records conducted by GSA as part of that agency's responsibility to recommend improvements in records management practices and programs, under authority of 44 U.S.C. 2904 and 2906. Such disclosure shall be made in accordance with the GSA regulations governing inspection of records for this purpose, and any other relevant (i.e., GSA or Commerce) directive. Such disclosure shall not be used to make determinations about individuals.
8. A record from this system of records may be disclosed, as a routine use, to the public after either publication of the application pursuant to 35 U.S.C. 122(b) or issuance of a patent pursuant to 35 U.S.C. 151. Further, a record may be disclosed, subject to the limitations of 37 CFR 1.14, as a routine use, to the public if the record was filed in an application which became abandoned or in which the proceedings were terminated and which application is referenced by either a published application, an application open to public inspection or an issued patent.
9. A record from this system of records may be disclosed, as a routine use, to a Federal, State, or local law enforcement agency, if the USPTO becomes aware of a violation or potential violation of law or regulation.

Notice of Allowability	Application No. 15/896,389	Applicant(s) Hong et al.	
	Examiner ISAAC SHOMER	Art Unit 1612	AIA (FITF) Status No

-- The MAILING DATE of this communication appears on the cover sheet with the correspondence address--

All claims being allowable, PROSECUTION ON THE MERITS IS (OR REMAINS) CLOSED in this application. If not included herewith (or previously mailed), a Notice of Allowance (PTOL-85) or other appropriate communication will be mailed in due course. **THIS NOTICE OF ALLOWABILITY IS NOT A GRANT OF PATENT RIGHTS.** This application is subject to withdrawal from issue at the initiative of the Office or upon petition by the applicant. See 37 CFR 1.313 and MPEP 1308.

1. ☑ This communication is responsive to Claims on 31 March 2020 and response on 21 May and 1 June 2020.
   ☐ A declaration(s)/affidavit(s) under **37 CFR 1.130(b)** was/were filed on _____.

2. ☐ An election was made by the applicant in response to a restriction requirement set forth during the interview on _____; the restriction requirement and election have been incorporated into this action.

3. ☑ The allowed claim(s) is/are 58-59,61-64,66-69 and 71-72 . As a result of the allowed claim(s), you may be eligible to benefit from the **Patent Prosecution Highway** program at a participating intellectual property office for the corresponding application. For more information, please see **http://www.uspto.gov/patents/init_events/pph/index.jsp** or send an inquiry to **PPHfeedback@uspto.gov.**

4. ☐ Acknowledgment is made of a claim for foreign priority under 35 U.S.C. § 119(a)-(d) or (f).

   Certified copies:

   a) ☐ All b) ☐ Some *c) ☐ None of the:

   1. ☐ Certified copies of the priority documents have been received.
   2. ☐ Certified copies of the priority documents have been received in Application No. _____ .
   3. ☐ Copies of the certified copies of the priority documents have been received in this national stage application from the International Bureau (PCT Rule 17.2(a)).

   * Certified copies not received: _____ .

Applicant has THREE MONTHS FROM THE "MAILING DATE" of this communication to file a reply complying with the requirements noted below. Failure to timely comply will result in ABANDONMENT of this application.
THIS THREE-MONTH PERIOD IS NOT EXTENDABLE.

5. ☐ CORRECTED DRAWINGS (as "replacement sheets") must be submitted.
   ☐ including changes required by the attached Examiner's Amendment / Comment or in the Office action of Paper No./Mail Date _____ .

   Identifying indicia such as the application number (see 37 CFR 1.84(c)) should be written on the drawings in the front (not the back) of each sheet. Replacement sheet(s) should be labeled as such in the header according to 37 CFR 1.121(d).

6. ☐ DEPOSIT OF and/or INFORMATION about the deposit of BIOLOGICAL MATERIAL must be submitted. Note the attached Examiner's comment regarding REQUIREMENT FOR THE DEPOSIT OF BIOLOGICAL MATERIAL.

Attachment(s)

1. ☑ Notice of References Cited (PTO-892)
2. ☐ Information Disclosure Statements (PTO/SB/08), Paper No./Mail Date _____.
3. ☐ Examiner's Comment Regarding Requirement for Deposit of Biological Material _____.
4. ☑ Interview Summary (PTO-413), Paper No./Mail Date. _____.
5. ☐ Examiner's Amendment/Comment
6. ☑ Examiner's Statement of Reasons for Allowance
7. ☐ Other _____.

/ISAAC SHOMER/
Primary Examiner, Art Unit 1612

REASONS FOR ALLOWANCE

The following is an examiner's statement of reasons for allowance:

As close prior art, the examiner cites Chou et al. (Journal of Bioscience and Bioengineering, Vol. 95, No. 4, 2003, pages 405-408), which was previously cited in the office action on 31 January 2020. Chou et al. (hereafter referred to as Chou) is drawn to a liposome comprising irinotecan, which has antitumor activity, as of Chou, page 405, title and abstract. Said liposome includes phospholipids such as phosphatidylcholines, as of Chou, page 405, title.

Chou differs from the instantly claimed invention because Chou does not teach sucrose octasulfate. The examiner takes the position that it would not have been prima facie obvious for the skilled artisan to have added sucrose octasulfate to the liposome of Chou. This determination is made in view of Yeh et al. (Molecular and Cellular Biology, Vol. 22, No. 20, October 2002, pages 7184-7192), which was previously cited on the PTO-892 added to the file record on 26 March 2020. Yeh teaches the following as of page 7184, right column, second paragraph below abstract, relevant text reproduced below with internal citations removed and examiner added text in bold brackets.

> Besides heparin, a number of chemically diverse low-molecular-weight sulfated sugars such as sucrose octasulfate (SOS) have been reported to potentiate FGF **[Examiner Note: FGF is fibroblast growth factor]** action. SOS has been shown to mimic heparin action in supporting FGF-induced neoangiogenesis and cell proliferation in vitro. Moreover, SOS facilitates wound healing by enhancing FGF-induced angiogenesis.

The skilled artisan would not have desired to have induced proliferation and neoangiogenesis when treating cancer. In the case of cancer, the skilled artisan would not have desired cell proliferation; this is because cancer is undesired overproliferation of cells. If the proliferating cells were cancer cells, then cell proliferation would have made cancer worse. In fact, in the case of treating cancer, the skilled artisan would have been motivated to have administered an agent that combats cell proliferation rather than an agent that causes cell proliferation.

Similarly, the skilled artisan would not have desired neoangiogenesis when treating cancer. The examiner notes that the term “neoangiogenesis” refers to the development of new blood vessels. The skilled artisan would not have desired the formation of new blood vessels at the site of a cancerous tumor as this would help the tumor get oxygen and nutrients and thereby would help the tumor grow.

As such, the skilled artisan would not have been motivated to have combined the composition of Chou, which is intended to treat cancer, with sucrose octasulfate. This is because, according to the teachings of Yeh indicates that sucrose octasulfate causes proliferation and neoangiogenesis, both of which would have been expected to have made cancer worse. It is improper to combine references where the references teach away from their combination. See MPEP 2145(X)(D)(2). In this case, that the teachings of Yeh indicate that sucrose octasulfate would have made cancer worse when Chou is trying to treat cancer indicate that the prior art teaches away from combining sucrose octasulfate with an irinotecan-containing liposome intended to treat cancer. Additionally, applicant proceeded against the accepted wisdom when adding sucrose octasulfate to an irinotecan-containing liposome intended to treat cancer. The totality of the prior art

must be considered, and proceeding contrary to accepted wisdom in the art is evidence of nonobviousness. See MPEP 2145(X)(D)(3).

With regard to the issue of double patenting, the examiner notes that there are a number of cases in the instant case family over which no double patenting rejections have been written and over which there is no terminal disclaimer. The examiner has noted the relevant references below and explained why no double patenting rejection is written in the table on the next page.

Patent	Explanation
8,329,213	Claims of '213 patent do not recite required lipid combination.
8,703,181	Claims of '181 patent do not recite required lipid combination.
8,658,203	Claims of '203 patent do not recite required lipid combination.
10,350,201	Claims of '201 patent do not recite sucrose octasulfate.
10,413,510	Claims of '510 patent do not recite sucrose octasulfate.

The examiner notes that the explanations here supersede explanations provided in the prior office action on 18 July 2019. This is due to claim amendments that have occurred on 17 January and 31 March 2020 that render the explanations provided in the prior office action on 18 July 2019 to be moot.

Any comments considered necessary by applicant must be submitted no later than the payment of the issue fee and, to avoid processing delays, should preferably accompany the issue fee. Such submissions should be clearly labeled "Comments on Statement of Reasons for Allowance."

Terminal Disclaimers

The terminal disclaimers filed on 21 May 2020 disclaiming the terminal portion of any patent granted on this application which would extend beyond the expiration date of the following patents and applications:

US application 15/664,970

US Patent 8,147,867

US Patent 9,737,528

US Patent 9,730,891

US Patent 9,717,723

US Patent 8,992,970

US Patent 9,724,303

US Patent 10,456,360

have been reviewed and is accepted. The terminal disclaimers have been recorded.

The terminal disclaimer filed on 1 June 2020 disclaiming the terminal portion of any patent granted on this application which would extend beyond the expiration date of **US Patent 9,782,349** has been reviewed and is accepted. The terminal disclaimer has been recorded.

Conclusion

Any inquiry concerning this communication or earlier communications from the examiner should be directed to ISAAC SHOMER whose telephone number is (571)270-7671. The examiner can normally be reached on 7:30 AM to 5:00 PM Monday Through Friday.

Examiner interviews are available via telephone, in-person, and video conferencing using a USPTO supplied web-based collaboration tool. To schedule an interview, applicant is encouraged to use the USPTO Automated Interview Request (AIR) at http://www.uspto.gov/interviewpractice.

If attempts to reach the examiner by telephone are unsuccessful, the examiner's supervisor, Frederick F Krass can be reached on (571)272-0580. The fax phone number for the organization where this application or proceeding is assigned is 571-273-8300.

Information regarding the status of an application may be obtained from the Patent Application Information Retrieval (PAIR) system. Status information for published applications may be obtained from either Private PAIR or Public PAIR. Status information for unpublished applications is available through Private PAIR only. For more information about the PAIR system, see https://ppair-my.uspto.gov/pair/PrivatePair. Should you have questions on access to the Private PAIR system, contact the Electronic Business Center (EBC) at 866-217-9197 (toll-free). If you would like assistance from a USPTO Customer Service Representative or access to the automated information system, call 800-786-9199 (IN USA OR CANADA) or 571-272-1000.

ISAAC . SHOMER
Primary Examiner
Art Unit 1612

/ISAAC SHOMER/
Primary Examiner, Art Unit 1612

Examiner-Initiated Interview Summary	Application No. 15/896,389	Applicant(s) Hong et al.		
	Examiner ISAAC SHOMER	Art Unit 1612	AIA (First Inventor to File) Status No	Page 1 of 2

All participants (applicant, applicants representative, PTO personnel):

1. ISAAC SHOMER (Primary Examiner); Telephonic 2. Deborah Herzfeld (Attomey of Record); Telephonic

Date of Interview: 29 May 2020

Claims Discussed: 58-59, 61-64, 66-69, 71-72

Prior Art Discussed: US Patent 9,782,349

Brief Description of the main topic(s) of discussion: Examiner requested terminal disclaimer to US Patent 9,782,349. Applicant filed this terminal disclaimer.

Issues Discussed:

Double Patenting:
In a phone message to representative of applicant on 29 May 2020, examiner took the position that a terminal disclaimer to US Patent 9,782,349 is needed to overcome double patenting issues over this patent. Applicant filed this terminal disclaimer on 1 June 2020. As such, this application is in condition for allowance.

The examiner notes that there was text in the office action on 18 July 2019, paragraph bridging pages 21-22, in which examiner has explained why no double patenting rejection had been written over the claims of US Patent 9,782,349. The examiner currently takes the position that the text in the office action on 18 July 2019, paragraph bridging pages 21-22 is not applicable to the currently pending claims in view of claim amendments that occurred on 17 January and 31 March 2020, which was after the mailing of the office action on 18 July 2019. These claim amendments render moot the position previously taken by the examiner in the office action on 18 July 2019, paragraph bridging pages 21-22.

Attachment(s): Other Attachment
{Notice of Allowance}

/ISAAC SHOMER/ Primary Examiner, Art Unit 1612	

Applicant is reminded that a complete written statement as to the substance of the interview must be made of record in the application file. It is the applicants responsibility to provide the written statement, unless the interview was initiated by the Examiner and the Examiner has indicated that a written summary will be provided. See MPEP 713.04
Please further see:
MPEP 713.04
Title 37 Code of Federal Regulations (CFR) § 1.133 Interviews, paragraph (b)
37 CFR § 1.2 Business to be transacted in writing

Applicant recordation instructions: It is not necessary for applicant to provide a separate record of the substance of interview .

Examiner recordation instructions: Examiners must summarize the substance of any interview of record. A complete and proper recordation of the substance of an interview should include the items listed in MPEP 713.04 for complete and proper recordation including the identification of the general thrust of each argument or issue discussed, a general indication of any other pertinent matters discussed regarding patentability and the general results or outcome of the interview, to include an indication as to whether or not agreement was reached on the issues raised.

UNITED STATES PATENT AND TRADEMARK OFFICE

UNITED STATES DEPARTMENT OF COMMERCE
United States Patent and Trademark Office
Address: COMMISSIONER FOR PATENTS
P.O. Box 1450
Alexandria, Virginia 22313-1450
www.uspto.gov

APPLICATION NO.	FILING DATE	FIRST NAMED INVENTOR	ATTORNEY DOCKET NO.	CONFIRMATION NO.
16/012,351	06/19/2018	Eliel Bayever	01208-0002-10US	3260

153749 7590 01/07/2020

McNeill Baur PLLC/Ipsen
Ipsen Bioscience, Inc.
125 Cambridge Park Drive
Suite 301
Cambridge, MA 02140

EXAMINER	
STRONG, TORI	

ART UNIT	PAPER NUMBER
1629	

NOTIFICATION DATE	DELIVERY MODE
01/07/2020	ELECTRONIC

Please find below and/or attached an Office communication concerning this application or proceeding.

The time period for reply, if any, is set in the attached communication.

Notice of the Office communication was sent electronically on above-indicated "Notification Date" to the following e-mail address(es):

docketing@mcneillbaur.com
eofficeaction@appcoll.com
patents.us@ipsen.com

Office Action Summary	Application No. 16/012,351	Applicant(s) Bayever et al.	
	Examiner TORI STRONG	Art Unit 1629	AIA (FITF) Status No

-- The MAILING DATE of this communication appears on the cover sheet with the correspondence address --

Period for Reply

A SHORTENED STATUTORY PERIOD FOR REPLY IS SET TO EXPIRE 3 MONTHS FROM THE MAILING DATE OF THIS COMMUNICATION.

- Extensions of time may be available under the provisions of 37 CFR 1.136(a). In no event, however, may a reply be timely filed after SIX (6) MONTHS from the mailing date of this communication.
- If NO period for reply is specified above, the maximum statutory period will apply and will expire SIX (6) MONTHS from the mailing date of this communication.
- Failure to reply within the set or extended period for reply will, by statute, cause the application to become ABANDONED (35 U.S.C. § 133). Any reply received by the Office later than three months after the mailing date of this communication, even if timely filed, may reduce any earned patent term adjustment. See 37 CFR 1.704(b).

Status

1)☑ Responsive to communication(s) filed on 06 September 2019.

☐ A declaration(s)/affidavit(s) under **37 CFR 1.130(b)** was/were filed on _____.

2a)☑ This action is **FINAL.** 2b) ☐ This action is non-final.

3)☐ An election was made by the applicant in response to a restriction requirement set forth during the interview on _____; the restriction requirement and election have been incorporated into this action.

4)☐ Since this application is in condition for allowance except for formal matters, prosecution as to the merits is closed in accordance with the practice under *Ex parte Quayle*, 1935 C.D. 11, 453 O.G. 213.

Disposition of Claims*

5) ☑ Claim(s) 21-32 is/are pending in the application.

5a) Of the above claim(s) _____ is/are withdrawn from consideration.

6) ☐ Claim(s) _____ is/are allowed.

7) ☑ Claim(s) 21-32 is/are rejected.

8) ☐ Claim(s) _____ is/are objected to.

9) ☐ Claim(s) _____ are subject to restriction and/or election requirement

* If any claims have been determined allowable, you may be eligible to benefit from the **Patent Prosecution Highway** program at a participating intellectual property office for the corresponding application. For more information, please see http://www.uspto.gov/patents/init_events/pph/index.jsp or send an inquiry to **PPHfeedback@uspto.gov.**

Application Papers

10)☐ The specification is objected to by the Examiner.

11)☐ The drawing(s) filed on _____ is/are: a)☐ accepted or b)☐ objected to by the Examiner.

Applicant may not request that any objection to the drawing(s) be held in abeyance. See 37 CFR 1.85(a).

Replacement drawing sheet(s) including the correction is required if the drawing(s) is objected to. See 37 CFR 1.121(d).

Priority under 35 U.S.C. § 119

12)☐ Acknowledgment is made of a claim for foreign priority under 35 U.S.C. § 119(a)-(d) or (f).

Certified copies:

a)☐ All b)☐ Some** c)☐ None of the:

1.☐ Certified copies of the priority documents have been received.

2.☐ Certified copies of the priority documents have been received in Application No. _____.

3.☐ Copies of the certified copies of the priority documents have been received in this National Stage application from the International Bureau (PCT Rule 17.2(a)).

** See the attached detailed Office action for a list of the certified copies not received.

Attachment(s)

1) ☐ Notice of References Cited (PTO-892)

2) ☑ Information Disclosure Statement(s) (PTO/SB/08a and/or PTO/SB/08b) Paper No(s)/Mail Date _____.

3) ☐ Interview Summary (PTO-413) Paper No(s)/Mail Date _____.

4) ☐ Other: _____.

DETAILED ACTION

Notice of Pre-AIA or AIA Status

The present application is being examined under the pre-AIA first to invent provisions.

Status of Claims

Claims 21-32 are pending in the instant application; claims 1-20 are cancelled; claims 21-32 are newly presented and are the subject of the Office Action below.

Information Disclosure Statement

The information disclosure statements (IDSs) submitted on 9/18/2019 and 11/04/2019 were filed after the mailing date of the application on June 19, 2018. The submission is in compliance with the provisions of 37 CFR 1.97. Accordingly, the information disclosure statement is being considered by the examiner. Enclosed with this Office Action are return copies of Form PTO/SB/08B with the Examiner's initials and signature indicating those references that have been considered.

Examination Considerations

Applicant's Amendments filed September 6, 2019 have been received and entered into the present application. Claims 21-32 are pending and are herein examined on the merits.

Applicant's Arguments, filed September 6, 2019 have been fully considered. Rejections not reiterated from previous Office Actions are hereby withdrawn. The following rejections are either reiterated or newly applied. They constitute the complete set of rejections presently being applied to the instant application.

Claim Rejections - 35 USC § 103 - Withdrawn

Claims 1-5 rejected under pre-AIA 35 U.S.C. 103(a) as being unpatentable over Kozuch *et al.* (*The Oncologist*, 2001, 6, pp. 488-495; cited in IDS) and Tsai *et al.* (*Journal of Gastrointestinal Oncology*, 2011, Vol. 2, No. 3, pp. 185-194; cited in IDS) in view of The American Cancer Society (ACS) (http://www.cancer.org/cancer/pancreaticcancer/detailedguide/pancreatic-cancer-what-is-pancreatic-cancer; cited in IDS) is ***withdrawn***.

Claims 6-20 rejected under pre-AIA 35 U.S.C. 103(a) as being unpatentable over Kozuch *et al.* (*The Oncologist*, 2001, 6, pp. 488-495; cited in IDS) and Tsai *et al.* *(Journal of Gastrointestinal Oncology*, 2011, Vol. 2, No. 3, pp. 185-194; cited in IDS) in view of American Cancer Society (ACS) (http://www.cancer.org/cancer/pancreaticcancer/detailedguide/pancreatic-cancer-what-is-pancreatic-cancer; cited in IDS), in further view of Yoo *et al.* (*British Journal of Cancer*, 2009, 101, pp. 1658-1663; cited in IDS) is ***withdrawn***.

Applicant has cancelled claims 1-20 thus rendering the rejections moot. Subsequent to cancellation, the rejections are withdrawn.

Double Patenting - Withdrawn

Claims 1-20 rejected on the ground of nonstatutory double patenting as being unpatentable over claims 1-11, 19-24 and 30-35 of U.S. Patent No. 9,452,162 B2; claims 1-20 and 23-28 of U.S. Patent No. 9,492,442; claims 1-27 of U.S. Patent No. 9,339,497; claims 1-29 of U.S. Patent No. 9,364,473 B2; and claims 1-24 of U.S. Patent No. 9,717,724 B2 is ***withdrawn***.

Claims 1-20 provisionally rejected on the ground of nonstatutory double patenting as being unpatentable over claims 1-20 of copending Application No. 16/012,372 is ***withdrawn***.

Applicant has cancelled claims 1-20 thus rendering the rejections moot. Subsequent to cancellation, the rejections are withdrawn.

Double Patenting – New Grounds (Necessitated by Amendment)

The nonstatutory double patenting rejection is based on a judicially created doctrine grounded in public policy (a policy reflected in the statute) so as to prevent the unjustified or improper timewise extension of the "right to exclude" granted by a patent and to prevent possible harassment by multiple assignees. A nonstatutory double patenting rejection is appropriate where the conflicting claims are not identical, but at least one examined application claim is not patentably distinct from the reference claim(s) because the examined application claim is either anticipated by, or would have

been obvious over, the reference claim(s). See, e.g., *In re Berg*, 140 F.3d 1428, 46 USPQ2d 1226 (Fed. Cir. 1998); *In re Goodman*, 11 F.3d 1046, 29 USPQ2d 2010 (Fed. Cir. 1993); *In re Longi*, 759 F.2d 887, 225 USPQ 645 (Fed. Cir. 1985); *In re Van Ornum*, 686 F.2d 937, 214 USPQ 761 (CCPA 1982); *In re Vogel*, 422 F.2d 438, 164 USPQ 619 (CCPA 1970); *In re Thorington*, 418 F.2d 528, 163 USPQ 644 (CCPA 1969).

A timely filed terminal disclaimer in compliance with 37 CFR 1.321(c) or 1.321(d) may be used to overcome an actual or provisional rejection based on nonstatutory double patenting provided the reference application or patent either is shown to be commonly owned with the examined application, or claims an invention made as a result of activities undertaken within the scope of a joint research agreement. See MPEP § 717.02 for applications subject to examination under the first inventor to file provisions of the AIA as explained in MPEP § 2159. See MPEP §§ 706.02(l)(1) - 706.02(l)(3) for applications not subject to examination under the first inventor to file provisions of the AIA. A terminal disclaimer must be signed in compliance with 37 CFR 1.321(b).

The USPTO Internet website contains terminal disclaimer forms which may be used. Please visit www.uspto.gov/patent/patents-forms. The filing date of the application in which the form is filed determines what form (e.g., PTO/SB/25, PTO/SB/26, PTO/AIA/25, or PTO/AIA/26) should be used. A web-based eTerminal Disclaimer may be filled out completely online using web-screens. An eTerminal Disclaimer that meets all requirements is auto-processed and approved immediately upon submission. For more information about eTerminal Disclaimers, refer to www.uspto.gov/patents/process/file/efs/guidance/eTD-info-I.jsp.

Claims 21-32 are rejected on the ground of nonstatutory double patenting as being unpatentable over claims 1-11, 19-24 and 30-35 of U.S. Patent No. 9,452,162 B2; claims 1-20 and 23-28 of U.S. Patent No. 9,492,442; claims 1-27 of U.S. Patent No. 9,339,497; claims 1-29 of U.S. Patent No. 9,364,473 B2; and claims 1-24 of U.S. Patent No. 9,717,724 B2. Although the claims at issue are not identical, they are not patentably distinct from each other because each of the disclosures set out to claim a method of treating pancreatic cancer refractory to gemcitabine therapy through intravenous administration of irinotecan as the MM-398 liposome, leucovorin as the (l)-form or racemic form and 5-fluorouracil. Each of the disclosures claim the combination in either a similar or identical dose for the therapeutic agents where the combination is administered in a two week cycle. The claims are obvious variants of each other.

Claims 21-32 are provisionally rejected on the ground of nonstatutory double patenting as being unpatentable over claims 21-41 of copending Application No. 16/012,372. Although the claims at issue are not identical, they are not patentably distinct from each other because each disclosure sets out to claim a method of treating pancreatic cancer refractory to gemcitabine therapy through intravenous administration of liposomal irinotecan in overlapping dosing range with leucovorin as the (l)-form or racemic form and 5-fluorouracil. The claims are obvious variants.

This is a provisional nonstatutory double patenting rejection because the patentably indistinct claims have not in fact been patented.

Conclusion

THIS ACTION IS MADE FINAL. Applicant is reminded of the extension of time policy as set forth in 37 CFR 1.136(a).

A shortened statutory period for reply to this final action is set to expire THREE MONTHS from the mailing date of this action. In the event a first reply is filed within TWO MONTHS of the mailing date of this final action and the advisory action is not mailed until after the end of the THREE-MONTH shortened statutory period, then the shortened statutory period will expire on the date the advisory action is mailed, and any extension fee pursuant to 37 CFR 1.136(a) will be calculated from the mailing date of the advisory action. In no event, however, will the statutory period for reply expire later than SIX MONTHS from the mailing date of this final action.

Any inquiry concerning this communication or earlier communications from the examiner should be directed to TORI STRONG whose telephone number is (571)272-6333. The examiner can normally be reached on Monday - Friday 8:00 am - 5:00 pm (EST).

Examiner interviews are available via telephone, in-person, and video conferencing using a USPTO supplied web-based collaboration tool. To schedule an interview, applicant is encouraged to use the USPTO Automated Interview Request (AIR) at http://www.uspto.gov/interviewpractice.

If attempts to reach the examiner by telephone are unsuccessful, the examiner's supervisor, Jeffrey Lundgren can be reached on (571)272-5541. The fax phone number for the organization where this application or proceeding is assigned is 571-273-8300.

Information regarding the status of an application may be obtained from the Patent Application Information Retrieval (PAIR) system. Status information for published applications may be obtained from either Private PAIR or Public PAIR. Status information for unpublished applications is available through Private PAIR only. For more information about the PAIR system, see http://pair-direct.uspto.gov. Should you have questions on access to the Private PAIR system, contact the Electronic Business Center (EBC) at 866-217-9197 (toll-free). If you would like assistance from a USPTO Customer Service Representative or access to the automated information system, call 800-786-9199 (IN USA OR CANADA) or 571-272-1000.

TORI STRONG
Examiner
Art Unit 1629

/TORI STRONG/
Examiner, Art Unit 1629

/JEFFREY S LUNDGREN/
Supervisory Patent Examiner, Art Unit 1629

UNITED STATES PATENT AND TRADEMARK OFFICE

UNITED STATES DEPARTMENT OF COMMERCE
United States Patent and Trademark Office
Address: COMMISSIONER FOR PATENTS
P.O. Box 1450
Alexandria, Virginia 22313-1450
www.uspto.gov

APPLICATION NO.	FILING DATE	FIRST NAMED INVENTOR	ATTORNEY DOCKET NO.	CONFIRMATION NO.
16/012,372	06/19/2018	Eliel Bayever	01208-0002-11US	1003

153749 7590 01/07/2020

McNeill Baur PLLC/Ipsen
Ipsen Bioscience, Inc.
125 Cambridge Park Drive
Suite 301
Cambridge, MA 02140

EXAMINER	
STRONG, TORI	

ART UNIT	PAPER NUMBER
1629	

NOTIFICATION DATE	DELIVERY MODE
01/07/2020	ELECTRONIC

Please find below and/or attached an Office communication concerning this application or proceeding.

The time period for reply, if any, is set in the attached communication.

Notice of the Office communication was sent electronically on above-indicated "Notification Date" to the following e-mail address(es):

docketing@mcneillbaur.com
eofficeaction@appcoll.com
patents.us@ipsen.com

Office Action Summary	Application No. 16/012,372	Applicant(s) Bayever et al.	
	Examiner TORI STRONG	Art Unit 1629	AIA (FITF) Status Yes

-- The MAILING DATE of this communication appears on the cover sheet with the correspondence address --

Period for Reply

A SHORTENED STATUTORY PERIOD FOR REPLY IS SET TO EXPIRE 3 MONTHS FROM THE MAILING DATE OF THIS COMMUNICATION.

- Extensions of time may be available under the provisions of 37 CFR 1.136(a). In no event, however, may a reply be timely filed after SIX (6) MONTHS from the mailing date of this communication.
- If NO period for reply is specified above, the maximum statutory period will apply and will expire SIX (6) MONTHS from the mailing date of this communication.
- Failure to reply within the set or extended period for reply will, by statute, cause the application to become ABANDONED (35 U.S.C. § 133). Any reply received by the Office later than three months after the mailing date of this communication, even if timely filed, may reduce any earned patent term adjustment. See 37 CFR 1.704(b).

Status

1)☑ Responsive to communication(s) filed on 06 September 2019.

☐ A declaration(s)/affidavit(s) under **37 CFR 1.130(b)** was/were filed on _____.

2a)☑ This action is **FINAL.** 2b) ☐ This action is non-final.

3)☐ An election was made by the applicant in response to a restriction requirement set forth during the interview on _____; the restriction requirement and election have been incorporated into this action.

4)☐ Since this application is in condition for allowance except for formal matters, prosecution as to the merits is closed in accordance with the practice under *Ex parte Quayle*, 1935 C.D. 11, 453 O.G. 213.

Disposition of Claims*

5) ☑ Claim(s) 21-41 is/are pending in the application.

5a) Of the above claim(s) _____ is/are withdrawn from consideration.

6) ☐ Claim(s) _____ is/are allowed.

7) ☑ Claim(s) 21-41 is/are rejected.

8) ☐ Claim(s) _____ is/are objected to.

9) ☐ Claim(s) _____ are subject to restriction and/or election requirement

* If any claims have been determined allowable, you may be eligible to benefit from the **Patent Prosecution Highway** program at a participating intellectual property office for the corresponding application. For more information, please see http://www.uspto.gov/patents/init_events/pph/index.jsp or send an inquiry to **PPHfeedback@uspto.gov.**

Application Papers

10)☐ The specification is objected to by the Examiner.

11)☐ The drawing(s) filed on _____ is/are: a)☐ accepted or b)☐ objected to by the Examiner.

Applicant may not request that any objection to the drawing(s) be held in abeyance. See 37 CFR 1.85(a).

Replacement drawing sheet(s) including the correction is required if the drawing(s) is objected to. See 37 CFR 1.121(d).

Priority under 35 U.S.C. § 119

12)☐ Acknowledgment is made of a claim for foreign priority under 35 U.S.C. § 119(a)-(d) or (f).

Certified copies:

a)☐ All b)☐ Some** c)☐ None of the:

1.☐ Certified copies of the priority documents have been received.

2.☐ Certified copies of the priority documents have been received in Application No. _____.

3.☐ Copies of the certified copies of the priority documents have been received in this National Stage application from the International Bureau (PCT Rule 17.2(a)).

** See the attached detailed Office action for a list of the certified copies not received.

Attachment(s)

1) ☐ Notice of References Cited (PTO-892)

2) ☑ Information Disclosure Statement(s) (PTO/SB/08a and/or PTO/SB/08b) Paper No(s)/Mail Date _____.

3) ☐ Interview Summary (PTO-413) Paper No(s)/Mail Date _____.

4) ☐ Other: _____.

DETAILED ACTION

Notice of Pre-AIA or AIA Status

The present application, filed on or after March 16, 2013, is being examined under the first inventor to file provisions of the AIA.

Status of Claims

Claims 21-41 are pending in the instant application; claims 1-20 are cancelled; claims 21-41 are newly presented; claims 21-41 are the subject of the Office Action below.

Information Disclosure Statement

The information disclosure statements (IDSs) submitted on 9/18/2019 and 11/04/2019 were filed after the mailing date of the application on June 19, 2018. The submission is in compliance with the provisions of 37 CFR 1.97. Accordingly, the information disclosure statement is being considered by the examiner. Enclosed with this Office Action are return copies of Form PTO/SB/08B with the Examiner's initials and signature indicating those references that have been considered.

Examination Considerations

Applicant's Amendments filed September 6, 2019 have been received and entered into the present application. Claims 21-41 are pending and are herein examined on the merits.

Applicant's Arguments, filed September 6, 2019 have been fully considered. Rejections not reiterated from previous Office Actions are hereby withdrawn. The following rejections are either reiterated or newly applied. They constitute the complete set of rejections presently being applied to the instant application.

Double Patenting - Withdrawn

Claims 1-20 rejected under 35 U.S.C. 101 as claiming the same invention as that of claims 1-20 of prior U.S. Patent No. 9,717,724 B2. This is a statutory double patenting rejection is ***withdrawn***.

Claims 1-20 rejected on the ground of nonstatutory double patenting as being unpatentable over claims 1-27 of U.S. Patent No. 9,339,497 B2; claims 1-29 of U.S. Patent No. 9,364,473 B2; claims 1-35 of U.S. Patent No. 9,452,162 B2; and claims 1-30 of U.S. Patent No. 9,492,442 B2; and claims 1-24 of U.S. Patent No. 9,717,724 B2 is ***withdrawn***.

Claims 1-20 provisionally rejected on the ground of nonstatutory double patenting as being unpatentable over claims 1-20 of copending Application No. 16/012,351 is ***withdrawn***.

Applicant has cancelled claims 1-20 thus rendering the rejections moot. Subsequent to cancellation, the rejections are withdrawn.

Double Patenting – New Grounds (Necessitated by Amendment)

The nonstatutory double patenting rejection is based on a judicially created doctrine grounded in public policy (a policy reflected in the statute) so as to prevent the unjustified or improper timewise extension of the "right to exclude" granted by a patent and to prevent possible harassment by multiple assignees. A nonstatutory double patenting rejection is appropriate where the conflicting claims are not identical, but at least one examined application claim is not patentably distinct from the reference claim(s) because the examined application claim is either anticipated by, or would have been obvious over, the reference claim(s). See, e.g., *In re Berg*, 140 F.3d 1428, 46 USPQ2d 1226 (Fed. Cir. 1998); *In re Goodman*, 11 F.3d 1046, 29 USPQ2d 2010 (Fed. Cir. 1993); *In re Longi*, 759 F.2d 887, 225 USPQ 645 (Fed. Cir. 1985); *In re Van Ornum*, 686 F.2d 937, 214 USPQ 761 (CCPA 1982); *In re Vogel*, 422 F.2d 438, 164 USPQ 619 (CCPA 1970); *In re Thorington*, 418 F.2d 528, 163 USPQ 644 (CCPA 1969).

A timely filed terminal disclaimer in compliance with 37 CFR 1.321(c) or 1.321(d) may be used to overcome an actual or provisional rejection based on nonstatutory double patenting provided the reference application or patent either is shown to be commonly owned with the examined application, or claims an invention made as a result of activities undertaken within the scope of a joint research agreement. See MPEP § 717.02 for applications subject to examination under the first inventor to file provisions of the AIA as explained in MPEP § 2159. See MPEP §§ 706.02(l)(1) - 706.02(l)(3) for applications not subject to examination under the first inventor to file provisions of the AIA. A terminal disclaimer must be signed in compliance with 37 CFR 1.321(b).

The USPTO Internet website contains terminal disclaimer forms which may be used. Please visit www.uspto.gov/patent/patents-forms. The filing date of the application in which the form is filed determines what form (e.g., PTO/SB/25, PTO/SB/26, PTO/AIA/25, or PTO/AIA/26) should be used. A web-based eTerminal Disclaimer may be filled out completely online using web-screens. An eTerminal Disclaimer that meets all requirements is auto-processed and approved immediately upon submission. For more information about eTerminal Disclaimers, refer to www.uspto.gov/patents/process/file/efs/guidance/eTD-info-I.jsp.

Claims 21-41 are rejected on the ground of nonstatutory double patenting as being unpatentable over claims 1-27 of U.S. Patent No. 9,339,497 B2; claims 1-29 of U.S. Patent No. 9,364,473 B2; claims 1-35 of U.S. Patent No. 9,452,162 B2; and claims 1-30 of U.S. Patent No. 9,492,442 B2; and claims 1-24 of U.S. Patent No. 9,717,724 B2. Although the claims at issue are not identical, they are not patentably distinct from each other because each disclosure sets out to claim treatment of pancreatic cancer with the antiproliferative therapeutic regimen that consist of liposomal irinotecan at a dosing of 60, 70 or 80 mg/m^2; leucovorin (*l*-form) at a dose if 200 mg/m^2; and 5-fluorouracil at a dose of 2,400 mg/m^2. Each disclosure teaches and claims treating patients refractory to gemcitabine therapy and treating patients who either are or not homozygous for the UGT1 A1*28 allele. The closest prior art, as indicated in the record of previous case App. No. 14/812,950 (now patented U.S. Patent No. 9,339,497 B2) is found in Yoo *et al.* (*British Journal of Cancer*, 2009, 101, pp. 1658-163); where Yoo teaches treating pancreatic cancer refractory to gemcitabine therapy with the

mFOIRIRI.3 regimen that consists of irinotecan, leucovorin and 5-fluorouracil. However, Yoo requires different dosing and that irinotecan is administered twice where the therapy provides the overall survival for the mFOIRIRI.3 regimen to be 16.6 weeks (or 4.2 months). The instantly claimed invention carves out a specific regimen that requires the dosing of the components and administers the drugs only once within a cycle and further provides for the unexpected result of improving clinical benefit of up to 80% and the increasing the patient population survival of at least 6 months. Therefore the claims are free of the art. However, the claims are obvious variants of the previously patented subject matter and therefore the nonstatutory double patenting rejection is applied.

Claims 21-41 are provisionally rejected on the ground of nonstatutory double patenting as being unpatentable over claims 21-32 of copending Application No. 16/012,351. Although the claims at issue are not identical, they are not patentably distinct from each other because each disclosure claims treating patients with pancreatic cancer refractory to gemcitabine therapy and treating patients the same general combination with overlapping dosing of liposomal irinotecan. The claims are obvious variants.

This is a provisional nonstatutory double patenting rejection because the patentably indistinct claims have not in fact been patented.

Conclusion

THIS ACTION IS MADE FINAL. Applicant is reminded of the extension of time policy as set forth in 37 CFR 1.136(a).

A shortened statutory period for reply to this final action is set to expire THREE MONTHS from the mailing date of this action. In the event a first reply is filed within TWO MONTHS of the mailing date of this final action and the advisory action is not mailed until after the end of the THREE-MONTH shortened statutory period, then the shortened statutory period will expire on the date the advisory action is mailed, and any extension fee pursuant to 37 CFR 1.136(a) will be calculated from the mailing date of the advisory action. In no event, however, will the statutory period for reply expire later than SIX MONTHS from the mailing date of this final action.

Any inquiry concerning this communication or earlier communications from the examiner should be directed to TORI STRONG whose telephone number is (571)272-6333. The examiner can normally be reached on Monday - Friday 8:00 am - 5:00 pm (EST).

Examiner interviews are available via telephone, in-person, and video conferencing using a USPTO supplied web-based collaboration tool. To schedule an interview, applicant is encouraged to use the USPTO Automated Interview Request (AIR) at http://www.uspto.gov/interviewpractice.

If attempts to reach the examiner by telephone are unsuccessful, the examiner's supervisor, Jeffrey Lundgren can be reached on (571)272-5541. The fax phone number for the organization where this application or proceeding is assigned is 571-273-8300.

Information regarding the status of an application may be obtained from the Patent Application Information Retrieval (PAIR) system. Status information for published applications may be obtained from either Private PAIR or Public PAIR. Status information for unpublished applications is available through Private PAIR only.

For more information about the PAIR system, see http://pair-direct.uspto.gov. Should you have questions on access to the Private PAIR system, contact the Electronic Business Center (EBC) at 866-217-9197 (toll-free). If you would like assistance from a USPTO Customer Service Representative or access to the automated information system, call 800-786-9199 (IN USA OR CANADA) or 571-272-1000.

TORI STRONG
Examiner
Art Unit 1629

/TORI STRONG/
Examiner, Art Unit 1629

/JEFFREY S LUNDGREN/
Supervisory Patent Examiner, Art Unit 1629

UNITED STATES PATENT AND TRADEMARK OFFICE

UNITED STATES DEPARTMENT OF COMMERCE
United States Patent and Trademark Office
Address: COMMISSIONER FOR PATENTS
P.O. Box 1450
Alexandria, Virginia 22313-1450
www.uspto.gov

APPLICATION NO.	FILING DATE	FIRST NAMED INVENTOR	ATTORNEY DOCKET NO.	CONFIRMATION NO.
16/012,372	06/19/2018	Eliel Bayever	01208-0002-11US	1003

153749 7590 07/27/2020

McNeill Baur PLLC/Ipsen
Ipsen Bioscience, Inc.
125 Cambridge Park Drive
Suite 301
Cambridge, MA 02140

EXAMINER	
STRONG, TORI	

ART UNIT	PAPER NUMBER
1629	

NOTIFICATION DATE	DELIVERY MODE
07/27/2020	ELECTRONIC

Please find below and/or attached an Office communication concerning this application or proceeding.

The time period for reply, if any, is set in the attached communication.

Notice of the Office communication was sent electronically on above-indicated "Notification Date" to the following e-mail address(es):

docketing@mcneillbaur.com
eofficeaction@appcoll.com
patents.us@ipsen.com

Office Action Summary	Application No. 16/012,372	Applicant(s) Bayever et al.	
	Examiner TORI STRONG	Art Unit 1629	AIA (FITF) Status Yes

-- The MAILING DATE of this communication appears on the cover sheet with the correspondence address --

Period for Reply

A SHORTENED STATUTORY PERIOD FOR REPLY IS SET TO EXPIRE 3 MONTHS FROM THE MAILING DATE OF THIS COMMUNICATION.

- Extensions of time may be available under the provisions of 37 CFR 1.136(a). In no event, however, may a reply be timely filed after SIX (6) MONTHS from the mailing date of this communication.
- If NO period for reply is specified above, the maximum statutory period will apply and will expire SIX (6) MONTHS from the mailing date of this communication.
- Failure to reply within the set or extended period for reply will, by statute, cause the application to become ABANDONED (35 U.S.C. § 133). Any reply received by the Office later than three months after the mailing date of this communication, even if timely filed, may reduce any earned patent term adjustment. See 37 CFR 1.704(b).

Status

1)☑ Responsive to communication(s) filed on 02 July 2020.

☐ A declaration(s)/affidavit(s) under **37 CFR 1.130(b)** was/were filed on _____.

2a)☐ This action is **FINAL.** 2b) ☑ This action is non-final.

3)☐ An election was made by the applicant in response to a restriction requirement set forth during the interview on _____; the restriction requirement and election have been incorporated into this action.

4)☐ Since this application is in condition for allowance except for formal matters, prosecution as to the merits is closed in accordance with the practice under *Ex parte Quayle*, 1935 C.D. 11, 453 O.G. 213.

Disposition of Claims*

5) ☑ Claim(s) 42-54 is/are pending in the application.

5a) Of the above claim(s) _____ is/are withdrawn from consideration.

6) ☐ Claim(s) _____ is/are allowed.

7) ☑ Claim(s) 42-54 is/are rejected.

8) ☐ Claim(s) _____ is/are objected to.

9) ☐ Claim(s) _____ are subject to restriction and/or election requirement

* If any claims have been determined allowable, you may be eligible to benefit from the **Patent Prosecution Highway** program at a participating intellectual property office for the corresponding application. For more information, please see http://www.uspto.gov/patents/init_events/pph/index.jsp or send an inquiry to **PPHfeedback@uspto.gov.**

Application Papers

10)☐ The specification is objected to by the Examiner.

11)☐ The drawing(s) filed on _____ is/are: a)☐ accepted or b)☐ objected to by the Examiner.

Applicant may not request that any objection to the drawing(s) be held in abeyance. See 37 CFR 1.85(a).

Replacement drawing sheet(s) including the correction is required if the drawing(s) is objected to. See 37 CFR 1.121(d).

Priority under 35 U.S.C. § 119

12)☐ Acknowledgment is made of a claim for foreign priority under 35 U.S.C. § 119(a)-(d) or (f).

Certified copies:

a)☐ All b)☐ Some** c)☐ None of the:

1.☐ Certified copies of the priority documents have been received.

2.☐ Certified copies of the priority documents have been received in Application No. _____.

3.☐ Copies of the certified copies of the priority documents have been received in this National Stage application from the International Bureau (PCT Rule 17.2(a)).

** See the attached detailed Office action for a list of the certified copies not received.

Attachment(s)

1) ☐ Notice of References Cited (PTO-892)

2) ☐ Information Disclosure Statement(s) (PTO/SB/08a and/or PTO/SB/08b) Paper No(s)/Mail Date _____.

3) ☐ Interview Summary (PTO-413) Paper No(s)/Mail Date _____.

4) ☐ Other: _____.

DETAILED ACTION

Notice of Pre-AIA or AIA Status

The present application, filed on or after March 16, 2013, is being examined under the first inventor to file provisions of the AIA.

Status of Claims

Claims 42-54 are pending in the instant application; claims 21-41 are cancelled; claims 42-54 are newly presented; claims 42-54 are the subject of the Office Action below.

Continued Examination Under 37 CFR 1.114

A request for continued examination under 37 CFR 1.114, including the fee set forth in 37 CFR 1.17(e), was filed in this application after final rejection. Since this application is eligible for continued examination under 37 CFR 1.114, and the fee set forth in 37 CFR 1.17(e) has been timely paid, the finality of the previous Office action has been withdrawn pursuant to 37 CFR 1.114. Applicant's submission filed on July 2, 2020 has been entered.

Examination Considerations

Applicant's Amendments filed July 2, 2020 have been received and entered into the present application. Claims 42-54 are pending and are herein examined on the merits.

Applicant's Arguments, filed July 2, 2020 have been fully considered. Rejections not reiterated from previous Office Actions are hereby withdrawn. The following rejections are either reiterated or newly applied. They constitute the complete set of rejections presently being applied to the instant application.

Double Patenting - Withdrawn

Claims 21-41 rejected on the ground of nonstatutory double patenting as being unpatentable over claims 1-27 of U.S. Patent No. 9,339,497 B2; claims 1-29 of U.S. Patent No. 9,364,473 B2; claims 1-35 of U.S. Patent No. 9,452,162 B2; and claims 1-30 of U.S. Patent No. 9,492,442 B2; and claims 1-24 of U.S. Patent No. 9,717,724 B2 is ***withdrawn***.

Claims 21-41 provisionally rejected on the ground of nonstatutory double patenting as being unpatentable over claims 1-20 of copending Application No. 16/012,351 is ***withdrawn***.

Applicant has cancelled claims 21-41 thus rendering the rejections moot. Subsequent to cancellation, the rejections are withdrawn.

Double Patenting – New Grounds (Necessitated by Amendment)

The nonstatutory double patenting rejection is based on a judicially created doctrine grounded in public policy (a policy reflected in the statute) so as to prevent the unjustified or improper timewise extension of the "right to exclude" granted by a patent

and to prevent possible harassment by multiple assignees. A nonstatutory double patenting rejection is appropriate where the conflicting claims are not identical, but at least one examined application claim is not patentably distinct from the reference claim(s) because the examined application claim is either anticipated by, or would have been obvious over, the reference claim(s). See, e.g., *In re Berg*, 140 F.3d 1428, 46 USPQ2d 1226 (Fed. Cir. 1998); *In re Goodman*, 11 F.3d 1046, 29 USPQ2d 2010 (Fed. Cir. 1993); *In re Longi*, 759 F.2d 887, 225 USPQ 645 (Fed. Cir. 1985); *In re Van Ornum*, 686 F.2d 937, 214 USPQ 761 (CCPA 1982); *In re Vogel*, 422 F.2d 438, 164 USPQ 619 (CCPA 1970); *In re Thorington*, 418 F.2d 528, 163 USPQ 644 (CCPA 1969).

A timely filed terminal disclaimer in compliance with 37 CFR 1.321(c) or 1.321(d) may be used to overcome an actual or provisional rejection based on nonstatutory double patenting provided the reference application or patent either is shown to be commonly owned with the examined application, or claims an invention made as a result of activities undertaken within the scope of a joint research agreement. See MPEP § 717.02 for applications subject to examination under the first inventor to file provisions of the AIA as explained in MPEP § 2159. See MPEP §§ 706.02(l)(1) - 706.02(l)(3) for applications not subject to examination under the first inventor to file provisions of the AIA. A terminal disclaimer must be signed in compliance with 37 CFR 1.321(b).

The USPTO Internet website contains terminal disclaimer forms which may be used. Please visit www.uspto.gov/patent/patents-forms. The filing date of the application in which the form is filed determines what form (e.g., PTO/SB/25, PTO/SB/26, PTO/AIA/25, or PTO/AIA/26) should be used. A web-based eTerminal Disclaimer may

be filled out completely online using web-screens. An eTerminal Disclaimer that meets all requirements is auto-processed and approved immediately upon submission. For more information about eTerminal Disclaimers, refer to www.uspto.gov/patents/process/file/efs/guidance/eTD-info-I.jsp.

Claims 42-54 are rejected on the ground of nonstatutory double patenting as being unpatentable over claims 1-27 of U.S. Patent No. 9,339,497 B2; claims 1-29 of U.S. Patent No. 9,364,473 B2; claims 1-35 of U.S. Patent No. 9,452,162 B2; and claims 1-30 of U.S. Patent No. 9,492,442 B2; and claims 1-24 of U.S. Patent No. 9,717,724 B2. Although the claims at issue are not identical, they are not patentably distinct from each other because each disclosure sets out to claim treatment of pancreatic cancer with the antiproliferative therapeutic regimen that consist of liposomal irinotecan at a dosing of 60, 70 or 80 mg/m^2; leucovorin (*l*-form) at a dose if 200 mg/m^2; and 5-fluorouracil at a dose of 2,400 mg/m^2. Each disclosure teaches and claims treating patients refractory to gemcitabine therapy and treating patients who either are or not homozygous for the UGT1 A1*28 allele. The closest prior art, as indicated in the record of previous case App. No. 14/812,950 (now patented U.S. Patent No. 9,339,497 B2) is found in Yoo *et al.* (*British Journal of Cancer*, 2009, 101, pp. 1658-163); where Yoo teaches treating pancreatic cancer refractory to gemcitabine therapy with the mFOIRIRI.3 regimen that consists of irinotecan, leucovorin and 5-fluorouracil. However, Yoo requires different dosing and that irinotecan is administered twice where the therapy provides the overall survival for the mFOIRIRI.3 regimen to be 16.6 weeks (or 4.2 months). The instantly claimed invention carves out a specific regimen that requires

the dosing of the components and administers the drugs only once within a cycle and further provides for the unexpected result of improving clinical benefit of up to 80% and the increasing the patient population survival of at least 6 months. Therefore the claims are free of the art. However, the claims are obvious variants of the previously patented subject matter and therefore the nonstatutory double patenting rejection is applied.

Claims 42-54 are provisionally rejected on the ground of nonstatutory double patenting as being unpatentable over claims 21-29 and 32-37 of copending Application No. 16/012,351; and claims 1-20 of copending Application 16/920,830. Although the claims at issue are not identical, they are not patentably distinct from each other because each disclosure claims treating patients with pancreatic cancer refractory to gemcitabine therapy and treating patients with the same general combination with overlapping dosing of liposomal irinotecan. The claims are obvious variants.

This is a provisional nonstatutory double patenting rejection because the patentably indistinct claims have not in fact been patented.

Conclusion

Any inquiry concerning this communication or earlier communications from the examiner should be directed to TORI STRONG whose telephone number is (571)272-6333. The examiner can normally be reached on Monday - Friday 8:00 am - 5:00 pm (EST).

Examiner interviews are available via telephone, in-person, and video conferencing using a USPTO supplied web-based collaboration tool. To schedule an

interview, applicant is encouraged to use the USPTO Automated Interview Request (AIR) at http://www.uspto.gov/interviewpractice.

If attempts to reach the examiner by telephone are unsuccessful, the examiner's supervisor, Jeffrey Lundgren can be reached on (571)272-5541. The fax phone number for the organization where this application or proceeding is assigned is 571-273-8300.

Information regarding the status of an application may be obtained from the Patent Application Information Retrieval (PAIR) system. Status information for published applications may be obtained from either Private PAIR or Public PAIR. Status information for unpublished applications is available through Private PAIR only. For more information about the PAIR system, see http://pair-direct.uspto.gov. Should you have questions on access to the Private PAIR system, contact the Electronic Business Center (EBC) at 866-217-9197 (toll-free). If you would like assistance from a USPTO Customer Service Representative or access to the automated information system, call 800-786-9199 (IN USA OR CANADA) or 571-272-1000.

/Kortney L. Klinkel/
Primary Examiner, Art Unit 1699

TORI STRONG
Examiner
Art Unit 1629

/TORI STRONG/
Examiner, Art Unit 1629

UNITED STATES PATENT AND TRADEMARK OFFICE

UNITED STATES DEPARTMENT OF COMMERCE
United States Patent and Trademark Office
Address: COMMISSIONER FOR PATENTS
P.O. Box 1450
Alexandria, Virginia 22313-1450
www.uspto.gov

APPLICATION NO.	FILING DATE	FIRST NAMED INVENTOR	ATTORNEY DOCKET NO.	CONFIRMATION NO.
16/302,050	11/15/2018	Bambang Adiwijaya	01208-0013-00US	4677

153749 7590 01/17/2020

McNeill Baur PLLC/Ipsen
Ipsen Bioscience, Inc.
125 Cambridge Park Drive
Suite 301
Cambridge, MA 02140

EXAMINER	
RONEY, CELESTE A	

ART UNIT	PAPER NUMBER
1612	

NOTIFICATION DATE	DELIVERY MODE
01/17/2020	ELECTRONIC

Please find below and/or attached an Office communication concerning this application or proceeding.

The time period for reply, if any, is set in the attached communication.

Notice of the Office communication was sent electronically on above-indicated "Notification Date" to the following e-mail address(es):

docketing@mcneillbaur.com
eofficeaction@appcoll.com
patents.us@ipsen.com

Office Action Summary	Application No. 16/302,050	Applicant(s) Adiwijaya et al.	
	Examiner CELESTE A RONEY	Art Unit 1612	AIA (FITF) Status Yes

-- The MAILING DATE of this communication appears on the cover sheet with the correspondence address --

Period for Reply

A SHORTENED STATUTORY PERIOD FOR REPLY IS SET TO EXPIRE 3 MONTHS FROM THE MAILING DATE OF THIS COMMUNICATION.

- Extensions of time may be available under the provisions of 37 CFR 1.136(a). In no event, however, may a reply be timely filed after SIX (6) MONTHS from the mailing date of this communication.
- If NO period for reply is specified above, the maximum statutory period will apply and will expire SIX (6) MONTHS from the mailing date of this communication.
- Failure to reply within the set or extended period for reply will, by statute, cause the application to become ABANDONED (35 U.S.C. § 133). Any reply received by the Office later than three months after the mailing date of this communication, even if timely filed, may reduce any earned patent term adjustment. See 37 CFR 1.704(b).

Status

1)☑ Responsive to communication(s) filed on 15 October 2019.

☐ A declaration(s)/affidavit(s) under **37 CFR 1.130(b)** was/were filed on _____.

2a)☐ This action is **FINAL.** 2b) ☑ This action is non-final.

3)☐ An election was made by the applicant in response to a restriction requirement set forth during the interview on _____; the restriction requirement and election have been incorporated into this action.

4)☐ Since this application is in condition for allowance except for formal matters, prosecution as to the merits is closed in accordance with the practice under *Ex parte Quayle*, 1935 C.D. 11, 453 O.G. 213.

Disposition of Claims*

5) ☑ Claim(s) 1-30 is/are pending in the application.

5a) Of the above claim(s) _____ is/are withdrawn from consideration.

6) ☐ Claim(s) _____ is/are allowed.

7) ☑ Claim(s) 1-30 is/are rejected.

8) ☐ Claim(s) _____ is/are objected to.

9) ☐ Claim(s) _____ are subject to restriction and/or election requirement

* If any claims have been determined allowable, you may be eligible to benefit from the **Patent Prosecution Highway** program at a participating intellectual property office for the corresponding application. For more information, please see http://www.uspto.gov/patents/init_events/pph/index.jsp or send an inquiry to **PPHfeedback@uspto.gov.**

Application Papers

10)☐ The specification is objected to by the Examiner.

11)☐ The drawing(s) filed on _____ is/are: a)☐ accepted or b)☐ objected to by the Examiner.

Applicant may not request that any objection to the drawing(s) be held in abeyance. See 37 CFR 1.85(a).

Replacement drawing sheet(s) including the correction is required if the drawing(s) is objected to. See 37 CFR 1.121(d).

Priority under 35 U.S.C. § 119

12)☑ Acknowledgment is made of a claim for foreign priority under 35 U.S.C. § 119(a)-(d) or (f).

Certified copies:

a)☑ All b)☐ Some** c)☐ None of the:

1.☑ Certified copies of the priority documents have been received.

2.☐ Certified copies of the priority documents have been received in Application No. _____.

3.☐ Copies of the certified copies of the priority documents have been received in this National Stage application from the International Bureau (PCT Rule 17.2(a)).

** See the attached detailed Office action for a list of the certified copies not received.

Attachment(s)

1) ☑ Notice of References Cited (PTO-892)

2) ☑ Information Disclosure Statement(s) (PTO/SB/08a and/or PTO/SB/08b) Paper No(s)/Mail Date 10/17/19; 10/18/19 (3).

3) ☐ Interview Summary (PTO-413) Paper No(s)/Mail Date _____.

4) ☐ Other: _____.

DETAILED ACTION

Notice of Pre-AIA or AIA Status

The present application, filed on or after March 16, 2013, is being examined under the first inventor to file provisions of the AIA. In the event the determination of the status of the application as subject to AIA 35 U.S.C. 102 and 103 (or as subject to pre-AIA 35 U.S.C. 102 and 103) is incorrect, any correction of the statutory basis for the rejection will not be considered a new ground of rejection if the prior art relied upon, and the rationale supporting the rejection, would be the same under either status.

Claim Rejections - 35 USC § 112 – Indefiniteness and Broad Limitation followed by Narrow Limitation

> The following is a quotation of 35 U.S.C. 112(b):
> (b) CONCLUSION.—The specification shall conclude with one or more claims particularly pointing out and distinctly claiming the subject matter which the inventor or a joint inventor regards as the invention.
>
> The following is a quotation of 35 U.S.C. 112 (pre-AIA), second paragraph:
> The specification shall conclude with one or more claims particularly pointing out and distinctly claiming the subject matter which the applicant regards as his invention.

Claims 1-30 are rejected under 35 U.S.C. 112(b) or 35 U.S.C. 112 (pre-AIA), second paragraph, as being indefinite for failing to particularly point out and distinctly claim the subject matter which the inventor or a joint inventor, or for pre-AIA the applicant regards as the invention.

A broad range or limitation together with a narrow range or limitation that falls within the broad range or limitation (in the same claim) is considered indefinite, since the resulting claim does not clearly set forth the metes and bounds of the patent protection

desired. See MPEP § 2173.05(c). Note the explanation given by the Board of Patent Appeals and Interferences in *Ex parte Wu*, 10 USPQ2d 2031, 2033 (Bd. Pat. App. & Inter. 1989), as to where broad language is followed by "such as" and then narrow language. The Board stated that this can render a claim indefinite by raising a question or doubt as to whether the feature introduced by such language is (a) merely exemplary of the remainder of the claim, and therefore not required, or (b) a required feature of the claims. Note also, for example, the decisions of *Ex parte Steigewald*, 131 USPQ 74 (Bd. App. 1961); *Ex parte Hall*, 83 USPQ 38 (Bd. App. 1948); and *Ex parte Hasche*, 86 USPQ 481 (Bd. App. 1949).

In the present instance, claims 1 and 9 recite the broad recitation "dose of liposomal irinotecan", and the claims also recite "(free base)" which is the narrower statement of the limitation. The Applicant is encouraged to remove the parenthesis () surrounding the phrase "free base", to obviate the 35 USC § 112 rejection.

Claim Rejections - 35 USC § 103 - Obviousness

The following is a quotation of 35 U.S.C. 103 which forms the basis for all obviousness rejections set forth in this Office action:

> A patent for a claimed invention may not be obtained, notwithstanding that the claimed invention is not identically disclosed as set forth in section 102, if the differences between the claimed invention and the prior art are such that the claimed invention as a whole would have been obvious before the effective filing date of the claimed invention to a person having ordinary skill in the art to which the claimed invention pertains. Patentability shall not be negated by the manner in which the invention was made.

Claims 1-3, 7-9, 11-16, 21-22 and 24-30 are rejected under 35 U.S.C. 103 as being unpatentable over Tardi et al (US 2016/0058704), in view of Madden et al (USP 7,244,448

B2) and further in view of the FDA (https://www.accessdata.fda.gov/drugsatfda_docs/label/2015/207793lbl.pdf).

Tardi disclosed irinotecan and cisplatin, co-administered in a blended liposome formulation, or administered as liposomal cisplatin alone or liposomal irinotecan alone, and given to mice bearing human small cell lung cancer solid tumors [0036-0038 and at Figures 7B-7C and Figure 8]. These compositions [0018] allowed the two agents to be delivered to the disease site in a coordinated fashion. This result was achieved whether the agents were co-encapsulated, or were separately encapsulated.

As such, Tardi taught [0021] delivery of a therapeutically effective amount of a platinum drug/therapeutic agent combination (e.g., preferred combinations were irinotecan and cisplatin or irinotecan and carboplatin, at [0020]), by administering a platinum-based drug stably associated with a first blended delivery vehicle and an additional therapeutic agent stably associated with a second delivery vehicle. The first and second delivery vehicles were contained in separate vials, the contents of the vials being administered to a patient simultaneously or sequentially (reads on treating small cell lung cancer with irinotecan, following disease progression on or after first-line platinum therapy).

Although Tardi exemplified the administration to mice, Tardi disclosed [0097] that the blended delivery vehicles may be administered to warm-blooded animals, including humans. For the treatment of human ailments, a qualified physician will determine dose, schedule and route of administration.

Although Tardi disclosed that the dosage and schedule could be determined by a qualified physician, Tardi did not specifically disclose administering liposomal irinotecan

every two weeks at 70 mg/m^2, as recited in claim 1. Tardi was silent as to the free base form of irinotecan, as recited in claim 1.

Madden disclosed [title and abstract] liposomal antineoplastic agents (e.g., camptothecin) for treating neoplasia. Madden disclosed that, for camptothecins (irinotecan disclosed at col 8, line 46) in the treatment of small cell lung cancer, the doses of active agent in humans are effective at ranges as low as from 0.015 mg/m^2, and are still tolerable at doses as high as 15 to 75 mg/m^2. Doses may be single or administered repeatedly, wherein preferred scheduling may employ a cycle of treatment that is repeated every two weeks, three weeks, four weeks, five weeks, six weeks or a combination thereof [col 9, line 63 to col 10, line 14].

Madden did not teach administering liposomal irinotecan following disease progression on or after first-line platinum-based therapy.

Since Tardi disclosed liposomal irinotecan for the treatment of small cell lung cancer in humans, it would have been prima facie obvious to one of ordinary skill in the art to administer the active once every two weeks, at a dosage of 70 mg/m^2. An ordinarily skilled artisan would have been so motivated because, for camptothecins (e.g., irinotecan) in the treatment of small cell lung cancer, the doses of active agent in humans are effective at ranges as low as from 0.015 mg/m^2, and are still tolerable at doses as high as 15 to 75 mg/m^2. Doses may be single or administered repeatedly, wherein preferred scheduling may employ a cycle of treatment that is repeated every two weeks, three weeks, four weeks, five weeks, six weeks or a combination thereof [col 9, line 63 to col 10, line 14].

The combined teachings of Tardi and Madden were silent the free base form of liposomal irinotecan.

However, the FDA disclosed [page 11, first paragraph] that liposomal irinotecan is commercially available as irinotecan freebase.

The FDA did not teach the treatment of small cell lung cancer.

It would have been prima facie obvious to one of ordinary skill in the art to include free base irinotecan within the combined teachings of Tardi and Madden. An ordinarily skilled artisan would have been motivated to formulate the liposome with the commercially available form of the active [FDA, page 11, first paragraph].

The combination of Tardi, Madden and FDA reads on claims 1-2, 7-8, 11-12, 14-15.

Claim 1 recites administration of liposomal irinotecan once every two weeks at a dosage of 70 mg/m^2. Claim 15 recites at least three six-week cycles. The combined teachings of Tardi, Madden and FDA taught 15 to 75 mg/m^2 in a single dosage or administered repeatedly, wherein preferred scheduling may employ a cycle of treatment that is repeated every two weeks, three weeks, four weeks, five weeks, six weeks or a combination thereof. In the case where the claimed ranges "overlap or lie inside ranges disclosed by the prior art", a prima facie case of obviousness exists. MPEP 2144.05 A.

Regarding claims 3 and 13, Tardi was silent the blood ANC of the human patients, as instantly recited. However, the FDA advised [page 4, section 5.1] that liposomal irinotecan should be administered when the ANC is $1500/mm^3$ or above, as both a warning and a precaution against severe neutropenia.

It would be prima facie obvious to one of ordinary skill in the art to administer Tardi's liposomal irinotecan to humans when the patient's ANC was 1500/mm^3 or above, as advised by the FDA. An ordinarily skilled artisan would be motivated to avoid severe or life-threatening neutropenia and fatal neutropenic sepsis, as advised by the FDA at page 4, section 5.1.

Regarding claims 9, 16 and 21-22, although Tardi disclosed [0098] intravenous administration, Tardi was silent the preparation of liposomal irinotecan, as instantly recited. However, the FDA disclosed [pages 2-3, sections 2.2 and 2.4] that liposomal irinotecan is prepared as a pharmaceutical injection composition, by diluting 70 mg/m^2 of the agent in 500 mL dextrose or 0.9 % sodium chloride, and mixing, followed by administration as an intravenous infusion over 90 minutes.

It would have been prima facie obvious to one of ordinary skill in the art to prepare Tardi's liposomal irinotecan, as taught by the FDA. An ordinarily skilled artisan would have been motivated by the FDAs teachings of liposomal irinotecan in its commercially available formulation, as previously discussed [FDA, sections 2.2 and 2.4]. An ordinarily skilled artisan would have been motivated to administer the liposomal irinotecan as an infusion, as recommended by the FDA for human administration [FDA, sections 2.2 and 2.4].

Regarding claims 24-30, although Tardi taught (encapsulation previously discussed) unilamellar vesicles [0052] having a diameter of less than 200 nm [0055], and formulated with DSPC, cholesterol [0034] and mPEG-DSPE [0054], Tardi was not specific the liposomal formulation instantly recited, wherein the aqueous space encapsulated irinotecan in a gelated or precipitated state as the sucrose octasulfate salt, as recited in

claim 24; the molecular weight of PEG, as recited in claims 26 and 29-30; amounts of phosphatidylcholine, cholesterol and mPEG, as recited in claims 26-28 and 30.

However, the FDA taught [page 11, 1st paragraph] that liposomal irinotecan is a dispersion, wherein the liposome is a unilamellar lipid bilayer vesicle, approximately 110 nm in diameter, which encapsulates an aqueous space containing irinotecan in a gelated or precipitated state as the sucrose octasulfate salt. The vesicle is composed of 1,2-distearoyl-sn-glycero-3-phosphocholine (DSPC) 6.81 mg/mL, cholesterol 2.22 mg/mL, and methoxy-terminated polyethylene glycol (MW 2000)-distearoylphosphatidyl ethanolamine (MPEG-2000-DSPE) 0.12 mg/mL.

It would have been prima facie obvious to one of ordinary skill in the art to formulate Tardi's liposomal irinotecan as taught by the guidance of the FDA. An ordinarily skilled artisan would be motivated to obtain liposomal irinotecan in its commercially available formulation, as previously discussed [FDA, page 11, 1st paragraph].

Claim 24 recites 110 nm diameter. Claim 27 recites one mPEG-2000-DSPE molecule per 200 phospholipid molecules. Claims 28 and 30 recite phosphatidylcholine, cholesterol and mPEG-2000-DSPE in a molar ratio of 3:2:0.015. Tardi taught liposomes at less than 200 nm; and, the FDA taught a vesicle approximately 110 nm in diameter, composed of DSPC 6.81 mg/mL, cholesterol 2.22 mg/mL, and MPEG-2000-DSPE 0.12 mg/mL. A prima facie case of obviousness exists because of overlap, as discussed above.

Claims 4-6 and 18 are rejected under 35 U.S.C. 103 as being unpatentable over Tardi et al (US 2016/0058704), in view of Madden et al (USP 7,244,448 B2), further in

view of the FDA (https://www.accessdata.fda.gov/drugsatfda_docs/label/2015/207793lbl.pdf) and further in view of Mirtsching et al (Am J Med Sci, 2014, 347(2), 167-169).

The 35 U.S.C. 103 rejection over Tardi, Madden and the FDA was previously discussed. The combined teachings of the prior art were silent the platelet count of the human patient, as recited in claims 4 and 18; the blood hemoglobin value, as recited in claims 5 and 18; the serum creatinine value, as recited in claims 6 and 18.

Mirtsching taught [title] drug-induced immune thrombocytopenia, wherein [page 3, last paragraph] a human patient had become sensitized to irinotecan during treatment cycles with the active agent. Before treatment, the patient's platelet count was 143,000/μL. Said counts were maintained between 113,000-150,000/μL during therapy.

However, after treatment, the patient had no platelet counts less than 100,000/μL, and no systemic symptoms during previous exposures to the active agent. Because cases of [page 3, last paragraph] acute, severe thrombocytopenia caused by irinotecan have now been identified, clinicians should consider this possible diagnosis in any patient who experiences an acute and isolated drop in the platelet levels after irinotecan administration. Other laboratory data included hemoglobin at 13.8 g/dL, and creatinine at 0.7 mg/dL [page 2, 2nd paragraph].

It would have been prima facie obvious to one of ordinary skill in the art to administer Tardi's liposomal irinotecan when the patient's blood platelet count was greater than 100,000/μL. An ordinarily skilled artisan would have been motivated to avoid a possible diagnosis of acute, severe thrombocytopenia [Mirtsching, page 3, last paragraph].

It would have been prima facie obvious to one of ordinary skill in the art to administer Tardi's liposomal irinotecan when the patient's blood hemoglobin was 13.8 g/dL, as taught by Mirtsching [page 2, 2nd paragraph]. An ordinarily skilled artisan would have been motivated to monitor the liver function, and the bone marrow reserve.

It would have been prima facie obvious to one of ordinary skill in the art to administer Tardi's liposomal irinotecan when the patient's serum creatinine was 0.7 mg/dL, as taught by Mirtsching [page 2, 2nd paragraph]. An ordinarily skilled artisan would have been motivated to monitor and ensure adequate renal function.

Claim 4 recites a platelet count greater than 100,000 cells per microliter. Claim 5 recites hemoglobin greater than 9 g/dL. Claim 6 recites creatinine less than or equal to 1.5xULN. Mirtsching taught a platelet count at 143,000/μL, hemoglobin at 13.8 g/dL and creatinine at 0.7 mg/dL, before treatment. A prima facie case of obviousness exists because of overlap, as previously discussed.

Further regarding claim 6, Mirtsching was silent the creatinine clearance, as instantly recited. However, it would be prima facie obvious to one of ordinary skill in the art to determine the creatinine clearance, as desired. An ordinarily skilled artisan would be motivated to monitor and ensure an adequate renal function.

Further, regarding claim 18, the claim instantly recites once every two weeks for a total of at least three six-week cycles. The combined teachings of Tardi and Madden taught administration in a single dosage, or repeatedly, wherein preferred scheduling may employ a cycle of treatment that is repeated every two weeks, three weeks, four weeks, five weeks, six weeks or a combination thereof. A prima facie case of obviousness exists because of overlap, as previously discussed.

Claims 10 and 17 are rejected under 35 U.S.C. 103 as being unpatentable over Tardi et al (US 2016/0058704), in view of Madden et al (USP 7,244,448 B2), further in view of the FDA (https://www.accessdata.fda.gov/drugsatfda_docs/label/2015/207793lbl.pdf) and further in view of Cassileth et al (Arch Intern Med, 1983, 143(7), 1347-1349) and Drug and Therapeutics Bulletin, 43(8), 2005, 57-62.

The 35 U.S.C. 103 rejection over Tardi, Madden and the FDA was previously described. Additionally, the FDA generally advised [page 3, Premedication section] administration of a corticosteroid and an anti-emetic prior to liposomal irinotecan infusion.

However, the combined teachings of the prior art did not specifically teach dexamethasone and a 5-HT3 blocker, as instantly recited.

Nevertheless, Cassileth taught [title] antiemetic efficacy of dexamethasone therapy in patients receiving cancer chemotherapy, wherein dexamethasone therapy has useful application in alleviating the emetic effects of cancer chemotherapy [abstract].

Moreover, the Drug and Therapeutics Bulletin taught [title] 5HT3-receptor antagonists as anti-emetics in cancer, wherein effective antiemetic therapy is crucial for patients undergoing chemotherapy or radiotherapy for cancer. Severe nausea and vomiting associated with such cancer treatment can lead to anxiety, anorexia, dehydration, electrolyte disturbance and renal failure, and may interrupt cancer therapy, demoralize patients or even cause them to abandon treatment [abstract].

Since the combined teachings of the prior art generally advised administration of a corticosteroid and an anti-emetic prior to liposomal irinotecan infusion, it would have been prima facie obvious to one of ordinary skill in the art to include dexamethasone and

a 5-HT3 blocker within the combination of said teachings. An ordinarily skilled artisan would have been motivated to alleviate the emetic effects of cancer chemotherapy, since the severe nausea and vomiting associated with cancer treatment can lead to anxiety, anorexia, dehydration, electrolyte disturbance and renal failure, and may interrupt cancer therapy, demoralize patients or even cause them to abandon treatment, as taught by the combined teachings of Cassileth and the Drug and Therapeutics Bulletin [abstracts and titles of each reference].

Generally, it is *prima facie* obvious to select a known material for incorporation into a composition, based on its recognized suitability for its intended use. See MPEP 2144.07. In the instant case, it is prima facie obvious to select both dexamethasone and a 5-HT3 blocker, for incorporation into a composition, based on their recognized suitability for the intended use as anti-emetics, as taught by the combined teachings of Cassileth and the Drug and Therapeutics Bulletin [abstracts and titles of each reference].

Claims 19-20 and 23 are rejected under 35 U.S.C. 103 as being unpatentable over Tardi et al (US 2016/0058704), in view of Madden et al (USP 7,244,448 B2), further in view of the FDA (https://www.accessdata.fda.gov/drugsatfda_docs/label/2015/207793lbl.pdf), further in view of Mirtsching et al (Am J Med Sci, 2014, 347(2), 167-169), further in view of Cassileth et al (Arch Intern Med, 1983, 143(7), 1347-1349) and further in view of Drug and Therapeutics Bulletin, 43(8), 2005, 57-62.

The 35 U.S.C. 103 rejection over Tardi, Madden and the FDA was previously described. Additionally, the FDA generally advised [page 3, Premedication section] administration of a corticosteroid and an anti-emetic prior to liposomal irinotecan infusion.

However, the combined teachings of the prior art did not specifically teach dexamethasone and a 5-HT3 blocker, as instantly recited.

Nevertheless, Cassileth taught [title] antiemetic efficacy of dexamethasone therapy in patients receiving cancer chemotherapy, wherein dexamethasone therapy has useful application in alleviating the emetic effects of cancer chemotherapy [abstract].

Moreover, the Drug and Therapeutics Bulletin taught [title] 5HT3-receptor antagonists as anti-emetics in cancer, wherein effective antiemetic therapy is crucial for patients undergoing chemotherapy or radiotherapy for cancer. Severe nausea and vomiting associated with such cancer treatment can lead to anxiety, anorexia, dehydration, electrolyte disturbance and renal failure, and may interrupt cancer therapy, demoralize patients or even cause them to abandon treatment [abstract].

Since the combined teachings of the prior art generally advised administration of a corticosteroid and an anti-emetic prior to liposomal irinotecan infusion, it would have been prima facie obvious to one of ordinary skill in the art to include dexamethasone and a 5-HT3 blocker within the combination of said teachings. An ordinarily skilled artisan would have been motivated to alleviate the emetic effects of cancer chemotherapy, since the severe nausea and vomiting associated with cancer treatment can lead to anxiety, anorexia, dehydration, electrolyte disturbance and renal failure, and may interrupt cancer therapy, demoralize patients or even cause them to abandon treatment, as taught by the

combined teachings of Cassileth and the Drug and Therapeutics Bulletin [abstracts and titles of each reference].

Generally, it is *prima facie* obvious to select a known material for incorporation into a composition, based on its recognized suitability for its intended use. See MPEP 2144.07. In the instant case, it is prima facie obvious to select both dexamethasone and a 5-HT3 blocker, for incorporation into a composition, based on their recognized suitability for the intended use as anti-emetics, as taught by the combined teachings of Cassileth and the Drug and Therapeutics Bulletin [abstracts and titles of each reference].

Regarding claims 20 and 23, although Tardi disclosed [0098] intravenous administration, Tardi was silent the preparation of liposomal irinotecan, as instantly recited. However, the FDA disclosed [pages 2-3, sections 2.2 and 2.4] that liposomal irinotecan is prepared, as a pharmaceutical injection composition, by diluting 70 mg/m^2 of the agent in 500 mL dextrose or 0.9 % sodium chloride, and mixing, followed by administration as an intravenous infusion over 90 minutes.

It would have been prima facie obvious to one of ordinary skill in the art to prepare Tardi's liposomal irinotecan as taught by the FDA. An ordinarily skilled artisan would have been motivated by the FDAs teachings of liposomal irinotecan in its commercially available formulation, as previously discussed [FDA, sections 2.2 and 2.4]. An ordinarily skilled artisan would have been motivated to administer the liposomal irinotecan as an infusion, as recommended by the FDA for human administration [FDA, sections 2.2 and 2.4].

Conclusion

Any inquiry concerning this communication or earlier communications from the examiner should be directed to CELESTE A RONEY whose telephone number is (571)272-5192. The examiner can normally be reached on Monday-Thursday; 7 AM-5 PM.

Examiner interviews are available via telephone, in-person, and video conferencing using a USPTO supplied web-based collaboration tool. To schedule an interview, applicant is encouraged to use the USPTO Automated Interview Request (AIR) at http://www.uspto.gov/interviewpractice.

If attempts to reach the examiner by telephone are unsuccessful, the examiner's supervisor, Frederick Krass can be reached on 571-272-0580. The fax phone number for the organization where this application or proceeding is assigned is 571-273-8300.

Information regarding the status of an application may be obtained from the Patent Application Information Retrieval (PAIR) system. Status information for published applications may be obtained from either Private PAIR or Public PAIR. Status information for unpublished applications is available through Private PAIR only. For more information about the PAIR system, see http://pair-direct.uspto.gov. Should you have questions on access to the Private PAIR system, contact the Electronic Business Center (EBC) at 866-217-9197 (toll-free). If you would like assistance from a USPTO Customer Service Representative or access to the automated information system, call 800-786-9199 (IN USA OR CANADA) or 571-272-1000.

/CELESTE A RONEY/
Primary Examiner, Art Unit 1612

UNITED STATES PATENT AND TRADEMARK OFFICE

UNITED STATES DEPARTMENT OF COMMERCE
United States Patent and Trademark Office
Address: COMMISSIONER FOR PATENTS
P.O. Box 1450
Alexandria, Virginia 22313-1450
www.uspto.gov

APPLICATION NO.	FILING DATE	FIRST NAMED INVENTOR	ATTORNEY DOCKET NO.	CONFIRMATION NO.
16/510,394	07/12/2019	Daryl C. Drummond	01208-0010-11US	1095

153749 7590 03/06/2020

McNeill Baur PLLC/Ipsen
Ipsen Bioscience, Inc.
125 Cambridge Park Drive
Suite 301
Cambridge, MA 02140

EXAMINER	
SHOMER, ISAAC	

ART UNIT	PAPER NUMBER
1612	

NOTIFICATION DATE	DELIVERY MODE
03/06/2020	ELECTRONIC

Please find below and/or attached an Office communication concerning this application or proceeding.

The time period for reply, if any, is set in the attached communication.

Notice of the Office communication was sent electronically on above-indicated "Notification Date" to the following e-mail address(es):

docketing@mcneillbaur.com
eofficeaction@appcoll.com
patents.us@ipsen.com

Office Action Summary	Application No. 16/510,394	Applicant(s) Drummond et al.	
	Examiner ISAAC SHOMER	Art Unit 1612	AIA (FITF) Status Yes

-- The MAILING DATE of this communication appears on the cover sheet with the correspondence address --

Period for Reply

A SHORTENED STATUTORY PERIOD FOR REPLY IS SET TO EXPIRE 3 MONTHS FROM THE MAILING DATE OF THIS COMMUNICATION.

- Extensions of time may be available under the provisions of 37 CFR 1.136(a). In no event, however, may a reply be timely filed after SIX (6) MONTHS from the mailing date of this communication.
- If NO period for reply is specified above, the maximum statutory period will apply and will expire SIX (6) MONTHS from the mailing date of this communication.
- Failure to reply within the set or extended period for reply will, by statute, cause the application to become ABANDONED (35 U.S.C. § 133). Any reply received by the Office later than three months after the mailing date of this communication, even if timely filed, may reduce any earned patent term adjustment. See 37 CFR 1.704(b).

Status

1)☑ Responsive to communication(s) filed on 27 February 2020.

☐ A declaration(s)/affidavit(s) under **37 CFR 1.130(b)** was/were filed on _____.

2a)☐ This action is **FINAL.** 2b) ☑ This action is non-final.

3)☐ An election was made by the applicant in response to a restriction requirement set forth during the interview on _____; the restriction requirement and election have been incorporated into this action.

4)☐ Since this application is in condition for allowance except for formal matters, prosecution as to the merits is closed in accordance with the practice under *Ex parte Quayle*, 1935 C.D. 11, 453 O.G. 213.

Disposition of Claims*

5) ☑ Claim(s) 1 is/are pending in the application.

5a) Of the above claim(s) _____ is/are withdrawn from consideration.

6) ☐ Claim(s) _____ is/are allowed.

7) ☑ Claim(s) 1 is/are rejected.

8) ☐ Claim(s) _____ is/are objected to.

9) ☐ Claim(s) _____ are subject to restriction and/or election requirement

* If any claims have been determined allowable, you may be eligible to benefit from the **Patent Prosecution Highway** program at a participating intellectual property office for the corresponding application. For more information, please see http://www.uspto.gov/patents/init_events/pph/index.jsp or send an inquiry to **PPHfeedback@uspto.gov.**

Application Papers

10)☐ The specification is objected to by the Examiner.

11)☐ The drawing(s) filed on _____ is/are: a)☐ accepted or b)☐ objected to by the Examiner.

Applicant may not request that any objection to the drawing(s) be held in abeyance. See 37 CFR 1.85(a).

Replacement drawing sheet(s) including the correction is required if the drawing(s) is objected to. See 37 CFR 1.121(d).

Priority under 35 U.S.C. § 119

12)☐ Acknowledgment is made of a claim for foreign priority under 35 U.S.C. § 119(a)-(d) or (f).

Certified copies:

a)☐ All b)☐ Some** c)☐ None of the:

1.☐ Certified copies of the priority documents have been received.

2.☐ Certified copies of the priority documents have been received in Application No. _____.

3.☐ Copies of the certified copies of the priority documents have been received in this National Stage application from the International Bureau (PCT Rule 17.2(a)).

** See the attached detailed Office action for a list of the certified copies not received.

Attachment(s)

1) ☑ Notice of References Cited (PTO-892)

2) ☐ Information Disclosure Statement(s) (PTO/SB/08a and/or PTO/SB/08b) Paper No(s)/Mail Date _____.

3) ☐ Interview Summary (PTO-413) Paper No(s)/Mail Date _____.

4) ☐ Other: _____.

DETAILED ACTION

Notice of Pre-AIA or AIA Status

The present application, filed on or after March 16, 2013, is being examined under the first inventor to file provisions of the AIA.

In the event the determination of the status of the application as subject to AIA 35 U.S.C. 102 and 103 (or as subject to pre-AIA 35 U.S.C. 102 and 103) is incorrect, any correction of the statutory basis for the rejection will not be considered a new ground of rejection if the prior art relied upon, and the rationale supporting the rejection, would be the same under either status.

Claim Interpretation

The instant claims are drawn to a composition comprising irinotecan. Irinotecan has the following structure, as obtained by the examiner from the CAS Registry Record for 97682-44-5 (Entered STN 18 August 1985, 2 printed pages), with an arrow drawn by the examiner pointing to a specific atom, the significance will be addressed below.

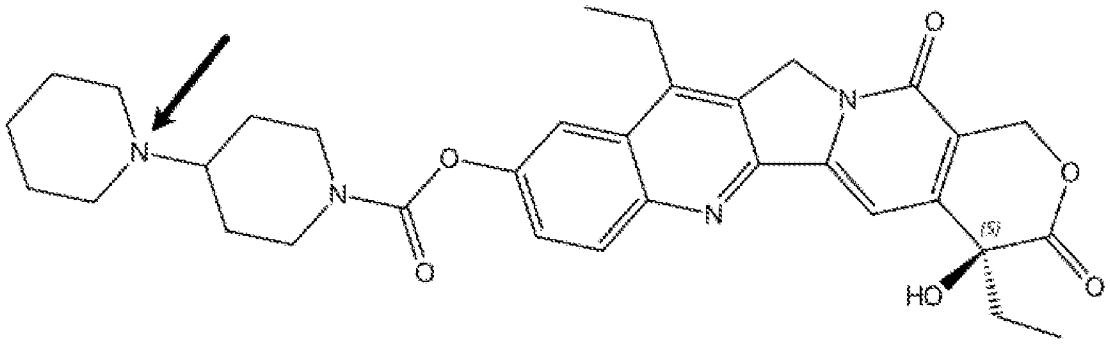

Absolute stereochemistry shown
Rotation (+)

As best understood by the examiner, irinotecan can exist either as a protonated salt (such as a hydrochloride salt) or a free base.

As best understood by the examiner, in the case wherein irinotecan is present as a salt, it is the tertiary nitrogen atom, to which an arrow is pointed in the above-reproduced diagram which becomes protonated. As best understood by the examiner, the pKa of a protonated tertiary aliphatic amine in the range of about 9-11. In support of this position, the examiner cites Evans pKa table http://evans.rc.fas.harvard.edu/pdf/evans_pKa_table.pdf (accessed 2 March 2020). This table shows the following on page 2, section regarding protonated nitrogen, reproduced below.

Substrate	pKa H_2O	(DMSO)
PROTONATED NITROGEN		
N^+H_4	9.2	(10.5)
EtN^+H_3	10.6	
$i\text{-}Pr_2N^+H_2$	11.05	
Et_3N^+H	10.75	(9.00)
PhN^+H_3	4.6	(3.6)
$PhN^+(Me)_2H$	5.20	(2.50)
$Ph_2N^+H_2$	0.78	
2-napthal-N^+H_3	4.16	
$H_2NN^+H_3$	8.12	
HON^+H_3	5.96	
Quinuclidine 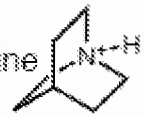	11.0	(9.80)
Morpholine 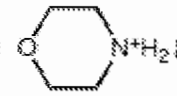	8.36	
N-Me morpholine	7.38	
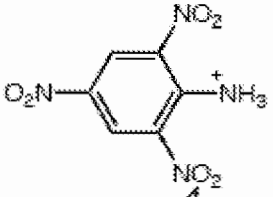	-9.3	
DABCO 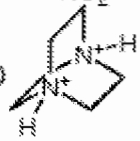	2.97, 8.82 (2.97, 8.93)	
	6.90, 9.95	
roton Sponge 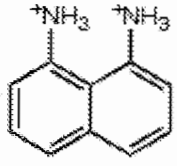	-9.0, 12.0 (--, 7.50)	
PhCN+H	-10	

The above-reproduced table indicates that ammonium, ethylammonium, diisopropylammonium, and triethylammonium have pKas ranging from 9.2-10.75 in

water. The examiner notes here that the nitrogen atom delineated with an arrow is an aliphatic amine. As such, the pKa range of 9.2-10.75, which is taught by the above-reproduced pKa table for protonated aliphatic amines, is understood to be applicable as an estimate of the pKa aliphatic amine nitrogen in irinotecan.

As such, the skilled artisan would have expected that at the claimed pH of 7.00-7.50, the majority of irinotecan would have been present in protonated form, with a small minority of irinotecan molecules being in the form of the free base. This determination is made in view of the Henderson-Hasselbalch equation, which is

$$pH = pKa + \log_{10}\frac{[conjugate\ base]}{[conjugate\ acid]}$$

which can be rewritten as

$$\frac{[conjugate\ base]}{[conjugate\ acid]} = 10^{pH-pKa}$$

or

$$\frac{[conjugate\ acid]}{[conjugate\ base]} = 10^{pka-pH}$$

The Henderson-Hasselbalch equation indicates that when pH=pKa, the conjugate acid is equal to the conjugate base in molar terms, but when pH<pKa, the concentration of the conjugate acid exceeds that of the conjugate base.

For the purposes of examination under prior art, a composition wherein the majority of irinotecan is present as a salt and a small minority is present as a free base is understood to meet the claim limitations.

Claim Rejections - 35 USC § 103 – Obviousness

The following is a quotation of 35 U.S.C. 103 which forms the basis for all obviousness rejections set forth in this Office action:

> A patent for a claimed invention may not be obtained, notwithstanding that the claimed invention is not identically disclosed as set forth in section 102, if the differences between the claimed invention and the prior art are such that the claimed invention as a whole would have been obvious before the effective filing date of the claimed invention to a person having ordinary skill in the art to which the claimed invention pertains. Patentability shall not be negated by the manner in which the invention was made.

The factual inquiries set forth in *Graham v. John Deere Co.*, 383 U.S. 1, 148 USPQ 459 (1966), that are applied for establishing a background for determining obviousness under 35 U.S.C. 103 are summarized as follows:

1. Determining the scope and contents of the prior art.

2. Ascertaining the differences between the prior art and the claims at issue.

3. Resolving the level of ordinary skill in the pertinent art.

4. Considering objective evidence present in the application indicating obviousness or nonobviousness.

This application currently names joint inventors. In considering patentability of the claims the examiner presumes that the subject matter of the various claims was commonly owned as of the effective filing date of the claimed invention(s) absent any evidence to the contrary. Applicant is advised of the obligation under 37 CFR 1.56 to point out the inventor and effective filing dates of each claim that was not commonly owned as of the effective filing date of the later invention in order for the examiner to consider the applicability of 35 U.S.C. 102(b)(2)(C) for any potential 35 U.S.C. 102(a)(2) prior art against the later invention.

Claims 1 is/are rejected under 35 U.S.C. 103 as being unpatentable over Hong et al. (US 2007/0116753 A1).

Hong et al. (hereafter referred to as Hong) is drawn to liposomes useful for drug delivery, as of Hong, title and abstract. Hong teaches one embodiment comprising liposomes comprising iriontecan (referred to as CPT-11) and sucrose octasulfate (referred to as "SOS"), as of Hong, at least as of page 23, Example 14, paragraph 0175. The liposomes of Hong include DSPC, cholesterol, and PEG-DSPE, as of Hong, paragraph 0142, wherein the PEG is methoxy terminated and has a molecular weight of 2000 Daltons, as of Hong, paragraph 0124. In one embodiment, Hong teaches about 500 mg of irinotecan per mmol of liposome phospholipid, as of Hong, paragraph 0169.

As to claim 1, the claim requires 4.3 mg of irinotecan per mL of the composition. Hong teaches that liposomes were stored at about 3.4-14.5 mg of CPT-11 (irinotecan) per mL, as of Hong, paragraph 0192, 5th line on page 26, top paragraph. While the prior art does not disclose the exact claimed values, but does overlap: in such instances even a slight overlap in range establishes a *prima facie* case of obviousness. See MPEP 2144.05(I).

As to claim 1, Hong teaches irinotecan, the relevant lipids, and the relevant concentrations, albeit in separate portions of the reference. Together these would provide a composition as claimed instantly. The prior art is not anticipatory insofar as these combinations must be selected from various lists/locations in the reference. It would have been obvious, however, to make the combination since each component is taught as being useful in making the compositions of the prior art. Since this modification of the prior art represents nothing more than "the predictable use of prior

art elements according to their established functions" a prima facie case of obviousness exists. See KSR v. Teleflex, 82 USPQ2d 1385, 1396 (2007). See also Ex parte Perrier, Appeal 2012-003888 (PTAB (2014)) (USSN 11/174,414) (applying the KSR standard of obviousness to selection of xanthan polymer and chloride of sebacic acid as polymer and crosslinker for forming prior art polymer networks since "this combination is merely a predictable used of prior art elements according to their established functions" – see fifth page of the decision).

As to claim 1, the claim requires a specific pH range of 7.00 to 7.50. Hong teaches a pH of from about 6.0 to about 7.5, as of Hong, paragraph 0115. This overlaps with the range of 7.00-7.50 required by the instant claims. While the prior art does not disclose the exact claimed values, but does overlap: in such instances even a slight overlap in range establishes a *prima facie* case of obviousness. See MPEP 2144.05(I). The skilled artisan would have expected that the majority of irinotecan would have existed is protonated form as a salt, but a minority of irinotecan would have been in free base form; see the section above entitled "Claim Interpretation."

As to claim 1, the claim requires that the composition is stabilized to form less than 20 mol% lysophosphatidylcholine during 6 months of storage at 4 °C. While this is not explicitly disclosed, Hong discloses that the composition is stable at 4 °C for six months to two years, as of Hong, paragraph 0112. As such, the skilled artisan would have expected that the phosphatidylcholine in the liposome of Hong would have successfully resisted degradation to lysophosphatidylcholine. Something which is old (e.g. the liposome of Hong) does not become patentable upon the discovery of a new property (that the phosphatidylcholine in the liposome would have resisted degradation

to lysophosphatidylcholine), and this feature need not have been recognized at the time of the invention. See MPEP 2112(I & II). Additionally, MPEP 2112(IV) posits that the examiner must provide rationale tending to show inherency. The teachings of Hong, paragraph 0112 regarding stability is understood by the examiner to be rationale/evidence tending toward inherency. This is because if the liposome composition is stable in the manner measured in paragraph 0112 of Hong, the skilled artisan would have expected that the liposome composition of Hong would have been stable if measured differently.

Non-Statutory Double Patenting

The nonstatutory double patenting rejection is based on a judicially created doctrine grounded in public policy (a policy reflected in the statute) so as to prevent the unjustified or improper timewise extension of the "right to exclude" granted by a patent and to prevent possible harassment by multiple assignees. A nonstatutory double patenting rejection is appropriate where the conflicting claims are not identical, but at least one examined application claim is not patentably distinct from the reference claim(s) because the examined application claim is either anticipated by, or would have been obvious over, the reference claim(s). See, e.g., *In re Berg*, 140 F.3d 1428, 46 USPQ2d 1226 (Fed. Cir. 1998); *In re Goodman*, 11 F.3d 1046, 29 USPQ2d 2010 (Fed. Cir. 1993); *In re Longi*, 759 F.2d 887, 225 USPQ 645 (Fed. Cir. 1985); *In re Van Ornum*,

686 F.2d 937, 214 USPQ 761 (CCPA 1982); *In re Vogel*, 422 F.2d 438, 164 USPQ 619 (CCPA 1970); *In re Thorington*, 418 F.2d 528, 163 USPQ 644 (CCPA 1969).

A timely filed terminal disclaimer in compliance with 37 CFR 1.321(c) or 1.321(d) may be used to overcome an actual or provisional rejection based on nonstatutory double patenting provided the reference application or patent either is shown to be commonly owned with the examined application, or claims an invention made as a result of activities undertaken within the scope of a joint research agreement. See MPEP § 717.02 for applications subject to examination under the first inventor to file provisions of the AIA as explained in MPEP § 2159. See MPEP §§ 706.02(l)(1) - 706.02(l)(3) for applications not subject to examination under the first inventor to file provisions of the AIA. A terminal disclaimer must be signed in compliance with 37 CFR 1.321(b).

The USPTO Internet website contains terminal disclaimer forms which may be used. Please visit www.uspto.gov/patent/patents-forms. The filing date of the application in which the form is filed determines what form (e.g., PTO/SB/25, PTO/SB/26, PTO/AIA/25, or PTO/AIA/26) should be used. A web-based eTerminal Disclaimer may be filled out completely online using web-screens. An eTerminal Disclaimer that meets all requirements is auto-processed and approved immediately upon submission. For more information about eTerminal Disclaimers, refer to www.uspto.gov/patents/process/file/efs/guidance/eTD-info-I.jsp.

Claim 1 is rejected on the ground of nonstatutory double patenting as being unpatentable over claims 1-31 of U.S. Patent No. 10,456,360. Although the

claims at issue are not identical, they are not patentably distinct from each other because of the following reasons:

Instant claim 1 is drawn to a storage stabilized liposome comprising irinotecan and sucrose octasulfate. Said liposome has a pH of 7.00-7.50, the lipids of cholesterol, DSPE, and MPEG-2000-DSPE. Said liposome is stabilized so that less than 20 mol% of lysophosphatidylcholine is formed during the first 6 months of storage at 4°C. Said liposome comprises 500 mg ± 10% irinotecan per millimole of total liposome phospholipid. The composition comprises 4.3 mg irinotecan per mL of the liposomal irinotecan composition.

Conflicting claim 1 is drawn to a storage stabilized liposomal irinotecan composition comprising irinotecan and sucrose octasulfate. The composition is stabilized such that there is less than 20 mol% formation of lysophosphatidylcholine after 6 months of storage at 2-8°C. Said liposome comprises DSPC, cholesterol, and MPEP-2000-DSPE. Said liposome comprises 500 mg ± 10% irinotecan per millimole of total liposome phospholipid. Conflicting claim 4 recites 4.3 mg/mL irinotecan. Conflicting claim 1 recites a pH of from about 7.25 to 7.50.

The instant and copending claims differ because conflicting claim 4 recites a pH of from about 7.25 to about 7.50, whereas instant claim 1 recites a pH of 7.00 to 7.50. Nevertheless, the subject matter of conflicting claim 4 is within the scope of that of instant claim 1, thereby effectively anticipating the subject matter of instant claim 1. This results in a prima facie case of anticipatory-type non-statutory double patenting.

Claim 1 is provisionally rejected on the ground of nonstatutory double patenting as being unpatentable over claims 24-59 of copending Application No. 16/567,902 (reference application). Although the claims at issue are not identical, they are not patentably distinct from each other because of at least the following reasons:

Instant claim 1 is drawn to a storage stabilized liposome comprising irinotecan and sucrose octasulfate. Said liposome has a pH of 7.00-7.50, the lipids of cholesterol, DSPE, and MPEG-2000-DSPE. Said liposome is stabilized so that less than 20 mol% of lysophosphatidylcholine is formed during the first 6 months of storage at 4°C. Said liposome comprises 500 mg ± 10% irinotecan per millimole of total liposome phospholipid. The composition comprises 4.3 mg irinotecan per mL of the liposomal irinotecan composition.

Copending claim 1 is drawn to a storage stabilized liposomal irinotecan composition. Said composition comprises irinotecan, sucrose octasulfate, cholesterol, and DSPC, and methoxy terminated PEG-DSPE. Said composition is stabilized to have less than 20 mol% lysophosphatidylcholine after about 180 days or 6 months in storage at a temperature of from 2-8°C. Said composition has a pH of from about 7.25 to about 7.50. Said composition has 500 grams ± 10% per mole of phospholipid (this is the same as 500 mg (± 10%) per mmol phospholipid). Copending claim 26 recites about 4.3 mg/mL.

The instant and copending claims differ because conflicting claim 4 recites a pH of from about 7.25 to about 7.50, whereas instant claim 1 recites a pH of 7.00 to 7.50. Nevertheless, the subject matter of the copending claims is within the scope of that of

instant claim 1, thereby effectively anticipating the subject matter of instant claim 1. This results in a prima facie case of anticipatory-type non-statutory double patenting.

This is a provisional nonstatutory double patenting rejection because the patentably indistinct claims have not in fact been patented.

Conclusion

No claim is allowed.

Any inquiry concerning this communication or earlier communications from the examiner should be directed to ISAAC SHOMER whose telephone number is (571)270-7671. The examiner can normally be reached on 7:30 AM to 5:00 PM Monday Through Friday.

Examiner interviews are available via telephone, in-person, and video conferencing using a USPTO supplied web-based collaboration tool. To schedule an interview, applicant is encouraged to use the USPTO Automated Interview Request (AIR) at http://www.uspto.gov/interviewpractice.

If attempts to reach the examiner by telephone are unsuccessful, the examiner's supervisor, Frederick F Krass can be reached on (571)272-0580. The fax phone number for the organization where this application or proceeding is assigned is 571-273-8300.

Information regarding the status of an application may be obtained from the Patent Application Information Retrieval (PAIR) system. Status information for published applications may be obtained from either Private PAIR or Public PAIR.

Status information for unpublished applications is available through Private PAIR only. For more information about the PAIR system, see https://ppair-my.uspto.gov/pair/PrivatePair. Should you have questions on access to the Private PAIR system, contact the Electronic Business Center (EBC) at 866-217-9197 (toll-free). If you would like assistance from a USPTO Customer Service Representative or access to the automated information system, call 800-786-9199 (IN USA OR CANADA) or 571-272-1000.

ISAAC . SHOMER
Primary Examiner
Art Unit 1612

/ISAAC SHOMER/
Primary Examiner, Art Unit 1612

UNITED STATES PATENT AND TRADEMARK OFFICE

UNITED STATES DEPARTMENT OF COMMERCE
United States Patent and Trademark Office
Address: COMMISSIONER FOR PATENTS
P.O. Box 1450
Alexandria, Virginia 22313-1450
www.uspto.gov

APPLICATION NO.	FILING DATE	FIRST NAMED INVENTOR	ATTORNEY DOCKET NO.	CONFIRMATION NO.
16/567,902	09/11/2019	Daryl C. Drummond	01208-0010-10US	3814

153749 7590 04/27/2020

McNeill Baur PLLC/Ipsen
Ipsen Bioscience, Inc.
125 Cambridge Park Drive
Suite 301
Cambridge, MA 02140

EXAMINER	
SHOMER, ISAAC	

ART UNIT	PAPER NUMBER
1612	

NOTIFICATION DATE	DELIVERY MODE
04/27/2020	ELECTRONIC

Please find below and/or attached an Office communication concerning this application or proceeding.

The time period for reply, if any, is set in the attached communication.

Notice of the Office communication was sent electronically on above-indicated "Notification Date" to the following e-mail address(es):

docketing@mcneillbaur.com
eofficeaction@appcoll.com
patents.us@ipsen.com

Office Action Summary	Application No. 16/567,902	Applicant(s) Drummond et al.	
	Examiner ISAAC SHOMER	Art Unit 1612	AIA (FITF) Status Yes

-- The MAILING DATE of this communication appears on the cover sheet with the correspondence address --

Period for Reply

A SHORTENED STATUTORY PERIOD FOR REPLY IS SET TO EXPIRE 3 MONTHS FROM THE MAILING DATE OF THIS COMMUNICATION.

- Extensions of time may be available under the provisions of 37 CFR 1.136(a). In no event, however, may a reply be timely filed after SIX (6) MONTHS from the mailing date of this communication.
- If NO period for reply is specified above, the maximum statutory period will apply and will expire SIX (6) MONTHS from the mailing date of this communication.
- Failure to reply within the set or extended period for reply will, by statute, cause the application to become ABANDONED (35 U.S.C. § 133). Any reply received by the Office later than three months after the mailing date of this communication, even if timely filed, may reduce any earned patent term adjustment. See 37 CFR 1.704(b).

Status

1)☑ Responsive to communication(s) filed on 22 November 2019.

☐ A declaration(s)/affidavit(s) under **37 CFR 1.130(b)** was/were filed on _____.

2a)☐ This action is **FINAL.** 2b) ☑ This action is non-final.

3)☐ An election was made by the applicant in response to a restriction requirement set forth during the interview on _____; the restriction requirement and election have been incorporated into this action.

4)☐ Since this application is in condition for allowance except for formal matters, prosecution as to the merits is closed in accordance with the practice under *Ex parte Quayle*, 1935 C.D. 11, 453 O.G. 213.

Disposition of Claims*

5) ☑ Claim(s) 24-59 is/are pending in the application.

5a) Of the above claim(s) _____ is/are withdrawn from consideration.

6) ☐ Claim(s) _____ is/are allowed.

7) ☑ Claim(s) 24-59 is/are rejected.

8) ☐ Claim(s) _____ is/are objected to.

9) ☐ Claim(s) _____ are subject to restriction and/or election requirement

* If any claims have been determined allowable, you may be eligible to benefit from the **Patent Prosecution Highway** program at a participating intellectual property office for the corresponding application. For more information, please see http://www.uspto.gov/patents/init_events/pph/index.jsp or send an inquiry to **PPHfeedback@uspto.gov.**

Application Papers

10)☐ The specification is objected to by the Examiner.

11)☐ The drawing(s) filed on _____ is/are: a)☐ accepted or b)☐ objected to by the Examiner.

Applicant may not request that any objection to the drawing(s) be held in abeyance. See 37 CFR 1.85(a).

Replacement drawing sheet(s) including the correction is required if the drawing(s) is objected to. See 37 CFR 1.121(d).

Priority under 35 U.S.C. § 119

12)☐ Acknowledgment is made of a claim for foreign priority under 35 U.S.C. § 119(a)-(d) or (f).

Certified copies:

a)☐ All b)☐ Some** c)☐ None of the:

1.☐ Certified copies of the priority documents have been received.

2.☐ Certified copies of the priority documents have been received in Application No. _____.

3.☐ Copies of the certified copies of the priority documents have been received in this National Stage application from the International Bureau (PCT Rule 17.2(a)).

** See the attached detailed Office action for a list of the certified copies not received.

Attachment(s)

1) ☑ Notice of References Cited (PTO-892)

2) ☑ Information Disclosure Statement(s) (PTO/SB/08a and/or PTO/SB/08b) Paper No(s)/Mail Date _____.

3) ☐ Interview Summary (PTO-413) Paper No(s)/Mail Date _____.

4) ☐ Other: _____.

DETAILED ACTION

Notice of Pre-AIA or AIA Status

The present application, filed on or after March 16, 2013, is being examined under the first inventor to file provisions of the AIA.

In the event the determination of the status of the application as subject to AIA 35 U.S.C. 102 and 103 (or as subject to pre-AIA 35 U.S.C. 102 and 103) is incorrect, any correction of the statutory basis for the rejection will not be considered a new ground of rejection if the prior art relied upon, and the rationale supporting the rejection, would be the same under either status.

Claim Interpretation

Claim 37 recites how the amount of free irinotecan is measured. The examiner provides the following explanation regarding claim 37.

The skilled artisan would have understood that the liposome of the instant claims is not indefinitely stable. As such, during storage, there is at least some degradation of the liposome. This degradation would likely contribute to irinotecan, which is the encapsulated drug, being prematurely released from encapsulation. It is this irinotecan which is released from liposomal encapsulation that is understood to read on the recited "free irinotecan." This does not lack antecedent basis because the skilled artisan would have expected that examples of irinotecan stored in a liposome would have resulted in free irinotecan because no storage is perfect, and said free irinotecan could have been

analyzed in the manner recited by claim 37. With that being said, the manner in which the free irinotecan is analyzed is not understood to further limit the claimed composition. See at least MPEP 2112(I & II), MPEP 2112.01(I & II), and MPEP 2114(II).

The examiner also clarifies that the "free irinotecan" recited by claim 37 differs from claim requirements of irinotecan in its free base form, e.g. as in claim 26. Irinotecan it its free base form is irinotecan that is not protonated; in contrast, free irinotecan is irinotecan that is outside the liposome.

Claim Rejections - 35 USC § 112(a) – New Matter

The following is a quotation of the first paragraph of 35 U.S.C. 112(a):

> (a) IN GENERAL.—The specification shall contain a written description of the invention, and of the manner and process of making and using it, in such full, clear, concise, and exact terms as to enable any person skilled in the art to which it pertains, or with which it is most nearly connected, to make and use the same, and shall set forth the best mode contemplated by the inventor or joint inventor of carrying out the invention.

The following is a quotation of the first paragraph of pre-AIA 35 U.S.C. 112:

> The specification shall contain a written description of the invention, and of the manner and process of making and using it, in such full, clear, concise, and exact terms as to enable any person skilled in the art to which it pertains, or with which it is most nearly connected, to make and use the same, and shall set forth the best mode contemplated by the inventor of carrying out his invention.

Claims 43 and 47-51 are rejected under 35 U.S.C. 112(a) or 35 U.S.C. 112 (pre-AIA), first paragraph, as failing to comply with the written description requirement. The claim(s) contains subject matter which was not described in the specification in such a way as to reasonably convey to one skilled in the relevant art that the inventor or

a joint inventor, or for pre-AIA the inventor(s), at the time the application was filed, had possession of the claimed invention.

Claim 43 recites an upper limit of 0.48 M sucrose octasulfate. There does not appear to be adequate support for this concentration.

Claims 47-51 recite the temperature at which the liposome is loaded. The temperature ranges recited by these claims do not appear to be adequately supported by the instant application as filed.

Non-Statutory Double Patenting

The nonstatutory double patenting rejection is based on a judicially created doctrine grounded in public policy (a policy reflected in the statute) so as to prevent the unjustified or improper timewise extension of the "right to exclude" granted by a patent and to prevent possible harassment by multiple assignees. A nonstatutory double patenting rejection is appropriate where the conflicting claims are not identical, but at least one examined application claim is not patentably distinct from the reference claim(s) because the examined application claim is either anticipated by, or would have been obvious over, the reference claim(s). See, e.g., *In re Berg*, 140 F.3d 1428, 46 USPQ2d 1226 (Fed. Cir. 1998); *In re Goodman*, 11 F.3d 1046, 29 USPQ2d 2010 (Fed. Cir. 1993); *In re Longi*, 759 F.2d 887, 225 USPQ 645 (Fed. Cir. 1985); *In re Van Ornum*, 686 F.2d 937, 214 USPQ 761 (CCPA 1982); *In re Vogel*, 422 F.2d 438, 164 USPQ 619 (CCPA 1970); *In re Thorington*, 418 F.2d 528, 163 USPQ 644 (CCPA 1969).

A timely filed terminal disclaimer in compliance with 37 CFR 1.321(c) or 1.321(d) may be used to overcome an actual or provisional rejection based on nonstatutory double patenting provided the reference application or patent either is shown to be commonly owned with the examined application, or claims an invention made as a result of activities undertaken within the scope of a joint research agreement. See MPEP § 717.02 for applications subject to examination under the first inventor to file provisions of the AIA as explained in MPEP § 2159. See MPEP §§ 706.02(l)(1) - 706.02(l)(3) for applications not subject to examination under the first inventor to file provisions of the AIA. A terminal disclaimer must be signed in compliance with 37 CFR 1.321(b).

The USPTO Internet website contains terminal disclaimer forms which may be used. Please visit www.uspto.gov/patent/patents-forms. The filing date of the application in which the form is filed determines what form (e.g., PTO/SB/25, PTO/SB/26, PTO/AIA/25, or PTO/AIA/26) should be used. A web-based eTerminal Disclaimer may be filled out completely online using web-screens. An eTerminal Disclaimer that meets all requirements is auto-processed and approved immediately upon submission. For more information about eTerminal Disclaimers, refer to www.uspto.gov/patents/process/file/efs/guidance/eTD-info-I.jsp.

Claims 24-59 are rejected on the ground of nonstatutory double patenting as being unpatentable over claims 1-31 of U.S. Patent No. 10,456,360. Although the claims at issue are not identical, they are not patentably distinct from each other because of the following reasons:

Instant claim 24 is drawn to an irinotecan sucrose octasulfate liposome. Said liposome has less than 20 mol% lysophosphatidylcholine after 6 months storage at 2-8°C. The instant claims recite a three step process by which this liposome is made as a product-by-process type claim limitation.

Conflicting claim 1 is drawn to an irinotecan sucrose octasulfate liposome. Said liposome has less than 20 mol% lysophosphatidylcholine after 6 months storage at 2-8°C. The conflicting claims recite a three step process by which this liposome is made as a product-by-process type claim limitation.

The instant and conflicting claims differ because step (b) of the three step process of instant claim 24 is drawn to incubating the liposomes with an aqueous solution comprising irinotecan at conditions effective to load the irinotecan. In contrast, step (b) of the three step process of conflicting claim 1 is drawn to contacting the liposomes with a solution comprising irinotecan, at a temperature above the transition temperature of the component phospholipids, thereby forming a preparation of liposomes encapsulating irinotecan sucrose octasulfate within the liposomes. Nevertheless, the product of the conflicting claims appears to be within the scope of the product of the instant claims, effectively anticipating the subject matter of the instant claims. This results in a prima facie case of anticipatory-type non-statutory double patenting.

Claims 24-59 are provisionally rejected on the ground of nonstatutory double patenting as being unpatentable over claim 1 of copending Application

No. 16/510,394 (reference application). Although the claims at issue are not identical, they are not patentably distinct from each other because of the following reasons:

Instant claim 24 is drawn to an irinotecan sucrose octasulfate liposome. Said liposome has less than 20 mol% lysophosphatidylcholine after 6 months storage at 2-8°C. The instant claims recite a three step process by which this liposome is made as a product-by-process type claim limitation. Said liposome comprises DSPC, cholesterol, and methoxy terminated polyethylene glycol distearoyl phosphatidylethanolamine (mPEG-DSPE).

Copending claim 1 is drawn to an irinotecan sucrose octasulfate liposome. Said liposome has less than 20 mol% lysophosphatidylcholine after 6 months storage at 2-8°C. Said liposome comprises cholesterol, DSPC, and mPEG-DSPE.

The instant and copending claims differ because the instant claims recite a pH range of about 7.25 to about 7.50, whereas the copending claims recite a pH range of 7.00 to 7.50. Nevertheless, the pH range of the copending claims overlaps with that of the instant claims, resulting in a prima facie case of obviousness-type non-statutory double patenting. See MPEP 2144.05(I).

The instant claims and copending claims differ because the copending claims recite the process by which the claimed composition is prepared, which is not recited by the instant claims. Nevertheless, the composition of the copending claims appears to be essentially the same as that of the instant claims with the exception of the overlap regarding pH range. An overlap of ranges results in a prima facie case of obviousness; see MPEP 2144.05(I). As such, this results in a prima facie case of obviousness-type non-statutory double patenting.

This is a provisional nonstatutory double patenting rejection because the patentably indistinct claims have not in fact been patented.

Cited Prior Art – No Prior Art Rejections Written

The examiner has cited the following close prior art, and has provided an explanation as to why no rejection has been written over the cited prior art. The following is taken mostly from the corrected reasons for allowance in prior application 15/768,352 (now US Patent 10,456,360), mailed on 28 August 2019; the issues in the instant case are very similar to those in the '352 application.

The instant claims are drawn to a liposomal composition comprising irinotecan and sucrose octasulfate. As close and relevant prior art, the examiner cites Drummond et al. (US 2007/0110798 A1) and Hong et al. (US 2007/0116753 A1), which are also drawn to liposomes comprising sucrose octasulfate and irinotecan. Also cited by the examiner is Saetern et al. (International Journal of Pharmaceutics, Vol. 288, 2005, pages 73-80).

The following reasons are provided by the examiner explaining why the instant claims have not been rejected as anticipated by these references or obvious over these references.

Summary of Examiner's Position: Liposomes are known to suffer from degradation when in storage. One such form of degradation involves the hydrolysis of phosphatidylcholine, which is a phospholipid molecule with two hydrocarbon chains that makes up the structural of the bilayer of the liposome, to lysophosphatidylcholine, which

has only one hydrocarbon chain. Such lysophosphatidylcholine is understood to have poor stability in the liposome bilayer, and a bilayer comprising sufficient amounts of lysophosphatidylcholine is subject to degradation. The instantly claimed invention is drawn to a liposome that has unexpectedly greater storage stability in that there is less degradation of phosphatidylcholine to lysophosphatidylcholine as compared with the liposomes of the Drummond and Hong prior art references cited above. The following reasons are presented by the examiner in support of this position.

A) pH Range: First, the instantly claimed liposome is stored in a medium wherein the pH is about 7.25 to about 7.50 (as in instant claim 24). Hong teaches that the liposome should be stored at a pH of between 6.0 and 7.5, with a pH of 6.5 as most optimal, as of Hong, paragraph 0115. However, additional relevant prior art shows that storage of a liposome in a pH of about 6.25 to 6.5 has the greatest storage stability, and that deviation from pH 6.25-6.5 results in more degradation during storage as compared to storage at pH 6.5. In support of this position, the examiner cites Saetern et al. (International Journal of Pharmaceutics, Vol. 288, 2005, pages 73-80). Saetern et al. (hereafter referred to as Saetern), teaches the following graph regarding degradation of phosphatidylcholine to lysophosphatidylcholine, as of page 77, right column, Figure 5, which is reproduced below.

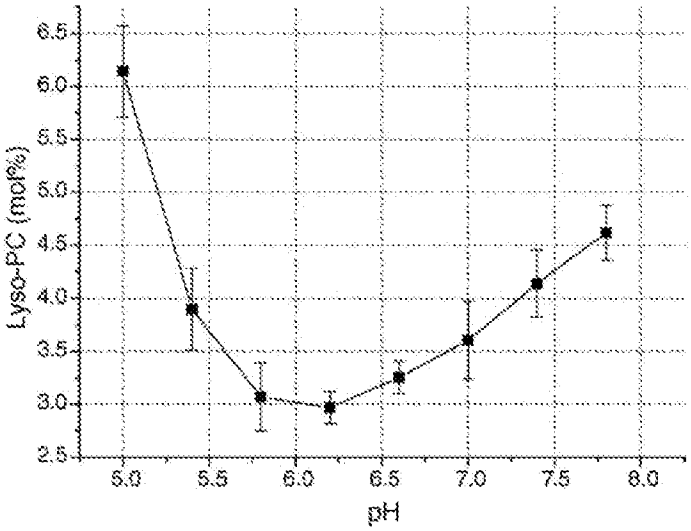

As such, the data of Saetern indicates that a pH of about 6.25 provides the greatest stability of a phosphatidylcholine containing liposome. The examiner also notes that the Saetern publication is especially relevant here because Saetern is drawn to encapsulating camptothecin as a drug, and the instant claims are drawn to a liposome that encapsulates irinotecan as a drug, wherein irinotecan is a derivative of camptothecin.

However, in the instant specification, applicant has presented data showing that a pH range of about 7.25 to about 7.50 unexpectedly provides increased stability as compared to a pH of about 6.5. In support of this position, the examiner cites table 1B on page 26 of the instant specification, which is reproduced below.

Table 1B: *Irinotecan Liposome Stability Ratio and Lyso-PC (after 6 months at 4 °C)*[b]

Sample	Molar (M) concentration of sulfate groups in the sucrosofate entrapped in the liposomes	Stability Ratio	pH	[mol% Lyso-PC] at 6 mos.
1	0.45	1047	6.5	19.5
2	0.475	992	6.5	17
3	0.5	942	6.5	26.5
4	0.6	785	6.5	30.2
5	0.45	1047	7.25	7.1
6	0.45	1047	6.5	14.6
7	0.45	1047	7.25	7.4
8	0.45	1047	7.5	5.4
9	0.6	785	6.5	29.8
10	0.6	785	7.25	24.1
11	0.6	785	7.5	22.8
13	0.45	1047	7.25	9.72

[b] Measured according to Method B, as described herein.

Instant table 1B discloses that a liposome at a pH of 6.5 and a sulfate group concentration of 0.45 M (Sample #1) shows 14.6 mol% or 19.5 mol% of lysophosphatidylcholine after 6 months, as of samples #6 and #1 respectively. In contrast, a sample with a pH of 7.25 and an identical sucrose octasulfate concentration of 0.45 M (Samples #5 and #7) shows only about 7.1 mol% or 7.4 mol% of lysophosphatidylcholine after 6 months of storage. As a greater percentage of lysophosphatidylcholine indicates a less stable liposome, the data presented in Table 1 show an increase in stability when the pH of a sucrose octasulfate containing irinotecan liposome is raised from 6.5 to 7.25.

This increase in stability with increase in pH is at odds with the teachings of the prior art, which indicate that a lower pH of 6.25 to 6.5 is optimal for achieving stability of the liposome. As applicant has shown that the claimed pH range is critical for achieving increased stability, this is understood to be evidence of non-obviousness. See MPEP 2144.05(III)(A). Additionally, proceeding contrary to accepted wisdom is evidence of

nonobviousness. See MPEP 2145(X)(D)(3), citing In re Hedges, 783 F.2d 1038, 228 USPQ 685 (Fed. Cir. 1986). In this case, applicant has proceeded contrary to the expected wisdom of the Saetern reference and has achieved beneficial results of increased stability.

B) Sucrose Octasulfate Loading Concentration: The instant claims were loaded at from 0.4 M to 0.5 M sucrose octasulfate. The following explanation is drawn to the reasons that this limitations is relevant to the examiner's decision not to reject the instant claims in view of this limitation.

B1 – Legal Information Regarding Product-by-Process Limitations: In the instantly claimed product-by-process, sucrose octasulfate was loaded in a concentration such that the sulfate groups are present in a concentration of 0.4 to 0.5 M based on sulfate groups, as of part (a) of claim 24.

As an initial matter, the examiner notes that, with regard to product-by-process claims, such claims are not limited to the manipulations of the recited steps, and are only limited to the structure implied by the steps. See MPEP 2113(I). Nevertheless, once the examiner provides a rationale tending to show that the claimed product appears to be the same or similar to that of the prior art, although produced by a different process, the burden shifts to applicant to come forward with evidence establishing an unobvious difference between the claimed product and the prior art product. See MPEP 2113(II). It is the examiner's position that applicant has provided such evidence. An explanation for why that is the case is provided below.

B2 – Explanation of Teachings of Hong Regarding Sucrose Octasulfate Concentration:

Hong teaches that the substituted ammonium and/or polyanion salt inside the liposome is in a concentration ranging from 10 mM to 1.0 M, with a preferred concentration range of about 0.65 M to about 1.0 M, as of Hong, paragraph 0104.

The examiner provides the following explanation of paragraph 0104 of Hong: Sucrose octasulfate is a polyanion (as it includes multiple sulfate anionic groups), and a salt of sucrose octasulfate is therefore a polyanion salt. Sucrose octasulfate as a substituted ammonium salt is taught in the examples of the Hong reference, e.g. as of paragraph 0138 in Example 7 of Hong and paragraph 0161 of Hong in Example 11. Paragraph 0161 of Hong teaches TEA-SOS, which is triethylammonium sucrose octasulfate.

As such, it is the examiner's best understanding that the "substituted ammonium and/or polyanion salt" in paragraph 0104 of Hong is a salt such as triethylammonium sucrose octasulfate (wherein triethylammonium is a substituted ammonium).

The examiner makes the following note regarding the chemistry of sucrose octasulfate. Sucrose octasulfate is a molecule comprising sucrose substituted with eight sulfate groups covalently attached thereto. Each sulfate group carries a formal charge of -1. As such, cations are needed to balance the negative formal charge in sucrose octasulfate. In the teachings of Hong, the most preferred cation is a substituted ammonium cation such as tetraethylammonium. The tetraethylammonium cation has a formal charge of +1, e.g. as of paragraph 0161 of Hong. As such, eight

tetraethylammonium cations are needed to balance the charge of one sucrose octasulfate anion.

The instant claims recites sucrose octasulfate concentration in terms of the sulfate concentration. Hong, in paragraph 0104, expresses polyanion (e.g. sucrose octasulfate) concentration in terms of the molarity of the substituted ammonium ion. These are equivalent concentrations, as one substituted ammonium ion is needed to balance the charge of one sulfate group.

As such, the value of 0.5 M in paragraph 0104 of Hong is the same as the recited value of 0.5 M. Nevertheless, any *prima facie* case of obviousness is overcome by unexpected results, as explained below.

B3 – Summary of Unexpected Results: In this case, any prima facie case of obviousness that may be present is overcome with unexpected results. See MPEP 716.01 and 716.02.

Data in the instant application show that loading with a level of sucrose octasulfate with a sulfate group concentration of 0.4 M to 0.5 M appears to provide a liposome with increased stability as compared with a liposome loaded at 0.60 to 0.65 M. In support of this position, the examiner cites table 1B on page 26 of the instant specification, which is reproduced above in section A of the reasons for allowance. Sample 10 of the instant specification shows loading at 0.60 M sucrose octasulfate and pH 7.25. In this example, there was 24.1 mol% lysophosphatidylcholine after 6 months of storage. In contrast, samples 5 and 7 are drawn to a liposome loaded with 0.45 M sucrose octasulfate and also a pH of 7.25, and these show 7.1% and 7.4% of lyosphosphatidylcholine respectively after 6 months of storage.

As a greater percentage of lysophosphatidylcholine indicates a less stable liposome, the data presented in Table 1 show an increase in stability when the concentration of sulfate groups from sucrose octasulfate is decreased from the preferred concentration in the prior art of 0.65 M to a lower concentration of 0.4 M to 0.5 M. This would not have been expected by the skilled artisan, and this also indicates that the concentration of sucrose octasulfate used in loading the liposome is critical to the liposome stability. This showing regarding the criticality of the claimed loading concentration of sucrose octasulfate is evidence of non-obviousness, and applicant's data show that the claimed range of sucrose octasulfate is critical with regard to the stability of the liposome that is ultimately formed. See MPEP 2144.05(III)(A).

B4 – Examiner's Statement Regarding MPEP 716.02(e) and the Prior Art: The examiner has included this section of the reasons for not rejection over prior art to make the case that applicant successfully compared the claimed invention to a comparative example that is at least as close as what is actually present in the prior art. See MPEP 716.02(e), especially 716.02(e)(II) and 716.02(e)(III). The following reasoning is presented by the examiner in support of this position.

The examiner notes here that while paragraph 0104 of Hong may teach sucrose octasulfate in amounts that overlap with the claimed amounts, most of the examples of Hong teach sucrose octasulfate in amounts that are greater than the claimed amount or that differ from the claimed invention in other ways. For example, Hong, paragraph 0072, Example 13, teaches sucrose octasulfate in an amount of 0.643 N. The same teaching is present on Hong, Example 15, paragraph 0176. Example 16, paragraph 0183 of Hong teaches sucrose octasulfate at 0.65 M based upon triethylammonium.

Hong teaches a higher concentration of 1.05 N sucrose octasulfate in Example 24, paragraph 0295.

The closest example in Hong appears to be a teaching of a liposome comprising 0.47 M triethylammonium sucrose octasulfate in Example 23, paragraph 0204 of Hong. However, this example is for the drug topotecan, which differs from the claimed irinotecan. Also, this example has a pH that of 6.27, which differs as compared with the claimed pH range of about 7.25 to about 7.50.

As such, Hong does not appear to teach an example comprising a liposome with irinotecan and sucrose octasulfate in a concentration of 0.4 M to 0.5 M.

In the case of determination of a prima facie case of obviousness, whether sucrose octasulfate in a concentration of 0.4 M to 0.5 M is taught in the examples or in the broad disclosure of Hong is not particularly relevant. This is because, regardless of whether the teaching is in the examples or in the broad disclosure, there is a prima facie case of obviousness. See MPEP 2123. However, in this case, the relevant issue being discussed in this section of the reasons for allowance is in regards to unexpected results rather than a prima facie case of obviousness. For the relevant analysis regarding unexpected results, the examiner cites MPEP 716.02(e), which states that the claimed invention must be compared with the closest prior art.

Crucially, MPEP 716.02(e)(III) states that [a]lthough evidence of unexpected results must compare the claimed invention with the closest prior art, applicant is not required to compare the claimed invention with subject matter that does not exist in the prior art. In this case, the examiner understands that an irinotecan liposome comprising 0.4-0.5 M sucrose octasulfate and a pH of about 7.25 to about 7.50, thought potentially

suggested by Hong through teachings at disparate portions of the reference, does not actually exist in Hong because it is not present in the examples of Hong.

As such, applicant's comparison of the claimed invention vs. a comparative example comprising 0.6 M sucrose octasulfate, as of Table 1B of the instant specification, which is reproduced above, is understood to successfully compare the claimed invention against a comparative example that is closer than the subject matter which actually exists in the prior art.

C) Combination of pH and Sucrose Octasulfate Concentration: The data shown above appear to indicate that it is not only the pH and the sucrose octasulfate concentration, but the combination of the pH and sucrose octasulfate concentration that lead to greater stability as compared with the prior art. For that matter, the only embodiments in Figure 1B, reproduced above, that form less than 10 mol% lysophosphatidylcholine after 6 months storage at 4°C have a pH of 7.25 or 7.5 and a sucrose octasulfate concentration of 0.45 M. Examples that differ by either pH, sucrose octasulfate concentration, or both, form a higher mol% of lysophosphatidylcholine after storage, which indicates lower stability.

As such, for at least these reasons, the examiner has not rejected the instant claims as prima facie obvious over Drummond et al. (US 2007/0110798 A1) or Hong et al. (US 2007/0116753 A1).

Conclusion

No claim is allowed at this time.

Any inquiry concerning this communication or earlier communications from the examiner should be directed to ISAAC SHOMER whose telephone number is (571)270-7671. The examiner can normally be reached on 7:30 AM to 5:00 PM Monday Through Friday.

Examiner interviews are available via telephone, in-person, and video conferencing using a USPTO supplied web-based collaboration tool. To schedule an interview, applicant is encouraged to use the USPTO Automated Interview Request (AIR) at http://www.uspto.gov/interviewpractice.

If attempts to reach the examiner by telephone are unsuccessful, the examiner's supervisor, Frederick F Krass can be reached on (571)272-0580. The fax phone number for the organization where this application or proceeding is assigned is 571-273-8300.

Information regarding the status of an application may be obtained from the Patent Application Information Retrieval (PAIR) system. Status information for published applications may be obtained from either Private PAIR or Public PAIR. Status information for unpublished applications is available through Private PAIR only. For more information about the PAIR system, see https://ppair-my.uspto.gov/pair/PrivatePair. Should you have questions on access to the Private PAIR system, contact the Electronic Business Center (EBC) at 866-217-9197 (toll-free). If you would like assistance from a USPTO Customer Service Representative or access

to the automated information system, call 800-786-9199 (IN USA OR CANADA) or 571-272-1000.

ISAAC . SHOMER
Primary Examiner
Art Unit 1612

/ISAAC SHOMER/
Primary Examiner, Art Unit 1612

UNITED STATES PATENT AND TRADEMARK OFFICE

UNITED STATES DEPARTMENT OF COMMERCE
United States Patent and Trademark Office
Address: COMMISSIONER FOR PATENTS
P.O. Box 1450
Alexandria, Virginia 22313-1450
www.uspto.gov

APPLICATION NO.	FILING DATE	FIRST NAMED INVENTOR	ATTORNEY DOCKET NO.	CONFIRMATION NO.
16/567,902	09/11/2019	Daryl C. Drummond	01208-0010-10US	3814

153749 7590 08/10/2020

McNeill Baur PLLC/Ipsen
Ipsen Bioscience, Inc.
125 Cambridge Park Drive
Suite 301
Cambridge, MA 02140

EXAMINER	
SHOMER, ISAAC	

ART UNIT	PAPER NUMBER
1612	

NOTIFICATION DATE	DELIVERY MODE
08/10/2020	ELECTRONIC

Please find below and/or attached an Office communication concerning this application or proceeding.

The time period for reply, if any, is set in the attached communication.

Notice of the Office communication was sent electronically on above-indicated "Notification Date" to the following e-mail address(es):

docketing@mcneillbaur.com
eofficeaction@appcoll.com
patents.us@ipsen.com

Office Action Summary	Application No. 16/567,902	Applicant(s) Drummond et al.	
	Examiner ISAAC SHOMER	Art Unit 1612	AIA (FITF) Status Yes

-- The MAILING DATE of this communication appears on the cover sheet with the correspondence address --

Period for Reply

A SHORTENED STATUTORY PERIOD FOR REPLY IS SET TO EXPIRE 3 MONTHS FROM THE MAILING DATE OF THIS COMMUNICATION.

- Extensions of time may be available under the provisions of 37 CFR 1.136(a). In no event, however, may a reply be timely filed after SIX (6) MONTHS from the mailing date of this communication.
- If NO period for reply is specified above, the maximum statutory period will apply and will expire SIX (6) MONTHS from the mailing date of this communication.
- Failure to reply within the set or extended period for reply will, by statute, cause the application to become ABANDONED (35 U.S.C. § 133). Any reply received by the Office later than three months after the mailing date of this communication, even if timely filed, may reduce any earned patent term adjustment. See 37 CFR 1.704(b).

Status

1)☑ Responsive to communication(s) filed on 27 July 2020.

☐ A declaration(s)/affidavit(s) under **37 CFR 1.130(b)** was/were filed on _____.

2a)☑ This action is **FINAL.** 2b) ☐ This action is non-final.

3)☐ An election was made by the applicant in response to a restriction requirement set forth during the interview on _____; the restriction requirement and election have been incorporated into this action.

4)☐ Since this application is in condition for allowance except for formal matters, prosecution as to the merits is closed in accordance with the practice under *Ex parte Quayle*, 1935 C.D. 11, 453 O.G. 213.

Disposition of Claims*

5) ☑ Claim(s) 24-59 is/are pending in the application.

5a) Of the above claim(s) _____ is/are withdrawn from consideration.

6) ☐ Claim(s) _____ is/are allowed.

7) ☑ Claim(s) 24-59 is/are rejected.

8) ☐ Claim(s) _____ is/are objected to.

9) ☐ Claim(s) _____ are subject to restriction and/or election requirement

* If any claims have been determined allowable, you may be eligible to benefit from the **Patent Prosecution Highway** program at a participating intellectual property office for the corresponding application. For more information, please see http://www.uspto.gov/patents/init_events/pph/index.jsp or send an inquiry to **PPHfeedback@uspto.gov.**

Application Papers

10)☐ The specification is objected to by the Examiner.

11)☐ The drawing(s) filed on _____ is/are: a)☐ accepted or b)☐ objected to by the Examiner.

Applicant may not request that any objection to the drawing(s) be held in abeyance. See 37 CFR 1.85(a).

Replacement drawing sheet(s) including the correction is required if the drawing(s) is objected to. See 37 CFR 1.121(d).

Priority under 35 U.S.C. § 119

12)☐ Acknowledgment is made of a claim for foreign priority under 35 U.S.C. § 119(a)-(d) or (f).

Certified copies:

a)☐ All b)☐ Some** c)☐ None of the:

1.☐ Certified copies of the priority documents have been received.

2.☐ Certified copies of the priority documents have been received in Application No. _____.

3.☐ Copies of the certified copies of the priority documents have been received in this National Stage application from the International Bureau (PCT Rule 17.2(a)).

** See the attached detailed Office action for a list of the certified copies not received.

Attachment(s)

1) ☑ Notice of References Cited (PTO-892)

2) ☑ Information Disclosure Statement(s) (PTO/SB/08a and/or PTO/SB/08b) Paper No(s)/Mail Date _____.

3) ☐ Interview Summary (PTO-413) Paper No(s)/Mail Date _____.

4) ☐ Other: _____.

DETAILED ACTION

Applicants' arguments, filed 27 July 2020, have been fully considered. Rejections and/or objections not reiterated from previous office actions are hereby withdrawn. The following rejections and/or objections are either reiterated or newly applied. They constitute the complete set presently being applied to the instant application.

The present application, filed on or after March 16, 2013, is being examined under the first inventor to file provisions of the AIA.

Withdrawn Rejections

The previously applied new matter rejection of claim 43 under 35 U.S.C. 112(a) has been withdrawn in view of the claim amendment.

The previously applied new matter rejection of claim 47 under 35 U.S.C. 112(a) has been withdrawn in view of the claim amendment and applicant's argument on page 9 of applicant's response on 27 July 2020 (hereafter referred to as applicant's response).

The previously applied new matter rejections of claims 48-51 have been withdrawn in view of the arguments provided on pages 9-10 of applicant's response.

Non-Statutory Double Patenting

The nonstatutory double patenting rejection is based on a judicially created doctrine grounded in public policy (a policy reflected in the statute) so as to prevent the unjustified or improper timewise extension of the "right to exclude" granted by a patent

and to prevent possible harassment by multiple assignees. A nonstatutory double patenting rejection is appropriate where the conflicting claims are not identical, but at least one examined application claim is not patentably distinct from the reference claim(s) because the examined application claim is either anticipated by, or would have been obvious over, the reference claim(s). See, e.g., *In re Berg*, 140 F.3d 1428, 46 USPQ2d 1226 (Fed. Cir. 1998); *In re Goodman*, 11 F.3d 1046, 29 USPQ2d 2010 (Fed. Cir. 1993); *In re Longi*, 759 F.2d 887, 225 USPQ 645 (Fed. Cir. 1985); *In re Van Ornum*, 686 F.2d 937, 214 USPQ 761 (CCPA 1982); *In re Vogel*, 422 F.2d 438, 164 USPQ 619 (CCPA 1970); *In re Thorington*, 418 F.2d 528, 163 USPQ 644 (CCPA 1969).

A timely filed terminal disclaimer in compliance with 37 CFR 1.321(c) or 1.321(d) may be used to overcome an actual or provisional rejection based on nonstatutory double patenting provided the reference application or patent either is shown to be commonly owned with the examined application, or claims an invention made as a result of activities undertaken within the scope of a joint research agreement. See MPEP § 717.02 for applications subject to examination under the first inventor to file provisions of the AIA as explained in MPEP § 2159. See MPEP §§ 706.02(l)(1) - 706.02(l)(3) for applications not subject to examination under the first inventor to file provisions of the AIA. A terminal disclaimer must be signed in compliance with 37 CFR 1.321(b).

The USPTO Internet website contains terminal disclaimer forms which may be used. Please visit www.uspto.gov/patent/patents-forms. The filing date of the application in which the form is filed determines what form (e.g., PTO/SB/25, PTO/SB/26, PTO/AIA/25, or PTO/AIA/26) should be used. A web-based eTerminal Disclaimer may

be filled out completely online using web-screens. An eTerminal Disclaimer that meets all requirements is auto-processed and approved immediately upon submission. For more information about eTerminal Disclaimers, refer to www.uspto.gov/patents/process/file/efs/guidance/eTD-info-I.jsp.

Claims 24-59 are rejected on the ground of nonstatutory double patenting as being unpatentable over claims 1-31 of U.S. Patent No. 10,456,360. Although the claims at issue are not identical, they are not patentably distinct from each other because of the following reasons:

Instant claim 24 is drawn to an irinotecan sucrose octasulfate liposome. Said liposome has less than 20 mol% lysophosphatidylcholine after 6 months storage at 2-8°C. The instant claims recite a three step process by which this liposome is made as a product-by-process type claim limitation.

Conflicting claim 1 is drawn to an irinotecan sucrose octasulfate liposome. Said liposome has less than 20 mol% lysophosphatidylcholine after 6 months storage at 2-8°C. The conflicting claims recite a three step process by which this liposome is made as a product-by-process type claim limitation.

The instant and conflicting claims differ because step (b) of the three step process of instant claim 24 is drawn to incubating the liposomes with an aqueous solution comprising irinotecan at conditions effective to load the irinotecan. In contrast, step (b) of the three step process of conflicting claim 1 is drawn to contacting the liposomes with a solution comprising irinotecan, at a temperature above the transition temperature of the component phospholipids, thereby forming a preparation of

liposomes encapsulating irinotecan sucrose octasulfate within the liposomes. Nevertheless, the product of the conflicting claims appears to be within the scope of the product of the instant claims, effectively anticipating the subject matter of the instant claims. This results in a prima facie case of anticipatory-type non-statutory double patenting.

Claims 24-59 are provisionally rejected on the ground of nonstatutory double patenting as being unpatentable over claim 1 of copending Application No. 16/510,394 (reference application). Although the claims at issue are not identical, they are not patentably distinct from each other because of the following reasons:

Instant claim 24 is drawn to an irinotecan sucrose octasulfate liposome. Said liposome has less than 20 mol% lysophosphatidylcholine after 6 months storage at 2-8°C. The instant claims recite a three step process by which this liposome is made as a product-by-process type claim limitation. Said liposome comprises DSPC, cholesterol, and methoxy terminated polyethylene glycol distearoyl phosphatidylethanolamine (mPEG-DSPE).

Copending claim 1 is drawn to an irinotecan sucrose octasulfate liposome. Said liposome has less than 20 mol% lysophosphatidylcholine after 6 months storage at 2-8°C. Said liposome comprises cholesterol, DSPC, and mPEG-DSPE.

The instant and copending claims differ because the instant claims recite a pH range of about 7.25 to about 7.50, whereas the copending claims recite a pH range of 7.00 to 7.50. Nevertheless, the pH range of the copending claims overlaps with that of

the instant claims, resulting in a prima facie case of obviousness-type non-statutory double patenting. See MPEP 2144.05(I).

The instant claims and copending claims differ because the copending claims recite the process by which the claimed composition is prepared, which is not recited by the instant claims. Nevertheless, the composition of the copending claims appears to be essentially the same as that of the instant claims with the exception of the overlap regarding pH range. An overlap of ranges results in a prima facie case of obviousness; see MPEP 2144.05(I). As such, this results in a prima facie case of obviousness-type non-statutory double patenting.

This is a provisional nonstatutory double patenting rejection because the patentably indistinct claims have not in fact been patented.

Response to Arguments Regarding Double Patenting Rejection

In applicant's response on 27 July 2020 (hereafter referred to as applicant's response), applicant requests that the double patenting rejections be held in abeyance, as of page 11, top paragraph of applicant's response. As such, these rejections have been maintained.

Cited Prior Art – No Prior Art Rejections Written

The examiner has cited the following close prior art, and has provided an explanation as to why no rejection has been written over the cited prior art. The

following is taken mostly from the corrected reasons for allowance in prior application 15/768,352 (now US Patent 10,456,360), mailed on 28 August 2019; the issues in the instant case are very similar to those in the '352 application.

The instant claims are drawn to a liposomal composition comprising irinotecan and sucrose octasulfate. As close and relevant prior art, the examiner cites Drummond et al. (US 2007/0110798 A1) and Hong et al. (US 2007/0116753 A1), which are also drawn to liposomes comprising sucrose octasulfate and irinotecan. Also cited by the examiner is Saetern et al. (International Journal of Pharmaceutics, Vol. 288, 2005, pages 73-80).

The following reasons are provided by the examiner explaining why the instant claims have not been rejected as anticipated by these references or obvious over these references.

Summary of Examiner's Position: Liposomes are known to suffer from degradation when in storage. One such form of degradation involves the hydrolysis of phosphatidylcholine, which is a phospholipid molecule with two hydrocarbon chains that makes up the structural of the bilayer of the liposome, to lysophosphatidylcholine, which has only one hydrocarbon chain. Such lysophosphatidylcholine is understood to have poor stability in the liposome bilayer, and a bilayer comprising sufficient amounts of lysophosphatidylcholine is subject to degradation. The instantly claimed invention is drawn to a liposome that has unexpectedly greater storage stability in that there is less degradation of phosphatidylcholine to lysophosphatidylcholine as compared with the liposomes of the Drummond and Hong prior art references cited above. The following reasons are presented by the examiner in support of this position.

A) pH Range: First, the instantly claimed liposome is stored in a medium wherein the pH is about 7.25 to about 7.50 (as in instant claim 24). Hong teaches that the liposome should be stored at a pH of between 6.0 and 7.5, with a pH of 6.5 as most optimal, as of Hong, paragraph 0115. However, additional relevant prior art shows that storage of a liposome in a pH of about 6.25 to 6.5 has the greatest storage stability, and that deviation from pH 6.25-6.5 results in more degradation during storage as compared to storage at pH 6.5. In support of this position, the examiner cites Saetern et al. (International Journal of Pharmaceutics, Vol. 288, 2005, pages 73-80). Saetern et al. (hereafter referred to as Saetern), teaches the following graph regarding degradation of phosphatidylcholine to lysophosphatidylcholine, as of page 77, right column, Figure 5, which is reproduced below.

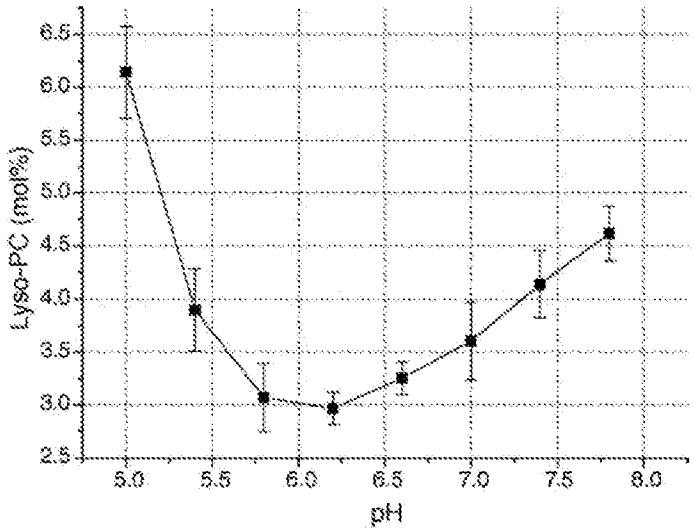

As such, the data of Saetern indicates that a pH of about 6.25 provides the greatest stability of a phosphatidylcholine containing liposome. The examiner also notes that the Saetern publication is especially relevant here because Saetern is drawn to encapsulating camptothecin as a drug, and the instant claims are drawn to a liposome

that encapsulates irinotecan as a drug, wherein irinotecan is a derivative of camptothecin.

However, in the instant specification, applicant has presented data showing that a pH range of about 7.25 to about 7.50 unexpectedly provides increased stability as compared to a pH of about 6.5. In support of this position, the examiner cites table 1B on page 26 of the instant specification, which is reproduced below.

Table 1B: *Irinotecan Liposome Stability Ratio and Lyso-PC (after 6 months at 4 °C)*[b]

Sample	Molar (M) concentration of sulfate groups in the sucrosofate entrapped in the liposomes	Stability Ratio	pH	[mol% Lyso-PC] at 6 mos.
1	0.45	1047	6.5	19.5
2	0.475	992	6.5	17
3	0.5	942	6.5	26.5
4	0.6	785	6.5	30.2
5	0.45	1047	7.25	7.1
6	0.45	1047	6.5	14.6
7	0.45	1047	7.25	7.4
8	0.45	1047	7.5	5.4
9	0.6	785	6.5	29.8
10	0.6	785	7.25	24.1
11	0.6	785	7.5	22.8
13	0.45	1047	7.25	9.72

[b] Measured according to Method B, as described herein.

Instant table 1B discloses that a liposome at a pH of 6.5 and a sulfate group concentration of 0.45 M (Sample #1) shows 14.6 mol% or 19.5 mol% of lysophosphatidylcholine after 6 months, as of samples #6 and #1 respectively. In contrast, a sample with a pH of 7.25 and an identical sucrose octasulfate concentration of 0.45 M (Samples #5 and #7) shows only about 7.1 mol% or 7.4 mol% of lyosphosphatidylcholine after 6 months of storage. As a greater percentage of lysophosphatidylcholine indicates a less stable liposome, the data presented in Table 1

show an increase in stability when the pH of a sucrose octasulfate containing irinotecan liposome is raised from 6.5 to 7.25.

This increase in stability with increase in pH is at odds with the teachings of the prior art, which indicate that a lower pH of 6.25 to 6.5 is optimal for achieving stability of the liposome. As applicant has shown that the claimed pH range is critical for achieving increased stability, this is understood to be evidence of non-obviousness. See MPEP 2144.05(III)(A). Additionally, proceeding contrary to accepted wisdom is evidence of nonobviousness. See MPEP 2145(X)(D)(3), citing In re Hedges, 783 F.2d 1038, 228 USPQ 685 (Fed. Cir. 1986). In this case, applicant has proceeded contrary to the expected wisdom of the Saetern reference and has achieved beneficial results of increased stability.

B) Sucrose Octasulfate Loading Concentration: The instant claims were loaded at from 0.4 M to 0.5 M sucrose octasulfate. The following explanation is drawn to the reasons that this limitations is relevant to the examiner's decision not to reject the instant claims in view of this limitation.

B1 – Legal Information Regarding Product-by-Process Limitations: In the instantly claimed product-by-process, sucrose octasulfate was loaded in a concentration such that the sulfate groups are present in a concentration of 0.4 to 0.5 M based on sulfate groups, as of part (a) of claim 24.

As an initial matter, the examiner notes that, with regard to product-by-process claims, such claims are not limited to the manipulations of the recited steps, and are only limited to the structure implied by the steps. See MPEP 2113(I). Nevertheless, once the examiner provides a rationale tending to show that the claimed product

appears to be the same or similar to that of the prior art, although produced by a different process, the burden shifts to applicant to come forward with evidence establishing an unobvious difference between the claimed product and the prior art product. See MPEP 2113(II). It is the examiner's position that applicant has provided such evidence. An explanation for why that is the case is provided below.

B2 – Explanation of Teachings of Hong Regarding Sucrose Octasulfate Concentration:

Hong teaches that the substituted ammonium and/or polyanion salt inside the liposome is in a concentration ranging from 10 mM to 1.0 M, with a preferred concentration range of about 0.65 M to about 1.0 M, as of Hong, paragraph 0104.

The examiner provides the following explanation of paragraph 0104 of Hong: Sucrose octasulfate is a polyanion (as it includes multiple sulfate anionic groups), and a salt of sucrose octasulfate is therefore a polyanion salt. Sucrose octasulfate as a substituted ammonium salt is taught in the examples of the Hong reference, e.g. as of paragraph 0138 in Example 7 of Hong and paragraph 0161 of Hong in Example 11. Paragraph 0161 of Hong teaches TEA-SOS, which is triethylammonium sucrose octasulfate.

As such, it is the examiner's best understanding that the "substituted ammonium and/or polyanion salt" in paragraph 0104 of Hong is a salt such as triethylammonium sucrose octasulfate (wherein triethylammonium is a substituted ammonium).

The examiner makes the following note regarding the chemistry of sucrose octasulfate. Sucrose octasulfate is a molecule comprising sucrose substituted with eight

sulfate groups covalently attached thereto. Each sulfate group carries a formal charge of -1. As such, cations are needed to balance the negative formal charge in sucrose octasulfate. In the teachings of Hong, the most preferred cation is a substituted ammonium cation such as tetraethylammonium. The tetraethylammonium cation has a formal charge of +1, e.g. as of paragraph 0161 of Hong. As such, eight tetraethylammonium cations are needed to balance the charge of one sucrose octasulfate anion.

The instant claims recites sucrose octasulfate concentration in terms of the sulfate concentration. Hong, in paragraph 0104, expresses polyanion (e.g. sucrose octasulfate) concentration in terms of the molarity of the substituted ammonium ion. These are equivalent concentrations, as one substituted ammonium ion is needed to balance the charge of one sulfate group.

As such, the value of 0.5 M in paragraph 0104 of Hong is the same as the recited value of 0.5 M. Nevertheless, any *prima facie* case of obviousness is overcome by unexpected results, as explained below.

B3 – Summary of Unexpected Results: In this case, any prima facie case of obviousness that may be present is overcome with unexpected results. See MPEP 716.01 and 716.02.

Data in the instant application show that loading with a level of sucrose octasulfate with a sulfate group concentration of 0.4 M to 0.5 M appears to provide a liposome with increased stability as compared with a liposome loaded at 0.60 to 0.65 M. In support of this position, the examiner cites table 1B on page 26 of the instant specification, which is reproduced above in section A of the reasons for allowance.

Sample 10 of the instant specification shows loading at 0.60 M sucrose octasulfate and pH 7.25. In this example, there was 24.1 mol% lysophosphatidylcholine after 6 months of storage. In contrast, samples 5 and 7 are drawn to a liposome loaded with 0.45 M sucrose octasulfate and also a pH of 7.25, and these show 7.1% and 7.4% of lyosphosphatidylcholine respectively after 6 months of storage.

As a greater percentage of lysophosphatidylcholine indicates a less stable liposome, the data presented in Table 1 show an increase in stability when the concentration of sulfate groups from sucrose octasulfate is decreased from the preferred concentration in the prior art of 0.65 M to a lower concentration of 0.4 M to 0.5 M. This would not have been expected by the skilled artisan, and this also indicates that the concentration of sucrose octasulfate used in loading the liposome is critical to the liposome stability. This showing regarding the criticality of the claimed loading concentration of sucrose octasulfate is evidence of non-obviousness, and applicant's data show that the claimed range of sucrose octasulfate is critical with regard to the stability of the liposome that is ultimately formed. See MPEP 2144.05(III)(A).

B4 – Examiner's Statement Regarding MPEP 716.02(e) and the Prior Art: The examiner has included this section of the reasons for not rejection over prior art to make the case that applicant successfully compared the claimed invention to a comparative example that is at least as close as what is actually present in the prior art. See MPEP 716.02(e), especially 716.02(e)(II) and 716.02(e)(III). The following reasoning is presented by the examiner in support of this position.

The examiner notes here that while paragraph 0104 of Hong may teach sucrose octasulfate in amounts that overlap with the claimed amounts, most of the examples of

Hong teach sucrose octasulfate in amounts that are greater than the claimed amount or that differ from the claimed invention in other ways. For example, Hong, paragraph 0072, Example 13, teaches sucrose octasulfate in an amount of 0.643 N. The same teaching is present on Hong, Example 15, paragraph 0176. Example 16, paragraph 0183 of Hong teaches sucrose octasulfate at 0.65 M based upon triethylammonium. Hong teaches a higher concentration of 1.05 N sucrose octasulfate in Example 24, paragraph 0295.

The closest example in Hong appears to be a teaching of a liposome comprising 0.47 M triethylammonium sucrose octasulfate in Example 23, paragraph 0204 of Hong. However, this example is for the drug topotecan, which differs from the claimed irinotecan. Also, this example has a pH that of 6.27, which differs as compared with the claimed pH range of about 7.25 to about 7.50.

As such, Hong does not appear to teach an example comprising a liposome with irinotecan and sucrose octasulfate in a concentration of 0.4 M to 0.5 M.

In the case of determination of a prima facie case of obviousness, whether sucrose octasulfate in a concentration of 0.4 M to 0.5 M is taught in the examples or in the broad disclosure of Hong is not particularly relevant. This is because, regardless of whether the teaching is in the examples or in the broad disclosure, there is a prima facie case of obviousness. See MPEP 2123. However, in this case, the relevant issue being discussed in this section of the reasons for allowance is in regards to unexpected results rather than a prima facie case of obviousness. For the relevant analysis regarding unexpected results, the examiner cites MPEP 716.02(e), which states that the claimed invention must be compared with the closest prior art.

Crucially, MPEP 716.02(e)(III) states that [a]lthough evidence of unexpected results must compare the claimed invention with the closest prior art, applicant is not required to compare the claimed invention with subject matter that does not exist in the prior art. In this case, the examiner understands that an irinotecan liposome comprising 0.4-0.5 M sucrose octasulfate and a pH of about 7.25 to about 7.50, thought potentially suggested by Hong through teachings at disparate portions of the reference, does not actually exist in Hong because it is not present in the examples of Hong.

As such, applicant's comparison of the claimed invention vs. a comparative example comprising 0.6 M sucrose octasulfate, as of Table 1B of the instant specification, which is reproduced above, is understood to successfully compare the claimed invention against a comparative example that is closer than the subject matter which actually exists in the prior art.

C) Combination of pH and Sucrose Octasulfate Concentration: The data shown above appear to indicate that it is not only the pH and the sucrose octasulfate concentration, but the combination of the pH and sucrose octasulfate concentration that lead to greater stability as compared with the prior art. For that matter, the only embodiments in Figure 1B, reproduced above, that form less than 10 mol% lysophosphatidylcholine after 6 months storage at 4°C have a pH of 7.25 or 7.5 and a sucrose octasulfate concentration of 0.45 M. Examples that differ by either pH, sucrose octasulfate concentration, or both, form a higher mol% of lysophosphatidylcholine after storage, which indicates lower stability.

As such, for at least these reasons, the examiner has not rejected the instant claims as prima facie obvious over Drummond et al. (US 2007/0110798 A1) or Hong et

al. (US 2007/0116753 A1). Also, for these reasons, the examiner has not written a double patenting rejection over patents issuing from the disclosures of either Drummond or Hong.

Additional Cited Prior Art

The examiner also searched for lysophosphatidylcholine as an excipient in lipid particles. The art found by the examiner would appear to indicate that lysophosphatidylcholine is generally not desirable as an excipient, at least for structures comprising lipid bilayers. As relevant prior art in this regard, the examiner cites Israelachvili et al. (Quarterly Reviews of Biophysics, Vol. 13(2), 1980, pages 121-200). Israelachvili teaches lysolecithin resulting in a hole forming in a lipid bilayer, as of page 175, figure 5.1, reproduced below.

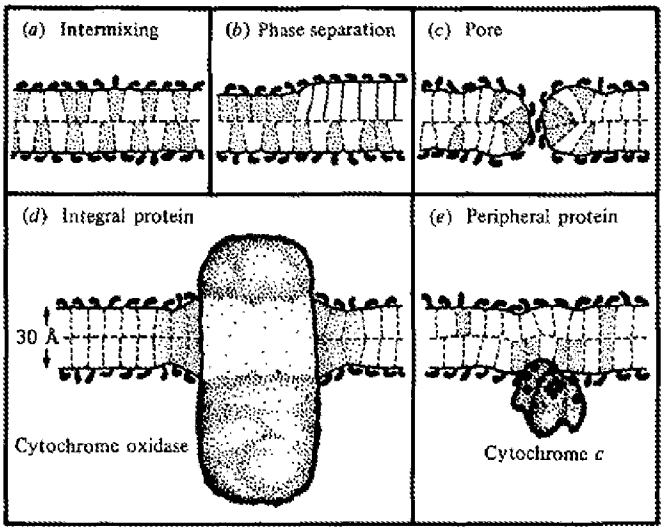

Fig. 5.1. Scaled drawings of mean packing conformations of mixed lipid and lipid–protein membranes. In each case the unperturbed bilayer hydrocarbon thickness is 30 Å. (*a*) Mixed lecithins of head-group area ~ 70 Å^2 but of different chain lengths, in the fluid state. (*b*) Solid-liquid phase separation in upper monolayer of a bilayer. Note that packing stresses must occur at the boundary. (*c*) Mixture of lecithin and lysolecithin where a transient local clustering of lysolecithin can produce a pore or channel. (*d*) Cytochrome oxidase in a lecithin bilayer. Note the perturbations at the protein boundary which may preferentially draw in certain lipids. Dimensions for cytochrome oxidase taken from Henderson *et al.* (1977); dimensions for lecithin are as discussed in Section IV. The detailed shape of cytochrome oxidase is still unknown. (*e*) Cytochrome *c* preferentially associating with charged lipids in a mixed-lipid bilayer via basic lysine residues of the protein surface. Dimensions for cytochrome *c* and positions of the haem and the five invariable lysine residues taken from Dickerson *et al.* (1971).

As best understood by the examiner, the above-reproduced diagram would appear to indicate that the presence of lysophosphatidylcholine (referred to as lysolecithin in the above-reproduced diagram) would appear to create a pore or hole in a lipid bilayer. The skilled artisan would have understood that such a pore or a hole would not have been desirable because it can result in drug leakage.

Therefore, the skilled artisan would have been motivated to have undertaken modifications to the liposome that would result in less degradation of phosphatidylcholine to lysophosphatidylcholine in order to have predictably reduced drug leakage. Nevertheless, the skilled artisan would not have known that the claimed lipids, product-by-process and sucrose octasulfate concentration would have resulted in

less degradation of phosphatidylcholine to lysophosphatidylcholine as compared with the prior art.

As such, Israelachvili further speaks to the practical utility of reducing degradation of phosphatidylcholine to lysophosphatidylcholine and further bolster's the examiner's case for not rejecting the instant claims over prior art.

Conclusion

No claim is allowed.

THIS ACTION IS MADE FINAL. Applicant is reminded of the extension of time policy as set forth in 37 CFR 1.136(a).

A shortened statutory period for reply to this final action is set to expire THREE MONTHS from the mailing date of this action. In the event a first reply is filed within TWO MONTHS of the mailing date of this final action and the advisory action is not mailed until after the end of the THREE-MONTH shortened statutory period, then the shortened statutory period will expire on the date the advisory action is mailed, and any extension fee pursuant to 37 CFR 1.136(a) will be calculated from the mailing date of the advisory action. In no event, however, will the statutory period for reply expire later than SIX MONTHS from the mailing date of this final action.

Any inquiry concerning this communication or earlier communications from the examiner should be directed to ISAAC SHOMER whose telephone number is (571)270-7671. The examiner can normally be reached on 7:30 AM to 5:00 PM Monday Through Friday.

Examiner interviews are available via telephone, in-person, and video conferencing using a USPTO supplied web-based collaboration tool. To schedule an interview, applicant is encouraged to use the USPTO Automated Interview Request (AIR) at http://www.uspto.gov/interviewpractice.

If attempts to reach the examiner by telephone are unsuccessful, the examiner's supervisor, Frederick F Krass can be reached on (571)272-0580. The fax phone number for the organization where this application or proceeding is assigned is 571-273-8300.

Information regarding the status of an application may be obtained from the Patent Application Information Retrieval (PAIR) system. Status information for published applications may be obtained from either Private PAIR or Public PAIR. Status information for unpublished applications is available through Private PAIR only. For more information about the PAIR system, see https://ppair-my.uspto.gov/pair/PrivatePair. Should you have questions on access to the Private PAIR system, contact the Electronic Business Center (EBC) at 866-217-9197 (toll-free). If you would like assistance from a USPTO Customer Service Representative or access to the automated information system, call 800-786-9199 (IN USA OR CANADA) or 571-272-1000.

ISAAC . SHOMER
Primary Examiner
Art Unit 1612

/ISAAC SHOMER/
Primary Examiner, Art Unit 1612

Notice of References Cited	Application/Control No. 16/567,902	Applicant(s)/Patent Under Reexamination Drummond et al.	
	Examiner ISAAC SHOMER	Art Unit 1612	Page 1 of 1

U.S. PATENT DOCUMENTS

*		Document Number Country Code-Number-Kind Code	Date MM-YYYY	Name	CPC Classification	US Classification
	A					
	B					
	C					
	D					
	E					
	F					
	G					
	H					
	I					
	J					
	K					
	L					
	M					

FOREIGN PATENT DOCUMENTS

*		Document Number Country Code-Number-Kind Code	Date MM-YYYY	Country	Name	CPC Classification
	N					
	O					
	P					
	Q					
	R					
	S					
	T					

NON-PATENT DOCUMENTS

*		Include as applicable: Author, Title Date, Publisher, Edition or Volume, Pertinent Pages)
	U	JN Israelachvili, SN Marcelja, and RG Horn. "Physical principles of membrane organization." Quarterly Reviews of Biophysics 13, 2 (1980), pp. 121-200. (Year: 1980)
	V	
	W	
	X	

*A copy of this reference is not being furnished with this Office action. (See MPEP § 707.05(a).)
Dates in MM-YYYY format are publication dates. Classifications may be US or foreign.

UNITED STATES PATENT AND TRADEMARK OFFICE

UNITED STATES DEPARTMENT OF COMMERCE
United States Patent and Trademark Office
Address: COMMISSIONER FOR PATENTS
P.O. Box 1450
Alexandria, Virginia 22313-1450
www.uspto.gov

APPLICATION NO.	FILING DATE	FIRST NAMED INVENTOR	ATTORNEY DOCKET NO.	CONFIRMATION NO.
16/586,609	09/27/2019	Sarah F. Blanchette	01208-0006-02US	9715

153749 7590 10/05/2020

McNeill Baur PLLC/Ipsen
Ipsen Bioscience, Inc.
125 Cambridge Park Drive
Suite 301
Cambridge, MA 02140

EXAMINER	
PACKARD, BENJAMIN J	

ART UNIT	PAPER NUMBER
1612	

NOTIFICATION DATE	DELIVERY MODE
10/05/2020	ELECTRONIC

Please find below and/or attached an Office communication concerning this application or proceeding.

The time period for reply, if any, is set in the attached communication.

Notice of the Office communication was sent electronically on above-indicated "Notification Date" to the following e-mail address(es):

docketing@mcneillbaur.com
eofficeaction@appcoll.com
patents.us@ipsen.com

Office Action Summary	Application No. 16/586,609	Applicant(s) Blanchette et al.	
	Examiner BENJAMIN J PACKARD	Art Unit 1612	AIA (FITF) Status Yes

-- The MAILING DATE of this communication appears on the cover sheet with the correspondence address --

Period for Reply

A SHORTENED STATUTORY PERIOD FOR REPLY IS SET TO EXPIRE 3 MONTHS FROM THE MAILING DATE OF THIS COMMUNICATION.

- Extensions of time may be available under the provisions of 37 CFR 1.136(a). In no event, however, may a reply be timely filed after SIX (6) MONTHS from the mailing date of this communication.
- If NO period for reply is specified above, the maximum statutory period will apply and will expire SIX (6) MONTHS from the mailing date of this communication.
- Failure to reply within the set or extended period for reply will, by statute, cause the application to become ABANDONED (35 U.S.C. § 133). Any reply received by the Office later than three months after the mailing date of this communication, even if timely filed, may reduce any earned patent term adjustment. See 37 CFR 1.704(b).

Status

1)☐ Responsive to communication(s) filed on _____.

☐ A declaration(s)/affidavit(s) under **37 CFR 1.130(b)** was/were filed on _____.

2a)☐ This action is **FINAL.** 2b) ☑ This action is non-final.

3)☐ An election was made by the applicant in response to a restriction requirement set forth during the interview on _____; the restriction requirement and election have been incorporated into this action.

4)☐ Since this application is in condition for allowance except for formal matters, prosecution as to the merits is closed in accordance with the practice under *Ex parte Quayle*, 1935 C.D. 11, 453 O.G. 213.

Disposition of Claims*

5) ☑ Claim(s) 21-37 is/are pending in the application.

5a) Of the above claim(s) _____ is/are withdrawn from consideration.

6) ☐ Claim(s) _____ is/are allowed.

7) ☑ Claim(s) 21-37 is/are rejected.

8) ☐ Claim(s) _____ is/are objected to.

9) ☐ Claim(s) _____ are subject to restriction and/or election requirement

* If any claims have been determined allowable, you may be eligible to benefit from the **Patent Prosecution Highway** program at a participating intellectual property office for the corresponding application. For more information, please see http://www.uspto.gov/patents/init_events/pph/index.jsp or send an inquiry to **PPHfeedback@uspto.gov.**

Application Papers

10)☐ The specification is objected to by the Examiner.

11)☐ The drawing(s) filed on _____ is/are: a)☐ accepted or b)☐ objected to by the Examiner.

Applicant may not request that any objection to the drawing(s) be held in abeyance. See 37 CFR 1.85(a).

Replacement drawing sheet(s) including the correction is required if the drawing(s) is objected to. See 37 CFR 1.121(d).

Priority under 35 U.S.C. § 119

12)☐ Acknowledgment is made of a claim for foreign priority under 35 U.S.C. § 119(a)-(d) or (f).

Certified copies:

a)☐ All b)☐ Some** c)☐ None of the:

1.☐ Certified copies of the priority documents have been received.

2.☐ Certified copies of the priority documents have been received in Application No. _____.

3.☐ Copies of the certified copies of the priority documents have been received in this National Stage application from the International Bureau (PCT Rule 17.2(a)).

** See the attached detailed Office action for a list of the certified copies not received.

Attachment(s)

1) ☐ Notice of References Cited (PTO-892)

2) ☑ Information Disclosure Statement(s) (PTO/SB/08a and/or PTO/SB/08b) Paper No(s)/Mail Date 67 pgs (5/15/20).

3) ☐ Interview Summary (PTO-413) Paper No(s)/Mail Date _____.

4) ☐ Other: _____.

DETAILED ACTION

Notice of Pre-AIA or AIA Status

The present application, filed on or after March 16, 2013, is being examined under the first inventor to file provisions of the AIA.

Obvious-Type Double Patenting

The nonstatutory double patenting rejection is based on a judicially created doctrine grounded in public policy (a policy reflected in the statute) so as to prevent the unjustified or improper timewise extension of the "right to exclude" granted by a patent and to prevent possible harassment by multiple assignees. A nonstatutory double patenting rejection is appropriate where the conflicting claims are not identical, but at least one examined application claim is not patentably distinct from the reference claim(s) because the examined application claim is either anticipated by, or would have been obvious over, the reference claim(s). See, e.g., *In re Berg*, 140 F.3d 1428, 46 USPQ2d 1226 (Fed. Cir. 1998); *In re Goodman*, 11 F.3d 1046, 29 USPQ2d 2010 (Fed. Cir. 1993); *In re Longi*, 759 F.2d 887, 225 USPQ 645 (Fed. Cir. 1985); *In re Van Ornum*, 686 F.2d 937, 214 USPQ 761 (CCPA 1982); *In re Vogel*, 422 F.2d 438, 164 USPQ 619 (CCPA 1970); *In re Thorington*, 418 F.2d 528, 163 USPQ 644 (CCPA 1969).

A timely filed terminal disclaimer in compliance with 37 CFR 1.321(c) or 1.321(d) may be used to overcome an actual or provisional rejection based on nonstatutory double patenting provided the reference application or patent either is shown to be commonly owned with the examined application, or claims an invention made as a result of activities undertaken within the scope of a joint research agreement. See MPEP § 717.02 for applications subject to examination under the first inventor to file provisions of the AIA as explained in MPEP § 2159. See MPEP § 2146 *et seq.* for applications not subject to examination under the first inventor to file provisions of the AIA. A terminal disclaimer must be signed in compliance with 37 CFR 1.321(b).

The USPTO Internet website contains terminal disclaimer forms which may be used. Please visit www.uspto.gov/patent/patents-forms. The filing date of the application in which the form is filed determines what form (e.g., PTO/SB/25, PTO/SB/26, PTO/AIA/25, or PTO/AIA/26) should be used. A web-based eTerminal Disclaimer may be filled out completely online using web-screens. An eTerminal Disclaimer that meets all requirements is auto-processed and approved immediately upon submission. For more information about eTerminal Disclaimers, refer to www.uspto.gov/patents/process/file/efs/guidance/eTD-info-I.jsp.

Claims 21-37 are rejected on the ground of nonstatutory double patenting as being unpatentable over claims 1-19 of U.S. Patent No. 9,895,365. Although the claims at issue are not identical, they are not patentably distinct from each other because the patent discloses the same actives with varying administration processes for the treatment of various cancers, including triple negative breast cancer. As such, the skilled artisan would find it obvious to treat the various cancers and to vary the dosage and times to optimize the treatment of the specific cancer.

Conclusion

Any inquiry concerning this communication or earlier communications from the examiner should be directed to BENJAMIN J PACKARD whose telephone number is (571)270-3440. The examiner can normally be reached on Mon and Wed-Fri (8am-6pm).

Examiner interviews are available via telephone, in-person, and video conferencing using a USPTO supplied web-based collaboration tool. To schedule an interview, applicant is encouraged to use the USPTO Automated Interview Request (AIR) at http://www.uspto.gov/interviewpractice.

If attempts to reach the examiner by telephone are unsuccessful, the examiner's supervisor, Frederick Krass can be reached on (571)272-0580. The fax phone number for the organization where this application or proceeding is assigned is 571-273-8300.

Information regarding the status of an application may be obtained from the Patent Application Information Retrieval (PAIR) system. Status information for published applications may be obtained from either Private PAIR or Public PAIR. Status information for unpublished applications is available through Private PAIR only. For more information about the PAIR system, see https://ppair-my.uspto.gov/pair/PrivatePair. Should you have questions on access to the Private PAIR system, contact the Electronic Business Center (EBC) at 866-217-9197 (toll-free). If you would like assistance from a USPTO Customer Service Representative or access to the automated information system, call 800-786-9199 (IN USA OR CANADA) or 571-272-1000.

/BENJAMIN J PACKARD/
Primary Examiner, Art Unit 1612

Int. J. Cancer: **80,** 134–137 (1999)

Publication of the International Union Against Cancer
Publication de l'Union Internationale Contre le Cancer

THERAPY OF A XENOGRAFTED HUMAN COLONIC CARCINOMA USING CISPLATIN OR DOXORUBICIN ENCAPSULATED IN LONG-CIRCULATING PEGYLATED STEALTH LIPOSOMES

Jan VAAGE[1]*, Dorothy DONOVAN[1], Eirin WIPFF[2], Robert ABRA[2], Gail COLBERN[2], Paul USTER[2] and Peter WORKING[2]

[1]*Department of Immunology, Roswell Park Cancer Institute, Buffalo, NY, USA*
[2]*SEQUUS Pharmaceuticals, Inc., Menlo Park, CA, USA*

We compared the therapeutic effects of low doses of cisplatin and doxorubicin hydrochloride encapsulated in long-circulating liposomes composed of cholesterol/hydrogenated soy phosphatidylcholine-polyethylene glycol-distearoyl-phosphatidyl-ethanolamine. The encapsulation of cisplatin and doxorubicin in these liposomes made ineffectively low doses of the free drugs able to inhibit the growth of and affect cures of a human colonic carcinoma growing in nude mice. Liposome-encapsulated cisplatin had minor systemic toxic side effects indicated by an average 9% weight loss which was recovered 3–4 weeks after the last treatment. Toxicity was not observed in mice treated with liposome-encapsulated doxorubicin. *Int. J. Cancer* 80:134–137, 1999.
1999 Wiley-Liss, Inc.

Studies in animal tumor models found that the therapeutic effects of anti-cancer drugs could be enhanced when the drugs were encapsulated in liposomes (Gabizon *et al.*, 1985; Szoka, 1991). The effectiveness of drugs in conventional liposomes was limited, however, by their rapid uptake by the cells of the reticuloendothelial system (RES), reducing the amount of the drug that reached the tumor (Gabizon *et al.*, 1991). The therapeutic efficacy of doxorubicin was found to be increased and its toxic side effects reduced (Vaage *et al.*, 1993*a*) when the drug was encapsulated in liposomes that had polyethylene glycol (PEG) conjugated to the lipid bilayers (pegylated liposomes) (Gabizon and Papahadjopoulos, 1988; Allen *et al.*, 1991). These liposomes have been given the trade name "Stealth liposomes" because of their reduced uptake by the cells of the RES (Lasic *et al.*, 1991) and their long (>20 hr in mice) circulation half-life (Allen *et al.*, 1991), which, consequently, results in an increased accumulation in tumors (Gabizon and Papahadjopoulos, 1988; Gabizon *et al.*, 1990; Huang *et al.*, 1992). When compared to free doxorubicin in saline, the pegylated liposomal doxorubicin formulation DOXIL showed increased therapeutic efficacy against mouse mammary carcinomas (Vaage *et al.*, 1992) and against xenografted human ovarian (Vaage *et al.*, 1993*b*), prostatic (Vaage *et al.*, 1993*a*) and pancreatic (Vaage *et al.*, 1997) carcinomas. DOXIL was significantly less toxic than free doxorubicin. A 95% lethal treatment of 4 weekly injections of 9 mg/kg doxorubicin in saline was reduced to 5% mortality when the drug was encapsulated in pegylated liposomes (Vaage *et al.*, 1993*a*). Empty liposomes were non-toxic and without effect on tumor growth (Vaage *et al.*, 1992).

The purpose of our investigation was to determine the relative efficacies of either cisplatin or doxorubicin in the regular saline formulations *vs.* the drugs in pegylated liposomes used as therapeutic agents against a human colonic carcinoma growing in athymic (nude) mice. Preliminary tests showed that the therapeutic advantage of encapsulating drugs in pegylated liposomes was clearer when the drugs were used at low, subtoxic doses. At higher doses the toxicity of free cisplatin and doxorubicin interfered with the long-term comparisons of therapeutic effects. Intraperitoneal tumor implantation and intraperitoneal therapy were not attempted in this colonic carcinoma mouse model because in clinical disease, intraperitoneal drug therapy after surgery could interfere with the healing of intestinal anastomoses and is therefore not a recommended procedure (Douglass *et al.*, 1993).

MATERIAL AND METHODS

Mice

The mice were fully mature 18-week-old female nude NCr. All of the mice were raised and kept in a pathogen-free environment and were handled according to U.S. Department of Agriculture and Roswell Park Cancer Institute guidelines.

Tumor

The colonic adenocarcinoma HT-29 is the cell repository line HTB 38 from the ATCC (Rockville, MD) human tumors. In this study, the tumor had an average volume doubling time of 5 days and a 100% probability of growth in untreated mice. Suspensions of 10^6 cultured tumor cells in 0.05 ml of saline were injected subcutaneously (s.c.) in the right and left posterior flanks of each mouse.

Liposome components

The liposome components were cholesterol (Croda, Fullerton, CA), hydrogenated soy phosphatidylcholine (HSPC) (Lipoid, Ludwigshafen, Germany) and distearoyl-phosphatidyl-ethanolamine (Genzyme, Cambridge, MA) conjugated at its amino position with a 1,900 molecular weight (m.w.) segment of methoxypolyethylene glycol carbamate (MPEG-1900-DSPE) in the molecular ratio 39:56:5.

Test material

Cisplatin (Platinol) was from Bristol-Myers Squibb (Princeton, NJ). Doxorubicin hydrochloride (Adriamycin) was from Farmitalia Carlo Erba (Milan, Italy). Liposome-encapsulated cisplatin (SPI-77, lot 6077-8) and doxorubicin (DOXIL, lot 7DOX-07) were provided by SEQUUS Pharmaceuticals. The cisplatin concentration in SPI-77 was 1.0 mg/ml, and the drug encapsulation efficiency was >90%, determined by gel permeation chromatography. The weight ratio of drug to lipid was 1 to 70. The particle size was 110 ± 10 nm, determined by dynamic laser scattering (Malvern Instruments, Malvern, UK). The doxorubicin concentration in DOXIL was 2.0 mg/ml, and the drug encapsulation efficiency was >95%. The weight ratio of drug to lipid was 1 to 8. The particle size was 95 ± 10 nm. Control mice received saline.

Treatment schedules

Treatments were started when the tumors had reached a mean diameter of 3–4 mm (10–25 mm^3) 5 days after implantation. The free drugs and liposomal drug formulations at dose levels of 3 mg cisplatin/kg body weight or 4 mg/kg doxorubicin were injected into a tail vein on a weekly schedule. Cisplatin and SPI-77 were given for 3 weeks; doxorubicin and DOXIL were given for 4 weeks. If one or both tumor implants grew to a size beyond possible regression (mean 1.5 cm^3), the mouse was euthanized by carbon

Grant sponsors: New York State Department of Health, American Cancer Society and SEQUUS Pharmaceuticals, Inc.

*Correspondence to: Department of Immunology, Roswell Park Cancer Institute, Elm and Carlton Streets, Buffalo, NY 14263, USA. Fax: (716) 845-3242.

Received 25 May 1998; Revised 23 July 1998

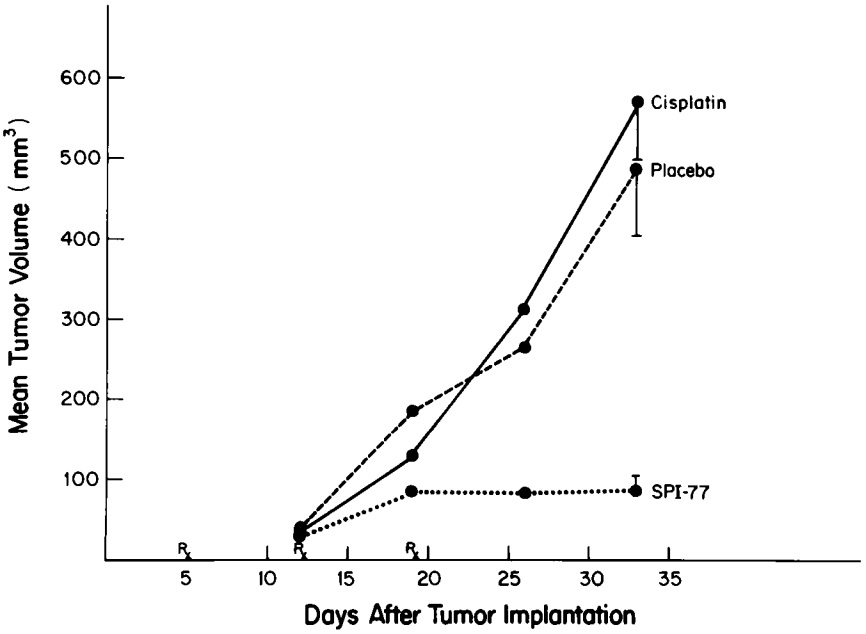

FIGURE 1 – The effects of treatments with saline (placebo), free cisplatin in saline (cisplatin) and cisplatin in pegylated liposomes (SPI-77) on the growth of s.c. implants of tumor HT-29. The values are the mean volumes of 30 tumors in each group of 15 mice. The standard errors of the means are shown only for the last time point of tumor measurements before some of the mice with large tumors were euthanized.

dioxide asphyxiation well before showing signs of discomfort. Mice with smaller tumors were euthanized at the termination of the study, 75 days after tumor implantation. Tumor-free mice and mice with palpable but non-progressing tumors were observed for an additional month before the mice were euthanized and the tumor implantation sites examined histologically for remaining viable tumor.

Statistical analysis

The mice were randomly assigned to therapy and control groups of 5 mice each. The effects of free and liposomal cisplatin were determined in 3 replicate tests. The effects of free and liposomal doxorubicin were determined in 2 replicate tests. The weight of the mice, the incidence of tumor growth and the tumor volumes were recorded weekly. Differences in final tumor incidence were evaluated with a 2×2 contingency test (Fisher's exact test). The tumor volumes were calculated by the formula $0.4\ (a \times b^2)$, where a was the larger and b was the smaller diameter. Differences in mean tumor volumes and in mean survival times were evaluated by Student's *t*-test. Differences were considered significant when the *p* value of comparison was less than 0.05.

RESULTS

Therapeutic effects

The data on the effects of the 2 cisplatin formulations on the growth of tumor HT-29 are presented in Figure 1 and the data on the final incidences of growing and cured tumors and on the mean survival are presented in Table I. The results of 3 replicate tests were similar, and the data have been combined. The data on the effects of the 2 doxorubicin formulations on the growth of tumor HT-29 are presented in Figure 2 and the data on the final incidences of growing and cured tumors and on the mean survival are presented in Table II. The results of 2 replicate tests were similar, and the data have been combined.

The results show that even at the low, easily tolerated doses used, SPI-77 and DOXIL were highly effective in inhibiting the growth of HT-29, significantly prolonged survival and resulted in a significant number of mice found tumor free by necropsy and histological examination of tumor implantation sites. The free drugs had little or no therapeutic effect.

TABLE I – COLONIC CARCINOMA HT-29 IN NUDE MICE: SURVIVAL AND INCIDENCE OF S.C. GROWTH WITH CISPLATIN TREATMENTS ON DAYS 5, 12 AND 19

Treatment[1]	Final incidence[2]	Mean survival (days)[3]
Placebo (saline)	30/30	50.7 ± 4.2
Cisplatin, 3 mg/kg	30/30	48.6 ± 3.6
SPI-77, 3 mg/kg	23/30*	70.7 ± 2.3**

[1]Cisplatin: free cisplatin in saline solution, SPI-77: cisplatin in pegylated liposomes.–[2]Incidence of tumors per group of 15 mice (2 implants per mouse) at the termination of the test on day 75.–[3]Deaths before day 75 were due to tumor progression.–*Significantly less than free cisplatin ($p = 0.01$). Three of the mice were tumor free.–**Significantly longer than free cisplatin ($p < 0.0001$).

Toxicity

Liposomal cisplatin caused an average loss of 9% body weight, which was recovered from 3 to 4 weeks after the last treatment. The other treatments caused transient weight losses of less than 3%, which were recovered from 1 to 2 weeks after the last treatment. Blood counts were made from tail vein punctures at the time of the last intravenous (i.v.) injections. The mean total white counts and differential counts were within the normal ranges in all treatment groups.

DISCUSSION

Earlier studies using human tumors implanted into nude mice found that doxorubicin encapsulated in conventional liposomes was no more effective therapeutically than was doxorubicin suspended in saline (Nagata *et al.*, 1990; Papahadjopoulos *et al.*, 1991). This was also observed in a mouse mammary tumor model (Vaage *et al.*, 1992). Long-circulating PEG-coated "pegylated" liposomes are taken up by the RES less readily than are conventional liposomes and therefore remain in the circulation longer (Gabizon and Papahadjopoulos, 1988; Allen *et al.*, 1991). This

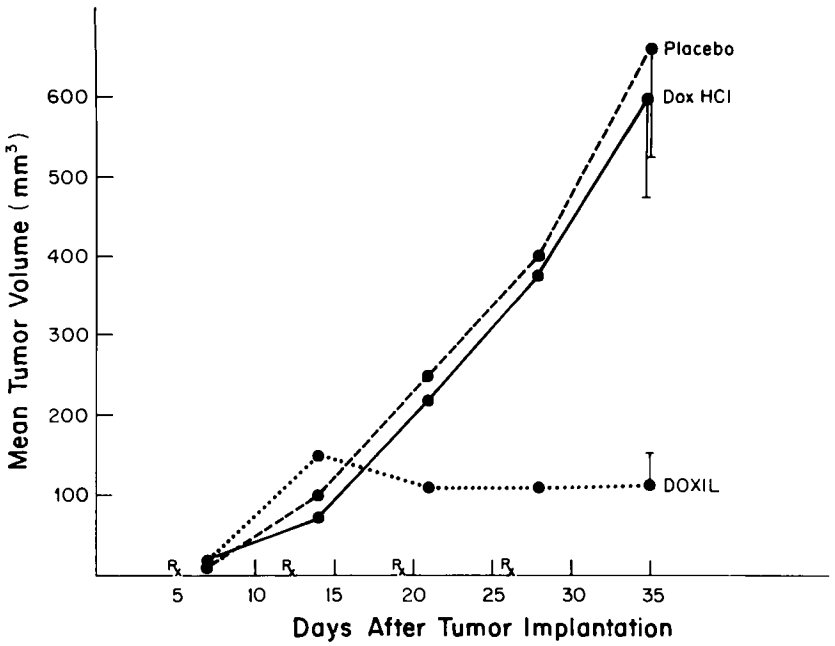

FIGURE 2.—The effects of treatments with saline (placebo), free doxorubicin in saline (Dox HCl) and doxorubicin in pegylated liposomes (DOXIL) on the growth of s.c. implants of tumor HT-29. The values are the mean volumes of 20 tumors in each group of 10 mice. The standard errors of the means are shown only for the last time point of tumor measurements before some of the mice with large tumors were euthanized.

TABLE II.—COLONIC CARCINOMA HT-29 IN NUDE MICE. SURVIVAL AND INCIDENCE OF S.C. GROWTH WITH DOXORUBICIN TREATMENTS ON DAYS 5, 12 AND 19

Treatment[1]	Final incidence[2]	Mean survival (days)[3]
Placebo (saline)	20/20	54.3 ± 4.2
Dox HCl, 4 mg/kg	20/20	58.6 ± 3.6
DOXIL, 4 mg/kg	14/20*	74.1 ± 0.9**

[1]Dox HCl: free doxorubicin in saline solution; DOXIL: doxorubicin in pegylated liposomes.—[2]Incidence of tumors per group of 10 mice (2 implants per mouse) at the termination of the test on day 75.—[3]Deaths before day 75 were due to tumor progression.—*Significantly less than free doxorubicin ($p = 0.02$). Three of the mice were tumor free.—**Significantly longer than free doxorubicin ($p < 0.0001$).

makes an increased accumulation of liposomes in tumors possible (Gabizon *et al.*, 1990; Huang *et al.*, 1992; Vaage *et al.*, 1997). Confocal laser scanning microscopy has shown that doxorubicin in pegylated liposomes entered a tumor in greater quantity, and remained detectable in the tumor longer (>7 days), than the free drug (<2 days). The liposome formulation produced a 6-fold increase in the area-under-the-curve for doxorubicin in a xenografted human pancreatic carcinoma (Vaage *et al.*, 1997). Analysis by atomic absorption spectroscopy of mice treated with cisplatin in pegylated liposomes found a similar increase in the platinum concentration in the murine colon tumor L26 and an enhanced therapeutic effect (Newman *et al.*, in press).

In the present study, using dose levels so low that the free drugs had little or no observable therapeutic effect, cisplatin and doxorubicin became distinctly effective against a human colonic carcinoma when encapsulated in pegylated liposomes. It is probable that the increased penetration into tumors, and the long presence with slow drug release from liposomes in the tumors, observed and measured in another tumor model (Vaage *et al.*, 1997) account for the enhanced therapeutic effect of the liposomal drugs. In view of the guarded optimism for the development of improved chemotherapy for disseminated colonic carcinomas (Connors *et al.*, 1995; Fong *et al.*, 1996), the present observations of the therapeutic efficacies of cisplatin and doxorubicin in pegylated liposomes against xenografts of a human colonic carcinoma, and the low systemic toxicity, are encouraging.

REFERENCES

ALLEN, T., HANSEN, C., MARTIN, F., REDEMANN, C. and YAU-YOUNG, A., Liposomes containing a synthetic lipid derivative of polyethylene glycol show prolonged circulation half-lives *in vivo*. *Biochim. biophys. Acta*, **1066**, 29–36 (1991).

CONNORS, T., DUNCAN, R. and KNOX, R., The chemotherapy of colon cancer. *Eur. J. Cancer*, **31**, 1373–1378 (1995).

DOUGLASS, H.O., JR., TEPPER, J. and LEICHMAN, L., Neoplasms of the exocrine pancreas. *In* J.F. Holland, E. Frei III, R.C. Bast, D.W. Kufe, D.L. Morton and R.R. Weichselbaum (eds.), *Neoplasms of the exocrine pancreas. Cancer medicine* (3rd ed.), pp. 1466–1484, Lea & Febiger, Philadelphia (1993).

FONG, Y., KEMENY, N., PATY, P., BLUMGART, L. and COHEN, A., Treatment of colorectal cancer: hepatic metastasis. *Semin. Surg. Oncol.*, **12**, 219–252 (1996).

GABIZON, A., CHISIN, R., AMSELEM, S., DRUCKMANN, S., COHEN, R., GOREN, D., FROMER, I., PERETZ, T., SULKES, A. and BARENHOLZ, Y., Pharmacokinetic and imaging studies in patients receiving a formulation of liposome-associated adriamycin. *Brit. J. Cancer*, **64**, 1125–1132 (1991).

GABIZON, A., GOREN, D., FUKS, Z., MESHORER, A. and BARENHOLZ, Y., Superior therapeutic activity of liposome-associated adriamycin in a murine metastatic tumor model. *Brit. J. Cancer*, **51**, 681–689 (1985).

GABIZON, A. and PAPAHADJOPOULOS, D., Liposome formulations with prolonged circulation time in blood and enhanced uptake by tumors. *Proc. nat. Acad. Sci. (Wash.)*, **85**, 6949–6953 (1988).

GABIZON, A., PRICE, D., HUBERTY, J., BRESALIER, R. and PAPAHADJOPOULOS, D., Effect of liposome composition and other factors on the targeting of liposomes to experimental tumors: biodistribution and imaging studies. *Cancer Res.*, **50**, 6371–6378 (1990).

HUANG, S., LEE, K.-D., HONG, K., FRIEND, D. and PAPAHADJOPOULOS, D., Microscopic localization of sterically stabilized liposomes in colon carcinoma-bearing mice. *Cancer Res.*, **52**, 5135–5143 (1992).

LASIC, D., MARTIN, F., GABIZON, A., HUANG, S. and PAPAHADJOPOULOS, D., Sterically stabilized liposomes: a hypothesis on the molecular origin of the extended circulation times. *Biochim. biophys. Acta*, **1070**, 187–192 (1991).

NAGATA, J., YAMAUCHI, M., TAKAGI, H., KOJIMA, N., HAYASHI, Y. and YAGI, K., Antitumor activity against human gastric cancers of sulfatide-inserted liposomes containing entrapped adriamycin. *J. clin. Biochem.*, **8**, 111–119 (1990).

NEWMAN, M., COLBERN, G., WORKING, P. and AMANTEA, M., Anti-tumor activity, pharmacokinetics and tumor disposition of cisplatin encapsulated in sterically stabilized (Stealth) liposomes in mice bearing the L26 colon carcinoma. *Cancer Chemother. Pharmacol.*, (1998) (In press).

PAPAHADJOPOULOS, D., ALLEN, T., GABIZON, A., MAYHEW, E., MATTHAY, K., HUANG, S.K., LEE, K.-D., WOODLE, M.C., LASIC, M.C., LASIC, D.D. and REDEMAN, C., Sterically stabilized liposomes: improvements in therapy against implanted tumors. *Proc. nat. Acad. Sci. (Wash.)*, **88**, 11460–11464 (1991).

SZOKA, F.C., Liposome drug delivery. *In* J. Wilschut and R. Hoekston (eds.), *Membrane fusion*, pp. 845–890, M. Dekker, New York (1991).

VAAGE, J., BARBERA-GUILLEM, E., ABRA, R., HUANG, A. and WORKING, P., Tissue distribution and therapeutic effect of intravenous free or encapsulated liposomal doxorubicin on human prostate carcinoma xenografts. *Cancer*, **73**, 1478–1484 (1993*a*).

VAAGE, J., DONOVAN, D., MAYHEW, E., ABRA, R. and HUANG, A., Therapy of human ovarian carcinoma xenografts using doxorubicin encapsulated in sterically stabilized liposomes. *Cancer*, **72**, 3671–3675 (1993*b*).

VAAGE, J., DONOVAN, D., USTER, P. and WORKING, P., Tumor uptake of doxorubicin in polyethylene glycol-coated liposomes and therapeutic effect against a xenografted human pancreatic carcinoma. *Brit. J. Cancer*, **75**, 482–486 (1997).

VAAGE, J., MAYHEW, E., LASIC, D. and MARTIN, F., Therapy of primary and metastatic mouse mammary carcinomas with doxorubicin encapsulated in long circulating liposomes. *Int. J. Cancer*, **51**, 942–948 (1992).

Join us for 24 Days of Stem Cells; a premiere virtual event featuring the latest advances in stem cell research.

This year's format will feature a new hour of cutting edge content every week day starting October 1st. Attend the sessions that are most relevant to your work - at your convenience and at your pace.

During the 24-day long event, you can:

- Access leading scientific presentations from thought leaders around the world
- Watch live training demonstrations from our stem cell experts
- Download key stem cell tools and resources
- Complete weekly challenges to earn points towards certification and prizes

Register today at
www.24daysofstemcells.com

ThermoFisher SCIENTIFIC

WILEY

British Journal of Cancer (2001) 84(8), 1029–1035
© 2001 Cancer Research Campaign
doi: 10.1054/ bjoc 2001.1723, available online at http://www.idealibrary.com on IDEAL

A phase I study in paediatric patients to evaluate the safety and pharmacokinetics of SPI-77, a liposome encapsulated formulation of cisplatin

GJ Veal[1], MJ Griffin[1], E Price[2], A Parry[2], GS Dick[3], MA Little[3], SM Yule[4], B Morland[5], EJ Estlin[6], JP Hale[2], ADJ Pearson[2], H Welbank[7] and AV Boddy[1]

[1]Cancer Research Unit and [2]Department of Child Health, Medical School, University of Newcastle-upon-Tyne, Newcastle-upon-Tyne NE2 4HH, UK; [3]Royal Marsden Hospital, Sutton, Surrey SM2 5PT, UK; [4]Yorkhill Hospital, Glasgow G3 8SJ, UK; [5]Birmingham Childrens Hospital, Birmingham B4 6NH, UK; [6]Royal Hospital for Sick Children, Bristol BS2 8BJ, UK; [7]ALZA Corporation, Mountain View, CA, USA

Summary Pre-clinical studies indicate that cisplatin encapsulated in STEALTH® liposomes (SPI-77) retains anti-tumour activity, but has a much reduced toxicity, compared to native cisplatin. A phase I study was conducted to determine the toxicity and pharmacokinetics of SPI-77 administered to children with advanced cancer not amenable to other treatment. Paediatric patients were treated at doses ranging from 40 to 320 mg m^{-2} by intravenous infusion every 4 weeks. Blood samples taken during, and up to 3 weeks after, administration and plasma and ultrafiltrate were prepared immediately. Urine was collected, when possible, for 3 days after administration. SPI-77 administration was well tolerated with the major toxicity being an infusion reaction which responded to modification of the initial infusion rate of SPI-77. Limited haematological toxicity and no nephrotoxicity were observed. No responses to treatment were seen during the course of this phase I study. Measurement of total plasma platinum showed that cisplatin was retained in the circulation with a half life of up to 134 h, with maximum plasma concentrations approximately 100-fold higher than those reported following comparable doses of cisplatin. Comparison of plasma and whole blood indicated that cisplatin was retained in the liposomes and there was no free platinum measurable in the ultrafiltrate. Urine recovery was less than 4% of the dose administered over 72 h. Results from this phase I study indicate that high doses of liposomal cisplatin can safely be given to patients, but further studies are required to address the issue of reformulation of liposomally bound cisplatin. © 2001 Cancer Research Campaign http://www.bjcancer.com

Keywords: SPI-77; liposomal cisplatin; pharmacokinetics; paediatrics; phase I

Cisplatin (cis-diammunedichloroplatinum) was first introduced into clinical practice in 1971 and has now been licensed for use in the treatment of cancer for over 20 years. Despite the continued search for new platinum complexes and cisplatin analogues with increased efficacy over the parent compound, cisplatin remains the mainstay of treatment for a number of solid tumour types. Cisplatin is currently an essential component in many clinical paediatric protocols for the treatment of osteogenic sarcoma, neuroblastoma and central nervous system tumours (Bramwell et al, 1992; Pearson et al, 1992; Buckner et al, 1999). In addition, cisplatin has a pivotal role in the foundation of curative regimens in ovarian and testicular cancers and is also effective in the treatment of bladder, cervical, oesophageal and small cell lung cancers, amongst others.

The clinical application of cisplatin is predominantly limited by the considerable side effects of cisplatin treatment, which include acute toxicity such as nausea and vomiting and chronic side effects of nephrotoxicity, ototoxicity and neurotoxicity (Krakoff, 1979; Vermorken et al, 1983; Cavaletti et al, 1992). While the search for superior platinum drugs continues, it is essential that methods are investigated to optimize the current clinical use of cisplatin in both paediatric and adult patient populations. Although a variety of different approaches have been undertaken to limit its side effects, none have proven wholly successful in reducing either the acute or chronic toxicities associated with cisplatin therapy.

Recent studies have shown that encapsulation of antineoplastic agents in liposomes can maintain antitumour activity whilst reducing drug toxicity (Rahman et al, 1990; Gill et al, 1995). Using this approach it is feasible that high plasma levels of free cisplatin, which are associated with the side effects of the drug, may be reduced whilst at the same time allowing more specific targeting of cisplatin to the tumour. This type of liposome delivery system has previously been used successfully for the delivery of doxorubicin in both animal and patient studies (Papahadjopoulous et al, 1991; Vaage et al, 1992; Uziely et al, 1995; Muggia et al, 1997).

SPI-77 (STEALTH® liposomal cisplatin) is a formulation of cisplatin encapsulated in sterically stabilized liposomes. These liposomes are thought to accumulate in tumours following extravasation through the tumour vasculature, due to their small size, long circulation time and reduced interaction with components of the blood including lipoproteins, cells, opsonins and other liposomes (Woodle and Lasic, 1992). Preclinical studies in tumour-bearing mice showed SPI-77 to have superior antitumour activity compared to the same cumulative dose of cisplatin with higher cumulative doses of SPI-77 being well tolerated and exhibiting increased antitumour affect (Newman et al, 1999). Significantly, SPI-77-treated animals had a 28-fold higher tumour

Received 11 August 2000
Revised 11 November 2000
Accepted 22 January 2001

Correspondence to: AV Boddy

exposure to platinum, as determined by area-under-the-curve (AUC), than cisplatin-treated animals, but a 4-fold lower exposure of platinum to the kidneys, which represents the primary target organ of toxicity associated with cisplatin treatment.

A phase I study of SPI-77 in children in the UK was conducted in parallel to the adult phase I study in the UK and Europe. This study was designed to determine the incidence of toxicity, maximum tolerated dose (MTD) and pharmacokinetics of SPI-77 when given every 4 weeks in paediatric patients with advanced cancer not amenable to other treatment.

PATIENTS AND METHODS

Patients

The study was performed between October 1997 and March 1999. Patients with different tumour types (Table 1) were recruited from 4 centres in the United Kingdom. Patients eligible for the study were aged 1–17 years with histologically confirmed malignancy for which no conventional therapy offered the possibility of cure or palliation. Previous chemotherapy must have ceased 4 weeks prior to recruitment to the study (6 weeks for nitrosourea) and 4 weeks must have elapsed since either cancer surgery or radiotherapy to measurable lesions. Further inclusion criteria were a Lansky performance status ≥ 30%, an adequate bone marrow function (absolute neutrophil count ≥ 1.0×10^9 l^{-1}, platelet count ≥100×10^9 l^{-1}), an adequate liver function (total bilirubin level within upper limit of normal, alanine aminotransferase and aspartate aminotransferase ≤ 1.5 upper limit of normal), an adequate renal function (glomerular filtration rate (GFR) > 50 ml min^{-1} 1.73 m^{-2}) and no clinical evidence of hearing loss determined by audiometry (i.e., no toxicity ≥ grade 2 Common Toxicity Criteria (CTC)). Written informed consent was obtained from the patient's parent or legal guardian and consent was also sought from the patient where deemed appropriate.

Excluded from the study were patients with a life expectancy of less than 6 weeks, signs or symptoms of acute infection requiring systemic therapy, neurotoxicity from previous anti-cancer treatment or significant neuropathy (> grade 1 CTC) from any cause. Further exclusion criteria were a history of allergic reaction to cisplatin- or platinum-containing compounds, use of another investigational agent within 30 days of dosing with SPI-77 or prior treatment with SPI-77.

Pretreatment evaluation consisted of radiologic assessment of disease, ECG and audiogram within 14 days prior to the first dose of SPI-77. Further evaluation included a full medical history, physical examination, neurologic examination, an estimate of the GFR by ^{51}Cr-EDTA plasma clearance, urine analysis, haematology including WBC with differential, red blood cell, haemoglobin, haematocrit and platelet count, and serum chemistry, glucose and a lipid profile. A urine pregnancy test was also carried out in female patients of childbearing potential. The study was approved by the appropriate Local Research Ethics Committee (LREC).

Drug formulation

SPI-77 was supplied by SEQUUS Pharmaceuticals, Inc (Brentford, UK) in single-dose sterile vials as an isotonic suspension containing a cisplatin concentration of 1 mg ml^{-1}. The total lipid content of the SPI-77 formulation was 71 mg ml^{-1} (hydrogenated soy phosphatidylcholine, cholesterol and the polymer MPEG-DSPE at an approximate 51:44:5 molar ratio), giving a drug-to-lipid ratio of approximately 14 μg cisplatin per 1 mg of lipid. The formulation also contained 10% sucrose, 1 mM sodium chloride and 10 mM histidine at pH 6.5. The mean liposome particle diameter was 110 nm and the cisplatin encapsulation exceeded 90%. Prior to infusion, SPI-77 was diluted to a final concentration of 0.2 mg ml^{-1} in normal saline or D5W (dextrose 5% in water). All doses of SPI-77 quoted in this study are given in cisplatin equivalents of mg m^{-2}.

Treatment plan

Patients received SPI-77 every 4 weeks for a total of 6 doses or until disease progression, whichever occurred earlier. 3 patients were initially enrolled for each dose level. SPI-77 was administered by intravenous (i.v.) infusion at a rate of 10 mg m^{-2} h^{-1} for the first 15 minutes, which increased to 40 mg m^{-2}h^{-1} for the remainder of the infusion, assuming no adverse reaction had occurred. All SPI-77 infusions were administered using a paediatric approved infusion pump. All patients received premedication with dexamethasone (0.15 mg kg^{-1} qds oral or i.v.), chlorpheniramine (0.05 mg kg^{-1} qds oral or i.v.) and ranitidine (3 mg kg^{-1} bd oral or 1 mg kg^{-1} i.v. tds) starting 24 h prior to SPI-77 infusion and continuing for 24 h after the infusion. The starting dose of SPI-77 was 40 mg m^{-2} for the first 3 patients with planned dose escalations as follows: 80, 120, 200, 320, 520, 840 mg m^{-2}, provided that no dose-limiting toxicities were observed. The last patient at each dose level was observed for at least 4 weeks before the first patient at the subsequent dose level was treated. If a dose-limiting toxicity (DLT) occurred in one of 3 patients at any given dose level, then 3 additional patients were treated at that level. The maximum tolerated dose (MTD) was defined as the dose immediately below that at which 2 out of 6 patients experienced a DLT.

DLT was defined as NCI CTC grade 3 thrombocytopenia or neutropenia lasting more than 7 days, grade 3 hepatic toxicity which does not resolve at least to grade 1 prior to the end of the cycle or any grade 3 or higher neurological or kidney/bladder toxicity. Any other grade 3 or 4 event, with the exception of nausea, vomiting, alopecia, weight change, fatigue and allergic reactions was also considered dose limiting.

Clinical evaluations

During each 4 week cycle of SPI-77 treatment, haematology and serum chemistry and electrolytes were checked on a weekly basis. Urine analysis and neurologic examination were performed at the end of each cycle and an audiogram and GFR measurement carried out by ^{51}Cr-EDTA plasma clearance at the end of cycles 2, 4 and 6. Upon completion of treatment, an electrocardiogram was also performed. Tumour evaluation and assessment of response was carried out at the end of cycles 2, 4 and 6 or at early withdrawal for patients not completing the entire course of treatment.

Pharmacokinetic sampling

During the first course of treatment, whole blood samples (approx. 3 ml) were collected in heparinized tubes prior to administration of SPI-77, hourly during infusion and at the end of infusion. Further samples were taken at 1, 3, 5, 24, 96, 120 and 168 hours post infusion and weekly thereafter for 2 additional weeks. For subsequent

courses at the same dose level, samples were taken at pre-dosing, hourly during infusion and at the end of infusion. A 400 µl aliquot of blood was removed from each sample and the remainder centrifuged for 10 minutes at 4°C (2000 *g*) to obtain the plasma fraction. Whole blood and plasma samples (400 µl) were diluted 10-fold with 0.1% triton-X-100 +0.2% nitric acid to a final volume of 4 ml. These samples were stored at −20°C prior to analysis. The remaining plasma was centrifuged for 30 minutes at 1500 *g* using Amicon Centrifree ultrafiltration devices to obtain a minimum of 200 µl of plasma ultrafiltrate and the samples stored at −20°C prior to analysis.

Urine samples were collected, where possible, beginning on the first day of treatment with the initiation of dosing and continuing each day for 3 consecutive days. 24 h pooled urine volumes were recorded and 10 ml of each pooled urine sample stored for analysis along with a 10 ml predose spot urine sample.

All platinum analyses were carried out at the Cancer Research Unit, Newcastle, by flameless atomic absorption spectrophotometry using a Perkin-Elmer AAnalyst 600 graphite furnace spectrometer (Perkin-Elmer Ltd, Beaconsfield, UK). Sample analysis was carried out using a 4-stage heating programme with temperatures ramping from 80 to 2800°C. Total platinum concentrations were determined in whole blood and plasma samples and free platinum levels determined in plasma ultrafiltrates (Peng et al, 1997). All samples were analysed in duplicate and the intra- and interassay coefficients of variation for a quality assurance sample had to be <10% for an assay to be valid. The limit of detection for the AAS was 0.10 µg ml^{-1}.

Data interpretation

The total and free platinum pharmacokinetic parameters in plasma and urine were calculated by standard non-compartmental analysis with actual sampling times used in the calculations. Analysis of all pharmacokinetic data was performed using WinNonlin.

RESULTS

Patients and treatment

A total of 18 patients were recruited to the study. Patient characteristics are shown in Table 1. 3 patients were treated at the starting dose of 40 mg m^{-2} (4 courses in total) and 4 patients were treated at 80 mg m^{-2} (4 courses) due to the withdrawal of 1 patient following a grade 3 infusion reaction. 3 patients were treated at 120 mg m^{-2} (6 courses), 4 patients at 200 mg m^{-2} (6 courses) and 3 patients at 320 mg m^{-2} (5 courses) giving a total of 25 courses administered overall. 10 patients received a single course of treatment, 4 patients received 2 courses (at doses of 40, 80, 120 and 320 mg m^{-2}) and 2 patients received 3 courses (doses of 120 and 200 mg m^{-2}). No further dose escalations were carried out due to concerns regarding the high doses of cisplatin being administered to patients in both the adult (Schellens et al, 1998) and paediatric phase I studies and the lack of detectable levels of free platinum measured in patient ultrafiltrate samples, indicating that the cisplatin was being retained within the liposomes. Following the occurrence of infusion reactions in 3 patients receiving doses of SPI-77 of 40 and 80 mg m^{-2}, in addition to similar adverse infusion-related reactions in the parallel phase I adult study, the initial infusion rate was decreased to 1 mg m^{-2} h^{-1} for the first 15 minutes, followed by a step increase up to 40 mg m^{-2} h^{-1} for the remainder of the infusion, giving an increased duration of infusion at doses of 120 mg m^{-2} and above. Due to this increased duration of infusion, the final concentration of SPI-77 was increased from 0.2 mg ml^{-1} to 0.3 mg ml^{-1}, in order to maintain the total infusion volumes at acceptable levels.

Table 1 Patient characteristics

Number of patients	18
Male/female	10/8
Median age (range)	10 (1–16)
Dose level (number of courses)	
40 mg m^{-2}	3 (4)
80 mg m^{-2}	4 (4)
120 mg m^{-2}	3 (6)
200 mg m^{-2}	4 (6)
320 mg m^{-2}	3 (5)
Diagnosis	
Neuroblastoma	5
Rhabdomyosarcoma	5
PNET (intra/extracranial)	2 (1/1)
Astrocytoma	1
Hepatocellular carcinoma	1
Ewings sarcoma	1
Small cell osteosarcoma	1
Medulloblastoma	1

Of the 18 patients recruited to the study, 1 patient did not receive SPI-77 due to disease progression prior to treatment. 1 patient was withdrawn following a serious infusion reaction and 3 patients died after the first course of therapy due to disease progression. No responses to treatment were observed in any of the patients studied. The remaining 13 patients went off-study following 1 (6 patients), 2 (5 patients) and 3 (2 patients) courses of SPI-77 treatment due to disease progression. Of the 5 patients who received 2 courses of treatment, 3 had rhabdomyosarcoma, 1 neuroblastoma and 1 PNET. Of the 2 patients who received 3 courses, 1 had hepatocellular carcinoma and the other neuroblastoma.

Toxicity

17 patients were evaluable for toxicity. Table 2 shows a summary of all the toxicities above CTC grade 1 recorded during this study. The most serious adverse event was a CTC grade 3 infusion reaction observed in 3 patients at doses of 40 and 80 mg m^{-2} during the first course of treatment in each case. This led to 1 patient being withdrawn from the study and resulted in modification of the initial infusion rate of SPI-77 for further dose escalation as described above. The other 2 patients were able to recommence administration on the same day, following resolution of the symptoms and treatment with antihistamines, steroids and oxygen. No subsequent infusion reactions were seen in patients treated under the reviewed guidelines for initial SPI-77 infusion. Gastrointestinal toxicities were the most commonly observed in children receiving SPI-77, with a total of 65% of patients (11/17) experiencing vomiting during the course of treatment and a further 18% of patients (3/17) experiencing nausea. Neither of these toxicities exceeded CTC grade 2 in any of the patients studied. 1 patient experienced a CTC grade 4 GI bleed, but this was not thought to be treatment related. Haematological toxicity was limited to grade 2/3 anaemia in 35% of patients (6/17) and grade 2 thrombocytopenia in 12% of patients (2/17). In 1 of these patients bone marrow disease is likely to have compromised platelet levels. Other toxicities observed included grade 3 hypertension (1/17), grade 1 fever (3/17), grade 1/2 allergic reaction (4/17) and grade 1 hyponatremia

Table 2 Patient toxicities

Toxicity	Grade	Number of patients (%)	Number of courses (%)
Gastrointestinal			
Vomiting	1,2	11 (64)	13 (52)
Nausea	1,2	4 (24)	4 (16)
GI bleed	4[a]	1 (6)	1 (4)
Haematologic			
Anaemia	2	4 (24)	5 (20)
	3[b]	2 (12)	3 (12)
Thrombocytopenia	2	2 (12)	2 (8)
Infusion reaction	3[c]	3 (18)	3 (12)
Dermatologic			
Allergy/rash	1,2	4 (24)	4 (16)
Alopecia	1	1 (6)	1 (4)
Other toxicities			
Fever	1	3 (18)	3 (12)
Hypertension	3[d]	1 (6)	1 (4)

[a]Dose level 120 mg m^{-2}; [b]Dose levels 40 and 120 mg m^{-2}; [c]Dose levels 40 and 80 mg m^{-2}; [d]Dose level 80 mg m^{-2}.

(2/17). Altered serum chemistry/electrolytes such as hypokalaemia, hyperbilirubinaemia and decreased phosphate were never greater than grade 1 and were never reported in more than 6% of patients (1/17).

Monitoring of blood lipids

Levels of cholesterol, HDL and LDL fractions and triglycerides were monitored during treatment with SPI-77 due to the high lipid content of the STEALTH® liposomes being administered. Peak cholesterol levels were observed at 8 days following administration of SPI-77 and then declined to levels approximating those seen prior to treatment by day 29. The relationship between dose of SPI-77 and corresponding increase in cholesterol levels is shown in Figure 1. Percentage increases in mean cholesterol levels at 8 days following SPI-77 administration were 77%, 102% and 244% at doses of 120, 200 and 320 mg m^{-2} respectively. Similar increases were seen in levels of HDL and LDL, for example at a SPI-77 dose of 320 mg m^{-2}. Mean percentage increases from pretreatment levels of HDL and LDL measured at 8 days were 300% and 143% respectively. Variations in triglyceride levels were less clearly defined, but increased levels were seen in the majority of patients over a 28 day period following treatment with SPI-77.

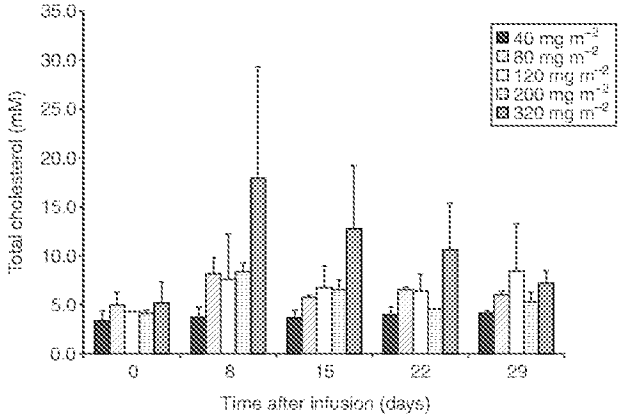

Figure 1 Mean plasma levels of total cholesterol following SPI-77 administration at doses of 40 to 320 mg m^{-2} following the first course of treatment. Error bars indicate standard error of the mean

Pharmacokinetics

Blood samples were taken for analysis of platinum during infusion of SPI-77 and for up to 3 weeks after administration. These platinum concentration data were used to derive pharmacokinetic parameters for total platinum in plasma and whole blood. Full pharmacokinetic data were obtained for 12 patients and are shown in Table 3. Despite the high concentrations of cisplatin administered to patients in this study, concentrations of free platinum measured in the plasma ultrafiltrate remained below the limit of detection (0.10 μg ml^{-1}) throughout the treatment period. Cisplatin was detectable in plasma and whole blood after SPI-77 administration in all patients. Individual patient plasma time profiles representative of the dose levels studied are shown in Figure 2. At the highest dose level, plasma platinum concentrations were still measurable prior to administration of the second course of treatment, i.e. 4 weeks after drug infusion. A plot of total platinum area under the plasma concentration–time curve (AUC) versus the dose of SPI-77 is shown in Figure 3. The half-life values for total platinum in plasma, determined following SPI-77 treatment, were within the range of 38 to 134 h in all but 1 patient, indicating an approximate 3-fold variation. Distribution of cisplatin within whole blood was determined by the blood/plasma ratio and ranged from approximately 0.5–0.8 in the majority of patients studied (Table 3), this generally reflected the haematocrit in these patients. The pharmacokinetic profile of patient 2 was notably different from that of the other patients studied, with a significantly greater clearance, reduced AUC and half-life and a blood/plasma ratio approaching 1. Patient 8 received multiple blood transfusions within 72 hours of SPI-77 administration, which resulted in an increased rate of elimination and disruption of whole blood distribution (Figure 4). Urine data was obtained from 6 patients and indicated prolonged and limited excretion, with a value of 3.8 ± 0.9% (mean ± SD) of the dose excreted in the first 72 hours.

Table 3 Pharmacokinetics of total platinum in plasma following SPI-77 treatment

Patient	Dose (mg m^{-2})	Infusion time (h)	C_{max} (μg ml^{-1})	AUC (mg ml^{-1} min)	Cl (ml h^{-1})	$t_{1/2}$ (h)	Blood/plasma[a]
1	40	2	34	145	20	38	0.72–0.88
2	40	4	8	4	255	11	0.69–1.00
3	40	5	37	181	17	65	0.54–0.66
5	80	3	71	402	5	56	0.49–0.80
7	80	5	103	818	13	134	0.60–0.88
8	120	4	88	442	18	41	0.31–0.79
9	120	3	111	679	19	86	0.57–0.85
10	120	4	151	1359	7	96	0.30–0.68
12	200	6	142	1412	9	78	0.55–0.76
13	200	6	177	1788	4	82	0.53–0.75
16	320	7	411	8027	2	132	0.54–0.73
18	320	6	187	2157	8	73	0.74–1.05

[a]Blood/plasma ratio given as a range determined over the 3 week sampling period.

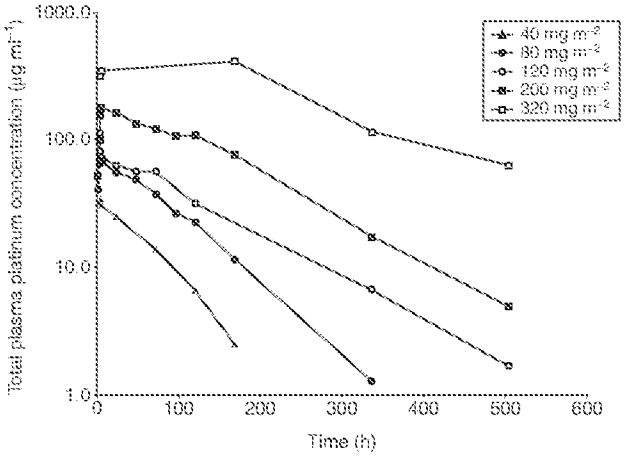

Figure 2 Plasma concentrations of total platinum following SPI-77 administration at doses of 40 to 320 mg m^{-2}. Data show individual patient data representative of each dose level of SPI-77

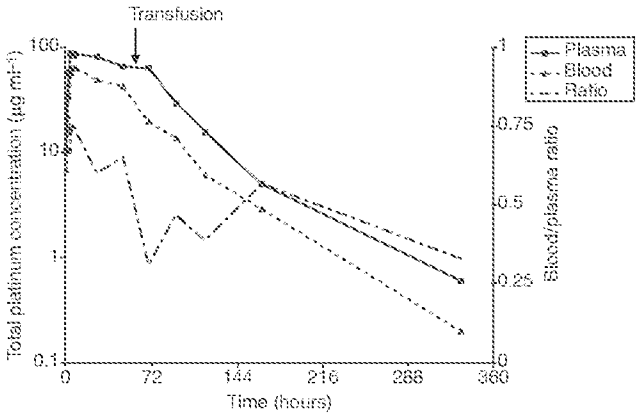

Figure 4 Concentrations of total platinum in plasma and whole blood following SPI-77 administration at a dose of 120 mg m^{-2} following the first course of treatment for patient 8. Patient received multiple blood transfusions within 72 h of SPI-77 administration

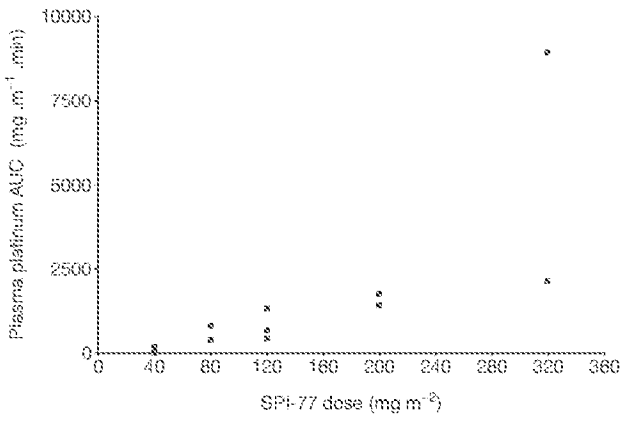

Figure 3 Relationship between total platinum area under the plasma concentration–time curve (AUC) and the dose of SPI-77 administered

DISCUSSION

The potential use of liposomes to deliver drugs to target sites of disease is a therapeutic approach that has been investigated with many different agents over the past 2 decades. Recent successes in this area of clinical research include the efficacy of liposomal doxorubicin in AIDS-related Kaposi's sarcoma and patients with refractory ovarian cancer (Muggia et al, 1997; Northfelt et al, 1997). Although the precise mechanisms by which liposomes selectively enter tumours and release drug are not completely understood, their successful application with doxorubicin has led to a resurgence of interest in this area. As liposome formulation issues and potential problems such as liposome stability and removal by elements of the immune system have been overcome with the STEALTH® liposomal system, the potential exists for improved delivery of a growing number of drugs for the treatment of many different types of disease. In addition, results from previous clinical trials give an indication as to how patients are likely to respond to the administration of STEALTH® liposomes

and the potential toxicities that may be associated with their use. Therefore the main issue regarding their use for the delivery of other therapeutic agents will largely be concerned with obtaining the desired balance between encapsulation and release of the drug of interest.

Preclinical results with SPI-77, a formulation of cisplatin encapsulated in STEALTH® liposomes, showed promising results in comparison with native cisplatin. Data from tumour-bearing mouse models showed a significantly greater antitumour activity compared to cisplatin and a significantly increased tumour exposure to platinum. This coincided with a decreased platinum exposure to the kidneys, the principal organ of cisplatin toxicity (Newman et al, 1999). On the basis of these preclinical results, in addition to the previous success of STEALTH® liposomal doxorubicin, phase I studies in both adult and paediatric patients, with advanced cancer not amenable to other cancer treatments, were performed in the UK and Europe. These studies were designed to determine the incidence of toxicity, MTD and pharmacokinetics of SPI-77 in these 2 separate patient populations. The rate of patient recruitment to the 2 studies was such that the adult phase I study was always one dose level ahead of the paediatric study, i.e. children were not enrolled for the next dose level until the specified number of adult patients had been treated at that dose.

Complete pharmacokinetic profiles were obtained from 12 of the patients taking part in this study. Cisplatin levels were determined in 2 different forms, total cisplatin concentrations were determined in both patient plasma and whole blood samples and concentrations of free platinum were determined in plasma ultrafiltrate samples. The cisplatin blood/plasma concentration ratio following SPI-77 treatment reflected the haematocrit in most patients. This contrasts with the equal distribution of platinum between plasma and red cells following native cisplatin administration (Manaka and Wolf, 1978). This information, in combination with the fact that there was no measurable free/active drug in plasma ultrafiltrate samples strongly suggests that the drug was retained within the liposomes following administration.

Plasma concentrations of total platinum following treatment with SPI-77 were considerably higher than those reported following administration of native cisplatin in children (Bues-Charbit et al, 1987; Dominici et al, 1989). For example, the total platinum AUC values obtained at a SPI-77 dose of 80 mg m^{-2} in this phase I study were approximately 100-fold higher than the total platinum AUC values previously reported following an equivalent dose of cisplatin (Pratt et al, 1981). This marked increase in total platinum AUC can largely be explained by the apparent decrease in clearance of total platinum and the low percentage of total platinum dose excreted in the urine of patients following SPI-77 administration. Total platinum clearance values observed for SPI-77 in the current study were ≤20 ml h^{-1} in all but 1 patient, approximately 100- to 1000-fold lower than clearance values of 10–20 l h^{-1} m^{-2} commonly reported for cisplatin (Bues-Charbit et al, 1987; Peng et al, 1997). Similarly, the limited excretion of cisplatin in the urine of children observed following SPI-77 administration, with approximately 4% of the administered dose excreted in the first 72 hours, was significantly less than seen with native cisplatin, with reported values of 27–35% of the dose excreted in 48 hours (Bues-Charbit et al, 1987; Peng et al, 1997). Overall, the half-life of cisplatin was prolonged following SPI-77 administration, but was not dissimilar to that of total plasma platinum reported following cisplatin administration in previous clinical studies (Pratt et al, 1981; Dominici et al, 1989). There was some evidence of non-linearity, with lower clearance and longer half-life of drug at the higher dose levels. This was also apparent from individual patient plasma time profiles representative of the dose levels studied (Figure 2).

One patient (patient 2) showed a different pharmacokinetic profile to the other patients with a blood/plasma ratio approaching unity and a much shorter half-life due to a higher clearance of cisplatin. As the data suggest that the drug was normally retained in the liposomes following administration of SPI-77, it seems likely that the different pharmacokinetics observed in this patient was due to altered handling of the liposomes. This may involve a decrease in liposome stability through interaction with plasma proteins or an increased clearance of liposome from the plasma. It is interesting to note that no increase in cholesterol levels was seen at 8 days after infusion of SPI-77 in this patient as compared to increases of 7 and 46% from pretreatment levels in the other 2 patients treated at the same dose level. The only other patient who exhibited a significantly different pharmacokinetic profile was patient 8 who received multiple blood transfusions within 72 hours of SPI-77 administration. This resulted in an increased rate of elimination and disruption of whole blood distribution (Figure 4).

The most striking clinical or biochemical observation was hyperlipidaemia with percentage increases in mean cholesterol levels at 8 days following administration being 77%, 102% and 244% at doses of 120, 200 and 320 mg m^{-2} respectively. Similar increases were seen in levels of HDL and LDL. Despite the fact that cholesterol levels returned to normal before the scheduled retreatment time, the apparent exaggeration of this adverse effect seen at a SPI-77 dose of 320 mg m^{-2} raises potential concerns with regards to further dose escalation. Other toxicities, including antiproliferative effects, were generally mild (CTC grade 1/2) with the only serious adverse event being a GI bleed which was not thought to be treatment related, due to a lack of related side effects and the length of time after administration that the toxicity occurred. Overall, administration of SPI-77 was well tolerated in paediatric patients with doses 3-fold higher than would be achievable with native cisplatin. However, despite this increase in cisplatin dosage and the high levels of total platinum in plasma, no responses were seen in any of the patients studied.

In summary, the data from this study indicate that the encapsulation of cisplatin in STEALTH® liposomes results in an altered toxicity profile and significantly different pharmacokinetics as compared with standard cisplatin administration in paediatric patients. This is in agreement with preliminary data obtained in a parallel phase I study of SPI-77 in adults (Schellens et al, 1998). The absence of nephrotoxicity following treatment with SPI-77 may be explained predominantly by the lack of detectable free platinum in the plasma, but may also be connected with the significantly decreased percentage of platinum excreted in the urine compared with cisplatin treatment. The major abnormal finding in the study was hypercholesterolaemia with low-grade anaemia and thrombocytopenia being the only observed antiproliferative effects. The pharmacokinetics of SPI-77 were significantly altered from those associated with cisplatin treatment and implied that the cisplatin was maintained inside the liposome with no detectable free cisplatin measured in plasma at any point following administration. Although preclinical data suggested that low plasma levels of free cisplatin would explain the lack of toxicity seen with SPI-77 in murine tumour models, the complete retention of cisplatin within the liposomes was not predicted as significant antitumour activity was observed (Newman et al, 1999). Both the paediatric

and adult phase I studies were stopped at a dose of 320 mg m^{-2} in order to address the issue of reformulation of liposomally bound cisplatin, i.e. to attempt to obtain an optimal balance between encapsulation and release of cisplatin. Despite the potential problems with formulation of liposomally bound cisplatin highlighted in this study, the limited toxicity reported in patients in the study does show that high doses of liposomal cisplatin can safely be given to patients. This would suggest that if the product can be reformulated to obtain the desired balance between encapsulation and release, this approach has the potential to lead to an improved method of administering cisplatin in a clinical setting.

REFERENCES

Bramwell VH, Burgers M, Sneath R, Souhami R, van Oosterom AT, Voûte PA, Rouesse J, Spooner D, Craft AW, Somers R, Pringle J, Malcolm AJ, van der Eijken J, Thomas D, Uscinska B, Machin D and van Glabbeke M (1992) A comparison of two short intensive adjuvant chemotherapy regimens in operable osteosarcoma of the limbs in children and young adults: the first study of the European Osteosarcoma Intergroup. *J Clin Oncol* **10**: 1579–1591

Buckner JC, Peethambaram PP, Smithson WA, Groover RV, Schomberg PJ, Kimmel DW, Raffel C, O'Fallon JR, Neglia J and Shaw EG (1999) Phase II trial of primary chemotherapy followed by reduced-dose radiation for CNS germ cell tumors. *J Clin Oncol* **17**: 933–940

Bues-Charbit M, Gentet JC, Bernard JL, Breant V, Cano JP and Raybaud C (1987) Continuous infusion of high-dose cisplatin in children: pharmacokinetics of free and total platinum. *Eur J Cancer Clin Oncol* **23**: 1649–1652

Cavaletti G, Marzorati L, Boglion G, Colombo N, Marzola M, Pittelli MR and Tredici G (1992) Cisplatin-induced peripheral neurotoxicity is dependent on total dose-intensity and single dose-intensity. *Cancer* **69**: 203–207

Dominici C, Petrucci F, Caroli S, Alimonti A, Clerico A and Castello MA (1989) A pharmacokinetic study of high-dose continuous infusion cisplatin in children with solid tumors. *J Clin Oncol* **7**: 100–107

Gill PS, Espina BM, Muggia F, Cabriales S, Tulpule A, Esplin JA, Liebman HA, Forssen E, Ross ME and Levine AM (1995) Phase I/II clinical and pharmacological evaluation of liposomal daunorubicin. *J Clin Oncol* **13**: 996–1003

Krakoff IH (1979) Nephrotoxicity of cis-dichlorodiammineplatinum (II). *Cancer Treat Rep* **63**: 1523–1525

Manaka RC and Wolf W (1978) Distribution of *cis*-platin in blood. *Chem Biol Interactions* **22**: 353–358

Muggia FM, Hainsworth JD, Jeffers S, Miller P, Groshen S, Tan M, Roman L, Uziely B, Muderspach L, Garcia A, Burnett A, Greco FA, Morrow CP, Paradiso LJ and Liang LJ (1997) Phase II study of liposomal doxorubicin in refractory ovarian cancer: antitumor activity and toxicity modification by liposomal encapsulation. *J Clin Oncol* **15**: 987–993

Newman MS, Colbern GT, Working PK, Engbers C and Amantia MA (1999) Comparative pharmacokinetics, tissue distribution, and therapeutic effectiveness of cisplatin encapsulated in long-circulating, pegylated liposomes (SPI-077) in tumor-bearing mice. *Cancer Chemother Pharmacol* **43**: 1–7

Northfelt DW, Dezube BJ, Thommes JA, Levine R, Von Roenn JH, Dosik GM, Rios A, Krown SE, DuMond C and Mamelok RD (1997) Efficacy of pegylated-liposomal doxorubicin in the treatment of AIDS-related Kaposi's sarcoma after failure of standard chemotherapy. *J Clin Oncol* **15**: 653–659

Papahadjopoulous D, Allen TN, Gabizon A, Mayhew E, Matthay K, Huang SK, Lee KD, Woodle MC, Lasic DD, Redemann C and Martin FJ (1991) Sterically stabilized liposomes: Improvement in pharmacokinetics and antitumor therapeutic efficacy. *Proc Natl Acad Sci (USA)* **88**: 11460–11464

Pearson AD, Craft AW, Pinkerton CR, Meller ST and Reid MM (1992) High-dose rapid schedule chemotherapy for disseminated neuroblastoma. *Eur J Cancer* **28A**: 1654–1659

Peng B, English M, Boddy AV, Price L, Wyllie R, Pearson ADJ, Tilby MJ and Newell DR (1997) Cisplatin pharmacokinetics in children. *Eur J Cancer* **33**: 1823–1828

Pratt CB, Hayes A, Green AA, Evans WE, Senzer N, Howarth CB, Ransom JL and Crom W (1981) Pharmacokinetic evaluation of cisplatin in children with malignant solid tumors: a phase II study. *Cancer Treat Rep* **65**: 1021–1026

Rahman A, Treat J, Roh JK, Potkul LA, Alvord WG, Forst D and Woolley PV (1990) A phase I clinical trial and pharmacokinetic evaluation of liposome encapsulated doxorubicin. *J Clin Oncol* **8**: 1093–1100

Schellens JHM, Meenum Terwogt J, Groenewegen G, Blijham GH, Ten Bokkel Huinink WW, Smart M, Maliepaard M, Floot B, Welbank H and Beijnen JH (1998) Phase I and pharmacologic study of SPI-77, a novel stealth liposomal encapsulated formulation of cisplatin (CDDP). *Eighty-ninth annual meeting, Proceedings American Association Cancer Research* **39**: P2218

Uziely B, Jeffers S, Isacson R, Kutsch K, Wei-Tsao D, Yehoshua Z, Libson E, Muggia FM and Gabizon A (1995) Liposomal doxorubicin (Dox-SL™): Antitumor activity and unique toxicities during two complementary phase I studies. *J Clin Oncol* **13**: 1777–1785

Vaage J, Mayhew E, Lasic D and Martin F (1992) Therapy of primary and metastatic mouse mammary carcinoma with doxorubicin encapsulated in long circulating liposomes. *Int J Cancer* **51**: 942–948

Vermorken JB, Kapteijn TS, Hart AAM and Pinedo HM (1983) Ototoxicity of cisdiamminedichloroplatinum (II): Influence of dose, schedule and mode of administration. *Eur J Cancer Clin Oncol* **19**: 53–58

Woodle MC and Lasic DD (1992) Sterically stabilized liposomes. *Biochem Biophys Acta* **1113**: 171

The Oncologist®
Gastrointestinal Cancer

Critical Evaluation of Current Treatments in Metastatic Colorectal Cancer

ALAN VENOOK

Division of Medical Oncology, Clinical Research Office, University of California Cancer Center, San Francisco, California, USA

Key Words. Fluorouracil · Irinotecan · Oxaliplatin · Bevacizumab · Cetuximab · Vascular endothelial growth factor · VEGF

LEARNING OBJECTIVES

After completing this course, the reader will be able to:

1. Describe the evolution of cancer chemotherapy for patients with colorectal cancer.
2. Discuss the current relevance of VEGF as a therapeutic target in colorectal cancer.
3. Discuss the current relevance of EGFR as a therapeutic target in colorectal cancer.

Access and take the CME test online and receive 1 hour of AMA PRA category 1 credit at CME.TheOncologist.com

ABSTRACT

Fluorouracil (FU) has been the mainstay of treatment for metastatic colorectal cancer (mCRC) for many years. However, in recent years, newer chemotherapeutic agents, particularly irinotecan (Campostar®; Pfizer Pharmaceuticals, New York, NY, http://www.pfizer.com) and more recently oxaliplatin (Eloxatin®; Sanofi-Aventis Inc., New York, NY, http://www.sanofi-aventis.com), have been shown to improve survival in combination with FU-based therapies. These agents were therefore incorporated into first- and second-line treatment strategies. The development of targeted agents that are tumor specific with better toxicity profiles than chemotherapeutic agents has widened the spectrum of therapies for this disease. The U.S. Food and Drug Administration (FDA) recently approved two targeted agents for treating mCRC: an antivascular endothelial growth factor monoclonal antibody (mAb), bevacizumab (Avastin®; Genentech, Inc., South San Francisco, CA, http://www.gene.com), in combination with first-line 5-FU-based chemotherapy regimens and the human epidermal growth factor receptor (HER-1/EGFR)-targeted mAb cetuximab (Erbitux®; ImClone Systems, Inc., New York, NY, http://www.imclone.com) as monotherapy or in combination with irinotecan as second-line therapy in refractory cancer. These newer, more effective agents are improving clinical outcome for patients with mCRC. However, as the number of agents has increased, choosing the most effective treatment strategy has become increasingly complex. This review discusses the role of the individual agents in the treatment of mCRC and identifies the most effective regimens. *The Oncologist* 2005;10:250–261

Correspondence: Alan Venook, M.D., Division of Medical Oncology, Clinical Research Office, University of California Cancer Center, Box 1705, 1600 Divisadero, San Francisco, California 94115-1705, USA. Telephone: 415-353-9888; Fax: 415-353-9959; e-mail: venook@cc.ucsf.edu Received August 12, 2004; accepted for publication February 15, 2005.

Introduction

Colorectal cancer is the third most common cancer in the U.S., with approximately 145,000 new cases expected in 2005 [1]. Estimated 5-year survival rates range from 90% for patients with stage I disease to <10% for patients with metastatic colorectal cancer (mCRC) [1]. For many years, the standard treatment for patients with mCRC was systemic chemotherapy with fluorouracil (FU). In the past 5 years, however, therapies for mCRC have progressed dramatically and shifted from monotherapy to combination therapy and, more recently, to sequential combination therapy. Because these more efficacious treatment regimens allow patients to survive longer and receive more lines of therapy, choosing the best treatment regimen is becoming increasingly complex. This review discusses the role of various agents/regimens in the treatment of mCRC and focuses on identifying the most effective regimens based on the available data.

Chemotherapeutic Agents/Regimens for mCRC

Fluorouracil/Leucovorin

For more than 40 years, FU was the standard of care for patients with mCRC. Because FU has a schedule-dependent mode of action, various strategies have been explored to maximize its cytotoxic effects, such as changing the dose, schedule, or route of administration. A brief overview of studies follows, comparing the efficacy and toxicity profiles of different modalities.

A pooled analysis, incorporating data from six randomized trials, showed that FU administered as a continuous i.v. infusion led to a significantly higher response rate than bolus i.v. FU (Mayo Clinic protocol) (22% versus 14%, respectively; odds ratio, 0.55; $p = .0002$), although the median survival times were similar (infusional FU 12.1 months versus bolus FU 11.3 months; hazards ratio, 0.88; $p = .04$) [2]. FU administered by continuous infusion allows for the delivery of more drug than bolus FU and shifts the dose-limiting toxicity from myelosuppression to hand-foot syndrome, which results in a more favorable toxicity profile [2, 3]. The change in toxicity profile is a result of a higher concentration of FU in the bone marrow following bolus administration versus continuous infusion [4].

The activity of FU also has been enhanced by the addition of the biochemical modulator folinic acid (leucovorin [LV]). In a recent meta-analysis of 3,300 patients randomized in 19 trials, the response rate was twofold greater in patients receiving FU/LV than in those receiving FU alone (21% versus 11%, respectively; $p < .0001$) [5]. There also was a slightly, but significantly, longer survival time in those receiving FU/LV [5]. Biomodulation of FU with LV also has, however, been associated with higher incidences of grade 3 and 4 diarrhea, stomatitis, and hematologic toxicities than either bolus or infusional FU [6].

Based on better response rates, bolus FU/LV therapy became the standard of care for patients with mCRC in the U.S. and remained as such until 2000. In Europe, oncologists were, however, more likely to use a modulated infusion regimen. The most commonly used approach there is the de Gramont regimen, an every-2-weeks protocol (LVFU2) that combines bolus with infusional FU/LV. De Gramont and colleagues reported that this regimen was more effective and had a better safety profile than the LV/FU bolus regimen [7]. However, U.S. oncologists have been reluctant to

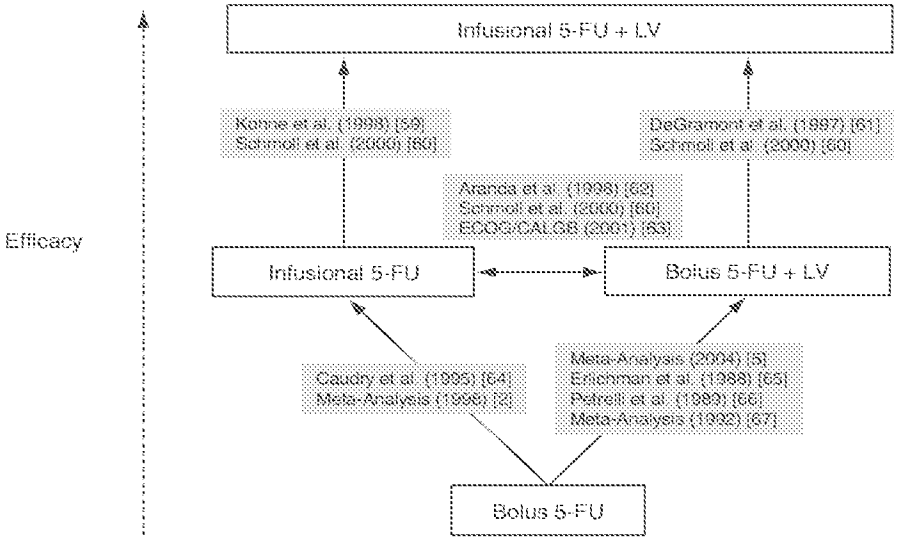

Figure 1. FU: the cornerstone of therapy for mCRC [2, 5, 59-67]. Abbreviations: CALGB = Cancer and Leukemia Group B; ECOG = Eastern Cooperative Oncology Group; FU = fluorouracil; LV = leucovorin; mCRC = metastatic colorectal cancer.

use infusional FU because of the inconvenience and higher costs associated with infusion access and pumps. Figure 1 shows key publications demonstrating the efficacy of bolus versus infusional 5-FU therapy.

Irinotecan, Oxaliplatin, and Capecitabine

In the past few years, newer chemotherapeutic agents, such as irinotecan (Camptosar®; Pfizer Pharmaceuticals, New York, NY, http://www.pfizer.com), oxaliplatin (Eloxatin®; Sanofi-Aventis Inc., Paris, France, http://www.sanofi-aventis.com), and capecitabine (Xeloda®; Hoffmann-La Roche Inc., Nutley, NJ, http://www.roche.us), used as monotherapy or in combination with 5-FU-based therapy have had a significant impact on treatment strategies for patients with mCRC.

Irinotecan, a topoisomerase I inhibitor, was initially introduced as monotherapy for patients with mCRC refractory to FU [8, 9]. In two pivotal phase III trials, therapy with single-agent irinotecan resulted in a longer survival time than best supportive care or infusional FU/LV therapy in FU-refractory patients [10, 11] (Table 1). Therefore, based on these data, irinotecan was approved for patients with mCRC who had failed treatment with FU/LV (Table 2).

Table 1. The efficacy of chemotherapeutic regimens, bevacizumab in combination with IFL, and single-agent cetuximab in first- or second-line mCRC

Study	*n* of patients	Response rate (%)	Median PFS (months, unless otherwise stated)	Overall survival (months)
Irinotecan first-line treatment				
Saltz et al. 2000 [12]				
IFL	231	39[a]	7.0	14.8
Bolus FU/LV	226	21[a]	4.3	12.6
Irinotecan	226	18[a]	4.2	12.0
Douillard et al. 2000 [13]				
FOLFIRI	198	34.8[b]	6.7	17.4
FU/LV	187	21.9[b]	4.4	14.1
Koehne et al. 2003 [14]				
FOLFIRI	214	54.2	8.5	20.1
FU/LV	216	31.5	6.4	16.9
Oxaliplatin first-line treatment				
de Gramont et al. 2000 [17]				
FOLFOX	210	50.7	9.0	16.2
LVFU2	210	22.3	6.2	14.7
Goldberg et al. 2004 [19]				
FOLFOX	267	45	8.7[c]	19.5
IFL	264	31	6.9[c]	15.0
IROX	264	35	6.5[c]	17.4
Grothey et al. 2002 [20]				
FUFOX	118	48.3	7.9	20.4
Bolus FU/LV	124	22.6	5.3	16.1
Tournigand et al. 2004 [22]				
FOLFOX followed by FOLFIRI	111	FOLFOX 54% FOLFIRI 4%	10.9	20.6
FOLFIRI followed by FOLFOX	111	FOLFIRI 56% FOLFOX 15%	14.2	21.5
Capecitabine first-line treatment				
Van Cutsem et al. 2001 [26]				
Capecitabine	301	18.9	5.2	13.2
FU/LV	301	15.0	4.7	12.1
Hoff et al. 2001 [27]				
Capecitabine	302	24.8	4.3	12.5
FU/LV	303	15.5	4.7	13.3

Table 1. The efficacy of chemotherapeutic regimens, bevacizumab in combination with IFL, and single-agent cetuximab in first- or second-line mCRC (continued)

Study	*n* of patients	Response rate (%)	Median PFS (months, unless otherwise stated)	Overall survival (months)
Bevacizumab first-line treatment				
Hurwitz et al. 2004 [41]				
IFL/bevacizumab	402	44.8	10.6	20.3
IFL	411	34.8	6.2	15.6
Irinotecan second-line treatment				
Cunningham et al. 1998 [10]				
Irinotecan	189	NA	NA	9.2
BSC	90	NA	NA	6.5
Rougier et al. 1998 [11]				
Irinotecan	133	NA	4.2	10.8
FU	134	NA	2.9	8.5
Oxaliplatin second-line treatment				
Rothenberg et al. 2003 [18]				
FOLFOX	152	9.9	4.6[c]	NA
FU/LV	151	0	2.7[c]	NA
Oxaliplatin	156	1.3	1.6[c]	NA
Cetuximab second-line treatment				
Saltz et al. 2004 [57]				
Cetuximab	57	8.8	1.4	6.4

Fluorouracil is by infusion unless otherwise stated.

[a]Confirmed response rate.

[b]Intent-to-treat population.

[c]Time to disease progression

Abbreviations: BSC = best supportive care; FU = fluorouracil; FOLFIRI = fluorouracil/leucovorin plus irinotecan; FOLFOX = fluorouracil/leucovorin plus oxaliplatin; FUFOX = infusional FU/LV given weekly and every 6 weeks plus oxaliplatin; IFL = bolus fluorouracil/leucovorin plus irinotecan; IROX = irinotecan plus oxaliplatin every 3 weeks; LV = leucovorin; LVFU2 = every-2-weeks chemotherapy regimen combining bolus with infusional fluorouracil/leucovorin; mCRC = metastatic colorectal cancer; NA = not available; PFS = progression-free survival.

Table 2. FDA-approved regimens for mCRC

Regimen	U.S. approval status		Year of approval
	First-line therapy	Second-line therapy	
Bevacizumab plus 5-FU-based regimens (IFL, FOLFIRI, FOLFOX, and FU/LV)	√		2004
Cetuximab (monotherapy or with irinotecan)		√	2004
FOLFOX	√	√	First line, 2004; second line, 2002
FOLFIRI	√		2000
IFL	√		2000
Irinotecan		√	1998
Capecitabine monotherapy	√		2002

Abbreviations: FDA = U.S. Food and Drug Administration; FOLFIRI = fluorouracil/leucovorin plus irinotecan; FOLFOX = fluorouracil/leucovorin plus oxaliplatin; FU/LV = fluorouracil/leucovorin; IFL = bolus fluorouracil/leucovorin plus irinotecan; mCRC = metastatic colorectal cancer.

Researchers then evaluated the addition of irinotecan to FU/LV as first-line treatment for mCRC. Saltz and colleagues showed that combining irinotecan with bolus FU/LV (IFL) resulted in a higher response rate, longer progression-free survival (PFS) time, and longer overall survival time in first-line mCRC treatment compared with bolus FU/LV alone [12] (Table 1). As expected, the incidence of grade 3 diarrhea was more common with irinotecan-based therapy than with bolus FU/LV alone. Similarly, in a European trial, Douillard and colleagues also showed that adding irinotecan to weekly or every-2-weeks regimens of FU/LV by infusion (FOLFIRI) improved the response rate and increased the PFS and survival times [13] (Table 1). Based on data from these trials, the U.S. Food and Drug Administration (FDA) and European regulatory authorities approved irinotecan in combination with both bolus and infusional FU/LV as first-line therapy for mCRC, replacing FU/LV as the standard of care (Table 2). U.S. oncologists were, however, partial to the bolus regimen, and European oncologists continued to use infusional FU/LV. Interestingly, a second European trial also examined irinotecan in combination with the AIO regimen (infusional FU/LV given weekly for 6 weeks) as first-line mCRC treatment [14]. Survival times in that trial were longer than those in the Saltz et al. and Douillard et al. trials (Table 1), but this may be explained by the extensive use of second- and third-line therapies, as both oxaliplatin and irinotecan were readily available in Europe at the time.

Oxaliplatin is a cisplatin derivative with a similar mechanism of action to other platinum compounds, although its antitumor profile differs from those of cisplatin (Platinol®; Bristol-Myers Squibb, Princeton, NJ, http://www.bms.com) and carboplatin (Paraplatin®; Bristol-Myers Squibb, http://www.bms.com) [15]. Indeed, experimental studies have shown that oxaliplatin inhibits colorectal cancer tumor cell lines that are resistant to cisplatin and carboplatin [16].

In a phase III trial, oxaliplatin was evaluated in combination with infusional FULV2 (FOLFOX regimen) as first-line therapy for patients with mCRC. The findings showed a higher response rate, longer median PFS time, and longer survival than those observed with FU/LV alone, although the survival difference was not statistically significant (Table 1) [17]. The lack of difference in survival benefit between the two groups may be explained by the small sample and crossover treatments that might have obscured any difference in survival [17]. Toxicities of oxaliplatin in combination with FU/LV2 also were mild, although dose-dependent and mostly reversible sensory neuropathy was a cumulative dose-limiting toxicity in the oxaliplatin arm. These data were submitted to the FDA in 2002, but oxaliplatin was denied approval because of the lack of a statistically significant survival benefit. A phase III trial demonstrated the efficacy of oxaliplatin-based therapy as second-line treatment for mCRC [18]. Rothenberg and colleagues showed a higher response rate and longer time to progression (TTP) with oxaliplatin plus infusional plus bolus FU than with oxaliplatin monotherapy and infusional FU/LV alone, although single-agent oxaliplatin and FU/LV had no meaningful activity (Table 1). These data led to the approval of oxaliplatin in combination with infusional FU/LV as second-line therapy following irinotecan and FU/LV for mCRC in the U.S. (Table 2).

A phase III trial recently suggested that FOLFOX first-line therapy is superior in efficacy and safety to IFL [19]. Goldberg and colleagues showed that FOLFOX produced a higher response rate (45%) and longer median survival time (19.5 months) than IFL (31% and 15 months, respectively) and than irinotecan and oxaliplatin given every 3 weeks (IROX; 35% and 17.4% months, respectively) (Table 1). With the exception of peripheral neuropathy, the toxicity profile for FOLFOX also was more favorable than that of either IFL or IROX.

The conclusion that the FOLFOX regimen is more effective than IFL or IROX for first-line mCRC therapy must be tempered by several nuances in the trial design. Notably, that an infusional FU-based combination regimen was compared with a bolus FU-based combination regimen, and therefore the individual contributions of irinotecan and oxaliplatin to an FU-based regimen cannot be determined. Also, crossover to second-line therapy was imbalanced because oxaliplatin was not readily available in the U.S. at the time of the trial, and therefore, most patients who received FOLFOX initially, as first-line therapy, received irinotecan at progression, whereas only a few patients who received first-line IFL received oxaliplatin at progression. The FDA, however, recently approved oxaliplatin as first-line therapy for mCRC (Table 2). In Europe, a second trial examined the AIO regimen plus oxaliplatin (FUFOX) versus bolus FU/LV in patients with advanced CRC [20]. It was shown that the oxaliplatin-based regimen significantly improved response rate, but not overall survival, although survival was longer (20.4 months versus 16.1 months) with the FUFOX regimen (Table 1). As with other European trials during that period, the long overall survival time may be attributed to the 75% of patients who received oxaliplatin- and/or irinotecan-based salvage therapies [20].

FOLFOX and FOLFIRI appear to be the most effective in terms of efficacy and tolerability. In a recent randomized trial, Colucci and colleagues showed that the two regimens were comparable [21]. Larger randomized studies comparing FOLFOX with FOLFIRI are ongoing and will help us to evaluate which is the more effective regimen.

Tournigand and colleagues also evaluated the FOLFOX and FOLFIRI regimens to find the best sequence for treating patients with mCRC [22]. Those authors showed that a sequence of first-line FOLFOX followed by second-line

FOLFIRI resulted in a similar survival time to that produced by the reverse sequence (Table 1). However, as at least 30% of patients did not receive second-line therapy, the authors highlighted the importance of choosing the most appropriate first-line therapy. Although both first-line therapies achieved similar response rates (FOLFIRI 56% versus FOLFOX 54%), second-line FOLFIRI achieved a significantly lower response rate than did FOLFOX (4% versus 15%). The toxicity profiles for the two regimens were also different. As expected from previous studies, grade 3/4 mucositis, nausea/vomiting, and grade 2 alopecia were more common with FOLFIRI, whereas grade 3/4 neutropenia and neurosensory toxicity were more common with FOLFOX. The authors noted that future studies should focus on the limitations of the trial, notably that neurotoxicity forces many patients to stop oxaliplatin before tumor resistance develops and that FOLFIRI has a relatively poor efficacy as a second-line therapy.

Importantly, it should be noted that phase III trials evaluating combination therapy have reported median overall survival times in the range of 14.8–21.5 months. As these were large, randomized trials conducted over a relatively short period, it is unlikely that patient selection or other factors outside the treatment strategy were responsible for these differences. It is most likely that second- or third-line therapies had an impact on overall survival. A recent meta-analysis analyzed results from seven phase III trials in mCRC to correlate the percentage of patients receiving: A) second-line therapy, and B) all three agents with the reported median overall survival [23]. The median overall survival was significantly correlated with the percentage of patients receiving all three agents over the disease course, but not with the proportion of patients receiving second-line therapy. To optimize clinical outcome, the authors suggested that it is important to make FU/LV, irinotecan, and oxaliplatin available to all patients with mCRC who are candidates for this type of therapy. However, possible study bias was noted, that is, patients who lived longer had a better chance of receiving all therapies, while patients with poorer performance statuses and shorter life expectancies were probably excluded from second-line therapy. Also, this analysis could not evaluate the best sequence of treatment, although ongoing and future randomized trials comparing different sequences should address these questions. Finally, as sequential therapies cannot be predefined in treatment protocols, overall survival may no longer be regarded as the most sensitive end point for assessing the efficacy of first-line therapy; other factors, such as PFS and TTP, should be considered.

Researchers are investigating alternative approaches to optimizing FU therapy. Capecitabine is an oral fluoropyrimidine carbamate, initially designed to deliver FU predominantly to tumor cells [24, 25]. In two randomized trials, the efficacy and toxicity of capecitabine as first-line treatment in patients with mCRC were evaluated [26, 27] (Table 1). Those trials showed that capecitabine had an efficacy that was at least equivalent to that of i.v. FU/LV. Grade 3 hand-foot syndrome was reported more frequently with capecitabine, although the condition was tolerated with a reduced dose. A higher incidence of grade 3/4 hyperbilirubinemia also was reported, but all cases were reversible. Against this background, capecitabine appears to offer equivalent efficacy and a better toxicity profile than the Mayo regimen, with the added convenience of an oral agent. Based on these data, capecitabine was approved in the U.S. as first-line therapy for patients with mCRC for whom combination therapy is not warranted (Table 2). Other phase II studies have examined the addition of oxaliplatin or irinotecan to capecitabine [28, 29]. So far, data have been encouraging, with toxicity profiles similar to that of infusional FU, and it appears that oxaliplatin/capecitabine is equivalent to irinotecan/ capecitabine therapy. Based on these data, randomized, phase III trials are planned to evaluate oxaliplatin or irinotecan in combination with capecitabine in patients with mCRC.

Targeted Agents in Combination with Chemotherapy—Moving Forward

Advances in chemotherapeutic agents have led to better outcomes for patients with mCRC. Chemotherapies, however, are limited by their lack of specificity and are often associated with frequent and potentially severe dose-limiting toxicities. Therefore, there is an urgent need for more effective, better-tolerated treatments that specifically target the processes pivotal to tumorigenesis and metastasis. Further advances in the understanding of molecular biology have led to the development of target-specific agents. The FDA recently approved two targeted agents: an antivascular endothelial growth factor (anti-VEGF) monoclonal antibody (mAb), bevacizumab (Avastin®; Genentech, Inc., South San Francisco, CA, http://www.gene.com), and a human epidermal growth factor receptor (HER-1/EGFR)-targeted mAb, cetuximab (Erbitux®; Imclone Systems, Inc., New York, NY, http://www.imclone.com), as first- and second-line mCRC therapy, respectively. These two agents are already having a significant impact on mCRC treatment strategies.

Bevacizumab

Rationale for Targeting VEGF

Over 20 years ago, researchers showed that tumors cannot grow beyond 1–2 mm without the establishment of a blood supply [30]. The formation of tumor blood vessels, or angiogenesis, not only allows tumors to absorb nutrients

and oxygen for their further growth and development but also allows a pathway for migrating tumor cells to access the systemic circulation and establish metastases. The transition, or switch, of a tumor to an angiogenic phenotype is caused by an increase in proangiogenic factors, including VEGF, basic fibroblast growth factor (bFGF), and transforming growth factor beta (TGF-β), and a decrease in antiangiogenic factors, such as interferon-α [31].

VEGF is a specific mitogen for the endothelial cell and one of the most potent proangiogenic factors. VEGF acts as a survival factor for endothelial cells through the inhibition of apoptosis and plays an important role in mobilizing endothelial cell precursors to sites of angiogenesis [32, 33]. VEGF is upregulated in most human tumors, including colorectal cancer [33]. This has been correlated with increased tumor invasion, microvessel density, disease recurrence, and a poor prognosis [34, 35]. Based on these observations, and its low levels in healthy tissue, VEGF appears to be a particularly attractive target for anticancer therapy.

There are a variety of strategies that target VEGF, although VEGF blockade with mAbs is the most studied approach. Bevacizumab is an anti-VEGF, humanized mAb that is the most advanced agent of its class in clinical development. Preclinical data show that this agent is active in colorectal cancer and other types of solid tumors and is better tolerated than conventional chemotherapeutic agents [36, 37]. Preclinical studies have also shown that combining anti-VEGF therapy with chemotherapeutic agents results in augmented antitumor activity [38, 39]. The mechanism by which bevacizumab enhances the efficacy of chemotherapy is not well understood, although it has been proposed that, as tumor blood vessels are chaotic, irregular, and leaky, relatively low doses of anti-VEGF therapy "normalize" tumor vasculature, reducing intratumoral pressure and allowing better delivery of therapeutic agents to the tumor, thereby maximizing antitumor activity [40]. Against this background, it was suggested that the most effective use of bevacizumab is in combination with chemotherapy.

Clinical Studies

Several studies have examined bevacizumab in combination with chemotherapy in the first- and second-line settings in patients with mCRC. Phase II and III trials of bevacizumab in combination with FU/LV and IFL are completed or ongoing (Table 1 and Table 3). Studies of bevacizumab in combination with oxaliplatin-based therapies are ongoing.

The phase III trial was the first phase III evaluation of the efficacy and safety of first-line bevacizumab and led to the recent approval of this agent in combination with i.v. FU-based therapy as first-line therapy for patients with mCRC (Table 2) [41]. In this trial, Hurwitz and colleagues examined bevacizumab in combination with IFL as first-line therapy for patients with mCRC. Over 900 patients were randomized to one of three treatments: IFL/placebo, IFL/bevacizumab, or FU/LV/bevacizumab. The FU/LV/bevacizumab arm was included because no previous study had examined IFL in combination with bevacizumab, but this arm was stopped when the safety of bevacizumab plus IFL was demonstrated in an interim analysis. Treatment could continue until disease progression, unacceptable toxicity, or 96 weeks. At progression, patients could receive second-line therapy. Oncologists treating patients in a bevacizumab-containing arm could choose to continue with bevacizumab during second-line therapy.

The addition of bevacizumab to IFL resulted in a significantly longer survival time, by almost 5 months (30% increase in survival) (20.3 months versus 15.6 months; $p < .001$) (Table 1 and Table 3). The addition of bevacizumab

Table 3. Completed or ongoing trials evaluating bevacizumab in combination with bolus FU/LV therapy in mCRC

Study	*n* of patients	Response rate (%)	Median PFS (months)	Overall survival (months)
Kabbinavar et al. 2003 [43]				
FU/LV/bevacizumab (high-dose)	33	24	7.2	16.1
FU/LV/bevacizumab (low-dose)	35	40	9.0	21.5
FU/LV	36	17	5.2	13.8
Kabbinavar et al. 2004 [44]				
FU/LV/bevacizumab	105	26	9.2	16.6
FU/LV	104	15	5.5	12.9
Hurwitz et al. 2004 [45]				
FU/LV/bevacizumab	110	40	8.8	18.3
IFL	100	37	6.8	15.1

Abbreviations: FU/LV = fluorouracil/leucovorin, IFL = bolus fluorouracil/leucovorin plus irinotecan; mCRC = metastatic colorectal cancer; PFS = progression-free survival

to IFL also resulted in a significantly greater overall response rate, duration of response, and PFS time. Survival benefit was observed for all patient subgroups and was independent of second-line therapy. For the subgroup of patients who received second-line therapy with oxaliplatin-containing regimens, overall survival times were 25.1 months and 22.2 months for the IFL/bevacizumab and IFL/placebo arms, respectively [42].

Overall, IFL with bevacizumab was generally well tolerated, with no overlapping toxicities. Although a number of adverse events, including bleeding, thrombosis, proteinuria, and hypertension, were observed in phase I/II trials, only hypertension (easily managed with standard blood pressure medications) had a higher incidence in the IFL/bevacizumab arm. However, six patients (1.5%) receiving IFL/bevacizumab had gastrointestinal events, including bowel perforation. Although this event was uncommon given the size of the trial, the risk of such events may be increased with bevacizumab. Studies are ongoing to understand further bevacizumab-related gastrointestinal perforation.

Phase II and III studies have evaluated the addition of bevacizumab to FU/LV as another standard option for the first-line treatment of mCRC [43–45] (Table 3). Indeed, these studies showed that FU/LV/bevacizumab compares favorably with FU/LV. Therefore, bevacizumab should be considered for the subgroup of patients for whom irinotecan- or oxaliplatin-based therapy is not recommended, as this subgroup of patients has few treatment options available.

Clinical trials are in progress or planned to evaluate the addition of bevacizumab to FOLFOX or FOLFIRI. For example, a recently completed phase III trial evaluated the addition of bevacizumab to FOLFOX in the second-line treatment of patients who have failed previous irinotecan plus FU therapy. Analyses of the findings are ongoing, but these data demonstrated that patients receiving bevacizumab plus FOLFOX had a 17% longer survival time than those receiving FOLFOX alone (12.5 months versus 10.7 months) and this regimen also had an acceptable toxicity profile [46]. Therefore, adding bevacizumab to chemotherapy results in a significant survival benefit for patients with untreated or relapsed mCRC. Figure 2 shows the survival benefit of bevacizumab plus chemotherapy relative to other regimens and best supportive care.

Other ongoing trials will provide further information on the efficacy and safety of bevacizumab in different settings. These studies will help us to define the extent to which bevacizumab can be used to treat mCRC. Finally, studies are examining bevacizumab plus FOLFOX in the adjuvant setting. This is a particularly important setting for antiangiogenic therapy, as targeting tumor neovasculature during early disease may contribute to curative treatment.

Cetuximab

Rationale for Targeting HER-1/EGFR

The HER-1/EGFR signaling pathway is thought to play a pivotal role in tumor growth and progression of various cancers, including colorectal cancer [47]. HER-1/EGFR belongs to the HER family of receptors. These receptors are transmembrane glycoproteins, comprising an extracellular ligand-binding domain, an intracellular tyrosine-kinase (TK) domain, and a transmembrane segment [47]. Various ligands can bind to the HER-1/EGFR extracellular domain inducing receptor homo- or heterodimerization with another HER-1/ EGFR receptor or other HER family members. This results in activation of the receptor's TK activity, initiating a downstream signaling cascade that ultimately leads to tumor cell proliferation, migration, adhesion and angiogenesis, and inhibition of apoptosis [48].

Various reports have shown that HER-1/EGFR signaling is dysregulated in colorectal cancer and other tumor types [49]. HER-1/EGFR overexpression has also been correlated with disease progression, poor prognosis, and reduced sensitivity to chemotherapy [50]. Therefore, several strategies have been developed to target HER-1/EGFR, including small-molecule TK inhibitors and mAbs. Cetuximab is the most advanced mAb targeting HER-1/EGFR in clinical development.

Cetuximab exerts its antitumor effects through ligand-independent processes, stimulating receptor internalization [51]. Preclinical and early clinical studies have shown that single-agent cetuximab primarily leads to cytostatic activity, whereas combining cetuximab with chemotherapeutic agents, such as cisplatin, topotecan (Hycamtin®; GlaxoSmithKline, Philadelphia, PA, http://www.gsk.com), and irinotecan leads to synergistic antitumor activity [51–54]. One hypothesis for this synergy is that, for the majority of cell lines, blocking HER-1/ EGFR signaling is insufficient for cytotoxicity, but HER-1/ EGFR inhibition may leave the cells more vulnerable to chemotherapy. Importantly, these studies consistently suggested that, at least in these models, HER-1/EGFR expression is required for cetuximab activity.

Clinical Data

A phase II study evaluated the activity and safety of cetuximab plus irinotecan in patients with irinotecan-refractory CRC. The response rate was 22.5% in 120 patients who had progressive disease on irinotecan [55]. Cunningham and colleagues also evaluated cetuximab alone and cetuximab plus irinotecan in patients with irinotecan-refractory CRC [56]. The response rates were 10.8% for cetuximab alone and 22.9% for cetuximab plus irinotecan. Finally, a more recent phase II trial also assessed the safety and efficacy of single-agent cetuximab in patients with chemotherapy-refractory mCRC who express HER-1/EGFR [57]. The findings were

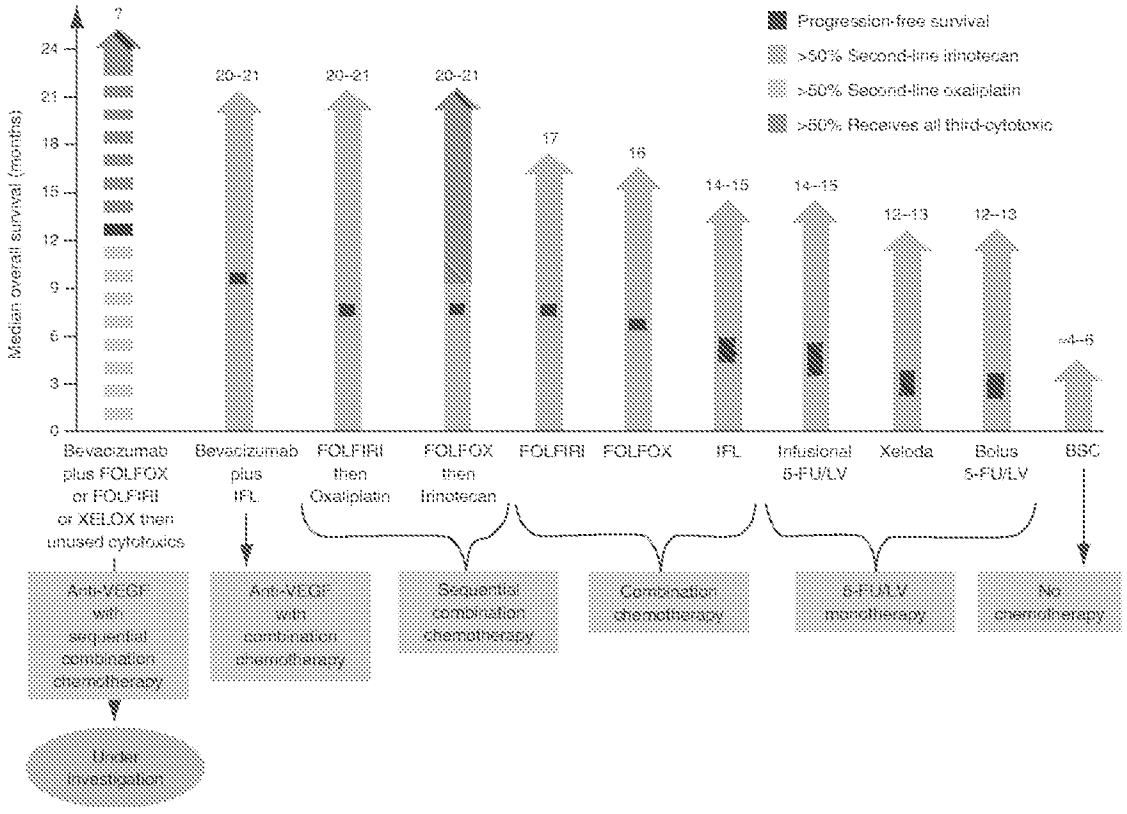

Figure 2. Survival benefit of bevacizumab plus first-line chemotherapy relative to other treatment strategies in patients with mCRC. Abbreviations: BSC = best supportive care; FOLFIRI = fluorouracil/leucovorin plus irinotecan; FOLFOX = every-2-weeks chemotherapy regimen combining bolus with infusional fluorouracil/leucovorin plus oxaliplatin; FU/LV = fluorouracil/leucovorin; IFL = bolus fluorouracil/leucovorin plus irinotecan; mCRC = metastatic colorectal cancer; VEGF = vascular endothelial growth factor; XELOX = capecitabine plus oxaliplatin.

similar to those of previous trials (Table 1). Unfortunately, response did not correlate with the degree of HER-1/EGFR expression as predicted by preclinical studies. This may be a result of the imprecision of quantifying HER-1/EGFR expression or possibly because HER-1/EGFR may not be the most appropriate marker for predicting response to therapy. Techniques such as gene expression profiling may help us to identify predictive markers of response, allowing the selection of patients most likely to respond to therapy.

Although different trials, particularly those with different regimens, should be compared with caution, the response rate from this trial was equivalent to the level of activity observed with second-line FOLFOX (9.9%) [18]. Based on these data, cetuximab was recently approved as second-line therapy for patients with mCRC in the U.S. and Europe (Table 2).

The side effects observed in this trial were manageable and similar to those previously reported. The most commonly reported grade 3/4 adverse events were severe hypersensitivity (managed with standard medications) and asthenia, fatigue, malaise, or lethargy. An acne-like rash typically associated with HER-1/EGFR inhibition was also observed in almost every patient, but none of the patients discontinued treatment because of the rash.

Finally, pilot trials have evaluated cetuximab in combination with IFL as first-line therapy for mCRC [58], and randomized phase III trials are examining cetuximab in combination with chemotherapy as first-line and adjuvant therapy. These studies will provide further information on the role of cetuximab in the treatment of CRC.

Conclusions

We have discussed some of the results from recently completed trials examining various chemotherapeutic regimens and/or targeted agents as first- and second-line mCRC therapy. We can conclude that the development of newer agents and the shift in treatment from monotherapy to sequential combination chemotherapy has improved clinical outcome for patients with mCRC, but the most appropriate setting for each of these agents/regimens still needs to be determined.

In terms of efficacy and tolerability, FOLFOX, FOLFIRI, and IFL plus bevacizumab are the most effective first-line regimens. However, we still cannot confirm which of these

regimens is the most effective for individual patients, although bevacizumab plus FOLFOX or FOLFIRI is likely to have the most clinical benefit (Fig. 2). In addition, important issues regarding the most effective sequence for these agents/regimens in the second- and third-line settings have yet to be clarified. For example, if patients progress after IFL, their options for second-line treatment include bevacizumab plus FOLFOX, cetuximab plus irinotecan, and capecitabine plus oxaliplatin. Recently, Grothey and colleagues [20] suggested that sequence is less important if all treatments are made available to all patients with mCRC. Ongoing, well-designed, comparative trials will hopefully provide a better understanding of how each regimen should be used to achieve maximum clinical benefit.

In addition, the optimal chemotherapy combinations, doses, and sequences of administration have yet to be defined. The addition of targeted agents has only added to the complexity. Indeed, it is likely that the optimal dose may vary with tumor location, growth rate, and previous therapy. Therefore, further studies are required to define the optimal dose and regimens for these agents in mCRC.

FU has been the cornerstone of treatment for mCRC for over 40 years. In the past few years, the introduction of more effective chemotherapeutic agents and targeted agents with their promising activities and mild toxicity profiles has pushed the overall median survival time from 12 months to 2 years. However, as discussed, there are still many challenges facing oncologists. Research is ongoing to understand these issues, and significant advances are expected through the implementation of well-designed clinical trials and continued preclinical investigation.

Disclosure of Potential Conflicts of Interest

The author indicated no potential conflicts of interest.

References

1 American Cancer Society. Cancer facts and figures. Atlanta, GA: American Cancer Society, 2005. http://www.cancer.org/downloads/STT/CAFF2005f4PWSecured.pdf. Accessed March 8, 2005.

2 Meta-analysis Group In Cancer. Efficacy of intravenous continuous infusion of fluorouracil compared with bolus administration in advanced colorectal cancer. J Clin Oncol 1998;16:301–308.

3 Perry M. The Chemotherapy Source Book. Philadelphia: Lippincott Williams & Wilkins, 1999:1–534.

4 Fraile RJ, Baker LH, Buroker TR et al. Pharmacokinetics of 5-fluorouracil administered orally, by rapid intravenous and by slow infusion. Cancer Res 1980;40:2223–2228.

5 Thirion P, Michiels S, Pignon JP et al. Modulation of fluorouracil by leucovorin in patients with advanced colorectal cancer: an updated meta-analysis. The Meta-Analysis Group in Cancer. J Clin Oncol 2004;22:3766–3775.

6 Kohne CH, Wils J, Lorenz M et al. Randomized phase III study of high-dose fluorouracil given as a weekly 24-hour infusion with or without leucovorin versus bolus fluorouracil plus leucovorin in advanced colorectal cancer: European Organization of Research and Treatment of Cancer Gastrointestinal Group Study 40952. J Clin Oncol 2003;21:3721–3728.

7 de Gramont A, Bosset JF, Milan C et al. Randomized trial comparing monthly low-dose leucovorin and fluorouracil bolus with bimonthly high-dose leucovorin and fluorouracil bolus plus continuous infusion for advanced colorectal cancer: a French intergroup study. J Clin Oncol 1997;15:808–815.

8 Hsiang YH, Hertzberg R, Hecht S et al. Camptothecin induces protein-linked DNA breaks via mammalian DNA topoisomerase I. J Biol Chem 1985;260:14873–14878.

9 Van Cutsem E, Rougier P, Droz J et al. Clinical benefit of irinotecan (CPT-11) in metastatic colorectal cancer (CRC) resistant to 5-FU. Proc Am Soc Clin Oncol 1997;8:268a.

10 Cunningham D, Pyrhonen S, James RD et al. Randomised trial of irinotecan plus supportive care versus supportive care alone after fluorouracil failure for patients with metastatic colorectal cancer. Lancet 1998;352:1413–1418.

11 Rougier P, Van Cutsem E, Bajetta E et al. Randomised trial of irinotecan versus fluorouracil by continuous infusion after fluorouracil failure in patients with metastatic colorectal cancer. Lancet 1998;352:1407–1412.

12 Saltz LB, Cox JV, Blanke C et al. Irinotecan plus fluorouracil and leucovorin for metastatic colorectal cancer. Irinotecan Study Group. N Engl J Med 2000;343:905–914.

13 Douillard JY, Cunningham D, Roth AD et al. Irinotecan combined with fluorouracil compared with fluorouracil alone as first-line treatment for metastatic colorectal cancer: a multicentre randomised trial. Lancet 2000;355:1041–1047.

14 Koehne C, Van Cutsem E, Wils J et al. Irinotecan improves the activity of the AIO regimen in metastatic colorectal cancer: results of EORTC GI Group Study 40986. Proc Am Soc Clin Oncol 2003;22:254a.

15 Woynarowski JM, Chapman WG, Napier C et al. Sequence- and region-specificity of oxaliplatin adducts in naked and cellular DNA. Mol Pharmacol 1998;54:770–777.

16 Rixe O, Ortuzar W, Alvarez M et al. Oxaliplatin, tetraplatin, cisplatin, and carboplatin: spectrum of activity in drug-resistant cell lines and in the cell lines of the National Cancer Institute's Anticancer Drug Screen panel. Biochem Pharmacol 1996;52:1855–1865.

17 de Gramont A, Figer A, Seymour M et al. Leucovorin and fluorouracil with or without oxaliplatin as first-line treatment in advanced colorectal cancer. J Clin Oncol 2000;18:2938–2947.

18 Rothenberg ML, Oza AM, Bigelow RH et al. Superiority of oxaliplatin and fluorouracil-leucovorin compared with either therapy alone in patients with progressive colorectal cancer after irinotecan and fluorouracil-leucovorin: interim results of a phase III trial. J Clin Oncol 2003;21:2059–2069.

19 Goldberg RM, Sargent DJ, Morton RF et al. A randomized controlled trial of fluorouracil plus leucovorin, irinotecan, and oxaliplatin combinations in patients with previously untreated metastatic colorectal cancer. J Clin Oncol 2004;22:23–30.

20 Grothey A, Deschler B, Kroening H et al. Phase III study of bolus 5-fluorouracil (5-FU)/folinic acid (FA) (Mayo) vs weekly high-dose 24h 5-FU infusion/FA + oxaliplatin (OXA) (FUFOX) in advanced colorectal cancer (ACRC). Proc Am Soc Clin Oncol 2002;21:129a.

21 Colucci G, Maiello E, Gebbia V et al. Preliminary results of a randomized multicenter trial of the Gruppo Oncologico Italia Meridionale (GOIM) comparing FOLFIRI vs FOLFOX in advanced colorectal (ACC) patients. Proc Am Soc Clin Oncol 2003;22:255a.

22 Tournigand C, Andre T, Achille E et al. FOLFIRI followed by FOLFOX6 or the reverse sequence in advanced colorectal cancer: a randomized GERCOR study. J Clin Oncol 2004;22:229–237.

23 Grothey A, Sargent D, Goldberg RM et al. Survival of patients with advanced colorectal cancer improves with the availability of fluorouracil-leucovorin, irinotecan, and oxaliplatin in the course of treatment. J Clin Oncol 2004;22:1209–1214.

24 Ishikawa T, Utoh M, Sawada N et al. Tumor selective delivery of 5-fluorouracil by capecitabine, a new oral fluoropyrimidine carbamate, in human cancer xenografts. Biochem Pharmacol 1998;55:1091–1097.

25 Miwa M, Ura M, Nishida M et al. Design of a novel oral fluoropyrimidine carbamate, capecitabine, which generates 5-fluorouracil selectively in tumours by enzymes concentrated in human liver and cancer tissue. Eur J Cancer 1998;34:1274–1281.

26 Van Cutsem E, Twelves C, Cassidy J et al. Oral capecitabine compared with intravenous fluorouracil plus leucovorin in patients with metastatic colorectal cancer: results of a large phase III study. J Clin Oncol 2001;19:4097–4106.

27 Hoff PM, Ansari R, Batist G et al. Comparison of oral capecitabine versus intravenous fluorouracil plus leucovorin as first-line treatment in 605 patients with metastatic colorectal cancer: results of a randomized phase III study. J Clin Oncol 2001;19:2282–2292.

28 Van Cutsem E, Twelves C, Tabernero JM et al. XELOX: mature results of a multinational, phase II trial of capecitabine plus oxaliplatin, an effective 1st line option for patients (pts) with metastatic colorectal cancer. Proc Am Soc Clin Oncol 2003;22:255a.

29 Patt Y, Lin E, Leibmann J et al. Capecitabine plus irinotecan for chemotherapy-naive patients with metastatic colorectal cancer (MCRC): US multicenter phase II trial. Proc Am Soc Clin Oncol 2003;22:281a.

30 Folkman J. Tumor angiogenesis. Adv Cancer Res 1974;19:331–358.

31 Hanahan D, Folkman J. Patterns and emerging mechanisms of the angiogenic switch during tumorigenesis. Cell 1996;86:353–364.

32 Ferrara N. Role of vascular endothelial growth factor in regulation of physiological angiogenesis. Am J Physiol Cell Physiol 2001;280:C1358–C1366.

33 Ferrara N, Davis-Smyth T. The biology of vascular endothelial growth factor. Endocr Rev 1997;18:4–25.

34 Frank RE, Saclarides TJ, Leurgans S et al. Tumor angiogenesis as a predictor of recurrence and survival in patients with node-negative colon cancer. Ann Surg 1995;222:695–699.

35 Choi HJ, Hyun MS, Jung GJ et al. Tumor angiogenesis as a prognostic predictor in colorectal carcinoma with special reference to mode of metastasis and recurrence. Oncology 1998;55:575–581.

36 Warren RS, Yuan H, Matli MR et al. Regulation by vascular endothelial growth factor of human colon cancer tumorigenesis in a mouse model of experimental liver metastasis. J Clin Invest 1995;95:1789–1797.

37 Gerber HP, Hillan KJ, Ryan AM et al. VEGF is required for growth and survival in neonatal mice. Development 1999;126:1149–1159.

38 Hu L, Hofmann J, Zaloudek C et al. Vascular endothelial growth factor immunoneutralization plus paclitaxel markedly reduces tumor burden and ascites in athymic mouse model of ovarian cancer. Am J Pathol 2002;161:1917–1924.

39 Sweeney CJ, Miller KD, Sissons SE et al. The antiangiogenic property of docetaxel is synergistic with a recombinant humanized monoclonal antibody against vascular endothelial growth factor or 2-methoxyestradiol but antagonized by endothelial growth factors. Cancer Res 2001;61:3369–3372.

40 Jain RK. Normalization of tumor vasculature: an emerging concept in antiangiogenic therapy. Science 2005;307:58–62.

41 Hurwitz HI, Fehrenbacher L, Novotny W et al. Bevacizumab plus irinotecan, fluorouracil, and leucovorin for metastatic colorectal cancer. N Engl J Med 2004;350:2335–2342.

42 Bedrick E, Hurwitz HI, Sarkar S et al. Post-progression therapy (PPT) effect on survival in AVF2107, a phase III trial of bevacizumab in first-line treatment of metastatic colorectal cancer (mCRC). Proc Am Soc Clin Oncol 2004;23:249a.

43 Kabbinavar F, Hurwitz HI, Fehrenbacher L et al. Phase II, randomized trial comparing bevacizumab plus fluorouracil (FU)/leucovorin (LV) with FU/LV alone in patients with metastatic colorectal cancer. J Clin Oncol 2003;21:60–65.

44 Kabbinavar F, Schulz J, McCleod M et al. Bevacizumab (Avastin), a monoclonal antibody to vascular endothelial growth factor, prolongs progression free survival in first-line colorectal cancer (CRC) in subjects who are not suitable candidates for first-line CPT-11. Proc Am Soc Clin Oncol 2004;23:249a.

45 Hurwitz HI, Fehrenbacher L, Hainsworth J et al. Bevacizumab in combination with 5-fluorouracil and leucovorin: a promising regimen for first-line metastatic colorectal cancer. Proc Gastrointest Cancer Symp 2004:182a.

46 Mitchell EP, Alberts SR, Schwartz MA et al. High-dose bevacizumab in combination with FOLFOX4 improves survival in patients with previously treated advanced colorectal cancer: results from the Eastern Cooperative Oncology Group (ECOG) study E3200. Proc Gastrointest Cancer Symp 2005.

47 Wells A. EGF receptor. Int J Biochem Cell Biol 1999;31:637–643.

48 Arteaga CL. The epidermal growth factor receptor: from mutant oncogene in nonhuman cancers to therapeutic target in human neoplasia. J Clin Oncol 2001;19(suppl 18):32S–40S.

49 Nicholson RI, Gee JM, Harper ME. EGFR and cancer prognosis. Eur J Cancer 2001;37(suppl 4):S9–S15.

50 Mendelsohn J, Baselga J. The EGF receptor family as targets for cancer therapy. Oncogene 2000;19:6550–6565.

51 Fan Z, Baselga J, Masui H et al. Antitumor effect of anti-epidermal growth factor receptor monoclonal antibodies plus cis-diamminedichloroplatinum on well established A431 cell xenografts. Cancer Res 1993;53:4637–4642.

52 Baselga J, Pfister D, Cooper MR et al. Phase I studies of anti-epidermal growth factor receptor chimeric antibody C225 alone and in combination with cisplatin. J Clin Oncol 2000;18:904–914.

53 Ciardiello F, Bianco R, Damiano V et al. Antitumor activity of sequential treatment with topotecan and anti-epidermal growth factor receptor monoclonal antibody C225. Clin Cancer Res 1999;5:909–916.

54 Prewett MC, Hooper AT, Bassi R et al. Enhanced antitumor activity of anti-epidermal growth factor receptor monoclonal antibody IMC-C225 in combination with irinotecan (CPT-11) against human colorectal tumor xenografts. Clin Cancer Res 2002;8:994–1003.

55 Saltz B, Rubin M, Hochster H et al. Cetuximab (IMC-C225) plus irinotecan (CPT-11) is active in CPT-11-refractory colorectal cancer (CRC) that expresses epidermal growth factor receptor (EGFR). Proc Am Soc Clin Oncol 2001;20:2a.

56 Cunningham D, Humblet Y, Siena S et al. Cetuximab monotherapy and cetuximab plus irinotecan-refractory metastatic colorectal cancer. N Engl J Med 2004;351:337–345.

57 Saltz LB, Meropol NJ, Loehrer PJ Sr et al. Phase II trial of cetuximab in patients with refractory colorectal cancer that expresses the epidermal growth factor receptor. J Clin Oncol 2004;22:1201–1208.

58 Folprecht G, Lutz M, Schoeffski P et al. Cetuximab/irinotecan/high-dose-5-fluorouracil/leucovorin (HD-5-FU/LV) in the first-line therapy of metastatic colorectal cancer (CRC). Proc Gastrointest Cancer Symp 2004:142.

59 Kohne CH, Schoffski P, Wilke H et al. Effective biomodulation by leucovorin of high-dose infusion fluorouracil given as a weekly 24-hour infusion: results of a randomized trial in patients with advanced colorectal cancer. J Clin Oncol 1998;16:418–426.

60 Schmoll HJ, Kohne C, Lorenz M et al. Weekly 24h infusion of high-dose (HD) 5-fluorouracil (5-FU24h) with or without folinic acid (FA) vs bolus 5-FU/FA (NCCTG/Mayo) in advanced colorectal cancer (CRC): a randomized phase III study of the EORTC Gastrointestinal Tract Cancer Cooperative Group and the AIO. J Clin Oncol 2000;19:241a.

61 de Gramont A, Louvet C, Andre T. A simplified bimonthly regimen with leucovorin and 5-fluorouracil for metastatic colorectal cancer. Proc Am Soc Clin Oncol 1997;16:287a.

62 Aranda E, Diaz-Rubio E, Cervantes A et al. Randomized trial comparing monthly low-dose leucovorin and fluorouracil bolus with weekly high-dose 48-hour continuous-infusion fluorouracil for advanced colorectal cancer: a Spanish Cooperative Group for Gastrointestinal Tumor Therapy (TTD) study. Ann Oncol 1998;9:727–731.

63 O'Dwyer PJ, Manola J, Valone FH et al. Fluorouracil modulation in colorectal cancer: lack of improvement with N-phosphonoacetyl-l-aspartic acid or oral leucovorin or interferon, but enhanced therapeutic index with weekly 24-hour infusion schedule—an Eastern Cooperative Oncology Group/Cancer and Leukemia Group B Study. J Clin Oncol 2001;19:2413–2421.

64 Caudry M, Bonnel C, Floquet A et al. A randomized study of bolus fluorouracil plus folinic acid versus 21-day fluorouracil infusion alone or in association with cyclophosphamide and mitomycin C in advanced colorectal carcinoma. Am J Clin Oncol 1995;18:118–125.

65 Erlichman C, Fine S, Wong A et al. A randomized trial of fluorouracil and folinic acid in patients with metastatic colorectal carcinoma. J Clin Oncol 1988;6:469–475.

66 Petrelli N, Douglass HO Jr, Herrera L et al. The modulation of fluorouracil with leucovorin in metastatic colorectal carcinoma: a prospective randomized phase III trial. Gastrointestinal Tumor Study Group. J Clin Oncol 1989;7:1419–1426.

67 Advanced Colorectal Cancer Meta-Analysis Project. Modulation of fluorouracil by leucovorin in patients with advanced colorectal cancer: evidence in terms of response rate. J Clin Oncol 1992;10:896–903.

Ferumoxytol as an MR imaging surrogate marker of liposomal drug deposition and longitudinal efficacy in a preclinical model of breast cancer

Manuela Ventura[1], Nicholas Bernards[1], Raquel De Souza[1†], Warren Foltz[1], Helen Lee[2†], Stephan Klinz[2†], Bart Hendriks[2†], Jonathan Fitzgerald[2†], and Jinzi Zheng[1,3]

[1]TECHNA Institute for the Advancement of Technology for Health, University Health Network, Toronto, Ontario, Canada

[2]Merrimack Pharmaceuticals, Inc., Cambridge, Massachusetts, USA

[3]Institute of Biomaterial and Biomedical Engineering, University of Toronto, Ontario, Canada

[†] Affiliation at the time of the study.

Background

Accurate identification of patients who are most likely to benefit from nanotherapies would help improving the chances of a positive therapeutic response.

Ferumoxytol (FMX), an FDA-approved iron replacement therapy, is also widely used off-label as an MRI contrast agent.

Similarities between FMX and Irinotecan liposome injection (Onivyde®, nal-IRI)

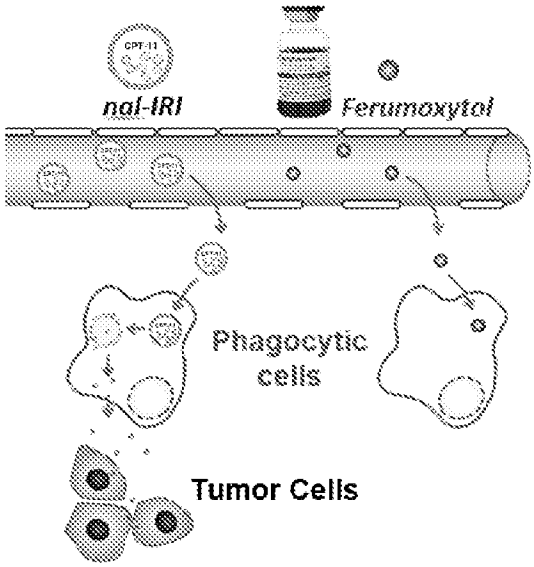

- Extended PK/Circulation
- Deposition in tumor through vasculature
- Uptake and retention by phagocytic cells and tumor cells
- Conversion of CPT-11 to SN-38 (nal-IRI only)

Aim

The aim of our study is to investigate the use of FMX as a macromolecular contrast agent to predict the efficacy of a multi-dose treatment with nal-IRI in a mouse xenograft model of breast cancer.

Methods

Mice bearing triple negative breast cancer MDA-MB-231 mammary fat pad tumors were injected with 50 mg/kg FMX and imaged on a 7T preclinical MRI, pre-contrast injection and at 4 and 24 h thereafter.

Six weekly doses of nal-IRI (20 mg/kg) were then administered, and response to treatment was monitored by caliper and MRI tumor volume measurements.

FMX tumor deposition variability, assessed by ICP-AES and MRI, was explored in SUM190, HT29, H2170 and A549 cancer models.

Agarose phantoms containing FMX-labeled J774A.1 macrophages, or corresponding concentrations of extracellular FMX, were used to explore the effect of cell bound vs. free FMX on T2 and T2* MR signal.

FMX deposition in tumors correlates with nal-IRI deposition

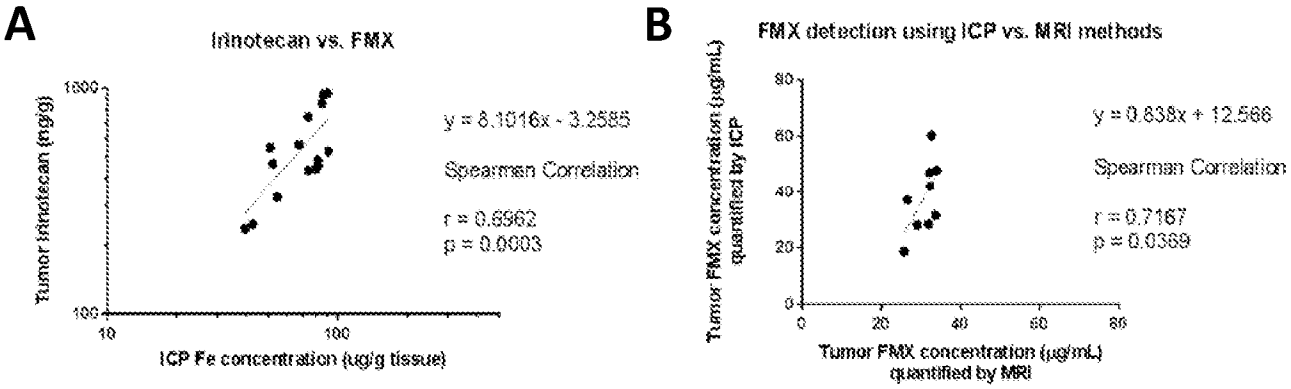

Figure 1. (A) Significant correlation between irinotecan and FMX tumor deposition, 24 h post-nal-IRI and immediately post-FMX injection, in MDA-MB-231 tumor bearing mice. This confirms the suitability of FMX as a potential tumor imaging surrogate marker for nal-IRI. **(B)** A weaker positive correlation was also found between CPT-11 tumor deposition, measured by HPLC, and FMX deposition, measured by MRI, suggesting that MR is less sensitive and less quantitative compared to *ex vivo* ICP-AES measurements of FMX concentration.

Variability of intratumoral FMX deposition

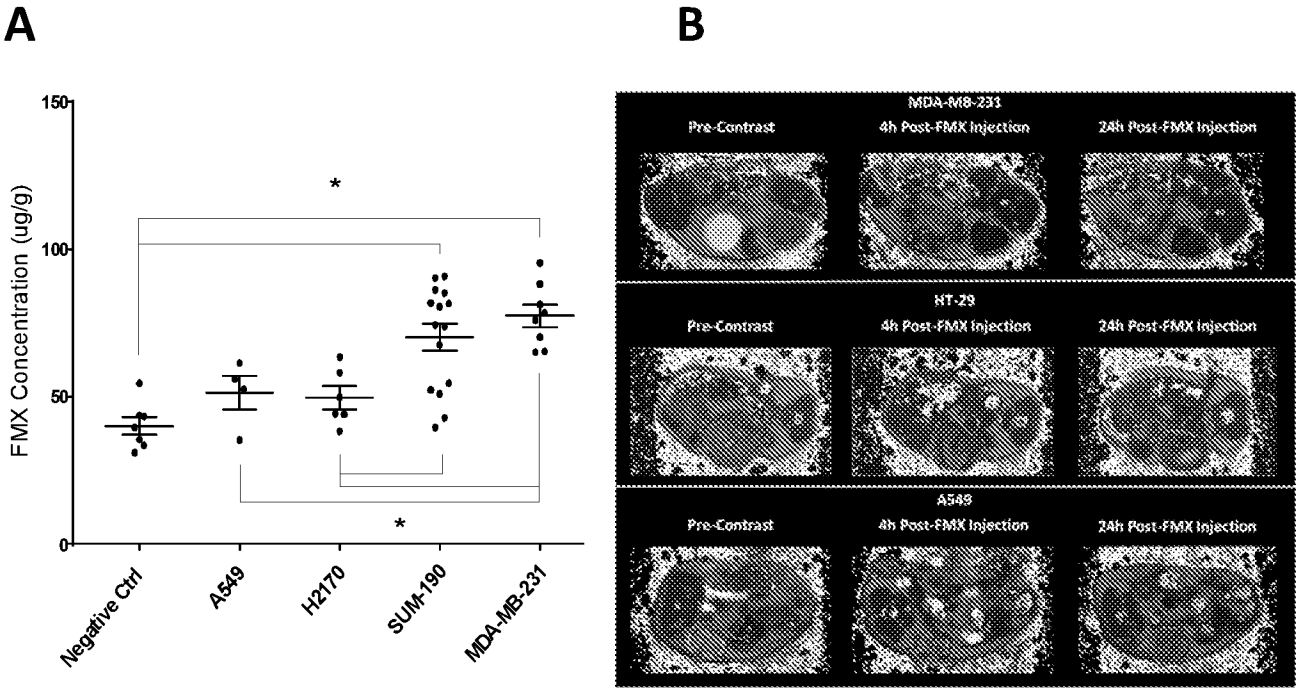

Figure 2. (A) Fe concentration measured by ICP-AES in different tumor models 24 h post FMX injection, compared to the non-FMX injected control tumors. The control group includes tumor tissue samples collected from all tumor models. The high variability in tumor uptake among different models is reflected in **(B)** T2 maps acquired on a preclinical 7T MRI, pre-FMX injection, 4 h and 24 h post-FMX injection.

R2 versus R2* imaging of FMX

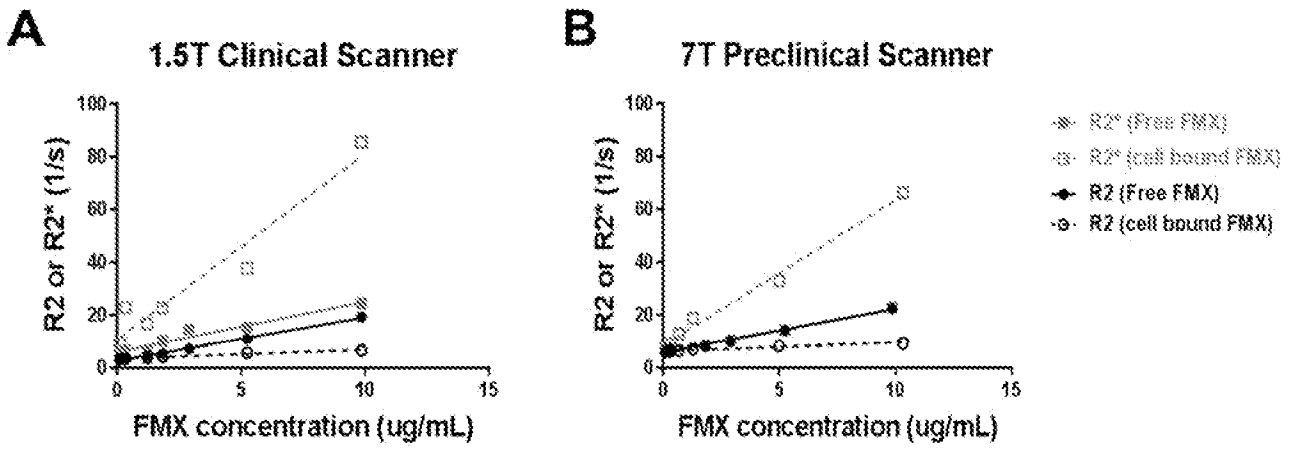

Figure 3. Illustration of the effect of the intracellular or extracellular distribution of FMX on R2 and R2* MR signal. Agarose phantoms containing FMX-labeled J774A.1 macrophage cells, or corresponding concentrations of extracellular FMX, were imaged on **(A)** a 1.5T clinical scanner (Siemens AERA) and **(B)** a 7T preclinical scanner (Bruker Biospec 70/30), showing comparable results upon signal quantification. The R2* for cell-bound FMX was approximately 3.7-fold higher than that for free FMX, whereas the R2 relaxivity for cell-bound SPIO was approximately 4.7-fold lower.

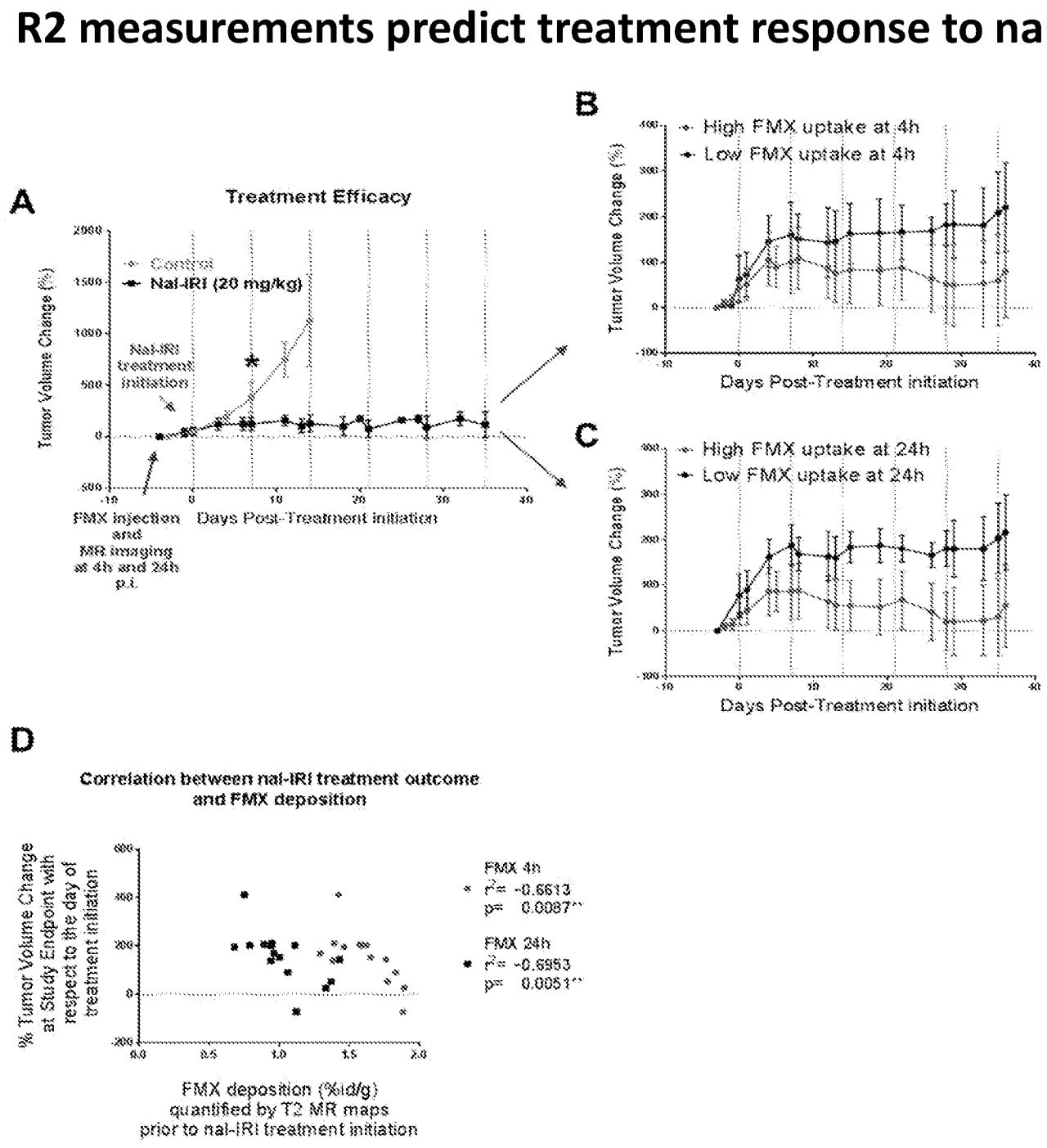

Figure 4. (A) Tumor growth curves, showed as % tumor volume change, relative to treatment day 0, for animals treated with nal-IRI or vehicle control. Vertical dashed lines indicate nal-IRI treatment administration. Animals in the treated group were further divided into two groups: (i) high FMX uptake and (ii) low FMX uptake, according to median FMX uptake values measured by R2 MRI at 4 h **(B)** and 24 h **(C)** post-FMX injection. **(D)** % tumor volume change on day 36 is shown as a function of the pretreatment FMX deposition at 4 h (red points) or 24 h (black points) On day 36 post treatment initiation (study end point), a statistically significant correlation was found between therapeutic outcome and the degree of FMX deposition quantified by T2 MRI maps prior to treatment initiation. Both the 4 h and the 24 h post-FMX injection imaging data show similar correlation to treatment outcome suggesting that both acute peak uptake and "late-stage" accumulation of FMX have predictive value for liposomal drug deposition and ultimately treatment efficacy.

Conclusions

In this study, we investigated the potential of ferumoxytol to predict the response to therapy of MDA-MB-231 triple negative breast cancer bearing mice, following a multi-dose treatment with nal-IRI.

Our results showed a positive correlation between intratumoral concentration of FMX (70.1 ± 17.6 μg/g) and irinotecan (548.1 ± 227.9 ng/g), observed at 24 h post injection.

In vivo, FMX quantification from MR T2 maps was not as sensitive in detecting small concentration changes, and more variable compared to *ex vivo* ICP measurements, although tumor FMX measurements at both 4 and 24 hours post injection strongly correlated with treatment outcomes, thus supporting the predictive potential of such imaging agent.

Acknowledgements

The authors would like to thank Maria Bisa, William Xiao and the Animal Resources Centre (ARC) staff for their technical support with animal handling and monitoring procedures, and Linyu Fan for performing ICP-AES.

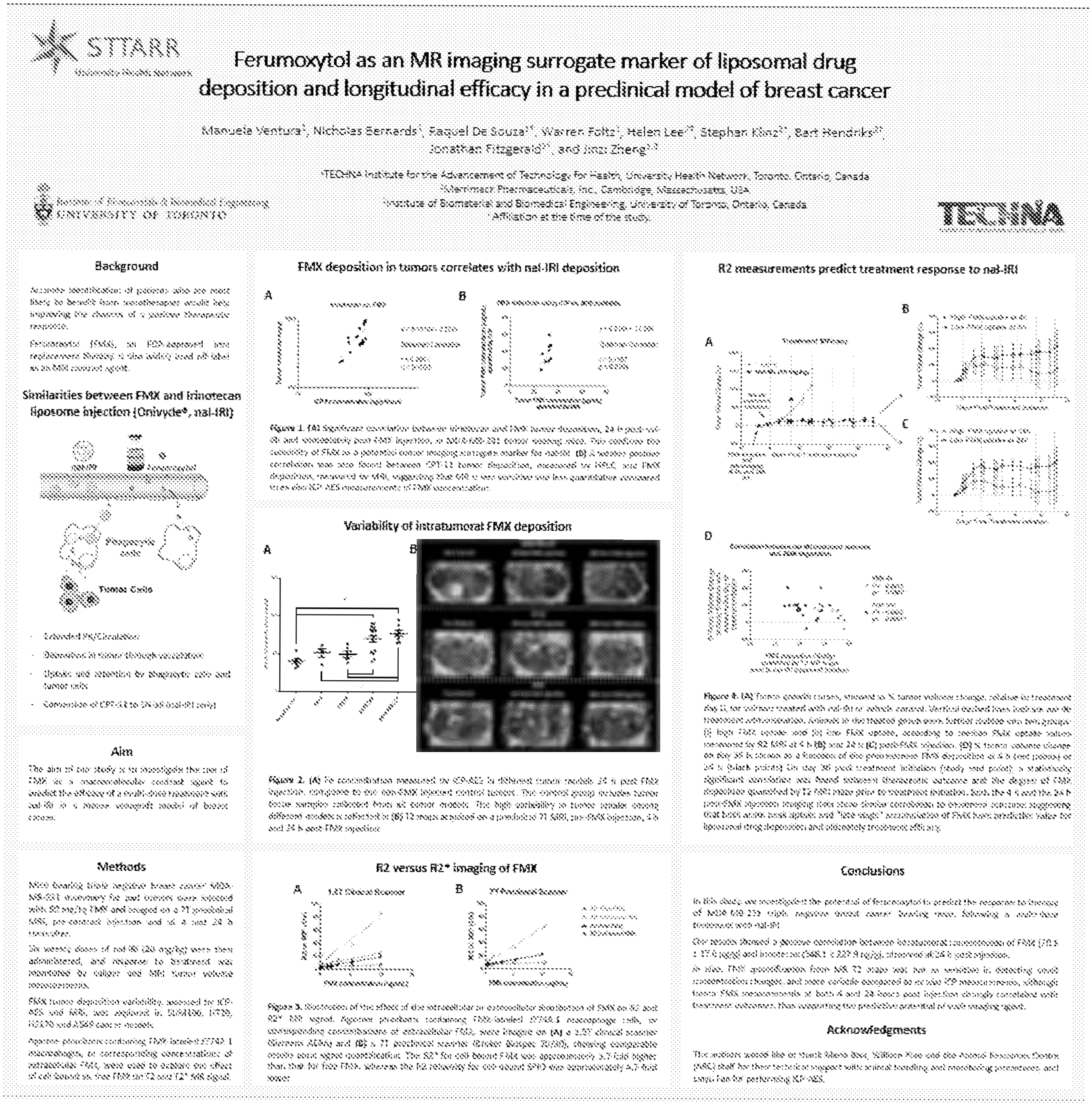
STTARR
Ferumoxytol as an MR imaging surrogate marker of liposomal drug deposition and longitudinal efficacy in a preclinical model of breast cancer
Manuela Ventura, Nicholas Bernards, Raquel De Souza, Warren Foltz, Helen Lee, Stephan Klinz, Bart Hendriks, Jonathan Fitzgerald, and Jinzi Zheng
TECHNA Institute for the Advancement of Technology for Health, University Health Network, Toronto, Ontario, Canada
Merrimack Pharmaceuticals, Inc., Cambridge, Massachusetts, USA
Institute of Biomaterials and Biomedical Engineering, University of Toronto, Ontario, Canada
Affiliation at the time of the study.
UNIVERSITY OF TORONTO
TECHNA
Background
Similarities between FMX and Irinotecan liposome injection (Onivyde®, nal-IRI)
Tumor Cells
Aim
Methods
FMX deposition in tumors correlates with nal-IRI deposition
A
B
Variability of intratumoral FMX deposition
A
B
R2 versus R2* imaging of FMX
A
B
R2 measurements predict treatment response to nal-IRI
A
B
C
D
Conclusions
Acknowledgements

Phase I Study of Low-Dose Suramin as a Chemosensitizer in Patients with Advanced Non-Small Cell Lung Cancer[1]

Miguel A. Villalona-Calero,[2]
M. Guillaume Wientjes, Gregory A. Otterson,
Steven Kanter, Donn Young, Anthony J. Murgo,
Beth Fischer, Carrie DeHoff, Danny Chen,
Teng-Kuang Yeh, SaeHeum Song,
Michael Grever, and Jessie L-S. Au

Department of Medicine and College of Pharmacy, The Ohio State University, The Arthur G. James Cancer Hospital & Richard J. Solove Research Institute, Columbus, Ohio 43210-1240, and The National Cancer Institute, Bethesda, Maryland 20892

ABSTRACT

Purpose: **Our preclinical studies have shown that acidic and basic fibroblastic growth factors confer broad spectrum chemoresistance and that low concentrations (10–50 μM) of suramin, a nonspecific fibroblastic growth factor inhibitor, enhance the antitumor activity of paclitaxel *in vivo*. The present Phase I study evaluated low-dose suramin in combination with paclitaxel/carboplatin in advanced non-small cell lung cancer patients.**

Experimental Design: **Patients received suramin followed by paclitaxel (175–200 mg/m^2) and carboplatin area under the concentration-time curve of 6 mg/ml/min, every 3 weeks. The initial suramin dose for the first cycle was 240 mg/m^2, and the doses for subsequent cycles were calculated based on the 72-h pretreatment plasma concentrations. The recommended suramin dose would yield plasma concentrations of 10–20 μM at 48 h in ≥5 of 6 patients.**

Results: **Fifteen patients (11 stage IV, 4 stage IIIB, 9 chemonaive, and 6 previously treated) received 85 courses. The most common toxicities were neutropenia, nausea/vomiting, malaise/fatigue, and peripheral neuropathy. No treatment-related hospitalizations, adrenal dysfunction, or episodes of sepsis occurred. The initial suramin dose resulted in the targeted concentrations of 10–20 μM at 48 h in 5 of the first 6 patients treated but also resulted in peak concentrations > 50 μM in all patients. Dividing the suramin dose to be administered in two doses, 24 h apart, yielded the target concentrations and avoided undesirable peak concentrations. Discernable antitumor activity occurred in 7 of 10 patients with measurable disease, including 2 with prior chemotherapy. The median time to tumor progression is 8.5 months (range, 3–27+ months) for 12 evaluable patients.**

Conclusions: **Low-dose suramin does not increase the toxicity of paclitaxel/carboplatin combination. The suramin dose can be calculated based on clinical parameters. Because of the preliminary antitumor activity observed, efficacy studies in chemonaive and chemorefractory patients are under way.**

INTRODUCTION

The polysulfonated naphtylurea suramin, an agent originally developed for the treatment of parasitic infestations (1–4), has long been a subject of interest as a candidate antitumor agent. Suramin inhibits reverse transcriptase in RNA tumor viruses (5), mitochondrial oxidative enzymes (6, 7), and the binding of growth factors to their respective receptors. The affected growth factors include platelet derived growth factor (8), epidermal growth factor (9, 10), vascular endothelial growth factor (11), transforming growth factor β (12), insulin-like growth factor 1 (13, 14), and FGFs[3] (15–18). Suramin also inhibits the activity of protein kinase C isoforms (19).

Suramin has shown concentration-dependent antiproliferative activity *in vitro* against cultured tumor cells and explanted human tumor specimens including colon, endometrium, kidney, non-small cell lung, and ovarian carcinoma, as well as malignant glioma, melanoma, and mesothelioma (20–23). However, at concentrations ≤ 50 μM, minimal antiproliferative activity was observed and several studies have shown growth stimulation of some tumor cells at these low suramin concentrations (22–26).

On the basis of these earlier preclinical findings, most studies evaluating suramin as a cytotoxic agent in humans have targeted concentrations of ≥200 μM. At these doses, suramin appears to have modest to moderate antitumor activity in hormone refractory prostate carcinoma (27–30), marginal activity in recurrent high-grade gliomas (31), and no or insignificant activity in non-small cell lung (32), breast (32), colorectal, (33) and renal carcinomas (34). Although careful clinical study has led to a strategy to circumvent its seemingly unpredictable pharmacokinetic behavior (35–37), a protean spectrum of toxicities including polyneuropathy (38), adrenal insufficiency (39), skin and appendages alterations (40–43), coagulopathy

Received 1/21/03; revised 4/23/03; accepted 4/26/03.
The costs of publication of this article were defrayed in part by the payment of page charges. This article must therefore be hereby marked *advertisement* in accordance with 18 U.S.C. Section 1734 solely to indicate this fact.
[1] This study was supported, in part, by National Cancer Institute, Department of Health and Human Services Research Grants R37CA49816, R21CA91547, and U01CA76576. Patients were treated at a General Clinical Research Center supported by NIH, Department of Health and Human Services Gram M01-RR00034.
[2] To whom requests for reprints should be addressed, at Arthur G. James Cancer Hospital, Ohio State University, B406 Starling-Loving Hall, 320 West 10th Avenue, Columbus, OH 43210-1240. Phone: (614) 293-7511; Fax: (614) 293-7529; E-mail, villalona-1@medctr.osu.edu.

[3] The abbreviations used are: FGF, fibroblast growth factor; ACTH, adrenocorticotropin hormone; AUC, area-under plasma concentration-time curve; DLT, dose-limiting toxicity; NSCLC, non-small cell lung cancer; PR, partial response; TTP, time to tumor progression.

(44, 45), and renal insufficiency (46) has limited its development as an anticancer agent. The onset of severe neurological toxicity (sensory motor axonal and progressively disabling demyelinating neuropathy) is generally associated with steady-state plasma concentrations of ≥275 μM (47–49).

In contrast to the high concentrations required for antiproliferative activity, inhibition of growth factor binding to receptors by suramin occurs at substantially lower concentrations. For example, basic FGF, a growth factor that has been implicated in neovascularization and tumor growth (18, 50), is inhibited at suramin concentrations <50 μM (51).

An *et al.* (51, 52) recently reported that elevated levels of acidic FGF and basic FGF in solid and metastatic tumors confer broad spectrum resistance to chemotherapy drugs with diverse structures and mechanisms of action and that low concentrations of suramin that are devoid of antitumor activity reverse the FGF-induced chemoresistance *in vitro*. In addition, in mice with well-established lung metastases, low and nontoxic doses of suramin (10 mg/kg, twice weekly × 3 weeks), yielding plasma concentrations of between 10 and 20 μM, enhanced the antitumor effect of paclitaxel; the combination resulted in tumor eradication in 42% of animals (none in the single agent paclitaxel group), a 9-fold greater reduction of the density of nonapoptotic cells and a 30% increase in the apoptotic cell fraction (53).

On the basis of the synergy of paclitaxel and low-dose suramin demonstrated in the preclinical studies and the observation that low-dose suramin had no or minimal toxicity in patients, we designed the present Phase I trial of low-dose suramin in combination with paclitaxel/carboplatin in patients with advanced NSCLC. The principal objectives of the study were to: (*a*) determine the dose of suramin that, when given in combination with commonly used doses of the paclitaxel/carboplatin regimen, would result in plasma concentrations of 10–20 μM (14–29 μg/ml) at 72 h (later adjusted to 48 h); (*b*) characterize the principal toxicities of the combination; and (*c*) seek preliminary evidence of antitumor activity.

MATERIALS AND METHODS

Eligibility. Patients with histologically confirmed stage IV NSCLC or patients with stage IIIB disease (not amenable to curative-intent radiation and chemotherapy) were eligible for this study. Eligibility criteria also included: (*a*) age, ≥18 years; (*b*) Eastern Cooperative Oncology Group performance status of 0–2 (ambulatory and capable of self care); (*c*) a life expectancy ≥3 months; (*d*) treatment with no more than one prior chemotherapy regimen; (*e*) no cytotoxic chemotherapy agents for at least 28 days; (*f*) adequate hematopoietic (WBC count ≥ 3,000/μl, absolute neutrophil count of ≥1,500/μl, platelets ≥ 100,000/μl, and hemoglobin level of ≥9.0 g/dl); hepatic (total serum bilirubin level <1.5 times institutional upper normal limits, aspartate amino transaminase and alanine amino transaminase <2.5 times upper normal limits); and renal functions (serum creatinine <1.5 mg/dl or calculated creatinine clearance ≥50 ml/min); (*g*) no brain metastases or leptomeningeal disease, unless the lesions had been previously irradiated, not being treated with corticosteroids, and were stable and asymptomatic; (*h*) no history of myocardial infarction within the previous 6 months, congestive heart failure requiring therapy, or unstable angina; (*i*) no known active serious infectious process or current treatment for HIV type 1 infection; (*j*) no uncontrolled diabetes mellitus; (*k*) no history of hypersensitivity to Cremophor EL; (*l*) baseline-corrected serum calcium of ≤11.5 mg/dl; and (*m*) no ≥grade 2 neuropathy. The treatment protocol and informed consent were approved by the Cancer Therapy Evaluation Program at the National Cancer Institute and the institutional review board at The Ohio State University. Patients gave written informed consent according to federal and institutional guidelines before treatment.

Dosage and Dose Escalation. The carboplatin dose was calculated using the Calvert equation (54) to yield an AUC of 6 mg/ml/min and remained fixed throughout the study. The starting dose of paclitaxel was 175 mg/m^2. The starting doses of paclitaxel and carboplatin were considered to be the minimal effective doses for the combination in the treatment of NSCLC. The initial suramin dose of suramin was 240 mg/m^2 given on day 1 and was calculated to yield target concentrations of 10–20 μM at 72 h (later changed to 48 h) after infusion; these target concentrations were selected based on the preclinical data (53). Treatment was repeated every 3 weeks. Subsequent treatment doses for paclitaxel and carboplatin were based on toxicity encountered during the prior cycle. Subsequent treatment doses of suramin were modified based on the residual suramin plasma concentrations at 72 h before treatment. Intrasubject dose escalation for paclitaxel and carboplatin was not permitted.

Modification of the starting doses of suramin in subsequent cohorts of at least three patients was to be performed if pharmacokinetic analyses of suramin plasma concentrations were off-target in ≥2 of the first 6 patients treated. The dose of paclitaxel was to be increased to 200 mg/m^2 in a subsequent cohort of at least 3 patients, once the target dose of suramin was defined, as long as DLTs did not occur in ≥2 of the first 6 patients during their first course of treatment. Paclitaxel was to be reduced to 135 mg/m^2 if treatment resulted in DLT in ≥2 of these patients.

Toxicities were graded according to the National Cancer Institute Common Toxicity Criteria version 2.0 (55). DLT was defined as one of the following: (*a*) an absolute neutrophil count <500/μl for >5 days or associated with any grade 2 fever (temperature, ≥38.5°C); (*b*) a platelet count <10,000/μl; (*c*) grade 3 nonhematological toxicity (including diarrhea, nausea, and vomiting) that resulted in interruption of treatment for >2 weeks; or (*d*) any grade 4 nonhematological toxicity. The recommended dose level was defined as the suramin dose that in combination with the highest tolerated dose of paclitaxel and carboplatin at an AUC of 6 resulted in concentrations of 10–20 μM at 72 h (later changed to 48 h) after infusion.

Drug Administration. Suramin was supplied by the National Cancer Institute, Division of Cancer Treatment and Diagnosis, as sterile, 600-mg, 10-ml vials. The vials were reconstituted with sterile water, resulting in a 100 mg/ml solution. The desired dose was additionally diluted in 0.9% sodium chloride or 5% dextrose in water. Commercially available paclitaxel (Taxol; Bristol Myers Squibb) was obtained from the hospital pharmacy in 30 (5 ml), 100 (16.7 ml), and 300 mg (50 ml) vials and was prepared according to the manufacturer's directions in glass or polyolefin containers diluted in 500–1000

ml of 5% dextrose or 0.9% sodium chloride. Commercially available carboplatin (Paraplatin; Bristol Myers Squibb) was obtained from the hospital pharmacy as sterile single-dose vials containing 50, 150, and 450 mg. The content of each vial was reconstituted with either sterile water, 5% dextrose in water, or 0.9% sodium chloride to produce concentrations of 10 mg/ml.

All three drugs were administered by i.v. infusion, using an infusion pump. Suramin was administered over 30 min, followed by paclitaxel over 3 h, and carboplatin over 1 h. Standard premedication included oral dexamethasone (20 mg 12 and 6 h before paclitaxel), diphenhydramine (50 mg i.v.), famotidine (20 mg i.v.), and ondasetron 16 mg p.o. given 30 min before paclitaxel.

Pretreatment Assessment and Follow-Up Studies. Histories, physical examinations, and routine laboratory studies were performed pretreatment and preceding each course of treatment. Routine laboratory studies included serum electrolytes, chemistries, and complete blood cell counts with differential white cell counts. Complete blood cell counts were also performed weekly, and blood clotting times, urinalysis, pregnancy tests (when indicated), chest radiographies, and electrocardiograms were performed before initiating treatment. If patients developed toxicity manifested by grade 3–4 abnormalities in hematological or biochemical laboratory parameters, the tests were repeated immediately and then daily until the toxicity resolved. Tumors were measured after every other course, and treatment was continued in the absence of progressive disease or intolerable toxicity. The RECIST criteria for response evaluation (56) was used to define objective responses, although measurable disease was not required to be eligible to participate in this trial. A complete response was defined as the disappearance of all target and nontarget lesions. A PR required at least a 30% reduction in the sum of the longest diameter of target lesions compared with pretreatment measures, and progressive disease required an increase of at least 20% in the sum of the longest diameter of target lesions. Objective responses required confirmation by a subsequent response evaluation separated by at least 4 weeks.

To evaluate if potential alterations in the adrenal axis are induced by the low dose suramin used in this study, as has been previously reported for higher doses (39), ACTH stimulation tests were performed pretreatment and after every three courses for patients remaining on treatment. Patients received 0.25 mg $ACTH_{1-24}$ (cosyntropin) i.m. or i.v., and samples for cortisol levels were obtained immediately before cosyntropin injection and 30 min after injection. To avoid potential interference with the test results caused by the oral dexamethasone premedication required before paclitaxel, ACTH stimulation tests were performed on day 15 of the cycle (*i.e.*, 2 weeks after dexamethasone).

Blood Sampling and Analysis. Blood samples were obtained from a site contralateral to the drug infusion during the first course of treatment. On treatment days 1 and 2, plasma samples (10 ml) were collected in heparin-containing vacutainer glass tubes before suramin treatment and at 1.5, 2.5, 3.5, 4, 4.5, 6, 9, 12, 15, 24, 48, and 72 h from the beginning of the suramin infusion. In addition, for subsequent courses, samples were obtained 72 h before treatment (to evaluate residual suramin concentrations), 1 h before the start of the suramin infusion, at the end of paclitaxel infusion, at the end of carboplatin infusion, as well as at 24, 48, and 72 h from the beginning of the suramin infusion. Plasma concentrations of suramin were determined using high performance liquid chromatography, as described previously (57).

Table 1 Patient characteristics

	No. of patients
Patients treated/toxicity evaluable	15/15
Activity evaluable	12
Male	10
Female	5
Median age (range), yr	62 (42–77)
Eastern Cooperative Oncology Group performance status:	
0	4
1	8
2	3
Stage	
IIIB (malignant pleural effusion)	4
IV	11
Previous radiotherapy	5
Previous chemotherapy	
None	9
One regimen	6

RESULTS

General. Fifteen patients received 85 courses (median number of courses, 6; range, 1–10) of suramin in combination with paclitaxel and carboplatin. Patient characteristics are listed in Table 1. Nine patients had no prior chemotherapy, whereas 6 patients had received one prior chemotherapy regimen. Five patients had received prior radiation treatment, including a patient previously irradiated for brain metastases. All patients were evaluable for toxicity. Three patients were taken off study early during the first course (within the first week); one individual because of a severe reaction to paclitaxel (did not receive carboplatin), a second subject because of spinal cord compression requiring immediate spine irradiation, and the third because of a revised pathological diagnosis to small cell lung cancer.

The number of new and total patients, courses, and rates of DLTs, per dose level, are listed in Table 2. The starting doses were suramin 240 mg/m^2, paclitaxel 175 mg/m^2, and carboplatin at an AUC of 6. At this dose, only 1 of the first 6 patients developed DLT (severe hypersensitivity reaction to paclitaxel). As described below, the final dose of suramin was calculated based on clinical parameters and was administered in two doses 24 h apart. At this new suramin dosing schedule, no DLTs were observed in the next 6 patients, including the 3 patients that received 200 mg/m^2 paclitaxel.

Pharmacokinetics of Low-Dose Suramin. Fig. 1 shows the plasma concentration-time profiles of suramin during the first cycle of treatment. Table 3 depicts the suramin plasma concentrations at the target time points. The target suramin concentration range of between 10 and 20 μM at 72 h was attained in 5 of 6 patients (range, 10–16 μM). However, peak concentrations of suramin attained at 1.5 h exceeded 50 μM in all patients (range, 56–97 μM), and concentrations attained immediately after paclitaxel infusion exceeded 50 μM in 5 of 6 patients (11 of 19 treatment courses).

Because of concerns of possible interference with the an-

Table 2 Dose escalation scheme

Suramin initial (mg/m²)[a]	Dose level paclitaxel (mg/m²)	Carboplatin AUC (mg/ml/min)[a]	No. of patients			Total courses	New patients with DLT/ total new patients[b]
			New	Reduced to this dose	Total		
240 d1	175	6	6	0	6	19	1/6
160 d1, 80 d2	175	6	3	6	9	38	0/3
160 d1, 80 d2	200	6	3	0	3	15	0/3
Individualized	200	6	3	0	3	13	0/3
Total			15			85	

[a] Suramin doses for second and subsequent courses were calculated based on the 72-h pretreatment plasma concentrations.
[b] First or second course.

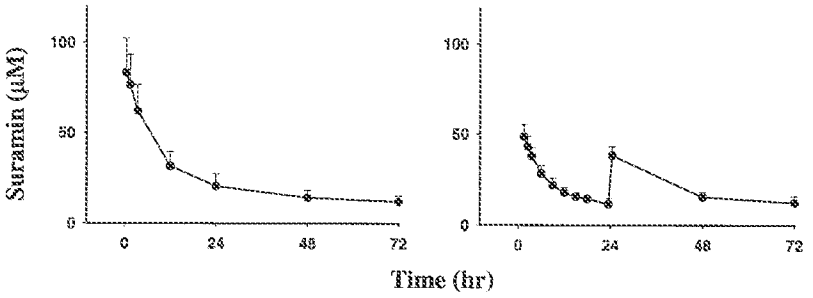

Fig. 1 Suramin plasma concentration-time profiles. Suramin was given by single dose (*left panel*, total of 19 treatments) or by split doses (*right panel*, total of 66 treatments) as described in "Materials and Methods" and "Results." Data are mean ± SD. Data points are connected by *straight lines*.

itumor effect of paclitaxel because of potential cell cycle arrest by >50 μM suramin, the treatment protocol was amended to split the administration of suramin during the first and subsequent treatment cycles, for current and subsequent patients, into two separate doses given 24 h apart; two-thirds of the dose on day 1 (before paclitaxel), and the remaining one-third on day 2 (24 h from first infusion). In addition, we found that the AUCs for paclitaxel and carboplatin attained in the first 48 h constituted >92 and >99% of their respective total AUCs (unpublished data). Hence, the doses of suramin for all subsequent and new treatments were revised to attain the target concentrations of 10–20 μM at 48 h instead of 72 h.

This new suramin dosing schedule yielded the targeted suramin concentrations of 10–20 μM at 48 h in all 66 treatments. The peak suramin concentrations exceeded 50 μM in only 2 of 6 patients (55 and 59 μM); this occurred only during the first treatment cycle that used a higher loading suramin dose and did not occur during the subsequent cycles that used lower suramin doses.

Because of its slow elimination, significant residual plasma concentrations deriving from the previous suramin dose were detected 72 h before the administration of the subsequent doses in all patients (Table 3). Hence, it was necessary to adjust the suramin dose for the subsequent treatments and to maintain the plasma levels within the narrow ranges required by this study. Furthermore, to eliminate the need of real-time pharmacokinetics in future studies, we derived an empirical equation to calculate the suramin dose.[4] This equation, depicted below, was derived using population pharmacokinetic analysis of the data of the first 12 patients and was tested in three additional patients: suramin dose in mg = FACTOR × (absolute value of body surface area, without units)^2. The value of the FACTOR was calculated based on the target suramin concentration (set at 15 μM at 48 h) and the volume of distribution and elimination rate constant of suramin. FACTOR equaled 110 divided by ($e^{-k} \times t$). k is the elimination rate constant and t is time. The results in the first 12 patients showed a 15% lower elimination rate constant in women ($n = 3$) compared with men ($n = 9$; 0.0022 h^{-1} *versus* 0.0026 h^{-1}). Accordingly, the numerical values of FACTOR were lower for women.

For the first dose, FACTOR was calculated to be 125 for males and 123 for females. For the ease of dose calculation, the value of FACTOR was set at 125 for both genders. To attain the same target concentrations of 15 μM at 48 h during subsequent treatment cycles, the dose administered during a subsequent cycle should replace the fraction of the dose that was eliminated during the interval between treatments. Hence, the value of FACTOR equaled the product of 125 × BSA^2 × ($1 - e^{-k} \times t$). Note that in contrast to the first cycle where t equaled 48 h, the value of t during subsequent cycles is a variable that equals the time lapsed since the previous cycle.

We evaluated the above suramin dose calculation method in 3 additional patients. The results showed that in all 13 treatments, the target concentration range of 10–20 μM at 48 h was attained, and the peak suramin concentration did not exceed 50 μM (Table 3).

Hematological Toxicity. Table 4 lists the number of courses associated with neutropenia, anemia, and thrombocytopenia. Overall, moderate to severe neutropenia was frequent. Grade 3 and 4 neutropenia occurred in 31 (36%) and 30 courses (35%), respectively. However, grade 4 neutropenia was in all

[4] D. Chen, S. Song, J. L.-S. Au, T. K. Yeh, M. Villalona-Calero, G. A. Otterson, S. Kanter, A. J. Murgo, M. Grever, and M. G. Wientjes. Pharmacokinetics of low dose suramin as a chemosensitizer in patients, manuscript in preparation.

Table 3 Plasma concentrations of suramin at target time points

Patient ID[a]	No. of treatments	Suramin (μM)[a] At 1.5 h after initiating suramin infusion	Immediately after paclitaxel infusion	At 48 h after initiating suramin infusion	At 72 h after initiating suramin infusion	At 72 h before the next suramin treatment
Single dose						
1	1[b]	89.2	77.4	18.6	15.6	NM[c]
2	5	97.2	40.9–77.5	19.3	9.9–15.0	2.0–5.0
3	5	64.0	40.5–63.2	11.4	9.4–13.1	3.0–4.5
4	1[b]	55.7	46.9	9.9	8.3	2.0
5	4	87.4	54.6–76.2	11.0	10.2–13.2	3.2–5.1
6	3	67.3	45.1–52.0	15.2	13.9–19.1	5.0–6.0
Split dose						
2	1	NM[c]	31.3	13.7	NM	NM
3	5	NM	24.0–32.3	12.4–17.7	11.5–13.0	4.8–6.7
5	6	NM	33.2–48.2	13.9–17.6	13.6–14.4	2.9–5.0
6	7	NM	27.1–37.1	14.4–20.4	13.3–14.7	5.0–6.0
7	4	55.5	30.4–42.4	14.7–18.1	NM	3.8–6.7
8	10	59.9	23.4–45.3	10.4–20.7	7.8–14.9	4.6–7.9
9	4	48.7	29.3–38.8	14.7–15.5	12.4	2.7–4.0
10	4	43.6	28.6–37.8	15.3–17.8	12.6–15.4	3.7–5.4
11	6	48.4	27.7–38.2	13.5–17.5	10.7–14.8	2.7–4.6
12	6	48.3	28.8–39.0	10.3–21.3	10.2–18.7	3.4–6.4
13	6	37.0	21.5–28.9	10.2–13.9	7.3–9.5	2.4–3.6
14	6	49.5	22.0–37.3	12.9–15.6	10.3–13.9	3.5–5.4
15	1[b]	47.9	36.0	19.4	16.3	NM

[a] Plasma samples were obtained on various times during first and subsequent treatment courses. Some samples (*e.g.*, 1.5-h postsuramin) were obtained only during the first treatment for the single dose schedule, whereas the other samples (*e.g.*, postpaclitaxel and 72-h postsuramin) were obtained during some or all treatments. The 48-h postsuramin samples were obtained during the first treatment in the single dose schedule and during all treatments in the split dose schedule. For the time points where samples were obtained during multiple treatments, the ranges of concentrations attained in different treatments are shown.

[b] Patients 1, 4, and 15 received only 1 treatment.

[c] NM, not measured.

Table 4 Toxicities of low-dose suramin with paclitaxel/carboplatin

Toxicity[a]	No. of courses with grade 0	1	2	3	4
Hematologic					
Neutropenia[b]	14		10	31	30
Anemia[b]	66		16	3	0
Thrombocytopenia	60	12	7	6	0
Non-hematologic					
Nausea/vomiting	26	36	22	1	0
Asthenia/fatigue	21	19	32	13	
Peripheral neuropathy	57	19	8	1	
Myalgias/arthralgias	33	47	5	0	
Hypersensitivity/rash	63	15	6	1	0
Diarrhea	70	14	0	1	0

[a] Toxicities are reported for all courses.

[b] Grade 1 neutropenia (absolute neutrophil count, 1500–1999/ml) and grade 1 anemia (hemaglobin, 10–11.9 g/dl) are not reported because they were permitted at study entry and re-treatment.

instances of short duration (<5 days) and never associated with fever. There were no episodes of grade 4 anemia or thrombocytopenia, and three and six courses were associated with grade 3 anemia and thrombocytopenia, respectively. These episodes were seldom clinically significant, requiring platelets and RBC transfusions in only two and one courses, respectively. No dose delays attributable to neutropenia or anemia occurred, and only 2 patients (a total of three courses) required dose delays because of thrombocytopenia. Overall, the observed hematological toxicities appeared no different from those expected from the paclitaxel/carboplatin combination.

Nonhematological Toxicity. The principal nonhematological toxicities of the combination are listed according to severity in Table 4. The most common nonhematological effects were nausea, vomiting, asthenia (fatigue, malaise), peripheral neuropathy, myalgias/arthralgias, hypersensitivity, and diarrhea.

Nausea and/or vomiting occurred frequently. However, these effects were generally mild to moderate; 36 (42%), 22 (26%), and 1 (1%) courses were associated with grades 1, 2, or 3 nausea and/or vomiting, respectively. All patients received prophylactic antiemetic treatment p.o. with a 5HT3 serotonin antagonist. Asthenia/fatigue/malaise were reported by 14 patients during 64 treatment courses. Although the contribution of therapy to this constellation of symptoms is hard to establish in patients with advanced malignancies, the transiency of the highest grade of these symptoms (*i.e.*, improving during the third week of each cycle) and its association with higher cumulative doses (10 of 13 episodes of grade 3 toxicity during a third or later course) indicate a possible relationship.

Neuropathy was generally mild to moderate, with grade 3 symptoms occurring in only 1 patient that developed spinal cord compression from metastatic disease to the spine, within 2 days after receiving the first course of treatment. Five of eight epi-

Table 5 Antineoplastic Activity

Dose level paclitaxel/carboplatin (mg/m^2/d)/ (AUC, mg/ml/min)	No. of courses	Stage	Metastatic sites	Prior therapy	Best response[a]	Time to tumor progression (mo)
175/6	6	IIIB	Pleura	Pleurodesis/cisplatin-XRT	SD (NM)	>27
	10	IV	Adrenal glands/mediastinum/ paraspinal muscle	Lobectomy	PR	18
	10	IV	Pericardium, lungs, bones	None	PR	8
	10	IV	Chest wall/mediastinum	None	PR	10
	4	IIIB	Mediastinum	None	PR	7.5
	6	IIIB	Pleura	None	SD (NM)	13
200/6	10	IV	Liver/bones	Paclitaxel/oxaliplatin	MR	9
	4	IV	Sternal mass/multiple lungs	XRT/cisplatin; paclitaxel/ carboplatin	PR	3
	4	IV	Lungs multiple/brain	Lobectomy/brain XRT	SD	5
	6	IV	Pleura/multiple lungs	Lobectomy/XRT; Wedge resection	SD	10
	6	IIIB	Pleura/lungs (two masses)	None	PR	7
	6	IV	Lungs multiple/liver	XRT, vinorelbine	SD	6

[a] XRT, radiation; PD, progressive disease; SD, stable disease; MR, minor response (15%); NM, nonmeasurable.

sodes of grade 2 toxicity occurred after three cycles of treatment with the combination and were characterized by painful dysesthesias of upper or lower extremities (five episodes) or decreases in motor strength in lower extremities (three episodes). Overall, these effects appeared no different from those expected from the paclitaxel/carboplatin combination. Similarly, myalgias and arthralgias commonly associated with paclitaxel were observed in 52 treatment courses.

Hypersensitivity reactions were observed during 22 courses. The most severe reaction occurred in a 67-year-old female with NSCLC metastatic to the mediastinum, bones, and adrenal gland, who had previously received treatment with paclitaxel (four courses) but had no history of idiosyncratic reaction to this agent. The patient had known coronary artery disease. Two and one-half hours into the paclitaxel infusion, the patient developed restlessness and some respiratory wheezing, which initially cleared spontaneously, allowing the paclitaxel infusion to finish. However, respiratory distress and loud wheezes, as well as chest discomfort, confusion, and increases in blood pressure, developed at the end of the infusion. The symptoms improved with sublingual nitroglycerine, i.v. hydrocortisone, and diphenhydramine. The confusion resolved the following morning. Because of safety concerns, the patient was removed from the trial, and a rechallenge with paclitaxel was not performed. Other episodes of hypersensitivity were mild and characterized by fascial flushing and/or erythematous rashes in face and upper extremities, which resolved without therapy. Mild to moderate nonhematological toxicities observed also included diarrhea, mucositis, and alopecia.

No clinical symptoms indicative of adrenal insufficiency were noted. In addition, ACTH stimulation tests were performed pretreatment in all patients, during course 3 in 10 patients, during course 6 in 7 patients, and in 2 subjects during a ninth or later course of treatment. No significant differences were observed between changes in cortisol levels after ACTH at baseline (mean ± SD = 12.9 ± 4.4 μg/dl) and after three cycles (11.1 ± 3.6; $P = 0.33$, paired t test) or between baseline and six cycles (10.6 ± 5.9) of treatment ($P = 0.30$).

Antitumor Activity. Relevant details pertaining to the antitumor effects of the combination in all 15 patients who participated in the study are depicted in Table 5. Twelve patients are evaluable for antitumor activity. Among these 12 patients, 10 had measurable disease and 2 had no measurable disease (metastatic disease to pleura). However, TTP data are available for all 12 patients. The remaining 3 nonevaluable patients were either withdrawn from the study within the first few days (severe reaction to paclitaxel in one patient and need for emergency radiation in the other) or were disqualified (1 patient) because of a revised pathological diagnosis from NSCLC to small cell lung cancer. Treatment in the latter patient was changed after the second course to a more conventional small cell lung cancer regimen (*i.e.*, etoposide and cisplatin), resulting in a complete response to treatment.

Seven of 10 patients with measurable disease experienced discernable antitumor activity. These include 6 patients who met the definition of PR as prospectively defined in this trial (RECIST Criteria). One additional patient, who progressed after two courses of paclitaxel/oxaliplatin and had metastases to liver and bones, experienced a 15% overall decrease in the sum of the longest diameter of measurable tumoral lesions (liver and lung) after eight courses of therapy. Tumor progression was demonstrated after two additional courses (overall TTP, 9 months). The 6 patients with PR included a previously surgically resected patient who develop biopsy proven recurrence to the adrenal glands, mediastinum, and paraspinal muscles. The treatment in this patient was discontinued after 10 cycles to receive radiation to the paraspinal muscle area, which was the only positron emission tomography avid and biopsy proven area of residual disease (adrenal gland was negative on rebiopsy) after treatment. Tumor progression (by positron emission tomography) did not occur until 18 months from initiation of the suramin/paclitaxel/carboplatin treatment. For all 12 evaluable patients, the median time to tumor progression is 8.5 months, and 1 patient (no measurable disease) does not have evidence of tumor after 27+ months follow-up.

DISCUSSION

The severity of the toxicities observed with suramin at the high concentrations required for antitumor activity has limited the development of this drug as a cytotoxic agent. The present study represents a novel approach to use low concentrations of suramin as a chemosensitizer. This is based on the preclinical observation that low-dose suramin, presumably by reversing the FGF-induced chemoresistance, potentiates the antitumor activity of chemotherapy in human xenograft tumors in mice (48–50).

To simulate the preclinical conditions, we targeted a narrow range for the trough and peak concentrations of suramin (10–50 μM), instead of the maximally tolerated doses typically targeted in Phase I trials. The results of this study show that at the range of targeted concentrations, low-dose suramin did not add to the toxicity profile of the paclitaxel/carboplatin combination (58, 59) and had no interference with the hypothalamic-pituitary-adrenal axis, although 33% of evaluable patients (4 of 12) received the relatively high number of 10 treatment cycles.

The present study successfully identified the suramin dose yielding a target plasma concentration range between 10 and 50 μM over the duration when paclitaxel and carboplatin were present at therapeutically significant levels. As described in detail in a separate study,[5] the relationships between suramin pharmacokinetic parameters and physiological parameters were used in conjunction with population pharmacokinetic analysis to establish an empirical equation that calculates the suramin dose needed to deliver the target concentrations. Results of the last 3 patients whose suramin dose was derived using this equation suggest the applicability of this equation. Additional studies in a larger patient population to confirm the predictive power of this equation are ongoing.

Most of the earlier pharmacokinetic studies of high-dose suramin were conducted in male patients with hormone refractory prostate cancer. The present study included 5 female patients, 3 of whom provided sufficient data for analysis of pharmacokinetic parameters. A preliminary analysis of the results suggests a slower elimination in female patients. These results need to be interpreted carefully because of the small number of female patients in the present study. Additional pharmacokinetic studies in patients with advanced metastatic breast cancer are under way.

Although the concept that optimal biological doses for molecularly targeted agents can be different from their maximally tolerated doses is not new, very seldom are clinical trials designed to have as their major end point the determination of the optimal biological dose. In many instances, this is because of the lack of reliable surrogates of biological activity, the rapid degradation in plasma of the targeted enzymes/proteins, and/or the difficulty of obtaining repetitive tumor samples. The present study used plasma concentrations of suramin as a surrogate biological end point because these concentrations were associated with the reversal of FGF-induced chemoresistance *in vitro* and had demonstrated synergy with chemotherapeutic agents such as doxorubicin and paclitaxel against human xenograft tumors *in vivo* (48–50). The relevance of such a design is that given the lack of toxicity or antitumor activity of single agent suramin at these concentrations, if increased antitumor activity is demonstrated in subsequent efficacy trials, this trial may set a new paradigm for the design of Phase I clinical trials of biological agents.

In the present trial, we were very mindful of avoiding peak concentrations of suramin that were substantially >50 μM. This concern arose from studies showing cell cycle perturbations by suramin. Suramin at >50 μM concentrations causes cell cycle arrest in the G_1 phase for human prostate tumor cells, NIH3T3 cells, and human neuroblastoma cells (60–63). In addition, arrest in the G_2-M phase for human breast and ovarian tumor cells and arrest in the G_2-M and S phases for meningioma cells have been reported (64–66). Likewise, preliminary results from our laboratory indicate that suramin at concentrations > 50 μM arrested human PC3 cells in G_1 phase, whereas lower concentrations did not produce cell cycle perturbations and that high suramin doses yielding ~200 μM plasma concentrations reduced the cell cycle progression in xenograft tumors, whereas low suramin doses yielding <50 μM concentrations did not (unpublished results). Although it is unclear if maintaining concentrations above these levels for a short period of time would result in antagonistic effects in humans, the concentrations resulting from low-dose suramin in our Phase I study were highly predictable, and the dose can be easily calculated in the clinical setting. Therefore, until careful evaluation of the clinical value of the concept discussed here is completed, it is our recommendation that efficacy trials should aim for the concentrations targeted in the present study.

Although it is beyond the purpose of a Phase I trial, it is of interest to comment on the antitumor activity observed. Despite the few patients and the potential bias introduced by patient selection that may exist in this small group of patients, encouraging antitumor activity was observed in both chemonaïve and previously treated patients. Two observations are noteworthy. First, antitumor activity was observed in 2 patients who had tumor progression after paclitaxel treatment. Second, the median TTP was an impressive 8.5 months, including 2 patients with ≥18 months before tumor progression was documented. These observations would encourage additional evaluation of low-dose suramin as a chemosensitizer not only in chemonaive patients in which the median TTP is typically 3–4 months (67) but also in chemorefractory patients. As is the case for most biological agents, TTP or progression-free rate at a particular time interval should be an important part of the analysis of such evaluations.

In summary, low-dose suramin can be combined with commonly administered doses of paclitaxel and carboplatin in NSCLC patients without an increase in toxicity, and the suramin concentration can be predicted based on clinical parameters. The preliminary antitumor activity observed encourages evaluation of the combination in efficacy trials.

REFERENCES

1. Anderson, J., Fuglsang, H., and de C. Marshall, T. F. Effects of suramin on ocular onchocerciasis. Tropenmed. Parasitol., *27*: 279–296, 1976.

2. Burchmore, R. J., Ogbunude, P. O., Enanga, B., and Barrett, M. P. Chemotherapy of human African trypanosomiasis. Curr Pharm Des, *8*: 256–267, 2002.

3. Mattock, N. M., and Peters, W. The experimental chemotherapy of leishmaniasis. II. The activity in tissue culture of some antiparasitic and antimicrobial compounds in clinical use. Ann. Trop. Med. Parasitol., *69:* 359–371, 1975.

4. Fairlamb, A. H., and Bowman, I. B. Uptake of the trypanocidal drug suramin by bloodstream forms of Trypanosoma brucei and its effect on respiration and growth rate *in vivo*. Mol. Biochem. Parasitol., *1:* 315–333, 1980.

5. De Clercq, E. Suramin: a potent inhibitor of the reverse transcriptase of RNA tumor viruses. Cancer Lett., *8:* 9–22, 1979.

6. Calcaterra, N. B., Vicario, L. R., and Roveri, O. A. Inhibition by suramin of mitochondrial ATP synthesis. Biochem. Pharmacol., *37:* 2521–2527, 1988.

7. Rago, R. P., Brazy, P. C., and Wilding, G. Disruption of mitochondrial function by suramin measured by rhodamine 123 retention and oxygen consumption in intact DU145 prostate carcinoma cells. Cancer Res., *52:* 6953–6955, 1992.

8. Hosang, M. Suramin binds to platelet-derived growth factor and inhibits its biological activity. J. Cell Biochem., *29:* 265–273, 1985.

9. Coffey, R. J., Jr., Leof, E. B., Shipley, G. D., and Moses, H. L. Suramin inhibition of growth factor receptor binding and mitogenicity in AKR-2B cells. J. Cell Physiol., *132:* 143–148, 1987.

10. Fujiuchi, S., Ohsaki, Y., and Kikuchi, K. Suramin inhibits the growth of non-small-cell lung cancer cells that express the epidermal growth factor receptor. Oncology, *54:* 134–140, 1997.

11. Waltenberger, J., Mayr, U., Frank, H., and Hombach, V. Suramin is a potent inhibitor of vascular endothelial growth factor. A contribution to the molecular basis of its antiangiogenic action. J. Mol. Cell Cardiol., *28:* 1523–1529, 1996.

12. Wade, T. P., Kasid, A., Stein, C. A., LaRocca, R. V., Sargent, E. R., Gomella, L. G., Myers, C. E., and Linehan, W. M. Suramin interference with transforming growth factor-beta inhibition of human renal cell carcinoma in culture. J. Surg. Res., *53:* 195–198, 1992.

13. Pollak, M., and Richard, M. Suramin blockade of insulin-like growth factor I-stimulated proliferation of human osteosarcoma cells. J. Natl. Cancer Inst. (Bethesda), *82:* 1349–1352, 1990.

14. Minniti, C. P., Maggi, M., and Helman, L. J. Suramin inhibits the growth of human rhabdomyosarcoma by interrupting the insulin-like growth factor II autocrine growth loop. Cancer Res., *52:* 1830–1835, 1992.

15. Basile, D. P., and Holzwarth, M. A. Basic fibroblast growth factor receptor in the rat adrenal cortex: effects of suramin and unilateral adrenalectomy on receptor numbers. Endocrinology, *134:* 2482–2489, 1994.

16. Bernardini, N., Giannessi, F., Bianchi, F., Dolfi, A., Lupetti, M., Citti, L., Danesi, R., and Del Tacca, M. Involvement of basic fibroblast growth factor in suramin-induced inhibition of V79/AP4 fibroblast cell proliferation. Br. J. Cancer, *67:* 1209–1216, 1993.

17. Pienta, K. J., Isaacs, W. B., Vindivich, D., and Coffey, D. S. The effects of basic fibroblast growth factor and suramin on cell motility and growth of rat prostate cancer cells. J. Urol., *145:* 199–202, 1991.

18. Pesenti, E., Sola, F., Mongelli, N., Grandi, M., and Spreafico, F. Suramin prevents neovascularisation and tumour growth through blocking of basic fibroblast growth factor activity. Br. J. Cancer, *66:* 367–372, 1992.

19. Khaled, Z., Rideout, D., O'Driscoll, K. R., Petrylak, D., Cacace, A., Patel, R., Chiang, L. C., Rotenberg, S., and Stein, C. A. Effects of suramin-related and other clinically therapeutic polyanions on protein kinase C activity. Clin. Cancer Res., *1:* 113–122, 1995.

20. Taylor, C. W., Lui, R., Fanta, P., and Salmon, S. E. Effects of suramin on *in vitro* growth of fresh human tumors. J. Natl. Cancer Inst. (Bethesda), *84:* 489–494, 1992.

21. Frommel, T. O. Suramin is synergistic with vinblastine in human colonic tumor cell lines: effect of cell density and timing of drug delivery. Anticancer Res., *17:* 2065–2071, 1997.

22. Kuratsu, J., Kurino, M., Fukunaga, K., Miyamoto, E., and Ushio, Y. Stimulatory effect of suramin on the proliferation of human glioma cells. Anticancer Res., *15:* 1263–1268, 1995.

23. Rubio, G. J., Pinedo, H. M., Virizuela, J., van Ark-Otte, J., and Giaccone, G. Effects of suramin on human lung cancer cell lines. Eur. J. Cancer, *31A:* 244–251, 1995.

24. Abdin, A., Larsson, S. E., Wasteson, A., and Walz, T. M. Suramin blocks growth-stimulatory effects of platelet-derived growth factor on malignant fibrous histiocytomas *in vitro*. Cancer Lett., *146:* 189–194, 1999.

25. Cardinali, M., Sartor, O., and Robbins, K. C. Suramin, an experimental chemotherapeutic drug, activates the receptor for epidermal growth factor and promotes growth of certain malignant cells. J. Clin. Investig., *89:* 1242–1247, 1992.

26. Mitchen, J., Rago, R., and Wilding, G. Effects of suramin on the proliferation of primary epithelial cell cultures derived from normal, benign hyperplastic and cancerous human prostates. Prostate, *22:* 75–89, 1993.

27. Eisenberger, M. A., Simbaldi, V. J., Reyno, L. M., Sridhara, R., Jodrell, D. I., Zuhowski, E. G., Tkaczuk, K. H., Lowitt, M. H., Hemady, R. K., Jacobs, S. C., *et al.* Phase I and clinical evaluation of a pharmacologically guided regimen of suramin in patients with hormone-refractory prostate cancer. J. Clin. Oncol., *13:* 2174–2186, 1995.

28. Rosen, P. J., Mendoza, E. F., Landaw, E. M., Mondino, B., Graves, M. C., McBride, J. H., Turcillo, P., deKernion, J., and Beildegrun, A. Suramin in hormone-refractory metastatic prostate cancer: a drug with limited efficacy. J. Clin. Oncol., *14:* 1626–1636, 1996.

29. Calvo, E., Cortes, J., Rodriguez, J., Sureda, M., Beltran, C., Rebollo, J., Martinez-Monge, R., Berian, J. M., de Iraia, J., and Brugarolas, A. Fixed higher dose schedule of suramin plus hydrocortisone in patients with hormone refractory prostate carcinoma a multicenter Phase II study. Cancer (Phila.), *92:* 2435–2443, 2001.

30. Small, E. J., Meyer, M., Marshall, M. E., Reyno, L. M., Meyers, F. J., Natale, R. B., Lenehan, P. F., Chen, L., Slichenmyer, W. J., and Eisenberger, M. Suramin therapy for patients with symptomatic hormone-refractory prostate cancer: results of a randomized Phase III trial comparing suramin plus hydrocortisone to placebo plus hydrocortisone. J. Clin. Oncol., *18:* 1440–1450, 2000.

31. Grossman, S. A., Phuphanich, S., Lesser, G., Rozental, J., Grochow, L. B., Fisher, J., and Piantadosi, S. Toxicity, efficacy, and pharmacology of suramin in adults with recurrent high-grade gliomas. J. Clin. Oncol., *19:* 3260–3266, 2001.

32. Mirza, M. R., Jakobsen, E., Pfeiffer, P., Lindebjerg-Clasen, B., Bergh, J., and Rose, C. Suramin in non-small cell lung cancer and advanced breast cancer. Two parallel Phase II studies. Acta Oncol., *36:* 171–174, 1997.

33. Falcone, A., Pfanner, E., Cianci, C., Danesi, R., Brunetti, I., Del Tacca, M., and Conte, P. F. Suramin in patients with metastatic colorectal cancer pretreated with fluoropyrimidine-based chemotherapy. A Phase II study. Cancer (Phila.), *75:* 440–443, 1995.

34. Dreicer, R., Smith, D. C., Williams, R. D., and See, W. A. Phase II trial of suramin in patients with metastatic renal cell carcinoma. Investig. New Drugs, *17:* 183–186, 1999.

35. Kobayashi, K., Vokes, E. E., Vogelzang, N. J., Janish, L., Soliven, B., and Ratain, M. J. Phase I study of suramin given by intermittent infusion without adaptive control in patients with advanced cancer. J. Clin. Oncol., *13:* 2196–2207, 1995.

36. Reyno, L. M., Egorin, M. J., Eisenberger, M. A., Sunbaldi, V. J., Zuhowski, E. G., and Sridhara, R. Development and validation of a pharmacokinetically based fixed dosing scheme for suramin. J. Clin. Oncol., *13:* 2187–2195, 1995.

37. van Rijswijk, R. E., van Loenen, A. C., Wagstaff, J., Meijer, E., Lopez, R., van Groeningen, C. J., Heimans, J. J., and Pinedo, H. M. Suramin: rapid loading and weekly maintenance regimens for cancer patients. J. Clin. Oncol., *10:* 1788–1794, 1992.

38. La Rocca, R. V., Meer, J., Gilliatt, R. W., Stein, C. A., Cassidy, J., Myers, C. E., and Dalakas, M. C. Suramin-induced polyneuropathy. Neurology, *40:* 954–960, 1990.

39. Kobayashi, K., Weiss, R. E., Vogelzang, N. J., Vokes, E. E., Janisch, L., and Ratain, M. J. Mineralocorticoid insufficiency due to suramin therapy. Cancer (Phila.), *78:* 2411–2420, 1996.

40. Katz, S. K., Medenica, M. M., Kobayashi, K., Vogelzang, N. J., and Soltani, K. Erythema multiforme induced by suramin. J. Am. Acad. Dermatol., *32:* 292–293, 1995.

41. Kobayashi, K., Pezen, D. S., Vogelzang, N. J., Medenica, M., Janisch, L., Ratain, M., Vokes, E. E., and Soltani, K. Keratoacanthomas and skin neoplasms associated with suramin therapy. Arch Dermatol., *132:* 96–98, 1996.

42. Holland, E. J., Stein, C. A., Palestine, A. G., LaRocca, R., Chan, C. C., Kuwabara, T., Myers, C. E., Thomas, R., McAtee, N., and Nussenblatt, R. N. Suramin keratopathy. Am. J. Ophthalmol., *106:* 216–220, 1988.

43. May, E., and Allolio, B. Fatal toxic epidermal necrolysis during suramin therapy. Eur. J. Cancer, *27:* 1338, 1991.

44. Horne, M. K., III, Wilson, O. J., Cooper, M., Grainick, H. R., and Myers, C. E. The effect of suramin on laboratory tests of coagulation. Thromb. Haemost., *67:* 434–439, 1992.

45. Arlt, W., Reincke, M., Siekmann, L., Winkelmann, W., and Allolio, B. Suramin in adrenocortical cancer: limited efficacy and serious toxicity. Clin. Endocrinol. (Oxf.), *41:* 299–307, 1994.

46. Figg, W. D., Cooper, M. R., Thibault, A., Headlee, D., Humphrey, J., Bergan, R. C., Reed, E., and Sartor, O. Acute renal toxicity associated with suramin in the treatment of prostate cancer. Cancer (Phila.), *74:* 1612–1614, 1994.

47. Stein, C. A., LaRocca, R. V., Thomas, R., McAtee, N., and Myers, C. E. Suramin: an anticancer drug with a unique mechanism of action. J. Clin. Oncol., *7:* 499–508, 1989.

48. Bitton, R. J., Figg, W. D., Venzon, D. J., Dalakas, M. C., Bowden, C., Headlee, D., Reed, E., Myers, C. E., and Cooper, M. R. Pharmacologic variables associated with the development of neurologic toxicity in patients treated with suramin. J. Clin. Oncol., *13:* 2223–2229, 1995.

49. Chaudhry, V., Eisenberger, M. A., Simbaldi, V. J., Sheikh, K., Griffin, J. W., and Cornblath, D. R. A prospective study of suramin-induced peripheral neuropathy. Brain, *119* (Pt. 6): 2039–2052, 1996.

50. Danesi, R., Del Bianchi, S., Soldani, P., Campagni, A., La Rocca, R. V., Myers, C. E., Paparelli, A., and Del Tacca, M. Suramin inhibits bFGF-induced endothelial cell proliferation and angiogenesis in the chick chorioallantoic membrane. Br. J. Cancer, *68:* 932–938, 1993.

51. Song, S., Wientjes, M. G., Gan, Y., and Au, J. L. Fibroblast growth factors: an epigenetic mechanism of broad spectrum resistance to anticancer drugs. Proc. Natl. Acad. Sci. USA, *97:* 8658–8663, 2000.

52. Zhang, Y., Song, S., Yang, F., Au, J. L., and Wientjes, M. G. Nontoxic doses of suramin enhance activity of doxorubicin in prostate tumors. J. Pharmacol. Exp. Ther., *299:* 426–433, 2001.

53. Song, S., Wientjes, M. G., Walsh, C., and Au, J. L. Nontoxic doses of suramin enhance activity of paclitaxel against lung metastases. Cancer Res., *61:* 6145–6150, 2001.

54. Calvert, A. H., Newell, D. R., Gumbrell, L. A., O'Reilly, S., Burnell, M., Boxall, F. E., Siddik, Z. H., Judson, I. R., Gore, M. E., and Wiltshaw, E. Carboplatin dosage: prospective evaluation of a simple formula based on renal function. J. Clin. Oncol., *7:* 1748–1756, 1989.

55. Trotti, A., Byhardt, R., Stetz, J., Gwede, C., Corn, B., Fu, K., Gunderson, L., McCormick, B., Morrisintegral, M., Rich, T., Shipley, W., and Curran, W. Common toxicity criteria: version 2.0, an improved reference for grading the acute effects of cancer treatment: impact on radiotherapy. Int. J. Radiat. Oncol. Biol. Phys., *47:* 13–47, 2000.

56. Therasse, P., Arbuck, S. G., Eisenhauer, E. A., Wanders, J., Kaplan, R. S., Rubinstein, L., Verweij, J., Van Glabbeke, M., van Oosterom, A. T., Christian, M. C., and Gwyther, S. G. New guidelines to evaluate the response to treatment in solid tumors. European Organization for Research and Treatment of Cancer, National Cancer Institute of the United States, National Cancer Institute of Canada. J. Natl. Cancer Inst. (Bethesda), *92:* 205–216, 2000.

57. Kassack, M., and Nickel, P. Rapid, highly sensitive gradient narrow-bore high-performance liquid chromatographic determination of suramin and its analogues. J. Chromatogr. B Biomed. Appl., *686:* 275–284, 1996.

58. Kelly, K., Crowley, J., Bunn, P. A., Jr., Presant, C. A., Grevstad, P. K., Moinpour, C. M., Ramsey, S. D., Wozniak, A. J., Weiss, G. R., Moore, D. F., Israel, V. K., Livingston, R. B., and Gandara, D. R. Randomized Phase III trial of paclitaxel plus carboplatin *versus* vinorelbine plus cisplatin in the treatment of patients with advanced non-small-cell lung cancer: a Southwest Oncology Group trial. J. Clin. Oncol., *19:* 3210–3218, 2001.

59. Langer, C. J., Leighton, J. C., Comis, R. L., O'Dwyer, P. J., McAleer, C. A., Bonjo, C. A., Engstrom, P. F., Litwin, S., and Ozols, R. F. Paclitaxel and carboplatin in combination in the treatment of advanced non-small-cell lung cancer: a Phase II toxicity, response, and survival analysis. J. Clin. Oncol., *13:* 1860–1870, 1995.

60. Howard, S. P., Park, S. J., Hughes-Davies, L., Coleman, C. N., and Price, B. D. Suramin increases p53 protein levels but does not activate the p53-dependent G_1 checkpoint. Clin. Cancer Res., *2:* 269–276, 1996.

61. Qiao, L., Pizzolo, J. G., and Melamed, M. R. Effects of suramin on expression of proliferation associated nuclear antigens in DU-145 prostate carcinoma cells. Biochem. Biophys. Res. Commun., *201:* 581–588, 1994.

62. Chatterjee, D., Wyche, J. H., and Pantazis, P. Induction of apoptosis in malignant and camptothecin-resistant human cells. Ann. N. Y. Acad. Sci., *803:* 143–156, 1996.

63. Sullivan, K. A., Kim, B., Buzdon, M., and Feldman, E. L. Suramin disrupts insulin-like growth factor II (IGF-II) mediated autocrine growth in human SH-SY5Y neuroblastoma cells. Brain Res., *744:* 199–206, 1997.

64. Foekens, J. A., Sieuwerts, A. M., Smurman-Smeets, E. M., Peters, H. A., and Klijn, J. G. Effects of suramin on cell-cycle kinetics of MCF-7 human breast cancer cells *in vitro*. Br. J. Cancer, *67:* 232–236, 1993.

65. Schrell, U. M., Gauer, S., Kiesewetter, F., Bickel, A., Hren, J., Adams, E. F., and Fahlbusch, R. Inhibition of proliferation of human cerebral meningioma cells by suramin: effects on cell growth, cell cycle phases, extracellular growth factors, and PDGF-BB autocrine growth loop. J. Neurosurg., *82:* 600–607, 1995.

66. Kikuchi, Y., Hirata, J., Hisano, A., Tode, T., Kita, T., and Nagata, I. Complete inhibition of human ovarian cancer xenografts in nude mice by suramin and *cis*-diamminedichloroplatinum(II). Gynecol. Oncol., *58:* 11–15, 1995.

67. Schiller, J. H., Harrington, D., Belani, C. P., Langer, C., Sandler, A., Krook, J., Zhu, J., and Johnson, D. H. Comparison of four chemotherapy regimens for advanced non-small-cell lung cancer. N. Engl. J. Med., *346:* 92–98, 2002.

Clinical Cancer Research

Phase I Study of Low-Dose Suramin as a Chemosensitizer in Patients with Advanced Non-Small Cell Lung Cancer

Miguel A. Villalona-Calero, M. Guillaume Wientjes, Gregory A. Otterson, et al.

Clin Cancer Res 2003;9:3303-3311.

ARTICLE

Simulation of Y-Site Compatibility of Irinotecan and Leucovorin at Room Temperature in 5% Dextrose in Water in 3 Different Containers

Scott E. Walker, Shirley Law, and Anitasha Puodziunas

ABSTRACT

Background: No data are available on the physical compatibility and chemical stability of irinotecan and leucovorin when these 2 drugs are mixed.

Objective: The objective of this study was to evaluate the physical compatibility and chemical stability of irinotecan diluted in 5% dextrose in water (D5W) and combined with the racemic form of leucovorin when stored at 23°C, unprotected from light, conditions that simulate Y-site administration of these drugs.

Methods: Six combinations of irinotecan and leucovorin were prepared (0.56 mg/mL and 0.94 mg/mL, 0.53 mg/mL and 0.74 mg/mL, 0.59 mg/mL and 0.66 mg/mL, 0.56 mg/mL and 0.27 mg/mL, 0.32 mg/mL and 3.60 mg/mL, and 0.30 mg/mL and 0.68 mg/mL, respectively), representing the concentrations (dose, volume, and infusion rate) most commonly administered in clinical practice. The stability of each solution was evaluated at room temperature (23°C) in 3 different types of containers: polyvinyl chloride (PVC), polypropylene–polyethylene copolymer, and glass (control). Each solution was visually inspected for precipitate, colour change, and evolution of gas, and the concentration of each drug was measured by high-performance liquid chromatography at time 0 (immediately after mixing) and at 0.5, 1, and 24 h. Each concentration measurement was completed in triplicate.

Results: All solutions remained clear and colourless throughout the 24-h study period. More than 96% of the initial concentration of leucovorin and more than 91% of the initial concentration of irinotecan remained after 0.5 h. Rapid degradation of irinotecan was observed in one mixture: irinotecan 0.30 mg/mL and leucovorin 3.60 mg/mL. In this mixture, the concentrations of irinotecan were between 91.57% and 95.09% of the original concentration at 0.5 h, but declined rapidly to between 76.30% and 78.34% by 24 h. This rapid degradation was likely due to the higher pH of the solution created by the high concentration of leucovorin (3.60 mg/mL, equivalent to a dose of 400 mg/m² body area, in 100 mL, for a 60-min infusion). For all mixtures, the mean

RÉSUMÉ

Historique : On ne dispose d'aucune donnée sur la compatibilité physique et la stabilité chimique de l'irinotécan et de la leucovorine lorsque ces deux médicaments sont mélangés ensemble.

Objectif : Évaluer la compatibilité physique et la stabilité chimique de l'irinotécan dilué dans une solution de dextrose à 5 % dans l'eau (D5W) et mélangé au composé racémique de leucovorine, puis entreposé à 23 °C, non protégé de la lumière, dans des conditions simulant l'administration de ces médicaments dans un raccord en Y.

Méthodes : Six mélanges d'irinotécan et de leucovorine ont été préparés (0,56 mg/mL et 0,94 mg/mL, 0,53 mg/mL et 0,74 mg/mL; 0,59 mg/mL et 0,66 mg/mL; 0,56 mg/mL et 0,27 mg/mL; 0,32 mg/mL et 3,60 mg/mL; et 0,30 mg/mL et 0,68 mg/mL, respectivement), représentant les concentrations (dose, volume et vitesse de perfusion) les plus fréquemment administrées en pratique clinique. On a évalué la stabilité de chaque solution à la température ambiante (23 °C) et dans trois différents types de contenants : polychlorure de vinyle (PVC), copolymère de polypropylène et polyéthylène, et verre (témoin). Chaque solution a été inspectée visuellement pour la présence d'un précipité, un changement de couleur et le dégagement de gaz, et la concentration de chaque médicament a été mesurée par chromatographie liquide à haute pression au temps 0 (immédiatement après le mélange) puis à 0,5, 1 et 24 h. La concentration de chaque médicament a été mesurée en triple.

Résultats : Toutes les solutions sont demeurées limpides et incolores au cours des 24 heures qu'a duré l'étude. Les solutions ont conservé plus de 96 % de la concentration initiale de leucovorine et plus de 91 % de la concentration initiale d'irinotécan après 0,5 h. On a observé une dégradation rapide de l'irinotécan dans un des mélanges : irinotécan à 0,30 mg/mL et leucovorine à 3,60 mg/mL. Dans ce mélange, les concentrations d'irinotécan étaient entre 91,57 % et 95,09 % des concentrations initiales à 0,5 h, et elles ont rapidement chuté entre 76,30 % et 78,34 % à 24 h. Cette dégradation rapide semblait être attribuable au pH

concentration of leucovorin at 24 h was greater than 96% of the initial concentration. There was no effect of container type on the rate of degradation of either drug.

Conclusions: Given that contact times are likely less than 3 min when standard IV tubing sets are used, it is concluded that irinotecan and leucovorin are physically compatible and chemically stable for a sufficient period of time to allow concurrent infusion via a Y site.

Key words: irinotecan, leucovorin, stability, compatibility

C an J Hosp Pharm 2005;58:212-22

plus élevé de la solution, causé par la forte concentration de leucovorine (3,60 mg/mL, équivalant à une dose de 400 mg/m² de surface corporelle, dans 100 mL, administrée par perfusion d'une durée de 60 minutes). Tous les mélanges ont retenu plus de 96 % de la concentration moyenne initiale de leucovorine à 24 h. Le type de contenant n'a pas eu d'effet sur le taux de dégradation de l'un ou l'autre médicament.

Conclusions : Étant donné que la durée de contact est probablement inférieure à trois minutes avec les tubulures IV standard, on peut conclure que l'irinotécan et la leucovorine sont physiquement compatibles et chimiquement stables durant une période de temps suffisante pour permettre la perfusion concomitante dans un raccord en Y.

Mots clés : irinotécan, leucovorine, stabilité, compatibilité

INTRODUCTION

Irinotecan (IR; Camptosar, 7-ethyl-10-[4-(1-piperidino)-1-piperidino] carbonyl oxycamptothecin, or CPT-11) was introduced in Canada in late 1997 for the treatment of relapsed or refractory colorectal cancer. The product monograph indicates that IR may be diluted with a variety of IV solutions, including 0.9% sodium chloride (normal saline; NS) and 5% dextrose in water (D5W), and that such solutions should be used within 12 h when stored at room temperature or 48 h when refrigerated.[1]

Previous evaluations of IR degradation have indicated that the first step involves hydrolysis of the lactone ring to form a ring-opened carboxylate derivative,[2] a reversible, pH-dependent process.[2,3] At a pH of less than 5 equilibrium favours IR, whereas at a pH of greater than 8, virtually all IR is present as the ring-opened carboxylate.[3] As the pH increases from 5 to 8, an increasing proportion of IR exists as the carboxylate at equilibrium. The rate of conversion from IR to the carboxylate is also pH-dependent, increasing 4-fold between pH 5 and pH 8,[2,3] such that equilibrium is established more rapidly at higher pH. The carboxylate derivative also appears to be more photosensitive than IR,[4] and at least 5 degradation products are produced under fluorescent light when the ring-opened carboxylate form is present.[4]

The period for which leucovorin (LV) is considered stable in solution ranges from 12 to 72 h.[4,5] The Novopharm product monograph indicates that when LV is diluted with D5W or dextrose 10% in water (D10W), infusion solutions of 0.06 to 1.0 mg/mL are stable for 12 h, whereas LV diluted with dextrose 10% in saline is stable for only 6 h.[4] The Lederle, Cyanamid Canada product monograph for LV states that the drug is stable for 24 h when diluted in D5W, D10W, or dextrose 10% in saline and stored at room temperature.[5] Lauper[6] and Benvenuto and others[7] reported that LV is stable for 24 h after mixing in D5W, whereas Smith and others[8] demonstrated stability with floxuridine over 72 h. Although these data may be limited to studies of short duration, they suggest that LV should be stable for at least 24 to 72 h when diluted in D5W and stored at room temperature.

Current protocols for treatment of metastatic colorectal cancer call for sequential administration of 180 mg/m² of IR and either 200 mg/m² of L-LV or 400 mg/m² of the racemic mixture of LV, followed by infusion of 5-fluorouracil (5FU). Approximately 3.5 h is required to sequentially administer the IR (90-min infusion) and LV (120-min infusion). Patients would spend much less time in the clinic, and more patients could potentially be treated in a given period of time, if IR and LV could be administered concurrently.

European data have indicated that IR and LV are stable when administered concurrently.[9] Although that study concluded that IR and LV were physically and chemically compatible (because both precipitate and degradation products were absent from the IR–LV mixture after a 2-h incubation) the L-isomer of LV was used in these experiments. Thus, the stability achieved with IR and racemic LV may not be accurately represented by these results.

The objective of this study was to evaluate the compatibility of IR diluted in D5W with the racemic mixture of LV also diluted in D5W when mixed together at concentrations typically encountered during Y-site administration at 23°C, in 3 types of containers, unprotected from light.

METHODS

Assay Development and Validation

HPLC Method for Simultaneous Analysis of Irinotecan and Leucovorin

A high-performance liquid chromatography (HPLC) method was developed that allowed simultaneous ana lyses of IR and LV and ensured separation of the 2 drugs from each other and their degradation products. The mobile phase consisted of a mixture of 10% acetonitrile and 90% 0.05 mol/L potassium phosphate monobasic (pH adjusted to 4.1), which was gradually changed to 35% acetonitrile and 65% 0.05 mol/L potassium phosphate monobasic (pH adjusted to 4.1) over 10 min. The pH of the mixed solution was adjusted to 4.1 with 1 mol/L phosphoric acid. Each sample was analyzed for 30 min. The mobile phase was pumped at 1 mL/min through a 15 cm × 4.6 mm reverse-phase C_{18}, 3-µm column (Supelcosil ABZ Plus, Supelco, Mississauga, Ontario) using a 600E system controller and pump (Waters Corp, Mississauga, Ontario). IR and LV were detected at 244 nm and 240 nm, respectively, using a scanning variable-wavelength detector (Spectra System UV6000LP, Thermo Separation Products, Freemont, California); the chromatograms were recorded directly into a computer database using ChromQuest software (Thermo Separation Products). The assay was developed using samples of IR, LV, and their respective degradation products to ensure accurate measurement of IR and LV stability. The UV spectral purity of the IR and LV peaks was compared between degraded and undegraded samples to demonstrate the specificity of the method. This method is unique and differs from previously published methods of IR analysis because of differences in type of column,[5,10] mobile-phase constituents,[5,9,10,12] temperature,[5] method or wavelength of detection,[5,9,10,12] and ability to separate IR from LV.

Accelerated Degradation of Irinotecan

During development of the HPLC method to separate IR and LV from their degradation products, the pH dependency of IR degradation and formation of the ring-opened carboxylate was evaluated, as was the formation of other irreversible degradation products. The ring-opened carboxylate product of IR was generated by the addition of sodium hydroxide to solutions of IR. A stock solution of IR was prepared by dissolving an accurately weighed quantity of approximately 10 mg of IR hydrochloride trihydrate powder (CPT-11, class A primary standard, Pharmacia Corporation, Mississauga, Ontario; lot C, expiry September 1, 2004) in 25 mL of distilled water to achieve a final IR concentration of 0.4 mg/mL. Eight separate samples with pH ranging from 4.12 to 10.14 were prepared by mixing 1 mL of the 0.4 mg/mL IR solution and 1 mL of sodium hydroxide ranging from 0.002 mol/L to 0.016 mol/L. The pH was determined immediately after mixing, and the concentration of IR was determined 30 min after addition of the sodium hydroxide. HPLC was used to monitor separation of IR and the primary degradation product, the ring-opened carboxylate. To the sample of pH 10.14, 1 mL of 0.016 mol/L hydrochloric acid was added. The pH was determined immediately after mixing and the concentration of IR was determined 30 min later.

Given that sodium hydroxide produces only the ring-opened product, a second set of experiments was performed, in which 10-µL aliquots of various sodium hypochlorite solutions ranging in concentration from 0.25% to 1% were added to 1-mL samples of 0.2 mg/mL IR (prepared by further dilution of the 0.4 mg/mL stock solution). These samples were immediately chromatographed, and the concentration of IR was determined.

Chromatograms from all solutions prepared above were inspected for the appearance of additional peaks, changes in retention time, and changes in peak shape. The ultraviolet (UV) spectral purity (200–365 nm, 6-nm bandwidth, determined with a UV3000LP deuterium lamp, Thermo Separation Products) of the leading edge, middle, and tail of the IR peak in a chromatogram of an authentic undegraded sample and the sample taken at time 0 were also compared. Samples of degraded IR were used to develop an HPLC method for simultaneous analysis of IR, LV, and their degradation products.

Degradation of Leucovorin

A degraded sample from an expired 10 mg/mL vial of LV calcium for injection USP (David Bull Laboratories; Vaudreuil, Quebec; lot 2024022, expiry December 1994) was analyzed by the HPLC method to separate LV from its degradation products. Chromatograms were inspected for the appearance of additional peaks, and the LV peak was compared to the LV peak obtained from HPLC analyses of a fresh sample of LV for changes in concentration, retention time, and peak shape.

Ultraviolet spectral purity (200–365 nm, 6-nm bandwidth, determined with a UV6000LP deuterium lamp, Thermo Separation Products) of the leading edge, middle, and tail of the LV peak in both the fresh and expired samples were compared. The expired LV was used to develop an HPLC method for separation of IR, LV, and their degradation products.

Accuracy and Reproducibility of the HPLC Assay

The accuracy and reproducibility of the HPLC method for simultaneous analysis of IR and LV was tested across 5 standard curves. Each sample containing both IR and LV standards was chromatographed in duplicate. Interday and intraday reproducibility were assessed using the coefficient of variation of the peak area for each compound determined in duplicate, and accuracy was determined on the basis of deviations from the known concentration.

Because the standard curve had an upper limit of 0.4 mg/mL for both IR and LV, all samples required dilution of either 1:2, 1:4, or 1:10. To evaluate the accuracy and reproducibility of an experimental solution that may need to be diluted, 5 replicates of samples containing 0.45 mg/mL of IR and 3.6 mg/mL of LV were prepared and diluted, and the concentrations of IR and LV were measured. All experimental solutions assessed by HPLC had concentrations of IR and LV above 0.00625 mg/mL, the lower limit of the standard curve for both drugs.

HPLC Analyses of Solutions for Compatibility Study

On each study day, fresh standards of IR and LV were prepared and chromatographed separately to construct standard curves. A stock solution of IR was prepared by dissolving an accurately weighed quantity of approximately 10 mg of IR hydrochloride trihydrate powder (CPT-11, class A primary standard, Pharmacia Corporation; lot C, expiry September 1, 2004) in 25 mL of distilled water. This stock solution (0.40 mg/mL) was then diluted to prepare 7 concentrations of IR: 0.00625, 0.0125, 0.025, 0.050, 0.100, 0.250, and 0.400 mg/mL. Four-microlitre aliquots of each of these 7 standards and a blank were directly chromatographed in duplicate to allow construction of the standard curve.

A stock solution of LV was prepared by diluting various volumes of a 10 mg/mL solution (leucovorin calcium for injection USP, Novopharm, Toronto, Ontario; lot 0271202001, expiry December 2004) in 10 mL of distilled water to prepare 7 concentrations of LV: 0.00625, 0.0125, 0.025, 0.050, 0.100, 0.250, and 0.400 mg/mL. Four-microlitre aliquots of each of these 7 standards and a blank were used to construct a standard curve.

IR and LV were quantified simultaneously each day using the newly developed HPLC method described above. The average peak area of 2 replicates from each sample of IR and LV was subjected to least-squares linear regression, the concentration of experimental solutions was interpolated from standard curves and

Table 1. Irinotecan–Leucovorin Treatment Scenarios and Calculation of Final Concentrations

Key Scenario Characteristic	Scenario Designation	Drug	Dose (mg/m^2)	Average Body Size (m^2)	Diluent Volume (mL)	Concentration* (mg/mL)	Infusion Duration (min)	Projected Mixed Final Concentration† (mg/mL)
Standard infusion times for both irinotecan (90 min) and leucovorin (120 min)	1a	IR	180	1.8	500	0.65	90	0.56
		LV	400	1.8	100	7.20	120	0.94
	1b	IR	180	1.7	500	0.61	90	0.53
		LV	400	1.7	250	2.72	120	0.74
Leucovorin infusion twice as long as irinotecan infusion	2a	IR	180	1.8	500	0.65	60	0.59
		LV	400	1.8	100	7.20	120	0.66
	2b	IR	180	1.7	500	0.61	60	0.56
		LV	200	1.7	250	1.36	120	0.27
Equal flow rates	3a	IR	180	1.8	500	0.65	300	0.32
		LV	400	1.8	100	7.20	60	3.60
	3b	IR	180	1.7	500	0.61	120	0.30
		LV	200	1.7	250	1.36	60	0.68

IR = irinotecan, LV = racemic leucovorin.

*This concentration represents the concentration in the bag. It considers dose and nominal bag volume but does not consider bag overfill or the volume of drug added to the bag and is calculated as dose/nominal volume.

†This concentration estimates the concentration after mixing of the 2 solutions based on the nominal bag volume and the infusion duration. For example, the IR concentration is calculated as follows: $\{[Conc_{IR}(Vol_{IR}/ID_{IR})]/[(Vol_{IR}/ID_{IR})+(Vol_{LV}/ID_{LV})]\}$ where Vol = nominal bag volume, ID = infusion duration, and Conc = concentration.

recorded. Concentrations were recorded to the nearest 0.001 mg/mL.

Study Design

This study was designed to simulate concurrent infusion of separate solutions of IR and LV using a Y-site connection and to evaluate the stability of these compounds under such conditions. Six treatment scenarios were designed, including those most frequently used in practice, as well as those representing potential extremes of practice (Table 1). In each scenario, IR at a concentration of 0.61 mg/mL was mixed with LV at concentrations of 1.36 mg/mL, 2.72 mg/mL, or 7.20 mg/mL. A concentration between 0.61 and 0.65 mg/mL of IR would be used for an average person (1.7 m^2 to 1.8 m^2 body surface area) receiving a dose of IR of 180 mg/m^2 diluted in D5W (concentrations of 300 to 324 mg/500 mL). Similarly, the concentrations of LV (1.36, 2.72, and 7.20 mg/mL) would be used for an average person (1.7 m^2 to 1.8 m^2) receiving a dose of LV of either 200 or 400 mg/m^2 diluted in 100-mL or 250-mL bags of D5W.

The final concentration of both drugs in a Y-site line after mixing depends not only on the concentration of the drugs in solution but also the flow rates of each solution. A more complete disclosure of volumes and rates used in the estimates of the final concentrations can be found in Table 1. These concentrations do not consider bag-overfill volumes or the volume of the drug solution added to the bag and so are slightly higher than might actually be encountered in practice under similar scenarios.

Each treatment scenario was implemented by combining IR hydrochloride trihydrate (Camptosar, 20 mg/mL, Pharmacia & UpJohn, Mississauga, Ontario; lot 18JAK, expiry June 2005) and LV calcium for injection USP (10 mg/mL, Novopharm, Toronto, Ontario; lot 027120201, expiry December 2004), each diluted in D5W. Each of the 6 treatment scenarios was evaluated in each of 3 different container types, to simulate different types of infusion tubing: glass test tubes (containing D5W from a PVC bag, Baxter Corporation, lot W2L12A1, expiry June 2004), which served as control; PVC bags (Baxter Corporation, lot W2L12A1, expiry June 2004); and polypropylene–polyethylene copolymer bags (partial additive bags [PAB®]; B. Braun Medical Inc, Irvine, California, lot J2D954, expiry July 2005). Thus, 18 separate experiments were designed, and each experiment was conducted in triplicate (n = 54 experimental solutions). All experiments were conducted at room temperature (25°C) under ambient fluorescent room lighting without protection from light.

The concentration of IR and LV in each solution was determined by HPLC at time 0 (immediately after mixing) and at 0.5 h, 1 h, and 24 h.

Determination of pH

Immediately before mixing, the pH of the IR solution (nominal concentrations of 0.61 mg/mL and 0.65 mg/mL, as listed in Table 1) and each of the 3 LV solutions (7.20, 2.72, and 1.36 mg/mL, as listed in Table 1) was measured. Immediately after the solution for each treatment scenario was mixed (in a glass container), its pH was measured. The pH meter (Accumet model 925, Fisher Scientific, Nepean, Ontario) was standardized on each day on which pH was to be measured using commercially available buffer solutions (Fisher Scientific). The pH was recorded to the nearest 0.001 unit but is reported to 2 decimal places.

Visual Inspection

Before and immediately after mixing (time 0) and after 0.5 h, 1 h, and 24 h, each of the 54 experimental solutions was visually inspected against both a black background and a white background for precipitate, colour changes, and clarity. The samples for physical inspection were removed from the respective containers and placed in glass test tubes before inspection to avoid misinterpretations related to the opacity of the container. After inspection, solutions were centrifuged (3000 rpm, 1500g) for 10 min to pellet any precipitate that might have formed. The supernatant was also visually inspected.

Data Reduction and Statistical Analysis

The data for each analysis are presented as mean ± standard deviation. Reproducibility was assessed by coefficient of variation. Mean concentrations of IR and LV in each solution were analyzed by least-squares linear regression to determine the percentage of the initial concentration remaining at each time point during the 24-h study period. Multiple linear regression and analysis of variance (SPSS for Windows, release 10.0.5, 1999) were used to determine whether container type (glass, PVC, or PAB) or concentration of IR or LV in the mixture at time 0 had any effect on rate of degradation of either drug. The commonly accepted cut-off for statistical significance of 5% was used for all analyses.

The concentration of IR or LV at any time point was considered within acceptable limits for degradation if the mean concentration had not declined below 90% of the final mixed concentration measured at time 0. A mixture

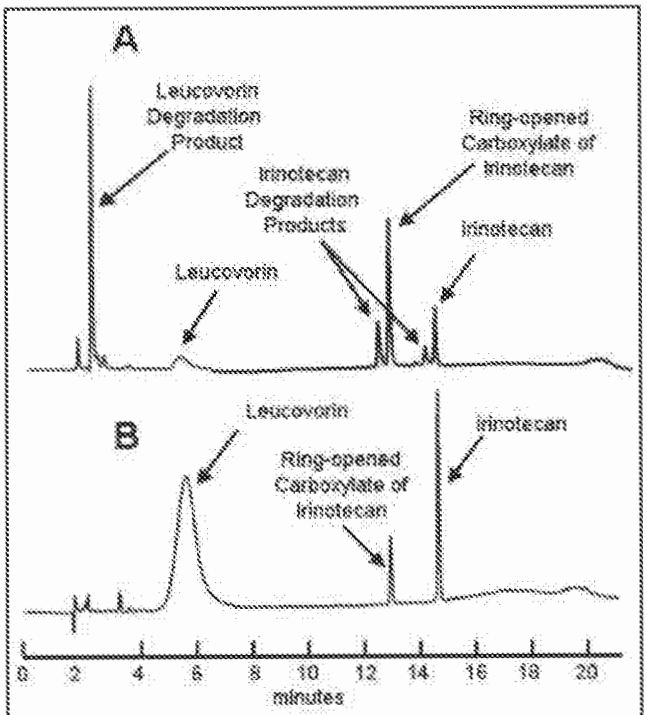

Figure 1. A: Chromatogram of a mixture of expired 10 mg/mL leucovorin and a sample of 0.2 mg/mL irinotecan with 10 µL of 0.5% sodium hypochlorite added. B: Chromatogram of a sample from the stability study (3.60 mg/mL leucovorin and 0.32 mg/mL irinotecan) 24 h after mixing, showing only undegraded leucovorin and irinotecan with about 22% as the ring-opened carboxylate.

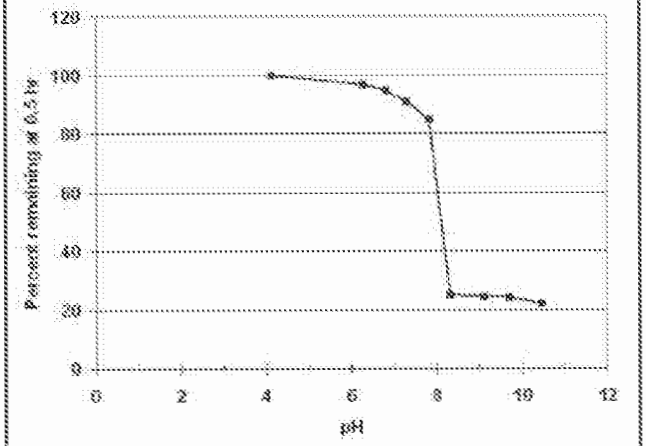

Figure 2. The pH dependency of irinotecan degradation. Eight samples ranging in pH from 4.12 to 10.14 (using concentrations of sodium hydroxide) were prepared, and the percentage of irinotecan remaining after 30 min was measured. Above pH 7, irinotecan degrades quickly. At pH 6.27, only 3% of the initial irinotecan concentration was lost, and at pH 6.79 only 5% of the irinotecan was lost at 30 min. These results are similar to those of Fassberg and Stell[2] and Dodds and others.[3]

was judged to be physically compatible if there was no visual change in the colour or clarity of the mixture, and no precipitate or other particulate formation was visually apparent.

RESULTS

Assay Development and Validation

Figure 1 is a typical chromatogram obtained using the newly developed HPLC method to simultaneously analyse IR and LV. With this separation method, IR eluted at 14.7 min and the ring-opened carboxylate, produced by the addition of either sodium hydroxide or sodium hypochlorite (pH 10), eluted at 13.0 min. Sodium hypochlorite also produces other degradation products (Figure 1A). The addition of increasing amounts of sodium hydroxide to an IR sample increases the formation of the ring-opened carboxylate as the pH increases from 4 to 8 (Figure 2). Above a pH of 8, the ring-opened carboxylate product is the predominate species in solution. Addition of hydrochloric acid to such a sample (e.g., a sample at pH 10.14 through the addition of sodium hydroxide), results in the re-formation of IR within 30 min (when the pH dropped to less than 5). LV and its primary degradation product eluted at 5.7 min and 2.5 min, respectively. The separation of the degradation products from both IR and LV, as well as the similarity of the UV spectra for peaks associated with IR and LV to authentic standards of each, indicates that the method is specific for both IR and LV.

Duplicate analysis of a 0.05 mg/mL IR quality control sample containing LV demonstrated that concentrations were estimated with less than 3% deviation between the observed and known concentrations of IR. The coefficient of variation on duplicate analysis of standards averaged less than 1.5% within days and less than 3% between days. These analyses indicated that the IR concentrations were measured accurately and reproducibly and that differences of 10% or more could be confidently detected with acceptable error rates.[10,14]

Duplicate analysis of a 0.20 mg/mL LV quality control sample containing IR demonstrated that concentrations were estimated with less than 0.7% deviation between the observed and known concentrations of LV. The coefficient of variation on duplicate analysis of standards averaged less than 1.6% within days and less than 0.9% between days.

Based on the separation of IR and LV from each other and from their degradation products and the

Table 2. Observed Mean Concentration (± Standard Deviation) of Irinotecan and Leucovorin in 5% Dextrose in Water Solutions Stored in Glass*

Characteristic	Scenario 1a (IR 0.56, LV 0.94)	Scenario 1b (IR 0.53, LV 0.74)	Scenario 2a (IR 0.59, LV 0.66)	Scenario 2b (IR 0.56, LV 0.27)	Scenario 3a (IR 0.32, LV 3.60)	Scenario 3b (IR 0.30, LV 0.68)
Irinotecan						
Initial concentration (mg/mL)	0.56±0.01	0.56±0.01	0.59±0.02	0.59±0.02	0.35±0.01	0.30±0.01
pH before mixing	3.12	3.12	3.06	3.06	4.02	4.02
% remaining						
At 0.5 h	99.40±2.50	98.67±0.84	99.68±0.04	99.89±0.97	95.09±3.14	98.54±1.95
At 1 h	98.12±1.56	97.84±1.64	99.69±0.20	100.10±0.76	89.08±4.83	98.00±1.36
At 24 h	92.48±0.99	92.78±0.66	96.47±1.10	97.56±2.04	77.23±4.59	95.52±1.03
Leucovorin						
Initial concentration (mg/mL)	0.91±0.02	0.73±0.00	0.68±0.01	0.26±0.00	3.65±0.11	0.62±0.05
pH before mixing	6.08	5.88	5.55	5.41	7.01	5.65
% remaining						
At 0.5 h	100.33±2.51	100.79±0.68	99.19±1.27	100.05±2.96	101.30±1.87	99.44±0.48
At 1 h	100.50±1.34	100.43±0.58	98.99±0.52	98.95±2.45	101.55±1.80	100.27±0.73
At 24 h	101.26±0.89	99.78±0.97	98.84±0.19	96.31±0.83	100.81±0.84	99.57±1.75
Mixture						
pH after mixing	5.56	5.42	5.33	4.76	6.50	5.52

*Scenario designations in column headings represent nominal concentration of each drug (mg/mL).

demonstration that concentrations of both IR and LV could be measured accurately and reproducibly (as indicated by within-day and between-day coefficients of variation), this method can be considered stability-indicating for both IR and LV.[15-17]

Physical Compatibility and Chemical Stability Studies

Physical Inspection and pH Measurements

Each individual solution of IR (nominal concentrations of 0.61 mg/mL and 0.65 mg/mL) and LV (7.20, 2.72, and 1.36 mg/mL) was initially clear and colourless. Mixing these individual solutions did not result in generation of gas, change in colour, or development of a precipitate in any of the 54 experimental solutions created for the 18 individual experiments.

The pH of each IR and LV solution used in the study (various concentrations) before mixing and the pH of each mixture (in glass) is reported in Table 2. These data show that before mixing, the pH of the LV solution was always greater than that of the IR solution. The pH of each mixture fell between the observed pH for the separate solutions, but was often driven by the component with the highest concentration. As a result, the solution containing 0.32 mg/mL IR and 3.60 mg/mL LV (treatment scenario 3a in Table 1) had the highest pH (6.50) of all mixtures.

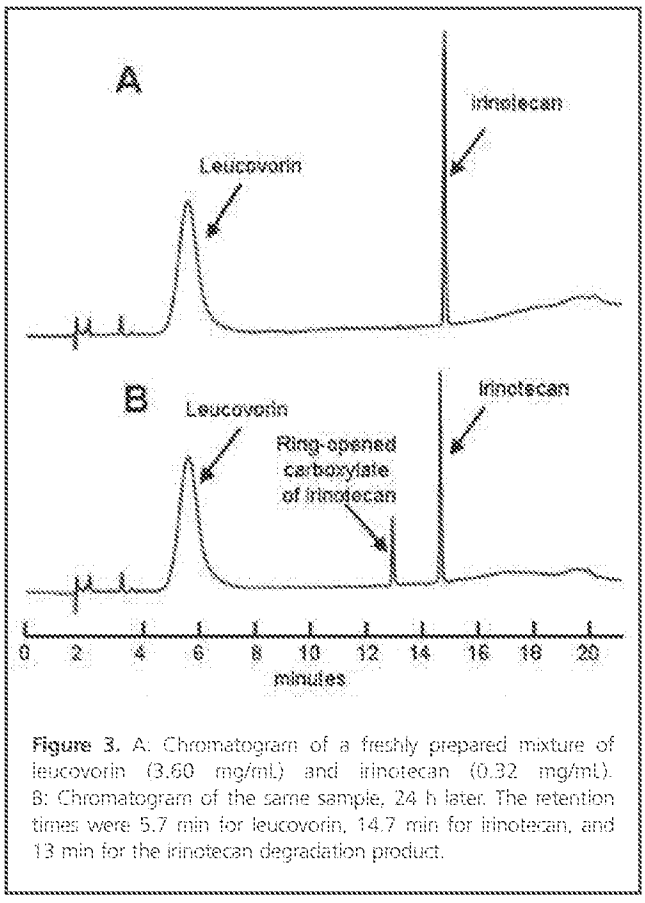

Figure 3. A: Chromatogram of a freshly prepared mixture of leucovorin (3.60 mg/mL) and irinotecan (0.32 mg/mL). B: Chromatogram of the same sample, 24 h later. The retention times were 5.7 min for leucovorin, 14.7 min for irinotecan, and 13 min for the irinotecan degradation product.

Table 3. Observed Mean Concentration (± Standard Deviation) of Irinotecan and Leucovorin in 5% Dextrose in Water Solutions stored in Polyvinyl Chloride*

Characteristic	Scenario 1a (IR 0.56, LV 0.94)	Scenario 1b (IR 0.53, LV 0.74)	Scenario 2a (IR 0.59, LV 0.66)	Scenario 2b (IR 0.56, LV 0.27)	Scenario 3a (IR 0.32, LV 3.60)	Scenario 3b (IR 0.30, LV 0.68)
Irinotecan						
Initial concentration (mg/mL)	0.65±0.03	0.55±0.01	0.47±0.12	0.54±0.00	0.31±0.00	0.34±0.00
% remaining						
At 0.5 h	99.08±0.41	98.70±0.18	99.15±0.78	99.40±0.25	91.76±0.28	99.45±1.26
At 1 h	97.50±0.27	98.10±0.19	99.42±0.89	98.82±0.04	88.69±0.67	97.03±0.34
At 24 h	92.00±0.50	92.58±0.32	96.17±0.23	97.33±0.26	78.34±0.81	95.08±0.32
Leucovorin						
Initial concentration (mg/mL)	0.87±0.03	0.70±0.02	0.68±0.02	0.26±0.00	3.55±0.01	0.66±0.01
% remaining						
At 0.5 h	101.02±1.79	99.67±2.25	99.65±1.21	99.77±0.10	103.39±2.87	98.98±1.32
At 1 h	100.52±0.86	100.94±0.69	100.62±0.79	100.05±0.19	101.83±0.39	99.78±0.58
At 24 h	100.36±1.32	100.03±1.49	99.42±1.06	99.14±0.26	101.57±0.51	100.69±5.20

*Scenario designations in column headings represent nominal concentration of each drug (mg/mL).

Table 4. Observed Mean Concentration (± Standard Deviation) of Irinotecan and Leucovorin in 5% Dextrose in Water Solutions Stored in Polypropylene–Polyethylene Copolymer Bags*

Characteristic	Scenario 1a (IR 0.56, LV 0.94)	Scenario 1b (IR 0.53, LV 0.74)	Scenario 2a (IR 0.59, LV 0.66)	Scenario 2b (IR 0.56, LV 0.27)	Scenario 3a (IR 0.32, LV 3.60)	Scenario 3b (IR 0.30, LV 0.68)
Irinotecan						
Initial concentration (mg/mL)	0.65±0.03	0.55±0.01	0.47±0.12	0.54±0.00	0.31±0.00	0.34±0.00
% remaining						
At 0.5 h	99.16±0.56	99.08±0.13	99.74±0.78	99.52±0.15	91.57±1.22	98.92±0.12
At 1 h	97.18±0.56	98.15±0.47	99.09±0.31	98.63±0.54	88.56±0.79	97.10±0.71
At 24 h	91.88±0.41	92.28±0.42	96.61±1.14	97.21±0.60	76.30±0.69	94.55±0.59
Leucovorin						
Initial concentration (mg/mL)	0.95±0.01	0.72±0.01	0.65±0.02	0.23±0.01	3.67±0.03	0.67±0.01
% remaining						
At 0.5 h	99.81±0.37	99.56±0.86	100.16±2.46	106.81±5.77	96.82±2.80	100.50±1.37
At 1 h	100.27±0.24	101.90±0.69	100.45±2.06	107.08±7.19	99.67±2.34	100.12±0.56
At 24 h	101.17±1.28	100.30±0.88	102.38±2.00	97.66±1.66	99.86±0.62	100.24±0.03

*Scenario designations in column headings represent nominal concentration of each drug (mg/mL).

Chemical Stability of Irinotecan and Leucovorin

To specifically evaluate the stability of IR and LV, HPLC was used to determine the concentrations in each experimental solution at time 0 and at 0.5 h, 1 h, and 24 h after mixing. Mean concentrations (3 determinations at each observation time) of IR and LV for solutions stored in glass, PVC, and PABs are reported in Tables 2, 3, and 4, respectively. These data show that the concentration of IR declined in all 18 experiments over the 24-h experimental period. In 5 of the 6 treatment scenarios (1a, 1b, 2a, 2b, and 3b), the mean concentration of IR was greater than 98% of the original concentration at 0.5 h and was greater than 91% of the original concentration at 24 h. The sixth treatment scenario (3a), with initial projected concentrations of IR 0.32 mg/mL and LV 3.60 mg/mL, had a more rapid degradation of IR. At 0.5 h, the mean concentration of IR was between 91.57% and 95.09%, but continued to decline (to 76.30% to 78.34% of the initial concentration) until 24 h. In these solutions, the only degradation product that was evident was the ring-opened carboxylate (Figure 3).

Analyses of these data by multiple linear regression demonstrated that there was no effect of container type ($p = 0.62$) or initial IR concentration ($p = 0.80$) on the rate of IR degradation, but there was a significant effect of initial LV concentration ($p < 0.0001$) and time ($p < 0.001$) on the rate of IR degradation. The significant effects of both time and initial LV concentration were entirely due to the loss of IR in the experimental solution containing

0.32 mg/mL IR and 3.60 mg/mL IV, in which the IR concentration degraded to 76.30% to 78.34% of the initial concentration at 24 h. It is noteworthy that the degradation of IR was not linear; IR concentration declined by approximately 12% on average in the first hour of incubation and then by a further approximately 12% over the next 23 h.

Analysis of IV concentrations by multiple linear regression demonstrated that there was no trend for a decrease in concentration and so there was no significant effect of container type ($p = 0.12$), initial IR concentration ($p = 0.80$), initial IV concentration ($p = 0.54$), or time ($p = 0.34$) over the 24-h period. The mean concentration of IV at 24 h was greater than 96% of the original concentration in all treatment scenarios.

The rapid degradation of IR observed in treatment scenario 3a was likely due to the higher pH of the solution created by high concentration of IV (Table 2). The pH dependency of IR stability was evaluated in a separate experiment undertaken as part of developing the new HPLC method. These data (Figure 2) indicate that at a pH above 7.82, IR converts rapidly to the ring-opened carboxylate. At pH 7.82, 14.9% of the initial IR concentration was lost in 30 min, whereas at pH 8.31, 74.9% of the initial IR concentration was lost in 30 min. The highest pH for any of the experimental solutions was observed for treatment scenario 3a (pH 6.50). In the pH dependency study, 3.0% of the initial IR concentration was lost in 30 min at pH 6.27 and 5.2% of the initial IR concentration was lost at pH 6.79. These results are in agreement with the percent remaining in all experiments conducted with the mixture of 0.32 mg/mL IR and 3.60 mg/L IV, in which between 4.9% and 8.4% of the inital IR concentration was lost in 0.5 h at pH 6.50.

DISCUSSION AND CONCLUSIONS

The studies reported here simulated the administration of IR and IV in most patient care areas. That is, all experimental solutions were continuously exposed to ambient fluorescent light, 3 types of containers simulating different types of tubing (PVC, PAB, and glass [control]) were used, and 6 concentration combinations representing 6 treatment scenarios (Table 1) were evaluated. PABs are made of a polypropylene–polyethylene copolymer and simulate the more rigid non-diethylhexyl phthalate PVC and polyethylene tubing sets used for administration of some drugs.

The final concentration of both drugs in the Y-site line after mixing depends not only on the concentration of the drugs in solution but also the flow rates of each solution. The concentration estimates in Table 1 do not consider bag-overfill volumes or the volume of the drug solution added to the bag and so are slightly higher than might actually be encountered in practice under similar scenarios.

Actual concentrations in clinical practice will also vary because of dose adjustments related to patients' body weight and because the infusion rate varies with calibration errors. However, the aim was to ensure that the estimated concentrations in Table 1 were closer to the concentrations likely encountered in clinical practice than those produced by the more common method of mixing equal volumes of each solution (scenarios 3a and 3b). Mixing equal volumes would yield IV concentrations 2- to 7-fold higher than those generally seen in clinical practice because of the longer infusion times and smaller bag volumes. To avoid this pitfall, numerous potential concentrations of mixtures were calculated, and concentration scenarios representing and/or encompassing concentrations likely to be observed in clinical practice were selected.

In all treatment scenarios, IR and IV were physically compatible for 24 h. The HPLC analyses of IR and IV concentrations at 0.5 h support these physical compatibility data. The mean concentrations of IV and IR at 0.5 h, as a percentage of the concentrations at time 0, were greater than 96% for IV and greater than 91% for IR in all treatment scenarios, which indicates that, based on a 10% threshold for degradation, both IR and IV were chemically stable for 0.5 h. In other words, concentrations of IR ranging from 0.30 to 0.59 mg/mL were chemically compatible with IV concentrations from 0.27 to 3.60 mg/mL for 0.5 h. Other treatment scenarios that might be used in clinical practice should have concentrations of IR and IV that fall within the ranges evaluated here. For example, if equal infusion times are used for treatment scenarios 2a and 2b, a concentration of 0.51 mg/mL for IR and 0.45 or 1.20 mg/mL for IV would be produced in the final mixuture. It can therefore be expected that the final mixed solution of IR and IV will be chemically stable at 0.5 h.

The stability of both IR and IV for 0.5 h supports the hypothesis that these 2 compounds can be administered simultaneously via Y-site connection because the contact time in the Y-site will be far less than 0.5 h. In fact, the period of contact will be less than 2 min with standard IV tubing set 81 cm (32 inches) long. Standard IV tubing 165 cm (65 inches) in length with an internal diameter of about 2.5 mm holds 9 mL of fluid (equivalent to 0.135 mL/inch or 0.055 mL/cm). Therefore, even if the Y-site is maximally separated from the site of infusion (32 inches or 81 cm) and the lowest flow rates for IR and IV are

employed (Table 1, scenario 3a), the mixing time will be limited to less than 2 min. These data also indicate that container type had no impact on stability, so either PVC or polyethylene-lined tubing could be used for Y-site infusion with IR and LV.

Data collected after 1 h and 24 h of incubation indicated that with each treatment scenario, there was a consistent and measurable decline in IR concentration. However, in 5 of the 6 treatment scenarios (1a, 1b, 2a, 2b, 3b), the concentration of IR remaining after 24 h was greater than 91% of that present at time 0. Therefore, IR remained within acceptable limits of degradation and was considered chemically stable for this time period. Treatment scenario 3a, which contained the highest concentration of LV (IR, 0.32 mg/mL; LV, 3.60 mg/mL) exhibited a higher rate of decline in IR concentration than the other 5 treatment scenarios. The mean concentration (± standard deviation [SD]) of IR remaining at 1 h, expressed as a percentage of the concentration at time 0, was between 88.56% ± 0.79% and 89.08% ± 4.83% (Tables 2–4). At 24 h the mean concentration (± SD) had further declined to 76.30% ± 0.69% to 78.34% ± 0.81% of that present at time 0. In addition to having the highest concentration of LV, treatment scenario 3a also had the highest pH (6.50) (Table 2). This relatively high pH contributed to the accelerated conversion of IR to the ring-opened carboxylate observed in treatment scenario 3a. The conversion of IR to the ring-opened carboxylate was pH-dependent (Figure 2); IR concentrations declined slowly between pH 4 and pH 6 and more rapidly above pH 6. The observation that treatment scenario 3a exhibited the most rapid decline in IR concentration should have been expected, because this was the only treatment scenario in which the pH of the mixture was greater than 6.

These data also show that the quantitative decline in IR observed in the pH dependency experiment (Figure 2) was similar to the decline observed at 0.5 h for each treatment scenario, supporting the notion that pH, possibly in combination with continuous exposure to fluorescent light,[8] is the only factor contributing to an accelerated decline in IR concentration. The decline in IR concentration in scenario 3a (Tables 2–4) resulted in mean concentrations (± SD) after 0.5 h that were between 91.57% ± 1.22% and 95.09% ± 3.14%, values that are in close agreement with concentrations remaining after 0.5 h in the pH dependency experiment (Figure 2). In the latter experiment, 96.79% and 94.82% of the IR remained at pH 6.27 and 6.79, respectively. Since these experiments did not control for exposure to light, it is impossible to separate the contribution of continuous exposure to fluorescent light from the contribution of pH to the decline in IR concentration. However, previous work by Dodds and others[3] demonstrated that the ring-opened carboxylate is a photolabile species and that photodegradation requires the presence of the ring-opened carboxylate. Nonetheless, during the stability study, analyses of IR exposed to both increasing pH and continuous light revealed only the ring-opened carboxylate product, which is produced by hydrolysis of the lactone ring that is in equilibrium with IR.[2,3] Other degradation products, produced by sodium hypochlorite oxidation or photodegradation[3] during continuous light exposure, were not observed.

The rates and proportion of the pH-dependent conversion of IR to the ring-opened carboxylate observed in this study were similar to those previously reported.[3] Both Fassberg and Stell[2] and Dodds and others[3] have demonstrated that IR is more stable in acidic solution (pH 5) than in neutral or basic solutions. Dodds and others[3] found that the photodegradation rate of IR in saline was 0.0245/h, which corresponds to a half-life of 28.28 h and a time of 4 h, 15 min to achieve 90% of the initial concentration. Commercially available IR solutions contain lactic acid, which lowers the pH and makes the product more stable[4,5] by preventing conversion to the ring-opened carboxylate (which undergoes photodegradation). The photodegradation rate of IR in 0.05 mol/L phosphate buffer at pH 5 was 0.0022/h,[3] which corresponds to a half-life of 315 h and a time of about 48 h to achieve 90% of the initial concentration. The dilution of commercial product in saline yields a solution with pH of about 3.[3] As a result, further investigations by Rivory and others[18] did not reveal significant degradation during infusions of 60 to 90 min.

Chamorey and Milano[9] have also evaluated the stability and compatibility of IR (0.36, 1.44, and 2.8 mg/mL in D5W) mixed with the L-isomer of LV (Elvorin, 0.4 and 4.0 mg/mL in D5W [Elvorin is the commercially available form of the L-isomer of LV in Europe]). The current study and the study conducted by Chamorey and Milano[9] evaluated similar concentrations of LV and IR in solutions of similar pH, and the 2 studies had similar results. However, Chamorey and Milano[9] reported a 32% loss in IR concentration immediately after mixing of a solution containing 0.36 mg/mL IR and 4 mg/mL L-LV. In contrast, in the study reported here there was little difference in the nominal and initial concentrations of IR at time 0 in any solution, including the solution containing 3.60 mg/mL LV. However, after

1.0 h the mean IR concentration had declined to between 88.56% ± 0.79% and 89.08% ± 4.83% of the concentration at time 0, and after 24 h the concentration had declined to between 76.30% ± 0.69% and 78.34% ± 0.81%. This difference in results may be explained by the fact that Chamorey and Milano[9] stored solutions at –20°C until "all samples were taken". Thus, conversion of IR to the ring-opened carboxylate might have occurred during storage at –20°C for at least 2 h or during the time required to allow the samples to thaw.

The studies reported here demonstrated conversion of IR to the ring-opened carboxylate following mixing with racemic LV. The 24-h stability data also suggest that IR (0.30 to 0.56 mg/mL) and LV (0.27 to 0.94 mg/mL) could be mixed in the same diluent bag and infused together, as suggested by Chamorey and Milano.[9] Future research should focus on evaluating additional concentrations of racemic LV between 0.94 and 3.6 mg/mL, to more precisely define the limits of LV concentration that can be used while maintaining IR stability.

In conclusion, IR and LV solutions, even those containing 3.60 mg/mL of LV, are physically compatible and chemically stable for a sufficient period of time to allow Y-site infusion, provided the period of contact (time from mixing to entry into the body) is short (less than 30 min).

References

1. Pharmacia & UpJohn Canada Inc. Irinotecan HCl trihydrate product monograph. Toronto (ON); 1999 Aug.
2. Fassberg J, Stell VJ. A kinetic and mechanistic study of the hydrolysis of camptothecin and some analogues. *J Pharm Sci* 1992;81:676-84.
3. Dodds HM, Craik DJ, Rivory LP. Photodegradation of irinotecan (CPT-11) in aqueous solutions: identification of fluorescent products and influence of solution composition. *J Pharm Sci* 1997;86:1410-6.
4. Novopharm Limited. Leucovorin calcium injection 10 mg/mL product monograph. Toronto (ON); 2000.
5. Lederle, Cyanamid Canada Inc. Lederle leucovorin calcium (calcium folinate) product monograph. Montreal (QC); 1989 Oct.
6. Lauper RD. Leucovorin calcium administration and preparation. *Am J Hosp Pharm* 1978;35:377-8.
7. Benvenuto JA, Anderson RW, Kerkof K, Smith RG, Loo TL. Stability and compatibility of antitumor agents in glass and plastic containers. *Am J Hosp Pharm* 1981;38:1914-8.
8. Smith JA, Morris A, Duafala ME, Bertino JR, Markman M, Kleinberg M. Stability of floxuridine and leucovorin calcium admixtures for intraperitoneal administration. *Am J Hosp Pharm* 1989;46(5):985-9.
9. Chamorey E, Milano G. Role of leucovorin-5FU2 and irinotecan in metastatic cancer of the colon. Physio-chemical stability of Campto® and Elvorine®. *Ther pratique hosp* 2000;11(56):2-7.
10. Dodds HM, Robert J, Rivory LP. The detection of photodegradation products of irinotecan (CPT-11, Campto, Camptosar), in clinical studies, using high-performance liquid chromatography/atmospheric pressure chemical ionisation/mass spectrometry. *J Pharm Biomed Anal* 1998;17:785-92.
11. de Bruijn P, Verweij J, Loos WJ, Nooter K, Stoter G, Sparreboom A. Determination of irinotecan (CPT-11) and its active metabolite SN-38 in human plasma by reversed-phase high-performance liquid chromatography with fluorescence detection. *J Chromatogr B Biomed Sci Appl* 1997;698:277-85.
12. Chourpa I, Riou JF, Millot JM, Lavelle F, Manfait M. Reactivity of the lactone ring of irinotecan (CPT-11) in the topoisomerase I-mediated cleavable complexes as studied by fluorescence spectroscopy [abstract]. *Proc Annu Meet Am Assoc Cancer Res* 1196;36:A2448.
13. Frieman JA, Chalmers TC, Smith H, Kuebler RR. The importance of beta, type II error and sample size in the design and interpretation of the randomized control trial. *N Engl J Med* 1978;299:690-4.
14. Stolley PD, Strom BL. Sample size calculations for clinical pharmacology studies. *Clin Pharmacol Ther* 1986;39:489-90.
15. Trissel LA. Avoiding common flaws in stability and compatibility studies of injectable drugs. *Am J Hosp Pharm* 1983;40:1159-60.
16. Trissel LA, Flora KP. Stability studies: five years later. *Am J Hosp Pharm* 1988;45:1569-71.
17. Policy for publication of chemical stability study manuscripts. *Can J Hosp Pharm* 1990;43:3-4.
18. Rivory LP, Dodds HM, Robert J. Stability of irinotecan (CPT-11) during administration to patients [abstract]. *Proc Ann Meet Am Assoc Cancer Res* 1997;38:A506.

Scott E. Walker, MScPhm, is Co-ordinator, Research and Quality Control, Department of Pharmacy and Division of Pharmacology, Sunnybrook and Women's College Health Sciences Centre, and Associate Professor, Faculty of Pharmacy, University of Toronto, Toronto, Ontario. He is also Editor of *CJHP*.

Shirley Law, DipPharmTech, is a Research Assistant in Quality Control, Department of Pharmacy, Sunnybrook and Women's College Health Sciences Centre, Toronto, Ontario.

Anitasha Puodziunas, BScPhm, BCOP, was, at the time of this study, Science Officer for Pharmacia Canada, and is now the Oncology Medical Liaison, Scientific Affairs, at Bristol-Myers Squibb Canada, Montreal, Quebec.

Acknowledgement

Funding for this study was provided by Pfizer Canada, Inc, Kirkland, Quebec.

Jpn J Clin Oncol 1998;28(1)16–19

Weekly 24-Hour Infusion of High-dose 5-Fluorouracil and Leucovorin in Patients with Advanced Colorectal Cancer: Taiwan Experience

Wei-Shu Wang[1], Po-Min Chen[1], Tzeon-Jye Chiou[1], Jin-Hwang Liu[1], Jen-Kou Lin[2], Tzu-Chen Lin[2], Wei-Shone Chen[2], Jeng-Kae Jiang[2], Chueh-Chuan Yen[1], Frank S Fan[1] and Ruey-Kuen Hsieh[1]

[1]Division of Medical Oncology, Department of Medicine and [2]Division of Colorectal Surgery, Department of Surgery, Veterans General Hospital-Taipei and National Yang-Ming University School of Medicine, Taipei, Taiwan

Between January 1994 and November 1995, 41 patients with metastatic colorectal carcinoma were enrolled in this study. All these patients had recurrent disease after a prior 5-fluorouracil based adjuvant chemotherapy or failed to achieve response by prior chemotherapy that included 5-fluorouracil. 5-Fluorouracil, 2600 mg/m^2, was administered concurrently with 100 mg/m^2 leucovorin over 24 hours of continuous intravenous infusion. The treatment was repeated every week until progressive disease was documented. Forty-one patients received a total of 810 courses of treatment. The overall response rate was 17.1% (95% confidence interval 5.6–28.6%). In two patients who achieved complete response, the liver was the metastatic site. The median survival was 18.4 months for responders and 12.6 months for non-responders. Gastrointestinal toxicities including diarrhea, stomatitis, nausea and vomiting were the major side-effects. Sixteen incidences (39.0 %) of grade 2–3 gastrointestinal toxicities were observed. One patient (2.4%) developed a grade 3 cardiac toxicity, and another one (2.4%) had a grade 2 neurotoxicity. Hematological toxicities were minimal with no evidence of severe (grade 2 or more) leukopenia or thrombocytopenia. We conclude that in patients with pretreated metastatic colorectal cancer, weekly 24-hour infusion of high-dose 5-fluorouracil and leucovorin is associated with higher efficacy and tolerable toxicity. This regimen is a good option as a second-line treatment for those whose diseases are recurrent from or refractory to prior 5-fluorouracil, and deserves a longer period of follow-up.

Key words: weekly high-dose continuous infusion – 5-fluorouracil – leucovorin – colorectal cancer

INTRODUCTION

Colorectal cancer is among the leading causes of cancer-related morbidity and mortality in Taiwan. Resection of the primary tumor is the mainstay of treatment for patients in early stages with localized disease and may offer a chance for cure, but for metastatic disease, cure is rarely achieved (1). Treatment of metastatic disease is mainly by chemotherapy. 5-Fluororuacil (5-FU) and leucovorin (LV) has remained the standard recommended chemotherapy (2). The reported response rate of 5-FU and LV in metastatic colorectal cancer varied between institutions, but generally the activity of all these regimens is limited to a response rate of about 20%, with no significant impact on survival (2).

Over the past decades, there have been numerous attempts to increase the efficacy of 5-FU by changing the dose, the schedule, or the route of administration (3). Recently, weekly 24-hour infusion of high-dose 5-FU with LV has become an important regimen in the treatment of various types of adenocarcinoma, including colorectal cancer. Ardalan et al. have conducted a phase II study of weekly 24-hour infusion of a maximal tolerable dose of 5-FU (2600 mg/m^2) and LV (500 mg/m^2) for treating advanced colorectal carcinoma (4). In their study, 22 patients received a total of 560 courses of treatment to achieve a response rate of 45% (10/22), without excessive toxicity. The response rate was higher than in other reported series. We were interested to know whether this regimen would be effective and tolerable in Chinese patients.

In this study, we report preliminary results on the efficacy and toxicity of weekly 24-hour infusion of high-dose 5-FU and LV in 41 Chinese patients with metastatic colorectal carcinoma.

Received May 9, 1997; accepted August 28, 1997

For reprints and all correspondence: Wei-Shu Wang, Division of Medical Oncology, Department of Medicine, Veterans General Hospital-Taipei, 201, Section 2, Shih-Pai Road, Taipei 11217, Taiwan

Abbreviations: 5-FU, 5-fluorouracil; LV, leucovorin; CT, computer tomographic; PS, performance status; CR, complete response; PR, partial response; SD, stable disease; PD, progressive disease; CBC, complete blood count; CEA, carcinoembryonic antigen; FdUMP, 5-fluorodeoxyuridine monophosphate; EF, ejection fraction.

SUBJECTS AND METHODS

PATIENTS

Between January 1994 and November 1995, 41 patients with metastatic colorectal carcinoma were enrolled in this study. All the patients were diagnosed as having metastatic adenocarcinoma of the colon or rectum. All of them had either recurrent disease after a prior 5-FU based adjuvant chemotherapy or failed to achieve response by prior chemotherapy that included the combination of 5-FU and LV. For a patient to be eligible, the disease had to be measurable in two dimensions by computer tomographic (CT) scan, ultrasound (lesions in liver) or chest X-ray (lesions in lung) or caliper measurement of palpable lesions elsewhere. All patients were required to have a performance status (PS) (Zubrod scale) of 2 or less (5) and to have adequate hematopoietic function as evidenced by leukocyte counts >3000/μl and platelet counts >100 000/μl. Patients with any active infection or previous history of any other malignancy were excluded from this study. Prior radiotherapy was allowed. All patients had normal serum creatinine levels. Patients' characteristics are shown in Table 1.

WEEKLY HIGH-DOSE 5-FU AND LV TREATMENT

All patients were hospitalized for treatment. Before the initiation of therapy all patients were required to have a Port-a-Cath in order to accommodate to protracted infusion. 5-FU 2600 mg/m^2 and LV 100 mg/m^2, admixed in 1000 ml 5% dextrose water, were given concurrently over 24 hours of continuous intravenous infusion with the aid of an infusion pump. We did not observe catheter blockages due to calcium LV crystals. The treatment was repeated every week. No dose escalation was allowed for either 5-FU or LV. If grade 3 hematologic or gastrointestinal toxicities were observed in any course of therapy, the 5-FU dose was reduced to 2100 mg/m^2. The treatment was continued until there was objective evidence of disease progression of intolerable toxicity, e.g. severe myelosuppression with sepsis or severe liver function impairment. All patients received a minimum of eight courses of treatment.

RESPONSE CRITERIA

Complete response (CR) was defined as complete disappearance of all known lesions documented by two separate observations at least 4 weeks apart and without the appearance of any new lesions. Partial response (PR) required at least a 50% reduction in the cross-sectional area of the indicator lesion (or sum of areas if there was more than one indicator lesion), again documented by two separate observations at least 4 weeks apart, with no individual lesion growing and no new lesion appearing. Stable disease (SD) was defined as <50% reduction or <25% increase in cross-sectional area of all measurable lesions with no appearance of new lesions for at least 4 weeks. Patients were considered to have progressive disease (PD) when any lesion grew >25% in cross-sectional area or when any new lesion appeared.

Table 1. Patients' characteristics

Characteristics	No.
No. of patients	41
Total courses of treatment	810
Age (yr)	
Median	62
Range	35–68
Sex	
Male	33
Female	8
Status	
Adjuvant	18
Refractory	23
Performance status	
0	18
1	15
2	8
Primary tumor	
Colon	29
Rectum	12
Site of metastases	
Liver only	16
Lung only	10
Liver and lung	11
Intra-abdominal, liver or lung	3
Intra-abdominal, liver and lung	1
Disease-free interval	
>6 mo	25
≥6 mo	16

Adjuvant, recurrent from a prior 5-FU based adjuvant chemotherapy; refractory, refractory to prior 5-FU based chemotherapy.

EVALUATION AND FOLLOW-UP

Before treatment, all patients underwent evaluation including a detailed history and physical examination, tumor measurement, chest X-ray, liver imaging (CT and sonogram), complete blood count (CBC), blood chemistry and carcinoembryonic antigen (CEA). All patients were asked to visit the outpatient clinic regularly for monthly physical examination and check-up of CBC, liver and renal functions and serum CEA level during treatment. Chest X-ray and sonogram of liver or CT scan of abdomen was examined every two months. Colonoscopy was performed annually. Adverse effects were evaluated according to the WHO criteria (6). Patients with CR, PR or SD remained in the protocol until progressive disease or unacceptable toxicity was documented.

RESULTS

RESPONSE TO THERAPY

The response data are summarized in Table 2. Forty-one patients who received a total of 810 courses of treatment achieved a response rate of 17.1% (2 CR, 5 PR). The 95% confidence interval is 5.6–28.6%. All responses of involved lesions were confirmed by sonogram, CT scan or chest X-ray.

Table 2. Response to chemotherapy

Response	%
CR	4.9 (2/41)
PR	12.2 (5/41)
SD	36.6 (15/41)
PD	46.3 (19/41)

CR, complete response; PR, partial response; SD, stable disease; PD, progressive disease.

Table 3. Treatment-related toxicities, graded according to WHO criteria

Toxicity	Grade				Total (%)
	1	2	3	4	
Nausea	9	2	0	0	11 (26.8)
Vomiting	4	1	0	0	5 (12.2)
Stomatitis	8	4	2	0	14 (34.1)
Diarrhea	6	5	2	0	13 (31.7)
Leukopenia	0	0	0	0	0 (0)
Thrombocytopenia	0	0	0	0	0 (0)
Hepatic	2	0	0	0	2 (4.9)
Renal	1	0	0	0	1 (2.4)
Cardiac	0	0	1	0	1 (2.4)
Neurological	0	1	0	0	1 (2.4)
Skin	0	2	0	0	2 (4.9)
Infection	0	0	0	0	0 (0)

Toxicity

Toxicities were evaluated and graded according to the WHO criteria (Table 3). These toxicities were generally tolerated by the majority of patients. Gastrointestinal toxicities including nausea, vomiting, stomatitis and diarrhea were the major side-effects, but they were generally tolerable and non life-threatening. Hematological toxicities were minimal with no evidence of severe (grade 2 or more) leucopenia or thrombocytopenia. Two patients developed a transient painful fissuring erythroderma over their palms and soles (the hand-foot syndrome) (7). Mild liver and renal toxicities were occasionally found. One patient developed a grade 3 cardiac dysfunction with clinical manifestation of shortness of breath and cardiomegaly after eight courses of treatment. Another patient developed a transient grade 2 neurotoxicity after 5 courses of treatment with clinical manifestation of somnolence and confusion.

Survival

The median survival was 18.4 months for the responders and 12.6 months for non-responders. Patients who had recurrent disease after a prior 5-FU based adjuvant chemotherapy had a medial survival of 14.0 months, which is similar to 12.9 months for those whose diseases failed to achieve response to prior 5-FU based chemotherapy.

DISCUSSION

Since its discovery by Heidelberger et al. about 30 years ago (8), 5-FU remains the most extensively studied drug and is considered the standard treatment in metastatic colorectal cancer. However, the optimal dose scheduling of 5-FU is still controversial. The most popular method of administration is monthly intravenous (iv) bolus injection, but it is generally accepted that iv bolus injection of 5-FU will produce an objective response rate of only 15–20% in metastatic colorectal cancer (9). These reports were disappointing and prompted us to explore different dose schedules of 5-FU to try to improve the response.

Over the past decades, there have been numerous attempts to increase the efficacy of 5-FU by changing the dose, the schedule or the route of administration. Several non-randomized trials have reported improved response rates when 5-FU is given as a continuous intravenous infusion (10,11). The reported response rates of these trials ranged from 31% to 53%. In a prospective randomized trial comparing continuous infusional 5-FU with a conventional bolus schedule, a higher response rate was achieved in the infusional arm (30% versus 7%, $P < 0.001$) (12).

A number of studies have indicated that the anti-tumor activity of 5-FU can be enhanced if the intracellular pools of reduced folates are expanded by adding LV (2). Enhanced activity of 5-FU in the presence of reduced folates is most probably a result of stabilization of the ternary complexes between 5-fluorodeoxyuridine monophosphate (FdUMP), thymidylate synthase and 5,10-methylenetetrahydrofolate, which occurs in the presence of 5–10 μmol/l of extracellular folate (4). Houghton et al. have shown that the optimal manner for administering LV is by intravenous infusion over several hours (13). In a phase I study conducted by Ardalan et al., the maximum tolerated dose of 5-FU (2600 mg/m^2) and LV (500 mg/m^2), infused concurrently over 24 hours every week, was determined (14). They then conducted a phase II study employing 5-FU 2600 mg/m^2 and LV 500 mg/m^2 over 24 hours intravenous infusion every week in 22 patients with advanced colorectal carcinoma (4). In their study, an overall response rate of 45%, including 3 CR, was noted. Several papers have reported that 5-FU and LV achieved only poor response rates in pretreated cases. In comparison with these papers, Ardalan's study showed a significantly higher response rate, which interested us.

In our study, 41 patients received a total of 810 courses of weekly 24-hour continuous infusion of 5-FU 2600 mg/m^2 and LV 100 mg/m^2. Two (4.9%) achieved CR while five (12.2%) showed PR. The overall response rate was 17.1%. In comparison with Ardalan's study, our study was not associated with a higher response rate in metastatic colorectal cancer. The probable reason is that all our patients had been previously treated with 5-FU. They had either recurrent diseases after prior 5-FU based adjuvant chemotherapy or failed to achieve response by prior therapy that included 5-FU. In Ardalan's study, only 10 patients had received 5-FU before entering the program, the remaining 12 being 5-FU naive. However, in our study, there were still 7 patients showing a response to the regimen, including 2 CR. The data suggest that weekly 24-hour infusion of high-dose 5-FU and

LV will produce a considerable response rate in pretreated metastatic colorectal cancer, and this is considered a good option for second-line treatment for pretreated metastatic colorectal cancer.

The cardiac toxicity of 5-FU was first identified by Dent and McColl in 1975 with the clinical manifestation of angina (15). Labianca et al. have reported a survey of 1083 patients receiving 5-FU; cardiotoxicities were found in 1.1% of all patients and in 4.6% of patients with prior heart diseases (16). 5-FU related cardiotoxicities, including precordial pain, ECG ST-T wave changes, acute myocardial infarction, arrhythmia, ventricular dysfunction and cardiac failure have been reported (17). In our study, a 48-year-old male patient without prior history of heart disease developed a grade 3 cardiac dysfunction with clinical manifestations of chest tightness and shortness of breath after eight courses of treatment. The ECG was not unusual but the echocardiogram revealed global ventricular dysfunction and four-chamber dilation. The chest X-ray showed profound cardiomegaly. The ejection fractions (EFs) of left and right ventricles were 43% and 32% respectively. Chemotherapy was discontinued and medical treatment for heart symptoms included prescription of oxygen and inotropic agents. After 2 weeks of treatment, the symptoms and signs of shortness of breath improved but cardiomegaly persisted and the EFs of both ventricles were 45% and 38% respectively, still below the normal limit. The patient was followed up at our out-patient department for 6 months; the symptoms of shortness of breath persisted and cardiomegaly with reduced EF was still noted.

5-FU related neurotoxicity is relatively rare. Neurological complications, including reversible somnolence, upper motor neuron signs, cerebellar ataxia, acute confusion and pyramidal tract signs may develop in <5% of patients receiving 5-FU (18). The biochemical basis for neurological toxicity secondary to 5-FU has not been elucidated. Previous reports have suggested that this toxicity may be due to further metabolism of the 5-FU catabolite 2-fluoro-beta-alanine to fluoroacetate and fluorocitrate, which are known neurotoxins (19). However, actual formation of fluoroacetate and fluorocitrate from 5-FU have not been documented. Acute confusion caused by 5-FU has been reported. Yeh et al. have reported a patient receiving 5-FU 2250 mg/m^2 and LV 500 mg/m^2 who developed deep coma, upward gaze and loss of verbal and motor response for about 40 hours (20). In our study, a 64-year-old male patient developed a transient neurotoxicity with clinical manifestations of confusion and somnolence on the fifth course of treatment. Physical examination revealed neither focal neurological symptoms nor sensory or motor function impairment. The pupils were isocoric with prompt light reflex. No pathologic reflex was identified. Oxygen was given via a nasal canula at the rate of 3 liters per minute. The status of confusion and somnolence persisted for about 6 hours, and recovered spontaneously without any neurological sequelae. No further neurological symptoms developed following subsequent treatments. In our study, it seemed that high-dose 5-FU related neurotoxicity was relatively rare, and tolerable in patients with metastatic colorectal cancer.

According to our study, in patients with pretreated metastatic colorectal cancer, weekly high-dose continuous infusion of 5-FU and LV is associated with a relatively higher efficacy and tolerable toxicity. This regimen is a good option as a second-line treatment for those who are recurrent from, or refractory to, prior 5-FU based chemotherapy, and deserves a longer period of follow-up.

Acknowledgments

This work was kindly supported by a grant from the Yen Tjing-Ling Medical Foundation.

References

1. Edler L, Heim ME, Quintero C, Brummer T, Queisser W. Prognostic factors of advanced colorectal cancer patients. *Eur J Cancer Clin Oncol* 1986;22:1231–7.
2. Erlichman C, Fine S, Wong A, Elhakim T. A randomized trial of fluorouracil and folinic acid in patients with metastatic colorectal carcinoma. *J Clin Oncol* 1988;6:469–75.
3. Buroker TR, Moertel CG, Fleming TR. A controlled evaluation of recent approaches to biochemical modulation or enhancement of 5-fluorouracil therapy in colorectal carcinoma. *J Clin Oncol* 1985;3:1624–31.
4. Ardalan B, Chua L, Tian EM, Reddy R, Sridhar K, Benedetto P, et al. A phase II study of weekly 24-hour infusion with high-dose fluorouracil with leucovorin in colorectal carcinoma. *J Clin Oncol* 1994;9:625–30.
5. Zubrod CG, Schneiderman M, Frei E, Brindley C, Gold GL, Schnider B. Appraisal of methods for the study of chemotherapy of cancer in man: comparative therapeutic trial of nitrogen mustard and triethylene thiophosphoramide. *J Chron Dis* 1960;11:7–33.
6. Miller AB, Hoogstraten B, Staquet M, Winkler A. Reporting results of cancer treatment. *Cancer* 1981;47:207–14.
7. Lokich JJ, Moore C. Chemotherapy-associated palmar-plantar erythrodysesthesia syndrome. *Ann Intern Med* 1984;101:798–800.
8. Heidelberger C, Chaudhari NK, Danneberg P. Fluorinated pyrimidine. A new class of tumor-inhibitory compounds. *Nature* 1957;179:663–6.
9. Petrelli N, Douglass Jr HO, Herrera L. The modulation of fluorouracil with leucovorin in metastatic colorectal carcinoma: a prospective randomized phase III trial. *J Clin Oncol* 1989;7:1419–26.
10. Seifert P, Baker LH, Reed ML. Comparison of continuously infused 5-fluorouracil with bolus injection in the treatment of patients with colorectal adenocarcinoma. *Cancer* 1975;36:123–8.
11. Shah A, MacDonald W, Goldie J, Gudauskas G, Brisebois B. 5-FU infusion in advanced colorectal cancer: a comparison of three dose schedules. *Cancer Treat Rep* 1985;69:739–42.
12. Lokich JJ, Ahlgren JD, Gullo JJ, Philips JA, Fryer JG. A prospective randomized comparison of continuous infusion fluorouracil with a conventional bolus schedule in metastatic colorectal carcinoma. *J Clin Oncol* 1989;7:425–32.
13. Houghton JA, Williams LG, Siebold SN. Relationship between dose rate of [6RS] leucovorin administration, plasma concentrations of reduced folates, and pools of 5, 10-methylenetetrahydrofolates and tetrahydrofolates in human colon adenocarcinoma xenografts. *Cancer Res* 1990;50:3493–502.
14. Ardalan B, Huessin A, Skaver L. Chemotherapy of advanced carcinoma with 5-fluorouracil with leucovorin [abstract]. *Proc Am Coc Clin Oncol* 1989;8:116.
15. Dent R, McColl I. 5-Fluorouracil and angina. *Lancet* 1975;1:347–8.
16. Labianca R, Beretta G, Clerici M, Fraschini P, Luporini G. Cardiac toxicity of 5-fluorouracil: a study of 1083 patients. *Tumori* 1982;68:505–10.
17. Freeman NJ, Costanza ME. 5-Fluorouracil-associated cardiotoxicity. *Cancer* 1988;61:36–45.
18. Lynch HT, Droszcz CP, Albano WA, Lynch JF. "Organic brain syndrome" secondary to 5-fluorouracil toxicity. *Dis Colon Rectum* 1981;24:130–1.
19. Koenig H, Patel A. Biochemical basis for fluorouracil neurotoxicity, the role of Krebs cycle inhibition by fluoroacetate. *Arch Neurol* 1970;23:155–60.
20. Yeh KH, Cheng AL. Acute confusion induced by a high-dose infusion of 5-fluorouracil and folinic acid. *J Formos Med Assoc* 1994;93:721–3.

Available online at www.sciencedirect.com

ScienceDirect

journal homepage: http://ees.elsevier.com/ajps/default.asp

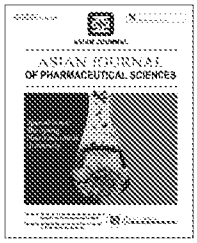

Original Research Paper

Active loading liposomal irinotecan hydrochloride: Preparation, in vitro and in vivo evaluation

Hongyan Wei[a], *Juan Song*[a], *Hao Li*[b], *Yang Li*[b], *Shanshan Zhu*[a], *Xiaodan Zhou*[a], *Xiwen Zhang*[a], *Li Yang*[a,*]

[a] *School of Pharmacy, Shenyang Pharmaceutical University, Shenyang, China*
[b] *Shenyang Shuangding Pharmaceutical Co., Ltd., Shenyang, China*

ARTICLE INFO

Article history:
Received 19 August 2013
Received in revised form
14 October 2013
Accepted 29 October 2013

Keywords:
Irinotecan hydrochloride
Liposomes
Transmembrane ammonium salts gradient
Pharmacokinetics
Cytotoxicity

ABSTRACT

The aim of the present study was to investigate the effect of various transmembrane ammonium salt gradients and different lipid composition on the loading efficiency of liposomal formulations of irinotecan hydrochloride (CPT-11), their behavior in vivo and cytotoxicity. Among ammonium salts studied, ammonium sulfate was successfully used to load CPT-11 into liposomes with the highest encapsulation efficiency. Subsequently, liposomal CPT-11 with different lipid composition was prepared by ammonium sulfate gradient method. CPT-11 can be loaded to a level over 90% into liposomes composed of soybean phospholipids/cholesterol (SPC-L) or hydrogenated natural soybean phospholipids/cholesterol (HSPC-L). In vitro release profiles were also investigated, indicating that HSPC-L had a lower release than that in SPC-L. In vivo, encapsulation of CPT-11 in both liposomal formulations showed higher area under the curve (AUC), a lower rate of clearance (CL) and smaller volume of distribution for CPT-11 than those of irinotecan hydrochloride solution (CPT-11-S). However, CL and AUC of 7-ethyl-10-hydroxycamptothecin (SN-38) were moderately improved in HSPC-L group. Based on the results of comparative pharmacokinetics of liposomal CPT-11 with different lipid composition, the in vitro cytotoxicity of HSPC-L was evaluated with human tumor cell. The result indicated that liposomal CPT-11 showed a great enhancement in vitro cytotoxicity. The results suggested that entrapment of CPT-11 in liposomes especially in those with high phase-transition temperature lipid by ammonium sulfate gradient would be a promising formulation with a better in vivo behavior.

* *Corresponding author*. Department of Pharmaceutics, School of Pharmacy, Shenyang Pharmaceutical University, 103 Wenhua Road, Shenyang 110016, China. Tel./fax: +86 024 23986349.
E-mail address: pharm305@126.com (L. Yang).

Peer review under responsibility of Shenyang Pharmaceutical University

Production and hosting by Elsevier

1818-0876/$ – see front matter © 2013 Shenyang Pharmaceutical University. Production and hosting by Elsevier B.V. All rights reserved.
http://dx.doi.org/10.1016/j.ajps.2013.10.006

1. Introduction

Irinotecan (CPT-11), a topoisomerase I inhibitor, has excellent antitumor activity against a variety of human xenografts [1–4]. The clinical introduction of CPT-11 had a significant impact on cancer treatment, particularly colorectal adenocarcinoma and small-cell lung cancers [5–9]. However CPT-11 is discovered to have serious side effects such as myelosuppression and gastrointestinal disorders (mainly diarrhea), which are recognized as constituting dose-limiting toxicity for this drug [10,11]. CPT-11 has a complicated pharmacologic profile and is extensively metabolized **in vivo** to yield a number of derivatives including the potent metabolite SN-38 which has 100- to 1000-fold more potent antitumor. Furthermore, it is worth mentioning that CPT-11 requires conversion to SN-38 for optimal activity yet must avoid inactivation via simple hydrolysis of the requisite lactone configuration to an inactive carboxylate. After intravenous administration of free CPT-11, less than 5% of CPT-11 is converted to SN-38, mainly in the liver. Use of drug delivery technologies focused on strategies to stabilize the lactone ring of CTP-11 [12,13]. Therefore, it is desired to find an effective drug delivery system to reduce toxicity and preserve the active form of the drug.

Recent reports have asserted that the liposomal formulations of CPT-11 can reduce the clearance of CPT-11 in vivo and increase antitumor activity [14,15]. The liposomal CPT-11 stabilized the lactone ring of CTP-11 as well. The physicochemical characteristics of CPT-11 make it amenable to efficient encapsulation in pharmaceutically viable liposome systems. CPT-11 can be trapped into liposomes with high encapsulation efficiency by pH-gradient, however, the acidified liposome can introduce instability by hydrolyzing lipid at acidic pH during long-term storage. Recently, a loading method was developed using copper adjusted to neutral pH with triethanolamine (TEA) without generation of a pH-gradient [16,17], whereas there is a possibility that serum copper causes systemic toxicity [18–20].

The transmembrane ammonium salts gradient approach differs from most other chemical approaches used for remote loading of liposomes, since it neither requires preparation of the liposomes in acidic pH, nor to alkalinize the extraliposomal aqueous phase. The stability of the ammonium ion gradient is related to the low permeability of its counterion, the anion which also stabilizes CPT-11 accumulation for prolonged storage periods. It can eliminate systemic toxicity caused by metal ion and load CPT-11 into liposomes with high encapsulation efficiency.

Now we developed a transmembrane ammonium ion gradient extensively in loading the amphipathic weak bases into liposomes to achieve high encapsulation efficiency. As for this method, we investigated the effect of different lipid composition and various transmembrane ammonium salt gradients on the loading efficiency of liposomal formulations. Characterizations of prepared liposomes in vitro were mainly measured. Meanwhile, comparative pharmacokinetics of CPT-11 liposomal formulations and CPT-11 injection (Sol) in rats were carried out. Nevertheless, few published reports have investigated in depth the pharmacokinetics of liposomal CPT-11 encapsulated by ammonium salt gradient method. Also, the study on in vitro cytotoxicity of liposomal CPT-11 was conducted.

2. Materials and methods

2.1. Materials

CPT-11 and camptothecin were obtained from Chengdu Lanbei Plant Chemical Science and Technology Co., Ltd (Chengdu, China). SN-38 was bought from Shanghai Junjie Biotechnology Co., Ltd (Shanghai, China). Hydrogenated natural soybean phospholipids (HSPC) and soybean phospholipids (SPC) were purchased from Lipoid Co. (Germany). All other reagents were of analytical grade and used as received.

2.2. Animals

Wistar male rats weighting between 180 and 220 g were used for pharmacokinetic study. The animals were provided by Experimental Animal Center of Shenyang Pharmaceutical University (Shenyang, China). All experimental procedures were carried out in accordance with the guidelines of the Experimental Animal Care and Use Committee of Shenyang Pharmaceutical University. The rats were fasted overnight before the experiments and water was available *ad libitum* throughout the experiments.

2.3. Synergistic effect of partition coefficient and different salt gradients on the loading efficiency of CPT-11 into liposomes

1-Octanol was used to represent the biomembrane. The partition coefficients of CPT-11 between 1-octanol and salt solutions at 25 °C were determined by the shake-flask method. Various salt solutions (200 mM), including ammonium salts of sulfate ($(NH_4)_2SO_4$), phytate (NH_4-PA), edetate (ETDA-2NH_4), pyrophosphate (NH_4PO_3), polyphosphate (NH_4-APP), chloride (NH_4Cl), citrate (NH_4-CA), and acetate (NH_4-AC), triethanolammonium salts of phytate (TEA-PA) and citrate (TEA-CA), and copper sulfate ($CuSO_4$), were investigated in this study. 1-Octanol and salt solution were co-saturated with each other for 24 h at 25 °C prior to use. 1-Octanol (4 volumes) and salt solution containing irinotecan (1 mg/ml) (1 volume) were mixed in the screw-capped glass scintillation vials and equilibrated under constant shaking at 25 °C for 24 h. The aqueous phase was then separated by centrifuging at 3000 rpm for 10 min and the concentration of CPT-11 in this phase was analyzed by HPLC. The 1-octanol/salt solution partition coefficients for CPT-11 were calculated.

The solutions of ammonium salts of ETDA-2NH_4, NH_4PO_3, NH_4-APP, NH_4-PA, and NH_4-CA were prepared by titration of edetic acid, pyrophosphoric acid, polyphosphoric acid, phytic acid, and citric acid solutions with concentrated ammonia and diluted to a final concentration of 200 mM, respectively. Also, the solutions of triethanolammonium salts of TEA-PA and TEA-CA were prepared by titration of phytic acid and citric acid solutions with TEA and diluted to a final concentration of

200 mM, separately. The rest salt solutions were prepared by dissolving corresponding commercial salts in water.

Meanwhile, various salts mentioned above were used to prepare CPT-11 liposomes by transmembrane salt gradient (shown in section 2.4) and encapsulation efficiency measurements were performed as described in section 2.5.2.

2.4. Preparation of CPT-11 containing liposomes

Lipids (SPC/Chol or HSPC/Chol) were dissolved in chloroform in a round bottom flask at the required ratio and dried to form a thin film under reduced pressure on a rotary evaporator, which was placed in a high vacuum to remove any residual solvent. Subsequently, the lipid films were hydrated with salt solution studied above to achieve multilamellar vesicles (MLVs) with a final lipid concentration of 100 mg/ml. The hydrated temperature of SPC/Chol or HSPC/Chol is 40 °C and 55 °C respectively. Following MLVs were sonicated by a probe tip sonicator and then passed through the filter of 0.22 μm pore size, to thereby prepare large unilamellar vesicles (LUVs). CPT-11 encapsulation into LUVs was achieved by remote loading method as followed: the external aqueous phase of LUVs was exchanged, using Sephadex G-50 size exclusion chromatography, with a 10 mM histidine/10% sucrose solution. The preformed liposomes were produced. The CPT-11 solution was added to the preformed liposomes and incubated at 60 °C for 10 min. After introduction, the sample was cooled in ice for 15 min. The liposome dispersions were passed through a 0.22 μm membrane to eliminate any microbes and then stored at 4–8 °C.

2.5. Characteristics of liposomal CPT-11

2.5.1. Particle size measurement

The particle size of prepared liposomes was measured by dynamic light scattering using NICOMP 380 submicron particle size analyzer (PSS, Santa Barbara, CA, USA) with a scattering angle of 90°. The samples were diluted with physiological saline to suitable optical density value prior to measurement.

2.5.2. Encapsulation efficiency measurement

The separation of liposomes from free CPT-11 was performed by size exclusion chromatography using a Sephadex G-50 column. After separation, the amount of CPT-11 in liposomes was determined at 370 nm by ultraviolet spectrophotometer (Unicom Instrument Co., Ltd, China) after lysis of the liposomes with Triton X-100. Then the total amount of CPT-11 in liposomal suspension was assayed by the same method mentioned above. The encapsulation efficiency was calculated.

2.5.3. In vitro release experiments

Because of the easy conversion of CPT-11 into carboxylate form in neutral medium, PBS with pH 5.0 was chosen as the release medium in release experiments in vitro. The release experiments were carried out in an isotonic PBS buffer with pH 5.0 at 37 °C. Briefly, 2.5 ml HSPC-L (equivalent to 10 mg CPT-11) was placed in a dialysis membrane bag with a molecular weight cut-off of 10 kDa, and immersed in 500 ml of PBS medium. The entire system was kept at 37 °C and stirred at a rate of 100 rpm. At predetermined time intervals, 3 ml of samples were collected, and the amounts of released CPT-11 from liposomes were determined at 370 nm by ultraviolet spectrophotometer, and the accumulated release rate was calculated. Each release experiment was run three times. The release experiment of SPC-L was conducted by the same method. Bring into comparison, the release of CPT-11 solution from the dialysis bag under the same conditions was also evaluated. The zero order kinetic equation, first-order kinetic equation, Higuchi's equation, and Peppas's equation were applied to fit release data.

Simultaneously, the release experiment of HSPC-L with rat plasma was investigated. The release experiment of CPT-11 solution with rat plasma was also conducted as control group. Briefly, equal volumes of the sample and rat plasma were mixed prior to the experiments. Subsequently, experiments were carried out according to the method mentioned above, except that the amounts of released CPT-11 from liposomes were determined by HPLC.

2.5.4. Conversion of liposomal CPT-11 to SN-38 in vitro

CPT-11 liposomes and rat plasma (1:8, v/v) were mixed together and incubated at 37 °C. At indicated time points, the concentration of SN-38 was evaluated by HPLC. The conversion rate was calculated by the molar ratio of SN-38 to CPT-11 (initial molar). The conversion of CPT-11 solution to SN-38 was also investigated. The experiments were repeated three times.

2.6. Pharmacokinetic study of CPT-11 liposomes

2.6.1. Analysis of CPT-11 and SN-38 in plasma

A simple HPLC method with fluorescence detection was developed for the determination of CPT-11 and SN-38 in rat plasma. The HPLC system (Jasco Corporation, Japan) consisted of PU-1580 pump with L-7485 fluorescence detector (Hitachi Co., Japan). HPLC separation was performed in a stainless-steel Diamonsil C_{18} column (150 × 4.6 mm I.D.; 5 μm particle size; Dikma) and the column temperature was maintained at 30 °C. The mobile phase consisted of acetonitrile-50 mM disodium hydrogen phosphate (30:70, v/v) containing 5 mM heptanesulphonate, adjusted to pH 3.0 with orthophosphoric acid. The flow-rate was set at 1.0 ml/min and the injection volume was 10 μl. The excitation wavelength was set at 556 nm, and the emission wavelength was 380 nm. Both concentrations of CPT-11 and SN-38 were calculated from the ratio of their peak areas to that of the I.S. Additionally, linearity, extraction recovery, precision and accuracy were carried out in method validation. The working solutions of CPT-11, SN-38 and CPT (I.S.) were prepared according to Hidetaka Sumiyoshi et al. [21].

2.6.2. Drug administration and sample preparation

Wistar rats were randomly divided into three groups, the HSPC-L, SPC-L, and Sol group and each group containing five rats. Each group was administrated at a dose of 20 mg/kg via the tail vein. After dosing, blood samples were collected at predetermined time intervals. Plasma was separated immediately by centrifugation with low temperature and 100 μl was collected for analysis by HPLC. Briefly, 100 μl I.S. solution (CPT, 1 μg/ml) and 300 μl acidified methanol (methanol-hydrochloride (9:1), v/v) were added to 100 μl plasma sequentially. All solutions were cooled in

ice before addition. Samples were then vortex-mixed for 1 min and separated by centrifugation at 14,000 rpm for 10 min. Finally, the 10 μl supernatant was injected into the HPLC system.

2.6.3. Data analysis

The data were analyzed by DAS version 2.0 software (Mathematical Pharmacology Professional Committee of China, Shanghai, China). The main pharmacokinetic parameters were calculated. A statistical comparison of the pharmacokinetic parameters was conducted using Student's *t*-test and one-way analysis of variance (ANOVA). The significance level was set to be 0.05.

2.7. In vitro cytotoxicity

Hela (cervical), Hos (osteosarcoma), BGC-823 (stomach), MCF-7 (breast) were used to investigated the in vitro cytotoxicity of liposomal CPT-11. The cells were maintained in RPMI1640 culture medium (Hos in MEM) in tissue culture flasks in a humidified incubator at 37 °C in an atmosphere of 95% air and 5% CO_2. Medium was changed 3 times a week and cells were passaged using trypsin/EDTA. For dose-dependent cytotoxicity assays, Cells were seeded in 96-well plates at 3000 cells/well with 3 replicates and pre-incubated for 24 h. Media were replaced with fresh medium. And then predetermined amounts of CPT-l1 and liposomal CPT-11. The in vitro cytotoxicities of CPT-l1 and liposomal CPT-11 were determined using MTT assay.

3. Results and discussion

3.1. Synergistic effect of partition coefficient and different salt gradients on the loading efficiency of CPT-11 into liposomes

Generally, it was considered that the partition coefficient of drug in 1-octanol and water (P-value) is an index to estimate whether the drugs can be encapsulated in liposomes easily or not. The hydrophilic (Log $P < -0.3$) or lipophilic (Log $P > 4.5$) drugs can be encapsulated in liposomes successfully and show the stable physicochemical characteristics [22]. Though the Log *P* octanol/water for CPT-11 was lower than −0.3 (showed in Table 1), CPT-11, a drug of amphipathic weak base, can not be trapped into liposomes with high encapsulation efficiency by passive loading method. As the partition coefficient of amphipathic weak base between 1-octanol and water was prone to be influenced by the pH and ionic strength of medium. Thus, CPT-11 was a good candidate to be trapped into liposomes by remote loading methods. The octanol/medium partition coefficient and state of the drug in intraliposomes may serve as crucial factors affecting the loading efficiency of drug into liposomes [23,24]. Thus, the effect of octanol/salt solution partition coefficient for CPT-11 and type of anion of salt on the encapsulation efficiency of CPT-11 liposomes were both investigated in this study.

As shown in Table 1, the Log partition coefficient (Log *P*) values for CPT-11 ranging from 0.21 to 1.50, indicating that the sort of salt solution could affect on the octanol/salt solution partition coefficient. Additionally, the Log *P* for CPT-11 in octanol/ammonium sulfate solution was the smallest, and the encapsulation efficiency was the highest. Whereas, no regular relationship was observed between the Log *P* values and the encapsulation efficiency. It was suggested that partition coefficient for CPT-11 was not the only factor affecting the encapsulation efficiency of liposomes in remote loading method. Ammonium salt anion, another factor, was found to influence on the encapsulation efficiency and the leakage of CPT-11 liposomes.

The role of ammonium salt anion is not only loading the amphipathic weak base but rather to control the stability of loading and the release rate of the amphipathic weak base from the liposomes to the external aqueous phase. Two major factors may influence the role of the ammonium salt anion. Firstly, their ability to induce precipitation/crystallization/gelation in the intraliposome aqueous phase, and secondly, their effect on the membrane/buffer or 1-octanol/buffer partition coefficient of the amphipathic weak base [24]. Among low molecular weight anions (inorganic and organic) used to achieve ammonium ion-drive loading, the order of loading stability for most amphipathic weak bases studied is sulfate > citrate > phosphate > chloride > glucuronate [25,26]. However, the results (showed in Table 1) in this study demonstrated that the order of loading stability for CPT-11 was sulfate > EDTA > phosphate > chloride > citrate > acetate, which might be concerned with the property of the drug.

On the other hand, the encapsulation efficiency of liposomes prepared by triethanolammonium salts gradient was

Table 1 – The octanol/aqueous solution partition coefficients for CPT-11.

Octanol/aqueous solutions	Partition coefficients (P)	Log P	Encapsulation efficiency (%)
Octanol/ammonium polyphosphate	31.27	1.50	81.67
Octanol/ammonium pyrophosphate	21.97	1.34	64.39
Octanol/*ammonium phytate*	15.84	1.20	84.50
Octanol/ammonium chloride	10.16	1.01	79.18
Octanol/ammonium EDTA	9.91	0.996	87.50
Octanol/ammonium citrate	8.57	0.93	16.20
Octanol/phytic acid (adjust pH to 6.5 with TEA)	7.26	0.86	4.16
Octanol/ammonium acetate	5.76	0.76	4.38
Octanol/citric acid (adjust pH to 6.5 with TEA)	4.64	0.67	2.42
Octanol/citric acid (adjust pH to 6.5 with TEA)	4.64	0.67	2.42
Octanol/$CuSO_4$	1.72	0.24	80.53
Octanol/ammonium sulfate	1.63	0.21	90.42
Octanol/water	0.355	−0.45	–

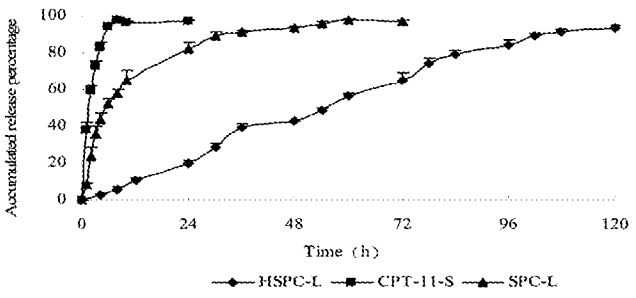

Fig. 1 – Release profiles of CPT-11 from SPC-L, HSPC-L and CPT-11-S in PBS (pH 5.0) (n = 3, mean ± SD).

much lower than that by ammonium salts. This could be attributed to the different permeability coefficients of the neutral ammonia and TEA. The higher permeability coefficient of neutral ammonia leads to fast diffusion of the NH_3 to the extraliposomal medium and a more stable pH-gradient is formed [27]. Therefore, transmembrane ammonium ion gradient was used to entrap the CPT-11 into liposomes.

Furthermore, high encapsulation efficiency (80.53%) of CPT-11 liposomes can be also obtained by transmembrane copper sulfate gradient. The reasons may be as follows: the lower solubility of the CPT-11 sulfate salt formed in the intraliposomal aqueous phase; the CPT-11 can complex the transition metal copper and then such complexation can promote drug loading into liposomes [28]. However, the toxicity of transition metal was inscrutable in vivo.

Base on these observations, lower octanol/salt solution partition coefficient and lower permeability coefficient of the anion through lipid bilayers were crucial factors in obtaining intraliposomal accumulation of CPT-11. An additional reason for having stable CPT-11 accumulation is the lower solubility of the CPT-11 salt formed in the intraliposomal aqueous phase. The Log P for CPT-11 in octanol/ammonium sulfate solution was the smallest, and the encapsulation efficiency was the highest. Therefore, transmembrane ammonium sulfate gradient method was chosen to prepare the CPT-11 liposomes. The encapsulation efficiency of CPT-11 liposomes in this study could reach over 90%.

3.2. *Encapsulation efficiency and particle size distribution of liposomes*

CPT-11, a drug of amphipathic weak base (pKa = 8.1), can be trapped into liposomes with high encapsulation efficiency by remote loading methods including pH-gradient, transmembrane ammonium ion gradient, and transition metal ion gradient [29–32]. Because of some disadvantages in pH-gradient and metal ion gradient [28,33], transmembrane ammonium ion gradient has been developed extensively in loading the amphipathic weak bases into liposomes to achieve high encapsulation efficiency. In this paper, transmembrane ammonium ion gradient was used to entrap the drug into liposomes.

The encapsulation efficiency of SPC-L and HSPC-L was 91.68% and 95.23%, respectively. It is thus clear that CPT-11 can be trapped into liposomes with high encapsulation efficiency by transmembrane ammonium ion gradient method. The mean diameter of SPC-L and HSPC-L possessed 92.2 ± 45.9 nm, 98.3 ± 52.2 nm, individually, measured by dynamic light scattering.

3.3. *In vitro release experiments*

Accumulated release profiles of CPT-11-S, SPC-L, and HSPC-L were shown in Fig. 1. It could be achieved from the profiles that the accumulated release percentage of CPT-11-S reached 83.13 ± 2.77% at 4 h, while it demonstrated merely 43.57 ± 3.87% and 2.68 ± 0.55%, respectively, for SPC-L and HSPC-L. The presence of the dialysis bag did not significantly affect the release rate of CPT-11. It was obvious that the release of CPT-11 from SPC-L was faster than that from HSPC-L, which could be due to the lower phase-transition temperature of SPC than that of HSPC. It was evident that HSPC-L has a sustained release in vitro.

The accumulated release profiles of CPT-11-S and HSPC-L, both with rat plasma, were shown in Fig. 2. A quicker release behavior of CPT-11 was observed in HSPC-L with rat plasma when compared with that in HSPC-L with PBS. It was thus evident that plasma could accelerate the release of CPT-11 from liposomes. The biological fate of liposomes might be affected by plasma factors. As various plasma components could influence the stability of liposomes and high density lipoprotein (HDL) was the essential one. Apolipoprotein A-1 (apoA-1) was liable to fall off from HDL, and interacted with phospholipids of liposomes. That was to say, exchange of apoA-1 and phospholipids occurred between HDL and liposomes, resulting the formation of hole on the liposomal membranes. Additionally, hydrolysis of phospholipids was caused by phospholipase existing in plasma, and a serum albumin-liposome complex was formed by the interaction of serum albumin with phospholipids of liposomes, which would decrease the stability of liposomes [34]. In addition, the different release patterns were also observed, the best fit with higher correlation coefficient was found in release data of HSPC-L with Peppas's equation, while the release behavior of HSPC-L at the presence of plasma was fit to the Higuchi's equation. The release data of SPC-L were best fit to first-order kinetic equation. The equations were shown as follows:

$$\text{Ln } Q = 1.06 \text{ Ln } t - 0.37,\ r = 0.9952 \text{ (Peppas's equation)}$$

$$Q = 15.67\, t^{1/2} - 3.64,\ r = 0.9969 \text{ (Higuchi's equation)}$$

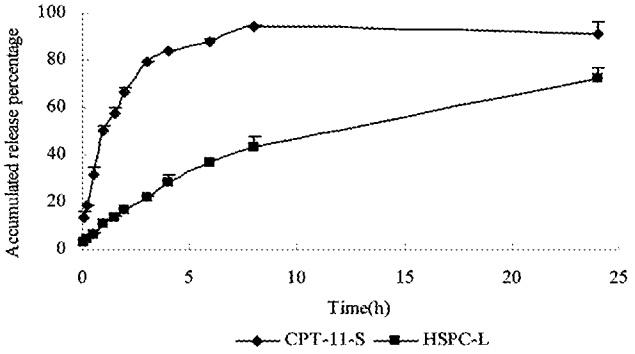

Fig. 2 – Release profiles of CPT-11 from HSPC-L, CPT-11-S with rat plasma in PBS (pH 5.0) (n = 3, mean ± SD).

$$\mathrm{Ln}\,(1-Q) = -0.052t + 4.22,\ r = 0.9761\ (\text{first}-\text{order kinetic equation})$$

3.4. Conversion of liposomal CPT-11 to SN-38 in vitro

The profiles of the conversion percentage of SN-38 from CPT-11 in rat plasma in vitro for HSPC-L and CPT-11-S were shown in Fig. 3. It was indicated that the conversion of SN-38 from CPT-11 in HSPC-L was slightly less than that in CPT-11-S group, but there were no significant statistical differences ($P > 0.05$) between the two groups. It was suspected that the conversion of SN-38 from CPT-11 also existed in the membranes of liposomes, which have been reported by Y. Sadzuka [35]. Though the conversion of SN-38 occurred, SN-38 was still entrapped in the intraliposomes. In this way, SN-38 could be refrained from metabolization by enzyme systems in plasma and high concentration of SN-38 was maintained simultaneously.

3.5. Pharmacokinetic study of CPT-11 liposomes

3.5.1. Assay validation

HPLC-Fluorescence method was used for the determination of CPT-11 and its metabolite SN-38 in plasma, and the results of validation were as follows:

The CPT-11, SN-38 and CPT were extracted from plasma by a methanol extraction, and their recoveries were over 90%. The mean ± SD absolute recovery of the I.S. (CPT 1 μg/ml plasma) was 99.33 ± 1.74%. The range of selected CPT-11 concentration was so wide that two standard curves of CPT-11 were established. The standard curve was established by plotting the ratio of the peak area to that of CPT against the concentration injected. Good standard curves were obtained for CPT-11 and SN-38, ranging from 20 to 1000 ng/ml, 600–24,000 ng/ml, and 2–200 ng/ml, respectively, which were sufficient for the pharmacokinetic studies of CPT-11. The lower limits of quantitation (LLQ) for CPT-11 and SN-38 were 20 and 2 ng/ml, respectively. The within-day and between-day reproducibility of the assay for CPT-11 and SN-38 were investigated. Both the precision and accuracy of this method were acceptable.

CPT-11 was easy to be converted into SN-38 in the presence of carboxylesterases existing in plasma at high level [36]. Therefore, immediate pretreatments were required for blood samples, which can inhibit the conversion of CPT-11 into SN-38 in plasma, so that the concentrations of CPT-11 and SN-38 in plasma can be determined with high accuracy. In addition, the aim of acidifying samples was to transform the carboxylate forms of CPT-11 and SN-38 to the closed lactone forms, and determine the total concentrations of CPT-11 and SN-38 in plasma.

3.5.2. Pharmacokinetics

The pharmacokinetic behavior of CPT-11 liposomes was investigated and compared with that of CPT-11 solution. Also, comparative pharmacokinetics of SPC-L and HSPC-L were conducted.

The plasma concentration versus time profiles of CPT-11 and SN-38 obtained after i.v. injection of SPC-L, HSPC-L, and Sol in rats were showed in Figs. 4 and 5, respectively. As shown in Figs. 4 and 5, there were several striking differences in pharmacokinetic properties between the liposomal CPT-11 formulations and CPT-11 solution. In the plasma, the CPT-11 concentrations at 5 min, 15 min, 0.5 h, and 1 h after injection of the SPC-L group increased 12.5-fold ($P < 0.01$), 6.3-fold ($P < 0.01$), 3.2-fold ($P < 0.01$), and 2.1-fold ($P < 0.01$), respectively, compared with that in the Sol group, but there were no significant differences ranging from 1.5 h to 12 h ($P > 0.05$). CPT-11 concentrations in plasma were below the detection limit at 24 h after dosing in both groups of SPC-L and Sol. In addition, the plasma concentrations of SN-38 were nearly the same ($P > 0.05$) at all indicated time between the SPC-L and Sol. Nevertheless, the plasma concentrations of CPT-11 were higher in HSPC-L than that in Sol or SPC-L at all time points. The CPT-11 concentration in plasma at 5 min, 15 min, 0.5 h, and 1 h after injection of the HSPC-L group was 70-fold ($P < 0.01$), 57-fold ($P < 0.01$), 43-fold ($P < 0.01$), and 38-fold ($P < 0.01$), respectively, higher than that in the Sol group. Moreover, the plasma concentrations of SN-38 were higher in HSPC-L than that in Sol or SPC-L at all time points especially ranging from 2 to 24 h.

The main pharmacokinetic parameters were shown in Table 2. It was exhibited that HSPC-L had a 32.6-fold ($P < 0.01$) increase in the AUC of CPT-11 when compared to Sol, while AUC for SPC-L was 3.3-fold ($P < 0.01$) greater than that of Sol.

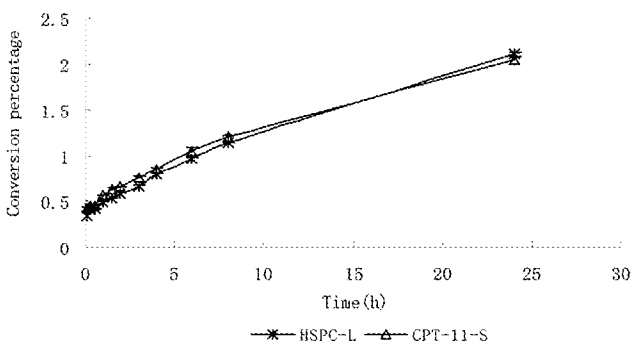

Fig. 3 – The profiles of conversion percentage of SN-38 from CPT-11 in vitro for HSPC-L and CPT-11-S in rat plasma.

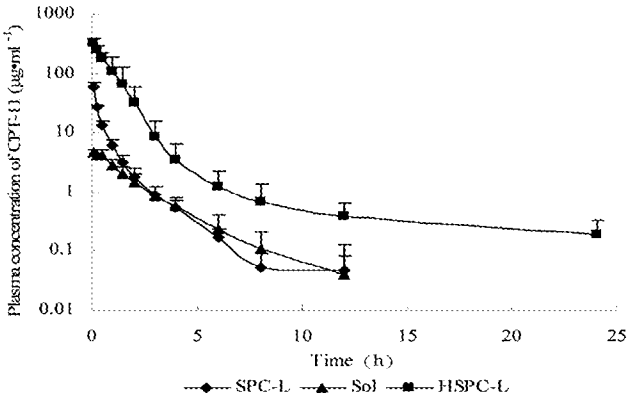

Fig. 4 – Plasma concentration of CPT-11 versus time curves after intravenous administration of HSPC-L, SPC-L and Sol, respectively (n = 5, mean ± SD).

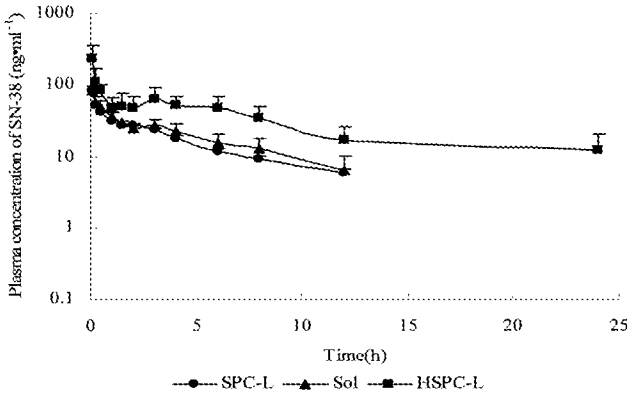

Fig. 5 – Plasma concentration of SN-38 versus time curves after intravenous administration of HSPC-L, SPC-L and Sol, respectively (n = 5, mean ± SD).

The CL and distribution volume (V) of CPT-11 in SPC-L group was 3.2 ($P < 0.01$) and 3.6 times ($P < 0.01$), respectively, lower than that in the Sol group. Furthermore, it was indicated that HSPC-L had a 29.5-fold and 29.4-fold decrease in the CL and V of CPT-11, respectively, compared with the Sol group. On the other hand, the $t_{1/2}$ of CPT-11 did not differ significantly between the liposomal formulations (HSPC-L, SPC-L) and solution ($P > 0.05$). Compared with SPC-L, HSPC-L exhibited 10.5-fold higher AUC of CPT-11, 8.8-fold lower of CL ($P < 0.01$), and 8.2-fold lower of V ($P < 0.01$). The pharmacokinetic parameters of SN-38 were comparable in both groups of SPC-L and Sol ($P < 0.05$). However, HSPC-L demonstrated 3.03- and 3.8-fold higher AUC of SN-38 ($P < 0.05$), respectively, than those in Sol and SPC-L group. Meanwhile, HSPC-L had a 2.57- and 3.12-fold decrease in clearance of SN-38 ($P < 0.05$), when compared with Sol and SPC-L group, respectively.

It was concluded that liposomes, as carriers of CPT-11, can significantly improve AUC, decrease CL and V of CPT-11. HSPC-L demonstrated superior pharmacokinetic behavior of CPT-11 or SN-38, when compared with SPC-L or Sol.

In vivo pharmacokinetics behavior differences between free and liposomal CPT-11 might be due to the differences of their stability in vivo. Compared with liposomal CPT-11, the free one, after i.v administration, eliminates fast by hydrolysis in plasma, transport to surrounding tissues and its elimination via the kidney. Simultaneously, owing to its encapsulation in the inner phase of liposomes, liposomal CPT-11 could escape hydrolysis in vivo after administration, which would result in higher plasma concentration of CPT-11 in active form. The following possible reasons can be explained for the different in vivo behaviors between HSPC-L and SPC-L. Liposomes with different lipid composition should have different in vivo behavior. The phase-transition temperature (about −20 °C) of SPC was lower than body temperature (37 °C), which would decrease the stability of SPC-L after administration, resulting in quick release of CPT-11. On the contrary, HSPC with high phase-transition temperatures (about 50 °C) should slow the leakage of CPT-11 from intraliposomes and warrant high drug level in blood circulation system.

On the other hand, the conversion of SN-38 occurring in CPT-11 liposomes (as shown in Fig. 3) and the pharmacokinetic behavior of CPT-11 liposomes, suggested that CPT-11, a pro-drug, can also be trapped effectively in liposomes. However, the blood circulation of CPT-11 was not improved greatly by liposomal formulation. The order of elimination $t_{1/2}$ value for CPT-11 and SN-38 was HSPC-L > Sol > SPC-L, but there is no significant difference between those values, suggested that the elimination of CPT-11 liposomes from blood circulation is still rapid. It might be due to that unmodified CPT-11 liposomes were unavoidable to be recognized by alternative pathways of complement activation and captured by macrophages in RES organs. Therefore, the next study point in this investigation may be the modification on the surface of the liposomes to achieve an improvement in both circulation time and plasma levels of CPT-11 and SN-38.

Table 3 – In vitro cytotoxic activity of liposomal CPT-11 and CPT-11 on different human tumor cells (IC_{50}, $n \geq 3$).

Cancer cells	Means ± SD	
	Liposomal CPT-11 (μg/ml)	CPT-11 (μg/ml)
Hela	3.118 ± 2.028[a]	16.08 ± 5.446
HOS	5.806 ± 3.001[a]	19.51 ± 6.083
BGC-823	2.115 ± 0.366[a]	>60
MCF-7	2.807 ± 0.346[a]	16.265 ± 6.170

[a] $P < 0.05$ compared to the CPT-11.

3.6. *In vitro cytotoxicity of liposomal CPT-11*

The biological activity of liposomal CPT-11 was investigated and compared with that of CPT-11 using Hela, Hos, BGC-823 and MCF-7. Liposome-entrapped CPT-11 showed a great

Table 2 – The main pharmacokinetic parameters of CPT-11 and SN-38 after i.v. administration of HSPC-L, SPC-L and Sol to rats, respectively (n = 5).

Parameters		$AUC_{0-\infty}$ (μg/ml h)	$t_{1/2}$ (h)	V (l/kg)	CL (l/h/kg)
CPT-11 (mean ± SD)	HSPC-L	306.24 ± 133.17[a]	1.81 ± 0.91	1.7 ± 0.05[a]	0.08 ± 0.03[a]
	SPC-L	29.22 ± 4.99[a]	1.36 ± 0.40	1.40 ± 0.60[a]	0.70 ± 0.12[a]
	Sol	2.17 ± 0.59	1.59 ± 0.57	5.04 ± 1.69	2.27 ± 0.66
SN-38 (mean ± SD)	HSPC-L	0.88 ± 0.37[b]	7.52 ± 4.24	243.87 ± 70.13	28.35 ± 17.72[a]
	SPC-L	0.23 ± 0.05	3.38 ± 0.60	426.96 ± 89.07	88.48 ± 15.40
	Sol	0.29 ± 0.07	4.04 ± 1.43	421.43 ± 175.92	72.73 ± 15.49

[a] $P < 0.01$ compared to the Sol.
[b] $P < 0.05$ compared to the Sol.

increased cytotoxicity versus CPT-11. IC_{50} value against Hela, Hos, BGC-823 and MCF-7 were 3.12, 5.81, 2,12 and 2.81 μg/ml for liposomal CPT-11 and 16.08, 19.51, >60, and 16.27 for CPT-11 (show in Table 3). The IC_{50} value of 48 exposure to liposome containing CPT-11 is 5.15-fold, 3.36-fold, more than 28.37-fold and 5.79-fold greater than free drug. The increased cytotoxicity derived from encapsulation may arise from preserving the active form of the CPT-11. Because the pH of medium was near physiological pH value and CPT-11 hydrolyzed to yield the inactive carboxylate species. But on the contrary, the internal acidic environment of the liposome limits hydrolysis of the lactone ring of camptothecins to the inactive carboxyl form. The CPT released from the liposomes into the culture medium slowly and maintained the effective concentration of the active form of the CPT-11 for a long time. But hydrolysis of free CPT-11 yielded a high percentage of inactive carboxyl form drug. So greatly enhanced cytotoxicity was obtained by encapsulating CPT-11 in liposome.

4. Conclusion

In this study, CPT-11 was entrapped into liposomes successfully by transmembrane ammonium sulfate gradient, possessing high encapsulation efficiency and sustained release in vitro. In vivo, encapsulation of CPT-11 in liposomes showed higher AUC, a lower rate of clearance and smaller volume of distribution for CPT-11 than those in Sol. The rate of clearance and AUC of SN-38 were improved in HSPC-L, but no obvious difference was observed in the pharmacokinetic parameters of SN-38 between SPC-L and Sol. HSPC-L demonstrated superior pharmacokinetic behavior of CPT-11 and SN-38, compared with SPC-L and Sol. The increased cytotoxicity of liposomes may be due to it can preserving more active form of the CPT-11. It appears that entrapment CPT-11 in liposomes especially in those with high phase-transition temperature by transmembrane ammonium salt gradient would be a promising formulation with a better in vivo behavior.

REFERENCES

[1] Yoshimatsu K, Kato H, Ishibashi K, et al. Second-line chemotherapy with low-dose CPT-11 and cisplatin for colorectal cancer resistant to 5-FU-based chemotherapy. Cancer Chemother Pharmacol 2003;52:465–468.

[2] Goldberg MG, Gill S. Recent phase III trials of fluorouracil, irinotecan and oxaliplatin as chemotherapy for metastatic colorectal cancer. Cancer Chemother Pharmacol 2004;54:57–64.

[3] Sugiyama T, Yakushiji M, Nishida T, et al. Irinotecan (CPT-11) combined with cisplatin in patients with refractory or recurrent ovarian cancer. Cancer Lett 1998;128:211–218.

[4] Ohyanagi F, Horiike A, Okano Y, et al. Phase II trial of gemcitabine and irinotecan in previously treated patients with small-cell lung cancer. Cancer Chemother Pharmacol 2008;61:503–508.

[5] Negoro S, Masuda N, Takada Y, et al. Randomised phase III trial of irinotecan combined with cisplatin for advanced nonsmall cell lung cancer. Br J Cancer 2003;88:335–341.

[6] Sone M, Uchida J, Tominaga M, et al. Small cell carcinoma of the larynx treated with irinotecan and cisplatin. Auris Nasus Larynx 2006;33:223–225.

[7] Muhr-Wilkenshoff F, Hinkelbein W, Ohmesorge J, et al. A pilot study of irinotecan (CPT-11) as single-agent therapy in patients with locally advanced or metastatic esophageal carcinoma. Int J Colorectal Dis 2003;18:330–334.

[8] Takahashi Y, Kitakata H, Yamashita K, et al. Pilot study of low-dose, divided maximum tolerated dose of CPT-11 in 21 consecutive patients with metastatic colorectal or gastric cancer. Surg Today 2004;34:246–250.

[9] Fadul CE, Kingman LS, Meyer LP, et al. A phase II study of thalidomide and irinotecan for treatment of glioblastoma multiforme. J Neurooncol 2008;90:229–235.

[10] Ohno R, Okada K, Masaoka T, et al. An early phase II study of CPT-11: a new derivative of camptothecin, for the treatment of leukemia and lymphoma. J Clin Oncol 1990;8:1997–1912.

[11] Bleiberg H, Cvitkovic E. Characterization and clinical management of CPT-11 (irinotecan)-induced adverse events: the European perspective. Eur J Cancer 1996;32:18–23.

[12] Cersosimo RJ. Irinotecan a new antineoplastic agent for the management of colorectal cancer. J Ann Pharmacother 1998;32:1324–1333.

[13] Yoshiyuki H, Li S, Wu XD. Novel irinotecan-loaded liposome using phytic acid with high therapeutic efficacy for colon tumors. J Control Release 2005;136:30–37.

[14] Sadzuka Y, Hirotsu S, Hirota S. Effect of liposomalization on the antitumor activity, side-effects and tissue distribution of CPT-11. Cancer Lett 1998;127: 99–106.

[15] Sadzuka Y, Hirotsu S, Hirota S. Effective irinotecan (CPT-11)-containing liposomes: Intraliposomal conversion to the active metabolite SN-38. Jpn J Cancer Res 1999;90:226–232.

[16] Ramsay E, Ainajim J, Ananthe M. Transition metal-mediated liposomal encapsulation of irinotecan (CPT-11) stabilizes the drug in the therapeutically active lactone conformation. Pharm Res 2006;23:2799–2808.

[17] Dicko A, Tardi P, Xie X, et al. Role of copper gluconate/triethanolamine in irinotecan encapsulation inside the liposomes. Int J Pharm 2007;337:219–228.

[18] Walsh FM, Crosson FJ, Bayley M, et al. Acute copper intoxication pathophysiology and therapy with a case report. Am J Dis Child 1977;131:149–151.

[19] Barcelouz DG. Copper. J Toxicol Clin Toxicol 1999;37:217–230.

[20] Kawanishi S, Inoue S, Yamamoto K, et al. Hydroxyl radical and singlet oxygen production and DNA damage induced by carcinogenic metal compounds and hydrogen peroxide. Biol Trace Elem Res 1989;21:367–372.

[21] Sumiyoshi H, Fujiwara Y, Ohune T, et al. High-performace liquid chromatographic determination of irinotecan (CPT-11) and its active metabolite (SN-38) in human plasma. J Chromatogr B 1995;670:309–316.

[22] Fan M, Xu S, Xia S, et al. Preparation of salidroside nanoliposomes by ethanol injection method and in vitro release study. Eur Food Res Technol 2008;227:167–174.

[23] Smith RN, Hansch C, Ames MM. Selection of a reference partitioning system for drug design work. J Pharm Sci 1975;64:599–606.

[24] Barenholz Y. Liposome application: problems and prospects. Colloid Interface Sci 2001;6:66–77.

[25] Gabizon A, Barenholz Y. Method for drug loading in liposomes. U.S Patent 988275/10 2005.

[26] Wasserman V. Development, characterization, optimization, and pharmacokinetic evaluation of liposome-based piperidine nitroxide formulation for treatment of pathological conditions: tumor and rheumatoid arthritis. Ph.D. thesis; 2002.

[27] Haran G, Cohen R, Bar LK, et al. Transmembrane ammonium sulfate gradients in liposomes produce efficient and stable

entrapment of amphipathic weak bases. Biochim Biophys Acta 1993;1151:201–215.
[28] Dicko A, Tardi P, Xie XW, et al. Role of copper gluconate/triethanolamine in irinotecan encapsulation inside the liposomes. Int J Pharm 2007;337:219–228.
[29] Bolotin EM, Cohen R, Bar LK. Ammonium sulfate gradients for efficient and stable remote loading of amphipathic weak bases into liposomes. J Liposome Res 1994;4:455–479.
[30] Chou TH, Chen SC, Chu IM, et al. Effect of composition on the stability of liposomal irinotecan prepared by a pH gradient method. J Biosci Bioeng 2003;95:405–408.
[31] Ramsay E, Alnajim J, Anantha M, et al. A novel liposomal irinotecan formulation with significant anti-tumour activity: use of the divalent cation ionophore A23187 and copper-containing liposomes to improve drug retention. Eur J Pharm Biopharm 2008;68:607–617.
[32] Lasic DD, Frederik PM, Stuart MCA, et al. Gelation of liposome interior: a novel method for drug encapsulation. FEBS Lett 1992;312:255–258.
[33] Damen J, Regts J, Scherphof G, et al. Transfer of [^{14}C] phosphatidylcholine between liposomes and human plasma high density lipoprotein. Biochim Biophys Acta 1982;712:444–452.
[34] Sadzuka Y, Hirotsu S, Hirota S. Effective irinotecan (CPT-11)-containing liposomes: intraliposomal conversion to the active metabolite SN-38. Jpn J Cancer Res 1999;90:226–232.
[35] Hennebelle I, Terret C, Chatelut E, et al. Characterization of CPT-11 converting carboxylesterase activity in colon tumor and normal tissues: comparison with p-nitro-phenylacetate converting carboxylesterase activity. Anti-Cancer Drugs 2000;6:465–470.

Convection-enhanced delivery of targeted quantum dot–immunoliposome hybrid nanoparticles to intracranial brain tumor models

Aim: The aim of this work is to evaluate combining targeting strategy and convection-enhanced delivery in brain tumor models by imaging quantum dot–immunoliposome hybrid nanoparticles. **Materials & methods:** An EGF receptor-targeted, quantum dot–immunoliposome hybrid nanoparticle (QD-IL) was synthesized. *In vitro* uptake was measured by flow cytometry and intracellular localization was imaged by confocal microscopy. In the *in vivo* study, QD-ILs were delivered to intracranial xenografts via convection-enhanced delivery and fluorescence was monitored noninvasively in real-time. **Results:** QD-ILs exhibited specific and efficient uptake *in vitro* and exhibited approximately 1.3- to 5.0-fold higher total fluorescence compared with nontargeted counterpart in intracranial brain tumor xenografts *in vivo*. **Conclusion:** QD-ILs serve as an effective imaging agent *in vitro* and *in vivo*, and the data suggest that ligand-directed liposomal nanoparticles in conjunction with convection-enhanced delivery may offer therapeutic benefits for glioblastoma treatment as a result of specific and efficient uptake by malignant cells.

Original submitted 15 June 2012; Revised submitted 12 November 2012; Published online 30 April 2013

KEYWORDS: brain tumor model • convection-enhanced delivery • drug delivery system • immunoliposome • *in vivo* imaging • nanomedicine • quantum dot • targeted cancer therapy • targeted nanoparticle

Kevin C Wang, Ryotaro Hashizume, Charles O Noble, Laura P Serwer, Daryl C Drummond, Dmitri B Kirpotin, Anne M Kuwabara, Lucy Y Chao, Fanqing F Chen, Charles D James & John W Park

Brain tumors remain a difficult malignancy to treat with high recurrence and poor prognosis even after multimodal therapy. While systemic chemotherapy is among the standard options in the therapeutic management of brain tumors, delivery of therapeutic agents to the CNS still presents a major challenge. Systemic side effects also limit the doses of chemotherapeutics required to convey the desired efficacy. As a result, clinical outcomes remain far from satisfactory [1,101].

The distribution of systemically administered therapeutic agents to brain tumors is significantly hindered by the blood–brain barrier [2]. Direct CNS application of drugs can bypass the blood–brain barrier, but reliance on passive diffusion typically results in limited intratumoral delivery. Convection-enhanced delivery (CED) was introduced to overcome the extremely poor diffusion-limited drug distribution associated with direct infusion [3]. It employs a pump-driven cannula to achieve bulk flow of drugs for improved volume of distribution [4]. The results brought about by this technique include higher concentrations achieved at the targeted site and reduced systemic toxicities. However, clinical development of CED for brain tumors has been compromised by technical issues including suboptimal cannula placement and control [5,6], indicating the need for an imaging-based strategy for CED infusion. Selection of an optimal therapeutic agent to be administered via CED is another key consideration. In recent studies, CED has been combined with advanced drug carriers, including liposome and nanoparticle drug delivery systems [7–14]. CED is well suited for the delivery of liposomes and particulate drug carriers that have the potential to provide a sustained level of drug and reach cellular targets with improved specificity [15,16]. CED of liposomal anticancer agents has shown greater target tissue retention, and effective antitumor activity in xenograft models, compared with free drug delivery [10,13,17]. Importantly, prolonged exposure to liposomal anticancer agents resulted in no measurable CNS toxicity, whereas free drugs induced severe CNS toxicity.

In this report, a multifunctional nanoparticle agent is described; EGF receptor (EGFR)-targeted immunoliposomes conjugated to quantum dots (QDs). This agent binds to and is internalized into EGFR-overexpressing brain tumor cells *in vitro*, and can be administered via CED for tumor cell targeting *in vivo*. A slow drug infusion rate was achieved by a microinfusion pump, coupled with a specially designed catheter, which is a 1-mm stepped design with a fused silica tubing into a 24-gauge needle. These optimized CED devices increase drug distribution and reduce reflux [18].

Targeting of malignant cells by immunoliposomes is a novel approach that has been shown to greatly improve efficacy via receptor-mediated internalization [19]. This mechanism allows nanoparticles to accumulate and release the drug intracellularly, thus greatly enhancing efficacy [20]. EGFR is a logical target for brain tumor treatment as it is frequently overexpressed in glioblastomas and can thereby delineate cancer cells from normal cells [20]. It is worth noting that although nontargeted and tumor-targeted nanocarriers typically show comparable extravasation via angiogenic vessels in solid tumors (i.e., both types rely upon passive targeting for initial tumor deposition), cellular internalization (immunotargeting) alone significantly improved therapeutic indices [20–22]. However, little is known about the biodistribution of targeted nanoparticles administered via CED.

Optical and spectroscopic probes can provide information on cellular and subcellular localization of nanoparticles. Semiconductor nanocrystals, or QDs, have emerged as reliable probes for biological imaging, particularly for tracking and imaging subcellular activities [23,24]. Compared with traditional dyes, they offer the advantages of narrow emission profiles and extraordinary photostability without suffering from photobleaching and biodegradation [25,26]. The near-infrared QDs are particularly suitable for *in vivo* imaging as their fluorescence transmits efficiently through the tissues and skin compared with QDs at the visible range. Near-infrared QDs have been used in mouse models and for tracking targeted agents in subcutaneous tumors [27–29]. Here, these optical properties of QDs are used in the tracking and monitoring of targeted liposomal nanoparticles in brain tumor models.

The overall aim of the study is to begin to explore hybrid multifunctional nanoparticles in the development of targeted imaging and drug delivery for brain tumors. While combining CED with liposomal formulations has been shown to improve therapeutic indices, the *in vivo* behavior of targeted nanoparticles in brain tumor models is still in very early stages and is not yet understood. The feasibility of imaging these multifunctional nanoparticles within tumor tissue is evaluated following CED.

Materials & methods

※ EGFR-targeted QD–immunoliposome hybrid nanoparticles

To synthesize nontargeted QD–liposome hybrid nanoparticles (QD-Ls) and EGFR-targeted QD–immunoliposome hybrid nanoparticles (QD-ILs), liposomes consisting of 2 mol% 1,2-distearoyl-*sn*-glycero-3-phosphoethanolamine-*N*-(amino[polyethylene glycol]$_{2000}$) (amine-PEG$_{2000}$-DSPE), approximately 0.5 mol% 1,2-distearoyl-*sn*-glycero-3-phosphoethanolamine-*N*-(maleimide[polyethylene glycol]$_{2000}$) (Mal-PEG$_{2000}$-DSPE) along with 60 mol% 1,2-distearoyl-*sn*-glycero-3-phosphocholine (Avanti Polar Lipids, AL, USA) and 37–38 mol% cholesterol (EMD Biosciences, CA, USA), were synthesized by extrusion using 100 nm pore polycarbonate membranes (Whatman, NJ, USA) in 5 mM 4-(2-hydroxyethyl)-1-piperazineethanesulfonic acid (HEPES), 135 mM sodium chloride buffer, pH 7.0. Cetuximab was first digested by pepsin and then reduced by cysteamine to yield the Fab′ fragments. CdSeTe/ZnS core/shell QDs with an emission peak at approximately 800 nM (Invitrogen, OR, USA) and carboxyl-derivatized surface were used to provide the functionality for chemical conjugation with primary amine groups of the lipid/liposome. A total of 0.2 μM carboxyl QDs and 7 mM liposomes were covalently linked by 1.8 mM zero-length crosslinker 1-ethyl-3-(3-dimethylaminopropyl)carbodiimide (EDC; Pierce, IL, USA) at room temperature for 2–4 h. The liposomal nanoparticles were purified by home-made dialyzers. For QD-ILs, Fab′ derived from cetuximab was incubated with liposomes for 6 h at room temperature, followed by dialysis purification. All buffers used for dialysis were freshly degassed by high-purity argon. All QD-liposomal formulations were characterized by dynamic light scattering and spectrofluorometry to confirm uniformity, conjugation efficiency and stability.

※ Flow cytometry

After treatment (typically incubation at 37°C for 2 h), cells were trypsinized and centrifuge-washed by sterile, filtered phosphate-buffered saline containing Ca^{2+} and Mg^{2+} (provided by the University of California, San Francisco Cell Culture Facility, CA, USA). Cell suspensions (0.5–0.6 ml) were analyzed by multichannel flow cytometry (FACS LSR II, BD Biosciences, CA, USA) for detection of QD fluorescence. The intensities of fluorescence collected from 10,000 cells were subtracted by the autofluorescence of control cells (cells without treatment) to eliminate dependence on instrument and settings. Mean area intensities were compared for quantitative and statistical analysis.

Confocal laser-scanning microscopy

Confocal laser-scanning microscopy was performed using the LSM 510 META (Zeiss, Jena, Germany) with an argon (488 nm) or titanium–sapphire (800 nm) laser for QD excitation (emission maximum at ~800 nm). A helium–neon laser (633 nm) was used for lipidic dye DiD (emission peak at 665 nm) excitation. The photomultiplier tube used was the H7422P-50 photosensor module (Hamamatsu, Shizuoka, Japan), which possesses a spectral response range from 380 to 890 nm. Cells were cultured on sterile, rounded coverglass (18-mm diameter) and were fixed on 25 × 75 × 1 mm glass slides (Fisher Scientific, PA, USA) with antifade VECTASHIELD® Mounting Medium including 4',6-diamidino-2-phenylindole (DAPI; Vector Laboratories, CA, USA) immediately after treatment. Plan-Apochromat 63×/1.4 numerical aperture oil-immersion and Plan-Neofluar 40×/1.3 numerical aperture oil-immersion objectives (Zeiss) were used for inspection and scanning.

Cell cultures

U-87 MG human glioblastoma cells and U87-EGFRvIII cells were obtained from the Department of Neurological Surgery Tissue Bank at the University of California, San Francisco. Cells were in high glucose Dulbecco's modified Eagle medium (DMEM) with 10% fetal calf serum, nonessential amino acids, penicillin and streptomycin. Before implantation, cells were washed in media without antibiotics. Cells were seeded into culture flasks 2 days before tumor implantation. For implantation, cells were harvested with trypsin, washed with Dulbecco's phosphate-buffered saline (DPBS), and resuspended in Hanks' balanced salt solution (HBSS) without Ca^{2+} and Mg^{2+}.

Modification of tumor cells with firefly luciferase-expressing reporter

U87-EGFRvIII and GBM39 cells were transduced with a lentiviral vector containing firefly luciferase (*Fluc*) under the control of the spleen focus-forming virus promoter. Lentiviral vectors were generated by transfection of 293T (human embryonal kidney) cells with plasmids encoding the vesicular stomatitis virus G envelope, gag-pol and *Fluc* genes [30]. Viral vectors were harvested from supernatant 48 h after transfection, filtered and then used to infect glioblastoma cells. Cells were screened for transfection efficiency by treatment with luciferin (D-luciferin potassium salt, 150 mg/kg, Gold Biotechnology, MO, USA) *in vitro* and examination by the IVIS® Lumina system (PerkinElmer, MA, USA). More than 80% of cells were transfected.

Animals

Six-week-old female athymic mice (nu/nu genotype, BALB/c background) were purchased from Simonsen Laboratories (CA, USA). Animals were housed in an animal facility and were maintained in a temperature- and light-controlled environment with an alternating 12 h light/dark cycle. All protocols were approved by the University of California, San Francisco Institutional Animal Care and Use Committee.

Human glioblastoma intracranial tumor model

Tumor cells were implanted into the brains of athymic mice, as previously described [31]. Briefly, animals were anesthetized with an intraperitoneal injection of ketamine (100 mg/kg) and xylazine (10 mg/kg), and were manually injected slowly with the U87-EGFRvIII or GBM39 cell suspension (3×10^5 cells in 3 µl Hanks' balanced salt solution) into the right caudate–putamen. All procedures were carried out under sterile conditions and this procedure typically resulted in a 100% tumor take.

In vivo bioluminescence monitoring (bioluminescence imaging)

In vivo bioluminescence imaging was performed with the IVIS Lumina system coupled to the data-acquisition Living Image® software (PerkinElmer, MA, USA). Mice were imaged 10 min after intraperitoneal injection of luciferin (D-luciferin potassium salt) mixed with ketamine (100 mg/kg) and xylazin (10 mg/kg). Luminescence signal intensity was quantified within a region of interest over the heads of mice, as defined by the Living Image software.

CED of QD–immunoliposome hybrid nanoparticles

All QD liposomes were administered intracranially by CED. To ensure the fluorescence intensities of QD-ILs and QD-Ls are equivalent before CED injection, 5 µl droplets of each solution were plated in three wells of a 96-well plate and imaged by the IVIS Lumina system. Photon flux showed the two formulations had average fluorescence intensities within approximately 5% difference. A step-design cannula was used to reduce reflux during the infusion and was assembled as previously described [4]. For the infusion, mice were anesthetized with ketamine

(100 mg/kg) and xylazine (10 mg/kg) and then placed in a stereotactic frame (Stoelting, IL, USA). Isofluorane was administered to the mice as needed to maintain a surgical plane of anesthesia. The burr hole created during tumor cell injection was exposed and used as the entry site for the cannula. The cannula was then positioned 3 mm below the surface of the skull and a syringe pump was attached to the cannula. The infusion ran at the following speeds: 0.1 µl/min for 5 min, 0.2 µl/min for 5 min, 0.5 µl/min for 5 min, and 0.8 µl/min for 7.5 min. The total infusion time was 22.5 min and the total volume infused was 10 µl. The infusion rates were chosen based on prior studies, which showed that this schedule both reduces infusate reflux and minimizes normal tissue damage during CED [4]. The infusion cannula remained in place for 1 min after the infusion ended. After the cannula was removed, the hole was sealed with bone wax and the scalp was closed with surgical staples (Stoelting).

Results & discussion

In this study, a multifunctional nanoparticle consisting of luminescent QDs, Fab′ moieties of cetuximab, and a spherical liposomal core capable of encapsulating chemotherapeutics was developed to investigate the interactions of EGFR-targeted immunoliposomal nanocarriers with glioblastoma cells *in vitro* and *in vivo*. To synthesize the hybrid nanoparticle via a modular assembly approach, Fab′ and carboxyl QDs were sequentially conjugated to maleimide and primary amine groups attached to the tip of pegylated lipids on surface-bifunctionalized liposomes, respectively. The functional components, that is, targeting moiety in Fab′ and luminescent reporters in QDs, were both linked onto separate lipids anchored in the bilayers of liposomes. It is thus important to ensure that both the affinity/specificity of Fab′ or the optical properties of QDs are not compromised by the bioconjugation reactions. Previously, the authors investigated a similar nanoconstruct that targets human epidermal growth factor receptor 2 (HER2/c-erbB2) in breast cancer models. However, the construction of anti-HER2 QD-ILs was achieved by the postinsertion of a scFv-PEG-DSPE micelle into preformed QD-conjugated liposomes rather than direct conjugation [28]. Therefore, it is important to assess the *in vitro* properties of the novel nanoconstruct synthesized through the sequential conjugation route and ensure the intactness of functional components incorporated into the hybrid nanoparticles. By using quantitative flow cytometry and confocal microscopy, the nanoconstruct was shown to be active for targeting and internalization to tumor cells while preserving the spectroscopic properties of QDs. These EGFR-targeted QD-ILs were first validated for use in the investigation of *in vivo* properties when administered via CED in the brain tumor models. Near-infrared QDs allowed for continuous postinfusion monitoring of QD-ILs and QD-Ls in intracranial brain xenografts and provided data for the activities of hybrid liposomal nanoparticles in the brain tumor model.

To take full advantage of liposomal formulations in cancer treatment, multiple factors need to be optimized; particularly spatial and temporal localization and distribution of the nanoparticles. Incorporating QDs potentially enables tracking the process *in vitro* and *in vivo* with the superior brightness and persistence of QDs. For anti-EGFR targeting, liposomes conjugated to Fab′ fragments of cetuximab (Erbitux®, ImClone Systems, Inc., NJ, USA), a recombinant chimeric monoclonal antibody used in cancer treatment, were prepared. To synthesize EGFR-targeted QD-ILs that incorporate both targeting and optical reporting functionalities, a two-step bioconjugation scheme was used to associate the molecular entities. The synthesis involves covalent linkage of carboxyl QDs and Fab′ fragments derived from cetuximab onto primary amine and maleimide functional groups on preformed liposome surfaces, respectively. Using this bioconjugation scheme, one must preclude cross-reactions, otherwise, the surface functional groups may be adversely consumed during the first step and compromise the efficiency of the next. In the hybrid nanoconstruct, 2 mol% amine-PEG_{2000}-DSPE and 0.5% Mal-PEG_{2000}-DSPE were incorporated. The composition was chosen so that the lipid bilayers maintain integrity and provide adequate targeting groups for ligand-directed delivery [32]. It was found that conjugating QDs prior to conjugation of Fab′ greatly reduced cell uptake, probably due to the steric hindrance of QDs blocking the available sites for Fab′ attachment (data not shown). Therefore, conjugation of Fab′ was performed before QDs. However, the biological reactivity of the synthesized QD-ILs would still be a concern if the conjugation of carboxyl onto Fab′-conjugated liposomes affected the affinity and specificity of Fab′, potentially via undesirable modification of amino/carboxyl groups presented on Fab′. Therefore, cell uptake and imaging were measured to verify the functionality of both Fab′ and QDs.

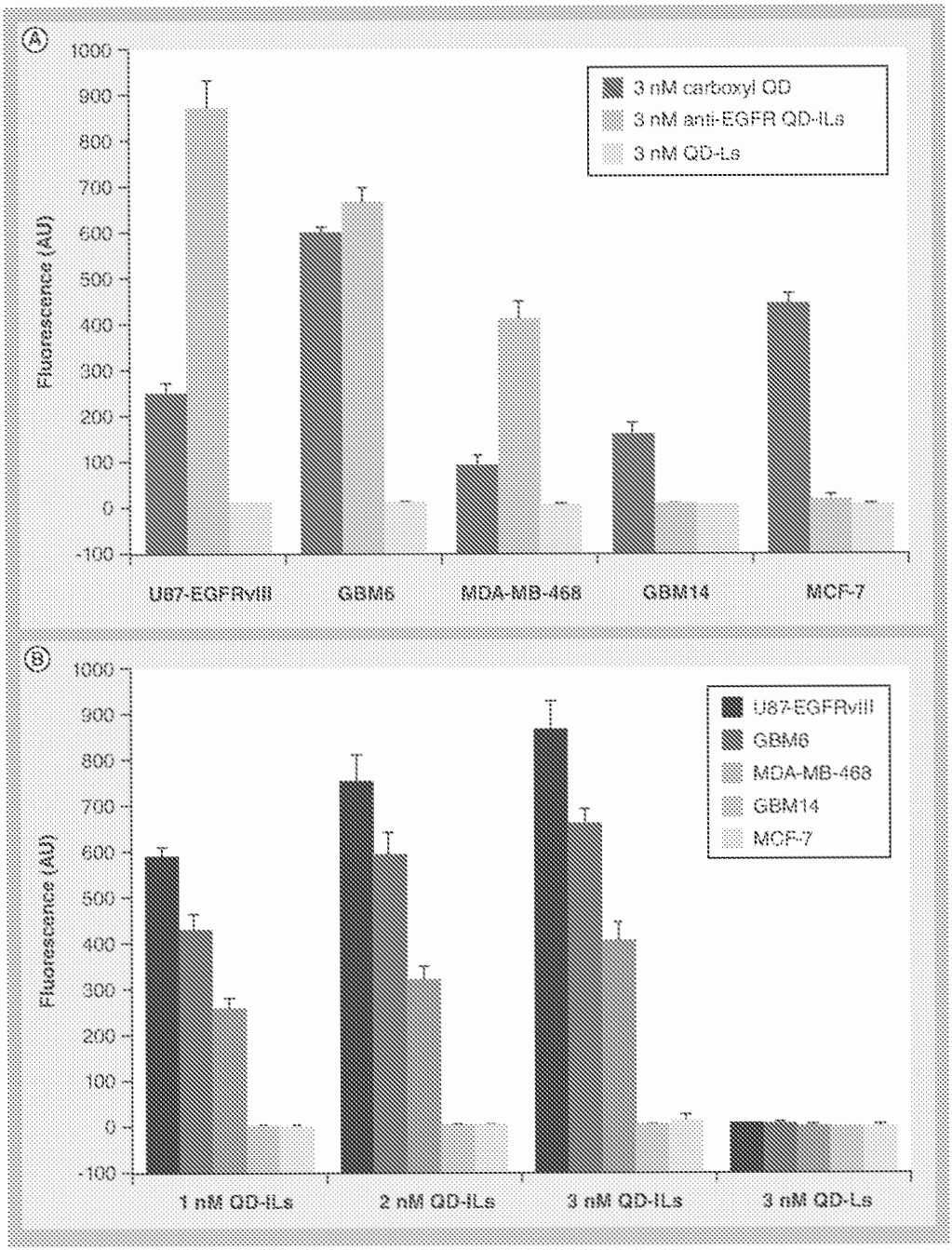

Figure 1. Flow cytometry comparison for concentration-dependent uptake of the various nanoparticle formulations by cancer cells. (A) Flow cytometry data for free carboxyl QD versus anti-EGFR QD-IL versus nontargeted QD-L uptake by U87-EGFRvIII (mutant EGFR-overexpressing cells), GBM6 (EGFR-overexpressing cells), MDA-MB-468 (EGFR-overexpressing cells), GBM14 (low EGFR-expressing cells) and MCF-7 (low EGFR-expressing cells). **(B)** Flow cytometry data for 1, 2 and 3 nM anti-EGFR QD-IL versus nontargeted QD-L uptake by U87-EGFRvIII, GBM6, MDA-MB-468, GBM14 and MCF-7.
EGFR: EGF receptor; QD: Quantum dot; QD-IL: Quantum dot–immunoliposome hybrid nanoparticle; QD-L: Quantum dot–liposome hybrid nanoparticle.

Cellular binding and uptake of free QDs, EGFR-targeted QD-ILs and nontargeted QD-Ls were evaluated by flow cytometry. Target cell lines included EGFRvIII-overexpressing U87 (U87-EGFRvIII), EGFR-overexpressing GBM6, MDA-MB-468, low EGFR-expressing GBM14 and MCF-7. U87-EGFRvIII is a cell line with mutant EGFR variant III (EGFRvIII) expression that has been established in glioma models. Free QDs are known to nonselectively absorb on the cell surface to varying extents [28,33]. A concentration-dependent binding of

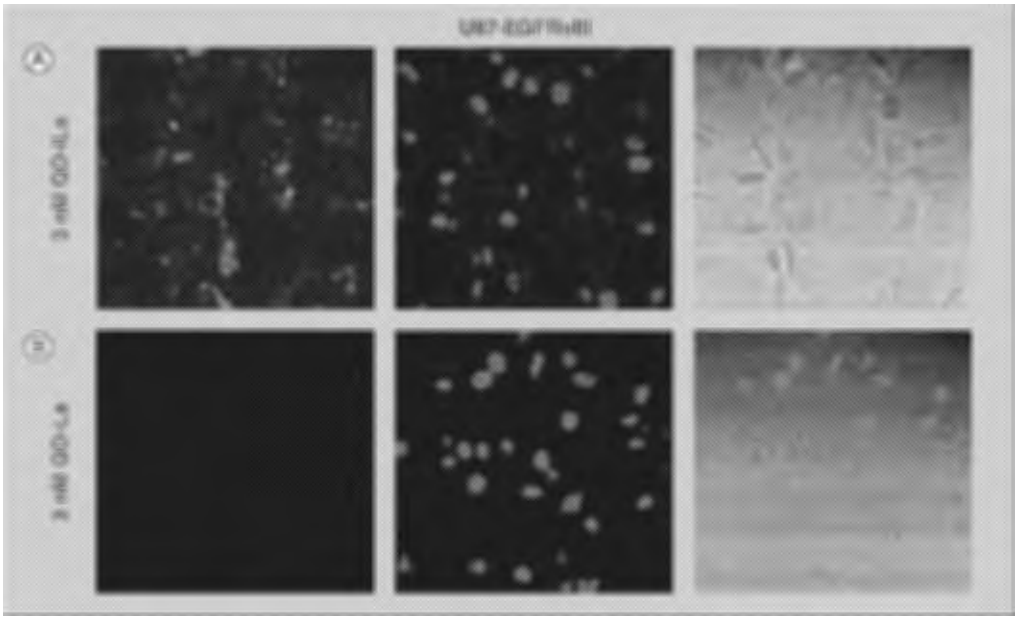

Figure 2. Confocal microscopy images of U87-EGFRvIII. (A) Confocal microscopy of EGF receptor-targeted QD-IL internalization by U87-EGFRvIII. **(B)** Uptake of nontargeted QD-Ls. Panels from left to right are quantum dot 800 (red), 4′,6-diamidino-2-phenylindole (blue) and composite images with differential interference contrast, respectively.
QD-IL: Quantum dot–immunoliposome hybrid nanoparticle; QD-L: Quantum dot–liposome hybrid nanoparticle.

free QDs on all cell lines was observed. Interestingly, the cell lines also exhibited markedly different amounts of binding by free QDs. As shown in Figure 1A, free carboxyl QDs, EGFR-targeted QD-ILs and nontargeted QD-Ls were administered to all cell lines at the same QD concentration (3 nM). In total, 3 nM of free QDs resulted in a significant increase in fluorescence signals for all cell lines. In the case for GBM6, it was nearly as high as the uptake of

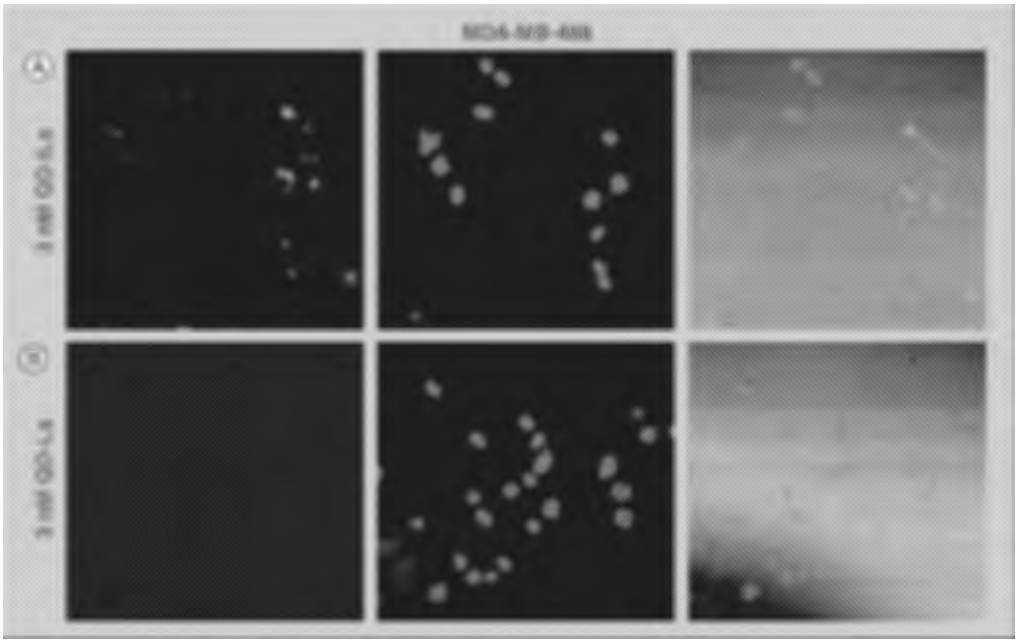

Figure 3. Confocal microscopy images of MDA-MB-468. (A) Confocal microscopy of QD-IL internalization by MDA-MB-468. **(B)** Uptake of QD-Ls (negligible). Panels from left to right are quantum dot 800 (red), 4′,6-diamidino-2-phenylindole (blue) and composite images with differential interference contrast, respectively.
QD-IL: Quantum dot–immunoliposome hybrid nanoparticle; QD-L: Quantum dot–liposome hybrid nanoparticle.

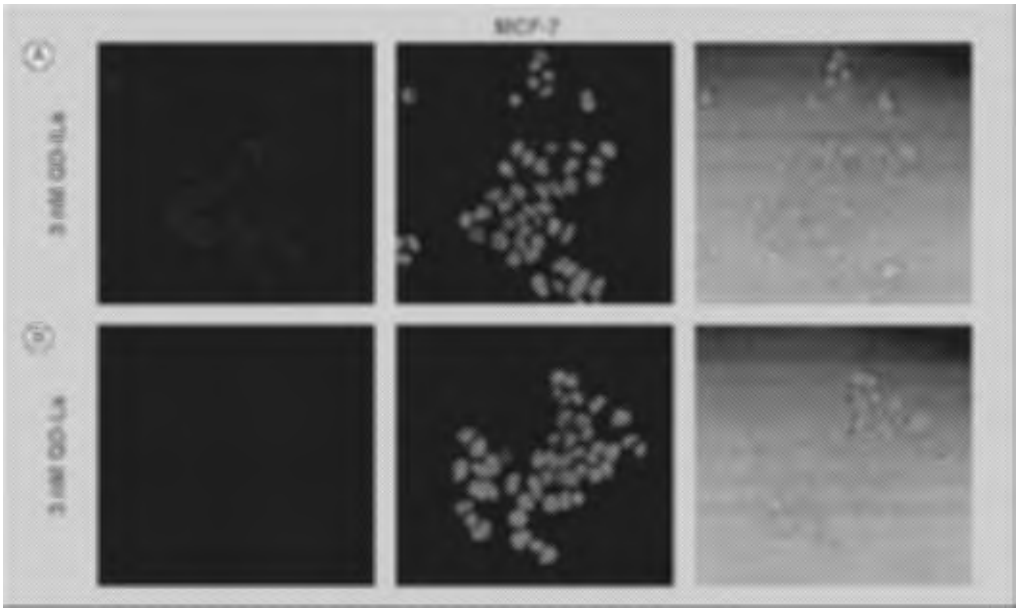

Figure 4. Confocal microscopy images of MCF-7. (A) Confocal microscopy of QD-IL internalization by MCF-7. **(B)** Uptake of QD-Ls (negligible). Panels from left to right are quantum dot 800 (red), 4',6-diamidino-2-phenylindole (blue) and composite images with differential interference contrast, respectively.
QD-IL: Quantum dot–immunoliposome hybrid nanoparticle; QD-L: Quantum dot–liposome nanoparticle.

QD-ILs. Uptake of 3 nM free carboxyl QDs by U87-EGFRvIII, GBM6, MDA-MB-468, GBM14 and MCF-7 is approximately 35-, 89-, 56-, 920- and 257-fold higher than nontargeted QD-Ls, respectively. Uptake of 3 nM of targeted QD-ILs by U87-EGFRvIII, GBM6 and MDA-MB-468 is approximately 126-, 99- and 261-fold higher than nontargeted QD-Ls, respectively. In Figure 1B, concentration-dependent uptake of the various nanoparticle formulations was shown. Nontargeted QD-Ls has negligible uptake at 3 nM, the highest concentration tested, for all cell lines, while the uptake of EGFR-targeted QD-ILs is markedly different between the three EGFR-overexpressing cells: U87-EGFRvIII, GBM14, MDA-MB-468, and low EGFR-expressing cells GBM14 and MCF-7.

In confocal microscopy examination, 3 nM QD-ILs and QD-Ls were administered to U87-EGFRvIII, MDA-MB-468 and MCF-7. In Figure 2, intracellular fluorescence is evident for U87-EGFRvIII, with the panels from the left showing fluorescence from QDs, the middle showing 4',6-diamidino-2-phenylindole for nucleus staining and the merged fluorescence images overlapped with differential interference contrast images to assist in delineating the boundaries of cells. In Figure 3, the intracellular localization of QD-ILs was also evident for MDA-MB-468. The fluorescence mainly came from the cytoplasm and near the peripherals of the nucleus. For MCF-7, neither QD-ILs nor QD-Ls exhibited uptake and detectable fluorescence across the view field, as shown in Figure 4. On the contrary, using the same microscope settings, no significant fluorescence was observed for nontargeted QD-Ls for all three cell lines imaged.

In *in vivo* studies, luciferase-modified U87-EGFRvIII glioblastoma cells overexpressing both EGFR and EGFRvIII were injected into the right supratentorial brain in mice and tumor growth was monitored by bioluminescence imaging, as shown in Figure 5. Intense luminescence signals were detected, corresponding with intracranial tumor growth. QD-Ls were infused into the intracranial tumor by CED and fluorescent signals from QD-Ls were detected at 2.5 h following CED by *in vivo* and *ex vivo* fluorescence imaging. The *ex vivo* fluorescence image in serial cross-sections showed intense fluorescent signals within the tumor. The whole brain and three serial sections collected from the nontargeted group indicates parenchymal penetration of QD-Ls. QD-ILs and QD-Ls were then delivered to intracranial U87-EGFRvIII and GBM39 xenografts, respectively, via CED. Fluorescence of QD-ILs and QD-Ls was monitored noninvasively in real-time using an *in vivo* imaging system. In the clinic, CED treatment can lead to variable agent distribution, due to reflux along the cannula track and infusate

leakage into low pressure areas of the brain, such as the subarachnoid space [34]. In this model, *in vivo* imaging was found to be useful in determining which mice, if any, had an unsuccessful infusion. If a mouse demonstrated a high fluorescence signal in the liver within 6 h of delivery, it was concluded that there may have been substantial infusate leakage, resulting in higher than expected levels of QD-ILs/QD-Ls systemic exposure. Such cases made assessment of QD-ILs/QD-Ls retention in the brain unreliable and were excluded from analysis. The QD-Ls and QD-ILs were evaluated *in vitro* before infusion to determine the fluorescence efficiency of each formulation. There was not a significant difference between the two formulations (<5%).

Figure 6 shows the *in vivo* fluorescence of the nanoparticle agents following CED in mice implanted with U87-EGFRvIII (Figure 6A) and GBM39 (Figure 6B) intracranial tumors. Both QD-Ls and QD-ILs produced detectable fluorescence through the skull. A time course experiment was performed at 2.5, 6, 24, 48, 73 and 94 h, respectively, on the mice with U87-EGFRvIII xenografts. At 2.5 h after infusion, both nanoparticle types were present in nearly equal amounts (QD-ILs:QD-Ls = 1.05); however, by 94 h the EGFR-targeted QD-ILs were retained to a greater extent (QD-ILs:QD-Ls = 1.71) (Figure 6A). The trend line showed an R^2 value of 0.9. In a second experiment over a longer time course with the GBM39 model, QD-ILs exhibited approximately 1.3-fold higher total fluorescence ($p < 0.05$; $n = 3$) on day 7 post-CED compared with nontargeted QD-Ls, confirming higher retention of QD-ILs in the brain (Figure 6B). Collectively, these results indicated that EGFR-targeted QD-ILs were selectively retained in tumor tissue following CED, compared with nontargeted QD-Ls. By contrast, it is now well established that antibody targeting of nanoparticles can result in no net increase in tumor localization over nontargeted nanoparticles following intravenous administration, even though they can provide significantly greater antitumor activity [21]. This apparent paradox is explained by the predominance of the enhanced permeability and retention (EPR) effect in mediating tumor localization of long circulating nanoparticles following systemic administration, as well as the importance of tumor cell targeting in overall treatment efficacy. It is therefore notable that CED, unlike systemic administration, can facilitate improved tumor retention due to immunotargeting. Both QD-ILs and QD-Ls showed half-lifes longer than 7 days, as the normalized fluorescence was higher than 50% at the end of the monitoring session, in agreement with the authors' previous study that showed a tissue half-life of 16.7 days for liposomes encapsulating CPT-11 (irinotecan) and 10.9 days for pegylated liposomal doxorubicin (Doxil®, Johnson and Johnson, NJ, USA) [12].

For the results shown in Figure 7, nontargeted QD-Ls and EGFR-targeted QD-ILs were infused into intracranial U87-EGFRvIII brain tumors by CED. Two mice in each group receiving QD-Ls and QD-ILs, respectively, were euthanized by transcardial perfusion with phosphate-buffered saline at 2.5 h following CED. Quantitation of relative fluorescence (QD-ILs/QD-Ls) by *ex vivo* imaging was for whole brain, as well as for brains sectioned in the coronal plane. Results are based on averages calculated for the two mice receiving QD-ILs, as well as for the two mice receiving QD-Ls. *In vivo* bioluminescence on the left panels showed intense luminescence signals corresponding to the intracranial GBM39 tumor. *Ex vivo* fluorescence images for mice injected with EGFR-targeted QD-ILs and nontargeted QD-Ls collected 2.5 h post-CED indicate areas covered by CED. Fluorescence quantitation by overhead view indicates five-times greater fluorescence in the brain infused with EGFR-targeted QD immunoliposomes compared with nontargeted QD-liposomes, whereas the cross-sectional view indicates a 4.4-times differential. A confocal microscope image of corresponding histological sections in Figure 7 shows parenchymal penetration of QD-ILs. With regards to clearance rate, QD-Ls and QD-ILs were infused into brain tumors by CED on day 25 after tumor cell implantation, which allowed a maximum of approximately 7 days of nanoparticle residence in mouse brains before the required sacrifice of animals due to tumor burden. At day 7 postadministration, there was readily detectable QD-L and QD-IL fluorescence remaining, suggesting that these particles are stable for an extended period of time *in vivo*.

One of the major advantages of formulating drugs in nanoparticle drug delivery systems for cancer treatment is the potentially favorable redirection of drugs to improve biodistribution. Targeting through specific interactions (e.g., immunotargeting) with tumor cells is often considered an important component to further enhance efficacy. Contrary to intuition, the authors of this article have reported that, irrespective of the presence of ligand-targeting components, sterically stabilized liposomes

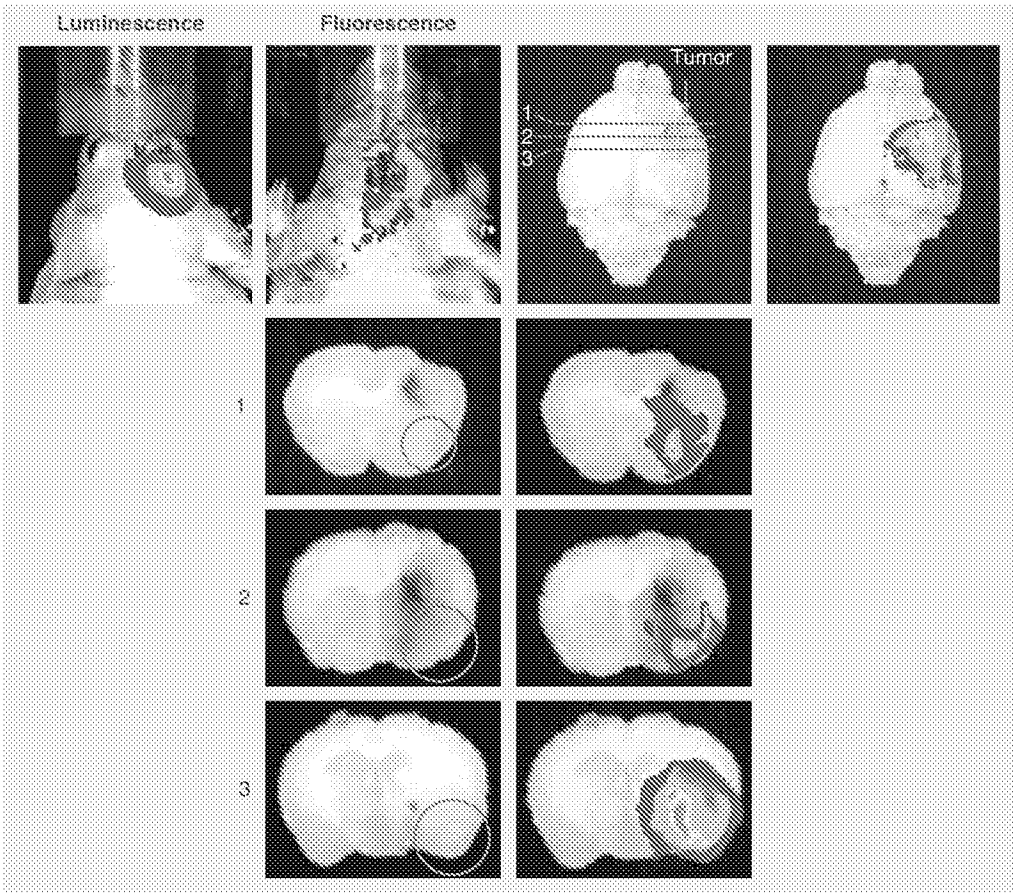

Figure 5. Convection-enhanced delivery of nontargeted quantum dot–liposome hybrid nanoparticles in U87-EGFRvIII intracranial tumor. *In vivo* bioluminescence and *ex vivo* fluorescence images of mice injected with nontargeted quantum dot–liposome hybrid nanoparticles, collected 2.5 h post-convection-enhanced delivery in U87-EGFRvIII intracranial tumor. Luciferase-modified U87-EGFRvIII glioblastoma cells were injected into the right supratentorial brain in mice and tumor growth was monitored by bioluminescence imaging. Intense luminescence signals were detected corresponding to intracranial tumor growth. Fluorescent nontargeted quantum dot–liposome hybrid nanoparticles were infused into the intracranial tumor by convection-enhanced delivery and fluorescent signals from quantum dot–liposome hybrid nanoparticles were detected at 2.5 h following convection-enhanced delivery by *in vivo* and *ex vivo* fluorescence imaging. The *ex vivo* fluorescence image in serial cross-sections showed intense fluorescent signals within the tumor, indicating parenchymal penetration of quantum dot–liposome hybrid nanoparticles. The numbers 1, 2 and 3 refer to the serial cross-sections. For color images see online at www.futuremedicine.com/doi/full/10.2217/NNM.12.209.

accumulate in solid tumors at comparable levels via the EPR effect [20,21]. Nevertheless, this group demonstrated that internalizing immunoliposomes do significantly enhance treatment efficacy via intracellular delivery of encapsulated chemotherapeutics, as opposed to extracellular accumulation of nontargeted counterparts with passive uptake by tumor cells [20,35]. Therefore, ligand-directed nanoparticles can indeed confer additional therapeutic advantages over nontargeted nanoparticles by exploiting the targeting mechanism at the cellular level. For example, EGFR-targeted immunoliposomes showed internalization in 92% of analyzed cells, while nontargeted liposomes internalized in <5% [20]. In the present study, EGFR targeting of lipidic nanoparticles was employed for brain tumor treatment, and specific tumor cell uptake *in vitro* and increased tumor tissue retention following CED *in vivo* due to immunotargeting was observed. In subsequent studies, the authors plan to evaluate drug-loaded versions of these nanoparticles for therapeutic delivery.

Conclusion

We describe multifunctional nanoparticles for tumor cell targeting and QD-mediated imaging in brain tumor models *in vitro* and *in vivo*. CED infusion of nanoparticles provided extensive tumor tissue distribution and retention over time. Further advantages were observed utilizing the cell-specific uptake and tissue retention

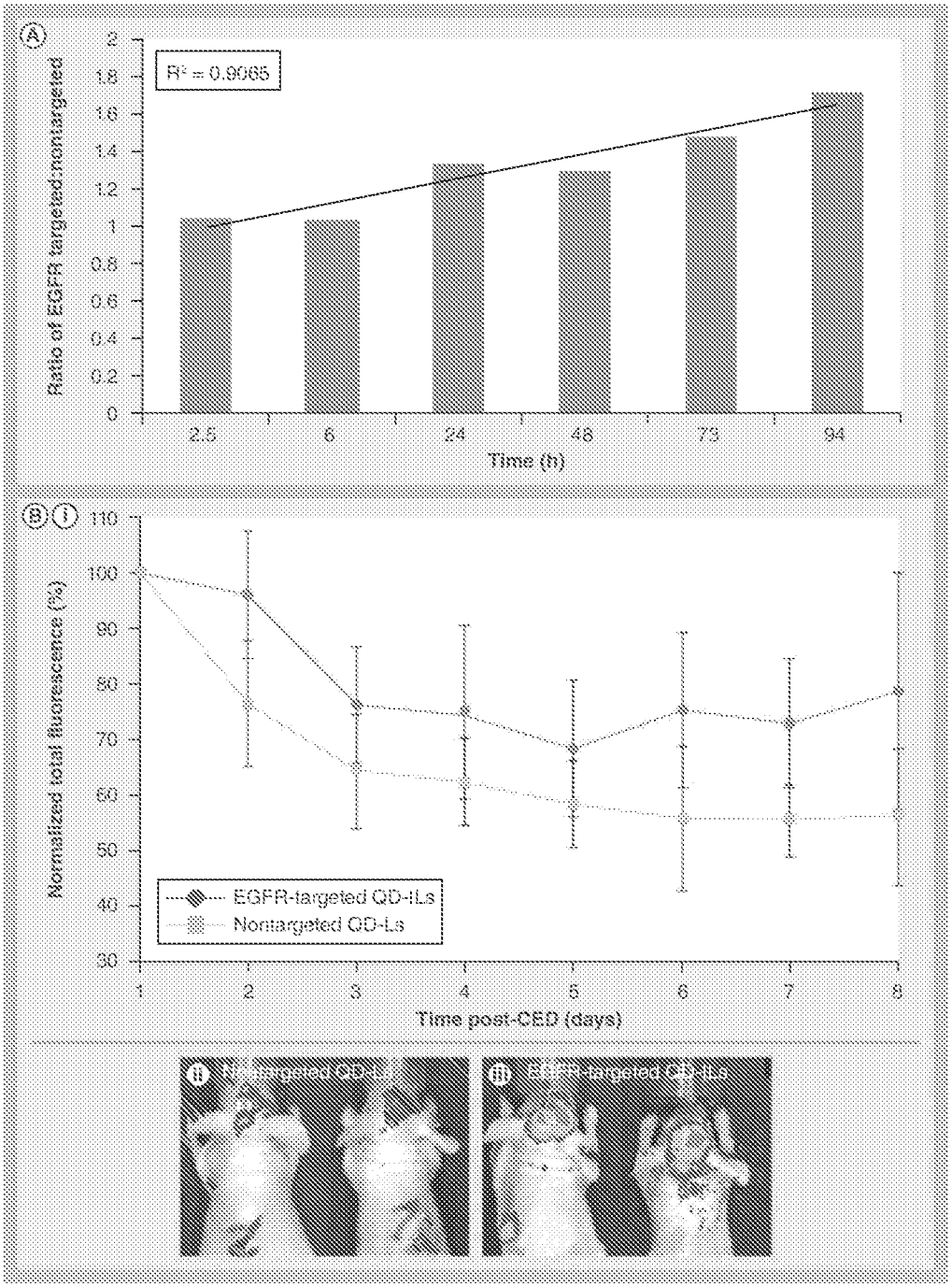

Figure 6. Retention of targeted quantum dot–immunoliposome hybrid nanoparticles versus nontargeted quantum dot–liposome hybrid nanoparticles delivered by convection-enhanced delivery in brain tumor models. (A) Two mice in each group with large intracranial U87-EGFRvIII tumors (bioluminescence: 2 x 10^5 photon/s/cm²) were infused with 10 µl of nontargeted QD-Ls and EGFR-targeted QD-ILs. Fluorescence values were taken in live mice on the IVIS® Lumina system. At 2.5 h after infusion, the liposomes were present in equal amounts (QD-ILs:QD-Ls = 1.05), but by 94 h, EGFR-targeted QD-ILs were retained at a greater rate (QD-ILs:QD-Ls = 1.71). The trend line formed has an R^2 value of 0.9 suggesting a statistically significant trend. **(Bi)** Normalized total intracranial fluorescence for EGFR-targeted QD-ILs and nontargeted QD-Ls. QD-ILs exhibited approximately 1.3-fold higher retention based on total fluorescence on day 7 post-CED ($p < 0.05$; $n = 3$) compared with nontargeted QD-Ls. Error bars indicate standard deviations. Results from mice infused with **(Bii)** nontargeted QD-Ls and **(Biii)** EGFR-targeted QD-ILs. Fluorescence signals were measured *in vivo* through the skull at 6 h after CED. For color images see online at www.futuremedicine.com/doi/full/10.2217/NNM.12.209.
CED: Convection-enhanced delivery; EGFR: EGF receptor; QD-IL: Quantum dot–immunoliposome hybrid nanoparticle; QD-L: Quantum dot–liposome hybrid nanoparticle.

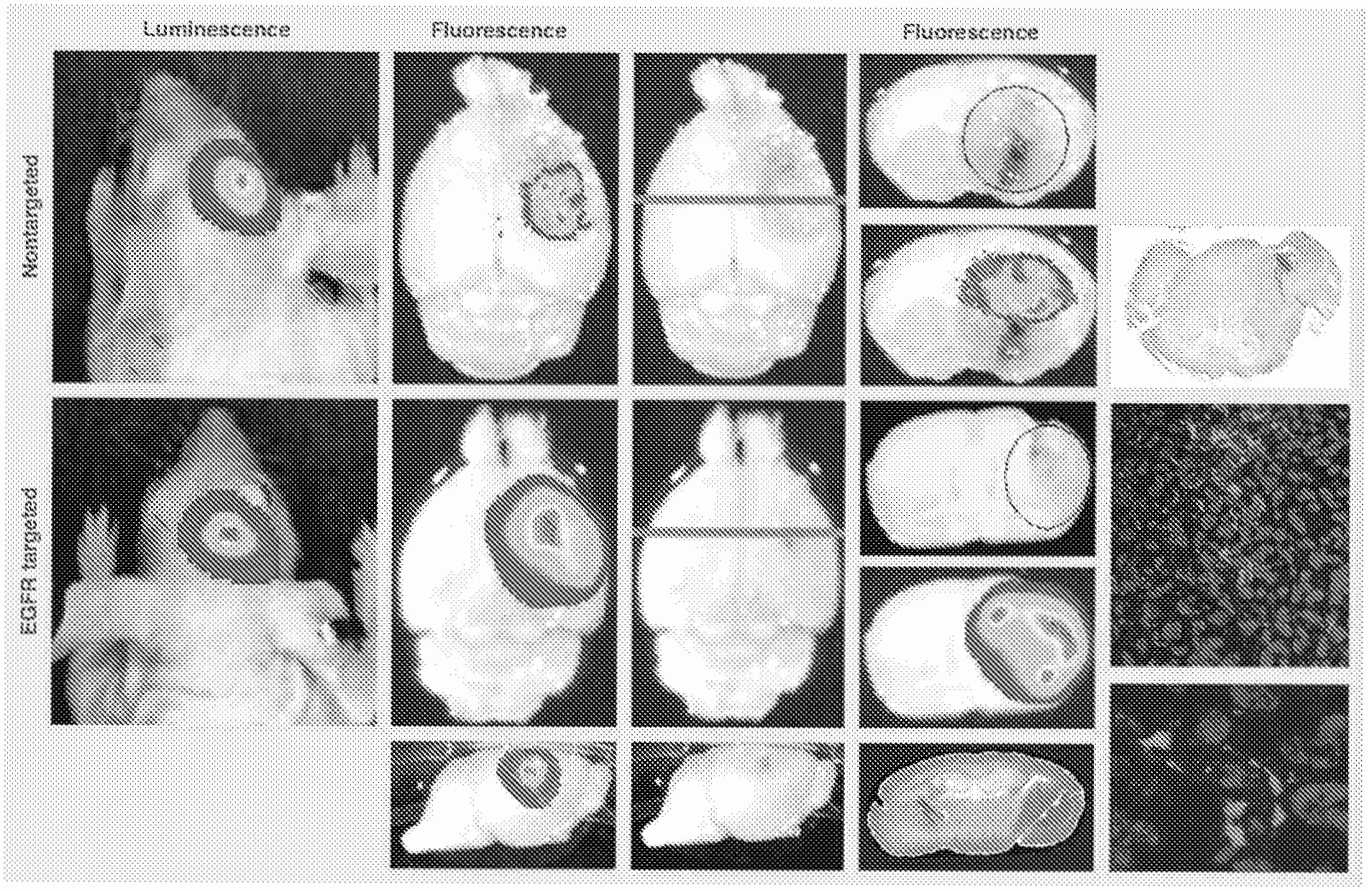

Figure 7. *In vivo* bioluminescence and *ex vivo* fluorescence images for mice injected with 10 µl EGF receptor-targeted quantum dot–immunoliposome hybrid nanoparticles and nontargeted quantum dot–liposome hybrid nanoparticles collected 2.5 h post-convection-enhanced delivery. Quantum dot–immunoliposome hybrid nanoparticles (QD-ILs) and quantum dot–liposome hybrid nanoparticles (QD-Ls) were infused into the GBM39 supratentorial tumor. Fluorescence quantitation by overhead view indicates five-times greater fluorescence in the brain injected with QD-ILs, whereas the cross-sectional view indicates a 4.4-times differential. Both QD-ILs and QD-Ls were detected within the tumor site at 6 h following convection-enhanced delivery. The confocal microscope images of corresponding histological sections show QD-ILs diffusely distributed into the tumor mass, indicating parenchymal penetration of QD-ILs. For color images see online at www.futuremedicine.com/doi/full/10.2217/NNM.12.209.
EGFR: EGF receptor

of immunotargeting. Introduction of QDs to immunoliposome technology allows for tracking of multifunctional nanoparticles at the cellular and subcellular levels, in addition to noninvasive monitoring after CED in orthotopic brain tumor models over time. QD-ILs represent a promising strategy for integrated imaging and drug delivery. These data suggest that antibody-directed lipidic nanoparticles, in conjunction with CED, may offer therapeutic benefits for glioblastoma treatment as a result of specific and efficient uptake by malignant cells.

Future perspective

In the years to come, one can expect the increasing use of nanotechnology-based agents in two areas. One is nanoparticle-based drug delivery systems in cancer treatment. New systems will build on the initial successes of liposome and other nanoparticle technologies. The other is theranostic systems that can integrate imaging and delivery capabilities at the nanoscale. Our proof-of-concept study describes one such system engineered to address these areas for brain tumor treatment.

Financial & competing interests disclosure

This work was supported by grants from the National Cancer Institute (NIH P50 CA 58207-01, NIH P50 CA CA097257 and NIH U54 CA90788). KC Weng is supported by the Delores R Malone American Brain Tumor Association Fellowship Award and the National Cancer Institute Cancer Center Support Grants Pilot Program. FF Chen is supported by the DOD BCRP BC045345 grant and Agilent Technologies Foundation Gift#NA270 and Gift#09-US-270. CO Noble, DC Drummond and DB Kirpotin are equity holders of Merrimack Pharmaceuticals, Inc. JW Park is a patent holder with the University of California, USA, and an advisor and equity holder of Merrimack Pharmaceuticals, Inc. The authors

have no other relevant affiliations or financial involvement with any organization or entity with a financial interest in or financial conflict with the subject matter or materials discussed in the manuscript apart from those disclosed.

No writing assistance was utilized in the production of this manuscript.

Ethical conduct of research

The authors state that they have obtained appropriate institutional review board approval or have followed the principles outlined in the Declaration of Helsinki for all human or animal experimental investigations. In addition, for investigations involving human subjects, informed consent has been obtained from the participants involved.

Executive summary

- To improve brain tumor treatment, the strategy of combining targeted nanoliposomal carriers and convection-enhanced delivery (CED) was evaluated in brain tumor models.
- An EGF receptor (EGFR)-targeted, quantum dot (QD)–immunoliposome hybrid nanoparticle (QD-IL) was synthesized by sequential bioconjugation of Fab' fragments derived from cetuximab and near-QDs to maleimide- and amine-bifunctionalized liposomes.
- QD-ILs were imaged *in vitro* and *in vivo* for cellular uptake and retention. QD liposome hybrid nanoparticles (QD-Ls) without EGFR-targeting moieties attached were measured as the nontargeted control.
- EGFR-overexpressing (GBM6 glioma and MDA-MB-468 breast cancer) and EGFRvIII-overexpressing (U87-EGFRvIII) cells all showed specific and efficient internalization of QD-ILs, while uptake by low EGFR-expressing (GBM14 and MCF-7) cells was negligible. The nontargeted counterpart, QD-Ls, also showed minimal uptake in all cell lines.
- In *in vivo* experiments, QD-ILs and QD-Ls were administered via CED in intracranial U87-EGFRvIII and GBM39 xenograft models, and fluorescence was noninvasively imaged in real-time. QD-ILs exhibited approximately 1.3–1.7-fold higher total fluorescence compared with nontargeted QD-Ls, indicating that imaging detected higher retention of QD-ILs in the brain tumors.
- Brains were also collected on day 1 after CED for *ex vivo* imaging and histological analysis. Fluorescence of whole brains *ex vivo* was found to be fivefold higher for QD-ILs compared with QD-Ls.
- QD-ILs serve as an effective imaging agent for tracking liposomal nanoparticles *in vitro* and *in vivo*.
- The data suggest that ligand-directed liposomal nanoparticles in conjunction with CED may offer therapeutic benefits for brain tumor treatment as a result of specific and efficient uptake by malignant cells.

References

Papers of special note have been highlighted as:
* of interest
** of considerable interest

1 Brem SS, Bierman PJ, Brem H *et al.* Central nervous system cancers. *J. Natl Compr. Canc. Netw.* 2011(9), 352–400 (2011).

2 Pardridge WM. Drug targeting to the brain. *Pharm. Res.* 24(9), 1733–1744 (2007).

3 Bobo RH, Laske DW, Akbasak A, Morrison PF, Dedrick RL, Oldfield EH. Convection-enhanced delivery of macromolecules in the brain. *Proc Natl Acad. Sci. USA* 91(6), 2076–2080 (1994).

4 Krauze MT, Saito R, Noble C *et al.* Reflux-free cannula for convection-enhanced high-speed delivery of therapeutic agents. *J. Neurosurg.* 103(5), 923–929 (2005).

5 Bidros DS, Liu JK, Vogelbaum MA. Future of convection-enhanced delivery in the treatment of brain tumors. *Future Oncol.* 6(1), 117–125 (2010).

6 Kunwar S, Chang S, Westphal M *et al.* Phase III randomized trial of CED of IL13-PE38QQR vs Gliadel wafers for recurrent glioblastoma. *Neuro Oncol.* 12(8), 871–881 (2010).

7 Mamot C, Nguyen JB, Pourdehnad M *et al.* Extensive distribution of liposomes in rodent brains and brain tumors following convection-enhanced delivery. *J. Neurooncol.* 68(1), 1–9 (2004).

8 Saito R, Bringas JR, McKnight TR *et al.* Distribution of liposomes into brain and rat brain tumor models by convection-enhanced delivery monitored with magnetic resonance imaging. *Cancer Res.* 64(7), 2572–2579 (2004).

9 Krauze Mt, Forsayeth J, Park JW, Bankiewicz KS. Real-time imaging and quantification of brain delivery of liposomes. *Pharm. Res.* 23(11), 2493–2504 (2006).

10 Noble CO, Krauze MT, Drummond DC *et al.* Novel nanoliposomal CPT-11 infused by convection-enhanced delivery in intracranial tumors: pharmacology and efficacy. *Cancer Res.* 66(5), 2801–2806 (2006).

** **This study, as well as [11] and [12], demonstrated convection-enhanced delivery of liposomal drugs in brain tumor models.**

11 Saito R, Krauze MT, Noble CO *et al.* Convection-enhanced delivery of Ls-TPT enables an effective, continuous, low-dose chemotherapy against malignant glioma xenograft model. *Neuro. Oncol.* 8(3), 205–214 (2006).

12 Krauze MT, Noble CO, Kawaguchi T *et al.* Convection-enhanced delivery of nanoliposomal CPT-11 (irinotecan) and pegylated liposomal doxorubicin (Doxil) in rodent intracranial brain tumor xenografts. *Neuro. Oncol.* 9(4), 393 (2007).

13 Yamashita Y, Krauze MT, Kawaguchi T *et al.* Convection-enhanced delivery of a topoisomerase I inhibitor (nanoliposomal topotecan) and a topoisomerase II inhibitor (pegylated liposomal doxorubicin) in intracranial brain tumor xenografts. *Neuro. Oncol.* 9(1), 20–28 (2007).

14 Mackay JA, Li W, Huang Z *et al.* HIV TAT peptide modifies the distribution of DNA nanolipoparticles following convection-enhanced delivery. *Mol. Ther.* 16(5), 893–900 (2008).

15 Saito R, Krauze MT, Noble CO *et al.* Tissue affinity of the infusate affects the distribution volume during convection-enhanced delivery into rodent brains: implications for local drug delivery. *J. Neurosci. Methods* 154(1–2), 225–232 (2004).

16 Murad GJA, Walbridge S, Morrison PF *et al.* Real-time, image-guided, convection-enhanced delivery of interleukin 13 bound to pseudomonas exotoxin. *Clin. Cancer Res* 12(10), 3145–3151 (2006).

17 Bidros DS, Vogelbaum MA. Novel drug delivery strategies in neuro-oncology. *Neurotherapeutics* 6(3), 539–546 (2009).

* Review of novel drug delivery strategies to brain tumors and the CNS.

18 Serwer L, Hashizume R, Ozawa T, James CD. Systemic and local drug delivery for treating diseases of the central nervous system in rodent models. *J. Vis. Exp.* 42, e1992 (2010).

19 Noble CO, Kirpotin DB, Hayes ME *et al.* Development of ligand-targeted liposomes for cancer therapy. *Expert Opin. Ther. Targets* 8(4), 335–353 (2004).

20 Mamot C, Drummond DC, Noble CO *et al.* Epidermal growth factor receptor-targeted immunoliposomes significantly enhance the efficacy of multiple anticancer drugs *in vivo*. *Cancer Res.* 65(24), 11631–11638 (2005).

» Data supporting EGF receptor-targeted immunoliposome drugs by intravenous administration in preclinical studies.

21 Kirpotin DB, Drummond DC, Shao Y *et al.* Antibody targeting of long-circulating lipidic nanoparticles does not increase tumor localization but does increase internalization in animal models. *Cancer Res.* 66(13), 6732–6740 (2006).

» Results demonstrated that long circulating immunoliposomes deposit in solid tumors at comparable amounts as nontargeted versions. The significant increase in efficacy with targeting was attributable to intracellular delivery of the encapsulated drug payload.

22 Pastorino F, Marimpieri D, Brignole C *et al.* Ligand-targeted liposomal therapies of neuroblastoma. *Curr. Med. Chem.* 14(29), 3070–3078 (2007).

23 Medintz IL, Uyeda HT, Goldman ER, Mattoussi H. Quantum dot bioconjugates for imaging, labelling and sensing. *Nat. Mater.* 4(6), 435–446 (2005).

24 Jaiswal JK, Goldman ER, Mattoussi H, Simon SM. Use of quantum dots for live cell imaging. *Nat. Methods* 1(1), 73–78 (2004).

25 Alivisatos AP, Gu W, Larabell C. Quantum dots as cellular probes. *Annu. Rev. Biomed. Eng.* 7, 55–76 (2005).

26 Klostranec JM, Chan WCW. Quantum dots in biological and biomedical research: recent progress and present challenges. *Adv. Mater.* 18(15), 1953–1964 (2006).

27 Ballou B, Ernst LA, Andreko S *et al.* Sentinel lymph node imaging using quantum dots in mouse tumor models. *Bioconjug. Chem.* 18(2), 389–396 (2007).

28 Weng KC, Noble CO, Papahadjopoulos-Sternberg B *et al.* Targeted tumor cell internalization and imaging of multifunctional quantum dot-conjugated immunoliposomes *in vitro* and *in vivo*. *Nano Lett.* 8(9), 2851–2857 (2008).

» First modularly assembled quantum dot–immunoliposome hybrid nanoparticles systemically administered and imaged *in vivo* in xenograft models.

29 Gao J, Chen X, Cheng Z. Near-infrared quantum dots as optical probes for tumor imaging. *Curr. Top. Med. Chem.* 10(12), 1147–1157 (2010).

30 Sarkaria JN, Yang L, Grogan PT *et al.* Identification of molecular characteristics correlated with glioblastoma sensitivity to EGFR kinase inhibition through use of an intracranial xenograft test panel. *Mol. Cancer Ther.* 6(3), 1167–1174 (2007).

31 Hashizume R, Gupta N, Berger MS *et al.* Morphologic and molecular characterization of ATRT xenografts adapted for orthotopic therapeutic testing. *Neuro. Oncol.* 12(4), 336–376 (2010).

32 Zhou Y, Drummond DC, Zou H *et al.* Impact of single-chain Fv antibody fragment affinity on nanoparticle targeting of epidermal growth factor receptor-expressing tumor cells. *J. Mol. Biol.* 371(4), 934–947 (2007).

33 Bentzen EL, Tomlinson ID, Mason J *et al.* Surface modification to reduce nonspecific binding of quantum dots in live cell assays. *Bioconjug. Chem.* 16(6), 1488–1494 (2005).

34 Sampson JH, Akabani G, Archer GE *et al.* Intracerebral infusion of an EGFR-targeted toxin in recurrent malignant brain tumors. *Neuro. Oncol.* 10(3), 320–329 (2008).

35 Park JW, Hong K, Kirpotin DB *et al.* Anti-HER2 immunoliposomes: enhanced efficacy attributable to targeted delivery. *Clin. Cancer Res.* 8(4), 1172–1181 (2002).

Website

101 CBTRUS 2012 statistical report tables, primary brain and central nervous system tumors diagnosed in the United States in 2004–2008, Brain Tumor Registry of the United States, Hinsdale, IL, USA, CBTRUS. www.cbtrus.org/2007-2008/2007-20081.html

NANO LETTERS
2008
Vol. 8, No. 9
2851-2857

Targeted Tumor Cell Internalization and Imaging of Multifunctional Quantum Dot-Conjugated Immunoliposomes in Vitro and in Vivo

Kevin C. Weng,[†] Charles O. Noble,[‡] Brigitte Papahadjopoulos-Sternberg,[§] Fanqing F. Chen,[||] Daryl C. Drummond,[‡] Dmitri B. Kirpotin,[‡] Donghui Wang,[†] Yun K. Hom,[†] Byron Hann,[†] and John W. Park*[,†]

UCSF Helen Diller Family Comprehensive Cancer Center, San Francisco, California 94115, Hermes Biosciences, South San Francisco, California 94080, NanoAnalytical Laboratory, San Francisco, California 94118, and Life Sciences Division, Lawrence Berkeley National Laboratory, Berkeley, California 94720

Received May 23, 2008; Revised Manuscript Received July 12, 2008

ABSTRACT

Targeted drug delivery systems that combine imaging and therapeutic modalities in a single macromolecular construct may offer advantages in the development and application of nanomedicines. To incorporate the unique optical properties of luminescent quantum dots (QDs) into immunoliposomes for cancer diagnosis and treatment, we describe the synthesis, biophysical characterization, tumor cell-selective internalization, and anticancer drug delivery of QD-conjugated immunoliposome-based nanoparticles (QD-ILs). Pharmacokinetic properties and in vivo imaging capability of QD-ILs were also investigated. Freeze-fracture electron microscopy was used to visualize naked QDs, liposome controls, nontargeted QD-conjugated liposomes (QD-Ls), and QD-ILs. QD-ILs prepared by insertion of anti-HER2 scFv exhibited efficient receptor-mediated endocytosis in HER2-overexpressing SK-BR-3 and MCF-7/HER2 cells but not in control MCF-7 cells as analyzed by flow cytometry and confocal microscopy. In contrast, nontargeted QD-Ls showed minimal binding and uptake in these cells. Doxorubicin-loaded QD-ILs showed efficient anticancer activity, while no cytotoxicity was observed for QD-ILs without chemotherapeutic payload. In athymic mice, QD-ILs significantly prolonged circulation of QDs, exhibiting a plasma terminal half-life ($t_{1/2}$) of ~2.9 h as compared to free QDs with $t_{1/2}$ < 10 min. In MCF-7/HER2 xenograft models, localization of QD-ILs at tumor sites was confirmed by in vivo fluorescence imaging.

A premise of nanomedicine is that it may be feasible to develop multifunctional constructs combining diagnostic and therapeutic capabilities, thus leading to better targeting of drugs to diseased cells. For example, it may be possible to track such constructs at the cellular and subcellular levels and to monitor their spatial and temporal interactions with tumor cells. Organic dyes have been used for optical detection of various agents including nanoparticles; however, they generally suffer from limitations such as narrow excitation/broad emission spectra, photobleaching, and biodegradation, which restrict the applicability of imaging techniques. More recently, semiconductor quantum dots (QDs) have emerged as a promising alternative to organic dyes as fluorescent markers for in vitro and in vivo imaging; their superior brightness and photostability[1−6] make them excellent candidates in the development of trackable multifunctional agents.

However, as molecular probes by themselves in medical applications, QDs have a number of potential limitations such as specificity, biocompatibility, and toxicology.[7] QDs have also been reported to aggregate nonselectively on the surface of cell membranes.[8−10] To target them to cells of interest, QDs have been conjugated to various biocompatible entities[11−13] or inserted into lipid bilayers.[14] These methods sometimes involve premodification of the target cell surface or use of large quantities and multilayer couplings of QDs, which limit their practicality.

As an alternative approach, we hypothesized that conjugation of QDs to immunoliposomes (ILs) would represent a feasible and novel strategy for QD-based cellular and in vivo tumor imaging, including integration of targeting, reporting,

* To whom correspondence should be addressed. Current address: UCSF Helen Diller Family Comprehensive Cancer Center, 1600 Divisadero St., 2nd Fl., San Francisco, CA 94115-1710. Tel: 415-502-3844. Fax: 415-353-9592. E-mail: jpark@cc.ucsf.edu.
[†] UCSF Helen Diller Family Comprehensive Cancer Center.
[‡] Hermes Biosciences.
[§] NanoAnalytical Laboratory.
[||] Lawrence Berkeley National Laboratory.

10.1021/nl801488u CCC: $40.75
Published on Web 08/20/2008

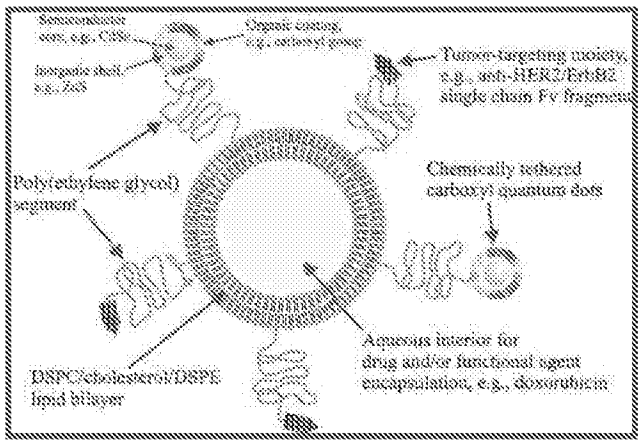

Figure 1. Schematic showing the structure of a QD-IL nanoparticle. The liposomal core is about 100 nm in diameter as visualized by ff-EM. Derivatized CdSe/ZnS core/shell QDs are represented as a sphere with a layer of organic coating (gray) covering the outer surface of the inorganic shell (yellow) and the semiconductor core (orange). They were also characterized by ff-EM, indicating an average diameter of ~11 nm. Surface-derivatized QDs were chemically linked to functionalized PEG-DSPE incorporated in extruded liposomes. Anti-HER2 single chain Fv fragments (scFv, arrowheads) are attached to the end of PEG chains. Nellis, D.F.; Ekstrom, D. L.; Kirpotin, D. B.; Zhu, J.; Andersson, R.; Broadt, T. L.; Ouellette, T. F.; Perkins, S. C.; Roach, J. M.; Drummond, D. C.; Hong, K.; Marks, J. D.; Park, J. W.; Giardina, S. L. Preclinical manufacture of an anti-HER2 scFv-PEG-DSPE, liposome-inserting conjugate. 1. Gram-scale production and purification. *Biotechnol. Prog.* **2005**, *21* (1), 205–220. scFv moieties (MW ~ 25 kDa) are not drawn to scale. QD-ILs retain an aqueous interior for loading and delivery of drugs/probes.

and drug delivery. Liposomes represent a prototypic nanoparticle system that has been fully optimized for in vivo human use as drug carriers.[15] Newer liposome-based approaches include ILs in which monoclonal antibody fragments are conjugated to liposomal drugs for targeted cell-specific delivery.[16] The continued evolution of ILs has led to optimized components and modular assembly strategies for specific functionalities.[17] For example, ILs against HER2[18,19] and EGFR[20,21] can efficiently deliver drugs to tumor cells and are in development for clinical testing. Our design for QD-conjugated ILs (QD-ILs) is schematically illustrated in Figure 1. To assemble the multifunctional QD-IL hybrid nanoparticles with imaging, targeting, and therapeutic modalities, a 0.2 μM concentration of carboxyl CdSe/ZnS core/shell QDs was chemically linked to 2−3 mol % amine-functionalized *N*-(polyethylene glycol)-1,2-distearoyl-*sn*-glycero-3-phosphoethanolamine (PEG-DSPE) incorporated in extruded liposomes through ~2 mM zero-length cross-linker 1-ethyl-3-(3-dimethylaminopropyl)carbodiimide (EDC). QD605 (λ_{max} ~ 605 nm) was used for in vitro analysis and pharmacokinetics (PK) studies. QD800 (λ_{max} ~ 800 nm) was used for in vivo imaging experiments for more efficient tissue penetration. Fluorescence spectrophotometry analysis of QD-conjugated liposomes (QD-Ls) indicated a mean phospholipid to QD ratio of ~42000, corresponding to 1.7−2.2 QDs per liposome (experimental methods are available in the Supporting Information). Higher ratios of QDs/phospholipid could be achieved; however, we observed a higher extent of cross-linking and reduced internalization in vitro with such constructs (data not shown).

Freeze-fracture electron microscopy (ff-EM) has been demonstrated to be a powerful technique to characterize nanoscale structures, including liposomes[22] and micelles.[23] Using ff-EM, we clearly visualized carboxyl QDs, both free (Figure 2a,b) and when conjugated to liposomes (Figure 2c) or HER2-targeted ILs containing doxorubicin (dox) (Figure 2d). QDs appeared as small, mostly spherical particles with shadowing behind the structure, typical for convex, hard-core particles. Diameters of the QDs investigated here ranged from 5 to 22 nm (mean, 11 nm). In contrast to QDs, liposomes and ILs displayed convex and concave fracture planes (shadow behind and shadow in front, respectively). Membrane-bound structures such as liposomes typically show fracture planes along the hydrophobic interior of bilayers as the area of weakest force interaction (hydrophobic interaction of the lipid−fatty acid tails). While both free QDs and QDs trapped in the interliposomal space showed equal diameters, QDs visible on liposomal fracture planes appeared less prominent. It is unlikely that such images depict actual QDs, which should be unable to penetrate into the hydrophobic interior of bilayers; rather, we hypothesize that these reflect imprints of surface-attached QDs showing through the semifluid, liquid−crystalline bilayers. Our ff-EM study demonstrated that conjugation of QDs resulted in some alteration of liposome size, which was also observed by dynamic light scattering measurements, showing an increase in both particle size and size distribution from 112 ± 27 to 212 ± 32 nm for extruded liposomes and QD-ILs, respectively. However, dynamic light scattering studies indicated no significant difference in size between targeted (212 ± 32 nm) and nontargeted (216 ± 37 nm) particles. Additionally, QDs were frequently observed at contact areas between liposomes/ILs. Using our methodology, the resolution limit for distinct, periodic structures in ff-EM micrographs is ~2 nm. Therefore, the fairly long but very small and flexible PEG chains that can adopt a "mushroom" conformation were not visible.

Cellular binding and uptake of free QDs and various QD-nanoparticle constructs were further evaluated by flow cytometry. Target cells included human breast carcinoma cell lines with HER2 overexpression via endogenous gene amplification (SK-BR-3) or transfection (MCF-7/HER2[24]). Parental MCF-7 was used as a negative control lacking HER2 overexpression. After 60 min of incubation at 37 °C, free carboxyl QDs bound nonspecifically to all tested cells (SK-BR-3, MCF-7/HER2, and MCF-7) in a concentration-dependent manner (Figure 3). At the highest concentration of free QD tested, 10 nM, uptake was slightly higher in MCF-7 cells than in MCF-7/HER2 cells ($p < 0.05$, two-tailed *t* test). In contrast, anti-HER2 QD-ILs showed specific uptake in HER2-overexpressing cells, with 16−30-fold greater uptake in SK-BR-3 and MCF-7/HER2 cells as compared with MCF-7 cells ($p < 0.05$ for all concentrations of QD-ILs). Furthermore, QD-ILs showed markedly greater uptake vs free QDs (50−300-fold) or vs nontargeted QD-Ls (900−1800-fold) in HER2-overexpressing cells at match-

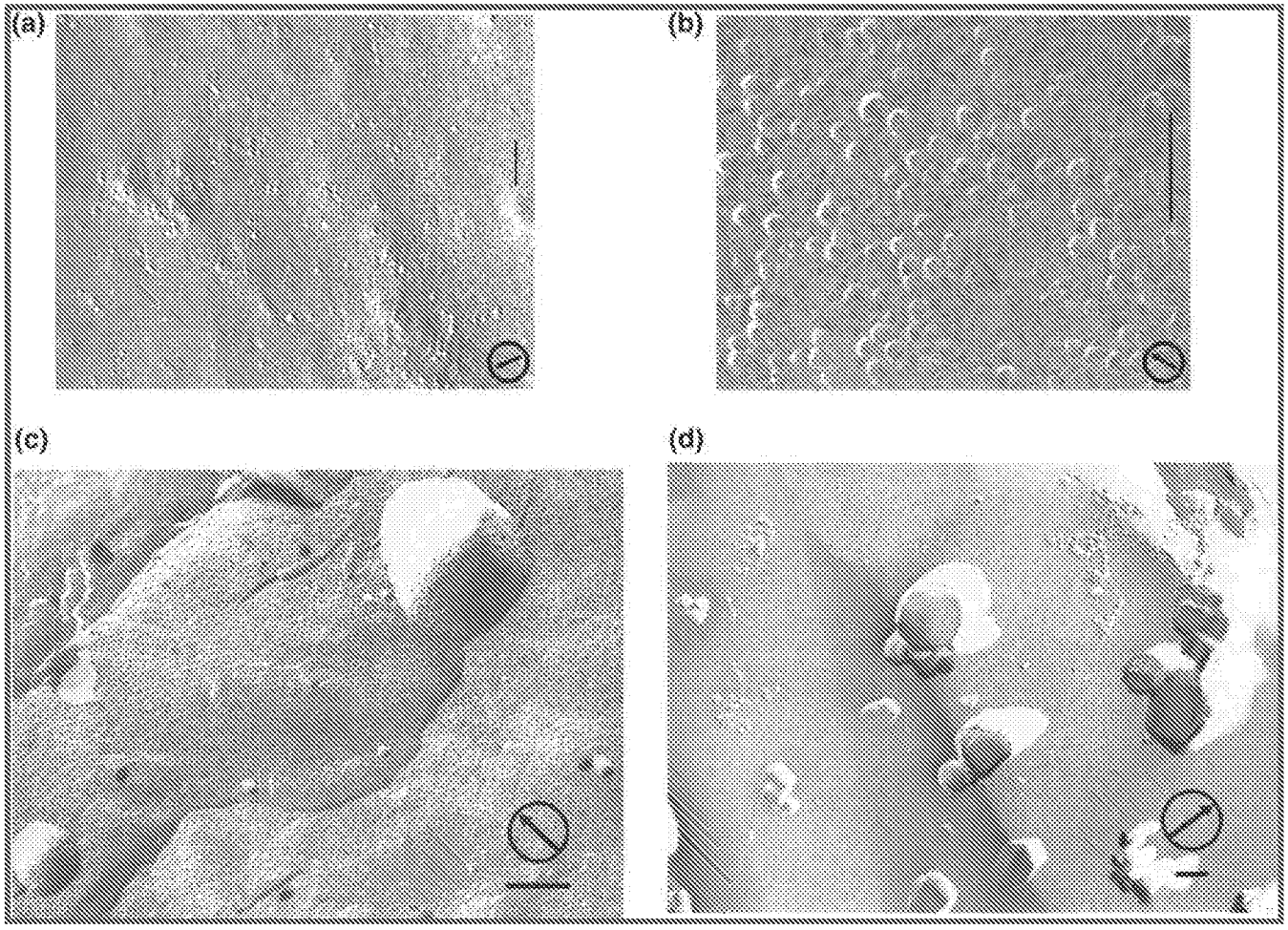

Figure 2. ff-EM micrographs of QD controls are shown. (a) QDs at 19300× and (b) QDs at 46700×. ff-EM micrographs of nanocomplexed QDs are shown. (c) QD-Ls and (d) dox-loaded QD-ILs (QD-ILs-Dox). On all electron micrographs, scale bars = 100 nm, and the shadow direction is indicated by the arrow. Panel d revealed the cross-linked structures of QDs and liposomes, as individual and aggregated liposomes were both observed. QD-ILs-Dox also showed occasionally angular features attributable to the crystalline form of dox precipitated in the interior of liposomes.

ing concentrations. For example, in SK-BR-3 cells, uptake of 2 nM QD-ILs was ~308-fold higher than the equivalent concentration of free QDs ($p < 0.05$); uptake remained ~21-fold higher than free QDs at the much higher concentration of 10 nM ($p < 0.05$). In non-HER2-overexpressing MCF-7 cells, QD-ILs showed equivalent and minimal uptake as nontarged QD-Ls. IL delivery of QDs corresponded to ~2.2 × 10^6 QDs per SK-BR-3 or MCF-7/HER2 cell. The extremely efficient uptake of QD-ILs also allowed use of significantly reduced amounts of QD material, with the lowest test concentration of 0.5 nM still yielding significant uptake, as compared to other methods typically requiring QDs in the high nanomolar to micromolar range.[11,14,25]

Internalization of QD-ILs was visualized using confocal microscopy. SK-BR-3 cells were treated with free QDs, QD-ILs, or QD-Ls for 60 min at 37 °C (Figure 4a−g). Free carboxyl QDs were observed in close association with the cell surface (Figure 4a,b) despite cell washing and specimen processing steps. Nontargeted QD-Ls showed minimal uptake (Figure 4c). Internalization of QD-ILs was confirmed by visualizing the subcellular distribution of the conjugated QD or a separate lipid-based DiD fluorescent label, indicating that ILs had accumulated mostly in the perinuclear region, consistent with endosomal routing (Figure 4d−f). Using the persistent fluorescence of QDs, we generated reconstructed three-dimensional images of cells treated by QD-ILs to map their intracellular localization (Figure 4g). This technique could be useful in studies of the spatial relations involved in intracellular trafficking of receptors. In MCF-7/HER2 cells, QD-ILs showed efficient internalization that was comparable to that observed in SK-BR-3 cells (Figure 4h); in contrast, QD-ILs showed minimal uptake in MCF-7 cells lacking HER2 overexpression (Figure 4i).

To verify that internalization of QD-ILs was mediated through HER2-dependent targeting, F5-PEG-DSPE micelles were added to cell cultures for competitive blockade prior to QD-ILs treatment. Incubation with F5-PEG-DSPE micelles at 5× molar excess (as compared to the amount of scFv in QD-ILs) for 30 min prior to adding QD-ILs effectively reduced IL uptake by ~70% in SK-BR-3 and ~90% in MCF-7/HER2 cells, respectively. Nontargeted QD-Ls were also used to treat SK-BR-3, MCF-7/HER2, and MCF-7 cells to evaluate nonspecific uptake. We observed virtually no uptake nor cell surface binding for nontargeted QD-Ls (Figure 4c).

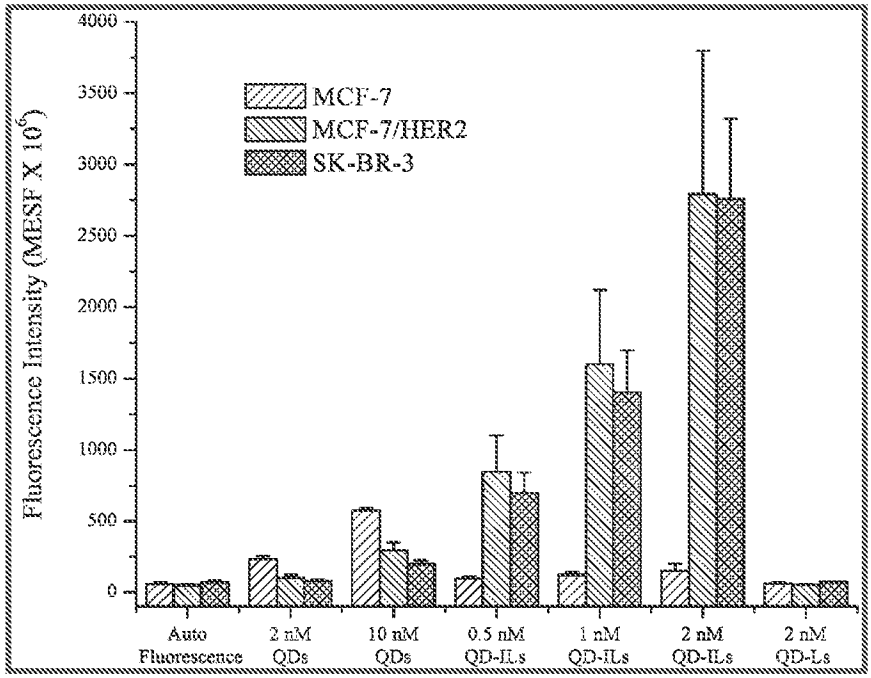

Figure 3. Quantitative flow cytometry results showing fluorescence intensities (mean ± SE; $n = 6$) of SK-BR-3, MCF-7/HER2 (both high HER2-overexpressing human breast cancer cell lines), and MCF-7 (low HER2-expressing human breast cancer cell line). Ten thousand cells were collected in each measurement. The columns, from left to right, represent autofluorescence, cells treated by carboxyl QDs at 2 and 10 nM, HER2-targeted QD-ILs at 0.5, 1, and 2 nM, and 2 nM nontargeted QD-Ls at 37 °C for 1 h. The fluorescence intensities were calibrated by standard fluorescent microbeads and presented in units of molecules of equivalent soluble fluorochrome (MESF) of phycoerythrin.

To install the therapeutic function, we loaded QD-Ls and QD-ILs with dox. Dox was encapsulated via the remote loading method[26] either before or after covalent linking of the liposomes to QDs. While drug loading into liposomes prior to QD conjugation was highly efficient (>90% of added drug was successfully encapsulated), loading into QD-Ls was associated with ~30% loading efficiency. Storage stability of dox encapsulated in QD-Ls and QD-ILs was evaluated, with approximately 15−30% of dox lost from QD-Ls and QD-ILs after storage in 20 mM MES buffer, pH 6, at 4 °C for 2 months.

The anticancer activity of the dox-loaded nanoparticles was evaluated in HER2-overexpressing SK-BR-3 cells (Table 1). Cells (7000−8000) were cultured in 96-well sterile black-walled assay plates (Corning, Corning, NY) and treated with various nanoparticle formulations at 37 °C for 1 h. The anticancer activity was assayed by ATP-activated luciferase assay (Promega, Madison, WI) after the cells were allowed to grow for 3 days. QD-ILs-Dox showed potent cytotoxicity against SK-BR-3 cells (IC_{50} ~ 0.5 μg/mL), which was comparable to ILs-Dox without QD (IC_{50} ~ 0.7 μg/mL). Nontargeted Ls-Dox with or without QDs showed ~10-fold less cytotoxicity than their IL counterparts [$p < 0.001$ by one-way analysis of variance (ANOVA)]. Consistent with previous results,[18] these studies confirmed that ILs but not liposomes provided intracellular dox delivery that was as efficient as the direct permeation of free dox in vitro and also indicated that this targeting effect was not compromised by QD conjugation. QD-ILs lacking dox showed minimal cytotoxicity, confirming that anticancer activity was due to drug delivery and not from the QD-IL carrier system. The slightly increased cytotoxicity of QD-conjugated nanoparticles vs their non-QD-containing counterparts (e.g., IC_{50} of 3.85 ± 0.24 μg/mL for QD-Ls-Dox vs 9.36 ± 0.83 μg/mL for Ls-Dox) likely resulted from some drug leakage in the presence of QDs, consistent with the stability data. It is notable that the highest concentration tested here was 5000-fold lower in QD content than the concentration of CdSe/ZnS core/shell QDs associated with normal tissue toxicity under other conditions.[27]

We evaluated in vivo properties of QD-ILs, including PK studies in nude mice, to address whether QD conjugation compromised the long circulation time of ILs. QD-ILs exhibited moderately prolonged circulation, with plasma terminal $t_{1/2}$ of ~2.9 h. This $t_{1/2}$ was somewhat less than that for non-QD-containing ILs ($t_{1/2}$ = ~7.7 h), possibly due to faster clearance associated with the positively charged amino groups on QD-ILs. However, $t_{1/2}$ of QDs carried by ILs was greatly prolonged over that of free QDs ($t_{1/2}$ < 10 min), which showed extremely rapid clearance to ~5% of the initial plasma level by 10 min and undetectable levels after 1 h. In addition, the mice ($n = 10$) were further monitored for weight change and gross toxicities for an additional 3 month period; no weight loss or obvious signs of toxicity were observed, although formal toxicology studies would be required for definitive evaluation of safety.

For tumor-targeted imaging, QD-ILs were injected i.v. in nude mice bearing HER2-overexpressing MCF-7/HER2 xenografts implanted s.c. in the flank. Twenty-four hours following injection, fluorescence signals were readily detected at the tumor site as well as in mononuclear phagocytic system (MPS) organs known to mediate liposome clearance

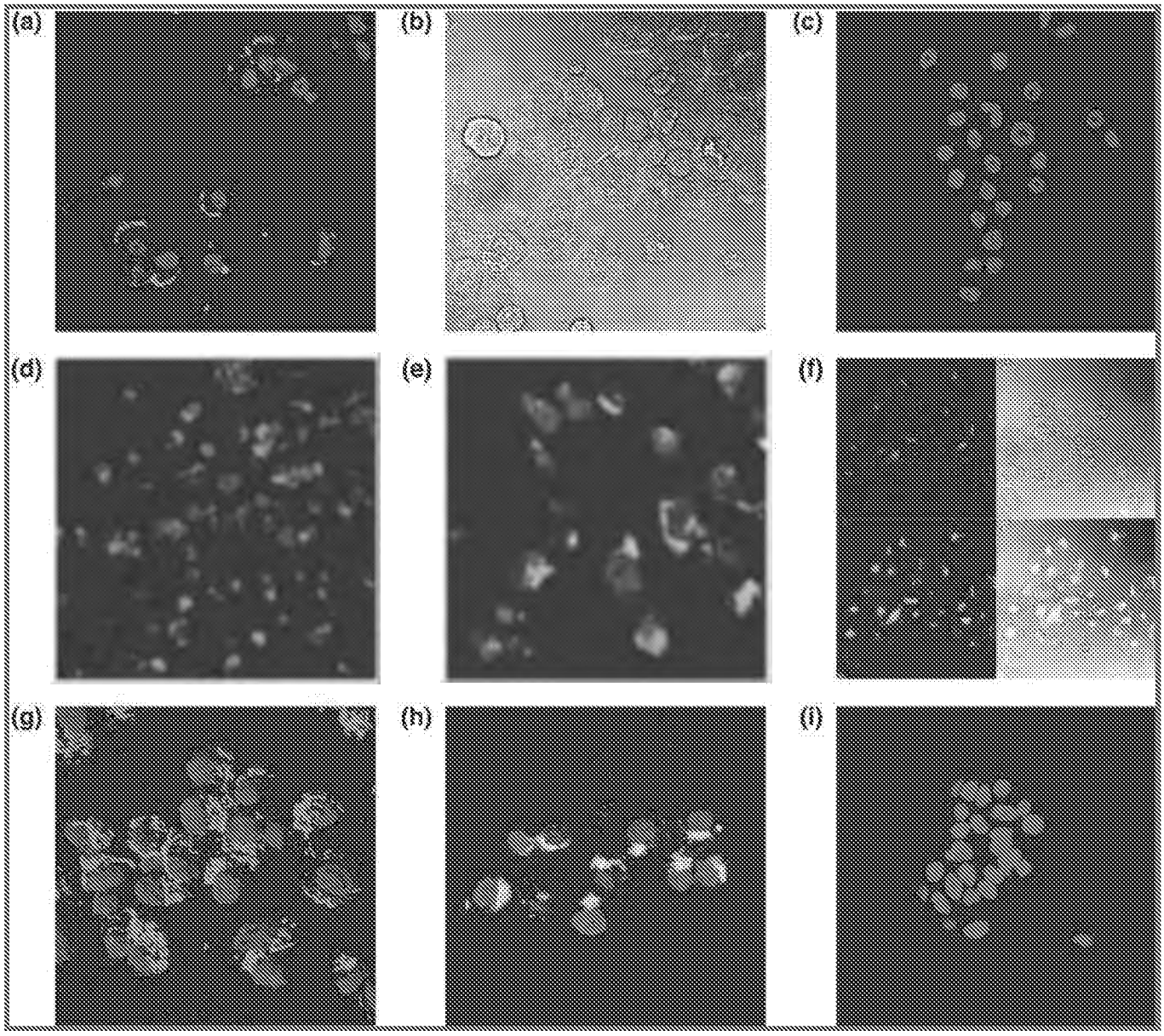

Figure 4. SK-BR-3 cells (panels a−g), MCF-7/HER2 (panel h), or MCF-7 cells (panel i) were treated with free QDs or QD-conjugated nanoparticles (red fluorescence) for 60 min at 37 °C. Cells were stained by DAPI (blue fluorescence). An argon laser (488 nm) or titanium: sapphire (800 nm) was used for QD excitation. A HeNe laser (633 nm) was used for lipidic dye DiD (emission peak at 665 nm) excitation. (a and b) SK-BR-3 cells treated with free carboxyl QDs, showing nonspecific association on the cell surface (image size = 235 μm × 235 μm, and magnification = 40×). In panel a, QD fluorescence (red) and nucleus DAPI staining (blue) are shown. In panel b, differential interference contrast (DIC) and QD fluorescence images are combined to reveal more vividly the binding of QDs along the outline of SK-BR-3 cells. (c) SK-BR-3 cells treated with nontargeted QD-liposomes (QD-Ls), showing virtually no detectable QDs (image size = 235 μm × 235 μm, and magnification = 40×). (d) QD-conjugated anti-HER2 ILs (QD-ILs) internalized in SK-BR-3 cells (image size = 235 μm × 235 μm, and magnification = 40×). (e) Dye-incorporated (green) QD-ILs internalized in SK-BR-3 cells (image size = 146 μm × 146 μm, and magnification = 63×). A 0.25−0.5 mol % amount of 1,1′-dioctadecyl-3,3,3′,3′-tetramethylindodicarbocyanine perchlorate (DiD oil) was included in the lipid mixture for dual labeling. (f) Subpanels of QDs (red, top left), DiD (green, bottom left), DIC (gray scale, top right), and composite (bottom right) images show the intracellular uptake of QD-ILs, in contrast to surface binding of free QDs in panels a and b (subpanel size = 235 μm × 235 μm, and magnification = 40×). (g) Reconstructed 3D image of QD-ILs (red) internalized within SK-BR-3 cells (nucleus in blue). The z-stack constitutes 11 panels that span a total 30 μm elevation (image size = 146 μm × 146 μm, and magnification = 63×). (h) QD-ILs internalized within MCF-7/HER2 cells (image size = 146 μm × 146 μm, and magnification = 63×). (i) MCF-7 cells treated with QD-conjugated anti-HER2 ILs (QD-ILs), showing minimal uptake of QD-ILs (image size = 235 μm × 235 μm, and magnification = 40×).

(Figure 5, left panel). Tumor fluorescence reached a plateau after 24 h, with up to 18 ± 5% (mean ± SD; n = 4) of total body fluorescence localizing to the tumor region. In separate experiments directly comparing tumor accumulation of targeted vs nontargeted nanoparticles, both versions of nanoparticles showed highly efficient tumor accumulation, with 14.2 ± 3.7 and 13.7 ± 2.4% (mean ± SD; n = 4), respectively, of total body fluorescence within the tumor at 24 h. Thus, tumor accumulation was extremely high and comparable for both targeted and nontargeted nanoparticles.

Table 1. Cytotoxicity of Free Dox and Dox-Loaded Nanoparticles against HER2-Overexpressing SK-BR-3 and Nonoverexpressing MCF-7 Cancer Cells in Vitro[a]

IC_{50} (μg/mL)	free Dox	Ls-Dox	ILs-Dox	QD-Ls-Dox	QD-ILs-Dox
SK-BR-3	1.30 ± 0.23	9.36 ± 0.83	0.79 ± 0.03	3.85 ± 0.24	0.45 ± 0.10
MCF-7	0.63 ± 0.03	9.55 ± 0.51	4.23 ± 0.99	3.90 ± 0.55	1.76 ± 0.25

[a] One hour at 37°C was used for incubation, and 3 days was allowed for regrowth after removal of nanoparticles. QD-ILs without dox were administered at equivalent QD concentrations and did not show any toxicity up to 8 nM QDs for 6 h. All values are expressed as IC_{50} (μg/mL) means ± standard errors with the number of replicates = 6; $p < 0.001$ by one-way ANOVA. Ls-Dox, dox-loaded liposomes; ILs-Dox, dox-loaded anti-HER2 ILs; QD-Ls-Dox, dox-loaded, QD-Ls nanoparticles; and QD-ILs-Dox, dox-loaded, QD-conjugated, anti-HER2 IL nanoparticles.

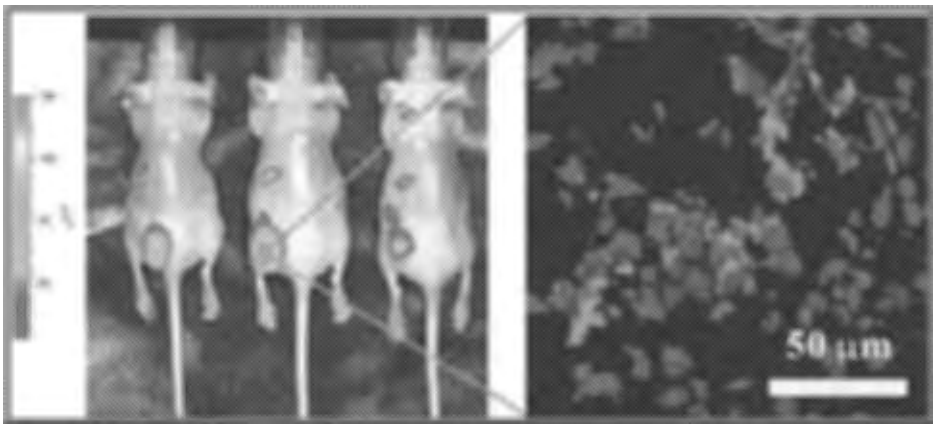

Figure 5. (Left panel) In vivo fluorescence imaging of three nude mice bearing MCF-7/HER2 xenografts implanted in the lower back 30 h after i.v. injection with anti-HER2 QD-ILs. The image was acquired by using an excitation filter of 580−610 nm and an emission band-pass filter of 695−770 nm. Imaging showed that QD-ILs had localized prominently in tumors as well as in MPS organs. Units: efficiency (the fractional ratio of fluorescence emitted per incident photon). (Right panel) A 5 μm section cut from frozen tumor tissues harvested at 48 h postinjection and examined by confocal microscopy by a 63× oil immersion objective (image size, 146 μm × 146 μm). The tumor section was examined in two-color scanning mode for nuclei stained by DAPI (blue) and QD-ILs (red). For the DAPI channel, an 800 nm (titanium:sapphire) two-photon excitation and 390−465 nm emission filter was used. For QD-ILs channel, 488 (argon) or 633 nm (HeNe) for excitation and 650 nm long pass for emission were used. The distribution of QD-ILs is similar to in vitro QD-ILs uptake in SK-BR-3 cells as in Figure 4c,d, where QD-ILs likely internalized to the cytosol of MCF-7/HER2 cells.

consistent with our previous reports that long circulating liposomes and ILs localize in tumors predominantly via the enhanced permeability and retention (EPR) effect rather than via antibody-mediated targeting.[21,28] Tissue sections of tumors collected 48 h postinjection were examined by confocal microscopy (Figure 5, right panel). QD-ILs showed extensive accumulation within tumor tissue and intracellularly within tumor cells; however, this technique did not allow quantitation of intracellular vs extracellular microdistribution.

In summary, we have synthesized QD-ILs that selectively and efficiently internalize in HER2-overexpressing tumor cells via receptor-mediated endocytosis. Uptake of QD-ILs in HER2-overexpressing cells was markedly greater than in nonoverexpressing cells as measured by flow cytometry assay and confocal microscopy. Systemic administration of QD-ILs resulted in tumor localization and in vivo fluorescence imaging in a xenograft mouse model, thus demonstrating how such constructs may facilitate QD use in vivo by exploiting the biocompatible properties of liposomes. Although conjugation of QDs to liposomes or ILs increased the average diameter of the labeled liposomal nanoparticles, it effectively eliminated the nonspecific binding observed with QDs alone and enabled extended circulation time in vivo. These studies indicate that QD-ILs were able to provide, in a single nanoscale construct, tumor cell-targeting, imaging, and drug delivery functions; to our knowledge, this is the first description of a targeted lipidic nanoparticle−QD system possessing all of these capabilities. Using QD-based labeling, nanoparticle biodistribution and penetration in solid tumors, intracellular fate in target cells, and real-time dynamics of drug delivery may be investigated in more detail. This targeted delivery system may also provide a strategy for tumor cell detection and labeling applications in vivo.

Acknowledgment. This work was supported by grants from the National Cancer Institute (NIH P50-CA58207-01, NIH P50-CA097257, and NIH U54-CA90788). K.C.W. is supported by the Delores R. Malone American Brain Tumor Association Fellowship Award and the National Cancer Institute Cancer Center Support Grants Pilot Program. F.F.C. is supported by DOD BCRP BC045345 grant, UCSF Prostate Cancer SPORE award (NIH Grant P50-CA89520), and CMC Institute of Nanotechnology and Nanomedicine (CMC-INN). This work was also performed under the auspices of the U.S. Department of Energy at the University of California/Lawrence Berkeley National Laboratory under contract no. DE-AC03-76SF00098. We thank Prof. C. David James, UCSF Department of Neurological Surgery and UCSF Brain Tumor Research Center, for assistance with in vivo imaging.

Supporting Information Available: Methods and three-dimensional images of anti-HER2 QD-ILs internalized by SK-BR-3 cells. This material is available free of charge via the Internet at http://pubs.acs.org.

References

(1) Jaiswal, J. K.; Simon, S. M. Potentials and pitfalls of fluorescent quantum dots for biological imaging. *Trends Cell Biol.* **2004**, *14* (9), 497–504.

(2) Jaiswal, J. K.; Goldman, E. R.; Mattoussi, H.; Simon, S. M. Use of quantum dots for live cell imaging. *Nat. Methods* **2004**, *1* (1), 73–78.

(3) Bruchez, M. P. Turning all the lights on: Quantum dots in cellular assays. *Curr. Opin. Chem. Biol.* **2005**, *9* (5), 533–537.

(4) Medintz, I. L.; Uyeda, H. T.; Goldman, E. R.; Mattoussi, H. Quantum dot bioconjugates for imaging, labelling and sensing. *Nat. Mater.* **2005**, *4* (6), 435–446.

(5) Michalet, X.; Pinaud, F. F.; Bentolila, L. A.; Tsay, J. M.; Doose, S.; Li, J. J.; Sundaresan, G.; Wu, A. M.; Gambhir, S. S.; Weiss, S. Quantum dots for live cells, in vivo imaging, and diagnostics. *Science* **2005**, *307* (5709), 538–544.

(6) So, M.-K.; Xu, C.; Loening, A. M.; Gambhir, S. S.; Rao, J. Self-illuminating quantum dot conjugates for in vivo imaging. *Nat. Biotechnol.* **2006**, *24* (3), 339–343.

(7) Alivisatos, A. P.; Gu, W.; Larabell, C. Quantum dots as cellular probes. *Annu. Rev. Biomed. Eng.* **2005**, *7*, 55–76.

(8) Bruchez, M. J.; Moronne, M.; Gin, P.; Weiss, S.; Alivisatos, A. P. Semiconductor nanocrystals as fluorescent biological labels. *Science* **1998**, *281* (5385), 2013–2016.

(9) Pathak, S.; Choi, S.-K.; Arnheim, N.; Thompson, M. E. Hydroxylated quantum dots as luminescent probes for in situ hybridization. *J. Am. Chem. Soc.* **2001**, *123* (17), 4103–4104.

(10) Benzen, E. L.; Tomlinson, I. D.; Mason, J.; Gresch, P.; Warnement, M. R.; Wright, D.; Sanders-Bush, E.; Blakely, R.; Rosenthal, S. J. Surface modification to reduce nonspecific binding of quantum dots in live cell assays. *Bioconjugate Chem.* **2005**, *16* (6), 1488–1494.

(11) Wu, X.; Liu, H.; Liu, J.; Haley, K. N.; Treadway, J. A.; Larson, J. P.; Ge, N.; Peale, F.; Bruchez, M. P. Immunofluorescent labeling of cancer marker HER2 and other cellular targets with semiconductor quantum dots. *Nat. Biotechnol.* **2003**, *21* (1), 41–46.

(12) Howarth, M.; Takao, K.; Hayashi, Y.; Ting, A. Y. Targeting quantum dots to surface proteins in living cells with biotin ligase. *Proc. Natl. Acad. Sci. U.S.A.* **2005**, *102* (21), 7583–7588.

(13) Gao, X.; Cui, Y.; Levenson, R. M.; Chung, L. W. K.; Nie, S. In vivo cancer targeting and imaging with semiconductor quantum dots. *Nat. Biotechnol.* **2004**, *22* (8), 969–976.

(14) Gopalakrishnan, G.; Danelon, C.; Izewska, P.; Prummer, M.; Bolinger, P.-Y.; Geissbühler, I.; Demurtas, D.; Dubochet, J.; Vogel, H. Multifunctional lipid/quantum dot hybrid nanocontainers for controlled targeting of live cells. *Angew. Chem. Int. Ed. Engl.* **2006**, *45* (33), 5478–5483.

(15) Drummond, D. C.; Meyer, O.; Hong, K.; Kirpotin, D. B.; Papahadjopoulos, D. Optimizing liposomes for delivery of chemotherapeutic agents to solid tumors. *Pharmacol. Rev.* **1999**, *51* (4), 691–743.

(16) Park, J. W.; Hong, K.; Kirpotin, D. B.; Papahadjopoulos, D.; Benz, C. C. Immunoliposomes for cancer treatment. *Adv. Pharmacol.* **1997**, *40*, 399–435.

(17) Park, J. W.; Benz, C. C.; Martin, F. J. Future directions of liposome- and immunoliposome-based cancer therapeutics. *Semin. Oncol.* **2004**, *31* (6, Suppl. 13), 196–205.

(18) Park, J. W.; Hong, K.; Carter, P.; Asgari, H.; Guo, L. Y.; Keller, G. A.; Wirth, C.; Shalaby, R.; Kotts, C.; Wood, W. I.; Papahadjopoulos, D.; Benz, C. C. Development of anti-p185^{HER2} immunoliposomes for cancer therapy. *Proc. Natl. Acad. Sci. U.S.A.* **1995**, *92* (5), 1327–1331.

(19) Park, J. W.; Hong, K.; Kirpotin, D. B.; Colbern, G.; Shalaby, R.; Baselga, J.; Shao, Y.; Nielsen, U. B.; Marks, J. D.; Moore, D.; Papahadjopoulos, D.; Benz, C. C. Anti-HER2 immunoliposomes: Enhanced efficacy attributable to targeted delivery. *Clin. Cancer Res.* **2002**, *8* (4), 1172–1181.

(20) Mamot, C.; Drummond, D. C.; Greiser, U.; Hong, K.; Kirpotin, D. B.; Marks, J. D.; Park, J. W. Epidermal growth factor receptor (EGFR)-targeted immunoliposomes mediate specific and efficient drug delivery to EGFR- and EGFRvIII-overexpressing tumor cells. *Cancer Res.* **2003**, *63* (12), 3154–3161.

(21) Mamot, C.; Drummond, D. C.; Noble, C. O.; Kallab, V.; Guo, Z.; Hong, K.; Kirpotin, D. B.; Park, J. W. Epidermal growth factor receptor-targeted immunoliposomes significantly enhance the efficacy of multiple anticancer drugs in vivo. *Cancer Res.* **2005**, *65* (24), 11631–11638.

(22) Torchilin, V. P.; Levchenko, T. S.; Rammohan, R.; Volodina, N.; Papahadjopoulos-Sternberg, B.; D'Souza, G. G. M. Cell transfection in vitro and in vivo with nontoxic TAT peptide-liposome-DNA complexes. *Proc. Natl. Acad. Sci. U.S.A.* **2003**, *100* (4), 1972–1977.

(23) Torchilin, V. P.; Lukyanov, A. N.; Gao, Z.; Papahadjopoulos-Sternberg, B. Immunomicelles: Targeted pharmaceutical carriers for poorly soluble drugs. *Proc. Natl. Acad. Sci. U.S.A.* **2003**, *100* (10), 6039–6044.

(24) Benz, C. C.; Scott, G. K.; Sarup, J. C.; Johnson, R. M.; Tripathy, D.; Coronado, E.; Shepard, H. M.; Osborne, C. K. Estrogen-dependent, tamoxifen-resistant tumorigenic growth of MCF-7 cells transfected with HER2/neu. *Breast Cancer Res. Treat.* **1993**, *24* (2), 85–95.

(25) Jaiswal, J. K.; Mattoussi, H.; Mauro, J. M.; Simon, S. M. Long-term multiple color imaging of live cells using quantum dot bioconjugates. *Nat. Biotechnol.* **2003**, *21* (1), 47–51.

(26) Haran, G.; Cohen, R.; Bar, L. K.; Barenholz, Y. Transmembrane ammonium sulfate gradients in liposomes produce efficient and stable entrapment of amphipathic weak bases. *Biochim. Biophys. Acta* **1993**, *1151* (2), 201–15.

(27) Derfus, A. M.; Chan, W. C. W.; Bhatia, S. N. Probing the cytotoxicity of semiconductor quantum dots. *Nano Lett.* **2004**, *4* (1), 11–18.

(28) Kirpotin, D. B.; Drummond, D. C.; Shao, Y.; Shalaby, M. R.; Hong, K.; Nielsen, U. B.; Marks, J. D.; Benz, C. C.; Park, J. W. Antibody targeting of long-circulating lipidic nanoparticles does not increase tumor localization but does increase internalization in animal models. *Cancer Res.* **2006**, *66* (13), 6732–6740.

NL801438U

Published in final edited form as:
Nat Med. 2004 February ; 10(2): 145–147. doi:10.1038/nm988.

Direct evidence that the VEGF-specific antibody bevacizumab has antivascular effects in human rectal cancer

Christopher G Willett[1], **Yves Boucher**[1,10], **Emmanuelle di Tomaso**[1,10], **Dan G Duda**[1,10], **Lance L Munn**[1,10], **Ricky T Tong**[1,10], **Daniel C Chung**[2], **Dushyant V Sahani**[3], **Sanjeeva P Kalva**[3], **Sergey V Kozin**[1], **Mari Mino**[4], **Kenneth S Cohen**[5], **David T Scadden**[5], **Alan C Hartford**[1], **Alan J Fischman**[6], **Jeffrey W Clark**[7], **David P Ryan**[7], **Andrew X Zhu**[7], **Lawrence S Blaszkowsky**[7], **Helen X Chen**[9], **Paul C Shellito**[8], **Gregory Y Lauwers**[4], and **Rakesh K Jain**[1]

1 *Department of Radiation Oncology, Massachusetts General Hospital and Harvard Medical School, Boston, Massachusetts 02114, USA*

2 *Division of Gastroenterology, Massachusetts General Hospital and Harvard Medical School, Boston, Massachusetts 02114, USA*

3 *Department of Radiology, Massachusetts General Hospital and Harvard Medical School, Boston, Massachusetts 02114, USA*

4 *Department of Pathology, Massachusetts General Hospital and Harvard Medical School, Boston, Massachusetts 02114, USA*

5 *AIDS Research Center/Experimental Hematology, Massachusetts General Hospital and Harvard Medical School, Boston, Massachusetts 02114, USA*

6 *Department of Nuclear Medicine, Massachusetts General Hospital and Harvard Medical School, Boston, Massachusetts 02114, USA*

7 *Division of Hematology/Oncology, Massachusetts General Hospital and Harvard Medical School, Boston, Massachusetts 02114, USA*

8 *Department of Surgery, Massachusetts General Hospital and Harvard Medical School, Boston, Massachusetts 02114, USA*

9 *Cancer Therapy Evaluation Program, National Cancer Institute, Bethesda, Maryland 20852, USA*

Abstract

The effects of vascular endothelial growth factor (VEGF) blockade on the vascular biology of human tumors are not known. Here we show here that a single infusion of the VEGF-specific antibody bevacizumab decreases tumor perfusion, vascular volume, microvascular density, interstitial fluid pressure and the number of viable, circulating endothelial and progenitor cells, and increases the fraction of vessels with pericyte coverage in rectal carcinoma patients. These data indicate that VEGF blockade has a direct and rapid antivascular effect in human tumors.

VEGF has a crucial role in physiological and pathological angiogenesis[1–3]. Although VEGF blockade, alone or in combination with cytotoxic therapies, is being tested in a number of

Correspondence should be addressed to C.G.W. (E-mail: cwillett@partners.org) or R.K.J. (E-mail: jain@steele.mgh.harvard.edu).
[10]These authors contributed equally to this work.

Note: Supplementary information is available on the Nature Medicine website.

COMPETING INTERESTS STATEMENT

The authors declare that they have no competing financial interests.

clinical trials[4], including the first successful phase 3 clinical trial[5], the effects of anti-VEGF treatment on the vascular biology of human tumors are not known. To this end, we recently initiated a National Cancer Institute–sponsored phase 1 clinical trial that integrates the VEGF-specific antibody bevacizumab (Avastin; Genentech) into a contemporary treatment program of preoperative chemotherapy and radiation therapy followed by surgery, for patients with primary and nonmetastatic rectal cancer. To gain insight into the mechanisms of action of bevacizumab, we designed the trial to evaluate the effects of bevacizumab alone on (i) tumor physiology (blood perfusion, blood volume, permeability–surface area product, microvascular density (MVD), perivascular coverage, interstitial fluid pressure (IFP) and 18-fluorodeoxyglucose (FDG) uptake); (ii) systemic response (VEGF level in blood, number of circulating endothelial cells (CECs) and progenitor cells); and (iii) tumor response (see Supplementary Note online for methods).

Six patients with primary and locally advanced adenocarcinoma of the rectum have been enrolled in a preoperative treatment protocol of bevacizumab administration alone (5 mg/kg intravenously), followed after 2 weeks—the approximate half-life of bevacizumab in circulation—by concurrent administration of bevacizumab with 5-fluorouracil and external beam radiation therapy to the pelvis and surgery, 7 weeks after treatment completion. Twelve days after bevacizumab infusion, flexible sigmoidoscopy (Fig. 1) revealed that bevacizumab induced tumor regression of >30% in patient 1, and no change in tumor size in the remaining five patients. Functional computed tomography (CT) scans at this time point indicated significant decreases in tumor blood perfusion (40–44%; $P < 0.05$) and blood volume (16–39% in four of five patients analyzed; $P < 0.05$; Figs. 1b and 2; see Supplementary Table 1 online for group statistics). This was accompanied by a significant decrease in tumor MVD (29–59% in five patients analyzed; $P < 0.05$; Fig. 2d). These three sets of data provide direct evidence of the antivascular effects of bevacizumab in human tumors, which is in line with preclinical findings[6,7].

Twelve days after bevacizumab treatment, IFP was reduced in four of four patients (Fig. 2f) and overall mean IFP decreased significantly from 15.0 ± 2.0 to 4.0 ± 2.2 mm Hg ($P < 0.01$). The decrease in IFP is in concert with our preclinical findings[6]. Elevated IFP, a hallmark of solid tumors, is a result of abnormalities in tumor vessels (such as abnormal structure of the vessel wall). The decrease in IFP after anti-VEGF treatment may be a result of 'normalization'; that is, the resumption of normal function in the tumor vasculature[8]. The increased fraction of vessels positive for α-smooth muscle actin in four of five patients (Fig. 2e and Supplementary Fig. 1 online) is supportive of vascular normalization[9]. As a result of the decrease in vascular volume and MVD, one would expect a reduction in vascular surface area, and hence a lowering of the permeability–surface area product. Surprisingly, four of five patients had no significant changes in permeability–surface area product (Fig. 2c and Supplementary Table 1), providing indirect evidence for improved extravasation of the CT contrast agent from the normalized vasculature. Finally, on day 12 the follow-up positron emission tomography (PET) scans indicated no change in tumor FDG uptake in five patients, and showed a 40% decrease in patient 3 (Fig. 2g). Collectively, these data suggest that the efficiency of blood vessels after bevacizumab treatment is improved. These clinical findings are consistent with previous preclinical data on tumor oxygenation[6] and drug uptake[10] after anti-VEGF treatment.

In addition to being a mitogen and survival factor for endothelial cells, VEGF mobilizes progenitor cells from the bone marrow into the circulation[11]. VEGF blockade decreased the number of progenitor cells circulating on day 3 (Fig. 2b). No decrease in circulating VEGF (plasma, serum and urine) was detected with the current assay (see Methods; data not shown). After bevacizumab treatment, the number of $CD31^{bright}CD45^{-}$ cells, but not the total number of $CD31^{+}CD45^{-}$ cells, decreased in all patients (Fig. 2h). Further analysis indicated that $CD31^{bright}CD45^{-}$ cells represented viable CECs (Supplementary Fig. 2 online). An increase

in the number and viability of CECs was recently found in lymphoma and breast cancer patients[12]. In addition, preclinical studies indicate that CEC kinetics might serve as a surrogate marker of response to treatment[13]. Based on these data, we suggest that the kinetics of progenitor cells or viable CECs in peripheral blood should be explored as an early indicator of tumor response to anti-VEGF agents.

Six weeks after completion of the bevacizumab, radiation therapy and chemotherapy regimen, follow-up PET scans (Fig. 1c) showed decreased tumor FDG uptake compared with pretreatment values in five patients (Fig. 2g). Tumor FDG uptake in patient 5 was low, and similar before and at the end of therapy (Fig. 2g). Notably, all six patients completed the combined treatment without dose-limiting toxicity, and underwent surgery without perioperative or postoperative complications. Macroscopic and histologic analysis of the surgical specimens revealed a marked response in all six patients, with only microscopic disease in five of the patients (Fig. 1a and Supplementary Note).

High doses of bevacizumab are more effective when used as monotherapy for highly VEGF-dependent tumors such as renal-cell carcinoma[14]. Our data from six consecutive patients show for the first time that even at low doses, bevacizumab alone can decrease perfusion, MVD and IFP in a solid tumor, and decrease the number of CECs. The decrease in IFP and increase in the fraction of vessels with pericyte coverage support the normalization hypothesis[8]. This normalization process may retard the shedding of metastatic cells in the circulation and improve the delivery of therapeutic agents in tumors. Bevacizumab may also sensitize the endothelium to cytotoxic agents. Collectively, these mechanisms may explain the unprecedented efficacy of bevacizumab in recent clinical trials, as well as the possible synergistic or additive interaction between antiangiogenic and cytotoxic therapies that has been observed in preclinical settings for more than a decade[4,15]. The identification of valid surrogate markers for antiangiogenic therapy, alone or combined with cytotoxic therapies, has been elusive. The results of this phase 1 study will hopefully facilitate and stimulate future research in this area.

Supplementary Material

Refer to Web version on PubMed Central for supplementary material.

Acknowledgments

This study was supported by two National Cancer Institute grants (R21 CA099237 to C.G.W. and PO1 CA80124 to R.K.J.). D.G.D. is a Cancer Research Institute fellow. R.T.T. is a fellow of the Susan G. Komen Breast Cancer Foundation. We thank T. Lee for his contribution to the CT analysis, M. Ancukiewicz, T.P. Padera and W. Strauss for helpful comments, and J. Tooredman for the ELISAs.

References

1. Carmeliet P, Jain RK. Nature 2000;407:249–257. [PubMed: 11001068]
2. Dvorak HF. J Clin Oncol 2002;20:4368–4380. [PubMed: 12409337]
3. Ferrara N, Gerber HP, LeCouter J. Nat Med 2003;9:669–676. [PubMed: 12778165]
4. Kerbel R, Folkman J. Nat Rev Cancer 2002;2:727–739. [PubMed: 12360276]
5. McCarthy M. Lancet 2003;361:1959. [PubMed: 12801743]
6. Lee C, et al. Cancer Res 2000;60:5565–5570. [PubMed: 11034104]
7. Yuan F, et al. Proc Natl Acad Sci USA 1996;93:14765–14770. [PubMed: 8962129]
8. Jain RK. Nat Med 2001;7:987–989. [PubMed: 11533692]
9. Jain RK. Nat Med 2003;9:685–693. [PubMed: 12778167]
10. Wildiers H, et al. Br J Cancer 2003;88:1979–1986. [PubMed: 12799646]
11. Rafii S, et al. Nat Rev Cancer 2002;2:826–835. [PubMed: 12415253]

12. Mancuso P, et al. Blood 2001;97:3658–3661. [PubMed: 11369666]
13. Monestiroli S, et al. Cancer Res 2001;61:4341–4344. [PubMed: 11389057]
14. Yang JC, et al. N Engl J Med 2003;349:427–434. [PubMed: 12890841]
15. Teicher BA. Cancer Metastasis Rev 1996;15:247–272. [PubMed: 8842498]

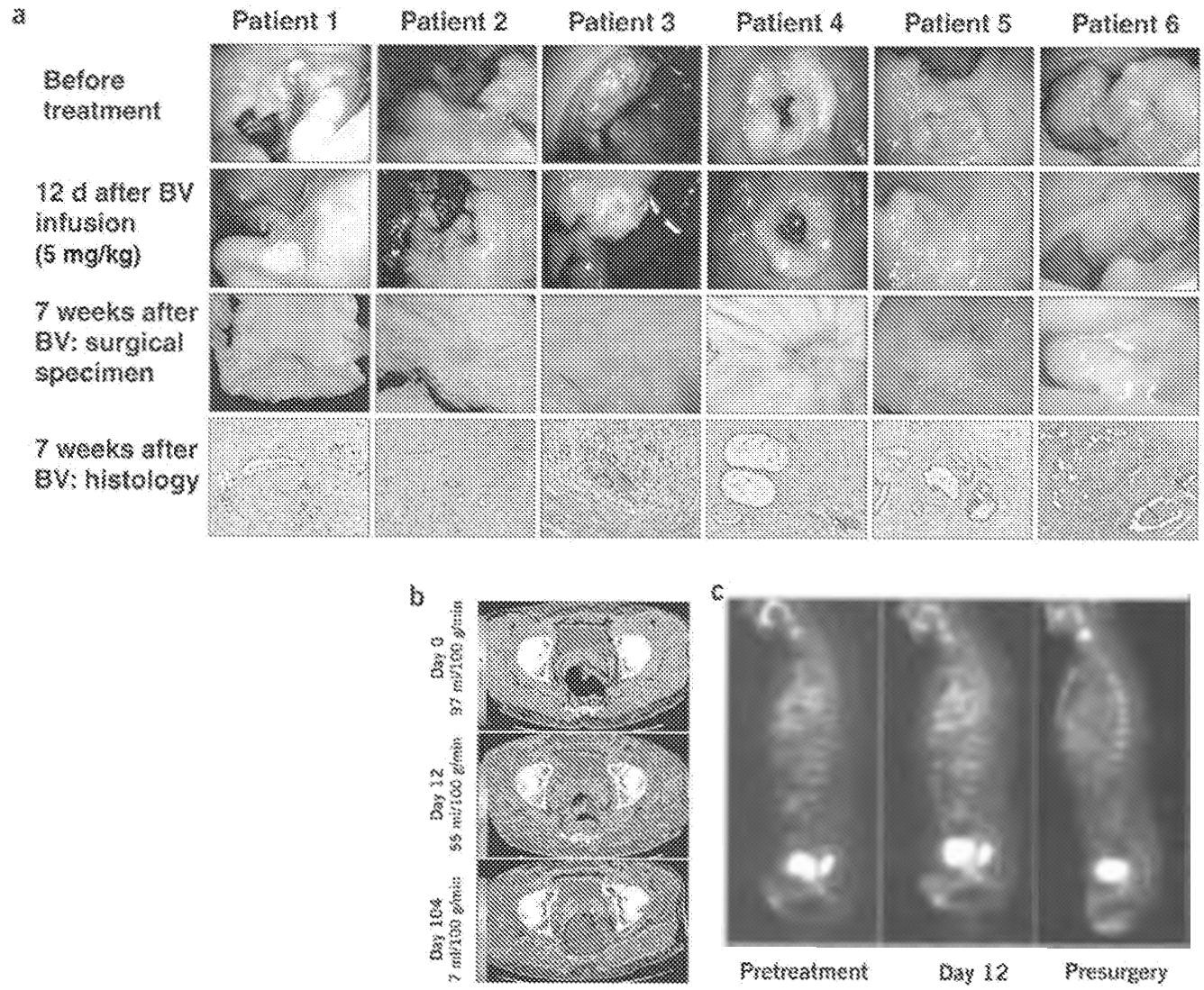

Figure 1.

Effect of treatment on tumors in patients who completed entire combined treatment regimen, and surgery. (**a**) Endoscopic and pathological evaluation of rectal tumors. Surgical specimens showed grade II tumor regression in patients 1–5 and grade III in patient 6, by Mandard criteria (see Supplementary Note). Endoscopic image (instead of surgical specimen) was taken for patient 6, 3.5 weeks before surgery. BV, bevacizumab. (**b**) Representative functional CT images of blood perfusion before treatment (day 0), after bevacizumab (day 12) and after completion of treatment (day 104) in patient 5. (**c**) Tumor FDG uptake before treatment (pretreatment), 12 d after bevacizumab treatment and 6–7 weeks after completion of all neoadjuvant therapy (presurgery). Sagittal projections of FDG-PET scans for patient 1 are shown. Tumor is outlined in box, posterior to bladder.

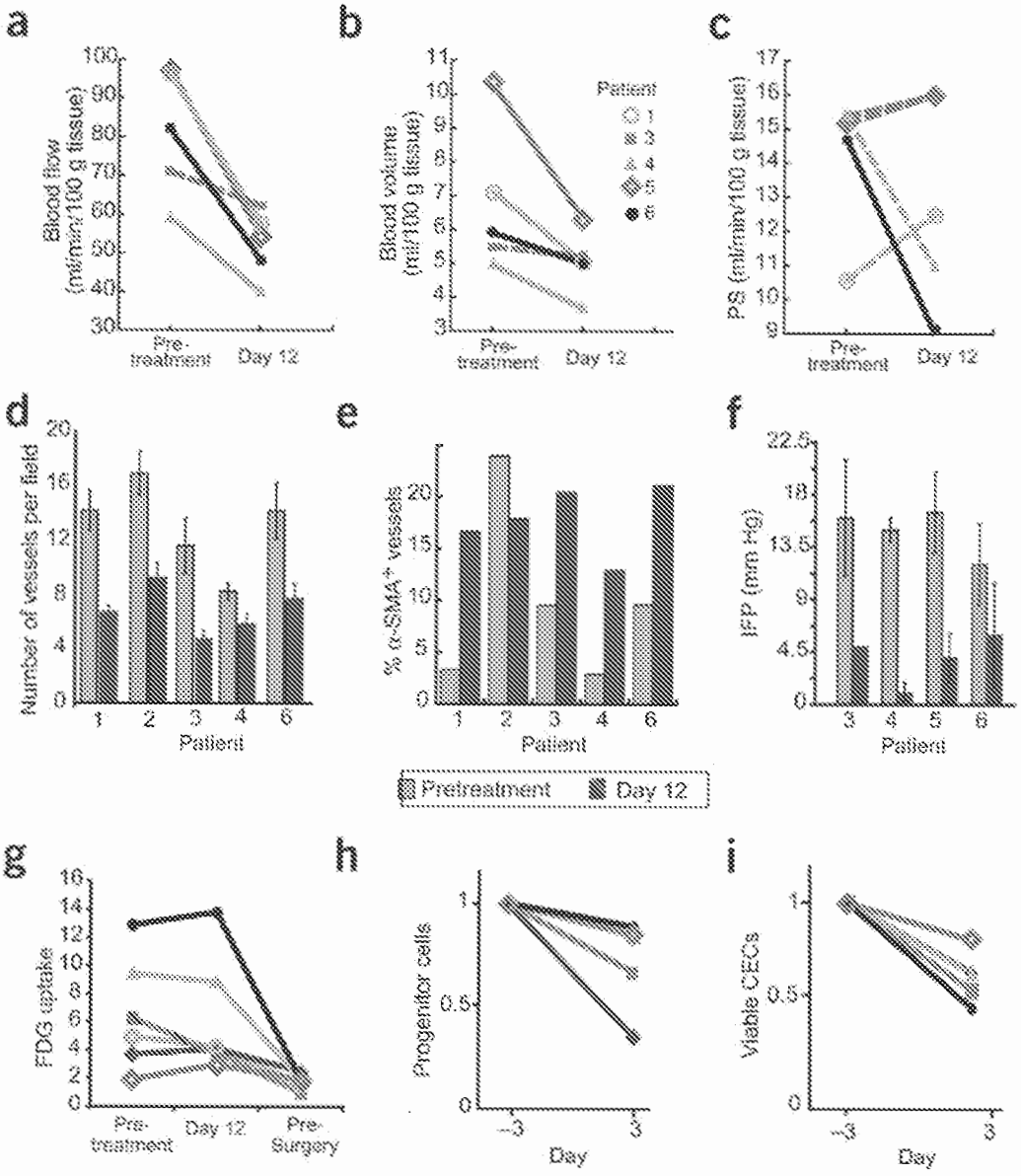

Figure 2.

Effect of a single injection of bevacizumab on tumor vasculature and FDG uptake. Parameters were obtained pretreatment and after one bevacizumab infusion. (a–c) Blood perfusion (a), blood volume (b) and permeability--surface area product (PS; c). Significant decreases after treatment are indicated by solid lines ($P < 0.05$ by t-test). Blood flow and blood volume decreased significantly in four of the patients. (d) Microvascular density. All patients showed significant decreases after treatment ($P < 0.05$ by t-test). (e) Fraction of vessels with pericyte coverage. The difference in the fraction of vessels positive for α-smooth muscle actin (α-SMA) in patient 2 was identified as an outlier by the Extreme Studentized Deviate test. Paired t-test analyses of the mean values that included and excluded the data of patient 2 had $P < 0.09$ and 0.001, respectively. (f) Mean tumor IFP decreased significantly after bevacizumab ($P < 0.01$ by paired t-test). (g) Tumor FDG uptake before treatment, on day 12 and presurgery (day 93), normalized for muscle values. On day 12 after bevacizumab treatment, a 40% decrease was observed in patient 3, and no change in the other patients. Lower levels were found in all

patients before surgery except for patient 5, who had low levels throughout the treatment. In comparison to pretreatment and day 12 values, the median standard uptake value was significantly lower on day 93 ($P < 0.01$; Supplementary Table 1). (**h**) Circulating progenitor/stem cells ($AC133^+$; left) and viable CECs (right) in peripheral blood. Samples were run to acquire 50,000 events in the mononuclear/lymphocyte gate. For both cell populations, bevacizumab induced a significant decrease in mean values ($P < 0.05$ by Wilcoxon signed-rank test). Key in b applies to a,c, g–i.